SENSING DNA IN ANTIVIRAL INNATE IMMUNITY

EDITED BY: Chunfu Zheng, Rongtuan Lin and Junji Xing
PUBLISHED IN: Frontiers in Immunology

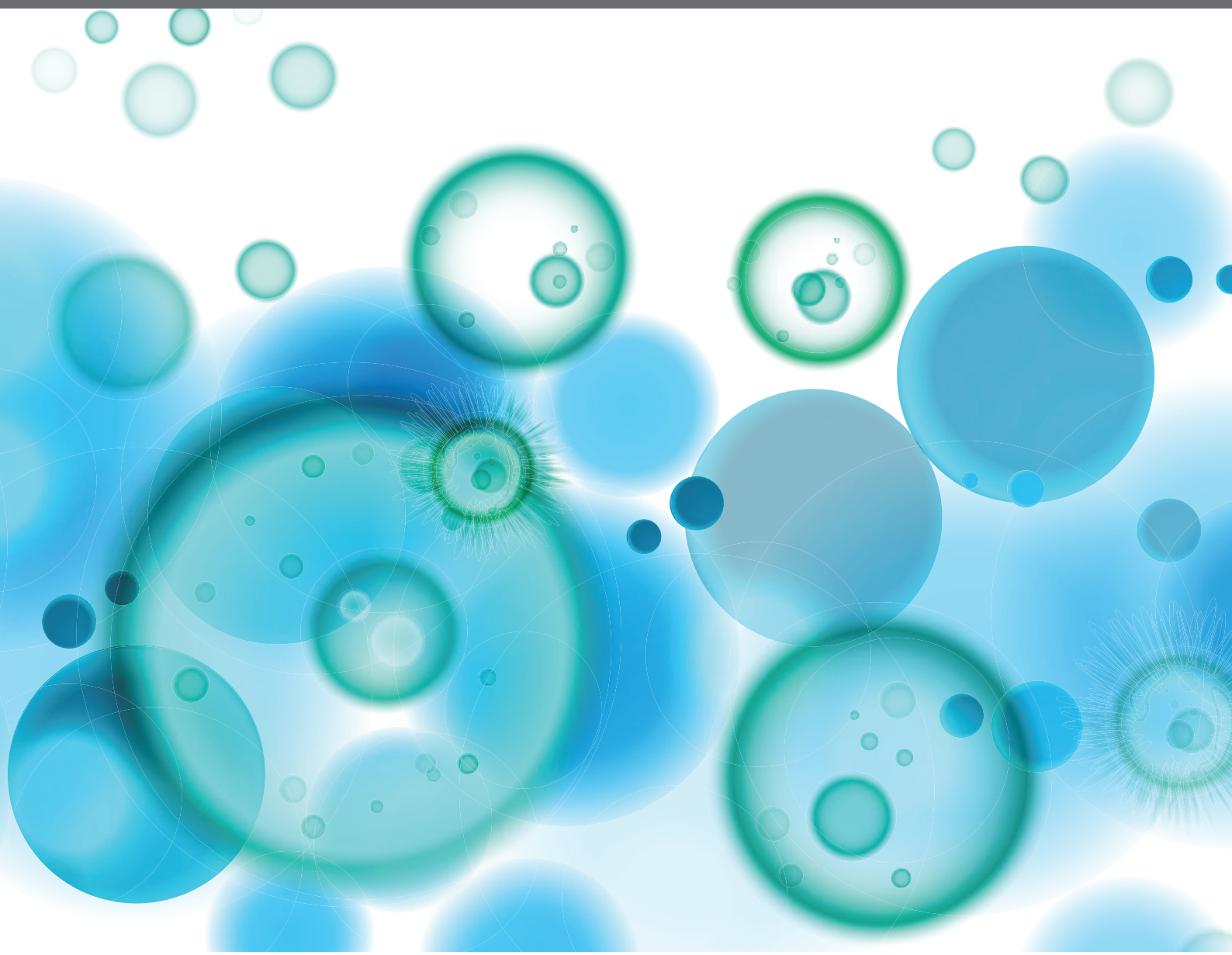

frontiers Research Topics

frontiers

ISSN 1664-8714
ISBN 978-2-88971-270-0
DOI 10.3389/978-2-88971-270-0

About Frontiers

Frontiers is more than just an open-access publisher of scholarly articles: it is a pioneering approach to the world of academia, radically improving the way scholarly research is managed. The grand vision of Frontiers is a world where all people have an equal opportunity to seek, share and generate knowledge. Frontiers provides immediate and permanent online open access to all its publications, but this alone is not enough to realize our grand goals.

Frontiers Journal Series

The Frontiers Journal Series is a multi-tier and interdisciplinary set of open-access, online journals, promising a paradigm shift from the current review, selection and dissemination processes in academic publishing. All Frontiers journals are driven by researchers for researchers; therefore, they constitute a service to the scholarly community. At the same time, the Frontiers Journal Series operates on a revolutionary invention, the tiered publishing system, initially addressing specific communities of scholars, and gradually climbing up to broader public understanding, thus serving the interests of the lay society, too.

Dedication to Quality

Each Frontiers article is a landmark of the highest quality, thanks to genuinely collaborative interactions between authors and review editors, who include some of the world's best academicians. Research must be certified by peers before entering a stream of knowledge that may eventually reach the public - and shape society; therefore, Frontiers only applies the most rigorous and unbiased reviews.
Frontiers revolutionizes research publishing by freely delivering the most outstanding research, evaluated with no bias from both the academic and social point of view. By applying the most advanced information technologies, Frontiers is catapulting scholarly publishing into a new generation.

What are Frontiers Research Topics?

Frontiers Research Topics are very popular trademarks of the Frontiers Journals Series: they are collections of at least ten articles, all centered on a particular subject. With their unique mix of varied contributions from Original Research to Review Articles, Frontiers Research Topics unify the most influential researchers, the latest key findings and historical advances in a hot research area! Find out more on how to host your own Frontiers Research Topic or contribute to one as an author by contacting the Frontiers Editorial Office: frontiersin.org/about/contact

SENSING DNA IN ANTIVIRAL INNATE IMMUNITY

Topic Editors:
Chunfu Zheng, University of Calgary, Canada
Rongtuan Lin, McGill University, Canada
Junji Xing, Houston Methodist Research Institute, United States

Citation: Zheng, C., Lin, R., Xing, J., eds. (2021). Sensing DNA in Antiviral Innate Immunity. Lausanne: Frontiers Media SA. doi: 10.3389/978-2-88971-270-0

Table of Contents

frontiers in Immunology

EDITORIAL
published: 01 July 2021
doi: 10.3389/fimmu.2021.644310

Editorial: Sensing DNA in Antiviral Innate Immunity

Rongtuan Lin[1]*, *Junji Xing*[2]* and *Chunfu Zheng*[3,4]*

[1] Department of Medicine, Lady Davis Institute-Jewish General Hospital, McGill University, Montreal, QC, Canada, [2] Immunobiology and Transplant Science Center, Department of Surgery, Houston Methodist Research Institute, Houston, TX, United States, [3] Department of Immunology, School of Basic Medical Sciences, Fujian Medical University, Fuzhou, China, [4] Department of Microbiology, Immunology and Infectious Diseases, University of Calgary, Calgary, AB, Canada

OPEN ACCESS

Edited by:
Alexis M. Kalergis,
Pontificia Universidad Católica de Chile, Chile

Reviewed by:
Dominic De Nardo,
Monash University, Australia
Julio Villena,
CONICET Centro de Referencia para Lactobacilos (CERELA), Argentina
Martin R. Jakobsen,
Aarhus University, Denmark

***Correspondence:**
Rongtuan Lin
rongtuan.lin@mcgill.ca
Junji Xing
jxing@houstonmethodist.org
Chunfu Zheng
zheng.alan@hotmail.com

Specialty section:
This article was submitted to Viral Immunology, a section of the journal Frontiers in Immunology

Received: 20 December 2020
Accepted: 21 June 2021
Published: 01 July 2021

Citation:
Lin R, Xing J and Zheng C (2021) Editorial: Sensing DNA in Antiviral Innate Immunity. Front. Immunol. 12:644310. doi: 10.3389/fimmu.2021.644310

Keywords: DNA sensors, pattern-recognition receptors, cyclic GMP-AMP synthase, STING, viruses, innate immune responses.

Editorial on the Research Topic

Sensing DNA in Antiviral Innate Immunity

The editorial team welcomes you to the specific Research Topic on "Sensing DNA in Antiviral Innate Immunity". We appreciate the hard work and outstanding contributions from all authors. Effective defense mechanisms against virus infection and pathogenesis rely on a prompt and robust induction of antiviral innate immunity. Central to antiviral innate immune responses is the detection of evolutionarily conserved structures, termed pathogen-associated molecular patterns (PAMPs), by a set of germline-encoded pattern-recognition receptors (PRRs) (1). In the case of DNA virus or retrovirus infection, cytosolic viral DNA or reverse transcription intermediates (RTI) is detected by DNA sensors cyclic GMP-AMP synthase (cGAS) as well as other cytosolic DNA binding proteins such as interferon-gamma inducible protein 16 (IFI16) (2, 3). Conversely, endosome-associated viral nucleic acids are recognized by toll-like receptor 7 (TLR7) and TLR9 (1).

Furthermore, a recent report identified heterogeneous nuclear ribonucleoprotein A2B1 (hnRNPA2B1) as a nuclear DNA sensor for viral double-stranded DNA, but not cellular DNA, in the nucleus (4). Additionally, cGAS is recently reported to sense nuclear DNA (5–11). Following the detection of specific viral PAMPs, PRRs trigger the activation of intracellular signaling cascades, ultimately leading to the activation of NF-κB, interferon regulatory factor (IRF) 3 and 7, and the production of type I interferons (IFN-I) and various inflammatory cytokines such as CXCL10, TNFα and IL-6 (12). The antiviral program is subsequently amplified by paracrine and autocrine signaling of IFN through IFN receptors and Janus kinase (JAK)-signal transducer and activator of transcription (STAT) signaling, resulting in the induction of antiviral IFN-stimulated genes (ISGs) (13). This Research Topic will feature different contributions providing the molecular and structural basis of endosomal, nuclear, and cytosolic DNA sensors in antiviral response, the dynamic regulations of DNA sensors and their adaptor protein activation, trafficking, and post-translational modifications, and virus evasion of the host DNA-sensing antiviral innate immune responses. These approaches could contribute to the development of novel antiviral therapies and oncolytic viruses in the future.

Zahid et al. introduced the PAMPs, PRRs, and the sources of cytotoxic DNA. The authors showed the structures of endosomal and cytosolic DNA sensors alone or complexed with DNA to provide insights on how binding the DNA to these sensors triggers the signaling pathways to activate the antiviral immune responses. They focused on the endosomal DNA sensor TLR9 and multiple cytosolic DNA sensors, including cGAS, IFI16, absent in melanoma 2 (AIM2), and DNA-dependent activator IRFs (DAI). The authors also covered other cytosolic DNA sensors, including DEAD-box helicase DDX41, RNA polymerase III, DNA-dependent protein kinase (DNA-PK), and meiotic recombination 11 homolog A (MRE11), as well as adaptor protein stimulator of interferon genes (STING).

To ensure successful antiviral defenses and avoid aberrant or dysregulation of host immune signaling, antiviral pathways need to be tightly regulated. PRRs and their adaptor proteins are regulated at multiple levels. Two papers have discussed the recent advances in DNA sensors' dynamic regulations and their adaptor protein STING. Zheng described the role of TLR9 dimerization, trafficking, and a multiprotein signaling complex formation in regulating endosomal DNA-sensing signaling. He also provided an update on the role of STING trafficking and polymerization in cGAS-STING signaling, how cellular proteins involve in cGAS-STING activation, and the evasion of cGAS-STING signaling by DNA viruses. Li et al. focused on trafficking and post-translational modifications in STING activation. They also summarized the proteins encoded by different DNA and RNA viruses to inhibit the intracellular trafficking and STING signaling activation.

Recent studies have identified nucleus-localized DNA and RNA sensors to detect pathogenic nucleic acids for triggering antiviral innate immune responses. IFI16, hnRNPA2B1, and nuclear cGAS are all defined as possible sensors for nuclear DNA that is unwinded from histone complexes. Zhang et al. summarized the recent advances in identifying nuclear DNA sensors IFI16, hnRNPA2B1, and nuclear cGAS and their roles in regulating antiviral innate immune responses and tumorigenesis. The authors also discussed the transcriptional, post-transcriptional, and post-translational regulations of these nuclear DNA sensors.

Viruses have evolved various strategies to inhibit and subvert the host's antiviral immune responses. Three papers have been contributed to discuss recent advances in DNA viruses-induced and antagonize innate immune responses *via* DNA sensors. Zhao et al. reviewed how herpes simplex viruses (HSVs) are detected by the cytosolic DNA sensor cGAS-STING, IFI16, AIM2, and DAI, and how HSV-encoded proteins antagonize the signaling pathways triggered by DNA sensors. The authors also provided an overview of RIG-I-like receptors (RLRs) and protein kinase R (PKR) in the antiviral immune responses against HSVs. A paper from El-Jesr et al. and another paper from Lu and Zhang reviewed the latest studies on how the cytosolic DNA sensors recognize vaccinia virus (VACV) and trigger the activation of innate immune responses, and the strategies evolved by VACV to antagonize innate immune responses induced *via* cytosolic DNA sensing pathways.

In a large genome-wide association study (GWAS) of the immune responses to primary smallpox vaccination, Kennedy et al. reported a cluster of SNPs on chromosome 5 (5q31.2) that were significantly associated with IFNα response to *in vitro* poxvirus stimulation. The authors identified rs1131769, a non-synonymous SNP in *TMEM173* causing an Arg-to-His change at position 232 in the STING protein (H232 STING), as a major regulator of cGAS-mediated IFN-I production. Compared to R232 homozygote, H232 homozygote has a 90% reduction in cGAMP-mediated IFNa secretion. Molecular modeling revealed that H232 has greater structural flexibility and mobility of the ligand-binding loop.

Cytosolic DNA sensors have not been studied in livestock animals. Zheng et al. reported the characterization of porcine cGAS, STING, and IFI16 and measured the function of porcine cGAS, STING, and IFI16 in regulating IFN-I, cytokine, and ISG gene expression. Porcine cGAS-STING signaling triggers the antiviral responses, while porcine IFI16 competitively binds with agonist DNA and STING to inhibit cGAS-STING signaling. Oliveira et al. used chicken macrophage-like cell line HD11 to characterize the function of cGAS-STING signaling in chicken. Knockout studies demonstrated that chicken cGAS-STING was essential for fowlpox- and intracellular DNA-induced IFN-I responses in chicken macrophage-like cells. Furthermore, chicken cGAS-STING signaling is also required for the regulation of macrophage effector functions.

The goal of our understanding of antiviral immune responses is to develop new therapeutics. Given that viral PAMP-PRR interaction is the initial trigger of the innate and adaptive immune response, an attractive strategy for developing an efficient therapy to inhibit virus replication is natural or synthetic molecules that mimic the viral PAMPs to activate the host innate immune defense. Shao et al. reported that poly(dA:dT) treatment induced the expression of IFNs and the multiple antiviral ISGs in the cervical epithelial cells and significantly inhibited HSV-2 infection. It has been demonstrated that poly (dA:dT) can be transcribed into a 5'pppRNA in the host cells, triggering RIG-I-dependent antiviral responses. The authors showed that knockout of RIG-I significantly compromised poly (dA:dT)-mediated activation of IFN signaling and inhibition of HSV-2 infection. With an alternative approach, Abraham et al. performed a high throughput screen to identify novel small molecules capable of stimulating IFN-I production. The authors reported a small molecule termed M04 that can activate a STING-dependent IFN-I production in human cells. Mechanistically, M04 induced STING phosphorylation and ER-Golgi trafficking.

Constitutive active mutation of STING is associated with the clinical syndrome known as STING-associated vasculopathy with onset in infancy (SAVI). Berthelot et al. reviewed the similarities between T and B cell responses in severe coronavirus disease 2019 (COVID-19) and human or animal models of SAVI syndromes. The authors proposed that a delayed overactivation of cGAS-STING signaling could play a central role in COVID-19 pathogenesis. Three potential models for SARS-CoV-2 mediated STING activation were discussed.

AUTHOR CONTRIBUTIONS

All authors listed have made a substantial, direct, and intellectual contribution to the work and approved it for publication.

FUNDING

Grant supports for this work: (1) RL lab is supported by the Canadian Institutes of Health Research grant (PJT-148657). (2) JX lab is supported by the American Heart Association Career Development Award 20CDA35260116 (Xing). (3) CZ lab is supported by the National Natural Science Foundation of China (82072263).

ACKNOWLEDGMENTS

We thank all the authors for contributing to this Research Topic.

REFERENCES

1. Kawai T, Akira S. The Role of Pattern-Recognition Receptors in Innate Immunity: Update on Toll-Like Receptors. *Nat Immunol* (2010) 11:373–84. doi: 10.1038/ni.1863
2. Chen Q, Sun L, Chen ZJ. Regulation and Function of the cGAS-STING Pathway of Cytosolic DNA Sensing. *Nat Immunol* (2016) 17:1142–9. doi: 10.1038/ni.3558
3. Unterholzner L, Keating SE, Baran M, Horan KA, Jensen SB, Sharma S, et al. IFI16 Is an Innate Immune Sensor for Intracellular DNA. *Nat Immunol* (2010) 11:997–1004. doi: 10.1038/ni.1932
4. Wang L, Wen M, Cao X. Nuclear Hnrnpa2b1 Initiates and Amplifies the Innate Immune Response to DNA Viruses. *Science* (2019) 365(6454): eaav0758. doi: 10.1126/science.aav0758
5. Zierhut C, Yamaguchi N, Paredes M, Luo JD, Carroll T, Funabiki H. The Cytoplasmic DNA Sensor cGAS Promotes Mitotic Cell Deat. *Cell* (2019) 178:302–15.e323. doi: 10.1016/j.cell.2019.05.035
6. Liu H, Zhang H, Wu X, Ma D, Wu J, Wang L, et al. Nuclear cGAS Suppresses DNA Repair and Promotes Tumorigenesis. *Nature* (2018) 563:131–6. doi: 10.1038/s41586-018-0629-6
7. Volkman HE, Cambier S, Gray EE, Stetson DB. Tight Nuclear Tethering of cGAS Is Essential for Preventing Autoreactivity. *Elife* (2019) 8:e47491. doi: 10.7554/eLife.47491
8. Zhao B, Xu P, Rowlett CM, Jing T, Shinde O, Lei Y, et al. The Molecular Basis of Tight Nuclear Tethering and Inactivation of cGAS. *Nature* (2020) 587:673–7. doi: 10.1038/s41586-020-2749-z
9. Michalski S, de Oliveira Mann CC, Stafford CA, Witte G, Bartho J, Lammens K, et al. Structural Basis for Sequestration and Autoinhibition of cGAS by Chromatin. *Nature* (2020) 587:678–82. doi: 10.1038/s41586-020-2748-0
10. Pathare GR, Decout A, Glück S, Cavadini S, Makasheva K, Hovius R, et al. Structural Mechanism of cGAS Inhibition by The Nucleosome. *Nature* (2020) 587:668–72. doi: 10.1038/s41586-020-2750-6
11. Boyer JA, Spangler CJ, Strauss JD, Cesmat AP, Liu P, McGinty RK, et al. Structural Basis of Nucleosome-Dependent cGAS Inhibition. *Science* (2020) 370:450–4. doi: 10.1126/science.abd0609
12. Sharma S, tenOever BR, Grandvaux N, Zhou GP, Lin RT, Hiscott J. Triggering the Interferon Antiviral Response Through an IKK-Related Pathway. *Science* (2003) 300:1148–51. doi: 10.1126/science.1081315
13. Platanias LC. Mechanisms of Type-I- and Type-II-Interferon-Mediated Signalling. *Nat Rev Immunol* (2005) 5:375–86. doi: 10.1038/nri1604

Conflict of Interest: The authors declare that the research was conducted in the absence of any commercial or financial relationships that could be construed as a potential conflict of interest.

frontiers in Immunology

REVIEW
published: 02 July 2020
doi: 10.3389/fimmu.2020.01255

Protein Dynamics in Cytosolic DNA-Sensing Antiviral Innate Immune Signaling Pathways

Chunfu Zheng [1,2*]

[1] Department of Immunology, School of Basic Medical Sciences, Fujian Medical University, Fuzhou, China, [2] Department of Microbiology, Immunology and Infectious Diseases, University of Calgary, Calgary, AB, Canada

Antiviral innate immunity works as the first line of host defense against viral infection. Pattern recognition receptors (PRRs) and adaptor proteins involved in the innate immune signaling pathways play critical roles in controlling viral infections via the induction of type I interferon and its downstream interferon-stimulated genes. Dynamic changes of adaptor proteins contribute to precise regulation of the activation and shut-off of signaling transduction, though numerous complex processes are involved in achieving dynamic changes to various proteins of the host and viruses. In this review, we will summarize recent progress on the trafficking patterns and conformational transitions of the adaptors that are involved in the antiviral innate immune signaling pathway during viral DNA sensing. Moreover, we aim to dissect the relationships between protein dynamics and DNA-sensing antiviral innate immune responses, which will reveal the underlying mechanisms controlling protein activity and maintaining cell homeostasis. By comprehensively revealing protein dynamics in cytosolic DNA-sensing antiviral innate immune signaling pathways, we will be able to identify potential new targets for the therapies of certain autoimmune diseases.

Keywords: protein dynamics, protein trafficking, conformational change, DNA sensing signaling, innate immunity

OPEN ACCESS

Edited by:
Gennady Bocharov, Institute of Numerical Mathematics (RAS), Russia

Reviewed by:
Hiroyuki Oshiumi, Kumamoto University, Japan
François J. M. A. Meurens, INRA UMR703 Ecole Nationale Vétérinaire, Agroalimentaire et de l'alimentation de Nantes-Atlantique, France

***Correspondence:**
Chunfu Zheng
zheng.alan@hotmail.com

Specialty section:
This article was submitted to Viral Immunology, a section of the journal Frontiers in Immunology

Received: *08 March 2020*
Accepted: *18 May 2020*
Published: *02 July 2020*

Citation:
Zheng C (2020) Protein Dynamics in Cytosolic DNA-Sensing Antiviral Innate Immune Signaling Pathways. Front. Immunol. 11:1255. doi: 10.3389/fimmu.2020.01255

INTRODUCTION

Cellular processes are dependent on transmembrane receptors to communicate and transmit various signals into intracellular compartments. Dynamic changes in proteins precisely regulate the activation and inhibition of the signaling transduction. As the host's frontline defense against viral infection, antiviral innate immunity is mainly triggered by the interaction between pattern recognition receptors (PRRs) and viral pathogen-associated molecular patterns (PAMPs), followed by the activation of downstream adaptor proteins, such as stimulator of interferon genes (STING), mitochondrial antiviral signaling protein (MAVS), tumor necrosis factor receptor-associated factor (TRAFs), Toll/IL-1 receptor domain-containing adaptor inducing IFN-β (TRIF), and some other adaptors, which contribute to the induction of type I interferons (IFN-I). Therefore, the expression of IFN-stimulated genes (ISGs) is significantly increased to restrict viral infection or replication (1).

In host antiviral innate immunity signaling pathways, protein trafficking is one of the primary protein dynamics essential for the activation of the signaling pathway. Until 2013, the cyclic GMP-AMP synthase (cGAS) had been identified as the only universal cytoplasmic DNA sensor in various cell types to sense double-stranded DNA (dsDNA) and catalyze the synthesis of cyclic GMP-AMP (cGAMP) (2). STING, the only receptor of cGAMP, moves from the endoplasmic reticulum

(ER) to the Golgi and recruits TANK binding kinase 1 (TBK1) and interferon regulatory factor 3 (IRF3). The location of TBK1 and IRF3 on Golgi engages their interaction with each other and phosphorylation transition. Activated IRF3 in the nucleus directly binds to the promoter region of IFN-I to enhance the transcription of IFN-β (3, 4). Toll-like receptors (TLRs) also play critical roles in antiviral innate immunity. TLR3, TLR7, and TLR9 are the first subgroup of PRRs identified in mammals. They traverse from ER to endosome by the transmembrane protein UNC93B1 to recognize viral PAMPs and induce innate immunity (5). The mitochondrially located protein MAVS transmits downstream signaling of antiviral innate immunity, with signaling complexes assembling on the mitochondrial-associated ER membrane (MAM) (6). Thus, protein trafficking and different sub-cellular localizations contribute significantly to the innate immune signal transduction.

The conformational transition is another type of protein dynamic for activation and signaling transduction. When sensing cytosolic dsDNA, cGAS needs to form into a polymer to bind to the dsDNA directly. Polymerization of cGAS is necessary for its enzymatic activity to catalyze the synthesis of cGAMP from ATP and GTP (7, 8). cGAMP works as the endogenous second messenger and binds to STING. Upon binding with cGAMP, STING undergoes the formation of the dimers and higher-order oligomers. A closed conformation of STING is formed following a 180° "twisting" of the STING dimer on its transmembrane domain upon ligand binding, leading to the oligomerization of STING through side-by-side packing of dimeric STING molecules, which is essential for STING trafficking and TBK1 trans-autophosphorylation (9, 10). Evidence indicates that homodimerization or heterodimerization of some TLRs in endosomes is critical for TLR-sensing PAMP (11). Besides, a recent study pointed out that the cleavage and release of the UNC93B-TLR9 complex in endosomes are required for activation of the signaling pathway (12). The retinoic acid-inducible gene I (RIG-I) is proposed to expose the N-terminal pair of caspase activation recruitment domains (CARDs), enabling an interaction with MAVS and thereby initiating downstream signaling (13). Thus, protein kinetics, including protein trafficking and conformational transition, play critical roles in the activation of innate immune signaling pathways. Revealing the working pattern of adaptors, especially how adaptors coordinate with other proteins in sub-cellular localization changing and conformational conversion in cytosolic DNA-sensing signaling pathways, is a matter of vital importance in innate immune responses.

PROTEIN TRAFFICKING PATTERNS IN cGAS-STING MEDIATING IFN-β PRODUCTION

DNA-sensing signaling is one of the main pathways in response to DNA virus infection that prevents viral invasion and replication intracellularly. Activation of DNA sensors and the adaptors directly regulates IFN-I production (14). Trafficking or different localizations of DNA sensors and their downstream adaptor proteins play essential roles in signal pathway activation. In the cGAS-STING signaling pathway, ER-retaining protein STING is usually thought to be activated by cGAMP (4). After its activation, STING traffics through the ER–Golgi intermediate compartment (ERGIC) and the Golgi apparatus in a process that is dependent on the cytoplasmic coat protein complex II (COPII) and ADP–ribosylation factor (ARF) GTPases (15). Located on Golgi, the kinase TBK1 and IRF3 are recruited by STING. A phosphorylation cascade allows signal transmission, leading to the activation of IRF3 and nuclear factor kappaB (NF-κB), which translocate into the nucleus to drive transcription of IFN-I and pro-inflammatory cytokines (16–18).

Host Proteins Regulate the Trafficking of Adaptors for cGAS-STING Signal Transduction

Mukai et al. demonstrated that the palmitoylation of STING undergone on the Golgi was necessary for STING activation (19, 20). Also, STING trafficking to the Golgi is the pre-requisite for TBK1 and IRF3 recruitment, which is followed by phosphorylation and signal transduction to induce IFN-I production (21). Inactive rhomboid protein 2 (iRhom 2) and translocon-associated protein (TRAPβ) form a complex with STING and facilitate the STING trafficking from ER to Golgi (22, 23). Mitochondrial E3 ubiquitin-protein ligase 1 (MUL1), autocrine motility factor receptor (AMFR), and insulin-induced gene 1 (INSIG1) were also reported to play positive regulatory roles in promoting STING translocation to Golgi and activation through polyubiquitination modification on STING (24, 25). Gui et al. found that secretion-associated and RAS-related protein (SAR1A) and the COPII cargo-binding protein SEC24C could interact with STING and accelerate STING's trafficking to Golgi (26). After activation on Golgi, STING moves to perinuclear or other organelles. Gonugunta et al. confirmed that STING quickly moved to Rab7-positive endo-lysosomes after activation on Golgi for degradation, turning off the downstream signaling (27), while it has also been shown that sentrin-specific protease (SENP2), a putative regulator, promotes STING degradation in autophagosome (28). A recent study demonstrated that post-Golgi trafficking of STING regulated the autophagy signaling (29). Autophagy related gene 9a (Atg9a) controls dsDNA-driven dynamic translocation of STING and the innate immune responses (30). The transcription factor IRF3 is exported from the nucleus via the CRM1-mediated pathway to locate in the cytosol at rest stage, while it is imported into the nucleus when receiving the signal upstream (31). Phosphorylated IRF3 forms dimers and shuttles into the nucleus, where they interact with the coactivator CBP/p300 and initiate transcription of IFN-I and inflammatory cytokines (32, 33). Fas-associated factor 1 (FAF1) and DEAD BOX Helicase 56 (DDX56) are found to physically associate with IRF3-IPO5/importin-β3 complex, and overexpression of FAF1 or DDX56 reduces the interaction between IRF3 and IPO5/importin-β3 and disrupts the nuclear translocation of IRF3 (34, 35). Interestingly, a recent study showed that the adaptor protein TRIF, mainly involved in TLR

signaling, also participates in cGAS-STING-mediated antiviral responses in a cell type-dependent manner (36).

Viral Proteins Interfere With Adaptors Trafficking During cGAS-STING Signaling

Trafficking of STING and IRF3 nuclear importation are essential for the activation of the cGAS-STING signaling pathway. Various host proteins interact with STING or IRF3 to regulate their translocation and signaling transduction and to maintain homeostasis. Viruses, especially DNA viruses, have evolved multiple strategies to impede the cGAS-STING signaling pathway by dampening the trafficking of STING and IRF3. Herpes simplex virus type I (HSV-1) serine protease VP24 and serine/threonine kinase US3 were shown to target IRF3 and block its dimerization and nuclear translocation, with a subsequent reduction of IFN-I (37, 38). HSV-1 tegument proteins UL24 and UL42 were found to bind to the endogenous NF-κB subunits p65 and p50, abrogating their nuclear translocation and NF-κB activation downstream of the cGAS-STING signaling pathway during viral infection (39, 40).

The Tegument protein UL82 of human cytomegalovirus (HCMV), one of the beta herpesviruses, was reported to impair STING-mediated signaling via two mechanisms. On the one hand, UL82 disrupts the STING-iRhom2-TRAPβ translocon complex and impedes the translocation of STING to Golgi. On the other hand, UL82 impairs the recruitment of TBK1 and IRF3 to the STING complex on Golgi, reducing IFN-I production (41). In addition, HCMV UL42 inhibits the trafficking and activation of STING by facilitating p62/LC3B-mediated degradation of TRAPβ (42). Recently, a study showed that vaccinia virus, a DNA virus replicating in the cytoplasm, encodes poxvirus immune nucleases (poxins) to restrict cGAS-STING signaling through cleaving 2′,3′- cGAMP and that deletion of poxin gene attenuates viral replication (43) (**Figure 1**).

TRANSLOCATION OF TLRs AFFECTS THE DNA-SENSING SIGNALING

TLRs are one of the main subgroups of PRRs for the primary sensing of virus-derived nucleic acids, leading to the production of IFN-I, pro-inflammatory cytokines, and chemokines by the host cells (44). Evidence indicates that the transduction of the TLR signaling pathway is mainly dependent on its intracellular trafficking. To date, UNC93B1 is the unique trafficking vector identified for TLR3, TLR7, and TLR9. The interaction between UNC93B1 and TLRs facilitates its loading into COPII vesicles and transport through ERGIC to endosome, resulting in the production of IFN-I (45–47). To date, TLR9 is the only known DNA sensor among human TLRs (48). TLR9 is mainly expressed in endosomes among B cells, macrophages, and dendritic cells (DCs) (49). TLR9 recognizes unmethylated 2′-deoxyribo cytidine-phosphate-guanosine (CpG) DNA, which is mostly expressed in bacteria (50). It has been demonstrated that infection by certain DNA viruses activates the TLR9 signaling pathway, in which TLR9 interacts with myeloid differentiation factor 88 (MyD88). Subsequently, TLR9 forms a multiprotein signaling complex with Interleukin-1 Receptor-Associated Kinase 4 (IRAK4), IRAK1, TNF Receptor-Associated Factor 6 (TRAF6), TRAF3, and IkB kinase α and activates IRF7, which induces the production of IFN-I (51). An FYVE (Phe-Tyr-Val-Glu) finger-containing phosphoinositide (PI) kinase, PIKfyve, appears to play an important role in TLR9 trafficking and signal transduction in DCs and macrophages (52). Adaptor protein-3 (AP-3) was required for late-endosome localization of TLR9 to induce the production of IFN-I (53). In sum, the DNA receptor TLR9 cooperates with other cellular proteins to accurately control DNA-sensing signaling.

PROTEIN CONFORMATIONAL TRANSITION MEDIATES THE SIGNALING ACTIVATION

cGAS is one of the critical receptors that account for DNA-driven innate immune responses. The nucleotidyltransferase (NTase) domain, which consists of a central catalytic pocket and two separate surfaces with positive charges in the C-terminal of cGAS, is critical for the dimer formation and enzymatic activity (54). Upon binding to dsDNA, cGAS assembles into a cGAS-dsDNA oligomeric complex with two molecules of dsDNA embedded in two cGAS molecules (55, 56). cGAS dimers form ladder-like networks between two separate stretches of dsDNA or on one long crooked dsDNA helix, which markedly enhances the stability of each individual cGAS-dsDNA complex along the dsDNA (8, 57). In addition, subcellular fractionation and bio-chemical analysis suggest that cGAS is predominantly located on the plasma membrane through the N-terminal unstructured domain but not in the cytosol at rest stage. After DNA transfection, cGAS translocates to the cytoplasm and forms large foci (probably liquid droplets of cGAS-DNA complex), to respond to extraneous DNA and viral infection (58, 59).

As the only receptor of the second messenger cGAMP, CDN-binding domain (CBD) of dimeric STING binds asymmetric 2′,3′ cGAMP preferentially and is essential for the translocation of STING from ER to Golgi (60). STING polymer formation is necessary for recruiting TBK1. Phosphorylation transition during STING-TBK1-IRF3 complex formation requires a 180° rotation of the ligand-binding domain in STING since the binding site of STING-TBK1 is far away from the kinase active center of TBK1 (10). cGAMP induces the closing of the human STING homodimer and release of the STING C-terminal tail, which exposes a polymerization interface on the STING dimer and leads to the formation of disulfide-linked polymers via cysteine residue 148 (61). The hyperactive STING mutation typically results in serious autoimmune diseases by its constitutive release of C-terminal tail and polymerization (61).

TLRs have been notoriously difficult to crystallize, while more and more evidence shows that the conformational change of TLR plays an essential role in the binding

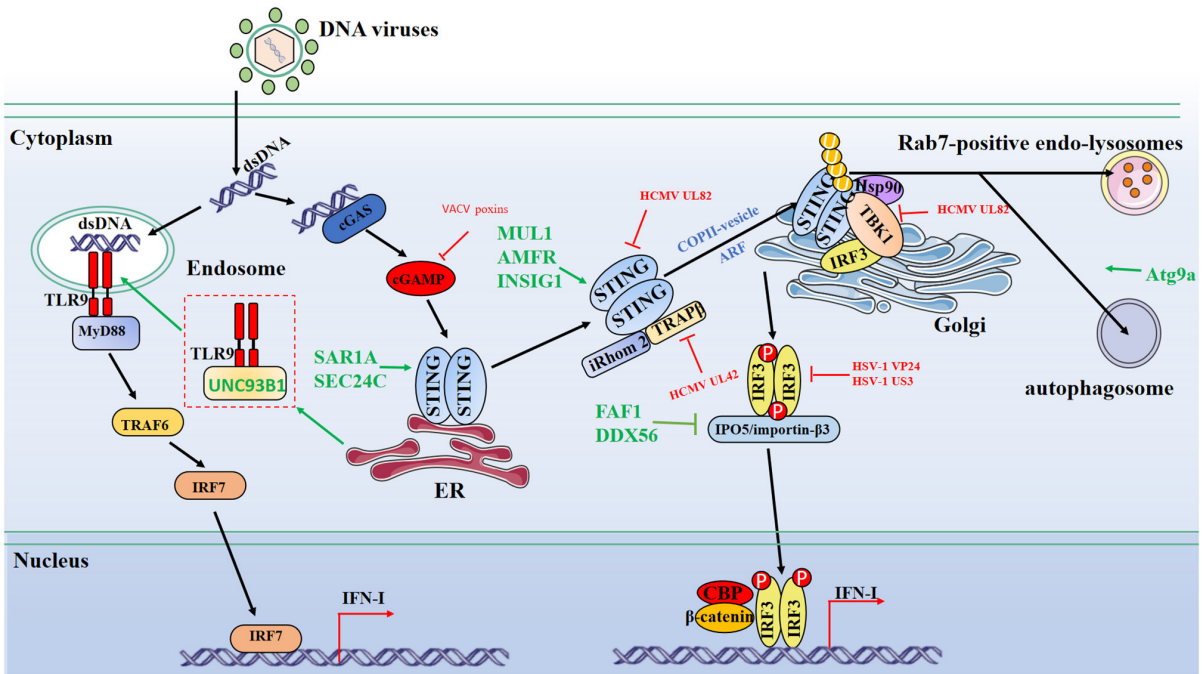

FIGURE 1 | Schematic diagram of protein dynamics of cytosolic DNA-sensing signaling antiviral innate immunity signaling pathways. Cytosolic DNA sensors, such as cGAS and TLR9, recognize dsDNA and trigger IFN-I production through the transmission of a series of signals. Multiple steps in the DNA-sensing signaling pathways can be modulated by host and viral proteins. Green lines indicate that host proteins target adaptors. Red lines indicate that viral proteins interfere with adaptors. CBP, CREB-binding protein; P, phosphate; U, ubiquitin.

of TLRs to its natural ligands. Upon addition of ligand, both TLR3 and TLR9 form dimers. However, full-length TLR9 in cells is suggested to exist as a pre-formed homodimer, and ligand binding simply induces a conformational change that is necessary for receptor activation (62).

CONCLUDING REMARKS AND FUTURE PERSPECTIVES

Evidence has shown that protein trafficking in innate immunity is critical to signaling transduction. In DNA-sensing signaling pathways, the cGAS-STING pathway plays the main role in response to cytosolic DNA and antiviral innate immunity. The activation of ER-retained STING requires translocation from the ER to ERGIC and then to the Golgi. During translocation, STING activates IRF3 and NF-κB transcription factors that induce the expression of IFN-I and inflammatory cytokines. The STING signaling cascade is reported to be regulated by multiple checks, which are involved in different stages of STING activation and inhibition. Many studies have demonstrated that COPII-dependent vesicles, together with some other transmembrane protein complexes, play critical roles in STING trafficking and conformational transition in the activation and signaling transduction of STING (23, 63–65). Also, studies have shown that the degradation of activated STING, which plays an important role in maintaining cell homeostasis, is mediated by the ubiquitin-proteasome, lysosomal, or autophagic degradation pathway (27). It remains elusive which mechanism contributes most to the degradation of activated STING. Studies on the stringent trafficking patterns of STING post-Golgi will be crucial for revealing the underlying mechanism of homeostatic regulation of STING protein after activation. Moreover, it will provide a potential way to cure the autoimmune diseases caused by aberrant activation of STING.

Working as another DNA-sensing PRR, TLR9, translocated into endosome and released from UNC93B-TLR9 complex, senses CpG dsDNA, which is leaked from mitochondria, induces IFN-I production, and subsequently moves to the lysosome for degradation (66) (**Figure 1**). In addition, cellular proteins involved in different signaling pathways work together with TLR9 and regulate the translocation or conformational conversion, leading to various signal transduction and innate immunity responses. TLR9 is the only known TLR that recognizes CpG dsDNA, while other TLR members like TLR2, TLR3, and TLR4 show the capability to respond to the infection of DNA viruses, even though they do not sense viral dsDNA (67–69). Previous reports showed that hetero-dimerization and homo-dimerization of certain TLRs are essential for ligand binding and signaling transduction. One possibility is that these TLRs might recognize the viral dsDNA when they form hetero- or homo-dimers. It will be interesting to reveal how other

TLRs function in DNA-sensing signaling, which will help our further understanding of how distinct TLR signal pathways are balanced.

AUTHOR CONTRIBUTIONS

CZ wrote, reviewed, and modified the manuscript.

ACKNOWLEDGMENTS

I apologize to all colleagues whose contributions were not discussed and cited owing to space constraints. I am grateful to Sisilia Zheng for a critical review of the manuscript. I thank previous lab members who have contributed papers for this review.

REFERENCES

1. Wu J, Chen ZJ. Innate immune sensing and signaling of cytosolic nucleic acids. *Annu Rev Immunol.* (2014) 32:461–88. doi: 10.1146/annurev-immunol-032713-120156
2. Li XD, Wu J, Gao D, Wang H, Sun L, Chen ZJ. Pivotal roles of cGAS-cGAMP signaling in antiviral defense and immune adjuvant effects. *Science.* (2013) 341:1390–4. doi: 10.1126/science.1244040
3. Chen Q, Sun L, Chen ZJ. Regulation and function of the cGAS-STING pathway of cytosolic DNA sensing. *Nat Immunol.* (2016) 17:1142–9. doi: 10.1038/ni.3558
4. Zhang X, Shi H, Wu J, Zhang X, Sun L, Chen C, et al. Cyclic GMP-AMP containing mixed phosphodiester linkages is an endogenous high-affinity ligand for STING. *Mol Cell.* (2013) 51:226–35. doi: 10.1016/j.molcel.2013.05.022
5. Kawai T, Akira S. The role of pattern-recognition receptors in innate immunity: update on Toll-like receptors. *Nat Immunol.* (2010) 11:373–84. doi: 10.1038/ni.1863
6. Horner SM, Wilkins C, Badil S, Iskarpatyoti J, Gale M Jr. Proteomic analysis of mitochondrial-associated ER membranes (MAM) during RNA virus infection reveals dynamic changes in protein and organelle trafficking. *PLoS ONE.* (2015) 10:e0117963. doi: 10.1371/journal.pone.0117963
7. Civril F, Deimling T, de Oliveira Mann CC, Ablasser A, Moldt M, Witte G, et al. Structural mechanism of cytosolic DNA sensing by cGAS. *Nature.* (2013) 498:332–7. doi: 10.1038/nature12305
8. Zhang X, Wu J, Du F, Xu H, Sun L, Chen Z, et al. The cytosolic DNA sensor cGAS forms an oligomeric complex with DNA and undergoes switch-like conformational changes in the activation loop. *Cell Rep.* (2014) 6:421–30. doi: 10.1016/j.celrep.2014.01.003
9. Shang G, Zhang C, Chen ZJ, Bai XC, Zhang X. Cryo-EM structures of STING reveal its mechanism of activation by cyclic GMP-AMP. *Nature.* (2019) 567:389–93. doi: 10.1038/s41586-019-0998-5
10. Zhang C, Shang G, Gui X, Zhang X, Bai XC, Chen ZJ. Structural basis of STING binding with and phosphorylation by TBK1. *Nature.* (2019) 567:394–8. doi: 10.1038/s41586-019-1000-2
11. Mahita J, Sowdhamini R. Investigating the effect of key mutations on the conformational dynamics of toll-like receptor dimers through molecular dynamics simulations and protein structure networks. *Proteins.* (2018) 86:475–90. doi: 10.1002/prot.25467
12. Majer O, Liu B, Woo BJ, Kreuk LSM, Van Dis E, Barton GM. Release from UNC93B1 reinforces the compartmentalized activation of select TLRs. *Nature.* (2019) 575:371–4. doi: 10.1038/s41586-019-1611-7
13. Beckham SA, Brouwer J, Roth A, Wang D, Sadler AJ, John M, et al. Conformational rearrangements of RIG-I receptor on formation of a multiprotein:dsRNA assembly. *Nucleic Acids Res.* (2013) 41:3436–45. doi: 10.1093/nar/gks1477
14. Desmet CJ, Ishii KJ. Nucleic acid sensing at the interface between innate and adaptive immunity in vaccination. *Nat Rev Immunol.* (2012) 12:479–91. doi: 10.1038/nri3247
15. Dobbs N, Burnaevskiy N, Chen D, Gonugunta VK, Alto NM, Yan N. STING activation by translocation from the ER is associated with infection and autoinflammatory disease. *Cell Host Microbe.* (2015) 18:157–68. doi: 10.1016/j.chom.2015.07.001
16. Lian Y, Duffy KJ, Yang J. STING activation and its application in immuno-oncology. *Curr topics med chem.* (2019) 19:2205–27. doi: 10.2174/1568026619666191010155903
17. Iurescia S, Fioretti D, Rinaldi M. Targeting cytosolic nucleic acid-sensing pathways for cancer immunotherapies. *Front Immunol.* (2018) 9:711. doi: 10.3389/fimmu.2018.00711
18. Abe T, Barber GN. Cytosolic-DNA-mediated, STING-dependent pro-inflammatory gene induction necessitates canonical NF-kappaB activation through TBK1. *J Virol.* (2014) 88:5328–41. doi: 10.1128/JVI.00037-14
19. Mukai K, Konno H, Akiba T, Uemura T, Waguri S, Kobayashi T, et al. Activation of STING requires palmitoylation at the Golgi. *Nat Commun.* (2016) 7:11932. doi: 10.1038/ncomms11932
20. Hansen AL, Mukai K, Schopfer FJ, Taguchi T, Holm CK. STING palmitoylation as a therapeutic target. *Cell Mol Immunol.* (2019) 16:236–41. doi: 10.1038/s41423-019-0205-5
21. Zhao B, Du F, Xu P, Shu C, Sankaran B, Bell SL, et al. A conserved PLPLRT/SD motif of STING mediates the recruitment and activation of TBK1. *Nature.* (2019) 569:718–22. doi: 10.1038/s41586-019-1228-x
22. Ishikawa H, Barber GN. STING is an endoplasmic reticulum adaptor that facilitates innate immune signalling. *Nature.* (2008) 455:674–8. doi: 10.1038/nature07317
23. Luo WW, Li S, Li C, Lian H, Yang Q, Zhong B, et al. iRhom2 is essential for innate immunity to DNA viruses by mediating trafficking and stability of the adaptor STING. *Nat Immunol.* (2016) 17:1057–66. doi: 10.1038/ni.3510
24. Wang Q, Liu X, Cui Y, Tang Y, Chen W, Li S, et al. The E3 ubiquitin ligase AMFR and INSIG1 bridge the activation of TBK1 kinase by modifying the adaptor STING. *Immunity.* (2014) 41:919–33. doi: 10.1016/j.immuni.2014.11.011
25. Ni G, Konno H, Barber GN. Ubiquitination of STING at lysine 224 controls IRF3 activation. *Sci Immunol.* (2017) 2:aah7119. doi: 10.1126/sciimmunol.aah7119
26. Gui X, Yang H, Li T, Tan X, Shi P, Li M, et al. Autophagy induction via STING trafficking is a primordial function of the cGAS pathway. *Nature.* (2019) 567:262–6. doi: 10.1038/s41586-019-1006-9
27. Gonugunta VK, Sakai T, Pokatayev V, Yang K, Wu J, Dobbs N, et al. Trafficking-mediated STING degradation requires sorting to acidified endolysosomes and can be targeted to enhance anti-tumor response. *Cell Rep.* (2017) 21:3234–42. doi: 10.1016/j.celrep.2017.11.061
28. Hu MM, Yang Q, Xie XQ, Liao CY, Lin H, Liu TT, et al. Sumoylation promotes the stability of the DNA sensor cGAS and the adaptor STING to regulate the kinetics of response to DNA virus. *Immunity.* (2016) 45:555–69. doi: 10.1016/j.immuni.2016.08.014
29. Liu Y, Gordesky-Gold B, Leney-Greene M, Weinbren NL, Tudor M, Cherry S. Inflammation-induced, STING-dependent autophagy restricts zika virus infection in the drosophila brain. *Cell Host Microbe.* (2018) 24:57–68.e53. doi: 10.1016/j.chom.2018.05.022
30. Saitoh T, Fujita N, Hayashi T, Takahara K, Satoh T, Lee H, et al. Atg9a controls dsDNA-driven dynamic translocation of STING and the innate immune response. *Proc Natl Acad Sci USA.* (2009) 106:20842–6. doi: 10.1073/pnas.0911267106
31. Yoneyama M, Suhara W, Fukuhara Y, Fukuda M, Nishida E, Fujita T. Direct triggering of the type I interferon system by virus infection: activation of a transcription factor complex containing IRF-3 and CBP/p300. *EMBO J.* (1998) 17:1087–95. doi: 10.1093/emboj/17.4.1087
32. Servant MJ, Grandvaux N, tenOever BR, Duguay D, Lin R, Hiscott J. Identification of the minimal phosphoacceptor site required for in vivo activation of interferon regulatory factor 3 in response to virus and double-stranded RNA. *J Biol Chem.* (2003) 278:9441–7. doi: 10.1074/jbc.M209851200

33. Takahasi K, Horiuchi M, Fujii K, Nakamura S, Noda NN, Yoneyama M, et al. Ser386 phosphorylation of transcription factor IRF-3 induces dimerization and association with CBP/p300 without overall conformational change. *Genes Cells.* (2010) 15:901–10. doi: 10.1111/j.1365-2443.2010.01427.x
34. Song S, Lee JJ, Kim HJ, Lee JY, Chang J, Lee KJ. Fas-Associated factor 1 negatively regulates the antiviral immune response by inhibiting translocation of interferon regulatory factor 3 to the nucleus. *Mol Cell Biol.* (2016) 36:1136–51. doi: 10.1128/MCB.00744-15
35. Li D, Fu S, Wu Z, Yang W, Ru Y, Shu H, et al. DDX56 inhibits type I interferon by disrupting assembly of IRF3-IPO5 to inhibit IRF3 nucleus import. *J Cell Sci.* (2019) 133:230409. doi: 10.1242/jcs.230409
36. Wang X, Majumdar T, Kessler P, Ozhegov, E, Zhang Y, Chattopadhyay S. STING requires the adaptor TRIF to trigger innate immune responses to microbial infection. *Cell host microbe.* (2016) 20:329–41. doi: 10.1016/j.chom.2016.08.002
37. Wang S, Wang K, Lin R, Zheng C. Herpes simplex virus 1 serine/threonine kinase US3 hyperphosphorylates IRF3 and inhibits beta interferon production. *J Virol.* (2013) 87:12814–27. doi: 10.1128/JVI.02355-13
38. Zhang D, Su C, Zheng C. Herpes simplex virus 1 serine protease VP24 blocks the DNA-sensing signal pathway by abrogating activation of interferon regulatory factor 3. *J Virol.* (2016) 90:5824–9. doi: 10.1128/JVI.00186-16
39. Zhang J, Wang S, Wang K, Zheng C. Herpes simplex virus 1 DNA polymerase processivity factor UL42 inhibits TNF-alpha-induced NF-kappaB activation by interacting with p65/RelA and p50/NF-kappaB1. *Med Microbiol Immunol.* (2013) 202:313–25. doi: 10.1007/s00430-013-0295-0
40. Xu H, Su C, Pearson A, Mody CH, Zheng C. Herpes simplex virus 1 UL24 abrogates the DNA sensing signal pathway by inhibiting NF-kappaB activation. *J Virol.* (2017) 91:17. doi: 10.1128/JVI.00025-17
41. Fu YZ, Su S, Gao YQ, Wang PP, Huang ZF, Hu MM, et al. Human cytomegalovirus tegument protein UL82 inhibits STING-mediated signaling to evade antiviral immunity. *Cell Host Microbe.* (2017) 21:231–43. doi: 10.1016/j.chom.2017.01.001
42. Fu YZ, Guo Y, Zou HM, Su S, Wang SY, Yang Q, et al. Human cytomegalovirus protein UL42 antagonizes cGAS/MITA-mediated innate antiviral response. *PLoS Pathog.* (2019) 15:e1007691. doi: 10.1371/journal.ppat.1007691
43. Eaglesham JB, Pan Y, Kupper TS, Kranzusch PJ. Viral and metazoan poxins are cGAMP-specific nucleases that restrict cGAS-STING signalling. *Nature.* (2019) 566:259–63. doi: 10.1038/s41586-019-0928-6
44. Korneev KV, Atretkhany KN, Drutskaya MS, Grivennikov SI, Kuprash DV, Nedospasov SA. TLR-signaling and pro-inflammatory cytokines as drivers of tumorigenesis. *Cytokine.* (2017) 89:127–35. doi: 10.1016/j.cyto.2016.01.021
45. Park A, Ra EA, Lee TA, Choi HJ, Lee E, Kang S, et al. HCMV-encoded US7 and US8 act as antagonists of innate immunity by distinctively targeting TLR-signaling pathways. *Nat Commun.* (2019) 10:4670. doi: 10.1038/s41467-019-12641-4
46. Jensen D, Schekman R. COPII-mediated vesicle formation at a glance. *J Cell Sci.* (2011) 124:1–4. doi: 10.1242/jcs.069773
47. Lee BL, Moon JE, Shu JH, Yuan L, Newman ZR, Schekman R, et al. UNC93B1 mediates differential trafficking of endosomal TLRs. *Elife.* (2013) 2:e00291. doi: 10.7554/eLife.00291
48. Latz E, Schoenemeyer A, Visintin A, Fitzgerald KA, Monks BG, Knetter CF, et al. TLR9 signals after translocating from the ER to CpG DNA in the lysosome. *Nat Immunol.* (2004) 5:190–8. doi: 10.1038/ni1028
49. Ishii KJ, Coban C, Kato H, Takahashi K, Torii Y, Takeshita F, et al. A toll-like receptor-independent antiviral response induced by double-stranded B-form DNA. *Nature immunol.* (2006) 7:40–8. doi: 10.1038/ni1282
50. Krieg AM, Yi AK, Matson S, Waldschmidt TJ, Bishop GA, Teasdale R, et al. CpG motifs in bacterial DNA trigger direct B-cell activation. *Nature.* (1995) 374:546–9. doi: 10.1038/374546a0
51. Shinohara ML, Lu L, Bu J, Werneck MBF, Kobayashi KS, Glimcher LH, et al. Osteopontin expression is essential for interferon-alpha production by plasmacytoid dendritic cells. *Nat immunol.* (2006) 7:498–506. doi: 10.1038/ni1327
52. Hayashi K, Sasai M, Iwasaki A. Toll-like receptor 9 trafficking and signaling for type I interferons requires PIKfyve activity. *Int Immunol.* (2015) 27:435–45. doi: 10.1093/intimm/dxv021
53. Sasai M, Linehan MM, Iwasaki A. Bifurcation of Toll-like receptor 9 signaling by adaptor protein 3. *Science.* (2010) 329:1530–4. doi: 10.1126/science.1187029
54. Gentili M, Lahaye X, Nadalin F, Nader GPF, Lombardi EP, Herve S, et al. The N-terminal domain of cGAS determines preferential association with centromeric DNA and innate immune activation in the nucleus. *Cell Rep.* (2019) 26:3798. doi: 10.1016/j.celrep.2019.03.049
55. Lee A, Park EB, Lee J, Choi BS, Kang SJ. The N terminus of cGAS de-oligomerizes the cGAS:DNA complex and lifts the DNA size restriction of core-cGAS activity. *FEBS Lett.* (2017) 591:954–61. doi: 10.1002/1873-3468.12598
56. Andreeva L, Hiller B, Kostrewa D, Lassig C, de Oliveira Mann CC, Jan Drexler D, et al. cGAS senses long and HMGB/TFAM-bound U-turn DNA by forming protein-DNA ladders. *Nature.* (2017) 549:394–8. doi: 10.1038/nature23890
57. Zhou W, Whiteley AT, de Oliveira Mann CC, Morehouse BR, Nowak RP, Fischer ES, et al. Structure of the human cGAS-DNA complex reveals enhanced control of immune surveillance. *Cell.* (2018) 174:300–11.e311. doi: 10.1016/j.cell.2018.06.026
58. Du M, Chen ZJ. DNA-induced liquid phase condensation of cGAS activates innate immune signaling. *Science.* (2018) 361:704–9. doi: 10.1126/science.aat1022
59. Hu MM, Shu HB. Innate immune response to cytoplasmic DNA: mechanisms and diseases. *Annu Rev Immunol.* (2019) 38:79–98. doi: 10.1146/annurev-immunol-070119-115052
60. Cong X, Yuan Z, Du Y, Wu B, Lu D, Wu X, et al. Crystal structures of porcine STING(CBD)-CDN complexes reveal the mechanism of ligand recognition and discrimination of STING proteins. *J Biol Chem.* (2019) 294:11420–32. doi: 10.1074/jbc.RA119.007367
61. Ergun SL, Fernandez D, Weiss TM, Li L. STING polymer structure reveals mechanisms for activation, hyperactivation, and inhibition. *Cell.* (2019) 178:290–301.e210. doi: 10.1016/j.cell.2019.05.036
62. Latz E, Verma A, Visintin A, Gong M, Sirois CM, Klein DC, et al. Ligand-induced conformational changes allosterically activate Toll-like receptor 9. *Nat Immunol.* (2007) 8:772–9. doi: 10.1038/ni1479
63. Sun MS, Zhang J, Jiang LQ, Pan YX, Tan JY, Yu F, et al. TMED2 Potentiates cellular IFN responses to DNA viruses by reinforcing MITA dimerization and facilitating its trafficking. *Cell Rep.* (2018) 25:3086–98.e3083. doi: 10.1016/j.celrep.2018.11.048
64. Ran Y, Xiong MG, Xu ZS, Luo WW, Wang SY, Wang YY. YIPF5 is essential for innate immunity to DNA virus and facilitates COPII-dependent STING trafficking. *J Immunol.* (2019) 203:1560–70. doi: 10.4049/jimmunol.1900387
65. Hiller B, Hornung V. STING signaling the enERGIC way. *Cell Host Microbe.* (2015) 18:137–9. doi: 10.1016/j.chom.2015.07.014
66. Piantadosi CA. Mitochondrial DNA, oxidants, innate immunity. *Free Radic Biol Med.* (2020) 152:455–61. doi: 10.1016/j.freeradbiomed.2020.01.013
67. Cai M, Li M, Wang K, Wang S, Lu Q, Yan J, et al. The herpes simplex virus 1-encoded envelope glycoprotein B activates NF-kappaB through the Toll-like receptor 2 and MyD88/TRAF6-dependent signaling pathway. *PLoS ONE.* (2013) 8:e54586. doi: 10.1371/journal.pone.0054586
68. Ahmad R, El Bassam S, Cordeiro P, Menezes J. Requirement of TLR2-mediated signaling for the induction of IL-15 gene expression in human monocytic cells by HSV-1. *Blood.* (2008) 112:2360–68. doi: 10.1182/blood-2008-02-137711
69. Zimmer B, Ewaleifoh O, Harschnitz O, Lee YS, Peneau C, McAlpine JL, et al. Human iPSC-derived trigeminal neurons lack constitutive TLR3-dependent immunity that protects cortical neurons from HSV-1 infection. *Proc Natl Acad Sci USA.* (2018) 115:E8775–E8782. doi: 10.1073/pnas.1809853115

Conflict of Interest: The author declares that the research was conducted in the absence of any commercial or financial relationships that could be construed as a potential conflict of interest.

frontiers in Immunology

ORIGINAL RESEARCH
published: 08 July 2020
doi: 10.3389/fimmu.2020.01430

Characterization of a Novel Compound That Stimulates STING-Mediated Innate Immune Activity in an Allele-Specific Manner

Jinu Abraham[1†], Sara Botto[1†], Nobuyo Mizuno[1], Kara Pryke[1], Bryan Gall[1], Dylan Boehm[1], Tina M. Sali[1], Haihong Jin[2], Aaron Nilsen[2], Michael Gough[3], Jason Baird[3], Marita Chakhtoura[4], Caroline Subra[5,6], Lydie Trautmann[1], Elias K. Haddad[4] and Victor R. DeFilippis[1]*

[1] Vaccine and Gene Therapy Institute, Oregon Health and Science University, Portland, OR, United States, [2] Veterans Affairs Medical Center, Portland, OR, United States, [3] Integrated Therapies Laboratory, Earle A. Chiles Research Institute, Portland, OR, United States, [4] Department of Medicine, Drexel University College of Medicine, Philadelphia, PA, United States, [5] U.S. Military HIV Research Program, Walter Reed Army Institute of Research, Silver Spring, MD, United States, [6] Henry M. Jackson Foundation for the Advancement of Military Medicine, Bethesda, MD, United States

OPEN ACCESS

Edited by:
Rongtuan Lin,
McGill University, Canada

Reviewed by:
Hong-Bing Shu,
Wuhan University, China
Andrew L. Mellor,
Newcastle University, United Kingdom

***Correspondence:**
Victor R. DeFilippis
defilipp@ohsu.edu

[†] These authors have contributed equally to this work

Specialty section:
This article was submitted to Molecular Innate Immunity, a section of the journal Frontiers in Immunology

Received: 27 March 2020
Accepted: 03 June 2020
Published: 08 July 2020

Citation:
Abraham J, Botto S, Mizuno N, Pryke K, Gall B, Boehm D, Sali TM, Jin H, Nilsen A, Gough M, Baird J, Chakhtoura M, Subra C, Trautmann L, Haddad EK and DeFilippis VR (2020) Characterization of a Novel Compound That Stimulates STING-Mediated Innate Immune Activity in an Allele-Specific Manner. Front. Immunol. 11:1430. doi: 10.3389/fimmu.2020.01430

The innate immune response to cytosolic DNA involves transcriptional activation of type I interferons (IFN-I) and proinflammatory cytokines. This represents the culmination of intracellular signaling pathways that are initiated by pattern recognition receptors that engage DNA and require the adaptor protein Stimulator of Interferon Genes (STING). These responses lead to the generation of cellular and tissue states that impair microbial replication and facilitate the establishment of long-lived, antigen-specific adaptive immunity. Ultimately this can lead to immune-mediated protection from infection but also to the cytotoxic T cell-mediated clearance of tumor cells. Intriguingly, pharmacologic activation of STING-dependent phenotypes is known to enhance both vaccine-associated immunogenicity and immune-based anti-tumor therapies. Unfortunately, the STING protein exists as multiple variant forms in the human population that exhibit differences in their reactivity to chemical stimuli and in the intensity of molecular signaling they induce. In light of this, STING-targeting drug discovery efforts require an accounting of protein variant-specific activity. Herein we describe a small molecule termed M04 that behaves as a novel agonist of human STING. Importantly, we find that the molecule exhibits a differential ability to activate STING based on the allelic variant examined. Furthermore, while M04 is inactive in mice, expression of human STING in mouse cells rescues reactivity to the compound. Using primary human cells in *ex vivo* assays we were also able to show that M04 is capable of simulating innate responses important for adaptive immune activation such as cytokine secretion, dendritic cell maturation, and T cell cross-priming. Collectively, this work demonstrates the conceivable utility of a novel agonist of human STING both as a research tool for exploring STING biology and as an immune potentiating molecule.

Keywords: interferon, cytokine, cytosolic DNA sensing, STING, adjuvant

INTRODUCTION

The innate immune response is a rapid cell-based reaction to microbial infection and diseased cellular states that predominantly involves secretion of immunologically functional cytokines. This results from activation of transcription factors or proteolytic caspases at the terminus of intracellular signaling cascades. These signaling pathways are initiated by pattern recognition receptor (PRR) proteins that directly engage and are induced by pathogen- or damage-associated molecular patterns (PAMPs, DAMPs). Among the most potent cytokines are the type I interferons (IFN-I) including IFNβ and multiple IFNα subtypes. IFN-I bind to the nearly ubiquitous IFNα/β receptor (IFNAR) which then activates via Janus kinases (JAK) the transcription factors signal transducer and activator of transcription 1 and 2 (STAT1/2) and IFN regulatory factor 9. The IFNAR-JAK-STAT pathway leads to the transcription of numerous IFN-stimulated genes (ISGs) that exhibit diverse phenotypic effects including generation of antiviral states and coordinating adaptive immunity (1). IFNs are thus essential for combating infectious (especially viral) diseases, anti-tumor T cell responses, and maintaining tissue homeostasis.

Synthesis of IFNβ mRNA specifically requires the transcription factor IFN regulatory factor 3 (IRF3) (2). Activation of this involves phosphorylation by the multi-target kinase TANK binding kinase 1 (TBK1). This, in turn, is activated by one of three adaptor proteins (TRIF, MAVS, and STING) that serve as signal integrators from upstream PRRs (3). Stimulator of IFN genes (STING, also called MITA, ERIS, MPYS, TMEM173) is an ER-associated protein that functions as an adaptor for signals from PRRs that react to cytosolic dsDNA [reviewed in (4)]. Importantly, STING is itself a PRR engaged by cyclic dinucleotides (CDNs) that are synthesized both during bacterial infection as well as by cyclic GMP-AMP synthase (cGAS), a cellular nucleotidyl transferase that is activated after binding to cytosolic DNA (5–7). cGAS uses ATP and GTP to produce a cyclic GMP-AMP molecule that contains G(2',5')pA and A(3',5')pG phosphodiester linkages that engages the C-terminal ligand binding domain (LBD) of dimerized STING proteins. Upon ligand binding, STING recruits TBK1 which phosphorylates STING, TBK1, and IRF3. Activated IRF3 then translocates to the nucleus where it drives synthesis of mRNA for IFNβ and a subset of ISGs, often in concert with other transcription factors such as NF-κB (8) and STAT6 (9) that potentiate expression of additional proinflammatory genes.

The STING-dependent activation of type I IFNs as well as other pro-inflammatory cytokines generates cellular and tissue states that are adverse for virus replication (10). Additionally, transient and localized activation of STING can also lead to stimulation of antigen presenting cell (APC) phenotypes involving cytokine, effector, and costimulatory protein expression that promote antigen uptake and processing and lymph node trafficking, and ultimately facilitate establishment of adaptive immune responses. As such, STING-dependent processes are important for antibody and cytotoxic T cell-mediated activity against infecting microbes as well as tumor cells [reviewed in (11)]. Intriguingly, STING activation can be triggered pharmacologically by synthetic small molecules and engineered macromolecules (12). This represents a potentially formidable strategy for eliciting broad-spectrum antiviral activity (13), generating anti-tumor immunity (14), and enhancing vaccine immunogenicity (15). In light of this, numerous efforts are underway to discover novel and safe STING-based immunomodulators that can be utilized for potentiating desirable clinical outcomes. Unfortunately, significant STING polymorphism exists in the human population, which affects both the molecular responses induced by the protein's activation and the degree of sensitivity to stimulatory ligands (16). Consequently, this can greatly impact the efficacy and safety of molecular entities pursued for clinical purposes. Here we describe a novel small molecule that activates the IFN-I response by way of STING that is differentially active in naturally occurring variants of the protein. In primary human cells this compound is also capable of inducing innate activity that is consistent with facilitation of adaptive immunity and as such may represent a new STING-directed molecular entity with clinical applications.

RESULTS

M04 Is a Small Molecule That Activates Type I IFN Signaling in Human Cells

Previous work from our group described a high throughput screen (HTS) undertaken to identify novel small molecules capable of stimulating the type I IFN response in human cells (17–19). From a library of >51,000 compounds, the second most reactive hit was 2-(cyclohexylsulfonyl)-N,N-dimethyl-4-tosylthiazol-5-amine (we term this M04 for simplicity; **Figure 1A**), which has a MW of 428.6 and LogP of 4.17. The original screen was performed on telomerase-transduced human foreskin fibroblasts (THF) into which a reporter cassette encoding the firefly luciferase (LUC) open reading frame controlled by IFN-stimulated responsive elements (ISRE) was also stably introduced. To validate the HTS results we therefore measured LUC expression in these cells following exposure to a range of M04 doses and, in parallel, cytotoxicity. As shown in **Figure 1B**, LUC signal was maximal at 100 μM with only minimal loss in cell viability. To examine efficacy of the molecule on human cells of a distinct ontology we employed myeloid-derived MonoMac6 (MM6) cells (20). These were stably transduced with the same ISRE-LUC reporter cassette and treated with a similar range of M04 doses. As shown in **Figure 1C**, MM6-ISRE exhibited higher sensitivity to M04 with maximum signal observed at 25 μM. While no detectable toxicity was observed at that concentration, higher doses showed significant cell death.

While these data show that M04 can clearly activate expression of an artificial IFN-sensitive reporter, we next aimed to establish whether the molecule is also capable of inducing transcription of endogenous IFN-stimulated genes (ISGs). For this we exposed MM6 cells to M04 as well as IFNβ and used semi-quantitative reverse transcriptase PCR (qPCR) to measure induced levels of IFIT1 (21) and Viperin (RSAD2) (22). As shown in **Figure 1D**, M04 led to levels of IFIT1 and Viperin mRNA synthesis

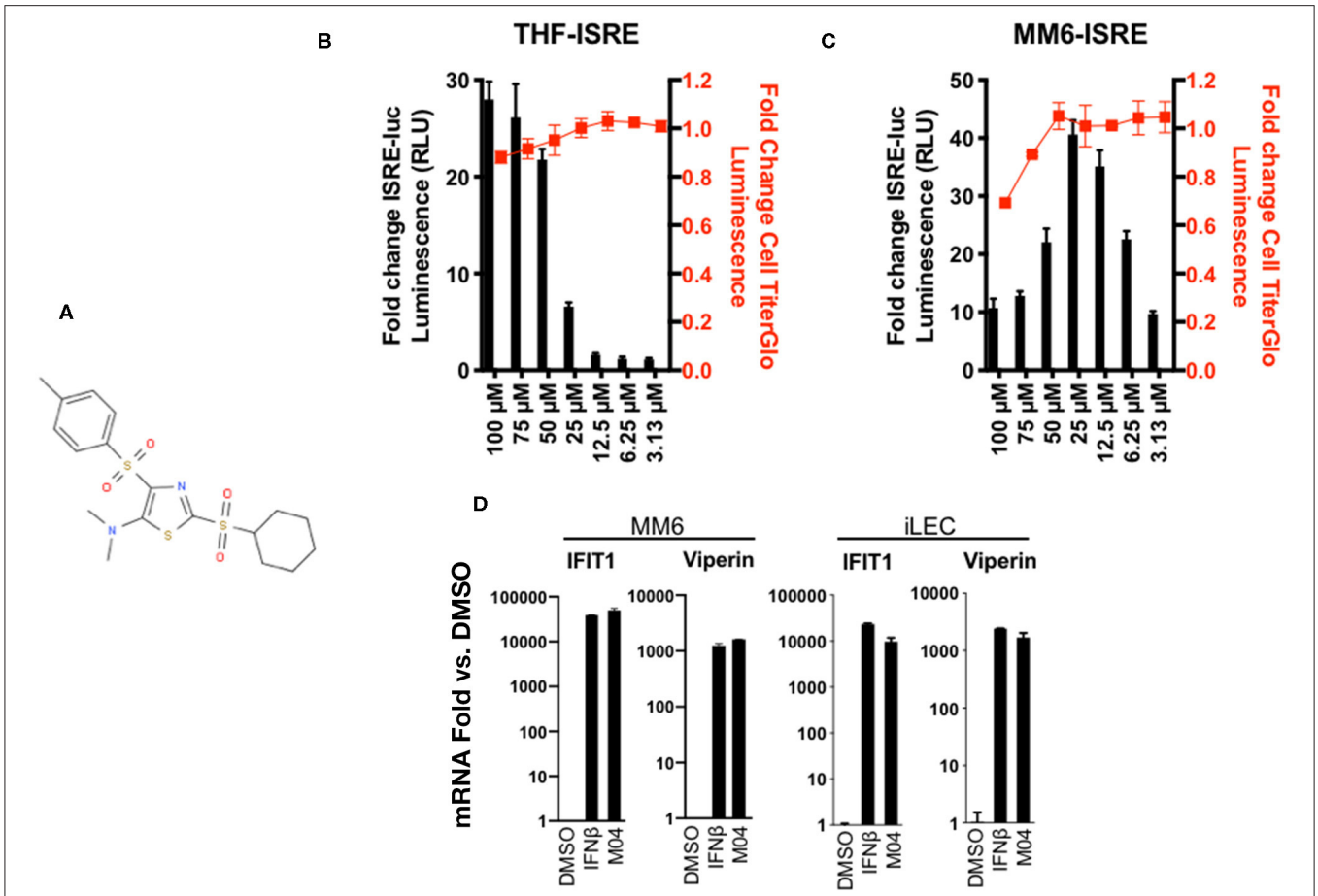

FIGURE 1 | Dose-Dependent Activation of Type I Interferon-Mediated Signaling and Cytotoxicity of M04 in Human Cells. **(A)** Chemical structure of 2-(cyclohexylsulfonyi)-N,N-dimethyl-4-tosylthiazol-5-amine ("M04"); **(B)** ISRE-dependent expression of Luciferase (LUC) as well as relative cellular viability as determined by Cell Titer Glo in THF **(B)** and MM6 **(C)** cells exposed to M04 at indicated concentrations (µM) for 8 h (RLU) or 24 h (Cell Titer Glow). Values presented are mean fold change ± SD relative to cells treated with 1% DMSO (RLU; black bars; left y-axis). Cell viability data are expressed as relative signal detected in DMSO-treated cells (red squares; right axis). Values displayed are based on four replicates; **(D)** Fold changes of IFIT1 or Viperin mRNA relative to 1% DMSO treatment in immortalized lymphatic endothelial cells (iLEC) or MM6 following 8 h exposure to 1000U/mL IFNβ or 50 µM M04 as indicated. Presented values represent average ± SD mRNA fold changes relative to cells exposed to untreated cells from duplicate experiments.

that resembled those induced by IFNβ. Since results thus far indicated that M04 was able to trigger IFN-associated activity in stromal and myeloid-derived cells, we next examined whether an unrelated cell type was also responsive to the molecule. For this we performed qPCR using immortalized human lymphatic endothelial cells (iLEC) treated as described for MM6 and observed similar levels of ISG induction (**Figure 1D**). Taken together, these data indicate that M04 is a novel small molecule capable of stimulating IFN-dependent responses across human cell types in a dose dependent manner without significant cytotoxicity at its active concentrations.

M04-Mediated Innate Stimulation Requires Activation of TBK1 and IRF3

Conventional initiation of the type I IFN response involves activation of the IRF3 transcription factor via phosphorylation of serine residues by TBK1 which then enables nuclear translocation and transcription of IFNβ (23). To examine whether this activity occurs following treatment with M04 we performed immunoblotting (IB) using whole cell lysates from MM6 and THF cells treated with M04 or the RIG-I/MAVS/IRF3-activating stimulus Sendai virus (SeV) (24). As shown in **Figure 2A**, both stimuli led to the phosphorylation of TBK1 and IRF3, indicating inducible activation of both proteins. Since activated IRF3 must accumulate in the nucleus to drive IFN and ISG transcription, we next examined its subcellular localization using indirect immunofluorescence assay (IFA). As shown in **Figure 2B**, THF cells treated with M04 as well as the STING/IRF3 agonist 2'3' cyclic GMP-AMP (cGAMP), but not the cytokine TNFα, displayed obvious nuclear IRF3 protein, consistent with its typical activated status.

While these data demonstrate standard activation of the TBK1-IRF3 signaling axis, whether this is essential to the IFN-associated innate induction triggered by M04 cannot be formally

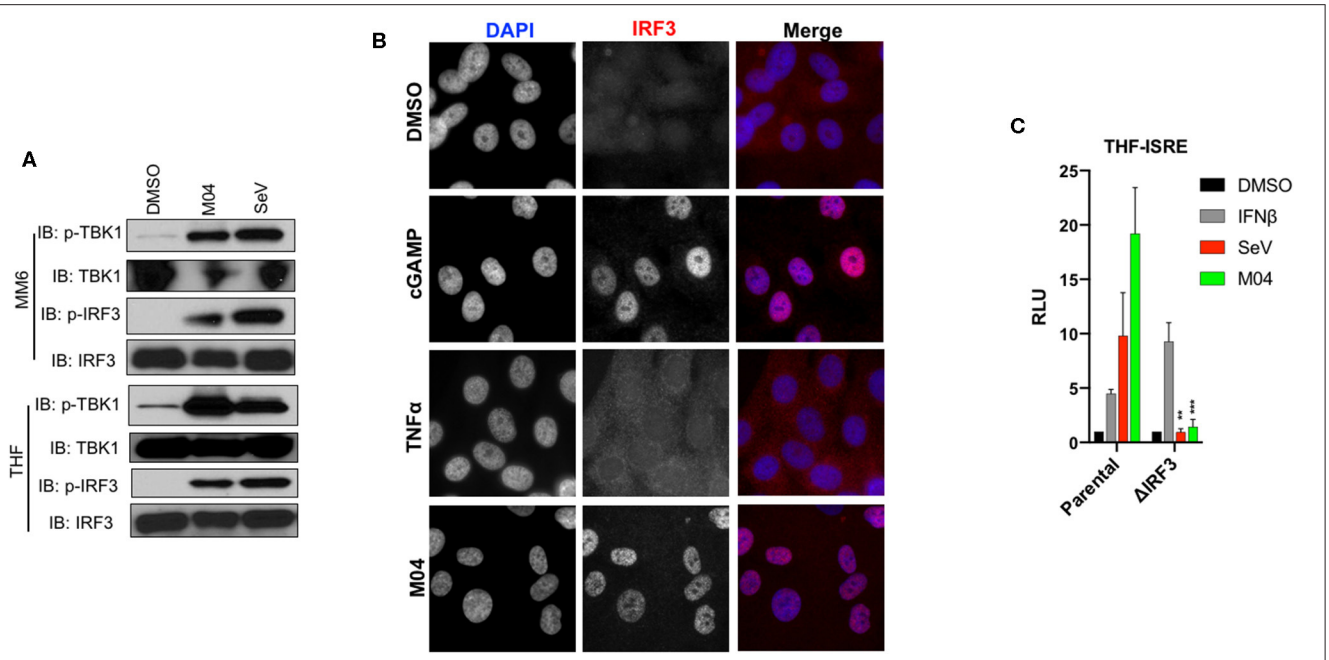

FIGURE 2 | M04 induces canonical activation of IRF3 which is essential to reporter signal generated by the compound. **(A)** Immunoblot showing phosphorylation status of TBK1 Ser172 and IRF3 Ser386 as well as corresponding total protein levels in MM6 cells (left) and THF (right) exposed for 4 h to 1% DMSO, 50 μM M04, or 1,000 HAU/mL SeV as indicated; **(B)** Indirect immunofluorescence showing subcellular localization of IRF3 in THF exposed for 4 h to 1% DMSO, transfected 2'3'cGAMP (10 μg/mL), 100 ng/mL TNFα, or 50 μM M04; **(C)** Reporter assay illustrating IFN-dependent LUC induction following overnight treatment with 1% DMSO, 1,000 U/mL IFNβ, 1,000 HAU/mL SeV, or 50 μM M04 in parental cells as well as those from which IRF3 was deleted as indicated. Data presented are mean ± SD relative luminescence units (RLU) using signal from DMSO-treated cells based on quadruplicate measurements. Student's *T*-test was used to compare RLU in the parental and ΔIRF3 cells $^{**}P < 0.01$; $^{***}P < 0.001$.

concluded. To address this, we utilized previously published THF reporter cells from which the IRF3 protein was deleted using CRISPR/Cas9-mediated genome editing (19). As shown in **Figure 2C**, derivative mutant cells are capable of producing reporter signal following treatment with IFNβ, which indicates that JAK/STAT signaling is intact. However, neither SeV nor M04 were able to elicit measurable reporter expression in these cells indicating that IRF3 is required for the induction of IFN-dependent signaling by both stimuli. Based on these data we conclude that M04 stimulates type I IFN responses through the canonical and necessary activation of TBK1 and IRF3.

M04 Does Not Stimulate Activation of Canonical NF-κB-Associated Transcription

The transcription factor NF-κB is activated by signaling initiated from multiple PRRs (including many that are also IRF3-directed) (25). Importantly, the protein also contributes to the expression of numerous proinflammatory cytokines, including type I IFNs (8, 9). Since M04 leads to conventional activation of IRF3, we therefore asked whether it also stimulates NF-κB. To address this we first exposed M04 to THF stably transduced with an NF-κB-dependent LUC reporter as described (18). As shown in **Figure 3A**, the compound was unable to activate LUC expression in these cells at a range of doses, in contrast to stimuli known to induce NF-κB such as SeV or the cytokine TNFα. Next, we examined whether M04 could induce nuclear accumulation of the NF-κB subunit proteins P50 and P65, a hallmark of canonical activation. For this we exposed THF to DMSO vehicle, TNFα, the STING ligand di-amidobenzimidazole (diABZI) (26), or M04 and used IFA to visualize subcellular localization of the proteins. As shown in **Figure 3B**, TNFα, but neither diABZI nor M04 led to nuclear localization of P65 and P50. Collectively, these data indicate that M04 does not lead to activation of NF-κB.

M04 Activates IRF3 and IFN-Terminal Signaling That Requires STING but Not MAVS, TRIF, or dsDNA PRRs

Three separate signaling cascades are known to elicit TBK1-IRF3 activation and these are defined by the adaptor proteins MAVS, TRIF, and STING [see (3)]. We therefore explored which, if any, of these proteins are required for M04-mediated induction of IRF3 and IFN. We began by utilizing THF-ISRE cell lines constructed previously that lack both MAVS and TRIF (17). **Figure 4A** shows that cGAMP [a STING-inducing IRF3/IFN activator (6, 7, 27, 28)] and M04 are able to elicit LUC expression in these cells suggesting that neither TRIF nor MAVS is required for their activity. We next examined whether M04 could activate IRF3 phosphorylation or ISG expression in these cells. In this case we included SeV as a control stimulus to demonstrate knockout as well as linked amidobenzimidazole (ABZI) as a control small molecule STING activator (26). As shown in **Figure 4B**, M04 and ABZI, but not SeV, were able

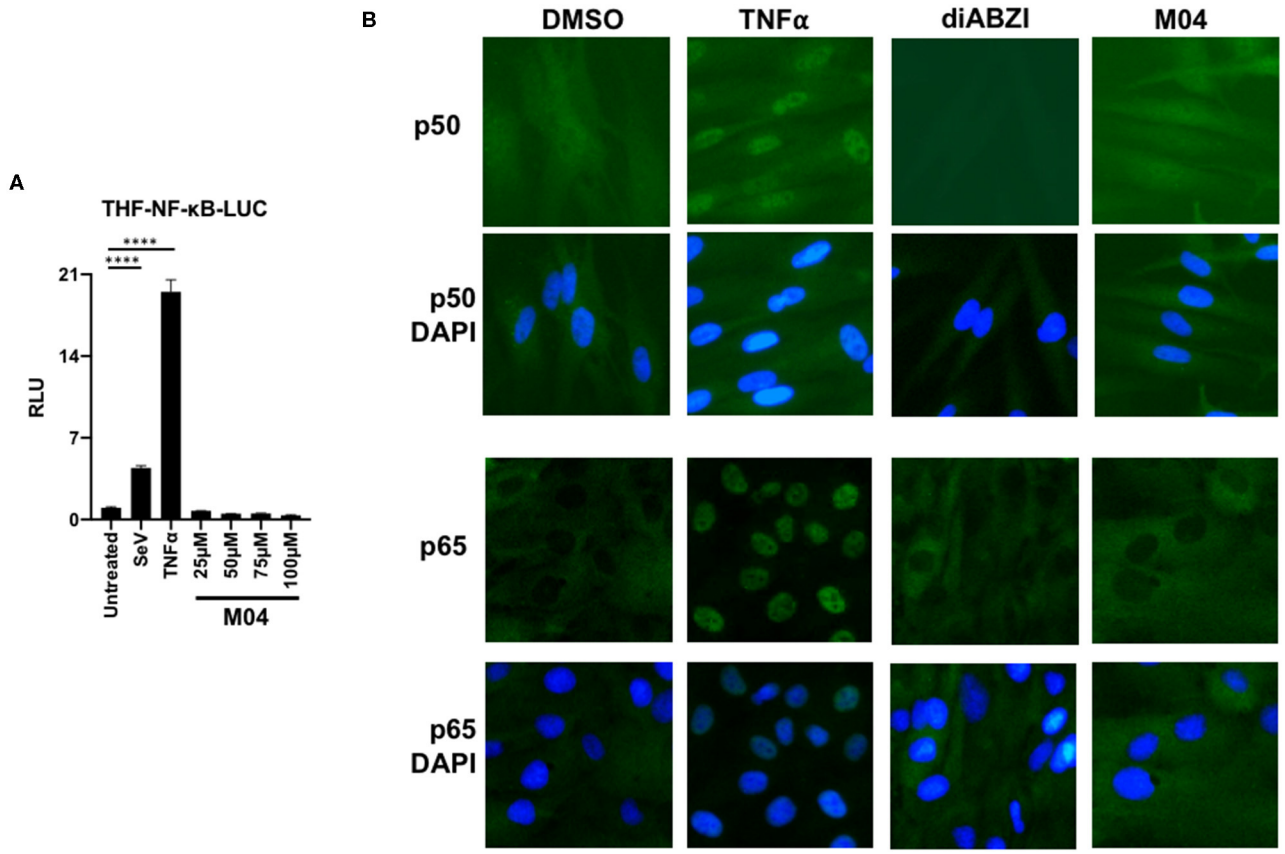

FIGURE 3 | M04 does not Activate NF-κB-Dependent Processes. **(A)** Reporter assay using THF cells responsive to activated NF-κB showing induction of LUC expression following 8 h treatment with 160 HAU/mL SeV, 10 ng/mL TNFα, or the indicated concentration of M04. Values displayed are average fold changes (±SD) based on four replicates compared to DMSO-treated cells; **(B)** Indirect immunofluorescence showing subcellular localization of NF-KB P65 subunit in THF exposed for 4 h to DMSO, 100 ng/mL TNFα, or 75 μM M04. Statistical significance between treated and untreated cells was then calculated using Student's *T*-test ****$p < 0.0001$.

to induce IRF3 phosphorylation. These results strongly suggest that both MAVS and TRIF are dispensable for M04-mediated IFN induction but that STING may play an important role. To address this issue we employed THF-ISRE from which STING was deleted (17–19). While the reporter cassette in these cells was reactive to IFNβ and SeV as expected, it was not induced by M04 (**Figure 4C**). Moreover, while SeV led to phosphorylation of IRF3 in these cells, neither M04 nor ABZI elicited a similar response (**Figure 4D**). To examine this further we assessed type I IFN secretion using a reporter cell-based bioassay on media from treated parental THF as well as those lacking MAVS and TRIF or STING as described (17). We exposed the cells to DMSO, SeV, transfected cGAMP, or M04 and measured secretion of all bioactive type I IFNs using a reporter-based assay. As expected, parental cells secreted IFN-I in response to the three innate stimuli (**Figure 4E**). Furthermore, MAVS/TRIF-deficient cells did not respond to SeV but were reactive to cGAMP and M04 while STING-deficient cells produced IFN-I in response to SeV but not cGAMP or M04. To explore the innate induction ability of M04 relative to other IRF3-terminal stimuli, we also performed a dose response on THF-ISRE that included SeV (MAVS agonist) and human cytomegalovirus (HCMV; STING agonist). As shown in **Supplemental Figure 1**, maximum activation by M04 approximates that induced by HCMV at an MOI of 0.25 and is higher than that induced by SeV at up to 160 HA units/mL.

These results indicate that STING, but not MAVS or TRIF is required for M04-mediated innate activation. STING is fundamentally involved in the innate intracellular response to cytosolic dsDNA (10, 29–31). In addition, multiple dsDNA-reactive PRRs including cGAS (32), DDX41 (33), IFI16 (34), and DAI/ZBP1 (35) are known to be associated with or upstream of STING-dependent responses. We therefore next asked whether M04-induced activity required any of these proteins. For this, RLU was measured using previously described THF-ISRE cells lacking each individual PRR after exposure to M04 (17). As shown in **Figure 4F**, M04 was active on all these cell lines, indicating that none of the deficient proteins are singularly essential for the compound's effects. Based on these results we conclude that M04 activates an IRF3- and IFN-terminal innate immune response in a manner that requires STING but not MAVS, TRIF, or canonical dsDNA PRRs.

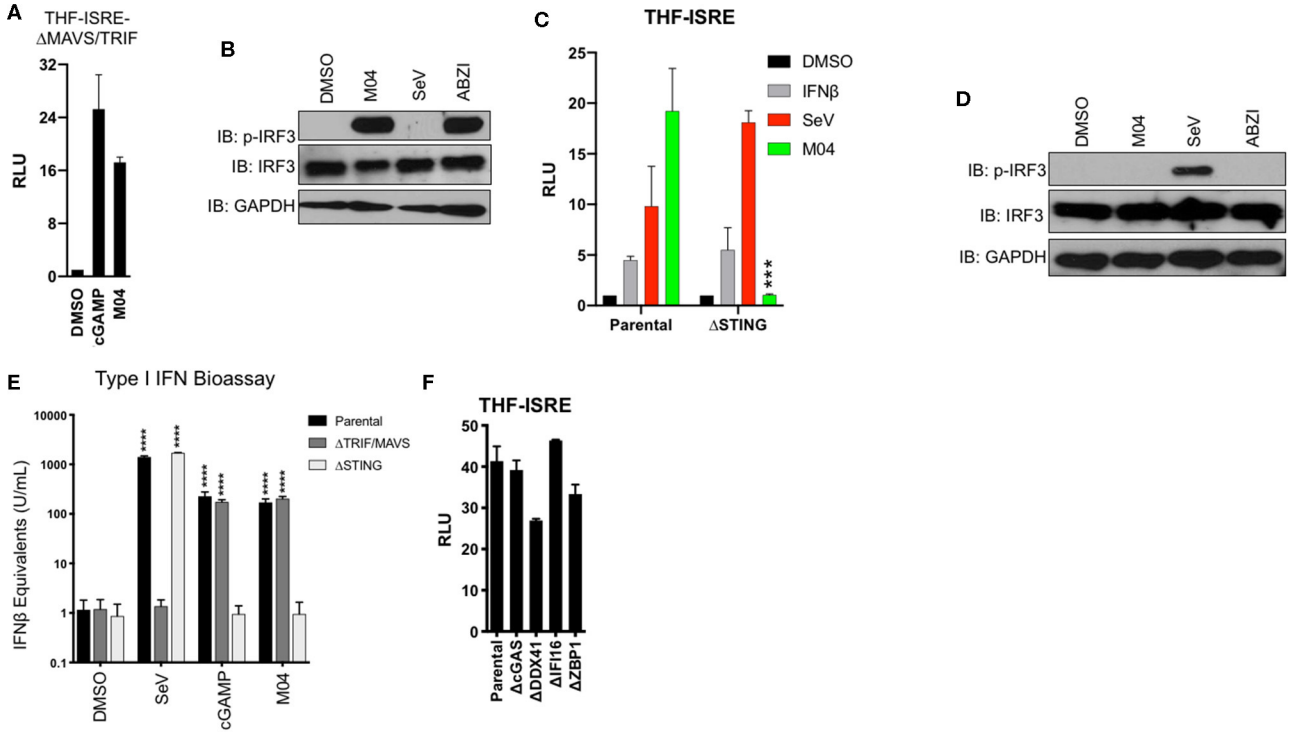

FIGURE 4 | Innate Activation by M04 requires STING but not MAVS, TRIF, or cytosolic DNA PRRs. **(A)** Reporter assay illustrating IFN-dependent LUC induction in THF-ISRE-ΔMAVS/TRIF following overnight treatment with 1% DMSO, transfected cGAMP (10 μg/mL), or 75 μM M04. Data presented are mean ± SD relative luminescence units (RLU) using signal from DMSO-treated cells as the basis ($n = 4$ treatments); **(B)** Immunoblot showing phosphorylation status of IRF3 Ser386, total IRF3, and GAPDH in THF-ISRE-ΔMAVS/TRIF following 8 h treatment with 1% DMSO, 75 μM M04, 1,000 HAU/mL SeV or 25 μM ABZI as indicated; **(C)** Reporter assay illustrating IFN-dependent LUC induction in THF-ISRE-ΔSTING following overnight treatment with 1% DMSO, 1,000 U/mL IFNβ, 1,000 HAU/mL SeV, or 75 μM M04. Data presented are mean RLU ± SD as described above; Student's *T*-test was used to compare RLU $^{***}p < 0.001$; **(D)** Immunoblot showing phosphorylation status of IRF3 Ser386, total IRF3 in THF-ISRE-ΔSTING following 4 h treatment with 1% DMSO, 50 μM M04, 1,000 HAU/mL SeV or 25 μM ABZI as indicated; **(E)** Secretion of bioactive type I IFN from parental THF as well as THF-ISRE-ΔMAVS/TRIF and THF-ISRE-ΔSTING treated in triplicate overnight with 1% DMSO, 1,000 HAU/mL SeV, transfected cGAMP (10 μg/mL), or 75 μM M04. Data are expressed as mean concentrations ± SD for IFNβ equivalent units. Statistical significance between treated and untreated cells of similar genetic background was calculated using Student's *T*-test. $^{****}p < 0.0001$; **(F)** Reporter assay from WT parental THF-ISRE cells as well as from cells from which indicated dsDNA-specific PRRs were deleted. Values presented are mean fold changes ± SD for duplicates relative to the value for DMSO-treated cells.

M04 Induces Phosphorylation and ER-Golgi Trafficking of STING

Canonical activation of STING involves phosphorylation of serine residue 366 (36) followed by translocation from the ER to the Golgi apparatus (37). Since M04 requires STING for IRF3 activation we predicted that the compound leads to these two outcomes. As shown in **Figure 5A**, immunoblots on whole cell lysates from MM6 and THF cells treated with M04 or ABZI displayed phosphorylation of STING Ser366 whereas lysates from untreated or SeV-treated cells did not. We next performed IFA to examine co-localization of STING with the standard Golgi protein marker GM130. **Figure 5B** shows that transfection of THFs with cGAMP or treatment with M04 leads to accumulation of STING in regions that also stain positive for GM130. These results are consistent with conventional intracellular activation of STING in response to M04. Since M04 induces IRF3 independently of any examined dsDNA PRRs or cGAMP synthesis, we next explored whether observations could be obtained that indicate direct interaction between the molecule and the STING protein. This was performed as part of previous studies measuring thermal shift of purified STING C-terminal domain (CTD) that includes the ligand binding domain (LBD) (17, 19). We expect that direct contact between the protein and an examined ligand will lead to an increase in the protein's thermal stability that is observable as emission of protein-associated SYPRO Orange at higher temperatures than those in the absence of the ligand (27, 38). As shown in **Figure 5C**, incubation of purified STING-CTD with cGAMP led to an increase in the temperature at which fluorescence was emitted relative to that with DMSO alone. However, the presence of M04 did not lead to a significant increase in such temperatures relative to that induced by DMSO. These results are not consistent with M04 directly interacting with STING-LBD as does cGAMP. While direct interaction cannot formally be ruled out, determining whether M04 activates STING by engaging the CTD in a manner that does not affect thermal stability or by engaging a region outside the CTD will require different experimental approaches such as affinity tagging and protein pulldown. Unfortunately, the

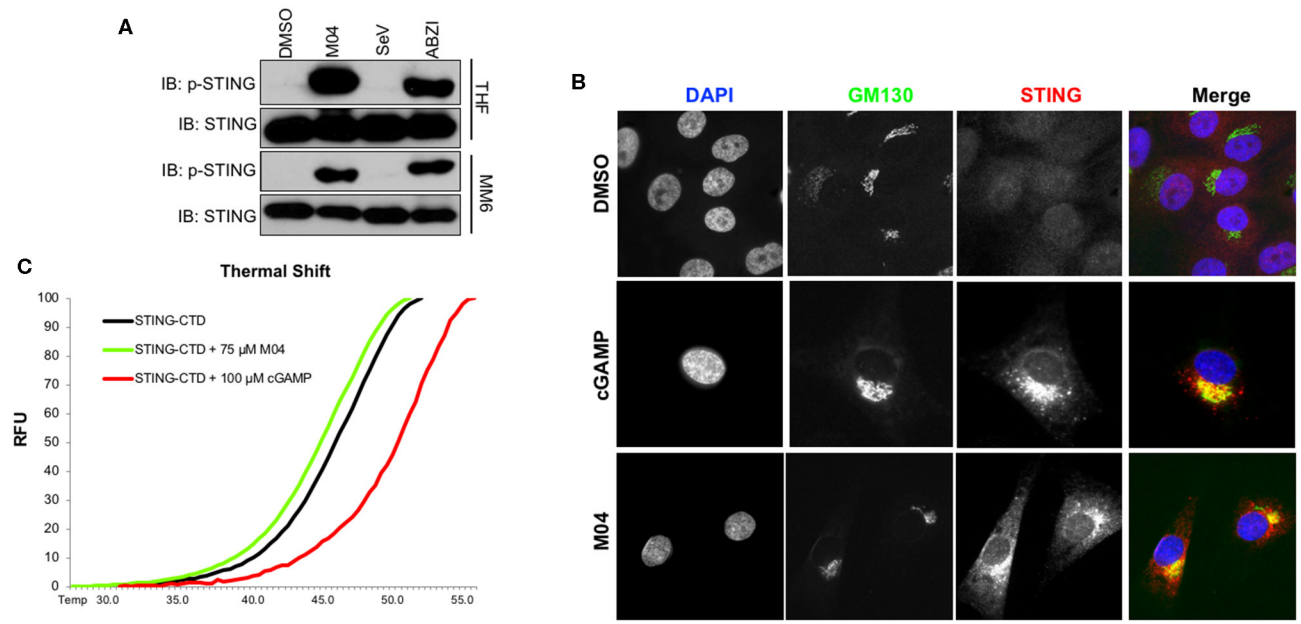

FIGURE 5 | M04 Induces Canonical STING Activation. **(A)** Immunoblot showing phosphorylation status of STING Ser366 as well as total STING in THF and MM6 following 4 h treatment with 1% DMSO, 50μM M04, 1,000 HAU/mL SeV or 25 μM ABZI as indicated; **(B)** Indirect immunofluorescence showing subcellular localization of Golgi marker GM130 and STING in THF exposed for 4 h to DMSO, transfected cGAMP (10 μg/mL), 100 ng/mL TNFα, or 50 μM M04; **(C)** Melting temperature shifts for human STING-CTD in the presence of DMSO, 75 μM M04, or 100 μM 2'3' cGAMP. Data presented are SYPRO orange relative fluorescent units (RFU).

innate activity of M04 is highly sensitive to chemical modification as indicated by the absence of ISRE activity in a group of 13 M04 derivatives as shown in **Supplemental Figure 2**. As such, adding moieties such as biotin to M04 will likely not represent appropriate pulldown bait.

M04 Stimulatory Capacity Is Dependent on STING Polymorphic Variant

In human populations multiple amino acid variants of STING are known to exist and these can be mechanistically associated with a range of phenotypic outcomes at the levels of molecular function and disease state [reviewed in (39)]. Since both THF and MM6 cells exhibit the most common and CDN-reactive STING allele (STING-WT), we chose to examine M04 activity in the presence of another variant. For this we used THP-1 promonocytic cells, which possess the R71H-G230A-R293Q (STING-HAQ) allele (7, 16, 40). We first used commercially available, IFN-sensitive THP-1-ISG-Lucia reporter cells. LUC signal was produced by these cells when exposed to SeV, IFNβ, a small molecule agonist of the TRIF pathway termed AV-C (18), but not M04 nor, interestingly, ABZI (**Figure 6A**). These results suggest that THP-1 cells are not responsive to these two compounds and this was validated by immunoblotting which showed that while SeV treatment led to S386-phosphorylated IRF3, neither M04 or ABZI did (**Figure 6B**). However, the cells were able to react to cGAMP, indicating that STING signaling is operational in these cells (**Figure 6B**). Based on this we hypothesized that the endogenous STING-HAQ protein was incapable of reacting to M04 and decided to ask whether ectopic expression of STING-WT could rescue M04 responsiveness in THP-1 cells. To pursue this, we first employed CRISPR/Cas9 to construct a THP-1 line from which the endogenous STING-HAQ protein was deleted and then used a lentivector to stably introduce into these edited cells a constitutively expressed open reading frame encoding the STING-WT protein (**Figure 6C**). These cells were then treated with SeV, M04, ABZI, or cGAMP and immunoblotting performed to examine IRF3 phosphorylation. As shown in **Figure 6D**, expression of STING-WT rendered the cells responsive to M04, suggesting that the compound is able to stimulate activity of this, but not the HAQ protein variant.

To verify the differential responsiveness of the protein variants to M04 using an independent method, we employed transiently transfected HEK293T cells. These cells are deficient in endogenous STING and as such will only respond to STING inducers during ectopic expression of the protein (29, 31). We constructed plasmid vectors that encode STING-WT, STING-HAQ, or STING-R232H (the third most common STING variant). We then transfected these along with a IFN-responsive LUC reporter vector and exposed the cells to DMSO, M04, cGAMP, or diABZI, a derivative of ABZI shown to be reactive with STING-HAQ (26). We then examined IRF3 phosphorylation and measured LUC expression from whole cell lysates. As shown in **Figure 7A**, while transfection of the vectors alone did not activate IRF3 phosphorylation, all three stimuli led to phosphorylation of IRF3 in the presence of STING-WT. However, M04 and diABZI elicited only weakly detectable phosphorylation in the presence of STING-HAQ. Furthermore, cGAMP appeared to induce a strong response in the presence of STING-HAQ and STING-WT but not

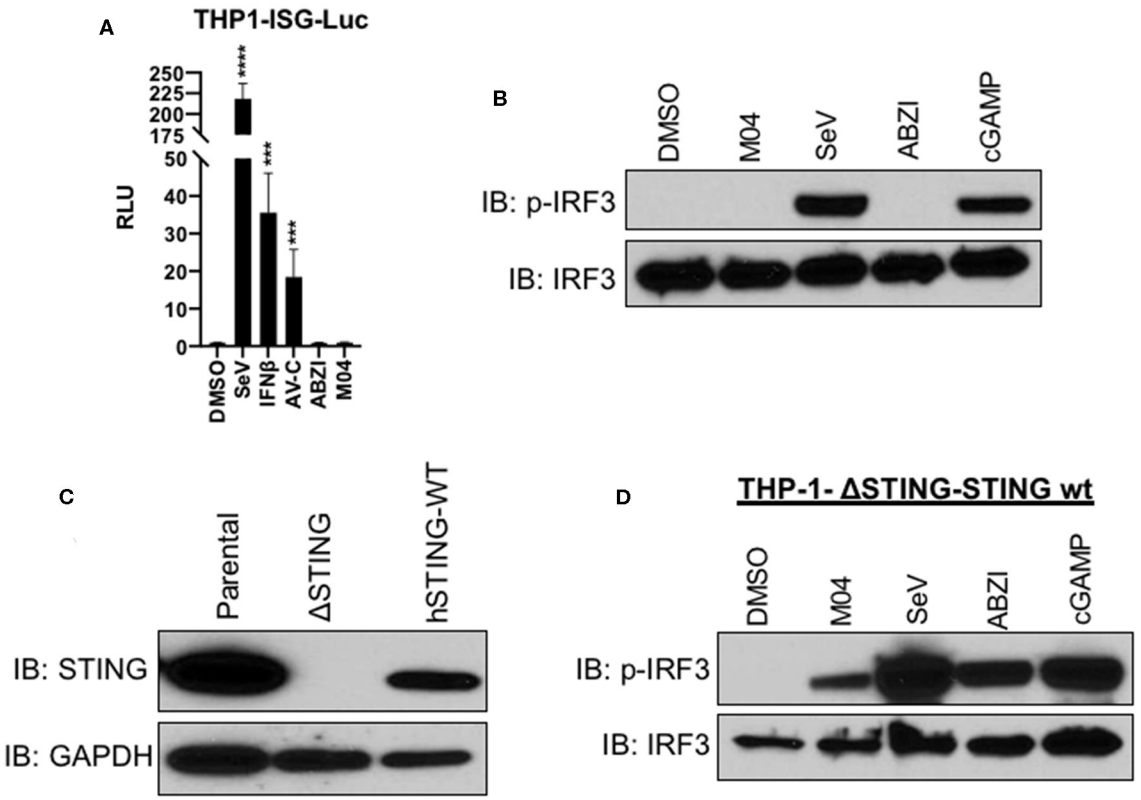

FIGURE 6 | Responsiveness to M04 can be Conferred through Introduction of WT STING Allelic Variant. **(A)** Reporter assay illustrating IFN-dependent LUC induction in THP-1-ISG-Lucia following overnight treatment with 1% DMSO, 1,000 HAU/mL SeV, 1,000 U/mL IFNβ, 75 μM TRIF agonist AV-C, 25 μM ABZI, or 75 μM M04. Data presented are mean ± SD relative luminescence units (RLU) using signal from DMSO-treated cells as the basis ($n = 4$ treatments). Student's *T*-test was used to compare RLU $^{***}p < 0.001$, $^{****}p < 0.0001$; **(B)** Immunoblot showing phosphorylation status of IRF3 Ser386 and total IRF3 in THP-1 whole cell lysates following 4 h treatment with 1% DMSO, 50 μM M04, 1,000 HAU/mL SeV, 25 μM ABZI, or 10 μg/mL cGAMP as indicated; **(C)** Immunoblot showing expression of endogenous or ectopically expressed WT hSTING in THP-1 as indicated. **(D)** Immunoblot showing phosphorylation status of IRF3 Ser386 in THP-1 cells from which endogenous STING was deleted and WT STING stably introduced following indicated treatment as described above.

STING-R232H (**Figure 7B**). This was surprising but consistent with results showing that this allele is comparatively less responsive to cGAMP (7, 16). These results were reflected in the IFN-dependent reporter signal with M04 and diABZI generating detectable signal in the presence of STING-WT and STING-R232H but weak or no signal in STING-HAQ transfected cells and cGAMP inducing highest LUC signal in STING-WT and STING-HAQ. These results also align with those generated in THP-1 cells.

A549 lung epithelial cells suppress expression of the endogenous STING mRNA (41) and, consequently, do not respond to M04 (**Figure 7C**). We therefore asked whether stable introduction of STING into these cells using methods described above could also rescue M04 responsiveness. As shown in **Figure 7C**, stable expression of hSTING-WT restores M04-associated ISG expression. Results described so far including these suggest that M04 activates STING in a manner that is independent of DNA PRRs (**Figure 4F**) and binding to the protein's CTD (**Figure 5C**). To rule out the unlikely possibility that M04 stimulates cGAS-independent synthesis of cGAMP we treated A549 cells with M04 and harvested lysates to measure cGAMP by ELISA. **Figure 7D** shows that while infection with HCMV induces cGAMP synthesis as described (42), treatment with M04 does not. Collectively, our results indicate that M04 activates STING in a cGAMP-independent manner either by directly engaging the protein or by stimulating a cellular factor common to THP-1, HEK293T, and A549 cells that regulates STING function.

hSTING Confers Responsiveness to M04 Across Species

Given that the efficacy of M04 associates with amino acid polymorphisms in the human STING allele, we believed it unlikely that the compound triggers an innate response in mouse cells. To address this, we first examined a commercially available RAW264.7 murine macrophage-like line that expresses an IFN-dependent reporter (RAW264.7-ISG-Lucia). In these, SeV and DMXAA [a mouse-specific STING agonist (43)], but not M04 were able to induce reporter expression (**Figure 8A**). To examine whether the compound might still be active in an *in vivo* setting, we injected it intraperitoneally into C57BL/6 mice and harvested spleens after 5 h. While DMXAA was able

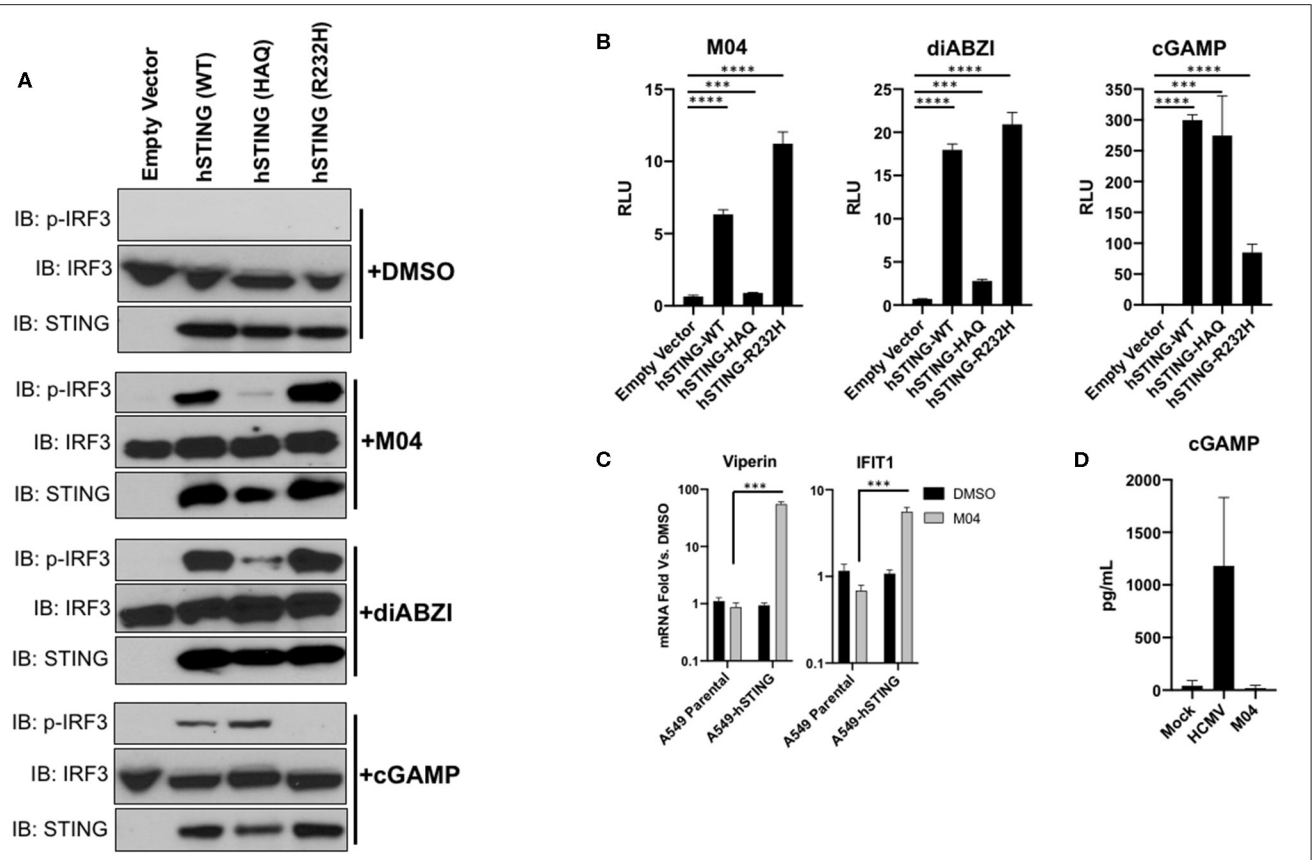

FIGURE 7 | Transient transfection of vectors encoding WT and R232H but not HAQ hSTING confer responsiveness to M04. **(A)** Immunoblot from HEK293T whole cell lysates showing expression of indicated STING variants following transient transfection, S386 phosphorylation status of IRF3 and total IRF3. Cells were left untreated or exposed to 75 μM M04, 100 nM diABZI, or 10 μg/mL cGAMP as indicated; **(B)** Reporter assay using cells ($n = 4$) treated as described in **(A)**. Values displayed are mean fold changes ± SD relative to cells transfected with empty vector; **(C)** Expression of IFIT1 and Viperin mRNA as determined by qPCR in parental A549 cells as well as those transduced with hSTING following treatment with 1% DMSO or 75 μM M04. Data are mean fodl changes ± SD relative to DMSO-treated cells based on duplicates; **(D)** Synthesis of cGAMP by A549-hSTING cells as determined by ELISA following overnight treatment with 1% DMSO, HCMV, or M04. Data presented are mean pg/mL ± SD based on duplicate samples. Student's *T*-test was used to compare RLU and mRNA levels $^{***}p < 0.001$, $^{****}p < 0.0001$.

to induce expression of Viperin and IFIT1 relative to DMSO-vehicle treated control mice, we observed no upregulation of these genes in response to M04 (**Figure 8B**). Since previous work has demonstrated functionality of hSTING in mouse cells (44), we next utilized a delete-and-replace approach as described above to see if responsiveness to M04 could be conferred to RAW264.7 cells by ectopic expression of hSTING-WT. **Figure 8C** shows expression of endogenous or human STING-WT in parental RAW264.7 cells as well as following CRISPR-mediated knockout and target hSTING protein stable introduction by lentivector. These cells were then exposed to DMSO, M04, SeV, or cGAMP. As shown in **Figure 8D**, SeV and cGAMP led to similar levels of phosphorylation IRF3 on serine residues 379 and 396. Surprisingly, however, M04 did not elicit detectable phosphorylation of IRF3 in either cell type. Since it is possible that IRF3 is activated by phosphorylation of C-terminal serine residues not detectable by available antibodies, we also examined M04-mediated induction of ISGs in these cells. As shown in **Figure 8E**, the compound induced minimal or no ISG expression in parental cells but substantial amounts in cells expressing hSTING. From these data we conclude that M04 leads to hSTING effects that can activate innate responses in non-human cells.

M04 Is Able to Elicit Secretion of Pro-inflammatory Cytokines From Primary Human Cells

STING agonism represents a potentially impactful pharmacologic strategy in the context of facilitating adaptive immune responses. However, thus far we only describe induction of STING-dependent responses in immortalized or telomerized cell lines. We therefore wished to determine whether M04 could activate innate phenotypes relevant for clinical uses. However, since M04 is inactive in conventional murine models, tractable options for exploring *in vivo* effects are not available. In light of this, we chose to utilize human peripheral blood mononuclear cells (PBMCs) to explore M04-mediated cellular

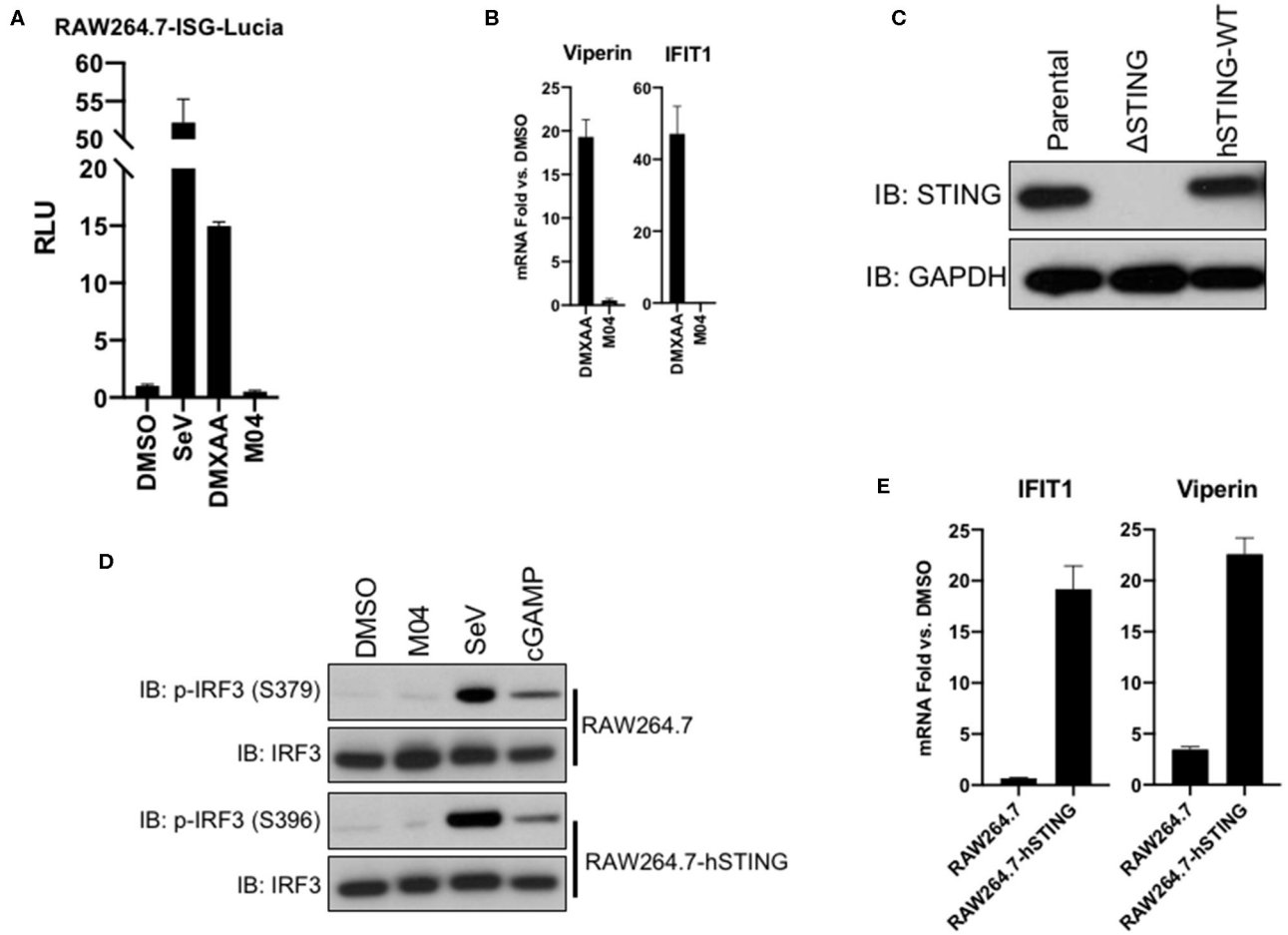

FIGURE 8 | Responsiveness to M04 can be conferred to murine cells by ectopic expression of human STING-WT variant. **(A)** Reporter assay illustrating IFN-dependent LUC induction in RAW264.7-ISG-Lucia cells followni g overnight treatment with 1% DMSO, 160 HAU/mL SeV, 25 μM DMXAA, or 75 μM M04.Data presented are mean ± SD relative luminescence units (RLU) using signal from DMSO-treated cells as the basis ($n = 4$ treatments); **(B)** qPCR examining *in vivo* ISG induction following IP injection of DMXAA or M04; **(C)** Immunoblot showing expression of endogenous or ectopically expressed hSTING-WT in RAW264.7 cells as indicated; **(D)** Immunoblot showing phosphorylation status of IRF3 Ser379 and Ser396 as well as total IRF3 in RAW264.7-hSTING cells following 4 h treatment with 1% DMSO, 75 μM M04, 160 HAU/mL SeV, or transfection of cGAMP as indicated; **(E)** qPCR examining transcription of IFIT1 or Viperin following overnight treatment of parental RAW264.7 and RAW264.7-hSTING cells with 75 μM M04 ($n = 3$). Data presented are mean fold changes ± SD of mRNA relative to cells treated with 1% DMSO.

outcomes. Since STING agonists are being pursued clinically as anti-cancer immunotherapeutics (45), we evaluated the response of a relevant population of patients with locally advanced or borderline resectable pancreatic cancer (46). PBMC isolated from patients prior to treatment were exposed to M04 overnight and media harvested for a multiplex assay to measure cyto/chemokines secreted in response to treatment. Cells were also left untreated, exposed to cyclic di-AMP (CDA) as a STING-specific positive control, or LPS as a STING-independent, IRF3-stimulating control. As shown in **Figure 9**, M04 significantly induced secretion of TNFα, IL-1β, IL12p70, and IL-10. Moreover, the patterns of M04-associated induction more closely resembled those observed for CDA than LPS, consistent with STING dependence of the two stimuli. Based on this we conclude that M04 is capable of inducing innate responses in primary human cells.

M04 Triggers Expression of Human Dendritic Cell Maturation Markers

Dendritic cells (DC) are essential for the establishment of adaptive immunity based on their capacity to present antigens and secrete immunologically potent cytokines. This process first involves their maturation, as denoted by surface marker expression, in response to appropriate innate immune stimuli that are often indicative of microbial infection or diseased cells. We therefore asked whether M04 was capable of eliciting induction of maturation markers on human cells. For this we employed PBMCs from six healthy human donors in an ex vivo

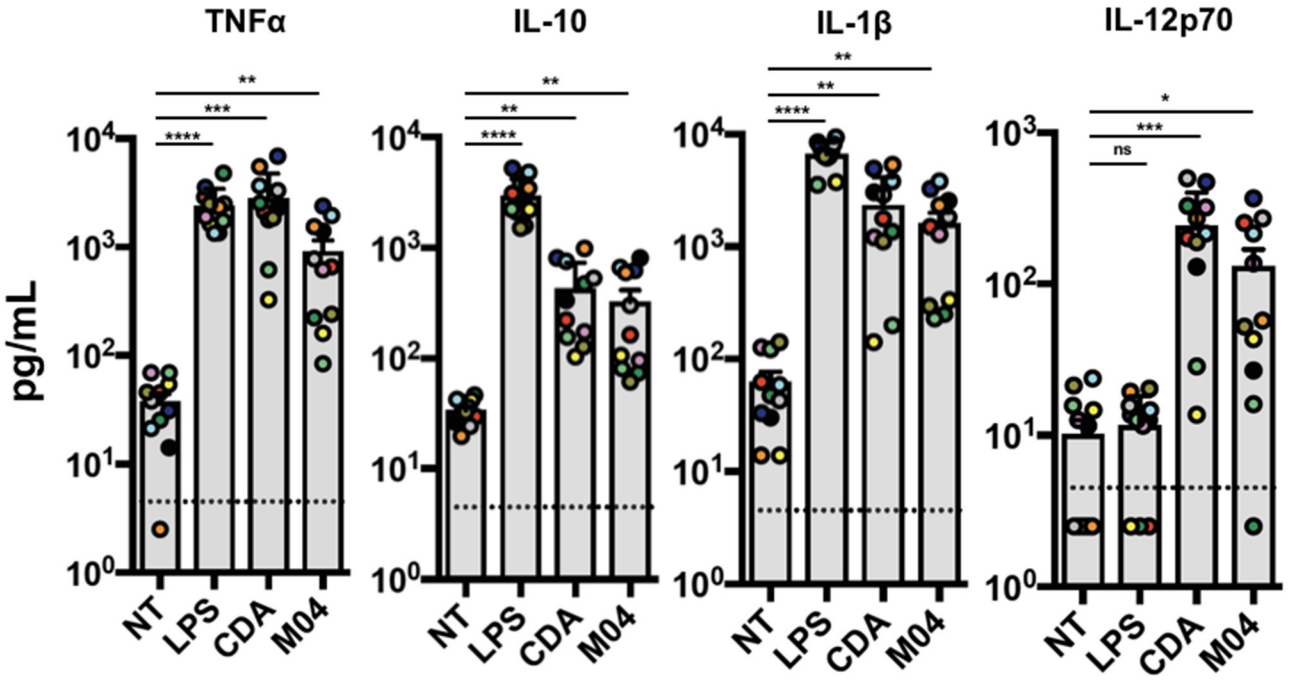

FIGURE 9 | Induction of cytokine expression by M04 on human primary cells. Peripheral blood mononuclear cells were harvested from ten human donors and treated overnight with 1OO ng/mL LPS, 10 μg/mL cyclic di-AMP (CDA), or 75 μM M04 as indicated. Luminex multiplex assay was then used to measure levels of TNFa, IL-10, IL-1β, or IL12p70 in cell culture supernatant. Donor specific data are indicated by colored circles. Statistical significance between treated and untreated cells was then calculated using Student's *T*-test. $^{*}p < 0.5$, $^{**}p < 0.01$, $^{***}p < 0.001$; $^{****}p < 0.0001$.

culture system. Immature monocyte-derived DCs cultured in IL-4 and GM-CSF were treated with two doses of M04. Control stimuli included DMSO (negative) and LPS + IFNγ (positive). Flow cytometry was then used to quantify expression of CD40, HLA-DR, CD80, CD83, and CD86. As shown in **Figure 10**, expression of HLA-DR and CD86 were significantly elevated after M04 exposure relative to vehicle-treated cells. Surprisingly, however, the compound did not similarly induce CD40, CD80, or CD83. These results suggest that M04 behaves as an innate stimulus that is capable of facilitating maturation of APCs and may thus exhibit adjuvant properties.

M04 Enables T Cell Cross Priming

Potent and adequate $CD8^+$ T cell responses against a specific antigen is a key component of the adaptive immune response. Induction of such high-quality T cell responses is crucial for many vaccination objectives. Adjuvants can enhance the function of antigen presenting cells, which through the priming process, will shape the immune response and induce naïve antigen-specific $CD8^+$ T cells into potent effector cytotoxic T lymphocytes. In an *ex vivo* assay using cryopreserved and unfractionated PBMCs adapted from (47), we recapitulated the priming, by dendritic cells, of $CD8^+$ T cells specific for the model antigen Melan-A, in the presence of M04. Antigen-specific $CD8^+$ T cells were detected by Melan-A-tetramer staining. As shown in **Figure 11**, both M04 and cGAMP induce significantly higher frequencies of primed Ag-specific $CD8^+$ T cells compared to the coculture without adjuvant. A 4.5-fold increase was observed in the presence of M04 while cGAMP enhanced this by 3.3 times the frequency of Ag-specific $CD8^+$ T cells. These results thus further demonstrate the adjuvant potential of M04 in human primary cells.

The M04 Transcriptome More Closely Resembles That Induced by cGAMP Than by LPS

Given the ability of M04 to induce STING-dependent transcription of targeted ISGs as well as innate phenotypes in primary human cells, we predicted the stimulation of substantial global transcriptional responses by the molecule in PBMCs. We also expected that qualitatively these would more closely resemble those triggered by an agonist of the STING pathway relative to another IRF3-terminal adaptor. To address this, we obtained PBMCs from two healthy human donors and treated them with DMSO vehicle, M04, cGAMP, or the TLR4/TRIF agonist LPS. RNA sequencing was then used to measure individual transcript levels in each sample and comparisons to vehicle-treated cells made (**Supplemental Table 1**). As shown in **Figure 12**, M04, cGAMP, and LPS led to the significant more than 2-fold upregulation of 314, 848, and 704 RNA transcripts, respectively. Importantly, however, the number of transcripts induced by M04 that were also uniquely upregulated by the other stimuli was much greater for cGAMP than for LPS (76 vs. 7, respectively). Furthermore, the quantitative similarity

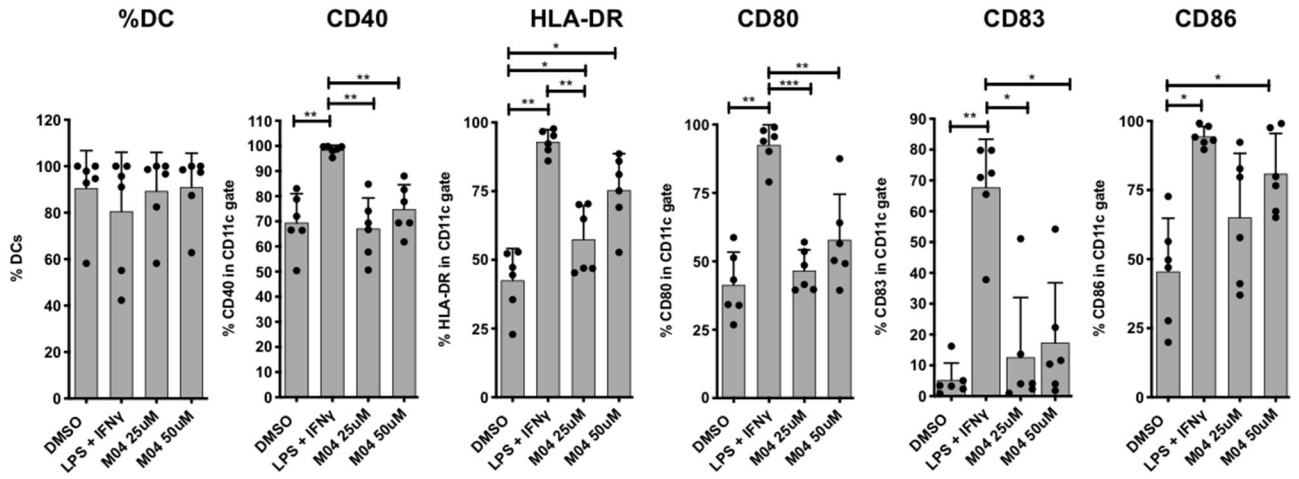

FIGURE 10 | M04 induces HLA and costimulatory molecule upregulation on human monocyte-derived dendritic cells. Human monocyte-derived dendritic cells (DCs) differentiated from healthy human PBMCs were treated with 1% OMSO or stimulated with 0.5 μg/ml LPS plus 40 ng/ml IFN-y and 25 μM or 50 μM M04 for 24 h. DCs were harvested (% DCs indicated PBMCs indicated at left) and analyzed by flow cytometry for the upregulation of surface C040, HLA-DR, CD80, CD83, and CD86 as indicated. Values are presented as mean ± the standard deviations (mean ± SD) for the indicated marker from 6 individual donors across 3 independent experiments (donor-specific values are represented by closed circles). $^{*}p < 0.5$, $^{**}p < 0.01$, $^{***}p < 0.001$.

in absolute fold changes of all observed transcripts was much higher between M04 and cGAMP (Pearson $r = 0.7554$) than between M04 and LPS ($r = 0.6141$) (**Figure 12C**). Finally, despite the failure of experiments to show canonical activation of NF-κB by M04 in fibroblasts, treatment of PBMCs with the compound led to induction of multiple RNAs whose transcription was predicted by two different computational tools (PASTAA and RegulatorTrail) to be associated with activity of this transcription factor (**Supplemental Tables 2** and **3**) (48, 49). This is consistent with previous work describing NF-κB activation by STING (8, 50, 51). We hypothesize that our results likely represent a phenomenon related to intrinsic differences in cell type whereby stromal and non-stromal cells are differentially reactive to NF-κB-associated, STING-mediated pro-inflammatory responses. This will require follow up mechanistic efforts to dissect, however.

DISCUSSION

The innate and adaptive immunostimulatory potential of synthetic STING activation has greatly incentivized the discovery and characterization of novel molecular entities that stimulate this pathway for anti-cancer therapies (45, 52) and as a strategy to enhance vaccination (53, 54). Currently the most clinically well-developed STING inducers are dithio-mixed linkage derivatives of cyclic dinucleotides such as ML-RR-S2 CDA (also known as ADU-S100) that are in clinical trials (NCT03172936) (55). Unfortunately, CDNs exhibit chemical liabilities including violation of Lipinski rules (56) for druglikeness, susceptibility to phosphodiesterase-mediated degradation (57, 58), and their size, hydrophilicity, and negative charge render them impermeable to cell membranes thus impairing exposure to cytosolic STING (59, 60). In general, the properties of small molecules such as M04 mitigate these issues and, as such, may ultimately represent a superior strategy for activating STING-mediated processes *in vivo*.

Our work demonstrates that M04 activates an innate response in human cells that requires STING and IRF3 but not an array of other described cytosolic PRRs of DNA (in particular cGAS). M04 also does not induce synthesis of cGAMP by a cGAS-dependent or independent process. Moreover, in addition to the loss of function approach used to demonstrate protein essentiality, we also used forward genetics methods that demonstrated conference of M04 responsiveness to non-responsive cells (including mouse cells) following ectopic expression of hSTING. These results strongly argue that the compound's mechanism of action involves direct engagement of the STING protein. Why thermal shift analysis showed no M04-mediated enhancement of STING-CTD stability is not clear but it is possible that the compound binds to a protein domain outside this region that leads to activation.

We also show that M04 is capable of inducing innate activation in a manner that requires specific variants of human STING. Surprisingly, diABZI showed similar patterns of allele-specific efficacy with poor responsiveness in STING-HAQ and normal activity in STING-R232H and STING-WT. This result is actually inconsistent with what was previously shown for diABZI in primary human cells homozygous for these alleles (26). Whether this disparity is associated with the cell type or model system we employed will require additional follow up studies. Overall, however, these data suggest that it is possible to identify small molecules that exhibit allele-specific activity, which may be important given the existing STING polymorphism in the human population (39). Interestingly, the alleles with which M04 and diABZI function best encode arginine or histidine amino acids at position 232 and arginine at position 293, which are both within

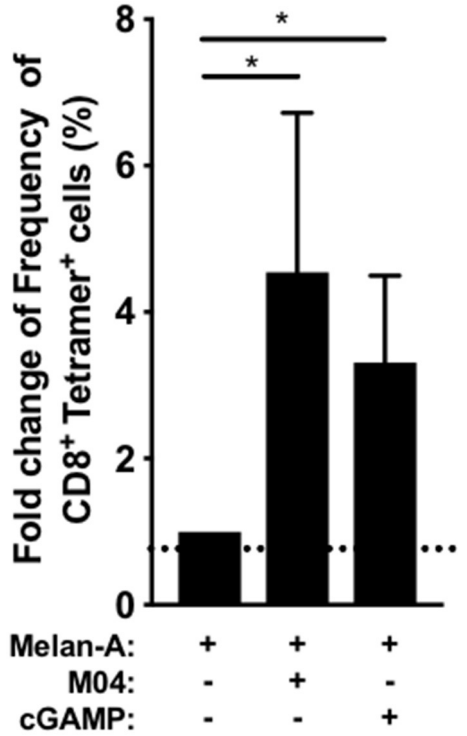

FIGURE 11 | *In vitro* $CD8^+$ T cell priming using unfractionated PBMC. Dendritic cell differentiation from healthy HLA-A2+ donor PBMCs ($n = 7$) was induced with GM-CSF (100 ng/ml) and IL-4 (20 ng/ml) and Melan A peptide (1O μg/ml) with M04 (50 μM) or 2,3' cGAMP (5 μg/ml) was added the next day when indicated. On day 11, the primed Metan-A specific $CD8^+$ T lymphocytes were detected using tetramer staining within the $CD3^+$ T cell population after aggregates and dead cell exclusion. The graph represents the fold increase of Metan-A - specific $CD8^+$ T lymphocytes frequency compared to the condition without STING agonists. A non-parametric Friedman signed rank test followed by Dunn's multiple comparison test was used to assess significance. $^*p < 0.05$.

the LBD. STING-HAQ differs from these alleles by encoding glutamine at position 293, alanine at 230 and histidine at position 71, which is in the transmembrane domain. Whether any of these individually are associated with our observations regarding M04 or diABZI activity will require additional examination. Furthermore, there exist other naturally occurring variants that exist with relatively high frequency that we also plan to examine. Surprisingly absent from the archive of studies examining the clinical value of STING agonists is exploration of genetic impacts. Given the breadth and frequency of human polymorphism in this protein as well as links between phenotype and variant, a more penetrative consideration of how this will affect STING-based therapeutics is clearly warranted. Understanding the spectrum of allele-associated molecule reactivity will be a very important step in the development of STING-directed pharmacophores.

It is worth noting that while STING activation is known to facilitate establishment of an adaptive immune response, its overall immune impact is more nuanced. In some models the protein is associated with tolerogenic responses likely through its induction of indoleamine 2,3-dioxygenase, as observed in our transcriptomic data for both M04 and cGAMP (61, 62). However, determining with precision the immune-mediated effects conferred by M04 and whether they have potential clinical utility is hindered by its inactivity in mice. Fortunately, primary human cells do display responses to M04 such as cytokine secretion, expression of DC maturation markers, and T cell cross-priming that associate with conventional immune activity. Previous work has identified similar phenomena induced by CDN-based agonists (63–65) as well as dsDNA (66) and diABZI (26). Why some of the DC markers were not induced as expected is unclear and could be related to donor-specific effects such as STING genotype or a skewed set of molecular processes induced in primary tissues by the compound. The key question regarding M04 in this regard is whether the innate processes induced by the molecule *ex vivo* would translate into meaningful immunological effects *in vivo*. If M04 elicits activity by binding directly to STING as we predict, obtaining this answer may be possible in mice that express hSTING. Previous work has shown that hSTING is functional and responsive to activating ligands in mouse cells (44). It is therefore possible that replacement of the endogenous mouse STING with a human allele could lead to an animal model useful for characterizing molecules with human but not mouse specificity (17, 19, 67). Accordingly, this would greatly expand the spectrum of potential compounds that could be explored for therapeutic activity.

MATERIALS AND METHODS

Reagents and Antibodies

Dimethyl sulfide (DMSO) was purchased from Thermo Fisher. Human recombinant IFNβ was obtained from PBL. Lipopolysaccharide (LPS) was obtained from Sigma. cGAMP was obtained from Invivogen. Stocks of M04 were originally obtained from Enamine. Larger stocks of M04 and ABZI were synthesized by the OHSU Medicinal Chemistry Core Facility. diABZI was obtained from MedChem Express. Puromycin was obtained from Invivogen and used at 3 μg/mL in resistant cell culture. Steady-Glo cell lysis/luciferin and CellTiter-Glo viability assay kits were obtained from Promega. Lipofectamine 3000 was obtained from Invitrogen. Sources and concentrations of antibodies used against the following antigens are indicated in parentheses: glyceraldehyde-3-phosphate dehydrogenase (GAPDH) (SC-51906; Santa Cruz) (1:10,000), IRF3 (4302; Cell Signaling), human phospho-IRF3 (76493; Abcam), mouse IRF3 (SC-9082; Santa Cruz), mouse phospho-S379 IRF3 (79945S; Cell Signaling), mouse phospho-S396 IRF3 (29047S; Cell Signaling), STING (13647S; Cell Signaling), phospho-S366 STING (19781S; Cell Signaling), TBK1 (3504S; Cell Signaling), phospho-TBK1 (5483S; Cell Signaling), NF-kB P65 (SC372; Santa Cruz), NF-kB P50 (3035; Cell Signaling), GM-130 (610823; BD Biosciences).

Cell Line Cultures and Virus

Telomerase-transduced human foreskin fibroblasts stably transduced with the IFN-responsive pGreenFire-ISRE lentivector

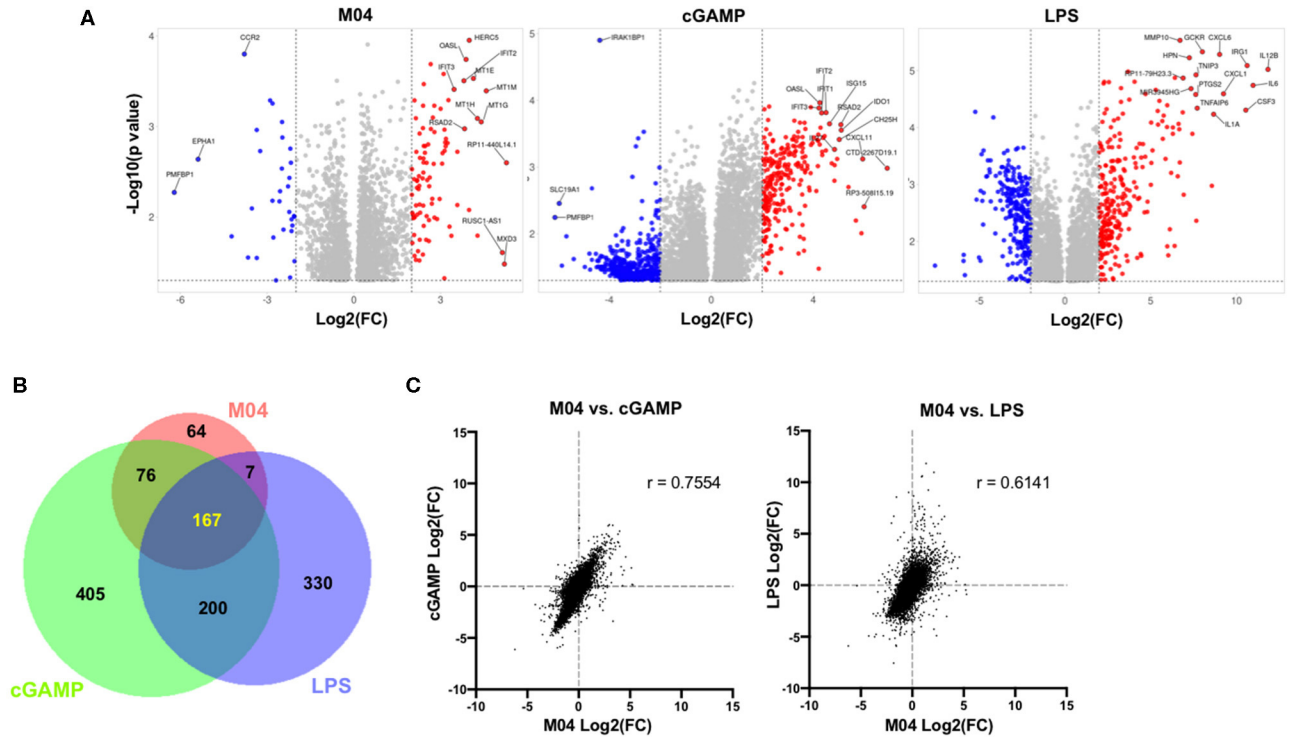

FIGURE 12 | Comparison of transcriptomic changes in PBMCs induced by M04, LPS, and cGAMP. **(A)** Volcano plots illustrating $-\log_{10}(p \text{ value})$ and fold change of significantly differentially regulated transcripts for indicated stimulus relative to cells exposed to DMSO vehicle treatment. Gene symbols of the top 15 transcripts as determined by Manhattan distance are labeled; **(B)** Venn diagram illustrating patterns of similarity in indicated stimulus-specific upregulated transcripts; **(C)** Fold change correlation of all detected transcripts between indicated stimuli. Pearson correlation coefficient (r) presented for each comparison.

(System Biosciences) were used as previously described (18, 19). A549 and HEK293T cells were a gift from Jay Nelson (Oregon Health and Science University). MonoMac6 (MM6) cells were a kind gift from Michael Gale (University of Washington) and used as described (17). THP-1-ISG-Lucia and RAW-ISG-Lucia were obtained from Invivogen. HEK293T, A549, THF, and RAW264.7 cells were maintained in Dulbecco's modified Eagle's medium (DMEM) containing 10% fetal bovine serum (FBS), penicillin (100 U/ml), and streptomycin (100 U/ml) and were transduced with a lentivector containing the pGreenFire ISRE cassette. THP-1 and MM6 cells were maintained in RPMI 1640 medium supplemented with 10% FBS, penicillin (100 U/ml), streptomycin (100 U/ml), and HEPES (10 mM). THP-1 ISG-lucia cells were differentiated by 2 h of treatment with 100 ng/mL PMA, and then the PMA was removed and replaced with complete medium for 72 h of incubation prior to all assays. All cells were grown at 37°C and 5% CO_2. Sendai virus (SeV) was obtained from Charles River Laboratories and used at 160 hemagglutination units (HAU)/ml. Human cytomegalovirus was grown and titered as described (68) and exposed to cells at a multiplicity of infection (MOI) of 3 unless otherwise indicated. cGAMP was transfected into cells using Lipofectamine 3000 following the manufacturer's protocol.

CRISPR/Cas9-Mediated Genome Editing and Ectopic Gene Expression

Genome editing using lentivector-mediated delivery of CRISPR/Cas9 components was performed as described previously (17–19). Briefly, we used the lentiCRISPRv2 vector (a gift from Feng Zhang; Addgene plasmid # 52961) (69). STING-specific guide RNAs (gRNA) were cloned into this vector (mouse STING gRNA: AGTATGACCAGGCCAGCCCG; human STING gRNA: CCCGTGTCCCAGGGGTCACG) and was then used to transduce the appropriate cells, selected using puromycin, and knockout validated by immunoblot. Stable and transient expression of hSTING variants was done by cloning target ORFs into the pLVX-EIF1α vector. Cells were then transduced and selected for antibiotic resistance as described previously (70). Transient transfection of these vectors into HEK293T cells was done using Lipfectamine 3000 according to the manufacturer's protocol (Invitrogen).

Luciferase Reporter Assay and Type I Interferon Bioassays

For reporter assays cells (THF-ISRE, RAW264.7-ISG-Lucia, THP-1-ISG-Lucia) were plated in white 96-well plates 24 h before stimulation. Treatments were performed in quadruplicate in

50 μL of either DMEM or RPMI plus 2% FBS overnight unless otherwise indicated. Steady-Glo lysis/luciferin reagent (Promega) was added (1:1 [vol/vol]) to each well, and luminescence was measured on a Synergy plate reader (BioTek). For cell viability assays, CellTiter-Glo reagent was used following the manufacturer's suggested protocol. For type I IFN bioassays, cells of interest were plated at 50,000 cells/well in 24-well-plates and serum starved in X-Vivo15 medium for 1 h prior to treatment. After treatment for 24 h, the media was harvested and clarified at 10,000 x g for 3 min. Recombinant IFNβ (at 40, 20, 10, 5, 2.5, 1.25, and 0.63 U/ml) was used to generate a standard response curve. The supernatant or standard was then added to THF-ISRE-ΔIRF3 cells (do not respond to STING/IRF3-inducing stimuli) plated as described above for 8 h, and luminescence was measured. IFN was quantitated by curve fitting relative to the signals generated from the standards.

Immunoblotting

Sodium dodecyl sulfate-polyacrylamide gel electrophoresis (SDS-PAGE) and immunoblotting were performed as follows. After cell pelleting at 2,000 × g for 10 min, whole-cell lysates were harvested in RIPA lysis buffer (50 mM Tris-HCl [pH 8.0], 150 mM NaCl, 1% NP-40, 0.5% sodium deoxycholate, and 0.1% SDS) supplemented with Halt protease and phosphatase inhibitor cocktail (Thermo Fisher). Lysates were electrophoresed in 8% polyacrylamide gels and then transferred onto polyvinylidene difluoride (PVDF) membranes (Millipore) by semidry transfer at 15 V mA for 15 min. The blots were blocked at room temperature for 2 h or overnight, using 5% non-fat milk in PBS containing 0.1% Tween 20. The blots were exposed to primary antibody in 5% non-fat milk in PBS containing 0.1% Tween 20 for 18 h at 4°C. The blots were then washed in PBS containing 0.1% Tween 20 for 20, 15, and 5 min, followed by deionized water for 5 min. A 1-h exposure to horseradish peroxidase-conjugated secondary antibodies and subsequent washes were performed as described for the primary antibodies. Antibodies were visualized using enhanced chemiluminescence (Pierce).

Indirect Immunofluorescence Assay

For the indirect immunofluorescence assays (IFA), cells were grown on coverslips in 24-well-plates and treated as described above. At room temperature, cells were washed twice with PBS, fixed for 30 min in 3.7% formalin, washed, and quenched for 10 min using 50 mM NH_4Cl. Cells were permeabilized with 0.1% Triton X-100 for 7 min and washed three times with PBS containing 2% bovine serum albumin (BSA). Cells were incubated with primary antibody in PBS containing 2% BSA at 37°C for 1 h, washed three times in PBS containing 2% BSA (10 min for each wash), and incubated with fluorescently conjugated secondary antibody diluted 1:1,000 in PBS containing 2% BSA for 1 h. Cells were washed twice in PBS containing 2% BSA (10 min for each wash) and once in PBS. Coverslips were mounted on a microscope slide with Vectashield mounting medium (Vector Laboratories, Burlingame, CA) containing DAPI, and imaging was performed on an Evos cell-imaging system.

RNA Isolation and Semiquantitative Reverse Transcription-PCR

Total RNA was isolated from cells, treated with the DNase provided in a DNA-free RNA isolation kit (Zymo Research) according to the manufacturer's protocol, and quantified by UV spectrometry. Single-stranded cDNA for use as a PCR template was made from total RNA and random hexamers to prime first-strand synthesis via a RevertAid First Strand cDNA synthesis kit (Thermo Fisher). Comparison of mRNA expression levels between samples was performed using semiquantitative real-time reverse transcription-PCR (qPCR) with an Applied Biosystems sequence detection system according to the $\Delta\Delta C_T$ method (71), with GAPDH as a control. Prevalidated Prime-Time 6-carboxyfluorescein qPCR primer/probe sets obtained from IDT were used for all genes.

STING Protein Purification and Thermal Shift Assays

Assays of the molecular interaction between the purified human STING C-terminal domain (amino acids 137 to 379; non-transmembrane domain) and M04 were performed as previously reported (19). Briefly, the 6xHis STING CTD open reading frame was cloned into pRSET-B (Invitrogen) and used to transform the Escherichia coli strain pLysS (Promega). The transformed *E. coli* cells were then induced to express the protein as induced by 1 mM IPTG (isopropyl-D-thiogalactopyranoside) at 16°C for 18 h. STING protein was purified by nickel-affinity chromatography (Clontech Laboratories) and then further purified by gel filtration chromatography (HiPrep 16/60 Sephacryl S-100 HR column; GE Healthcare Life Sciences). Eluted proteins were concentrated using Amicon centrifugal filters (10-kDa cutoff). For thermal shift assays, SYPRO Orange dye was used, following the manufacturer's suggested protocol, to determine protein stability in the presence and absence of cGAMP (Invivogen) or M04.

Human Samples

Peripheral blood mononuclear cells (PBMCs) were collected and analyzed at two separate institutions for cytokine secretion measurements, maturation marker analysis, and cross-priming assays. All procedures were performed accordance with the Institutional Review Boards of the respective institutions (Drexel University College of Medicine, Earle A. Chiles Research Institute). Donor samples analyzed at Drexel University were obtained from Martin Health System (Stuart, Florida). The study was approved by the Institutional Review Board of Martin Health System and Drexel University College of Medicine (Philadelphia). All donors signed informed consent from all participants. Patients with locally advanced or borderline resectable pancreatic cancer enrolled on a clinical study (46) provided a pre-treatment blood sample. Studies were approved by the institutional review board at Providence Portland Medical Center, Portland OR with study ID numbers PHS 10-141B and PHS 13-026A. The clinical trial registration numbers are NCT01342224 and NCT01903083. All patients provided written informed consent for treatment and participation in these

studies, including analysis of serum and blood parameters over the course of the study.

Luminex Analysis

PBMCs were plated at 4×10^5 per well in 96-well-plates, stimulated with DMSO, M04 (50 μM), LPS (100 ng/mL), or cyclic-di-AMP (10 μg/mL) diluted in RPMI, and incubated at 37°C and 5% CO_2 for 24 h. Supernatants were then removed and used in a multiplex cytokine bead-based assay according to the manufacturer's protocol (BD Biosciences human inflammation cytokine bead array, catalog number 551,811, or BioLegend human IL-12p70 enzyme-linked immunosorbent assay [ELISA] Max).

Generation of Human Monocyte-Derived Dendritic Cells (mDCs)

Human PBMCs from healthy donors were obtained immediately after blood withdrawal using the Ficoll-Paque (GE Healthcare) gradient method and stored in liquid nitrogen until usage. Cells were thawed in RPMI 1640 (Corning) supplemented with 10% fetal bovine serum (Access Biologicals) and 1% penicillin/streptomycin (Gibco). $CD14^+$ $CD16^+$ monocytes were then enriched from total PBMCs by negative selection using the EasySep™ human monocyte enrichment kit without CD16 depletion (STEMCELL Technologies) according to the manufacturer's protocol and counted. Cells were then resuspended in serum-free CellGenix GMP dendritic cell medium (CellGenix) with 100 ng/ml of recombinant human GM-CSF (BioLegend) and 20 ng/ml of recombinant human IL-4 (Gemini Bio-Products) at a density of 2×10^6 per ml in 24-well plates. After 48 h of incubation, cells were stimulated with 0.5 ug/ml of LPS (Invivogen) plus 40 ng/ml of IFNγ (Gemini Bio-Products) in medium or with two concentrations 25 and 50uM of the STING agonist MO4 (source) in DMSO, and compared to the DMSO control. Dendritic cells were harvested after 24 h of stimulation, and analyzed by flow cytometry.

Flow Cytometric Analysis of Stimulated Human mDCs

Harvested mDCs were incubated with TruStain FcγR block (BioLegend) and fluorochrome-conjugated antibodies for 15–20 min on ice in the dark. The following BioLegend fluorochrome-conjugated anti-human antibodies were used: CD3 (clone HIT3α), CD19 (clone HIB19), CD14 (clone M5E2), CD11c (clone 3.9), HLA-DR (clone L243), CD86 (clone IT2.2), CD83 (clone HB15e), CD40 (clone 5C3), and CD80 (clone 2D10). Dead cells were identified using both LIVE/DEAD fixable Aqua Dead Cell Stain Kit for flow cytometry (Vivid) (Life Technologies) and Annexin V (BD Biosciences). mDC samples were washed then resuspended in PBS plus 2% FBS then acquired on a BD LSR II and analyzed with FlowJo software (Treestar). The gating strategy excluded doublet cells and mDCs were gated on live ($Vivid^-$ $Annexin\ V^-$) $CD3^-$ $CD19^-$ $CD11c^+$ cells.

Peptides

The HLA-A2-restricted Melan-A/ MART-1 modified peptide (ELAGIGILTV, residues 26-35_{A27L}) was used for *in vitro* priming and was obtained from Biosynthesis. The tetramer HLA-A*02:01- ELAGIGILTV (Melan-A/MART-1) was obtained from the NIH Tetramer Core Facility (Emory University).

In vitro Priming of Naive Melan-A/MART-1 Ag-Specific $CD8^+$ T Cells

Naïve $CD8^+$ T cells precursors for the Melan-A/MART-1 epitope ELA were primed *in vitro* using unfractionated PBMC protocol as described in [1] with minor modifications. Briefly, PBMC from HLA-$A2^+$ healthy donors were thawed and seeded at 5×10^6 cells/ml in CellGro® DC medium (CellGenix™), supplemented with human GM-CSF (100 ng/ml; MACS Miltenyi Biotec) and IL-4 (20 ng/ml; Gemini Bio-products) in a 24-well tissue culture plate. After 24 h, Melan-A/MART-1 antigen (at 10 μg/ml) was added, in presence of M04 (final 50 μM) or 2'3'cGamp (5 μg/ml, Invitrogen) to induce maturation of resident dendritic cells. Twenty-four hours later and every 3 days, half of the media was replaced by fresh RPMI 1640 (Corning) supplemented with 8% human serum (Atlanta Biologicals) and IL-2 (20 U/ml, Miltenyi Biotech). On day 11, the $CD8^+$ T cells frequency and were assessed by flow cytometry within the $CD3^+CD8^+$ T cell population using Melan-A –HLA-A2 tetramer staining after exclusion of dead cells.

In vivo Administration of M04

All animal procedures for *in vivo* administration of M04 were conducted in accordance with and approved by the Oregon Health and Science University Institutional Animal Care and Use Committee (IACUC) under protocol 0913. The Oregon Health and Science University IACUC adheres to the NIH Office of Laboratory Animal Welfare standards (OLAW welfare assurance A3304-1). C57BL/6J mice (5–7 weeks of age; Jackson Laboratories) were housed in cage units, fed *ad-libitum*, and cared for under USDA guidelines for laboratory animals. M04 at 25 mg/kg of body weight or DMXAA (or DMSO alone) was prepared in DMSO plus PBS to 200 μL and injected intraperitoneally. Animals were euthanized at 5 h post-injection by isoflurane overdose. Spleens were harvested, RNA isolated, and qPCR performed as described above.

RNA-seq

PBMCs from two healthy adult donors were obtained from StemCell Technologies, grown in 12 well-dishes in RPMI + 10% FBS, and treated in duplicate for 6 h with 1% DMSO vehicle, 50 μM M04, 100 ng/mL LPS, or 15 μg/mL cGAMP. Total RNA was isolated using Direct-zol RNA mini-prep kit (Zymo Research) in accordance with manufacturer's instructions and profiled for intactness on a Bioanalyzer (Agilent). Libraries were then prepared using the Tru-Seq RNA Sample Preparation kit (Illumina). Briefly, poly(A)+ RNA was isolated from 500 ng of total RNA per sample. The isolated RNA was fragmented using divalent cations and heat. First strand cDNA was generated using random hexamer priming. The RNA template was removed and the second strand was synthesized. The ends of the cDNAs were repaired, followed by adenylation of the 3′ termini. Indexing adapters were ligated to the cDNA ends. The ligation products were amplified using polymerase chain reaction (PCR).

The amplification product was cleaned using AMPure XP beads (Beckman Coulter). Libraries were profiled on the Tapestation 2200 (Agilent). The concentration of the libraries was determined using real time PCR on a StepOne or StepOnePlus Real Time PCR Workstation (Thermo) using a library quantification kit (Kapa Biosystems). Samples were mixed for multiplexing and run on a HiSeq 2500 (Illumina) using a 100 cycle single read protocol. Base call files were converted to fastq format using Bcl2fastq (Illumina).

Gene Expression and Transcription Factor Prediction Analysis

The quality of the raw sequencing files were first evaluated using FastQC combined with MultiQC (72) (http://multiqc.info/). The files were imported into the Oregon National Primate Center's DISCVR-Seq, LabKey (73) server-based system, PRIMe-Seq. Trimmomatic (74) was used to remove any remaining Illumina adapters. Reads were aligned to the Homo_sapiens.GRCh38 genome in Ensembl along with its corresponding annotation, release 84. The program STAR (v020201) (75) was used to align the reads to the genome. STAR has been shown to perform well-compared to other RNA-seq aligners (76). Two-pass mode was used with default parameters. Since STAR utilizes the gene annotation file, it calculated the number of reads aligned to each gene. RNA-SeQC (v1.1.8.1) (77) was utilized to ensure alignments were of sufficient quality. Samples had an average of 45 M mapped reads, an average exonic rate of 83%, and an average of 22 K genes detected (>5 reads) per sample. Gene-level raw counts were normalized using DEseq2 (78) which were then transformed using regularized log transformation (rlog) to stabilize variance in R. After data processing, gene-wise general linear models with compound symmetry covariance structure was used (to account for repeated response measures on the same subject) to identify differentially expressed genes in SAS9.4. We used criteria to designate genes as differentially regulated in each stimulus vs. control with fold change ≥ 2 (up or down) and raw $p < 0.05$. Transcription factor prediction analysis was performed by submitting all genes found to be significantly upregulated by M04 to the online tools PASTAA and RegulatorTail (48, 49) using default settings. Venn diagrams were made using BioVenn (79). Volcano plots were made using VolcanoNoseR (https://huygens.science.uva.nl/VolcaNoseR/).

DATA AVAILABILITY STATEMENT

The raw data supporting the conclusions of this article will be made available by the authors, without undue reservation. The transcriptomics data has been deposited in the Gene Expression Omnibs under accession Series (GSE152179).

ETHICS STATEMENT

The animal study was reviewed and approved by Oregon Health and Science University IACUC.

AUTHOR CONTRIBUTIONS

VD, MG, LT, AN, JB, JA, and BG: conceived of experiments. JA, SB, NM, KP, BG, DB, TS, HJ, JB, MC, and CS: performed experiments. JA, AN, MG, LT, EH, and VD: interpreted experiments. VD: wrote manuscript. All authors contributed to the article and approved the submitted version.

FUNDING

This work was supported by NIH AI143660, HHSN272201400055C, and AI109680.

SUPPLEMENTARY MATERIAL

The Supplementary Material for this article can be found online at: https://www.frontiersin.org/articles/10.3389/fimmu.2020.01430/full#supplementary-material

REFERENCES

1. Schoggins JW. Interferon-stimulated genes: what do they all do? *Annu Rev Virol.* (2019) 6:567–84. doi: 10.1146/annurev-virology-092818-015756
2. Schafer SL, Lin R, Moore PA, Hiscott J, Pitha PM. Regulation of type I interferon gene expression by interferon regulatory factor-3. *J Biol Chem.* (1998) 273:2714–20. doi: 10.1074/jbc.273.5.2714
3. Liu S, Cai X, Wu J, Cong Q, Chen X, Li T, et al. Phosphorylation of innate immune adaptor proteins MAVS, STING, and TRIF induces IRF3 activation. *Science.* (2015) 347:aaa2630. doi: 10.1126/science.aaa2630
4. Hu M-M, Shu H-B. Innate immune response to cytoplasmic DNA: mechanisms and diseases. *Annu Rev Immunol.* (2019) 38:79–98. doi: 10.1146/annurev-immunol-070119-115052
5. Sun L, Wu J, Du F, Chen X, Chen ZJ. Cyclic GMP-AMP synthase is a cytosolic DNA sensor that activates the type I interferon pathway. *Science.* (2013) 339:786–91. doi: 10.1126/science.1232458
6. Gao P, Ascano M, Wu Y, Barchet W, Gaffney BL, Zillinger T, et al. Cyclic [G(2',5')pA(3",5")p] is the metazoan second messenger produced by DNA-activated cyclic GMP-AMP synthase. *Cell.* (2013) 153:1094–107. doi: 10.1016/j.cell.2013.04.046
7. Diner EJ, Burdette DL, Wilson SC, Monroe KM, Kellenberger CA, Hyodo M, et al. The innate immune DNA sensor cGAS produces a noncanonical cyclic dinucleotide that activates human STING. *Cell Rep.* (2013) 3:1355–61. doi: 10.1016/j.celrep.2013.05.009
8. Fang R, Wang C, Jiang Q, Lv M, Gao P, Yu X, et al. NEMO-IKKβ are essential for IRF3 and NF-κB activation in the cGAS-STING pathway. *J Immunol.* (2017) 199:3222–33. doi: 10.4049/jimmunol.1700699
9. Chen H, Sun H, You F, Sun W, Zhou X, Chen L, et al. Activation of STAT6 by STING is critical for antiviral innate immunity. *Cell.* (2011) 147:436–46. doi: 10.1016/j.cell.2011.09.022
10. Ishikawa H, Ma Z, Barber GN. STING regulates intracellular DNA-mediated, type I interferon-dependent innate immunity. *Nature.* (2009) 461:788–92. doi: 10.1038/nature08476
11. Motwani M, Pesiridis S, Fitzgerald KA. DNA sensing by the cGAS–STING pathway in health and disease. *Nat Rev Genet.* (2019) 20:657–74. doi: 10.1038/s41576-019-0151-1
12. Zhu G, Xu Y, Cen X, Nandakumar KS, Liu S, Cheng K. Targeting pattern-recognition receptors to discover new small molecule immune modulators. *Eur J Med Chem.* (2018) 144:82–92. doi: 10.1016/j.ejmech.2017.12.026

13. Es-Saad S, Tremblay N, Baril M, Lamarre D. Regulators of innate immunity as novel targets for panviral therapeutics. *Curr Opin Virol.* (2012) 2:622–8. doi: 10.1016/j.coviro.2012.08.009
14. Bourquin C, Pommier A, Hotz C. Harnessing the immune system to fight cancer with Toll-like receptor and RIG-I-like receptor agonists. *Pharmacol Res*. (2019) 154:104192. doi: 10.1016/j.phrs.2019.03.001
15. Probst P, Grigg JB, Wang M, Muñoz E, Loo Y-M, Ireton RC, et al. A small-molecule IRF3 agonist functions as an influenza vaccine adjuvant by modulating the antiviral immune response. *Vaccine*. (2017) 35:1964–71. doi: 10.1016/j.vaccine.2017.01.053
16. Yi G, Brendel VP, Shu C, Li P, Palanathan S, Cheng Kao C. Single nucleotide polymorphisms of human STING can affect innate immune response to cyclic dinucleotides. *PLoS ONE*. (2013) 8:e77846. doi: 10.1371/journal.pone.0077846
17. Gall B, Pryke K, Abraham J, Mizuno N, Botto S, Sali TM, et al. Emerging alphaviruses are sensitive to cellular states induced by a novel small-molecule agonist of the STING pathway. *J Virol.* (2018) 92:e01913–17. doi: 10.1128/JVI.01913-17
18. Pryke KM, Abraham J, Sali TM, Gall BJ, Archer I, Liu A, et al. A novel agonist of the TRIF pathway induces a cellular state refractory to replication of zika, chikungunya, dengue viruses. *mBio.* (2017) 8:e00452–17. doi: 10.1128/mBio.00452-17
19. Sali TM, Pryke KM, Abraham J, Liu A, Archer I, Broeckel R, et al. Characterization of a novel human-specific STING agonist that elicits antiviral activity against emerging alphaviruses. *PLoS Pathog.* (2015) 11:e1005324. doi: 10.1371/journal.ppat.1005324
20. Ziegler-Heitbrock HW, Thiel E, Fütterer A, Herzog V, Wirtz A, Riethmüller G. Establishment of a human cell line (Mono Mac 6) with characteristics of mature monocytes. *Int J Cancer.* (1988) 41:456–61. doi: 10.1002/ijc.2910410324
21. Chebath J, Merlin G, Metz R, Benech P, Revel M. Interferon-induced 56,000 Mr protein and its mRNA in human cells: molecular cloning and partial sequence of the cDNA. *Nucleic Acids Res.* (1983) 11:1213–26. doi: 10.1093/nar/11.5.1213
22. Chin KC, Cresswell P. Viperin (cig5), an IFN-inducible antiviral protein directly induced by human cytomegalovirus. *Proc Natl Acad Sci USA*. (2001) 98:15125–30. doi: 10.1073/pnas.011593298
23. Sharma S, tenOever BR, Grandvaux N, Zhou G-P, Lin R, Hiscott J. Triggering the interferon antiviral response through an IKK-related pathway. *Science.* (2003) 300:1148–51. doi: 10.1126/science.1081315
24. Seth RB, Sun L, Ea C-K, Chen ZJ. Identification and characterization of MAVS, a mitochondrial antiviral signaling protein that activates NF-kappaB and IRF 3. *Cell.* (2005) 122:669–82. doi: 10.1016/j.cell.2005.08.012
25. Hiscott J. Convergence of the NF-kappaB and IRF pathways in the regulation of the innate antiviral response. *Cytokine Growth Factor Rev.* (2007) 18:483–90. doi: 10.1016/j.cytogfr.2007.06.002
26. Ramanjulu JM, Pesiridis GS, Yang J, Concha N, Singhaus R, Zhang S-Y, et al. Design of amidobenzimidazole STING receptor agonists with systemic activity. *Nature.* (2018) 564:439–43. doi: 10.1038/s41586-018-0705-y
27. Zhang X, Shi H, Wu J, Zhang X, Sun L, Chen C, et al. Cyclic GMP-AMP containing mixed phosphodiester linkages is an endogenous high-affinity ligand for STING. *Mol Cell.* (2013) 51:226–35. doi: 10.1016/j.molcel.2013.05.022
28. Ablasser A, Goldeck M, Cavlar T, Deimling T, Witte G, Röhl I, et al. cGAS produces a 2"-5-"linked cyclic dinucleotide second messenger that activates STING. *Nature.* (2013) 498:380–84. doi: 10.1038/nature12306
29. Sun W, Li Y, Chen L, Chen H, You F, Zhou X, et al. ERIS, an endoplasmic reticulum IFN stimulator, activates innate immune signaling through dimerization. *Proc Natl Acad Sci USA*. (2009) 106:8653–8. doi: 10.1073/pnas.0900850106
30. Zhong B, Yang Y, Li S, Wang Y-Y, Li Y, Diao F, et al. The adaptor protein MITA links virus-sensing receptors to IRF3 transcription factor activation. *Immunity.* (2008) 29:538–50. doi: 10.1016/j.immuni.2008.09.003
31. Ishikawa H, Barber GN. STING is an endoplasmic reticulum adaptor that facilitates innate immune signalling. *Nature.* (2008) 455:674–8. doi: 10.1038/nature07317
32. Wu J, Sun L, Chen X, Du F, Shi H, Chen C, et al. Cyclic GMP-AMP is an endogenous second messenger in innate immune signaling by cytosolic DNA. *Science.* (2013) 339:826–30. doi: 10.1126/science.1229963
33. Zhang Z, Yuan B, Bao M, Lu N, Kim T, Liu Y-J. The helicase DDX41 senses intracellular DNA mediated by the adaptor STING in dendritic cells. *Nat Immunol.* (2011) 12:959–65. doi: 10.1038/ni.2091
34. Unterholzner L, Keating SE, Baran M, Horan KA, Jensen SB, Sharma S, et al. IFI16 is an innate immune sensor for intracellular DNA. *Nat Immunol.* (2010) 11:1004. doi: 10.1038/ni.1932
35. Takaoka A, Wang Z, Choi MK, Yanai H, Negishi H, Ban T, et al. DAI (DLM-1/ZBP1) is a cytosolic DNA sensor and an activator of innate immune response. *Nature.* (2007) 448:501–5. doi: 10.1038/nature06013
36. Tanaka Y, Chen ZJ. STING specifies IRF3 phosphorylation by TBK1 in the cytosolic DNA signaling pathway. *Sci Signal.* (2012) 5:ra20. doi: 10.1126/scisignal.2002521
37. Saitoh T, Fujita N, Hayashi T, Takahara K, Satoh T, Lee H, et al. Atg9a controls dsDNA-driven dynamic translocation of STING and the innate immune response. *Proc Natl Acad Sci USA.* (2009) 106:20842–6. doi: 10.1073/pnas.0911267106
38. Niesen FH, Berglund H, Vedadi M. The use of differential scanning fluorimetry to detect ligand interactions that promote protein stability. *Nat Protoc.* (2007) 2:2212–21. doi: 10.1038/nprot.2007.321
39. Patel S, Jin L. TMEM173 variants and potential importance to human biology and disease. *Genes Immun.* (2019) 20:82–89. doi: 10.1038/s41435-018-0029-9
40. Sivick KE, Surh NH, Desbien AL, Grewal EP, Katibah GE, McWhirter SM, et al. Comment on "The common R71H-G230A-R293Q human TMEM173 is a null Allele". *J Immunol.* (2017) 198:4183–85. doi: 10.4049/jimmunol.1700294
41. Olagnier D, Brandtoft AM, Gunderstofte C, Villadsen NL, Krapp C, Thielke AL, et al. Nrf2 negatively regulates STING indicating a link between antiviral sensing and metabolic reprogramming. *Nat Commun.* (2018) 9:3506. doi: 10.1038/s41467-018-05861-7
42. Paijo J, Döring M, Spanier J, Grabski E, Nooruzzaman M, Schmidt T, et al. cGAS senses human cytomegalovirus and induces type I interferon responses in human monocyte-derived cells. *PLoS Pathog.* (2016) 12:e1005546. doi: 10.1371/journal.ppat.1005546
43. Conlon J, Burdette DL, Sharma S, Bhat N, Thompson M, Jiang Z, et al. Mouse, but not human STING, binds and signals in response to the vascular disrupting agent 5,6-dimethylxanthenone-4-acetic acid. *J Immunol.* (2013) 190:5216–25. doi: 10.4049/jimmunol.1300097
44. Gao P, Zillinger T, Wang W, Ascano M, Dai P, Hartmann G, et al. Binding-pocket and lid-region substitutions render human STING sensitive to the species-specific drug DMXAA. *Cell Rep.* (2014) 8:1668–76. doi: 10.1016/j.celrep.2014.08.010
45. Flood BA, Higgs EF, Li S, Luke JJ, Gajewski TF. STING pathway agonism as a cancer therapeutic. *Immunol Rev.* (2019) 290:24–38. doi: 10.1111/imr.12765
46. Crocenzi T, Cottam B, Newell P, Wolf RF, Hansen PD, Hammill C, et al. A hypofractionated radiation regimen avoids the lymphopenia associated with neoadjuvant chemoradiation therapy of borderline resectable and locally advanced pancreatic adenocarcinoma. *J Immuno Ther Cancer.* (2016) 4:45. doi: 10.1186/s40425-016-0149-6
47. Lissina A, Briceno O, Afonso G, Larsen M, Gostick E, Price DA, et al. Priming of qualitatively superior human effector CD8+ T cells using TLR8 ligand combined with FLT3 ligand. *J Immunol.* (2015) 196:256–63. doi: 10.4049/jimmunol.1501140
48. Roider HG, Manke T, O'Keeffe S, Vingron M, Haas SA. PASTAA: identifying transcription factors associated with sets of co-regulated genes. *Bioinformatics.* (2009) 25:435–42. doi: 10.1093/bioinformatics/btn627
49. Kehl T, Schneider L, Schmidt F, Stöckel D, Gerstner N, Backes C, et al. RegulatorTrail: a web service for the identification of key transcriptional regulators. *Nucleic Acids Res.* (2017) 45:W146–53. doi: 10.1093/nar/gkx350
50. Balka KR, Louis C, Saunders TL, Smith AM, Calleja DJ, D'Silva DB, et al. TBK1 and IKKε Act redundantly to mediate STING-induced NF-κB responses in myeloid cells. *Cell Rep.* (2020) 31:107492. doi: 10.1016/j.celrep.2020.03.056
51. Abe T, Barber GN. Cytosolic-DNA-mediated, STING-dependent proinflammatory gene induction necessitates canonical NF- B activation through TBK1. *J Virol.* (2014) 88:5328–41. doi: 10.1128/JVI.00037-14
52. Berger G, Marloye M, Lawler SE. Pharmacological modulation of the STING pathway for cancer immunotherapy. *Trends Mol Med*. (2019) 25:412–27. doi: 10.1016/j.molmed.2019.02.007

53. Libanova R, Becker PD, Guzmán CA. Cyclic di-nucleotides: new era for small molecules as adjuvants. *Microb Biotechnol.* (2012) 5:168–76. doi: 10.1111/j.1751-7915.2011.00306.x
54. Dubensky TW, Kanne DB, Leong ML. Rationale, progress and development of vaccines utilizing STING-activating cyclic dinucleotide adjuvants. *Ther Adv Vaccines.* (2013) 1:131–43. doi: 10.1177/2051013613501988
55. Corrales L, Glickman LH, McWhirter SM, Kanne DB, Sivick KE, Katibah GE, et al. Direct activation of STING in the tumor microenvironment leads to potent and systemic tumor regression and immunity. *Cell Rep*. (2015) 11:1018–30. doi: 10.1016/j.celrep.2015.04.031
56. Lipinski CA, Lombardo F, Dominy BW, Feeney PJ. Experimental and computational approaches to estimate solubility and permeability in drug discovery and development settings. *Adv Drug Deliv Rev.* (2001) 46:3–26. doi: 10.1016/S0169-409X(00)00129-0
57. Li L, Yin Q, Kuss P, Maliga Z, Millán JL, Wu H, et al. Hydrolysis of 2"3-"cGAMP by ENPP1 and design of nonhydrolyzable analogs. *Nat Chem Biol.* (2014) 10:1043–48. doi: 10.1038/nchembio.1661
58. Gao J, Tao J, Liang W, Zhao M, Du X, Cui S, et al. Identification and characterization of phosphodiesterases that specifically degrade 3"3-"cyclic GMP-AMP. *Cell Res.* (2015) 25:539–50. doi: 10.1038/cr.2015.40
59. Torchilin VP. Recent approaches to intracellular delivery of drugs and DNA and organelle targeting. *Annu Rev Biomed Eng.* (2006) 8:343–75. doi: 10.1146/annurev.bioeng.8.061505.095735
60. Koshy ST, Cheung AS, Gu L, Graveline AR, Mooney DJ. Liposomal delivery enhances immune activation by STING agonists for cancer immunotherapy. *Adv Biosyst*. (2017) 1:1600013. doi: 10.1002/adbi.201600013
61. Lemos H, Huang L, Chandler PR, Mohamed E, Souza GR, Li L, et al. Activation of the STING adaptor attenuates experimental autoimmune encephalitis. *J Immunol.* (2014) 192:5571–8. doi: 10.4049/jimmunol.1303258
62. Huang L, Li L, Lemos H, Chandler PR, Pacholczyk G, Baban B, et al. Cutting edge: DNA sensing via the STING adaptor in myeloid dendritic cells induces potent tolerogenic responses. *J Immunol.* (2013) 191:3509–13. doi: 10.4049/jimmunol.1301419
63. Lirussi D, Ebensen T, Schulze K, Trittel S, Duran V, Liebich I, et al. Type I IFN and not TNF, is essential for cyclic Di-nucleotide-elicited CTL by a cytosolic cross-presentation pathway. *EBIOM.* (2017) 22:100–11. doi: 10.1016/j.ebiom.2017.07.016
64. Karaolis DKR, Means TK, Yang D, Takahashi M, Yoshimura T, Muraille E, et al. Bacterial c-di-GMP is an immunostimulatory molecule. *J Immunol.* (2007) 178:2171–81. doi: 10.4049/jimmunol.178.4.2171
65. Borriello F, Pietrasanta C, Lai JCY, Walsh LM, Sharma P, O'Driscoll DN, et al. Identification and characterization of stimulator of interferon genes as a robust adjuvant target for early life immunization. *Front Immunol.* (2017) 8:1772. doi: 10.3389/fimmu.2017.01772
66. Kis-Toth K, Szanto A, Thai T-H, Tsokos GC. Cytosolic DNA-activated human dendritic cells are potent activators of the adaptive immune response. *J Immunol.* (2011) 187:1222–34. doi: 10.4049/jimmunol.1100469
67. Zhang X, Liu B, Tang L, Su Q, Hwang N, Sehgal M, et al. Discovery and mechanistic study of a novel human-stimulator-of-interferon-genes agonist. *ACS Infect Dis*. (2019) 5:1139–49. doi: 10.1021/acsinfecdis.9b00010
68. Defilippis VR, Sali T, Alvarado D, White L, Bresnahan W, Früh KJ. Activation of the interferon response by human cytomegalovirus occurs via cytoplasmic double-stranded DNA but not glycoprotein B. *J Virol.* (2010) 84:8913–25. doi: 10.1128/JVI.00169-10
69. Sanjana NE, Shalem O, Zhang F. Improved vectors and genome-wide libraries for CRISPR screening. *Nat Meth.* (2014) 11:783–84. doi: 10.1038/nmeth.3047
70. Botto S, Abraham J, Mizuno N, Pryke K, Gall B, Landais I, et al. Human Cytomegalovirus immediate early 86-kDa protein blocks transcription and induces degradation of the immature interleukin-1β protein during virion-mediated activation of the AIM2 inflammasome. *mBio.* (2019) 10:257. doi: 10.1128/mBio.02510-18
71. Livak KJ, Schmittgen TD. Analysis of relative gene expression data using real-time quantitative PCR and the $2^{-\Delta\Delta}C_T$) method. *Methods.* (2001) 25:402–8. doi: 10.1006/meth.2001.1262
72. Ewels P, Magnusson M, Lundin S, Käller M. MultiQC: summarize analysis results for multiple tools and samples in a single report. *Bioinformatics*. (2016) 32:3047–8. doi: 10.1093/bioinformatics/btw354
73. Nelson EK, Piehler B, Eckels J, Rauch A, Bellew M, Hussey P, et al. LabKey server: an open source platform for scientific data integration, analysis and collaboration. *BMC Bioinformatics.* (2011) 12:71. doi: 10.1186/1471-2105-12-71
74. Bolger AM, Lohse M, Usadel B. Trimmomatic: a flexible trimmer for Illumina sequence data. *Bioinformatics.* (2014) 30:2114–20. doi: 10.1093/bioinformatics/btu170
75. Dobin A, Davis CA, Schlesinger F, Drenkow J, Zaleski C, Jha S, et al. STAR: ultrafast universal RNA-seq aligner. *Bioinformatics.* (2012) 29:15–21. doi: 10.1093/bioinformatics/bts635
76. Engström PG, Steijger T, Sipos B, Grant GR, Kahles A, Rätsch G, et al. Systematic evaluation of spliced alignment programs for RNA-seq data. *Nat Meth.* (2013) 10:1185–91. doi: 10.1038/nmeth.2722
77. DeLuca DS, Levin JZ, Sivachenko A, Fennell T, Nazaire M-D, Williams C, et al. RNA-SeQC: RNA-seq metrics for quality control and process optimization. *Bioinformatics.* (2012) 28:1530–32. doi: 10.1093/bioinformatics/bts196
78. Love MI, Huber W, Anders S. Moderated estimation of fold change and dispersion for RNA-seq data with DESeq2. *Genome Biol.* (2014) 15:550. doi: 10.1186/s13059-014-0550-8
79. Hulsen T, de Vlieg J, Alkema W. BioVenn - a web application for the comparison and visualization of biological lists using area-proportional Venn diagrams. *BMC Genomics*. (2008) 9:488. doi: 10.1186/1471-2164-9-488

Disclaimer: The views expressed are those of the authors and should not be construed to represent the positions of the U.S. Army, the Department of Defense, the National Institutes of Health, the Department of Health and Human Services, or HJF. The investigators have adhered to the policies for protection of human subjects as prescribed in AR-70.

Conflict of Interest: The authors declare that the research was conducted in the absence of any commercial or financial relationships that could be construed as a potential conflict of interest.

frontiers in Immunology

ORIGINAL RESEARCH
published: 14 August 2020
doi: 10.3389/fimmu.2020.01669

Porcine IFI16 Negatively Regulates cGAS Signaling Through the Restriction of DNA Binding and Stimulation

Wanglong Zheng[1,2,3,4†], *Rongyun Zhou*[1,2,3,4†], *Shuangjie Li*[1,2,3,4], *Shan He*[1,2,3,4], *Jia Luo*[1,2,3,4], *Meiqin Zhu*[1,2,3,4], *Nanhua Chen*[1,2,3,4], *Hongjun Chen*[5], *François Meurens*[6] and *Jianzhong Zhu*[1,2,3,4*‡]

[1] Comparative Medicine Research Institute, Yangzhou University, Yangzhou, China, [2] College Veterinary Medicine, Yangzhou University, Yangzhou, China, [3] Jiangsu Co-innovation Center for Prevention and Control of Important Animal Infectious Diseases and Zoonoses, Yangzhou, China, [4] Joint International Research Laboratory of Agriculture and Agri-Product Safety, Yangzhou, China, [5] Shanghai Veterinary Research Institute, Chinese Academy of Agriculture Sciences, Shanghai, China, [6] BIOEPAR, INRAE, Oniris, Nantes, France

The innate immunity DNA sensors have drawn much attention due to their significant importance against the infections with DNA viruses and intracellular bacteria. Among the multiple DNA sensors, IFI16, and cGAS are the two major ones, subjected to extensive studies. However, these two DNA sensors in livestock animals have not been well defined. Here, we studied the porcine IFI16 and cGAS, and their mutual relationship. We found that both enable STING-dependent signaling to downstream IFN upon DNA transfection and HSV-1 infection, and cGAS plays a major role in DNA signaling. In terms of their relationship, IFI16 appeared to interfere with cGAS signaling as deduced from both transfected and knockout cells. Mechanistically, IFI16 competitively binds with agonist DNA and signaling adaptor STING and thereby influences second messenger cGAMP production and downstream gene transcription. Furthermore, the HIN2 domain of porcine IFI16 harbored most of its activity and mediated cGAS inhibition. Thus, this study provides a unique insight into the porcine DNA sensing system.

Keywords: innate immunity, DNA sensor, signaling, porcine, mutual relationship

OPEN ACCESS

Edited by:
Leon Grayfer, George Washington University, United States

Reviewed by:
Sabine Hammer, University of Veterinary Medicine Vienna, Austria
Chunfu Zheng, Fujian Medical University, China

***Correspondence:**
Jianzhong Zhu
jzzhu@yzu.edu.cn

[†] These authors have contributed equally to this work

[‡] ORCID:
Jianzhong Zhu
orcid.org/0000-0002-7082-1993

Specialty section:
This article was submitted to Comparative Immunology, a section of the journal Frontiers in Immunology

Received: *14 March 2020*
Accepted: *22 June 2020*
Published: *14 August 2020*

Citation:
Zheng W, Zhou R, Li S, He S, Luo J, Zhu M, Chen N, Chen H, Meurens F and Zhu J (2020) Porcine IFI16 Negatively Regulates cGAS Signaling Through the Restriction of DNA Binding and Stimulation. Front. Immunol. 11:1669. doi: 10.3389/fimmu.2020.01669

INTRODUCTION

The innate immune system acts as the first line of host defense and senses multiple danger signals from pathogens by recognizing the pathogen-associated molecular patterns (PAMPs) (1). It also detects damage-associated molecular patterns (DAMPs) to maintain homeostasis (1, 2). The PAMPs and DAMPs are both recognized by innate immune pattern recognition receptors (PRRs), which include Toll-like receptors (TLRs), RIG-I-like receptors (RLRs), NOD-like receptors (NLRs), C-type lectin like receptors (CLRs), and cytosolic DNA receptors (CDRs). Upon activation, the PRRs trigger intracellular signaling to initiate either gene transcription or protease-dependent cytokine secretion, resulting in the production of anti-viral interferons (IFNs), proinflammatory cytokines, and chemokines to directly combat pathogens and shape subsequent adaptive immunity.

The DNA sensors consist of a broad range of receptors, including membrane-bound TLR9 and various CDRs. TLR9 was the first identified DNA sensor localized in the ER/endosome. It

recognizes endolysosomal under-methylated CpG DNA to activate transcription factors IRF7 and NF-κB and stimulate type I IFN production (3). TLR9 expression is immune cell specific, mainly expressed in plasmacytoid dendritic cells (pDCs) and B cells. Two CDRs, DExD/H-box helicases DHX36 and DHX9, are required in pDCs for TLR9-dependent IFNα and TNF-α productions, respectively, thus possible accessory receptors for TLR9 (4, 5). In addition to DHX36 and DHX9, CDRs include also DAI, AIM2, RNA Pol III, LRRFIP1, IFI16, DDX41, DNA-PK, MRE11, cGAS, and STING (5).

DAI (or ZBP-1) was the first discovered CDR, able to induce IFNs through IRF3 and NF-κB activations (6). However, DAI knockout mice demonstrated normal DNA-mediated cytokine production; thus, the role of DAI as a DNA sensor has been controversial and it also indicated the existence of other CDRs (7). AIM2 belongs to PYHIN family proteins containing Pyrin and HIN domains. It binds viral double-stranded (ds) DNA using the C-terminal HIN domains to subsequently recruit downstream adaptor ASC via its N-terminal Pyrin domain through homotypic interaction. Further, ASC is able to recruit and activate caspase-1 by a homotypic CARD domain interaction to formulate inflammasome. In turn, caspase-1 causes proteolytic cleavage and maturation of the proinflammatory cytokines IL1β and IL18 (5, 8, 9). RNA polymerase III (Pol III) was described as a DNA sensor because of the transcription of AT-rich dsDNA, such as poly (dA:dT), into 5-triphosphate RNA, which can then activate RIG-I leading to IFNβ induction (10, 11). LRRFIP1 was reported to bind both dsDNA and dsRNA, and then interact with and activate β-catenin, which increases IFNβ expression as a co-activator by binding with IRF3 and recruiting the acetyltransferase p300 to the IFNβ enhanceosome (12). DDX41, an additional DExD/H-box helicase, was shown to bind with DNA and activate STING/TBK1-dependent IRF3 and NF-κB, and subsequent cytokine production (13). Besides dsDNA from transfection and virus infection, DDX41 was further reported to bind with bacterial cyclic dinucleotides (CDNs), cyclic-di-GMP, and cyclic di-AMP to activate similar downstream signaling (14). DNA-PK and MRE11 are both nuclear DNA damage sensor proteins, with the former comprising heterocomplex of Ku70, Ku80, and the catalytic subunit DNA-PKcs. Both protein complexes in cytosol were reported to be involved in DNA sensing and trigger STING-dependent cytokine production (15, 16).

STING (also called MITA, MPYS, and ERIS) was discovered in 2008 by several groups independently (17–20). STING acts as the signaling adaptor for DNA sensing pathways even though there are reports of its direct DNA sensing (21). Furthermore, STING also directly recognizes CDNs such as bacterial c-di-GMP and mammalian second messenger cGAMP to induce a type I IFN response (22, 23). IFI16 was the first reported STING-dependent DNA sensor in 2010 and is also a PYHIN family protein mediating IFN induction (24). IFI16 at steady state is present in the cell nucleus, but also shuttles between nucleus and cytosol depending on the acetylation status of its nuclear localization sequence (25). Moreover, nuclear IFI16 also engages in inflammasome formation (26), but the mechanisms by which IFI16 initiates signal to both STING and inflammasome are still unknown (5). cGAS was identified in 2013 as a cytosolic DNA sensor; upon DNA stimulation, it utilized substrates ATP and GTP to synthesize second messenger 2′5′-cGAMP, which directly activates STING signaling (27). Since its discovery, the cGAS-cGAMP-STING pathway has been subjected to extensive studies (28).

IFI16 and cGAS are the most extensively studied and best-characterized DNA sensors. However, these two DNA sensors are not well defined in livestock animals. In this study, we investigated porcine DNA sensors IFI16 and cGAS. Our study found that both porcine DNA sensors trigger STING-dependent signaling, and IFI16 negatively regulates cGAS signaling to IFN mainly through competitive binding to agonist DNA and adaptor STING.

MATERIALS AND METHODS

Cells and Reagents

HEK-293T and porcine kidney-15 (PK15) cells were cultured in Dulbecco's modified Eagle medium (DMEM, Hyclone Laboratories, USA) containing 10% fetal bovine serum (FBS) and 100 IU/ml of penicillin plus 100 μg/ml streptomycin. Porcine alveolar macrophages (PAMs) were cultured in Roswell Park Memorial Institute 1640 (RPMI, Hyclone) containing 10% FBS with penicillin/streptomycin. All cells were maintained at 37°C with 5% CO_2 in a humidified incubator. Restriction endonucleases, Phusion Hot Start High Fidelity DNA polymerase (M0203S), and T4 DNA ligase (M0203S) were all purchased from New England Biolabs (Beijing, China). Gateway™ LR Clonase™ II Enzyme mix, Lipofectamine™ 2000, and Goat Anti-Mouse IgG (H+L) Antibody DyLight 488 were from ThermoFisher Scientific (Shanghai, China). Pro Ligation-Free Cloning Kit (Cat No: E086/E087) was from Applied Biological Materials Inc. (Richmond, Canada). TRIpure Reagent for RNA extraction was from Aidlab (Beijing, China). EasyScript Reverse Transcriptase, 2×EasyTag PCR SuperMix, BluePlus Protein Marker, anti-HA mAb, anti-FLAG mAb, anti-GFP mAb, anti-Actin mAb, HRP anti-mouse IgG, HRP anti-rabbit IgG, and TransDetect Double-Luciferase Reporter Assay Kit were bought from Transgen Biotech (Beijing, China). The anti-HA rabbit pAb and anti-FLAG rabbit pAb were from Sangon Biotech (Shanghai, China). The anti-p-TBK1 (D52C2) and anti-p-IRF3 (4D4G) were from Cell Signaling Technology (Danvers, MA, US). Phanta Max Super-Fidelity DNA Polymerase, PCR Purification Kit, Gel Extraction Kit, Plasmid Mini-prep Kit were from Vazyme Biotech Co., Ltd. (Nanjing, China). Forty-five-base pair (45-bp) dsDNA (TACAGATCTACTAGTGATCTAT-GACTGATCTGTACATGATCTACA) as a DNA agonist was synthesized by GENEWIZ (Shouzhou, China). HSV-1 (KOS strain, whose VP26 was fused with GFP) was a gift from Dr.

Tony Wang in SRI International USA. The second messenger or STING agonist 2′3′-cGAMP was bought from InvivoGen (Hong Kong, China).

Molecular Cloning and Gene Mutations

Total RNA was extracted from primary PAMs using TRIzol® reagent (ThermoFisher Scientific). From the total RNA, porcine cGAS (XM_013985148) and IFI16 (XM_013996900) open reading frames (ORFs) were amplified by RT-PCR using the designed primers shown in **Supplementary Table 1**. The PCR products were digested with *Nco*I/*EcoR*V and *Sal*I/*EcoR*V, respectively, and cloned into the corresponding sites of the Gateway entry vector pENTR4-2HA, which was adapted from pENTR4 (Addgene) by inserting a 2HA sequence behind *EcoR*V to express C-terminal HA tagged genes. The sequence confirmed that HA-tagged pcGAS and pIFI16 were transferred from pENTR4 vectors to Destination vectors pDEST47 (Addgene) by LR recombination to obtain the final pcDNA recombinant expression vectors. If not specifically mentioned, cGAS and IFI16 in this paper refer to porcine cGAS and porcine IFI16, respectively.

For IFI16 subcloning and mutations, the Pyrin1, HIN1, Pyrin2, HIN2, ΔPyrin1, and ΔHIN2 fragments were amplified by PCR using Phanta Max Super-Fidelity DNA Polymerase from IFI16 plasmid template using the designed primer pairs shown in **Supplementary Table 1**. For IFI16 deletion mutants ΔHIN1 and ΔPyrin 2, the two fragments flanking the deletion site were amplified by PCR from IFI16 plasmid; next, the two flanking fragments together with the Bridge fragment were joined together by the fusion PCR. The Pyrin1, HIN1, Pyrin2, and HIN2 domain fragments were digested with *Nhe*I and *EcoR*V and cloned into pcDNA3.1 vector expressing C-terminal 2HA as we described previously (29), whereas the deletion fragments ΔPyrin1, ΔHIN1, ΔPyrin 2, and ΔHIN2 were cloned into the same sites of the above pcDNA3.1-2HA vector using the Pro Ligation-Free Cloning Kit.

CRISPR gRNA Design, gRNA Expressing Lentiviruses, and Stable KO Cells

The CRISPR gRNAs targeting porcine cGAS and IFI16 were designed using the web tool from Benchling (www.benchling.com). For porcine cGAS and IFI16, three gRNAs were chosen based on the predicted high scores, respectively, and the encoding DNA sequences are shown in **Supplementary Table 2**. The annealed gRNA encoding DNA pairs were ligated with *BsmB1*-digested lentiCRISPRv2 vector (Addgene), and the efficacy and specificity of these gRNA expressing lentiviral vectors targeting porcine cGAS and IFI16 were demonstrated as shown in **Supplementary Figures 2, 3**. The gRNA expressing lentiviruses were generated by co-transfecting lentiCRISPRv2-gRNAs with package plasmids psPAX2 and pMD2.G into 293T cells using Lipofectamine 2000. The supernatants containing three gRNA expressing lentiviruses were mixed equally and used to infect the PK15 cells and PAMs, respectively. Then, the infected PK15 cells were selected with 1.5 μg/ml puromycin, whereas infected PAMs were selected with 1 μg/ml puromycin. After puromycin selection, the CRISPR vector control, pcGAS KO, IFI16 KO stable PAMs, and CRISPR vector control, cGAS KO, and IFI16 KO stable PK15 cells were all prepared and ready for use.

DsDNA Binding Assay and Co-immunoprecipitation

The 5′-biotin-labeled 45-bp dsDNA was also synthesized and obtained from GENEWIZ (Shouzhou, China). Streptavidin Agarose (Cat No: S951, ThermoFisher Scientific) was washed three to five times with PBS by centrifugation at 10,000 *g* and suspended in PBS. Each milliliter of streptavidin agarose was mixed with 20 nmol 5′-biotin-labeled 45-bp dsDNA, incubated at RT for 30 min, and washed three to five times with PBS, and the resultant 45-bp dsDNA-agarose was stored at 4°C for protein pull-down assay. For protein pull-down assay, cells in a six-well plate (8×10^5 cells/well) were transfected for 48 h, harvested, and lysed in 500μl of RIPA buffer (50 mM Tris, pH 7.2, 150 mM NaCl, 1% sodium deoxycholate, and 1% Triton X-100) containing protease inhibitors on ice for 30 min. The 50 μl of cleared lysate was used as input control, and the remainder was incubated with 20 μl of dsDNA-agarose at 4°C overnight with shaking. Next day, the dsDNA agarose was washed three times by centrifugation, and bound proteins were eluted with 20 μl of 2×SDS sample buffer by heating at 100°C for 10 min. The elution supernatants from centrifugation together with input controls were subjected to Western blot analysis. For co-immunoprecipitation, the cleared cell lysate from transfected cells was incubated with 1 μg of specific antibody at 4°C overnight with shaking and further incubated with Protein A/G PLUS-Agarose (sc-2003, Santa Cruz Biotechnology) for 2–3 h. The agarose was similarly washed and eluted with 20 μl of 2×SDS sample buffer. The elution and input were both subjected to Western blot analysis.

Western Blot Analysis

Cell lysates or precipitated samples were resolved on 10% SDS-polyacrylamide gels in the presence of 2-mercaptoethanol. The protein bands on gels were transferred onto PVDF membranes and the membranes were blocked with 5% non-fat dry milk Tris-buffered saline, pH 7.4, with 0.1% Tween-20 (TBST), incubated with various primary antibodies. After washing with TBST, the membranes were incubated with HRP-conjugated goat anti-mouse IgG or goat anti-rabbit IgG (1:10,000 dilutions). The bound secondary antibody signals were detected with enhanced chemiluminescence (ECL) substrate (Tanon, China) and visualized by Western blot imaging system (Tanon, China).

Fluorescence Microscopy

PAMs grown on coverslips in 24-well culture plate (1×10^5 cells/well) or 293T cells grown on coverslips in 12-well plates (4×10^5 cells) were transfected with pcGAS-HA, pIFI16-HA, and GFP-pSTING plasmids, respectively, using Lipofectamine 2000. Forty-eight hours later, the transfected pcGAS and pIFI16 cells on coverslips were fixed with 4% paraformaldehyde at RT for 15 min and permeabilized with 0.5% Triton X for 10 min. After washing with PBS, the

cells were sequentially incubated with primary anti-HA mAb (1:500) and goat anti-mouse IgG (H+L) DyLight 488 second antibody (1:200). The stained cells and fixed GFP-pSTING cells were counterstained with 0.5 μg/ml 4′,6-diamidino-2-phenylindole (DAPI, Beyotime, China) at 37°C for 15 min to stain the cell nucleus and the coverslips sealed with nail polish. Lastly, the 293T cells were visualized under fluorescence microscope (Olympus, Japan) and the PAMs were observed under laser-scanning confocal microscope (LSCM, Leica SP8, Solms, Germany) at the excitation wavelengths 340 and 488 nm, respectively.

Promoter-Driven Luciferase Reporter Gene Assays

293T cells grown in 96-well plates (3×10^4 cells/well) were co-transfected by Lipofectamine 2000 with ISRE-luciferase reporter or ELAM (NF-κB)-firefly luciferase (Fluc) reporter (10 ng/well) and β-actin *Renilla* luciferase (Rluc) reporter (0.2 ng/well), together with the indicated plasmids or vector control (5–40 ng/well). The total DNA per well was normalized to 50 ng by adding empty vector. About 36 h post-transfection, the cells were harvested and lysed, and both Fluc and Rluc activities were sequentially measured using the TransDetect Double-Luciferase Reporter Assay Kit. The results were expressed as fold induction of ISRE or ELAM (NF-κB)-Fluc compared with that of vector control after Fluc normalization by corresponding Rluc.

RT-PCR and Quantitative RT-PCR

293T, PAMs, or PK15 cells grown in 24-well plates (3×10^5 cells) were subjected to different treatments. The treated cells were harvested and RNA extracted with TRIpure Reagent. The extracted RNA was reverse transcribed into cDNA with EasyScript Reverse Transcriptase, and then the target gene expressions were measured by PCR or quantitative PCR with 2×EasyTag PCR SuperMix by using StepOnePlus equipment (Applied Biosystems). The PCR program is denaturation at 94°C for 30 s followed by 25 cycles of 94°C for 5 s, 60°C for 30 s, and 72°C for 30 s, whereas the qPCR program is denaturation at 94°C for 30 s followed by 40 cycles of 94°C for 5 s and 60°C for 30 s. The PCR primers for hIFN-β, hISG56, hIL8, hRPL32, pIFNβ, pISG56, pISG60, pIL-8, and pβ-actin are shown in **Supplementary Table 3**. The PCR products were analyzed by agarose gel electrophoresis and visualized by imaging, whereas in qPCR, the transcriptional levels of IFN-β, ISG56, ISG60, and IL-8 were calculated using $\Delta\Delta C_T$ method.

Statistical Analysis

All the experiments are representative of three similar experiments and the representative experimental data in graphs were shown as the mean ± SD of duplicate wells. The statistical analysis was performed with the Student *t*-test or one-way ANOVA where appropriate, which are built within the software GraphPad Prism 5.0.

RESULTS

Characterization of Porcine cGAS and IFI16 Signaling Activity

The porcine cGAS has an amino acid (AA) sequence identity of 75.13% to human cGAS, while porcine IFI16 has only 45.61% identity of AA to human IFI16. Considering the low sequence identities of the two receptors between porcine and human, it is important to investigate the signaling

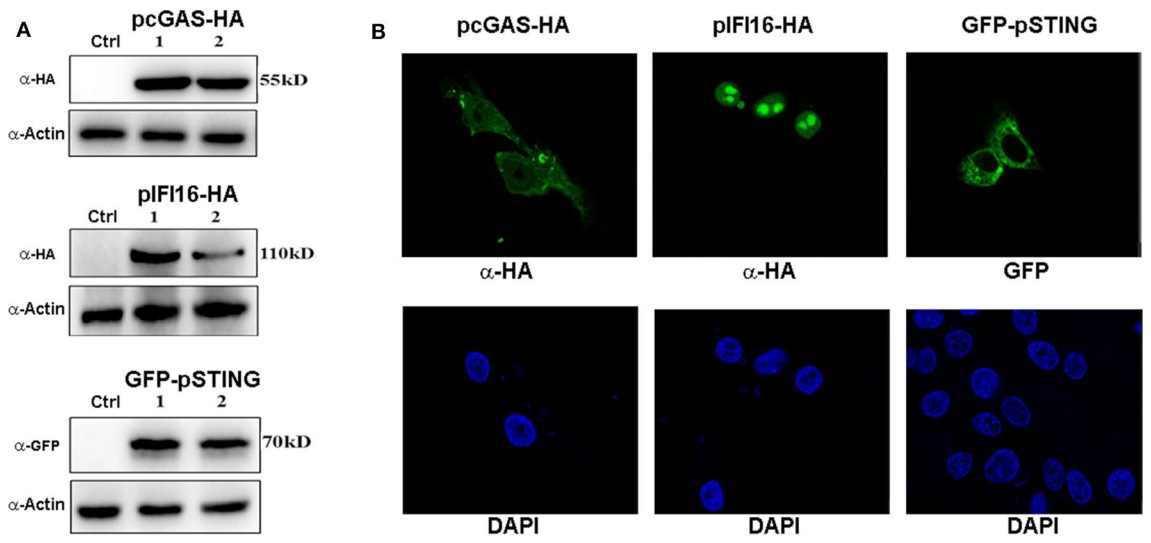

FIGURE 1 | The expressions of porcine DNA sensors cGAS, IFI16, and STING. **(A)** The pcDNA-cGAS, pcDNA-IFI16, pEGFP-STING, and control plasmids (0.5 μg each) were transfected into 293T cells (4×10^5 cells/well in a 24-well plate) using the Lipofectamine 2000. Forty-eight hours post-transfection, the protein expressions were detected by Western blotting with the indicated antibodies. Numbers 1 and 2 denote the two expression clones. **(B)** PAMs on coverslips in a 24-well plate (1×10^5 cells/well) were transfected with pcDNA-cGAS, pcDNA-IFI16, and pEGFP-STING as in **(A)**, and the fixed and stained PAMs were examined by confocal microscopy.

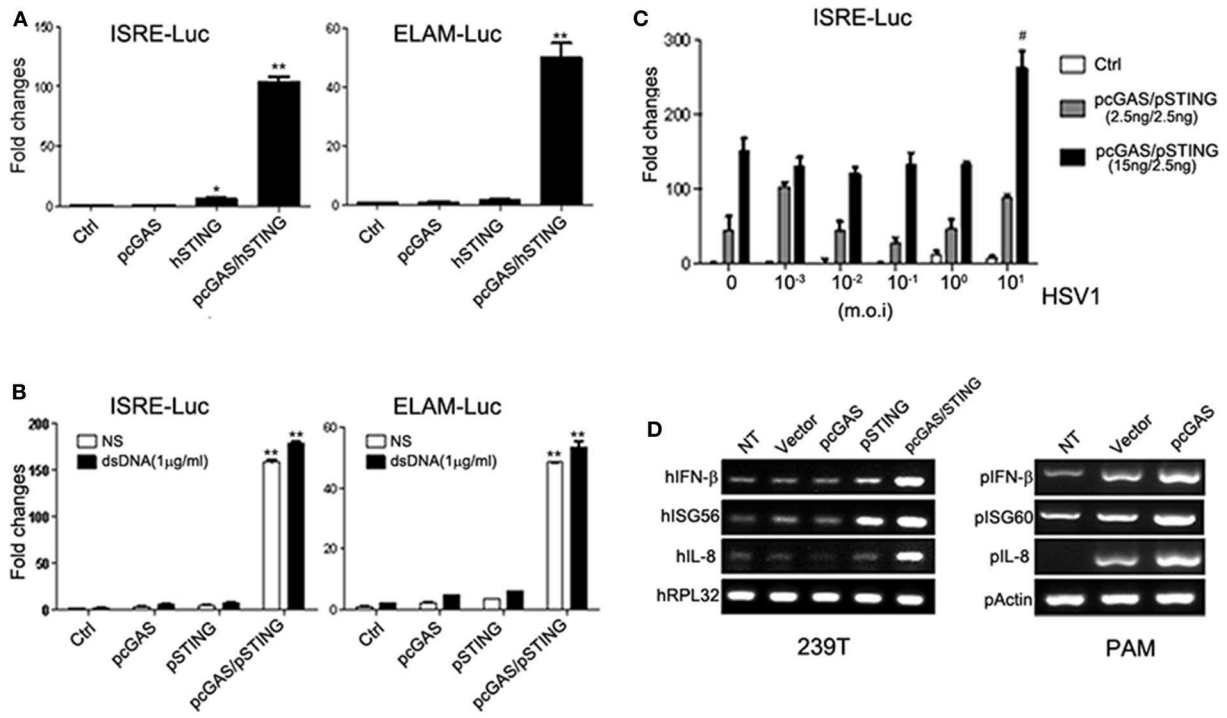

FIGURE 2 | Characterization of porcine DNA sensor cGAS. **(A)** 293T cells grown in 96-well plates were transfected with pcGAS (20 ng), hSTING (10 ng) plus ISRE-Fluc/ELAM-Fluc (10 ng), and Rluc (0.2 ng), which was normalized to 50 ng/well. Twenty-four hours post-transfection, the luciferase activities were measured with Double-Luciferase Reporter Assay. **(B)** 293T cells were transfected as in **(A)** with pSTING replacing hSTING, and 24 h later were mock stimulated (NS) or stimulated with dsDNA by transfection. Twelve hours post-stimulation, the luciferase activities were measured. **(C)** 293T cells were transfected as indicated, and 24 h later stimulated with HSV-1. Twelve hours post-stimulation, luciferase activities were measured. **(D)** 293T cells and PAM grown in 24-well plates were not transfected (NT) or transfected with 0.5 μg each recombinant plasmid and 24 h later the downstream gene transcription was examined by RT-PCR. $^{*}p < 0.05$, $^{**}p < 0.01$ vs. controls. $\#p < 0.05$ vs. non-HSV-1 stimulation.

functions of the two porcine receptors especially porcine IFI16. To study the signaling functions of the two porcine DNA receptors, the porcine cGAS and IFI16 gene cDNAs were amplified and both cloned into the Gateway pENTR4-2HA vector. Following sequence confirmation, cDNAs were further transferred into destination pcDNA expression vectors by LR reaction. The pcDNA expression constructs of porcine cGAS and IFI16 were transfected into 293T cells and PAMs, and their expressions were examined by Western blotting and IFA using the anti-HA antibody. As shown in **Figure 1** and **Supplementary Figure 1**, the porcine cGAS was expressed as a 55-kD protein, mainly localized in the cytoplasm similar to previously reported (27, 30). Conversely, the porcine IFI16 was expressed predominantly in cell nucleus, as a 110-kD protein. We also examined the expression of signaling adaptor porcine STING we previously cloned in pEGFP-C1 vector, and the GFP-STING fusion protein with M.W. of 70 kD was localized in the cytoplasm.

The signaling function of porcine cGAS was first examined together with the functionally known human adaptor STING. Porcine cGAS alone did not show any activity in either ISRE promoter or ELAM (NF-κB) promoter assay whereas human STING alone had weak ISRE activity. When porcine cGAS was transfected together with human STING, it showed strong activity in both ISRE and NF-κB promoter assays (**Figure 2A**). Next, the porcine cGAS was tested with porcine STING, which gave similar results (**Figure 2B**). Upon dsDNA agonist treatment, the porcine cGAS/STING activity had a modest increase in both ISRE and NF-κB promoter assays (**Figure 2B**). When stimulated with HSV-1, the porcine cGAS/STING activity showed significant increase in ISRE promoter assay at the high concentration of virus (**Figure 2C**). The downstream gene inductions including IFNβ, ISG56, and IL8 were obvious in porcine cGAS/STING transfected 293T cells, which normally lack both protein expressions (left panel, **Figure 2D**). In PAMs, the transfection of porcine cGAS alone was sufficient to induce downstream IFNβ, ISG60, and IL8 productions (right panel, **Figure 2D**).

Porcine IFI16 alone did not have any activity in promoter assay in 293T cells. When co-transfected with either human STING or porcine STING, the porcine IFI16/STING exhibited ISRE promoter activity but not as strong as that of porcine cGAS/STING (**Figures 3A,B**). The porcine IFI16/STING ISRE activity was significantly upregulated by dsDNA (left panel, **Figure 3B**) and by high titers of HSV-1 (**Figure 3C**). In the NF-κB promoter assay, porcine IFI16/STING showed no activity

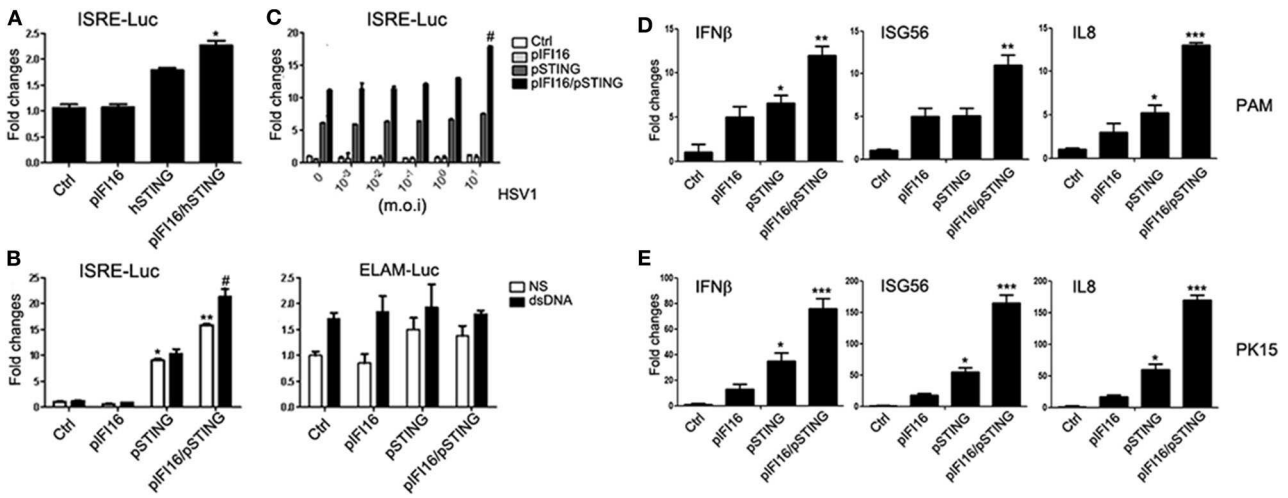

FIGURE 3 | Characterization of porcine DNA sensor IFI16. **(A)** 293T cells grown in 96-well plates were transfected with pIFI16 (20 ng), hSTING (10 ng) plus ISRE-Fluc (10 ng), and Rluc (0.2 ng), which was normalized to 50 ng/well. Twenty-four hours post-transfection, the luciferase activities were measured. **(B)** 293T cells were transfected as in **(A)** using ISRE-Fluc (*left*) or ELAM-Fluc (*right*) with pSTING replacing hSTING, and 24 h later, the cells were stimulated with 1 μg/ml dsDNA by transfection. Twelve hours post-stimulation, the luciferase activities were measured. **(C)** 293T cells were transfected as in **(B)**, and 24 h later stimulated with HSV-1. Twelve hours post-stimulation, luciferase activities were measured. **(D,E)** PAMs and PK15 cells grown in 24-well plates were transfected with 0.5 μg of each recombinant plasmid, and 24 h later, the downstream gene transcription was examined by RT-qPCR. $^{*}p < 0.05$, $^{**}p < 0.01$, $^{***}p < 0.001$ vs. controls. $\#p < 0.05$ vs. non-HSV-1 stimulation.

due to its weak signaling activity (right panel, **Figure 3B**). The downstream gene inductions of IFNβ, ISG56, and IL8 were observed in both PAMs and PK15 cells transfected with porcine IFI16 alone, porcine STING alone, or both (**Figures 3D,E**).

The Porcine IFI16 Interferes With cGAS Signaling and Downstream Gene Transcription

Several previous studies on human and mouse cGAS and IFI16 investigated their mutual relationship and revealed the cooperation between these two DNA receptors (30–34). To understand whether the two porcine DNA receptors also have cooperative relationship, we first co-transfected IFI16 with cGAS/STING in 293T cells and PK15 cells and examined the downstream gene transcription by RT-qPCR. As shown in **Figures 4A,B**, the downstream expressions of IFNβ and IL8 genes in 293T and ISG56 and IL8 genes in PK15 (activated by cGAS/STING) were both significantly decreased with IFI16 when compared with those without IFI16. The results indicated that porcine IFI16 does not promote cGAS signaling; instead, it inhibits cGAS activity. Next, we observed a similar inhibition of cGAS/STING ISRE activity by IFI16 in the promoter assay (**Figure 4C**). We also monitored the activation of DNA signaling pathway molecules with or without IFI16 using Western blotting; it turned out that the phosphorylated TBK1 (p-TBK1) and IRF3 (p-IRF3) activated by cGAS/STING were both slightly downregulated by IFI16 (**Figure 4D**).

To dissect the signaling relationship between porcine cGAS and IFI16 more accurately, we sought to utilize porcine cGAS and IFI16 knockout cells. The CRISPR gRNAs targeting porcine cGAS and IFI16 were designed and cloned into lentiviral vector. The efficacy and specificity of these gRNA expressing lentiviral vectors were verified in transfected cells by Western blotting (**Supplementary Figures 2**, **3**). The packaged lentiviruses were used to infect PAMs and PK15 cells and subjected to puromycin selection to make stable KO cells. As shown in **Figure 5**, upon stimulation by 45-bp dsDNA and plasmid pcDNA3.1, the downstream IFNβ and ISG56 genes were induced in control PAMs. However, the gene inductions were largely absent in cGAS KO PAMs, which is consistent with the strong cGAS/STING signaling activity observed in transfected cells, suggesting that cGAS is the major DNA sensor in these cells (**Figure 5A**). Intriguingly, in IFI16 KO PAMs, the DNA-activated IFNβ and ISG56 were both significantly increased compared with those in control PAMs (**Figure 5A**). HSV-1 stimulated IFNβ and IL8 productions in control PAMs, but the gene inductions were largely decreased in cGAS KO PAMs whereas the same genes were significantly increased in IFI16 KO cells relative to those in control cells (**Figure 5B**). We also stimulated the PK15 cGAS and IFI16 KO cells with plasmid pcDNA3.1 and HSV-1, and obtained similar results (**Supplementary Figures 4A,B**). Altogether, the obtained data clearly suggest that porcine IFI16 negatively regulates cGAS signaling and downstream gene transcription.

Porcine IFI16 Inhibits cGAS Signaling by Competitively Binding With Agonist dsDNA and Adaptor Porcine STING

cGAS is responsible for second messenger 2′5′-cGAMP production, which then directly activates STING for downstream signaling. First, we wondered if porcine IFI16 influences cGAMP production during cGAS activation. We first treated IFI16 KO,

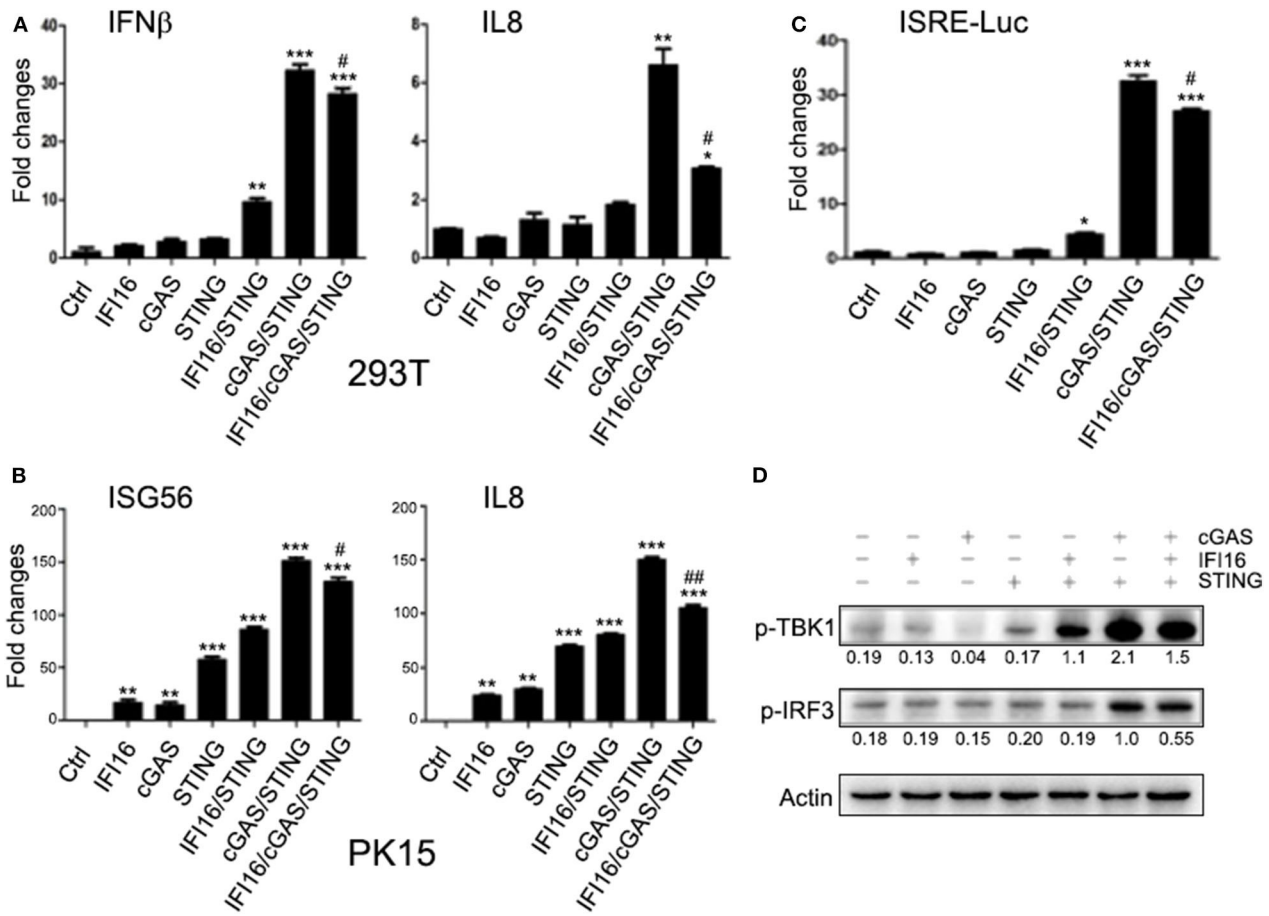

FIGURE 4 | Effects of ectopic porcine IFI16 on porcine cGAS-STING signaling. 293T **(A)** and PK15 cells **(B)** in a 24-well plate were transfected with 0.5 μg of each plasmid, and normalized to 1.5 μg of total DNA each well. Next day, cells were subjected to RT-qPCR analysis. **(C)** 293T cells in a 96-well plate were transfected with the indicated combinations of porcine cGAS (5 ng), IFI16 (20 ng), and STING (2 ng) plus Fluc and Rluc reporters. Twenty-four hours post-transfection, the cells were examined for Fluc and Rluc activities. **(D)** 293T cells (5×10^5 cells/well in a 24-well plate) were transfected with 0.5 μg of each plasmid, and normalized to 1.5 μg each well. Forty-eight hours later, the cells were subjected for Western blot analysis. The densitometry values of p-TBK1 and p-IRF3 after normalization by actin were indicated at the bottom of the bands. $^*p < 0.05$, $^{**}p < 0.01$, $^{***}p < 0.001$ vs. controls. #$p < 0.05$, ##$p < 0.01$ vs. cGAS/STING samples.

cGAS KO, and control stable PK15 cells with HSV-1, and then co-cultured the treated PK15 cells, respectively, with porcine STING transfected ISRE luciferase reporter cells we described before (35). The reporter gene expressions were measured to reflect the cGAMP productions during cGAS activation by HSV-1 infection. As shown in **Figure 6A**, the control PK15 cells stimulated with HSV-1 produced significant higher levels of reporter gene expression reflecting high level of cGAMP. Compared with control PK15 cells, the cGAS KO PK15 cells had lower amount of cGAMP whereas the IFI16 KO PK15 produced slightly but significantly higher amount of cGAMP compared to control PK15 cells, suggesting that porcine IFI16 might control cGAMP production through cGAS. On the other hand, we would like to know if porcine IFI16 modulated the cGAMP-triggered STING-dependent downstream signaling. The IFI16 KO and cGAS KO PK15 were directly stimulated with cGAMP and downstream gene transcription was examined. The results showed that there was no difference of downstream IFNβ, ISG56, and IL8 levels in IFI16 KO and cGAS KO PK15 cells relative to control cells (**Figures 6B–D**). It indicates that porcine IFI16 is not likely to regulate cGAMP downstream STING signaling.

Based on the above results and previous reports (31, 33), we hypothesized that porcine IFI16 might interfere with cGAS for agonist DNA binding to produce cGAMP. Indeed, normally, the biotin-streptavidin conjugated dsDNA agarose could pull down porcine cGAS from cell lysate (**Figure 7A**), but in the presence of porcine IFI16, the binding of cGAS with dsDNA was impaired (**Figure 7B**). We also checked the interaction between porcine cGAS and STING in Co-IP and found that there was interaction between these two proteins despite no requirement of this interaction for STING function and signaling (**Figure 7C**). Further, in the presence of porcine IFI16, the interactions between cGAS and STING became weak as shown by Co-IP in both ways (**Figures 7D,E**).

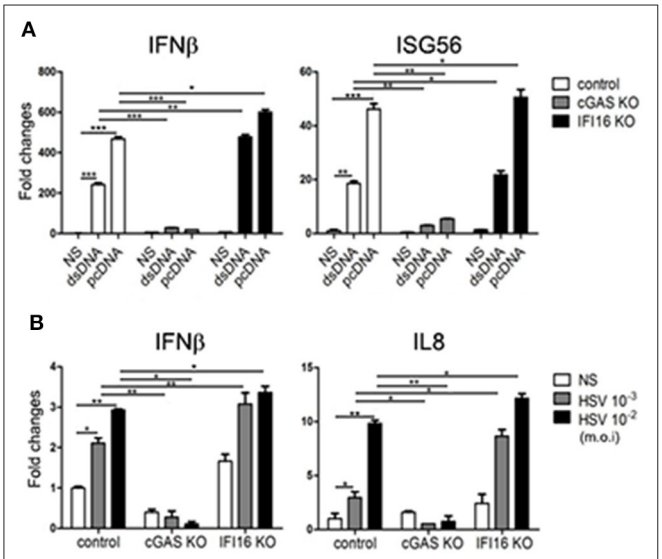

FIGURE 5 | Effects of IFI16 and cGAS KO on DNA and HSV-1 stimulated gene transcription. PAM cGAS KO, IFI16 KO, and control stable cells in a 24-well plate (2×10^5 wells/well) were stimulated with 1 μg/ml dsDNA, 1 μg/ml pcDNA3.1 by transfection for 12 h **(A)**, or HSV-1 at the indicated concentrations for 8 h **(B)**. The stimulated cells were harvested and subjected for RT-qPCR analysis. NS denotes mock stimulation. $^*p < 0.05$, $^{**}p < 0.01$, $^{***}p < 0.001$.

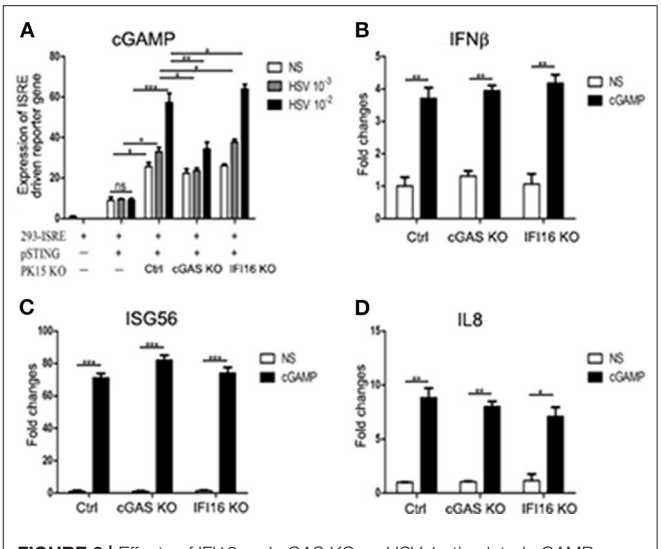

FIGURE 6 | Effects of IFI16 and cGAS KO on HSV-1 stimulated cGAMP production and cGAMP stimulated and STING activated gene transcription. **(A)** ISRE reporter cells in a 24-well plate (2×10^5 cells/well) were transfected with 0.5 μg of pEGFP-pSTING, and 24 h later, the transfected cells were collected by trypsin digestion and cell number was calculated. Simultaneously, PK15 cGAS KO, IFI16 KO, and control stable cells in a 24-well plate (3×10^5 cells/well) were stimulated with HSV-1 at the indicated MOIs for 12 h, then the stimulated cells harvested and cell number calculated. Next, 0.3×10^5 pSTING transfected ISRE reporter cells were incubated with 1.2×10^5 of each type of PK15 stable cells (1:4) in a 24-well plate for 12 h. The incubated pool cells were examined for Fluc and Rluc activities. **(B–D)** The PK15 cGAS KO, IFI16 KO, and control stable cells in a 24-well plate (3×10^5 cells/well) were stimulated with 10 μg/ml 2′3′-cGAMP by transfection for 24 h, and the stimulated PK15 cells were examined for downstream gene transcription by RT-qPCR. NS denotes mock stimulation. $^*p < 0.05$, $^{**}p < 0.01$, $^{***}p < 0.001$, ns, not significant.

Because of the low sequence identity between porcine and human IFI16, we speculated that species specificity exists. The protein domain prediction by the online software PROSITE from ExPASy (www.ExPASy.org) showed that there is one extra Pyrin domain (Pyrin 2) in porcine IFI16 protein (**Figure 8A**). To pinpoint the individual roles of each domain in the IFI16 function, we made deletions of each domain and cloned each domain. While the expressions of deletion mutants could be detected by Western blotting, the individual domain expressions were not detectable (**Figure 8A**). Nevertheless, we proceeded to analyze IFI16 mutants for downstream signaling and gene transcription. In ISRE promoter assay, all the mutants showed activity but much less than full-length IFI16 (**Figure 8B**). In transfected PK15 cells, all mutants were able to induce downstream IFNβ, ISG56, and IL8 gene transcription, among which domain HIN2 induced close gene transcription to full-length IFI16, while mutant ΔHIN2 had the lowest activity (**Figures 8C–E**). Correspondingly, similar to full-length IFI16, domain HIN2 significantly inhibited cGAS induced IFNβ and IL8 transcript production, while mutant ΔHIN2 lost the inhibitory ability (**Figures 8F,G**).

DISCUSSION

In this study, we functionally assessed the porcine DNA sensors cGAS and IFI16, the two most studied DNA sensors in human and mice, both capable of eliciting STING-dependent signaling (36, 37). IFI16 was identified as a DNA sensor (24); however, IFI16 is a multifunctional protein, once implicated in cell senescence and cell growth control (37, 38). Although IFI16 is a nuclear protein at steady state, as confirmed in our study (**Figure 1B**), it shuttles between nucleus and cytosol, and its cellular localization appears cell type specific (39). In monocytes and macrophages, it may have significant cytosolic moiety where it exerts canonical DNA sensing function (32, 34), while in non-immune cells such as fibroblasts, it is predominantly localized in nucleus and acts as nuclear DNA sensor, suppressing viral gene expression epigenetically and activating IFN and IFN-stimulated gene (ISG) transcription directly in a non-canonical way (40, 41). More recently, nuclear IFI16 was shown to activate STING via forming complex with p53 and TRAF6 in response to DNA damage (42). The porcine IFI16 has not been studied before despite that the IFI16 from monkey kidney Marc-145 cells was reported to suppress porcine reproductive and respiratory syndrome virus (PRRSV) replication in the cells (43). Regarding porcine cGAS, it has been investigated directly in only one study (44) and for its antiviral properties in several other reports (45–47). We showed here that both porcine cGAS and IFI16 are capable of eliciting IFN signaling dependent on porcine STING, which is exchangeable to human STING (**Figures 2**, **3**). The triple of cytosolic cGAS, IFI16, and STING constitutes the canonical DNA signaling pathway to induce IFN.

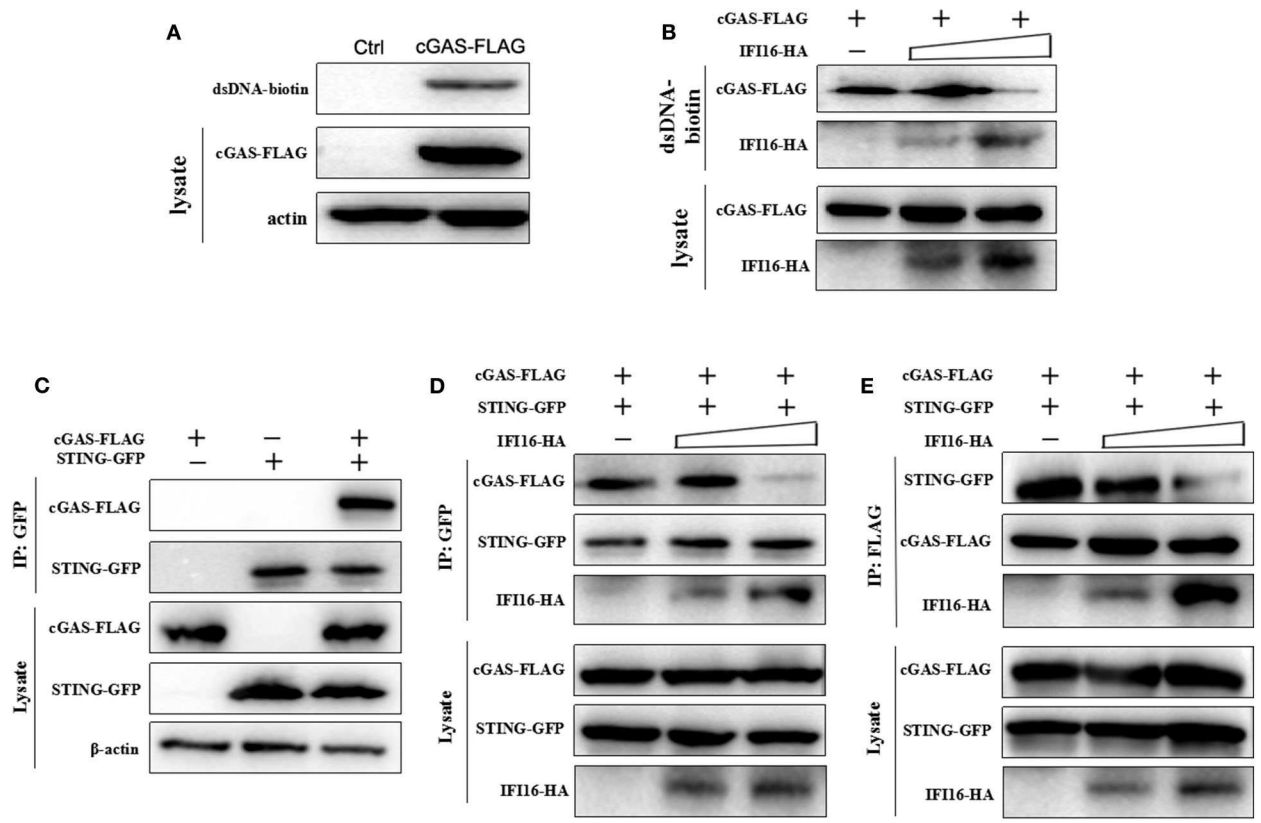

FIGURE 7 | The binding of dsDNA and STING by porcine cGAS in the presence or absence of porcine IFI16. **(A)** 293T cells in a six-well plate (8×10^5 cells/well) were transfected with 0.5 μg of pcGAS or control pcDNA3.1 for 48 h, the transfected cells were lysed, and cell lysates were subjected for dsDNA binding assay with the bound cGAS analyzed by Western blotting using anti-FLAG mAb. **(B)** 293T cells were transfected as in **(A)** without or with 0.5 μg and 1.0 μg porcine IFI16, respectively, and examined for dsDNA binding. **(C)** 293T cells in a six-well plate (8×10^5 cells/well) were transfected with 0.5 μg of pcGAS and 0.5 μg of pSTING for 48 h, and the cell lysates were subjected for Co-IP using anti-GFP antibody and subsequent Western blot analysis. **(D,E)** 293T cells were transfected as in **(C)** without or with 0.5 μg and 1.0 μg porcine IFI16, respectively, and cell lysates were subjected for Co-IP using anti-GFP antibody **(D)** or anti-FLAG antibody **(E)** and subsequent Western blot analysis.

In the canonical pathway, STING, as an ER resident protein, upon DNA activation traffics from ER to Golgi apparatus and finally to the perinuclear region for degradation. During its trafficking, STING recruits and activates TBK1. In turn, the activated TBK1 phosphorylates IRF3, leading to downstream IFN induction (48).

Importantly, we studied the relationship between porcine IFI16 and cGAS signaling and we did not observe any cooperation between these two DNA receptors. Instead, we found that porcine IFI16 interferes with cGAS for downstream signaling. In comparison, the relation of cGAS and IFI16 in human and mice is quite different. Indeed, several previous studies showed the cooperation between these two DNA receptors during DNA transfection or pathogen infections (30–34). Specifically, human IFI16 was shown to amplify the cGAS-STING canonical pathway to induce IFNβ in response to *Listeria monocytogenes* infection and the subsequent presence of bacterial DNA in the cytosol of human macrophages (32). Mouse IFI16 counterpart p204 cooperated with cGAS to engage in STING-dependent type I IFN production in response to *Francisella novicida* infection and the bacterial DNA in the cytosol of murine macrophages (34). Human IFI16 could positively influence cGAS-STING pathway signaling in macrophages through the increase of second messenger cGAMP production by cGAS and the enhanced recruitment of TBK1 to STING (33), while human IFI16 cooperated with cGAS in keratinocytes by only targeting STING activation (31). Additionally, IFI16 in nucleus could be stabilized by cGAS in human fibroblasts during HSV-1 infection and thus the heightened non-canonical function of IFI16 was obtained (30). In our study, ectopic porcine IFI16 suppressed porcine cGAS/STING-induced phosphorylation of TBK1 and IRF3, ISRE promoter activation, and downstream IFNβ, ISG56, and IL8 transcription (**Figure 4**). Whereas in porcine IFI16 KO PAMs and PK15 cells, the dsDNA and HSV-1 activated, porcine cGAS-induced downstream genes including IFNβ, ISG56, and IL8 were increased (**Figure 5** and **Supplementary Figure 4**). Therefore, the results clearly showed that porcine IFI16 interferes with cGAS signaling. We speculated the reason that may lead to the discrepancy and thought that could be due to the nature of IFI16, which belongs

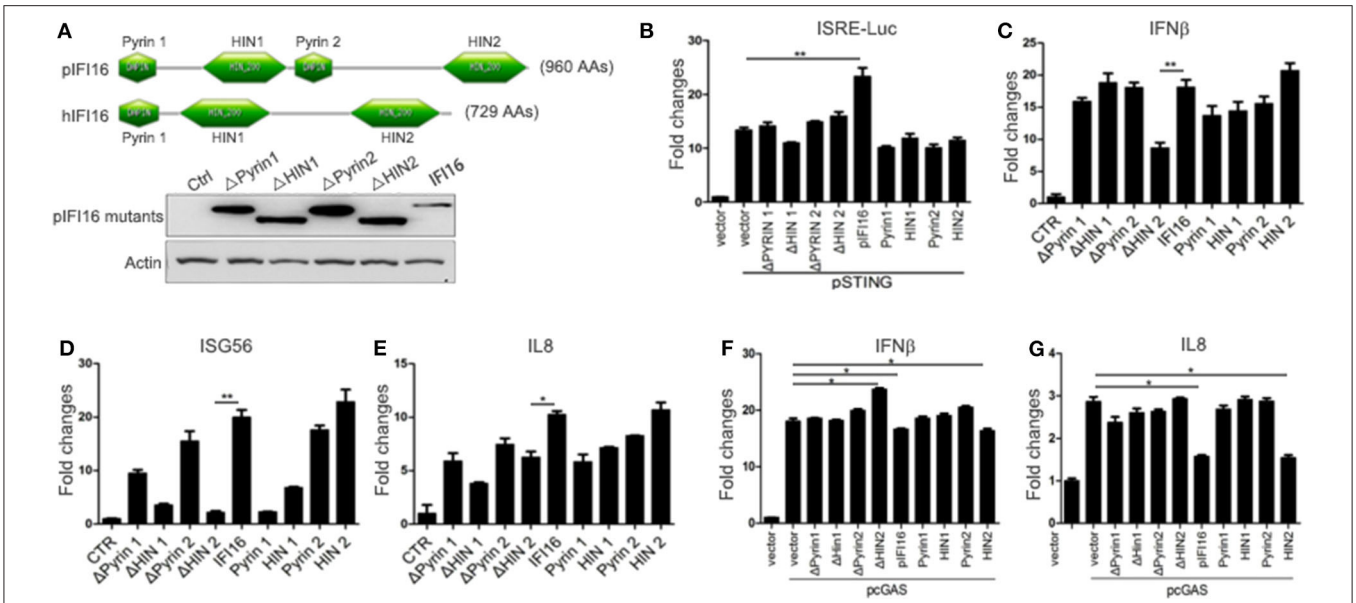

FIGURE 8 | Functional characterization of porcine IFI16 domains. **(A)** The comparison of pIFI16 and hIFI16 domains and expressions of pIFI16 deletion mutants by Western blotting using anti-HA antibody. **(B)** 293T cells in a 96-well plate were transfected with 10 ng of pSTING and 20 ng of each IFI16 mutant together with Fluc and Rluc, and 36 h post-transfection cells were examined for Fluc and Rluc activities. **(C–E)** PK15 in a 24-well plate were transfected with 0.5 μg of each IFI16 mutant for 24 h, and downstream gene transcription was analyzed by RT-qPCR. **(F,G)** PK15 cells in a 24-well plate were transfected with 0.5 μg of pcGAS together with 0.5 μg of each IFI16 mutant for 24 h, and downstream gene transcription was analyzed by RT-qPCR. $^{*}p < 0.05$, $^{**}p < 0.01$.

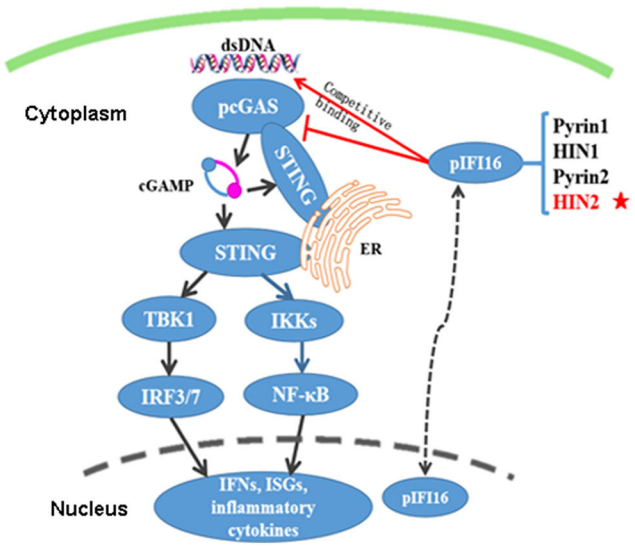

FIGURE 9 | The schematic illustration of porcine cGAS regulation by IFI16. Porcine cGAS, upon recognition of agonist dsDNA, produces second messenger 2′3′-cGAMP, which directly binds with and activates the adaptor STING. The activated STING traffics from ER to Golgi apparatus to the perinuclear region; during the process, it recruits and activates TBK1 that phosphorylates IRF3/7. However, how STING exactly activates NF-κB is still open. In turn, the activated IRF3/7 and NF-κB drive IFN and other gene transcription. Steady-state porcine IFI16 is mainly in the nucleus, but it shuttles into cytosol where it competes with cGAS for binding to agonist DNA and STING mainly via its HIN2 domain, thus modulating the cGAMP production and downstream signaling.

to the very diverse PYHIN family. In this family, human has four members including IFI16, IFIX, MNDA, and AIM2, whereas mice have 13 members with p204 usually considered as the functional ortholog of human IFI16 (49, 50). In fact, among the 13 mouse members, there are varying degrees of functional redundancy; thus, it is difficult to define the exact functional homolog of IFI16 in mice (49). In contrast, the information in porcine PYHIN family is very limited, and current porcine IFI16 is the only available PYHIN protein that has low identity to human IFI16 and harbors one extra Pyrin 2 domain (**Figure 8A**). Whether there is another functional homolog of human IFI16 in porcine is now unknown and warrants further investigation.

Regarding the molecular mechanism of action by porcine IFI16 to suppress cGAS signaling, we showed here that both porcine IFI16 and cGAS bind with dsDNA (**Figures 7A,B**). Furthermore, IFI16 was observed to compete with cGAS for DNA binding (**Figures 7A,B**). Previous studies showed that both cGAS and IFI16 recognize dsDNA in a sequence-independent way (50, 51); thus, it provides the possibility that these two DNA sensors can compete for dsDNA binding. The competition for agonist dsDNA by IFI16 coincided well with the increased cGAMP level in IFI16 KO cells during HSV-1 infection (**Figure 6A**). We also found that porcine cGAS and STING interact with each other and that this interaction can be disturbed by porcine IFI16 (**Figures 7C–E**). However, this disturbance seems not to affect porcine STING activation and downstream gene transcription (**Figures 6B–D**). Even though STING function was not affected, it could not

be excluded that porcine cGAS function might be affected, contributing to reduced cGAMP production. By dissecting the individual domains of porcine IFI16, we found that each domain contributes more or less to IFI16 activity dependent on STING while the HIN2 domain activity is closer to full-length IFI16 (**Figures 8B–E**). Among the IFI16 domains, the HIN domains are responsible for binding with DNA, while the Pyrin domain mediates homotypic interaction and IFI16 oligomerization (39, 51, 52). In porcine IFI16, HIN2 domain had not only prominent STING dependent activity but also the significant ability to inhibit porcine cGAS activity (**Figures 8F,G**). Since the HIN2 is the most critical domain for dsDNA binding (48, 53), it also explains well the role of HIN2 in competitive binding agonist dsDNA of cGAS by porcine IFI16 (**Figures 7A,B**).

Collectively, this study isolated two porcine DNA sensors cGAS and IFI16, confirmed their STING-dependent IFN-inducing activity, analyzed the relation between these two DNA sensors, and explored the mechanism of action utilized by porcine IFI16 to regulate cGAS signaling (**Figure 9**), and therefore revealed unique insights into innate immune biology in the pig, which is the promising model for human diseases.

DATA AVAILABILITY STATEMENT

All datasets generated for this study are included in the article/**Supplementary Material**.

AUTHOR CONTRIBUTIONS

JZ conceived and designed the experiments. WZ, RZ, SL, SH, JL, and MZ performed the experiments. WZ, NC, HC, FM, and JZ analyzed the data. WZ and JZ wrote the paper. All authors contributed to the article and approved the submitted version.

FUNDING

This work was partly supported by the National Key Research and Development Program of China (2017YFD0502301), the National Natural Science Foundation of China (31672523 and 31872450), and a project funded by the Priority Academic Program Development of Jiangsu Higher Education Institutions (PAPD).

ACKNOWLEDGMENTS

We thank Dr. Saumendra N. Sarkar at University of Pittsburgh, USA, for critical reading and advice.

SUPPLEMENTARY MATERIAL

The Supplementary Material for this article can be found online at: https://www.frontiersin.org/articles/10.3389/fimmu.2020.01669/full#supplementary-material

Supplementary Figure 1 | The pcDNA-cGAS, pcDNA-IFI16, pEGFP-STING (0.5 μg each) were transfected into 293T cells (4×10^5 cells/well on coverslips in 12-well plate) using lipofectamine 2000. Forty-eight hours post transfection, the protein expressions were examined by fluorescence microscopy after fixation and staining.

Supplementary Figure 2 | The validation of efficacy and specificity of gRNA lentiviral plasmids targeting porcine cGAS. 293 T cells (5×10^5 cells/well) were transfected with 0.5 μg porcine cGAS or IFI16 together with 0.5 and 1 μg cGAS gRNAs, respectively, 48 h later, the transfected cells were analyzed by Western blotting using anti-HA antibody.

Supplementary Figure 3 | The validation of efficacy and specificity of gRNA lentiviral plasmids targeting porcine IFI16. 293 T cells (5×10^5 cells/well) were transfected with 0.5 μg porcine IFI16 or cGAS together with 0.5 and 1 μg IFI16 gRNAs, respectively, 48 h later, the transfected cells were analyzed by Western blotting using anti-HA antibody.

Supplementary Figure 4 | Effects of IFI16 and cGAS KO on DNA and HSV-1 stimulated gene transcription. PK15 cGAS KO, IFI16 KO, and control stable cells in 24-well plate (2×10^5 wells/well) were stimulated with 1 μg/ml pcDNA3.1 by transfection for 12 h **(A)**, or HSV-1 at the indicated concentrations for 8 h **(B)**. The stimulated cells were harvested and subjected for RT-qPCR analysis. NS denotes mock stimulation. $^*p < 0.05$, $^{**}p < 0.01$, $^{***}p < 0.001$.

Supplementary Table 1 | The PCR primers used for gene cloning and mutations.

Supplementary Table 2 | The CRISPR gRNA encoding DNA sequences for porcine cGAS and IFI16.

Supplementary Table 3 | Primers for RT-PCR and RT-qPCR in this study.

REFERENCES

1. Takeuchi O, Akira S. Pattern recognition receptors and inflammation. *Cell.* (2010) 140:805–20. doi: 10.1016/j.cell.2010.01.022
2. Cui J, Chen Y, Wang HY, Wang RF. Mechanisms and pathways of innate immune activation and regulation in health and cancer. *Hum Vaccines Immunother.* (2014) 10:3270–85. doi: 10.4161/21645515.2014.979640
3. Hemmi H, Takeuchi O, Kawai T, Kaisho T, Sato S, Sanjo H, et al. A toll-like receptor recognizes bacterial DNA. *Nature.* (2000) 408:740–5. doi: 10.1038/35047123
4. Kim T, Pazhoor S, Bao M, Zhang Z, Hanabuchi S, Facchinetti V, et al. Aspartate-glutamate-alanine-histidine box motif (DEAH) /RNA helicase a helicases sense microbial DNA in human plasmacytoid dendritic cells. *Proc Natl Acad Sci USA.* (2010) 107:15181–6. doi: 10.1073/pnas.1006539107
5. Dempsey A, Bowie AG. Innate immune recognition of DNA: a recent history. *Virology.* (2015) 480:146–52. doi: 10.1016/j.virol.2015.03.013
6. Takaoka A, Wang Z, Choi MK, Yanai H, Negishi H, Ban T, et al. DAI (DLM-1/ZBP1) is a cytosolic DNA sensor and an activator of innate immune response. *Nature.* (2007) 448:501–5. doi: 10.1038/nature06013
7. Ishii KJ, Kawagoe T, Koyama S, Matsui K, Kumar H, Kawai T, et al. TANK-binding kinase-1 delineates innate and adaptive immune responses to DNA vaccines. *Nature.* (2008) 451:725–9. doi: 10.1038/nature06537
8. Hornung V, Ablasser A, Charrel-Dennis M, Bauernfeind F, Horvath G, Caffrey DR, et al. AIM2 recognizes cytosolic dsDNA and forms a caspase-1-activating inflammasome with ASC. *Nature.* (2009) 458:514–8. doi: 10.1038/nature07725
9. Fernandes-Alnemri T, Yu JW, Juliana C, Solorzano L, Kang S, Wu J, et al. The AIM2 inflammasome is critical for innate immunity to *Francisella tularensis*. *Nat Immunol.* (2010) 11:385–93. doi: 10.1038/ni.1859
10. Ablasser A, Bauernfeind F, Hartmann G, Latz E, Fitzgerald KA, Hornung V. RIG-I-dependent sensing of poly(dA:dT) through the induction of an RNA polymerase III-transcribed RNA intermediate. *Nat Immunol.* (2009) 10:1065–72. doi: 10.1038/ni.1779

11. Chiu YH, Macmillan JB, Chen ZJ. RNA polymerase III detects cytosolic DNA and induces type I interferons through the RIG-I pathway. *Cell.* (2009) 138:576–91. doi: 10.1016/j.cell.2009.06.015
12. Yang P, An H, Liu X, Wen M, Zheng Y, Rui Y, et al. The cytosolic nucleic acid sensor LRRFIP1 mediates the production of type I interferon via a beta-catenin-dependent pathway. *Nat Immunol.* (2010) 11:487–94. doi: 10.1038/ni.1876
13. Zhang Z, Yuan B, Bao M, Lu N, Kim T, Liu YJ. The helicase DDX41 senses intracellular DNA mediated by the adaptor STING in dendritic cells. *Nat Immunol.* (2011) 12:959–65. doi: 10.1038/ni.2091
14. Parvatiyar K, Zhang Z, Teles RM, Ouyang S, Jiang Y, Iyer SS, et al. The helicase DDX41 recognizes the bacterial secondary messengers cyclic di-GMP and cyclic di-AMP to activate a type I interferon immune response. *Nat Immunol.* (2012) 13:1155–61. doi: 10.1038/ni.2460
15. Ferguson BJ, Mansur DS, Peters NE, Ren H, Smith GL. DNA-PK is a DNA sensor for IRF-3-dependent innate immunity. *eLife.* (2012) 1:e00047. doi: 10.7554/eLife.00047
16. Kondo T, Kobayashi J, Saitoh T, Maruyama K, Ishii KJ, Barber GN, et al. DNA damage sensor MRE11 recognizes cytosolic double-stranded DNA and induces type I interferon by regulating STING trafficking. *Proc Natl Acad Sci USA.* (2013) 110:2969–74. doi: 10.1073/pnas.1222694110
17. Ishikawa H, Barber GN. STING is an endoplasmic reticulum adaptor that facilitates innate immune signalling. *Nature.* (2008) 455:674–8. doi: 10.1038/nature07317
18. Jin L, Waterman PM, Jonscher KR, Short CM, Reisdorph NA, Cambier JC. MPYS, a novel membrane tetraspanner, is associated with major histocompatibility complex class II and mediates transduction of apoptotic signals. *Mol Cell Biol.* (2008) 28:5014–26. doi: 10.1128/MCB.00640-08
19. Zhong B, Yang Y, Li S, Wang YY, Li Y, Diao F, et al. The adaptor protein MITA links virus-sensing receptors to IRF3 transcription factor activation. *Immunity.* (2008) 29:538–50. doi: 10.1016/j.immuni.2008.09.003
20. Sun W, Li Y, Chen L, Chen H, You F, Zhou X, et al. ERIS, an endoplasmic reticulum IFN stimulator, activates innate immune signaling through dimerization. *Proc Natl Acad Sci USA.* (2009) 106:8653–8. doi: 10.1073/pnas.0900850106
21. Abe T, Harashima A, Xia T, Konno H, Konno K, Morales A, et al. STING recognition of cytoplasmic DNA instigates cellular defense. *Mol Cell.* (2013) 50:5–15. doi: 10.1016/j.molcel.2013.01.039
22. Burdette DL, Monroe KM, Sotelo-Troha K, Iwig JS, Eckert B, Hyodo M, et al. STING is a direct innate immune sensor of cyclic di-GMP. *Nature.* (2011) 478:515–8. doi: 10.1038/nature10429
23. Gao P, Ascano M, Zillinger T, Wang W, Dai P, Serganov AA, et al. Structure-function analysis of STING activation by c[G(2',5')pA(3',5')p] and targeting by antiviral DMXAA. *Cell.* (2013) 154:748–62. doi: 10.1016/j.cell.2013.07.023
24. Unterholzner L, Keating SE, Baran M, Horan KA, Jensen SB, Sharma S, et al. IFI16 is an innate immune sensor for intracellular DNA. *Nat Immunol.* (2010) 11:997–1004. doi: 10.1038/ni.1932
25. Li T, Diner BA, Chen J, Cristea IM. Acetylation modulates cellular distribution and DNA sensing ability of interferon-inducible protein IFI16. *Proc Natl Acad Sci USA.* (2012) 109:10558–63. doi: 10.1073/pnas.1203447109
26. Kerur N, Veettil MV, Sharma-Walia N, Bottero V, Sadagopan S, Otageri P, et al. IFI16 acts as a nuclear pathogen sensor to induce the inflammasome in response to kaposi sarcoma-associated herpesvirus infection. *Cell Host Microbe.* (2011) 9:363–75. doi: 10.1016/j.chom.2011.04.008
27. Sun L, Wu J, Du F, Chen X, Chen ZJ. Cyclic GMP-AMP synthase is a cytosolic DNA sensor that activates the type I interferon pathway. *Science.* (2013) 339:786–91. doi: 10.1126/science.1232458
28. Li T, Chen ZJ. The cGAS-cGAMP-STING pathway connects DNA damage to inflammation, senescence, and cancer. *J Exp Med.* (2018) 215:1287–99. doi: 10.1084/jem.20180139
29. Zhu J, Lai K, Brownile R, Babiuk LA, Mutwiri GK. Porcine TLR8 and TLR7 are both activated by a selective TLR7 ligand, imiquimod. *Mol Immunol.* (2008) 45:3238–43. doi: 10.1016/j.molimm.2008.02.028
30. Orzalli MH, Broekema NM, Diner BA, Hancks DC, Elde NC, Cristea IM, et al. cGAS-mediated stabilization of IFI16 promotes innate signaling during herpes simplex virus infection. *Proc Natl Acad Sci USA.* (2015) 112:E1773–81. doi: 10.1073/pnas.1424637112
31. Almine JF, O'Hare CA, Dunphy G, Haga IR, Naik RJ, Atrih A, et al. IFI16 and cGAS cooperate in the activation of STING during DNA sensing in human keratinocytes. *Nat Commun.* (2017) 8:14392. doi: 10.1038/ncomms14392
32. Hansen K, Prabakaran T, Laustsen A, Jorgensen SE, Rahbaek SH, Jensen SB, et al. Listeria monocytogenes induces IFNbeta expression through an IFI16-, cGAS- and STING-dependent pathway. *EMBO J.* (2014) 33:1654–66. doi: 10.15252/embj.201488029
33. Jonsson KL, Laustsen A, Krapp C, Skipper KA, Thavachelvam K, Hotter D, et al. IFI16 is required for DNA sensing in human macrophages by promoting production and function of cGAMP. *Nat Commun.* (2017) 8:14391. doi: 10.1038/ncomms14391
34. Storek KM, Gertsvolf NA, Ohlson MB, Monack DM. cGAS and Ifi204 cooperate to produce type I IFNs in response to *Francisella* infection. *J Immunol.* (2015) 194:3236–45. doi: 10.4049/jimmunol.1402764
35. Zhu J, Smith K, Hsieh PN, Mburu YK, Chattopadhyay S, Sen GC, et al. High-throughput screening for TLR3-IFN regulatory factor 3 signaling pathway modulators identifies several antipsychotic drugs as TLR inhibitors. *J Immunol.* (2010) 184:5768–76. doi: 10.4049/jimmunol.0903559
36. Christensen MH, Paludan SR. Viral evasion of DNA-stimulated innate immune responses. *Cell Mol Immunol.* (2017) 14:4–13. doi: 10.1038/cmi.2016.06
37. Knipe DM. Nuclear sensing of viral DNA, epigenetic regulation of herpes simplex virus infection, innate immunity. *Virology.* (2015) 480:153–9. doi: 10.1016/j.virol.2015.02.009
38. Xin H, Pereira-Smith OM, Choubey D. Role of IFI 16 in cellular senescence of human fibroblasts. *Oncogene.* (2004) 23:6209–17. doi: 10.1038/sj.onc.1207836
39. Diner BA, Lum KK, Cristea IM. The emerging role of nuclear viral DNA sensors. *J Biol Chem.* (2015) 290:26412–21. doi: 10.1074/jbc.R115.652289
40. Thompson MR, Sharma S, Atianand M, Jensen SB, Carpenter S, Knipe DM, et al. Interferon gamma-inducible protein (IFI) 16 transcriptionally regulates type i interferons and other interferon-stimulated genes and controls the interferon response to both DNA and RNA viruses. *J Biol Chem.* (2014) 289:23568–81. doi: 10.1074/jbc.M114.554147
41. Diner BA, Lum KK, Toettcher JE, Cristea IM. Viral DNA sensors IFI16 and cyclic GMP-AMP synthase possess distinct functions in regulating viral gene expression, immune defenses, and apoptotic responses during herpesvirus infection. *mBio.* (2016) 7:e01553-16. doi: 10.1128/mBio.01553-16
42. Dunphy G, Flannery SM, Almine JF, Connolly DJ, Paulus C, Jonsson KL, et al. Non-canonical activation of the DNA sensing adaptor STING by ATM and IFI16 mediates NF-kappaB signaling after nuclear DNA damage. *Mol Cell.* (2018) 71:745–60.e5. doi: 10.1016/j.molcel.2018.07.034
43. Chang X, Shi X, Zhang X, Wang L, Li X, Wang A, et al. IFI16 inhibits porcine reproductive and respiratory syndrome virus 2 replication in a MAVS-dependent manner in MARC-145 cells. *Viruses.* (2019) 11:1160. doi: 10.3390/v11121160
44. Wang J, Chu B, Du L, Han Y, Zhang X, Fan S, et al. Molecular cloning and functional characterization of porcine cyclic GMP-AMP synthase. *Mol Immunol.* (2015) 65:436–45. doi: 10.1016/j.molimm.2015.02.002
45. Huang B, Zhang L, Lu M, Li J, Lv Y. PCV2 infection activates the cGAS/STING signaling pathway to promote IFN-beta production and viral replication in PK-15 cells. *Vet Microbiol.* (2018) 227:34–40. doi: 10.1016/j.vetmic.2018.10.027
46. Wang X, Wu J, Wu Y, Chen H, Zhang S, Li J, et al. Inhibition of cGAS-STING-TBK1 signaling pathway by DP96R of ASFV China 2018/1. *Biochem Biophys Res Commun.* (2018) 506:437–43. doi: 10.1016/j.bbrc.2018.10.103
47. Garcia-Belmonte R, Perez-Nunez D, Pittau M, Richt JA, Revilla Y. African swine fever virus armenia/07 virulent strain controls interferon beta production through the cGAS-STING pathway. *J Virol.* (2019) 93:e02298-18. doi: 10.1128/JVI.02298-18
48. Ma Z, Ni G, Damania B. Innate sensing of DNA virus genomes. *Ann Rev Virol.* (2018) 5:341–62. doi: 10.1146/annurev-virology-092917-043244
49. Brunette RL, Young JM, Whitley DG, Brodsky IE, Malik HS, Stetson DB. Extensive evolutionary and functional diversity among mammalian AIM2-like receptors. *J Exp Med.* (2012) 209:1969–83. doi: 10.1084/jem.20121960
50. Orzalli MH, Knipe DM. Cellular sensing of viral DNA and viral evasion mechanisms. *Ann Rev Microbiol.* (2014) 68:477–92. doi: 10.1146/annurev-micro-091313-103409

51. Jin T, Perry A, Jiang J, Smith P, Curry JA, Unterholzner L, et al. Structures of the HIN domain:DNA complexes reveal ligand binding and activation mechanisms of the AIM2 inflammasome and IFI16 receptor. *Immunity.* (2012) 36:561–71. doi: 10.1016/j.immuni.2012.02.014
52. Morrone SR, Wang T, Constantoulakis LM, Hooy RM, Delannoy MJ, Sohn J. Cooperative assembly of IFI16 filaments on dsDNA provides insights into host defense strategy. *Proc Natl Acad Sci USA.* (2014) 111:E62–71. doi: 10.1073/pnas.1313577111
53. Ni X, Ru H, Ma F, Zhao L, Shaw N, Feng Y, et al. New insights into the structural basis of DNA recognition by HINa and HINb domains of IFI16. *J Mol Cell Biol.* (2016) 8:51–61. doi: 10.1093/jmcb/mjv053

Conflict of Interest: The authors declare that the research was conducted in the absence of any commercial or financial relationships that could be construed as a potential conflict of interest.

frontiers in Immunology

MINI REVIEW
published: 28 August 2020
doi: 10.3389/fimmu.2020.01637

DNA-Sensing Antiviral Innate Immunity in Poxvirus Infection

Yue Lu [1,2,3,4] *and Leiliang Zhang* [1,2,3,4,5]*

[1] Department of Laboratory Medicine, The First Affiliated Hospital of Shandong First Medical University, Jinan, China, [2] Institute of Basic Medicine, Shandong First Medical University and Shandong Academy of Medical Sciences, Jinan, China, [3] Key Laboratory for Biotech-Drugs of National Health Commission, Jinan, China, [4] Key Laboratory for Rare and Uncommon Diseases of Shandong Province, Jinan, China, [5] Science and Technology Innovation Center, Shandong First Medical University, Shandong Academy of Medical Sciences, Jinan, China

As pattern recognition receptors, cytosolic DNA sensors quickly induce an effective innate immune response. Poxvirus, a large DNA virus, is capable of evading the host antiviral innate immune response. In this review, we summarize the latest studies on how poxvirus is sensed by the host innate immune system and how poxvirus-encoded proteins antagonize DNA sensors. A comprehensive understanding of the interplay between poxvirus and DNA-sensing antiviral immune responses of the host will contribute to the development of new antiviral therapies and vaccines in the future.

Keywords: poxvirus, cGAS, DNA-PK, IFI16, STING

OPEN ACCESS

Edited by:
Chunfu Zheng,
Fujian Medical University, China

Reviewed by:
Kai Huang,
University of Texas Medical Branch at Galveston, United States
Guanqun L. Liu,
University of Chicago, United States

***Correspondence:**
Leiliang Zhang
armzhang@hotmail.com

Specialty section:
This article was submitted to Viral Immunology, a section of the journal Frontiers in Immunology

Received: *15 April 2020*
Accepted: *18 June 2020*
Published: *28 August 2020*

Citation:
Lu Y and Zhang L (2020) DNA-Sensing Antiviral Innate Immunity in Poxvirus Infection. Front. Immunol. 11:1637. doi: 10.3389/fimmu.2020.01637

INTRODUCTION

Poxvirus is a double-stranded DNA (dsDNA) virus (1, 2) that replicates completely in the cytoplasm. Members of the *Poxviridae* family include variola virus (VARV), vaccinia virus (VACV), ectromelia virus (ECTV), and monkeypox virus (MPXV). VACV is a prototype member of the *Orthopoxvirus* genus of the *Poxviridae* family and has been used as a live vaccine for smallpox eradication (3). Interest in VACV persists because it is an excellent model for studying host pathogen interactions and cell biology (4). ECTV is a mouse-specific pathogen that has been used as a model to study the pathogenesis and immunobiology of *Orthopoxvirus* infection (5, 6).

The innate immune response against viruses is not only the first line of defense against viral infection but is also important for the establishment of adaptive immunity against viruses. The recognition of the viral DNA genome by DNA sensors, including cyclic GMP–AMP synthase (cGAS), DNA-dependent protein kinase (DNA-PK), and IFN-γ inducible protein 16 (IFI16), is the first step in the innate immune response (7, 8). Next, innate immune signal transduction is initiated by activating adaptor proteins, such as stimulator of interferon genes (STING), resulting in the production of a large number of defense molecules in the host, including interferons (IFNs) and pro-inflammatory cytokines and chemokines (9–11).

The evolutionary arms race between the virus and the host leads to the virus-mediated antagonism of antiviral immunity. Viruses hide their DNA from cellular sensing systems and/or inactivate sensors and downstream signal transduction pathways. These viral strategies include separation or modification of viral nucleic acids, interfering with specific post-translational modifications of pattern recognition receptors (PRRs) or their adaptors, degradation or cleavage of PRRs or adaptors, and separating or repositioning PRRs. For instance, there are a variety of proteins that inhibit the activation of the transcription factors interferon regulatory factor 3 (IRF3) and nuclear factor kappa B (NF-κB) or the Janus kinase (JAK)/signal transducer and activator of transcription (STAT) pathway (2).

Poxvirus encodes the largest number of immune antagonistic virus proteins, thereby showing the most diverse immune escape strategies (4). During infection, these immunomodulatory

proteins are delivered to the cytoplasm of the host cell to combat the innate immune response (12, 13). The conserved central region of the poxvirus genome encodes the open reading frames (ORFs) essential for virus replication. The other ORFs are non-essential for viral replication in cell culture (14), with most associated with targeting the innate immune system (15, 16).

In this review, we summarize the DNA-sensing signal pathways in poxvirus-infected cells. In particular, we focus on DNA sensors (cGAS/DNA-PK/IFI16), an adaptor protein (STING), and host defense molecules (IFNs/cytokines). We also describe how poxvirus targets DNA sensors to abrogate the antiviral immune response. Understanding antiviral immunity and poxvirus-mediated antagonism mechanisms may guide the development of live attenuated vaccines and antiviral therapies.

cGAS

In 2013, Sun et al. discovered a new DNA sensor, cGAS, which advanced our understanding of innate DNA sensing (17). cGAS, an enzyme belonging to the ancient oligoadenylate synthase (OAS) protein family (18), is a universal cytoplasmic DNA sensor upstream of STING. cGAS recognizes a large number of cytoplasmic DNA viruses (HSV-1, KSHV, and VACV) and retroviruses (HIV-1, HIV-2) (19–24). cGAS is activated upon binding to DNA, which catalyzes the production of 2'3'-cGAMP from ATP and GTP, resulting in the binding of second messenger cyclic GMP–AMP (cGAMP) to STING (17, 25–29). As an adaptor protein, STING recruits TBK1, which phosphorylates IRF3. Then, IRF3 is relocated to the nucleus to induce IFN and thus establishes an antiviral state (19, 30–33). NF-κB is also activated by STING (32).

The cGAS–STING pathway is very important for sensing ECTV infection, inducing type I IFN production and controlling ECTV replication (34). In the lymph nodes of mice infected with ECTV, inflammatory monocytes (IMOs) are the main cells producing type I IFN in draining lymph nodes (DLNs). To induce the expression of IFN and pro-inflammatory cytokines, IMOs require STING–IRF7 and STING–NF-κB (10).

By using cGAS-deficient mice, researchers showed that type I IFN is not produced during VACV infection (35, 36). In addition, cGAMP, produced by cGAS in virus-infected cells, can be transferred to uninfected neighboring cells through gap junctions, where it promotes STING activation and antiviral immunity reactions independent of type I IFN (37).

Interferon-induced oligoadenylate synthetase-like (OASL) binds specifically to cGAS and inhibits cGAS enzyme activity in the process of DNA virus infection, which inhibits IFN induction and promotes DNA virus replication through the cGAS–STING DNA sensing pathway (38). Deletion of human OASL and mouse OASL2 can inhibit DNA virus infection. OASL1 and OASL2 are negative feedback regulators of cGAS and inhibit cGAS-mediated type I IFN induction (38).

The modified VACV Ankara strain (MVA) has been designed as a vaccine vector (39–41), and it can effectively prevent VARV and MPXV infection (42, 43). IFN in MVA-infected conventional dendritic cells (cDCs) is produced independently of the RNA-sensing pathway mediated by MDA5, MAVS, TLR3, or TRIF and is not affected by the absence of TLR9/MyD88 in the DNA sensing pathway *in vivo*. The cGAS/STING-mediated DNA-sensing pathway plays a key role in MVA-induced IFN production in CDCs. MVA infection of cDCs triggers the phosphorylation of TBK1 and IRF3, which is abolished in the absence of cGAS and STING. Similar results were also observed in mouse models (44).

TLR9

Of the 10 TLRs found in humans, TLR9 is the only known DNA sensor. TLR9 specifically recognizes the unmethylated CpG motif in dsDNA (CpG DNA), which is common in bacterial and viral genomes (32, 45–47). TLR9 recruits the adaptor protein MyD88 and then recruits tumor necrosis factor receptor associated factor 6 (TRAF6) and IκB kinase (IKK) complexes; the former leads to the activation of IRF7 and ultimately induces the production of type I IFN (48, 49), and the latter leads to the activation of NF-κB, resulting in the induction of inflammatory cytokines (50).

TLR9/MyD88 sensing increased the expression of the NKG2D ligand in virus-infected migratory dendritic cells (mDCs), and induced production of IFN-γ in classical NK cells and innate lymphoid cells (ILCs). IFN-γ induces CXCL9 in uninfected IMOs and induces the recruitment of protective NK cells to DLNs (51). In $CD11c^+$ cells, MyD88–IRF7 recruit IMOs to DLNs, and although the TLR9–MyD88–IRF7 signaling pathway is necessary for IMOs recruitment to DLNs, it is not directly necessary for type I IFN production. The induction of type I IFN in DLNs during ECTV infection is due to the indirect recognition of the virus by the TLR9–MyD88–IRF7 and STING–IRF7/NF-κB pathways (52). Compared with wild-type mice, mice lacking TLR9 and MyD88 showed higher viral loads, more severe pathological liver and spleen conditions, and increased susceptibility to ECTV infection (53–55). C57BL/6 mice lacking IRF7 and NF-κB, which are downstream targets of TLR9–MyD88 and STING, are highly susceptible to ECTV infection (52).

AIM2

Absent in melanoma 2 (AIM2), a member of the PYHIN protein family, is a receptor of cytoplasmic DNA. AIM2 senses viral DNA and can activate the inflammasome pathway (56, 57), which plays an important role in the production of pro-inflammatory cytokines and the clearance of infected cells through pyroptosis (58). After AIM2 binds to DNA through its HIN200 domain, caspase-1 is recruited and activated, leading to the production of inflammatory cytokines, including IL-1β and IL-18. Disabling AIM2 inhibits caspase-1 activation by cytoplasmic dsDNA and VACV infection (59, 60). More importantly, AIM2-deficient cells have a defective innate immune response to VACV (61).

IFI16, DNA-PK, AND OTHER DNA SENSORS

IFI16, a member of the PYHIN protein family, recognizes the DNA virus genome in the nucleus and activates antiviral

gene expression and the inflammasome-mediated immune response. IFI16 is mainly located in the nucleus but can also shuttle between the cytoplasm and nucleus in different types of cells (62). IFI16 could bind to the dsDNA fragment of 70 bp from the VACV genome (48). It can also interact with STING to induce the TBK1-dependent IFN-β response. The nuclear induction of IFI16 upon cell exposure to viral DNA activates the inflammasome pathway through ASC and caspase-1, resulting in the production of IL-1β and IL-18 (63).

Both IFI16 and cGAS are necessary for the activation of STING, which is induced by cGAMP. They interact with STING to promote its phosphorylation and translocation. IFI16 is the main nuclear DNA receptor, while cGAS plays an auxiliary role. For example, upon the stabilization of IFI16 to initiate or prolong signal enhancement, the synergistic effect of IFI16 and cGAS can induce immune signaling in response to exogenous DNA in the nucleus (64, 65).

DNA-PK is a protein kinase that binds to cytoplasmic DNA. It is composed of Ku70, Ku80, and catalytic subunit DNA-PKCs. In the case of VACV infection, DNA-PK relies on STING, TBK1, and IRF3 to induce cytokine production (32, 45–47). PRR detection of DNA triggers the production of type I IFN, cytokines, and chemokines through the STING pathway (51).

DNA viruses usually release genomic DNA into the nucleus of host cells after entry. Heterogeneous nuclear ribonucleoprotein A2B1 (HnRNPA2B1) recognizes viral DNA, undergoes homodimerization, and is demethylated by arginine demethylase JMJD6 at Arg226. This modification results in hnRNPA2B1 translocation to the cytoplasm and activation of the TBK1–IRF3 pathway, which enhances IFN-α/β production. In addition, hnRNPA2B1 promotes the modification of N6-methyladenosine (m6A) and the nuclear and cytoplasmic transport of cGAS, IFI16, and spiny mRNA. These factors mediate the amplified activation of the cytoplasmic TBK1–IRF3 pathway. Therefore, nuclear hnRNPA2B1 initiates and amplifies the innate immune response to DNA viruses (52).

RNA polymerase III is a new type of dsDNA cytoplasmic DNA sensor, and RIG-I is pivotal in sensing viral RNA. AT-rich dsDNA serves as a template for this DNA sensor, RNA polymerase III converts poly(dA:dT) to poly(A:U)-rich dsRNA, which, in turn, serves as a RIG-I agonist. Then, activation of RIG-I by this dsRNA induces the production of type I IFN and activation of the transcription factor NF-κB (53–55).

VIRAL ANTAGONISM

Poxvirus inhibits innate immunity through diverse mechanisms that involve multiple players including sensors, adaptors, and effectors. In this review, we focus on sensors and the most recent studies on adaptors and effectors. Therefore, only a small number of poxvirus immune antagonistic proteins are discussed. More poxvirus immune evasion mechanisms have been summarized in previous studies (4, 66–69).

DNA SENSORS

cGAS is the main sensor that mediates IRF activation and ISG response to VACV lacking F17 (44, 70). The poxvirus F17 protein hijacks the mammalian target of rapamycin (mTOR) regulatory factors Raptor and Rictor, leading to an mTOR imbalance. Excess mTOR accumulates in the Golgi apparatus and causes mTOR-dependent cGAS degradation, thus inactivating the cGAS–STING pathway (71). In contrast, when VACV lacking F17 infects the cells, cGAS activates STING. Then, STING is phosphorylated, dimerized, and translocated from the endoplasmic reticulum (ER) to the perinuclear region, where it mediates the activation of IRF3 (72).

DNA-PK can be antagonized by VACV proteins C16 and C4. C16 and C4 bind to Ku and block the binding of Ku to DNA (73), resulting in the reduced production of cytokines and chemokines, decreased recruitment of inflammatory cells, and inhibition of IRF3 signaling. The response to VACV infection is weakened in cells and mice lacking DNA-PK components (49). A model infected with C16-knockout VACV show fewer signs of disease and upregulated cytokine synthesis (73, 74). C4 inhibits NF-κB signaling (75) and cytokine production *in vitro* and *in vivo*. The loss of C4 enhances the recruitment and activation of cells involved in innate and acquired immunity.

ADAPTORS

Georgana et al. studied the activation of innate immune signals by four different VACV prototypes. They found that the virulent Copenhagen and Western Reserve VACV strains inhibited STING dimerization and phosphorylation during infection and in response to transfected DNA and cGAMP, thus effectively inhibiting DNA sensing and the activation of IRF3. However, an attenuated MVA strain showed the opposite result, and IRF3 was activated by cGAS and STING after infection (70). Georgana et al. found that virus-encoded protein C16 is a viral DNA sensing inhibitor that acts upstream of STING and has the ability to block STING activation (70).

DOWNSTREAM SIGNALING MOLECULES

The mutation of serine to alanine in the IκBα-like motif of A49 prevented β-TrCP binding, stabilized p-IκBα and inhibited the activation of NF-κB (76). B14 targets IKK complex and inhibits the activation of NF-κB in response to TNF-α, IL-1β, Poly(I:C), and PMA (77). The intracellular immunomodulatory proteins K1L, N1L, and A52R can inhibit the NF-κB signaling pathway (44, 78, 79).

VACV virulence factor N1 is a 14 kDa cytoplasmic protein that facilitates an increase in virulence (80, 81) and plays an inhibitory role in the cGAS–STING–IRF3-dependent cytoplasmic DNA-sensing pathway and in IFN-β gene induction (82).

Poxvirus protein serine protease inhibitor 2 (SPI-2) and cytokine response modifier (CrmA) are involved in a variety of poxvirus immune escape strategies. SPI-2 and CrmA target caspase-1 to prevent apoptosis and cytokine activation. The ectopic expression of SPI-2 or CrmA inhibits the induction of

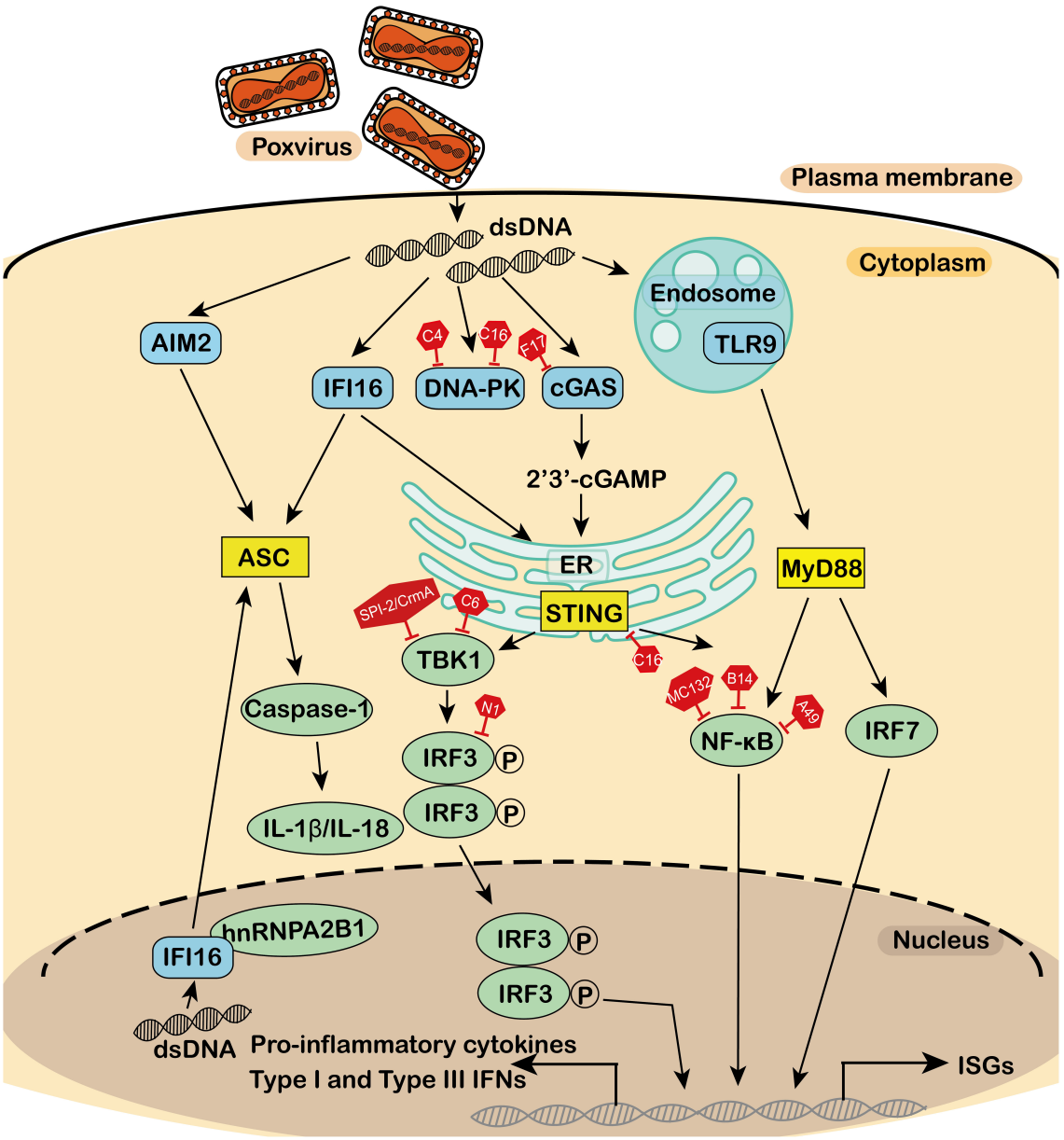

FIGURE 1 | Antagonism of the DNA sensor by poxvirus. During poxvirus infection, the cytosolic DNA sensor activates the adaptor, which in turn activates a series of downstream effectors to produce interferons, cytokines, and interleukins for an antiviral immune response. DNA sensors, adaptors, effectors, and virus-encoded inhibitors are in blue, yellow, green, and red, respectively. dsDNA, double-stranded DNA; TLR9, toll-like receptor 9; IFI16, interferon-γ inducible protein 16; cGAS, cyclic guanosine monophosphate-adenosine monophosphate synthase; DNA-PK, DNA-dependent protein kinase; AIM2, absent in melanoma 2; MyD88, myeloid differentiation factor 88; STING, stimulator of interferon genes; ASC, apoptosis-associated speck-like protein containing a CARD; IFN, interferons; CK, cytokines; NF-κB, nuclear factor κB; TBK1, TANK-binding kinase 1; IRF3, interferon regulatory factor 3; P, phosphorylation; IRF7, interferon regulatory factor 7; IL, interleukin; HnRNPA2B1, heterogeneous nuclear ribonucleoprotein A2B1; ER, endoplasmic reticulum; ISGs, IFN stimulating genes.

IFN-β and its downstream genes. SPI-2 and CrmA can also bind to TBK1 and IKKε to disrupt the STING-TBK1/IKK ε-IRF3 complex, which is a newly discovered mechanism of the SPI-2/CrmA–mediated immune escape of poxvirus (83).

VACV expresses many proteins that antagonize the IFN system. C6 is a multifunctional IFN inhibitor expressed prior to viral genome replication and resides in the cytoplasm and nucleus. It can reduce IFN production and inhibit IFN-induced signal transduction, thus inhibiting ISG expression (84). C6 inhibits the activation of IRF3 by binding to TBK1 in the cytoplasm, thus blocking the induction of IFN by IRF3 (84).

Poxvirus encodes several soluble IFN receptors. For instance, VACV B8 interacts with IFN-γ and prevents it from binding to IFN-γ receptors (85–87). VACV B18 binds to type I IFN and blocks the signal transduction of IFNAR (88–91).

CONCLUSION AND PERSPECTIVES

In this review, we discussed the interplay between poxvirus and host antiviral innate immune factors, particularly focusing on the STING pathway (**Figure 1**). The sensor proteins upstream of STING are cGAS, DNA-PK, and IFI16. There are two pathways of downstream STING effectors: TBK1-IRF3 and IKK-NF-κB. These two signaling pathways induce the production of IFNs and cytokines. In addition, we also described other signaling pathways that trigger the innate immune response.

Subcellular compartments are involved in the spatiotemporal interplay between poxviruses and DNA sensing molecules. TLR9 is located in endosomes, while STING is located in the ER. Yip1 Domain Family Member 5 (YIPF5) is recycled between the ER and the Golgi, involving the maintenance of the Golgi structure. YIPF5 recruits STING to COPII vesicles and facilitates STING trafficking from the ER to the Golgi apparatus, triggering type I IFN production (92). Interestingly, cGAS and IFI16 are located in the nucleus and cytoplasm. Acetylation of nuclear localization signal sequences targets IFI16 to the cytoplasm, thus fine-tuning the subcellular distribution of IFI16. Endogenous cGAS seems to be uniformly distributed in the cytoplasm and nucleus (93). Although poxvirus replicates in the cytoplasm, many viral proteins are located in the nucleus. cGAS and IFI16 are partially localized to the nucleus; however, no nuclear poxvirus proteins are reported to antagonize cGAS or IFI16 in the nucleus.

To successfully survive, the poxvirus genome encodes a number of immunomodulatory proteins to escape the innate immune response. The key challenge is to translate the viral evasion mechanism into useful applications for the development of new vaccines and antiviral drugs. Knockouts of immunomodulatory proteins or the depletion of specific viral PRR antagonistic mechanisms may lead to changes in virulence and/or the immune response, which may effectively induce long-lasting immune antiviral responses and may improve the immunogenicity of viral vectors.

Through these recent achievements, we have gained a richer understanding of viral evasion mechanisms in host cells. However, there are gaps that need to be investigated further. Firstly, how the interplay between poxvirus and innate immune response affects human viral diseases is unknown. Secondly, what are the relative contributions of the many DNA sensors required for poxvirus sensing? There is no definite answer to date. Finally, what might be the unique viral ligands that activate distinct DNA sensors? Are these DNA sensors involved in different cell types? Determining the molecular mechanism of poxvirus evasion will not only greatly contribute to important insights for the development of antiviral drugs and vaccines but will also provide a viral model for the future study of viral antagonism to host immunity.

AUTHOR CONTRIBUTIONS

LZ conceived the work and modified the manuscript. YL drafted the manuscript. All authors contributed to the article and approved the submitted version.

FUNDING

This work was supported by grants from National Natural Science Foundation of China (81871663 and 81672035) and Academic Promotion Programme of Shandong First Medical University (2019LJ001).

REFERENCES

1. Moss, B. (2015). Poxvirus membrane biogenesis. *Virology.* 479–80:619–26. doi: 10.1016/j.virol.2015.02.003
2. Smith GL, Talbot-Cooper C, Lu Y. How does vaccinia virus interfere with interferon? *Adv Virus Res.* (2018) 100:355–78. doi: 10.1016/bs.aivir.2018.01.003
3. Andzhaparidze OG, Slepushkin AN. The 30th anniversary of the adoption by the World Health Organization of the program for smallpox eradication throughout the world. *Vopr Virusol.* (1988) 33:517–23.
4. Smith GL, Benfield CTO, Maluquer de Motes C, Mazzon M, Ember SWJ, Ferguson BJ, et al. Vaccinia virus immune evasion: mechanisms, virulence and immunogenicity. *J Gen Virol.* (2013) 94:2367–92. doi: 10.1099/vir.0.055921-0
5. Garver J, Weber L, Vela EM, Anderson M, Warren R, Merchlinsky M, et al. Ectromelia virus disease characterization in the BALB/c mouse: a surrogate model for assessment of smallpox medical countermeasures. *Viruses.* (2016) 8:70203. doi: 10.3390/v8070203
6. Usme-Ciro JA, Paredes A, Walteros DM, Tolosa-Perez EN, Laiton-Donato K, Pinzon MD, et al. Detection and molecular characterization of zoonotic poxviruses circulating in the Amazon Region of Colombia, 2014. *Emerg Infect Dis.* (2017) 23:649–53. doi: 10.3201/eid2304.161041
7. Luecke S, Paludan SR. Molecular requirements for sensing of intracellular microbial nucleic acids by the innate immune system. *Cytokine.* (2017) 98:4–14. doi: 10.1016/j.cyto.2016.10.003
8. Ma Z, Ni G, Damania B. Innate sensing of DNA virus genomes. *Annu Rev Virol.* (2018) 5:341–62. doi: 10.1146/annurev-virology-092917-043244
9. Orzalli MH, Conwell SE, Berrios C, DeCaprio JA, Knipe DM. Nuclear interferon-inducible protein 16 promotes silencing of herpesviral and transfected DNA. *Proc Natl Acad Sci USA.* (2013) 110:E4492–501. doi: 10.1073/pnas.1316194110
10. Wu J, Chen ZJ. Innate immune sensing and signaling of cytosolic nucleic acids. *Annu Rev Immunol.* (2014) 32:461–88. doi: 10.1146/annurev-immunol-032713-120156
11. Brubaker SW, Bonham KS, Zanoni I, Kagan JC. Innate immune pattern recognition: a cell biological perspective. *Annu Rev Immunol.* (2015) 33:257–90. doi: 10.1146/annurev-immunol-032414-112240
12. Hwang S, Kim KS, Flano E, Wu TT, Tong LM, Park AN, et al. Conserved herpesviral kinase promotes viral persistence by inhibiting the IRF-3-mediated type I interferon response. *Cell Host Microbe.* (2009) 5:166–78. doi: 10.1016/j.chom.2008.12.013
13. Schmidt FI, Bleck CK, Reh L, Novy K, Wollscheid B, Helenius A, et al. Vaccinia virus entry is followed by core activation and proteasome-mediated release of the immunomodulatory effector VH1 from lateral bodies. *Cell Rep.* (2013) 4:464–76. doi: 10.1016/j.celrep.2013.06.028
14. Gubser C, Hue S, Kellam P, Smith GL. Poxvirus genomes: a phylogenetic analysis. *J Gen Virol.* (2004) 85:105–17. doi: 10.1099/vir.0.19565-0
15. Bowie AG, Unterholzner L. Viral evasion and subversion of pattern-recognition receptor signalling. *Nat Rev Immunol.* (2008) 8:911–22. doi: 10.1038/nri2436
16. Elde NC, Child SJ, Eickbush MT, Kitzman JO, Rogers KS, Shendure J, et al. Poxviruses deploy genomic accordions to adapt rapidly against host antiviral defenses. *Cell.* (2012) 150:831–41. doi: 10.1016/j.cell.2012.05.049

17. Sun L, Wu J, Du F, Chen X, Chen ZJ. Cyclic GMP-AMP synthase is a cytosolic DNA sensor that activates the type I interferon pathway. *Science.* (2013) 339:786–91. doi: 10.1126/science.1232458
18. Kranzusch PJ, Wilson SC, Lee AS, Berger JM, Doudna JA, Vance RE. Ancient origin of cGAS-STING reveals mechanism of universal 2',3' cGAMP signaling. *Mol Cell.* (2015) 59:891–903. doi: 10.1016/j.molcel.2015.07.022
19. Sun W, Li Y, Chen L, Chen H, You F, Zhou X, et al. ERIS, an endoplasmic reticulum IFN stimulator, activates innate immune signaling through dimerization. *Proc Natl Acad Sci USA.* (2009) 106:8653–8. doi: 10.1073/pnas.0900850106
20. Gao D, Wu J, Wu YT, Du F, Aroh C, Yan N, et al. Cyclic GMP-AMP synthase is an innate immune sensor of HIV and other retroviruses. *Science.* (2013) 341:903–6. doi: 10.1126/science.1240933
21. Lahaye X, Satoh T, Gentili M, Cerboni S, Conrad C, Hurbain I, et al. The capsids of HIV-1 and HIV-2 determine immune detection of the viral cDNA by the innate sensor cGAS in dendritic cells. *Immunity.* (2013) 39:1132–42. doi: 10.1016/j.immuni.2013.11.002
22. Gao J, Tao J, Liang W, Jiang Z. Cyclic (di)nucleotides: the common language shared by microbe and host. *Curr Opin Microbiol.* (2016) 30:79–87. doi: 10.1016/j.mib.2015.12.005
23. Tao J, Zhou X, Jiang Z. cGAS-cGAMP-STING: the three musketeers of cytosolic DNA sensing and signaling. *IUBMB Life.* (2016) 68:858–70. doi: 10.1002/iub.1566
24. Kieser KJ, Kagan JC. Multi-receptor detection of individual bacterial products by the innate immune system. *Nat Rev Immunol.* (2017) 17:376–90. doi: 10.1038/nri.2017.25
25. Ablasser A, Goldeck M, Cavlar T, Deimling T, Witte G, Rohl I, et al. cGAS produces a 2'-5'-linked cyclic dinucleotide second messenger that activates STING. *Nature.* (2013) 498:380–4. doi: 10.1038/nature12306
26. Diner EJ, Burdette DL, Wilson SC, Monroe KM, Kellenberger CA, Hyodo M, et al. The innate immune DNA sensor cGAS produces a noncanonical cyclic dinucleotide that activates human STING. *Cell Rep.* (2013) 3:1355–61. doi: 10.1016/j.celrep.2013.05.009
27. Gao P, Ascano M, Wu Y, Barchet W, Gaffney BL, Zillinger T, et al. Cyclic [G(2',5')pA(3',5')p] is the metazoan second messenger produced by DNA-activated cyclic GMP-AMP synthase. *Cell.* (2013) 153:1094–107. doi: 10.1016/j.cell.2013.04.046
28. Wu J, Sun L, Chen X, Du F, Shi H, Chen C, et al. Cyclic GMP-AMP is an endogenous second messenger in innate immune signaling by cytosolic DNA. *Science.* (2013) 339:826–30. doi: 10.1126/science.1229963
29. Zhang X, Shi H, Wu J, Zhang X, Sun L, Chen C, et al. Cyclic GMP-AMP containing mixed phosphodiester linkages is an endogenous high-affinity ligand for STING. *Mol Cell.* (2013) 51:226–35. doi: 10.1016/j.molcel.2013.05.022
30. Ishikawa H, Barber GN. STING is an endoplasmic reticulum adaptor that facilitates innate immune signalling. *Nature.* (2008) 455:674–8. doi: 10.1038/nature07317
31. Zhong B, Yang Y, Li S, Wang YY, Li Y, Diao F, et al. The adaptor protein MITA links virus-sensing receptors to IRF3 transcription factor activation. *Immunity.* (2008) 29:538–50. doi: 10.1016/j.immuni.2008.09.003
32. Tanaka Y, Chen ZJ. STING specifies IRF3 phosphorylation by TBK1 in the cytosolic DNA signaling pathway. *Sci Signal.* (2012) 5:ra20. doi: 10.1126/scisignal.2002521
33. Liu S, Cai X, Wu J, Cong Q, Chen X, Li T, et al. Phosphorylation of innate immune adaptor proteins MAVS, STING, and TRIF induces IRF3 activation. *Science.* (2015) 347:aaa2630. doi: 10.1126/science.aaa2630
34. Cheng WY, He XB, Jia HJ, Chen GH, Jin QW, Long ZL, et al. The cGas-sting signaling pathway is required for the innate immune response against ectromelia virus. *Front Immunol.* (2018) 9:1297. doi: 10.3389/fimmu.2018.01297
35. Li XD, Wu J, Gao D, Wang H, Sun L, Chen ZJ. Pivotal roles of cGAS-cGAMP signaling in antiviral defense and immune adjuvant effects. *Science.* (2013) 341:1390–4. doi: 10.1126/science.1244040
36. Schoggins JW, MacDuff DA, Imanaka N, Gainey MD, Shrestha B, Eitson JL, et al. Pan-viral specificity of IFN-induced genes reveals new roles for cGAS in innate immunity. *Nature.* (2014) 505:691–5. doi: 10.1038/nature12862
37. Ablasser A, Schmid-Burgk JL, Hemmerling I, Horvath GL, Schmidt T, Latz E, et al. Cell intrinsic immunity spreads to bystander cells via the intercellular transfer of cGAMP. *Nature.* (2013) 503:530–4. doi: 10.1038/nature12640
38. Ghosh A, Shao L, Sampath P, Zhao B, Patel NV, Zhu J, et al. Oligoadenylate-synthetase-family protein OASL inhibits activity of the DNA sensor cGAS during DNA virus infection to limit interferon production. *Immunity.* (2019) 50:51–63 e55. doi: 10.1016/j.immuni.2018.12.013
39. Meyer H, Sutter G, Mayr A. Mapping of deletions in the genome of the highly attenuated vaccinia virus MVA and their influence on virulence. *J Gen Virol.* (1991) 72:1031–8. doi: 10.1099/0022-1317-72-5-1031
40. McCurdy LH, Larkin BD, Martin JE, Graham BS. Modified vaccinia Ankara: potential as an alternative smallpox vaccine. *Clin Infect Dis.* (2004) 38:1749–53. doi: 10.1086/421266
41. Vollmar J, Arndtz N, Eckl KM, Thomsen T, Petzold B, Mateo L, et al. Safety and immunogenicity of IMVAMUNE, a promising candidate as a third generation smallpox vaccine. *Vaccine.* (2006) 24:2065–70. doi: 10.1016/j.vaccine.2005.11.022
42. Sutter G, Staib C. Vaccinia vectors as candidate vaccines: the development of modified vaccinia virus Ankara for antigen delivery. *Curr Drug Targets Infect Disord.* (2003) 3:263–71. doi: 10.2174/1568005033481123
43. Gomez CE, Najera JL, Krupa M, Esteban M. The poxvirus vectors MVA and NYVAC as gene delivery systems for vaccination against infectious diseases and cancer. *Curr Gene Ther.* (2008) 8:97–120. doi: 10.2174/156652308784049363
44. Dai P, Wang W, Cao H, Avogadri F, Dai L, Drexler I, et al. Modified vaccinia virus Ankara triggers type I IFN production in murine conventional dendritic cells via a cGAS/STING-mediated cytosolic DNA-sensing pathway. *PLoS Pathog.* (2014) 10:e1003989. doi: 10.1371/journal.ppat.1003989
45. Ishii KJ, Kawagoe T, Koyama S, Matsui K, Kumar H, Kawai T, et al. TANK-binding kinase-1 delineates innate and adaptive immune responses to DNA vaccines. *Nature.* (2008) 451:725–9. doi: 10.1038/nature06537
46. Zyzak J, Mitkiewicz M, Leszczyńska E, Reniewicz P, Moynagh PN, Siednienko J. HSV-1/TLR9-mediated IFNβ and TNFα induction is mal-dependent in macrophages. *J Innate Immun.* (2019) 18:1–12. doi: 10.1159/000504542
47. Ishikawa H, Ma Z, Barber GN. STING regulates intracellular DNA-mediated, type I interferon-dependent innate immunity. *Nature.* (2009) 461:788–92. doi: 10.1038/nature08476
48. Unterholzner L, Keating SE, Baran M, Horan KA, Jensen SB, Sharma S, et al. IFI16 is an innate immune sensor for intracellular DNA. *Nat Immunol.* (2010) 11:997–1004. doi: 10.1038/ni.1932
49. Ferguson BJ, Mansur DS, Peters NE, Ren H, Smith GL. DNA-PK is a DNA sensor for IRF-3-dependent innate immunity. *Elife.* (2012) 1:e00047. doi: 10.7554/eLife.00047.012
50. Kawai T, Akira S. Toll-like receptors and their crosstalk with other innate receptors in infection and immunity. *Immunity.* (2011) 34:637–50. doi: 10.1016/j.immuni.2011.05.006
51. Wong E, Xu RH, Rubio D, Lev A, Stotesbury C, Fang M, et al. Migratory dendritic cells, group 1 innate lymphoid cells, and inflammatory monocytes collaborate to recruit NK cells to the virus-infected lymph node. *Cell Rep.* (2018) 24:142–54. doi: 10.1016/j.celrep.2018.06.004
52. Xu RH, Wong EB, Rubio D, Roscoe F, Ma X, Nair S, et al. Sequential activation of two pathogen-sensing pathways required for type i interferon expression and resistance to an acute DNA virus infection. *Immunity.* (2015) 43:1148–59. doi: 10.1016/j.immuni.2015.11.015
53. Samuelsson C, Hausmann J, Lauterbach H, Schmidt M, Akira S, Wagner H, et al. Survival of lethal poxvirus infection in mice depends on TLR9, and therapeutic vaccination provides protection. *J Clin Invest.* (2008) 118:1776–84. doi: 10.1172/JCI33940
54. Sutherland DB, Ranasinghe C, Regner M, Phipps S, Matthaei KI, Day SL, et al. Evaluating vaccinia virus cytokine co-expression in TLR GKO mice. *Immunol Cell Biol.* (2011) 89:706–15. doi: 10.1038/icb.2010.157
55. Rubio D, Xu RH, Remakus S, Krouse TE, Truckenmiller ME, Thapa RJ, et al. Crosstalk between the type 1 interferon and nuclear factor kappa B pathways confers resistance to a lethal virus infection. *Cell Host Microbe.* (2013) 13:701–10. doi: 10.1016/j.chom.2013.04.015
56. Burckstummer T, Baumann C, Bluml S, Dixit E, Durnberger G, Jahn H, et al. An orthogonal proteomic-genomic screen identifies AIM2 as a

cytoplasmic DNA sensor for the inflammasome. *Nat Immunol.* (2009) 10:266–72. doi: 10.1038/ni.1702
57. Roberts TL, Idris A, Dunn JA, Kelly GM, Burnton CM, Hodgson S, et al. HIN-200 proteins regulate caspase activation in response to foreign cytoplasmic DNA. *Science.* (2009) 323:1057–60. doi: 10.1126/science.1169841
58. Kanneganti TD. Central roles of NLRs and inflammasomes in viral infection. *Nat Rev Immunol.* (2010) 10:688–98. doi: 10.1038/nri2851
59. Fernandes-Alnemri T, Yu JW, Datta P, Wu J, Alnemri ES. AIM2 activates the inflammasome and cell death in response to cytoplasmic DNA. *Nature.* (2009) 458:509–13. doi: 10.1038/nature07710
60. Hornung V, Ablasser A, Charrel-Dennis M, Bauernfeind F, Horvath G, Caffrey DR, et al. AIM2 recognizes cytosolic dsDNA and forms a caspase-1-activating inflammasome with ASC. *Nature.* (2009) 458:514–8. doi: 10.1038/nature07725
61. Rathinam VA, Jiang Z, Waggoner SN, Sharma S, Cole LE, Waggoner L, et al. The AIM2 inflammasome is essential for host defense against cytosolic bacteria and DNA viruses. *Nat Immunol.* (2010) 11:395–402. doi: 10.1038/ni.1864
62. Dell'Oste V, Gatti D, Giorgio AG, Gariglio M, Landolfo S, De Andrea M. The interferon-inducible DNA-sensor protein IFI16: a key player in the antiviral response. *New Microbiol.* (2015) 38:5–20.
63. Kerur N, Veettil MV, Sharma-Walia N, Bottero V, Sadagopan S, Otageri P, et al. IFI16 acts as a nuclear pathogen sensor to induce the inflammasome in response to Kaposi Sarcoma-associated herpesvirus infection. *Cell Host Microbe.* (2011) 9:363–75. doi: 10.1016/j.chom.2011.04.008
64. Hemmi H, Takeuchi O, Kawai T, Kaisho T, Sato S, Sanjo H, et al. A Toll-like receptor recognizes bacterial DNA. *Nature.* (2000) 408:740–5. doi: 10.1038/35047123
65. Latz E, Schoenemeyer A, Visintin A, Fitzgerald KA, Monks BG, Knetter CF, et al. TLR9 signals after translocating from the ER to CpG DNA in the lysosome. *Nat Immunol.* (2004) 5:190–8. doi: 10.1038/ni1028
66. Rahman MM, McFadden G. Modulation of NF-κB signalling by microbial pathogens. *Nat Rev Microbiol.* (2011) 9:291–306. doi: 10.1038/nrmicro2539
67. Brady G, Bowie AG. Innate immune activation of NFκB and its antagonism by poxviruses. *Cytokine Growth Factor Rev.* (2014) 25:611–20. doi: 10.1016/j.cytogfr.2014.07.004
68. Bidgood SR, Mercer J. Cloak and dagger: alternative immune evasion and modulation strategies of poxviruses. *Viruses.* (2015) 7:4800–25. doi: 10.3390/v7082844
69. Shisler JL. Immune evasion strategies of molluscum contagiosum virus. *Adv Virus Res.* (2015) 92:201–52. doi: 10.1016/bs.aivir.2014.11.004
70. Georgana I, Sumner RP, Towers GJ, Maluquer de Motes C. Virulent poxviruses inhibit DNA sensing by preventing STING activation. *J Virol.* (2018) 92:17. doi: 10.1128/JVI.02145-17
71. Meade N, King M, Munger J, Walsh D. mTOR dysregulation by vaccinia virus F17 controls multiple processes with varying roles in infection. *J Virol.* (2019) 93:19. doi: 10.1128/JVI.00784-19
72. Meade N, Furey C, Li H, Verma R, Chai Q, Rollins MG, et al. Poxviruses evade cytosolic sensing through disruption of an mTORC1-mTORC2 regulatory circuit. *Cell.* (2018) 174:1143–57 e1117. doi: 10.1016/j.cell.2018.06.053
73. Peters NE, Ferguson BJ, Mazzon M, Fahy AS, Krysztofinska E, Arribas-Bosacoma R, et al. A mechanism for the inhibition of DNA-PK-mediated DNA sensing by a virus. *PLoS Pathog.* (2013) 9:e1003649. doi: 10.1371/journal.ppat.1003649
74. Fahy AS, Clark RH, Glyde EF, Smith GL. Vaccinia virus protein C16 acts intracellularly to modulate the host response and promote virulence. *J Gen Virol.* (2008) 89:2377–87. doi: 10.1099/vir.0.2008/004895-0
75. Ember SWJ, Ren H, Ferguson BJ, Smith GL. Vaccinia virus protein C4 inhibits NF-kappaB activation and promotes virus virulence. *J Gen Virol.* (2012) 93:2098–108. doi: 10.1099/vir.0.045070-0
76. Mansur DS, Maluquer de Motes C, Unterholzner L, Sumner RP, Ferguson BJ, Ren H, et al. Poxvirus targeting of E3 ligase beta-TrCP by molecular mimicry: a mechanism to inhibit NF-kappaB activation and promote immune evasion and virulence. *PLoS Pathog.* (2013) 9:e1003183. doi: 10.1371/journal.ppat.1003183
77. Chen RA, Ryzhakov G, Cooray S, Randow F, Smith GL. Inhibition of IkappaB kinase by vaccinia virus virulence factor B14. *PLoS Pathog.* (2008) 4:e22. doi: 10.1371/journal.ppat.0040022
78. Lynch HE, Ray CA, Oie KL, Pollara JJ, Petty IT, Sadler AJ, et al. Modified vaccinia virus Ankara can activate NF-kappaB transcription factors through a double-stranded RNA-activated protein kinase (PKR)-dependent pathway during the early phase of virus replication. *Virology.* (2009) 391:177–86. doi: 10.1016/j.virol.2009.06.012
79. Willis KL, Patel S, Xiang Y, Shisler JL. The effect of the vaccinia K1 protein on the PKR-eIF2alpha pathway in RK13 and HeLa cells. *Virology.* (2009) 394:73–81. doi: 10.1016/j.virol.2009.08.020
80. Kotwal GJ, Hugin AW, Moss B. Mapping and insertional mutagenesis of a vaccinia virus gene encoding a 13,800-Da secreted protein. *Virology.* (1989) 171:579–87. doi: 10.1016/0042-6822(89)90627-2
81. Bartlett N, Symons JA, Tscharke DC, Smith GL. The vaccinia virus N1L protein is an intracellular homodimer that promotes virulence. *J Gen Virol.* (2002) 83:1965–76. doi: 10.1099/0022-1317-83-8-1965
82. DiPerna G, Stack J, Bowie AG, Boyd A, Kotwal G, Zhang Z, et al. Poxvirus protein N1L targets the I-kappaB kinase complex, inhibits signaling to NF-kappaB by the tumor necrosis factor superfamily of receptors, and inhibits NF-kappaB and IRF3 signaling by toll-like receptors. *J Biol Chem.* (2004) 279:36570–8. doi: 10.1074/jbc.M400567200
83. Qin Y, Li M, Zhou SL, Yin W, Bian Z, Shu HB. SPI-2/CrmA inhibits IFN-beta induction by targeting TBK1/IKKepsilon. *Sci Rep.* (2017) 7:10495. doi: 10.1038/s41598-017-11016-3
84. Unterholzner L, Sumner RP, Baran M, Ren H, Mansur DS, Bourke NM, et al. Vaccinia virus protein C6 is a virulence factor that binds TBK-1 adaptor proteins and inhibits activation of IRF3 and IRF7. *PLoS Pathog.* (2011) 7:e1002247. doi: 10.1371/journal.ppat.1002247
85. Alcami A, Smith GL. Vaccinia, cowpox, and camelpox viruses encode soluble gamma interferon receptors with novel broad species specificity. *J Virol.* (1995) 69:4633–9. doi: 10.1128/JVI.69.8.4633-4639.1995
86. Mossman K, Upton C, Buller RM, McFadden G. Species specificity of ectromelia virus and vaccinia virus interferon-gamma binding proteins. *Virology.* (1995) 208:762–9. doi: 10.1006/viro.1995.1208
87. Symons JA, Tscharke DC, Price N, Smith GL. A study of the vaccinia virus interferon-gamma receptor and its contribution to virus virulence. *J Gen Virol.* (2002) 83:1953–64. doi: 10.1099/0022-1317-83-8-1953
88. Colamonici OR, Domanski P, Sweitzer SM, Larner A, Buller RM. Vaccinia virus B18R gene encodes a type I interferon-binding protein that blocks interferon alpha transmembrane signaling. *J Biol Chem.* (1995) 270:15974–8. doi: 10.1074/jbc.270.27.15974
89. Symons JA, Alcami A, Smith GL. Vaccinia virus encodes a soluble type I interferon receptor of novel structure and broad species specificity. *Cell.* (1995) 81:551–60. doi: 10.1016/0092-8674(95)90076-4
90. Alcami A, Symons JA, Smith GL. The vaccinia virus soluble alpha/beta interferon (IFN) receptor binds to the cell surface and protects cells from the antiviral effects of IFN. *J Virol.* (2000) 74:11230–9. doi: 10.1128/JVI.74.23.11230-11239.2000
91. Montanuy I, Alejo A, Alcami A. Glycosaminoglycans mediate retention of the poxvirus type I interferon binding protein at the cell surface to locally block interferon antiviral responses. *FASEB J.* (2011) 25:1960–71. doi: 10.1096/fj.10-177188
92. Ran Y, Xiong MG, Xu ZS, Luo WW, Wang SY, Wang YY. YIPF5 is essential for innate immunity to DNA virus and facilitates COPII-dependent STING trafficking. *J Immunol.* (2019) 203:1560–70. doi: 10.4049/jimmunol.1900387
93. Orzalli MH, Broekema NM, Diner BA, Hancks DC, Elde NC, Cristea IM, et al. cGAS-mediated stabilization of IFI16 promotes innate signaling during herpes simplex virus infection. *Proc Natl Acad Sci USA.* (2015) 112:E1773–81. doi: 10.1073/pnas.1424637112

Conflict of Interest: The authors declare that the research was conducted in the absence of any commercial or financial relationships that could be construed as a potential conflict of interest.

frontiers in Immunology

REVIEW
published: 29 September 2020
doi: 10.3389/fimmu.2020.02064

When STING Meets Viruses: Sensing, Trafficking and Response

*Zhaohe Li[1], Siqi Cai[1], Yutong Sun[1], Li Li[1,2,3], Siyuan Ding[4] and Xin Wang[1,2,3]**

[1] Key Laboratory of Marine Drugs of Ministry of Education, School of Medicine and Pharmacy, Ocean University of China, Qingdao, China, [2] Center for Innovation Marine Drug Screening and Evaluation, Pilot National Laboratory for Marine Science and Technology, Qingdao, China, [3] Marine Biomedical Research Institute of Qingdao, Qingdao, China, [4] Department of Molecular Microbiology, School of Medicine, Washington University in St. Louis, St. Louis, MO, United States

To effectively defend against microbial pathogens, the host cells mount antiviral innate immune responses by producing interferons (IFNs), and hundreds of IFN-stimulated genes (ISGs). Upon recognition of cytoplasmic viral or bacterial DNAs and abnormal endogenous DNAs, the DNA sensor cGAS synthesizes 2',3'-cGAMP that induces STING (stimulator of interferon genes) undergoing conformational changes, cellular trafficking, and the activation of downstream factors. Therefore, STING plays a pivotal role in preventing microbial pathogen infection by sensing DNAs during pathogen invasion. This review is dedicated to the recent advances in the dynamic regulations of STING activation, intracellular trafficking, and post-translational modifications (PTMs) by the host and microbial proteins.

Keywords: STING, DNA viruses, cellular trafficking, post translational modifications, immune responses

OPEN ACCESS

Edited by:
Chunfu Zheng,
Fujian Medical University, China

Reviewed by:
Qi Wang,
Harbin Veterinary Research Institute (CAS), China
Junji Xing,
Houston Methodist Research Institute, United States

****Correspondence:***
Xin Wang
wx8399@ouc.edu.cn

Specialty section:
This article was submitted to Viral Immunology, a section of the journal Frontiers in Immunology

Received: *02 June 2020*
Accepted: *29 July 2020*
Published: *29 September 2020*

Citation:
Li Z, Cai S, Sun Y, Li L, Ding S and Wang X (2020) When STING Meets Viruses: Sensing, Trafficking and Response. Front. Immunol. 11:2064. doi: 10.3389/fimmu.2020.02064

INTRODUCTION

The immune response is a complicated process in which the body defends against pathogen infections and confines the disease progression, leading to the eventual recovery, and conferring protective immunity. Innate immunity is the first line to resist viral invasion. A myriad of host factors, such as interferons (IFNs), cytokines, and chemokines, respond quickly to viral invading, and trigger adaptive immunity (1). Due to the special biological features of viruses and their unique relationships with host cells, antiviral immunity not only shares commonalities with antibacterial immunity but also has unique characteristics. Invading viruses trigger innate immunity during and after entry into host cells via germline-encoded molecules termed pattern recognition receptors (PRRs), which detect pathogens by recognition of their conserved molecular structures, called pathogen-associated molecular patterns (PAMPs) (2). In this process, different PRRs jointly participate in the complicated and delicate immune responses by collaboration between multiple PRRs and their downstream factors. Until now, stimulator of interferon genes (STING) is the most important adaptor protein in immune responses against DNA viruses, in cooperation with other well-identified molecules, including cGAS, TBK1, IRF3, and NF-κB (3–5).

DNA VIRUS INFECTION, IMMUNE RESPONSE, AND DISEASES

To date, more than 6,000 types of viruses have been identified according to the International Committee on Taxonomy of Viruses (ICTV). There are approximately 400 kinds of viruses of human health concerns and many are double-stranded DNA (dsDNA) viruses or retroviruses.

For instance, the retrovirus human immunodeficient virus (HIV) is considered as a DNA virus here because of the viral dsDNA produced by reverse transcription process, leading to Acquired Immune Deficiency Syndrome (AIDS). Similarly, chronic infection with human hepatitis B virus (HBV), which is harboring a partial double-stranded genomic DNA and belongs to *Hepadnaviridae*, leads to liver fibrosis and cancers (6). Other pathogenic human DNA viruses mostly belong to the *Poxviridae*, *Herpesviridae*, *Adenoviridae*, *Papillomaviridae*, and *Polyomaviridae* families. In the *Herpesviridae* family, human cytomegalovirus (HCMV) causes immunocompromised symptoms of the brain, liver, spleen, and lung (7). Infection by the herpes simplex virus 1 (HSV-1) results in painful blisters or ulcers (8). What's more, it might lead to more serious symptoms including encephalitis. HSV-2 infection is a typical sexually transmitted disease (STD) with the symptom of different genital warts (9). Epstein-Barr virus (EBV) is involved in numerous types of lymphomas and gastric cancers (10). Kaposi's sarcoma–associated herpesvirus (KSHV) is found in Kaposi's sarcoma, primary effusion lymphoma, and multicentric Castleman's disease. The incidence of Kaposi's sarcoma is much higher in immunosuppressed individuals, because of the deficiency of host immunity (10, 11). Especially, Kaposi's sarcoma has a high fatality rate among AIDS patients (12). Virulent adenoviruses lead to the common cold, fever, sore throat, acute bronchitis, pneumonia, and neurologic disease (in rare cases) (13–15, 187). In the *Papillomaviridae* and *Polyomaviridae* families, high-risk human papillomaviruses (HPVs) are admittedly oncogenic and significantly related to cervical cancer and head and neck cancers (16), while low-risk HPVs are responsible for anogenital condyloma, genital warts, and other skin diseases (17). Merkle cell polyomavirus (MCPyV) integration is found in Merkle cell carcinoma. JC polyomavirus and BK polyomavirus are found in organ transplant patients (18, 19). Therefore, a thorough understanding of the arms race between DNA viruses and host immunity is required to develop therapeutic strategies for viral infections.

Innate immunity is vital to restrict viral infections at the early stages of host antiviral immunity (20). After the invasion, viral PAMPs stimulate IFN production in a variety of cells, which possess a broad-spectrum antiviral effect (21). Thus, they would induce antiviral albumin to block viral propagation (22). For innate immune responses to viral invasion, although PRRs and IFN signaling are constituently components in nearly all somatic cells to control early infections in our body, it is believed that leukocytes are the protagonists in the stage to clear propagating viruses, by either secreted IFNs, and cytokines or cell killing. In innate immune cells, macrophages are tissue-residents, and clear virions and infected cells by phagocytosis. Natural killer cells (NK cells) account for 5–10% of the total number of lymphocytes and are constantly undertaking "patrol" tasks in the body. Infected host cells that lack MHC-I molecules are within the scope of NK cell attacking (23, 24). Additionally, dendritic cells (DCs) are the main bridge between innate and adaptive immunity by antigen presentation. DCs are also the major producers of IFNs in the peripheral blood (25, 26).

CELLULAR SENSORS OF ABNORMAL DNA

Several DNA sensing PRRs have been characterized so far, including Toll-like receptors (TLRs), NOD-like receptors (NLRs), C-type lectin receptors (CLRs), and cytosolic DNA sensors including cyclic GMP–AMP synthase (cGAS), IFN-γ (IFN-γ)-inducible protein 16 (IFI16), heterogeneous nuclear ribonucleoprotein A2/B1 (hnRNPA2B1), absent in melanoma 2 (AIM2), DNA-dependent activator of IRFs (DAI), RNA polymerase III, DEAD box helicase 41 (DDX41), DEAH box protein 9 (DHX9)/DEAH box protein 36 (DHX36), leucine-rich repeat flightless-interacting protein 1 (LRRFIP1), Ku70, and Sox2 (3, 27, 28). As the first discovered DNA recognition molecule, DAI binds to dsDNA and induces type I IFN (IFN-I) (29, 30). However, the knockdown of DAI does not affect the innate immune response of mice to B-DNA stimulation in later studies, raising controversy (31). AIM2 is an IFN induced cytosolic protein containing a pyrin domain (PYD) and a HIN200 domain. The HIN domain promotes its binding to DNA. The PYD binds to ASC, the apoptosis-associated speck-like protein containing a caspase recruitment domain (CARD), forming an activated caspase-1 inflammasome to promote releases of IL-1β, and IL-18 (32). RNA polymerase III converts dsDNA poly (dA:dT) into 5′- triphosphate double-stranded RNA, delivering signals to the RIG-I pathway (33, 34). DDX41 (DEAD box polypeptide 41) promotes IFN and IFN-stimulated genes (ISGs) expression in a STING-dependent way. It recognizes intracellular DNA or bacterial c-*di*-GMP and c-*di*-AMP and then activates IRF3 by TBK1 (35, 36). IFI16 is predominantly a nuclear protein sensing abnormal DNA in the nucleus (37). HnRNPA2B1 is another recently reported nuclear initiation factor that detects and limits DNA virus infection (38).

Potentiating signals from many other DNA sensors and cyclic dinucleotides (CDNs) binding, places STING a nodal position to restrict DNA viruses. The first promised DNA sensor IFI16 implicating in IFN induction by DNA stimulation localizes both in the nucleus and the cytoplasm but may sense abnormal DNA in the nucleus (39), because HSV-1 ICP0 re-localizes IFI16 from the nucleus to the cytoplasm, hampering IFN responses to viruses (40). Active IFI16 recruits STING to facilitate a TBK1-dependent gene induction. Knockdown of IFI16 or its mouse ortholog p204 impairs IFN-I induction in response to dsDNA or HSV-1 genomic DNA (39). As the PYHIN protein AIM2, IFI16 can activate inflammasome-mediated immune responses (41, 42). DDX41 scaffolds DNA and STING in the cytosol for ISG induction. Knockdown of DDX41 blocks TBK1 phosphorylation, and IRF3- or NF-κB- dependent gene expression in mouse DCs (35). Nuclear protein Ku70 and hnRNPA2B1 also induce IFN expression by STING (43, 44). Ku70 is an important component in the DNA damage repair (DDR) machinery (45), collaborating with STING to maintain the host genomic integrity and clear damaged cells. However,

DNA viruses utilize host DDR components during viral DNA replication (46, 47), and the crosstalk between Ku70-STING might also contribute to antiviral immune responses. The newly-identified DNA sensor hnRNPA2B1 senses viral genomic DNA in the nucleus. Undergoing homodimerization and demethylation at the Arg226 site by JMJD6, hnRNPA2B1 translocate into the cytoplasm, where STING and TBK1 are recruiting. HnRNPA2B1 simultaneously promotes cGAS, IFI16, and STING expression, which in turn amplifies cGAS-STING signaling (38). It is noting that STING signals may crosstalk with the RIG-I-MAVS pathway during viral infections (48, 49).

The discovery of cGAS in DNA sensing process greatly expanded the understanding of intracellular exogenous or abnormal DNA sensing (3). Unlike other DNA sensors, cGAS catalyzes and releases the second messenger cGAMP from ATP and GTP after DNA recognitions, instead of directly binding to the adaptor protein STING (50, 51). Cytosolic cGAMP inserts into STING dimer and induces a conformation change, leading to the exposure of C-terminal tail (CTT) of STING for TBK1 recruitment (52, 53). Moreover, cGAS-deficient mice show a complete loss of IFN production in response to DNA stimulation or DNA virus infection (HSV-1, vaccinia virus, and murine γ herpesvirus). It indicates the importance of cGAS in DNA-induced immune responses. cGAMP can be transferred from infected cells to uninfected neighboring cells through gap junctions or exosomes, where it amplifies immune responses to DNA stimulation independent on IFN signaling (54). Leucine-rich repeat containing 8 VRAC subunit A (LRRC8) volume-regulated anion channel facilitates this process (55). These findings uncover a novel host strategy that rapidly conveys antiviral immunity to bystander cells independent of the paracrine signaling of IFNs.

RNA viruses, such as dengue virus, induce mitochondria DNA (mtDNA) leakage into the cytosol and trigger STING signaling (56, 57). This interesting observation partially explained the reduction of IFN expression response to RNA virus infection in STING-deficient cells. Adaptor protein TRIF facilitates STING signaling by the interaction with STING on its carboxyl-terminal domains to promote its dimerization and translocation (58). The crosstalk between adaptor protein STING, MAVS, and TRIF become interesting and elucidated now. Noticeably, these adaptor proteins share some common behaviors, such as phosphorylation patterns and oligomerization (59–61). Although these adaptor proteins seem to all play roles in detecting cytosolic DNA, their contributions to DNA-mediated gene induction are either partial or cell type specific.

THE STRUCTURE AND SUBCELLULAR LOCALIZATION OF STING

Abnormal cytosolic DNA molecules trigger a dsDNA sensing process, which consequently induces IFNs and ISGs expression (62). As mentioned above, nuclear DNA sensors also potentiate the signaling in the cytoplasm after intracellular translocation. STING locates in the ER and consists of four transmembrane regions, which is expressing in a variety of endothelial cells, epithelial cells, and hematopoietic hepatocytes (61, 63). Human STING encodes a protein of 379 amino acids (aa), containing a predicted transmembrane portion (1-173aa) in the N-terminus and an intracellular soluble portion (174-379aa) in the C-terminus (64). The N-terminus regulates its cellular localization and homodimerization, since the transmembrane domains cross the ER membrane (61, 65). The C-terminal domain (CTD) functionally docks downstream molecules, including TBK1/IKKε, and IRF3/IRF7 (66–68). To potentiate the signaling, the native ligand cGAMP binds to the V-shaped hydrophilic pocket in STING dimer (50). Undergoing a conformational change, the hidden CTT of STING is exposed to TBK1 and IRF3 (69–73). During this process, STING is transported from the ER to the ER-Golgi intermediate compartment (ERGIC), Golgi, and then perinuclear regions (74). Although the cGAMP induced STING activation via a closed conformation, the artificial agonist diABZI activates STING with an open conformation (75). It is still unclear that if STING conformation changes are required for the following intracellular translocation. Studies should be pursued to elucidate the details.

The classical STING signaling starts on the appearance of DNA in the cytoplasm, which is considered as an abnormal signal. Once triggered by free DNA in cytoplasm, cytoplasmic cGAS catalyzes the synthesis of cGAMP to activate STING (50, 76). Alternatively, other PRRs directly bind to STING, such as hnRNPA2B1 and IFI16 (38, 77). After activation, STING travels to the endosome through the ER and the Golgi apparatus via intracellular trafficking or autophagy process (78). STING dimers are closely arranged side by side in the lipid membrane under the active state. Dimerized STING can be connected to adjacent dimers, and these connections are stabilized by connecting the dimer's ring at its interface (79). Without cGAMP bound, the connecting element may stabilize the inhibitory direction of the interface loop. It is hypothesized that the rearrangement of the connecting element on cGAMP binding is related to the STING activation. Although it is still hard to understand how to form chemical bonds between adjacent STING dimers for the side by side oligomer maintenance, there is no other better explanation at this moment.

TBK1 dimer associates with STING at the perinuclear region after cellular trafficking. It docks on top of the cGAMP binding domain of STING. This interaction is mediated by the conserved eight amino acid residues in the CTT domain of STING, which is highly flexible, and hard to be crystalized (72). The peptide linker between cGAMP binding pocket and C-terminus of STING, allows TBK1, and STING to adopt different orientations with each other (50). The ligand cGAMP might be an initiator in the pathway and not needed in the following intracellular trafficking and TBK1 binding. Thus, cGAMP binds to dimerized STING in ER, triggers its conformation change and oligomerization to initiate signaling (50, 80). In the process, STING is transported to the ERGIC, Golgi, and perinuclear regions, where it meets downstream factors, including protein kinase TBK1/IKKε, transcription factors IRF3 and NF-κB, and other cellular factors. Ultimately, IRF3 is phosphorylated by

TBK1 and enters into the nucleus to induce IFN and cytokine production (4, 81–84).

STING-RELATED SIGNALING PATHWAY

As shown in **Figure 1**, in the presence of cytosolic DNA, STING translocates sequentially from the ER to ERGIC, Golgi apparatus, and eventually relocates to perinuclear regions where activated STING recruits TBK1 (63, 74). TBK1 phosphorylates and activates IFN regulatory factors (IRFs) and NF-κB, which induces IFN-I, IFN-III, and other pro-inflammatory genes (85, 86). IRF3 and TBK1 dock on polymerized STING complex, thus phosphorylated IRF3 dissociates from the complex and translocate into the nucleus to potentiate gene transcription (51, 84, 87). The regulation of STING signaling mainly focuses on the activation, trafficking, post-translational modifications (PTMs), and downstream pathway. Notably, TOLLIP exerts an important role in STING-mediated immune response and maintain the immune homeostasis. As a stabilizer of STING, TOLLIP interacts with STING directly and maintain the stabilization of STING protein by inhibiting the ER stress sensor IRE1α which suppresses resting-state of STING turnover. Knockdown of TOLLIP reduced the phosphorylation of IRF3 (88). In addition to the activation of STING signaling pathway, STING-mediated immune response also needs to maintain the stabilization of STING protein to ensure an effective response.

As activation, silencing is also critical in signal transduction. The negative feedback loop of STING signals is not clearly understood. To prevent chronic signaling, the active STING together with TBK1 are eventually degraded in a lyso-endosome dependent way (53, 84). STING colocalizes with Rab7 containing vesicles, which are late endosomes or lysosomes, but not early endosomes (Rab5-containing vesicles), or recycling endosomes (Res; Rab11-containing vesicles). Inhibiting acidification of the endo-lysosome pathway prevents activation-induced STING degradation (89, 90). Moreover, cytosolic dsDNA would be cleared in STING induced autophagosomes to prevent chronic cGAS activation. Cells deficient in either cGAS or STING fail to induce autophagy in response to dsDNA (91, 92). In macrophages, the autophagosomal marker LC3 colocalizes with dsDNA as well as cGAS, STING, and TBK1, suggesting the direct role of autophagy in dsDNA clearance and STING degradation (93–95). Cyclic GMP-AMP would be degraded

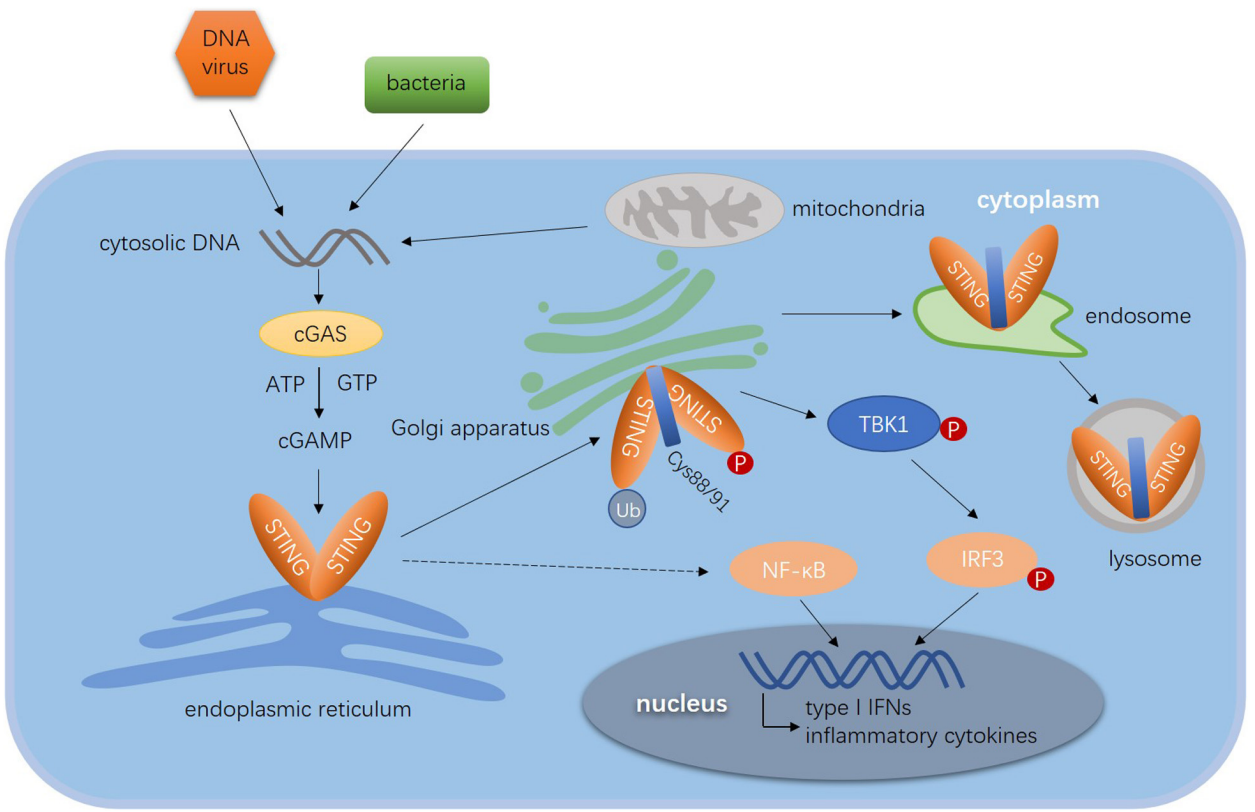

FIGURE 1 | Diagram of STING-mediated immune response to viruses. The cytosolic dsDNA derived from DNA viruses, bacteria CDNs and mitochondria are sensed by cGAS, which catalyzes ATP and GTP to generate cGAMP. Cyclic GAMP directly binds to the pocket of STING dimer and initiates the translocation of STING. STING translocates from the ER to ERGIC, Golgi apparatus and endosome, where it is degraded in the lysosome. The phosphorylation, ubiquitination, and palmitoylation are essential for the activation of STING. The activated STING dimer recruits TBK1 to form the translocation complex. By recruiting and phosphorylating IRF3, the complex promoted IRF3 to entry into nucleus. STING induces the expression of type I IFN genes and other pro-inflammatory cytokines through the TBK1–IRF3 axis and NF-κB signal pathway.

by the extracellular phosphodiesterase ENPP1 to terminate STING signals (96). Besides, it is reported that the cytosolic nuclease poxins (poxvirus immune nucleases) from the vaccinia virus and its homologs from moths, butterflies, and their pathogenic baculovirus, also act as cGAMP-degrading enzymes to prevent cGAS-STING activation (97). More detailed regulation by ubiquitination-mediated degradation would be discussed later. The STING signaling is negatively regulated by protein degradation as well as clearance of the stimulus. Besides ubiquitination, many other posttranslational modifications regulate STING signal transduction and the crosstalk of the STING pathway with other cellular processes. Understanding these mechanistic details may be important for uncovering STING intracellular trafficking and signal transduction.

STING TRAFFICKING AND ISG INDUCTION

STING trafficking is critical in IRF3 and NF-κB induced ISG expression in response to cytosolic DNA (98). As shown in **Figure 2**, it is regulated by multiple factors and has not been fully elucidated yet. STING mostly locates in the ER and partially in the mitochondria and mitochondria-associated membranes in resting cells (48, 63, 99). Immediately after ligand binding, dimeric STING translocates between intracellular membranes, from the ER to ERGIC, Golgi apparatus, and perinuclear microsomes or punctate structures (74, 100, 101). Constitutively active STING mutants aggregate in the ERGIC in the absence of ligands, suggesting the ligand-binding itself is not required during the intracellular trafficking process (100). To date, many proteins are known to involved in the regulation of STING trafficking, including the translocon-associated protein β (TRAPβ), the translocon adapter Sec61β, exocyst complex component Sec5, iRhom2, SCAP, SNX8, and YIF5 (63, 102–106). Because STING mutant induced disordered STING translocation and ligand-independent activation contributes to autoinflammatory and autoimmune diseases in patients (107, 108), detailed investigations of STING trafficking become both biological and clinical meaningful (100).

Several pathogen-encoded antagonists of STING have been characterized. The ERGIC localizes between the ER exit sites and the Golgi apparatus as a bridge. The ERGIC sorts ER-derived COPII vesicles for anterograde transport to the Golgi or retrograde transport to the ER (109). The *Shigella* effector protein IpaJ efficiently inhibits gene induction by blocking STING trafficking from the ER to the ERGIC via de-myristoylating the ARF1 GTPase. After exiting from the ERGIC or Golgi, STING translocates to perinuclear punctate structures where it meets TBK1. The VirA protein from *Shigella* blocks STING trafficking from the ERGIC to Golgi by hydrolyzing the Rab1-GTP to Rab1-GDP (74). Even in the presence of STING ligands, inhibition of the translocation either from the ER to ERGIC by IpaJ, or from the ERGIC to Golgi by VirA, hampers STING induced IFN-I expression (99, 100).

Studies on iRhom2 furtherly elucidate the intracellular trafficking in STING signal transduction. iRhom2 is originally

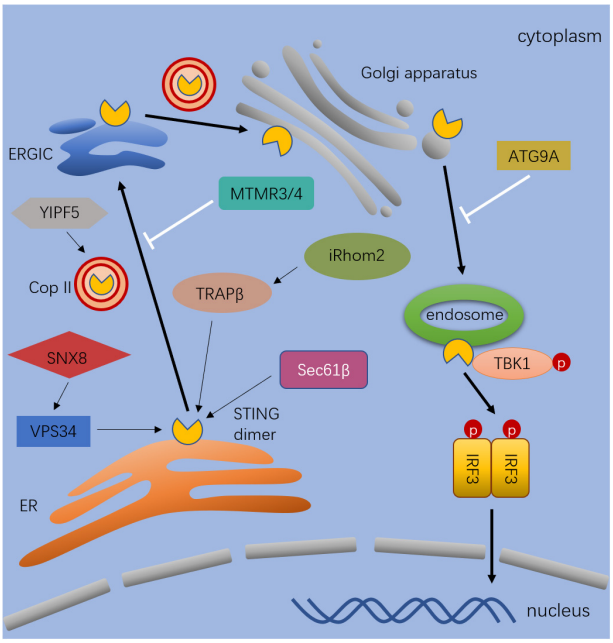

FIGURE 2 | The process and regulation of STING trafficking. After stimulated by cytosolic dsDNA, STING dimer exist from the ER to ERGIC, Golgi, and endosomes. The process of trafficking is mediated by diverse proteins. The thick black arrows indicate the pathway that lead to activation and trafficking of STING. The thin black arrows indicate the regulators which positively regulates the trafficking of STING. The white arrows indicate the regulators which negatively regulates the trafficking of STING. Full name of the abbreviations: VPS34 (Vacuolar protein sorting-associated protein 34); SNX8 (Sorting nexin-8); YIPF5 (Yip1 Domain Family Member 5); MTMR3/4 (Myotubularin Related Protein 3); TRAPβ (Translocon-associated protein β); Sec61β (SEC61 Translocon Subunit Beta); iRhom2 (inactive rhomboid 2); ATG9A (Autophagy-related protein 9A); and Cop II (Coat protein II).

reported to promote the trafficking of TACE (TNFα convertase) from the ER to the cell surface and facilitates LPS induced TNFα expression (110). Recent studies are showing that iRhom2 is essential to the immune responses to DNA viruses (106), which is transported from the ER to ERGIC/Golgi apparatus and perinuclear punctate structures together with STING after HSV-1 infection. STING fails to leave ER in iRhom2 deficiency cells, suggesting that viral DNA induced STING translocation is dependent on iRhom2. iRhom2 might adapt STING to interact with TRAPβ, an important translocon-associated protein because knockdown of TRAPβ inhibits STING trafficking and gene induction (106).

In addition to proteins, STING trafficking is also regulated by small molecules, such as phospholipids. Cellular levels of PtdIns (phosphatidylinositol) and PtdIns5P are regulated by myotubularin related protein MTMR3 and MTMR4, which dephosphorylate 3′ position in phosphatidylinositol (PtdIns). MTMR3 and MTMR4 generate PtdIns5P and PtdIns from PtdIns (3, 5) and PtdIns3P, respectively, (111). Increased PtdIns3P is accumulated in enlarged cytosolic puncta in MTMR3 and MTMR4 double knockout (DKO) cells, and STING is aberrantly accumulated in PtdIns3P positive puncta after DNA stimulation.

In DKO cells, STING rapidly translocates from the ER to Golgi and produces an enhanced IFN expression in response to IFN-stimulatory DNA (ISD) and HSV-1 infection (111). As shown in **Figure 2**, MTMR3 and MTMR4 are suppressing STING trafficking in response to DNA stimulation by regulating cellular phospholipid metabolism.

STING is tracking the native vesicular transporters in response to the stimulus, which might inherit from its ancestral functions in autophagy machinery (112). YIPF5 maintains the integrity of Golgi and ER (113, 114), and low levels of YIPF5 are still able to preserve a relatively normal ER network (115). It is essential for viral or intracellular DNA triggered production of IFN and ISGs, by interacting with both STING and components of COPII to facilitate STING recruitment into COPII-coated vesicles and the cellular trafficking from the ER to the Golgi apparatus (105). SNX8, a protein involving in endocytosis and endosomal sorting, belongs to the sorting nexin protein family, which is previously found as a component of IFNγ-triggered non-canonical signaling pathway (116, 117). SNX8 boosts DNA-triggered innate immune responses by recruitment of class III phosphatylinositol 3-kinase VPS34 to STING (118). VPS34 is the key component in STING trafficking from the ER to perinuclear microsomes. SNX8$^{-/-}$ mice fail to respond to HSV-1 infection and exhibiting a lower level of serum cytokines and higher viral titers in mouse brains (118). NLRC3 (nucleotide-binding, leucine-rich-repeat containing protein) negatively regulates STING translocation in response to DNA viral infection. In the presence of NLRC3, STING trafficking to the perinuclear region is prevented (119). NLRC3 is originally reported as an inhibitor in the PI3K-mTOR pathway (120). It is suggesting that STING trafficking may share some common factors in mTOR signals.

In addition to STING, TBK1 and IRF3 also translocate to perinuclear regions in dsDNA stimulated cells. Since the integration of TBK1, IKKs, IRF3, and NF-κB is a later event in the evolutional history of the STING pathway, it is hypothesized that the translocation of TBK1 and IRF3 is dependent on STING trafficking (112). In perinuclear puncta, STING recruits TBK1 to activate transcription factor IRF3 by phosphorylation. STING deficiency leads to the retention of TBK1 to perinuclear regions after dsDNA stimulation. The ATPase inhibitor Brefeldin A (BFA) prevents STING-mediated IRF3 phosphorylation and ISG expression by restriction of STING trafficking (121). Sec5, the exocyst complex component, is essential for the antiviral responses to recruit and activate TBK1 (122). DNA stimulation leads to translocation of STING to Sec5-containing endosome from the ER or ERGIC (63, 102). During this process, TRAPβ, and Sec61β are needed. TMED2 that belongs to the transmembrane emp24 domain/p24 (TMED) family promotes STING-TRAPβ interaction and enhances STING trafficking and gene induction (123). Knockdown of TRAPβ, Sec61β, and Sec5 inhibits STING dependent gene expression. These studies suggest that STING links cytosol DNA stimulation to TBK1 activation through the intracellular trafficking between the ER and perinuclear punctate structures. Similarly, SCAP recruits IRF3 into STING complex and translocates from the ER to perinuclear microsomes after viral infection (124). It could be interesting to disrupt scaffold proteins between STING-IRF3 and STING-TBK1 to figure out the driver factor in the orchestrated process.

Notably, endocytosed cyclic di-nucleotides (eCDNs) released from damaged or dying infected cells could activate bystander cells. Upon binding to eCDNs, cGAS undergoes a conformational change and promotes its interaction with STING. It facilitates the formation of eCDNs/cGAS/STING perinuclear signalosomes to enable STING activation (125). This finding provides an insight into the differences between eCDNs and cGAMP in STING activation and trafficking. Detailed molecular mechanisms are still remaining to be elucidated.

VIRAL INFECTION AND STING TRAFFICKING

Viral DNA and virus-induced leakage of mtDNA trigger STING activation and trafficking (98, 126). Viruses have to evolve certain strategies to defeat host immunity for efficient infection. For example, HSV-1 encodes series of proteins to antagonize STING signals, including viral ubiquitin ligase ICP0, deubiquitylase (DUB) UL36USP, protein kinases (US3, VP24), and protein-protein interaction inhibitors (PPis) (127). Since ubiquitination regulates protein trafficking, it is natural to wonder if viral ICP0 and UL36USP would change intracellular trafficking of STING and components in STING signaling. Adenovirus E1A and human papillomavirus E7 inhibit cGAS-STING signals by direct interaction between the LXCXE motifs of viral oncoproteins and STING (128). NS4B of hepatitis C virus and NS2B3 protein of dengue virus directly cleave STING (129, 130). VP24 of HSV-1 and vIRF1 of KSHV impair STING-TBK1 interaction (128, 131). HSV-1 VP1-2 and HTLV-1 Tax protein deubiquitinate STING and inhibit its downstream signals (132, 133). Interestingly, the conserved hemagglutinin fusion peptide of RNA virus influenza virus A (IVA) interacts STING and abolishes STING dependent IFN induction by membrane fusion (134). It reflects a cGAS- and CDNs- independent STING activation.

Increased studies are showing that viruses inhibit the intracellular trafficking of STING. HSV-1 $\gamma_1$34.5 protein perturbs STING trafficking from the ER to Golgi by interaction with STING on its N-terminus. STING is colocalizing with ER marker calreticulin in cells infected by wild type virus, while it forms puncta with GM130 (Golgi apparatus) in cells infected by $\gamma_1$34.5 deletion viruses (135). It is still unknown how viral $\gamma_1$34.5 protein inhibits STING trafficking. HCMV tegument protein UL82 is a negative regulator of the STING pathway by direct interaction with STING. It inhibits STING trafficking from the ER to perinuclear punctate structures by breaking the iRhom2-mediated assembly of the STING-TRAPβ translocation complex. STING fails to recruit TBK1 and IRF3 (101). Moreover, virulent African swine fever virus (ASFV) strain Armenia/07 attenuated STING-dependent IFN induction by re-localizing STING. ASFV is

a complex, cytoplasmic dsDNA virus. STING colocalizes with clathrin adaptor protein AP1 outside from perinuclear structures in attenuated strain ASFV/NH/P68 but not in virulent strain Armenia/07 infected cells (136). With the increasing understanding of STING signaling transduction, more and more viral proteins would be found to manipulate the intracellular trafficking of the STING pathway.

STING TRAFFICKING, AUTOPHAGY AND RECYCLING

Autophagy possesses important functions, including innate immune responses, and inflammation. Of note, dsDNA-induced STING trafficking involves autophagy (78). The autophagy-related gene ATG9A negatively regulates dsDNA-induced IFN expression by inhibiting the trafficking of STING. In ATG9A-deficient cells, translocation of STING to the perinuclear puncta and the assembly of STING-TBK1-IRF3 complexes are raised upon dsDNA stimulation (103). Moreover, knockdown of VPS34 (PI3KC3) inhibits STING trafficking and IFN induction by dsDNA stimulation. The Beclin-1-PI3KC3 (VPS34) core complex manipulates autophagy by generating PtdIns 3-phosphate-rich membranes, which are regarded as the platform for the recruitment of autophagy-related proteins and autophagosome maturation (137, 138). Beclin-1 interacts with cGAS and decreases STING induced IFN expression by repressing the enzymatic activity of cGAS (94). cGAS is required for dsDNA-induced Beclin-1 dependent autophagy (94). The cGAS–STING axis orchestrates ISGs and autophagy pathways to boost host immune responses to DNA viruses (93, 139–141). However, STING triggers autophagy independent of TBK1 activation and IFN induction. Above all, upon binding cGAMP, STING translocation to the Golgi is dependent on the COP-II complex and ARF GTPases. STING-coated ERGIC is the membrane source for LC3 lipidation, which initiates autophagosome maturation. cGAMP triggers LC3 lipidation by WIPI2 and ATG5 but independent of the ULK and VPS34-beclin-1 (78). LC3-positive membranes enfold dsDNA, bacteria, and viruses to form autophagosomes (142). Prabakaran and colleagues have found the interaction between STING and the selective autophagy receptor p62/SQSTM1, which attenuates cGAS-STING signaling. P62 is activated by TBK1-mediated phosphorylation. Phosphorylated p62 ubiquitinates STING and facilitates STING degradation by autophagy (143).

The translocation of STING plays a crucial role in the activation of downstream pathways. At the same time, dsDNA-induced autophagy is important for the removal of DNA and viruses in the cytoplasm. Upon cGAMP stimulation, STING induces autophagy but not IFN expression, indicating that autophagy induction is the original function of the cGAS-STING pathway (78, 144). Although the relationship between STING re-localization and autophagy has been established, the precision mechanism by which STING translocation is initiated remains unclear. Regarding the question of whether STING preferentially recruits IRF3 to perinuclear microsomes or via autophagosomes to activate the related immune response needs further exploration.

Moreover, STING translocates to the REs, and then to the p62-positive compartments/lysosomes after exiting from the Golgi apparatus (143). Chloroquine or BFA prevents the lysosomal degradation of STING and enhances STING-induced antiviral gene expression. The palmitoylation of STING is not required for its degradation because the palmitoylation-deficiency mutant (C88/91S) cannot prevent STING degradation. There are still controversies about the effect of the autophagic process in STING degradation (98).

POST TRANSLATIONAL MODIFICATIONS AND STING REGULATION

Post-translational modification is important in the initiation, dynamic regulation, and silence of signal transduction pathways. It affects the pathway by regulation of protein localization, stabilization, and conformational changes (145). Examples of these regulations include ligand-dependent EGFR activation, Janus kinase (JAKs) regulated STAT signals, and ISG15-dependent regulation in TLR signals (146–148). The common types of PTMs are ubiquitination, phosphorylation (including serine/threonine phosphorylation and tyrosine phosphorylation), palmitoylation, glycation, lipidation, acetylation, methylation, and so on (149–151). It has been reported that ubiquitination, phosphorylation, and palmitoylation regulate the innate immune responses to dsDNA by STING. These modifications occur on all components in the pathway, including cGAS, STING, TBK1, and IRF3 (148).

Monoubiquitination and polyubiquitination regulate protein trafficking and degradation. K48-linked polyubiquitination is related to proteasomal degradation, while K63-linked polyubiquitination is related to signal transduction. Mostly, ubiquitin covalently binds to the lysine residue in substrate proteins through a multi-enzyme cascade, and the de-ubiquitination of proteins involves deubiquitinating enzymes (DUBs) (151, 152). However, it is clear now that polyubiquitin chains can also bind to substrates non-covalently. The E3-ligases TRIM32 and TRIM56 promote the recruitment of TBK1 by STING in response to the stimulus, by targeting STING for K63-linked ubiquitination at K150. Overexpression of these E3 ligases enhances IFNβ expression while knockout of either could abrogate STING-dependent responses. In a later study, researchers could not observe polyubiquitinations of STING in the presence of TRIM32 and TRIM56. The question about the precise coordination of TRIM32 and TRIM56 to STING in the process still remains to be elucidated (153–155).

Together with insulin-induced gene 1 (INSIG1), the autocrine motility factor receptor (AMFR) boost STING signaling by catalyzing a K27-linked polyubiquitination. Wang et al. reported that K27-linked di-ubiquitin chains bind the ubiquitin-like domain (ULD) of TBK1 directly (156). Four lysine residues of STING, K137, K150, K224, and K236, may involve in this process. However, it becomes controversial if the K27-linked polyubiquitination of STING is essential for TBK1 recruitment,

since earlier studies are showing that TBK1 binds *Escherichia coli* derived recombinant STING fragments (84). RNF5 impairs STING signaling by modification of STING at K150 with K48-linked polyubiquitination, which promotes STING degradation. RNF26 catalyzes a K11-linked polyubiquitination at the same residue to antagonize RNF5-mediated STING degradation (157–159). The detailed regulations of TRIM32-, TRIM56-, RNF5-, and RNF26- dependent STING K150 polyubiquitination are worth exploring. Meanwhile, TRIM30α negatively regulates the STING pathway by the K48-linked ubiquitination of STING on K275. Knockdown and deficiency of TRIM30α enhance the production IFN-I and IL-6 upon dsDNA stimulation, and TRIM30α$^{-/-}$ mice are more resistant to HSV-1 infection than wild type mice. Detailed studies show that TRIM30 interacts with STING through its SPRY domain (160, 161). Since TRIM30 could be induced by STING-NF-κB in response to dsDNA, it suggests that TRIM30 is a self-negative regulation component in STING signaling (161). It is worth noting that TRIM30α is absent in human (162). The E3-ligases TRIM29 inhibits the expression of STING and catalyzes the K48-linked ubiquitination of STING on K370. In the presence of cytoplasmic DNA, TRIM29 is highly expressed and impairs the expression of IFN-I. It is suggested that TRIM29$^{-/-}$ mice are less susceptible to HSV-1 or adenovirus infection than wild type mice. TRIM29 plays a similar role as TRIM30 to inhibit innate immune responses (163). In addition, CD40 is reported to regulate the K48-linked ubiquitination of STING. The ubiquitin-ligase TRAFs are involved in the ubiquitination and stability of STING. Increased level of CD40 competes with STING to interact with TRAFs, reduces the degradation of STING, and promotes STING-mediated IFN-I responses (164). The mitochondrial E3 ubiquitin protein ligase 1 (MUL1) catalyzes K63-linked polyubiquitination of STING at K224, and deliver TBK1 to IRF3. It is found that the ubiquitination-deficient mutant STING K224R fails to translocate to perinuclear puncta in response to the stimulus, suggesting K63-linked polyubiquitination of STING at K224 is essential for STING trafficking (165). Interestingly, the MUL1-mediated STING ubiquitination is required in STING-IRF3 activation but not STING-NF-κB signals. It is noting that the dominant ubiquitination of STING on K236 and K338 are found in the same study (165).

As mentioned above, iRhom2 boosts gene induction by STING in responses to DNA viruses. It recruits the eukaryotic translation initiation factor 3, subunit 5 (EIF3S5) to STING, which removes K48-linked polyubiquitin of STING and inhibits STING degradation by the proteasome (106). USP13, a deubiquitinating enzyme, interacts with STING and catalyzed removal of K27 O- or K33 O-linked but not K27 R-linked polyubiquitin chains from STING. It impairs the recruitment of TBK1 by STING (166). USP13$^{m/m}$ mice are more resistant to HSV-1 infection with a higher survival rate and a robuster IFN and cytokines in sera (166). Many viral proteins have already been found to de-ubiquitinate STING, which is discussed earlier in this review.

Palmitoylation is an important form of protein posttranslational lipid modification for regulating protein transport, stability, and cellular localization (167, 168). Palmitoylation of STING is found after trafficking to the Golgi apparatus, which is essential for the activation of STING (169, 170). The palmitoylation inhibitor 2-bromopalmitate (2-BP) impairs IFN induction via STING. The STING C88/91S mutant, which is deficient in palmitoylation, cannot induce ISGs expression in the presence of STING stimulus. It is demonstrated that STING is palmitoylated at the Golgi, and this PTM is essential for STING signaling (98, 169). Small molecules C-178 and its derivatives inhibit STING- mediated gene expression by antagonizing palmitoylation of STING with a covalent bond between C88/91 residue of STING and compound (171). This unique lipidation of protein may be maintaining the active STING oligomer on ERGIC or Golgi apparatus.

Protein phosphorylation is involved in almost all biological processes and is regulated by both kinases and phosphatases. Phosphorylation of STING at residue S366 by TBK1 promoted the recruitment and activation of IRF3. However, it is reported that phosphorylation of activated STING at S366 by ULK1 inhibits the activation of IRF3 at an earlier time (121). In both studies, S366A mutant that mimics unphosphorylated STING has a greatly reduced IFNβ expression in response to the stimulus, it is more convinced to conclude that phosphorylation of STING at S366 residue is a positive regulation. Besides, the residue S358 of STING is reported to carry through the phosphorylation process (172). Protein phosphatase Mg^{2+}/Mn^{2+} dependent 1A (PPM1A) dephosphorylates STING at S358 and suppresses the formation of perinuclear puncta, which leads to reduced responses. The relationships between S358 and S366 phosphorylation are still unclear. Collectively, these studies reveal the positive effect of phosphorylation on STING activation (173). Currently, it is reported that the ribosomal protein S6 kinase 1 (S6K1) interacts with phosphorylated STING and TBK1 to form the transduction complex (174). It is a piece of the missed parts in the regulation of STING pathways, and partially explains the function of phosphorylation of STING in this signal.

Although tyrosine phosphorylation accounts for a small percentage of all protein phosphorylation modifications, it is critical in many processes. Tyrosine phosphorylation of STING has been identified in a preliminary experiment, in which STING (MPYS in this work) has been detected in immunoprecipitated samples by anti-pTyr antibodies (175). In the following years, less has been known for tyrosine phosphorylation of STING. In 2015, researchers found that Bruton's tyrosine kinase (BTK) positively regulates STING-dependent signaling. BTK belongs to the Tec family of cytoplasmic tyrosine kinases. It is vital for B cell receptor signaling and lymphopoiesis (176). BTK interacts with STING and DDX41 and then phosphorylates DDX41. Y364 and Y414 of DDX41 are critical for DNA recognition and binding to STING. Y414 phosphorylation increases its affinity to STING by increasing the number of hydrogen bonds and salt bridges with STING. The finding indicates the interaction between DDX41 and the transmembrane region of STING by the tyrosine phosphorylation of DDX41 (177). Later, it is found that phosphorylation of Y245 in STING is important for STING activation. PTPN1 and PTPN2 dephosphorylated STING at Y245 and then facilitated STING degradation by 20S proteasome (178).

THERAPEUTIC AGENTS TARGETING STING

Considering the nodal role of STING in the innate immune responses against abnormal DNA and viral invasion, it is tempting to harness this activity for therapy. The STING agonists and antagonists are immunotherapy drugs suitable for a variety of diseases. STING antagonists are supposed to cure autoimmune diseases, while STING agonists would be used in anti-tumor and antiviral therapies. We summarize the recent advances of STING agonists here.

STING agonists could activate innate and following adaptive immune responses for the treatment of many diseases, especially for cancers, and infectious diseases. Vascular disrupting agents DMXAA (also known as Vadimezan or ASA404) is the first STING agonist utilized in clinical trials, which directly interacts with mouse STING to activate TBK1-IRF3 and induces IFNs and cytokines. DMXAA reduces HBV DNA replication intermediates in the livers of HBV-injected mice. Unfortunately, DMXAA can only bind to mouse STING (179). It has extremely good efficacy in the mouse model, but the clinical trials failed in phase III (73). Meanwhile, immunotherapy based on STING agonists has always been considered to sweep the field of tumor immunotherapy (180–182). Researchers have discovered and designed a series of molecules to develop an effective activator of STING. To mimic the native agonist, nucleotidic agonist ADU-S100 (also called ML-RR-S2-CDA or MIW815) was designed and tested in clinical trials (180). Following this strategy, Merck, GlaxoSmithKline, and Bristol-Myers Squibb have patented different nucleotidic agonists of STING. Non-nucleotidic agonist diABZI was optimized from a small molecule lead compound amidobenzimidazole (ABZI). It binds to STING with an IC_{50} of 20 $\pm$ 0.8 nM and inhibits STING induced IFN-I expression in cells with an EC_{50} of 130 $\pm$ 40 nM (75). Until now, many other STING agonists or activators were reported, including IACS-8803, IACS-8779, and CL656 (183–185). Except for DMXAA, other STING agonists are developed for tumor immunotherapy. It is also believed that STING agonists might be used in antiviral therapies. One of the potential advantages of these new molecules is that they can be transported through blood (186). This new immunotherapy drug greatly enhanced the adaptive immune function. On one hand, the immune mechanism targeting STING provides new ideas for the entire anti-tumor and antiviral immunotherapy researches. On the other hand, the new STING agonists have also promoted the emergence and clinical application of new immune drugs.

CONCLUDING REMARKS

A series of studies in the recent years demonstrated a critical role of STING signaling in the recognition of pathogenic DNA as well as endogenous DNA, and therefore in autoimmune diseases and tumor immunity. However, there remains a number of key questions unaddressed. For instance, the precise mechanism of regulation of the STING trafficking from the ER to the Golgi complex remains to be determined. In addition, STING has TBK1-independent and cGAS-independent functions. How these processes are regulated is not yet completely clear.

There is also substantial interest in identifying STING agonists and antagonists. DMXAA activates murine STING *in vitro* and *in vivo*, and CDNs activate human STING, potentially inhibiting metastatic tumors. It has shown that STING agonists may become another dark horse for immunotherapy. Given that direct IFN administration causes flu-like symptoms and other adverse effects, using CDNs or other small-molecules may reduce these side effects and lead to a more plausible therapy strategy.

AUTHOR CONTRIBUTIONS

All authors listed have made contributions to the manuscript and approved it for publication.

FUNDING

This research was supported by the National Natural Science Foundation of China (31700755 and 81991525), the Taishan Scholars Program (tsqn201909170), and the Fundamental Research Funds for the Central Universities and the Innovative Leader of Qingdao Program (19-3-2-26-zhc).

REFERENCES

1. Takeuchi O, Akira S. Innate immunity to virus infection. *Immunol Rev.* (2009) 227:75–86. doi: 10.1111/j.1600-065X.2008.00737.x
2. Wu J, Chen ZJ. Innate immune sensing and signaling of cytosolic nucleic acids. *Annu Rev Immunol.* (2014) 32:461–88. doi: 10.1146/annurev-immunol-032713-120156
3. Xia P, Wang S, Gao P, Gao G, Fan Z. DNA sensor cGAS-mediated immune recognition. *Protein Cell.* (2016) 7:777–91. doi: 10.1007/s13238-016-0320-3
4. Balka KR, Louis C, Saunders TL, Smith AM, Calleja DJ, D'Silva DB, et al. TBK1 and IKKepsilon act redundantly to mediate STING-Induced NF-kappaB responses in myeloid cells. *Cell Rep.* (2020) 31:107492. doi: 10.1016/j.celrep.2020.03.056
5. Xu L, Yu D, Peng L, Wu Y, Fan Y, Gu T, et al. An Alternative Splicing of tupaia STING modulated anti-RNA virus responses by targeting MDA5-LGP2 and IRF3. *J Immunol.* (2020) 204:3191–204. doi: 10.4049/jimmunol.1901320
6. Masrour-Roudsari J, Ebrahimpour S. Causal role of infectious agents in cancer: an overview. *Caspian J Intern Med.* (2017) 8:153–8. doi: 10.22088/cjim.8.3.153
7. Nogalski MT, Collins-McMillen D, Yurochko AD. Overview of human cytomegalovirus pathogenesis. *Methods Mol Biol.* (2014) 1119:15–28. doi: 10.1007/978-1-62703-788-4_2
8. Kurt-Jones EA, Orzalli MH, Knipe DM. Innate immune mechanisms and herpes simplex virus infection and disease. *Adv Anat Embryol Cell Biol.* (2017) 223:49–75. doi: 10.1007/978-3-319-53168-7_3
9. Bassett I, Donovan B, Bodsworth NJ, Field PR, Ho DW, Jeansson S, et al. Herpes simplex virus type 2 infection of heterosexual men attending a sexual health centre. *Med J Aust.* (1994) 160:697–700.
10. Taylor GS, Long HM, Brooks JM, Rickinson AB, Hislop AD. The immunology of Epstein-Barr virus-induced disease. *Annu Rev Immunol.* (2015) 33:787–821. doi: 10.1146/annurev-immunol-032414-112326

11. Dittmer DP, Damania B. Kaposi sarcoma-associated herpesvirus: immunobiology, oncogenesis, and therapy. *J Clin Invest.* (2016) 126:3165–75. doi: 10.1172/JCI84418
12. Zucman D, Mellot F, Couderc L. HIV-associated cancers and related diseases. *N Engl J Med.* (2018) 378:2144–5. doi: 10.1056/NEJMc1804812
13. Siew JX, Seah XFV, Chew YR, Thoon KC, Chong CY, Yung CF, et al. Epidemiology of adenovirus infections and outcomes of cidofovir treatment in severely Ill children. *Pediatr Infect Dis J.* (2020). doi: 10.1097/INF.0000000000002726
14. Li L, Woo YY, de Bruyne JA, Nathan AM, Kee SY, Chan YF, et al. Epidemiology, clinical presentation and respiratory sequelae of adenovirus pneumonia in children in Kuala Lumpur, Malaysia. *PLoS One.* (2018) 13:e0205795. doi: 10.1371/journal.pone.0205795
15. Schwartz KL, Richardson SE, MacGregor D, Mahant S, Raghuram K, Bitnun A. Adenovirus-associated central nervous system disease in children. *J Pediatr.* (2019) 205:130–7. doi: 10.1016/j.jpeds.2018.09.036
16. Gillison ML, Chaturvedi AK, Anderson WF, Fakhry C. Epidemiology of human papillomavirus-positive head and neck squamous cell carcinoma. *J Clin Oncol.* (2015) 33:3235–42. doi: 10.1200/JCO.2015.61.6995
17. Reuschenbach M, Mihm S, Wolle R, Schneider KM, Jacob C, Braun S, et al. Burden of HPV related anogenital diseases in young women in Germany – an analysis of German statutory health insurance claims data from 2012 to 2017. *BMC Infect Dis.* (2020) 20:297. doi: 10.1186/s12879-020-05002-w
18. Imperiale MJ, Jiang M. Polyomavirus persistence. *Annu Rev Virol.* (2016) 3:517–32. doi: 10.1146/annurev-virology-110615-042226
19. Wang X, Li J, Schowalter RM, Jiao J, Buck CB, You J. Bromodomain protein Brd4 plays a key role in Merkel cell polyomavirus DNA replication. *PLoS Pathog.* (2012) 8:e1003021. doi: 10.1371/journal.ppat.1003021
20. Ma Z, Ni G, Damania B. Innate sensing of DNA virus genomes. *Annu Rev Virol.* (2018) 5:341–62. doi: 10.1146/annurev-virology-092917-043244
21. Barrat FJ, Crow MK, Ivashkiv LB. Interferon target-gene expression and epigenomic signatures in health and disease. *Nat Immunol.* (2019) 20:1574–83. doi: 10.1038/s41590-019-0466-2
22. Ragu S, Matos-Rodrigues G, Lopez BS. Replication stress, DNA damage, inflammatory cytokines and innate immune response. *Genes(Basel).* (2020) 11:409. doi: 10.3390/genes11040409
23. Hua Z, Hou B. The role of B cell antigen presentation in the initiation of CD4+ T cell response. *Immunol Rev.* (2020) 296:24–35. doi: 10.1111/imr.12859
24. Balz K, Trassl L, Hartel V, Nelson PP, Skevaki C. Virus-induced T cell-mediated heterologous immunity and vaccine development. *Front Immunol.* (2020) 11:513. doi: 10.3389/fimmu.2020.00513
25. Candolfi M, King GD, Yagiz K, Curtin JF, Mineharu Y, Muhammad AK, et al. Plasmacytoid dendritic cells in the tumor microenvironment: immune targets for glioma therapeutics. *Neoplasia.* (2012) 14:757–70. doi: 10.1593/neo.12794
26. Hermant P, Michiels T. Interferon-lambda in the context of viral infections: production, response and therapeutic implications. *J Innate Immun.* (2014) 6:563–74. doi: 10.1159/000360084
27. Holm CK, Paludan SR, Fitzgerald KA. DNA recognition in immunity and disease. *Curr Opin Immunol.* (2013) 25:13–8. doi: 10.1016/j.coi.2012.12.006
28. Zhang X, Flavell RA, Li HB. hnRNPA2B1: a nuclear DNA sensor in antiviral immunity. *Cell Res.* (2019) 29:879–80. doi: 10.1038/s41422-019-0226-8
29. Hornung V, Latz E. Intracellular DNA recognition. *Nat Rev Immunol.* (2010) 10:123–30. doi: 10.1038/nri2690
30. Rebsamen M, Heinz LX, Meylan E, Michallet MC, Schroder K, Hofmann K, et al. DAI/ZBP1 recruits RIP1 and RIP3 through RIP homotypic interaction motifs to activate NF-kappaB. *EMBO Rep.* (2009) 10:916–22. doi: 10.1038/embor.2009.109
31. Barber GN. Cytoplasmic DNA innate immune pathways. *Immunol Rev.* (2011) 243:99–108. doi: 10.1111/j.1600-065X.2011.01051.x
32. Jones JW, Kayagaki N, Broz P, Henry T, Newton K, O'Rourke K, et al. Absent in melanoma 2 is required for innate immune recognition of Francisella tularensis. *Proc Natl Acad Sci USA.* (2010) 107:9771–6. doi: 10.1073/pnas.1003738107
33. Ablasser A, Bauernfeind F, Hartmann G, Latz E, Fitzgerald KA, Hornung V. RIG-I-dependent sensing of poly(dA:dT) through the induction of an RNA polymerase III-transcribed RNA intermediate. *Nat Immunol.* (2009) 10:1065–72. doi: 10.1038/ni.1779
34. Chiu YH, Macmillan JB, Chen ZJ. RNA polymerase III detects cytosolic DNA and induces type I interferons through the RIG-I pathway. *Cell.* (2009) 138:576–91. doi: 10.1016/j.cell.2009.06.015
35. Zhang Z, Yuan B, Bao M, Lu N, Kim T, Liu YJ. The helicase DDX41 senses intracellular DNA mediated by the adaptor STING in dendritic cells. *Nat Immunol.* (2011) 12:959–65. doi: 10.1038/ni.2091
36. Parvatiyar K, Zhang Z, Teles RM, Ouyang S, Jiang Y, Iyer SS, et al. The helicase DDX41 recognizes the bacterial secondary messengers cyclic di-GMP and cyclic di-AMP to activate a type I interferon immune response. *Nat Immunol.* (2012) 13:1155–61. doi: 10.1038/ni.2460
37. Hurst TP, Aswad A, Karamitros T, Katzourakis A, Smith AL, Magiorkinis G. Interferon-inducible protein 16(IFI16) has a broad-spectrum binding ability against ssDNA targets: an evolutionary hypothesis for antiretroviral checkpoint. *Front Microbiol.* (2019) 10:1426. doi: 10.3389/fmicb.2019.01426
38. Wang L, Wen M, Cao X. Nuclear hnRNPA2B1 initiates and amplifies the innate immune response to DNA viruses. *Science.* (2019) 365:eaav0758. doi: 10.1126/science.aav0758
39. Unterholzner L, Keating SE, Baran M, Horan KA, Jensen SB, Sharma S, et al. IFI16 is an innate immune sensor for intracellular DNA. *Nat Immunol.* (2010) 11:997–1004. doi: 10.1038/ni.1932
40. Orzalli MH, DeLuca NA, Knipe DM. Nuclear IFI16 induction of IRF-3 signaling during herpesviral infection and degradation of IFI16 by the viral ICP0 protein. *Proc Natl Acad Sci USA.* (2012) 109:E3008–17. doi: 10.1073/pnas.1211302109
41. Goubau D, Rehwinkel J, Reis SC. PYHIN proteins: center stage in DNA sensing. *Nat Immunol.* (2010) 11:984–6. doi: 10.1038/ni1110-984
42. Schattgen SA, Fitzgerald KA. The PYHIN protein family as mediators of host defenses. *Immunol Rev.* (2011) 243:109–18. doi: 10.1111/j.1600-065X.2011.01053.x
43. Takaoka A, Wang Z, Choi MK, Yanai H, Negishi H, Ban T, et al. DAI(DLM-1/ZBP1) is a cytosolic DNA sensor and an activator of innate immune response. *Nature.* (2007) 448:501–5. doi: 10.1038/nature06013
44. Sui H, Zhou M, Imamichi H, Jiao X, Sherman BT, Lane HC, et al. STING is an essential mediator of the Ku70-mediated production of IFN-lambda1 in response to exogenous DNA. *Sci Signal.* (2017) 10:5054. doi: 10.1126/scisignal.aah5054
45. Fell VL, Schild-Poulter C. Ku regulates signaling to DNA damage response pathways through the Ku70 von Willebrand A domain. *Mol Cell Biol.* (2012) 32:76–87. doi: 10.1128/MCB.05661-11
46. Wang X, Helfer CM, Pancholi N, Bradner JE, You J. Recruitment of Brd4 to the human papillomavirus type 16 DNA replication complex is essential for replication of viral DNA. *J Virol.* (2013) 87:3871–84. doi: 10.1128/JVI.03068-12
47. Mirabello L, Yeager M, Yu K, Clifford GM, Xiao Y, Zhu B, et al. HPV16 E7 genetic conservation is critical to carcinogenesis. *Cell.* (2017) 170:1164–74.e66. doi: 10.1016/j.cell.2017.08.001
48. Zhong B, Yang Y, Li S, Wang YY, Li Y, Diao F, et al. The adaptor protein MITA links virus-sensing receptors to IRF3 transcription factor activation. *Immunity.* (2008) 29:538–50. doi: 10.1016/j.immuni.2008.09.003
49. Zevini A, Olagnier D, Hiscott J. Crosstalk between Cytoplasmic RIG-I and STING sensing pathways. *Trends Immunol.* (2017) 38:194–205. doi: 10.1016/j.it.2016.12.004
50. Zhang C, Shang G, Gui X, Zhang X, Bai XC, Chen ZJ. Structural basis of STING binding with and phosphorylation by TBK1. *Nature.* (2019) 567:394–8. doi: 10.1038/s41586-019-1000-2
51. Yum S, Li M, Chen ZJ. Old dogs, new trick: classic cancer therapies activate cGAS. *Cell Res.* (2020) 30:639–48. doi: 10.1038/s41422-020-0346-1
52. Abdullah Z, Knolle PA. Scaling of immune responses against intracellular bacterial infection. *EMBO J.* (2014) 33:2283–94. doi: 10.15252/embj.201489055
53. Abe T, Harashima A, Xia T, Konno H, Konno K, Morales A, et al. STING recognition of cytoplasmic DNA instigates cellular defense. *Mol Cell.* (2013) 50:5–15. doi: 10.1016/j.molcel.2013.01.039
54. Guo H, Konig R, Deng M, Riess M, Mo J, Zhang L, et al. NLRX1 sequesters STING to negatively regulate the interferon response, thereby facilitating the

replication of HIV-1 and DNA viruses. *Cell Host Microbe.* (2016) 19:515–28. doi: 10.1016/j.chom.2016.03.001
55. Zhou C, Chen X, Planells-Cases R, Chu J, Wang L, Cao L, et al. Transfer of cGAMP into bystander cells via LRRC8 volume-regulated anion channels augments sting-mediated interferon responses and anti-viral immunity. *Immunity.* (2020) 52:767–81.e66. doi: 10.1016/j.immuni.2020.03.016
56. Aguirre S, Fernandez-Sesma A. Collateral damage during dengue virus infection: making sense of DNA by cGAS. *J Virol.* (2017) 91:16. doi: 10.1128/JVI.01081-16
57. Aarreberg LD, Esser-Nobis K, Driscoll C, Shuvarikov A, Roby JA, Gale M Jr. Interleukin-1beta induces mtDNA release to activate innate immune signaling via cGAS-STING. *Mol Cell.* (2019) 74:801–15.e06. doi: 10.1016/j.molcel.2019.02.038
58. Wang X, Majumdar T, Kessler P, Ozhegov E, Zhang Y, Chattopadhyay S, et al. STING requires the adaptor TRIF to trigger innate immune responses to microbial infection. *Cell Host Microbe.* (2017) 21:788. doi: 10.1016/j.chom.2017.05.007
59. Liu S, Cai X, Wu J, Cong Q, Chen X, Li T, et al. Phosphorylation of innate immune adaptor proteins MAVS, STING, and TRIF induces IRF3 activation. *Science.* (2015) 347:aaa2630. doi: 10.1126/science.aaa2630
60. Hou F, Sun L, Zheng H, Skaug B, Jiang QX, Chen ZJ. MAVS forms functional prion-like aggregates to activate and propagate antiviral innate immune response. *Cell.* (2011) 146:448–61. doi: 10.1016/j.cell.2011.06.041
61. Shang G, Zhang C, Chen ZJ, Bai XC, Zhang X. Cryo-EM structures of STING reveal its mechanism of activation by cyclic GMP-AMP. *Nature.* (2019) 567:389–93. doi: 10.1038/s41586-019-0998-5
62. Lin Y, Zheng C. A Tug of War: DNA-sensing antiviral innate immunity and herpes simplex virus type I infection. *Front Microbiol.* (2019) 10:2627. doi: 10.3389/fmicb.2019.02627
63. Ishikawa H, Barber GN. STING is an endoplasmic reticulum adaptor that facilitates innate immune signalling. *Nature.* (2008) 455:674–8. doi: 10.1038/nature07317
64. Ran JS, Jin J, Zhang XX, Wang Y, Ren P, Li JJ, et al. Molecular characterization, expression and functional analysis of chicken sting. *Int J Mol Sci.* (2018) 19:706. doi: 10.3390/ijms19123706
65. Surpris G, Chan J, Thompson M, Ilyukha V, Liu BC, Atianand M, et al. Cutting edge: novel tmem173 allele reveals importance of sting N terminus in trafficking and type I IFN production. *J Immunol.* (2016) 196:547–52. doi: 10.4049/jimmunol.1501415
66. Zhao B, Shu C, Gao X, Sankaran B, Du F, Shelton CL, et al. Structural basis for concerted recruitment and activation of IRF-3 by innate immune adaptor proteins. *Proc Natl Acad Sci USA.* (2016) 113:E3403–12. doi: 10.1073/pnas.1603269113
67. Ouyang S, Song X, Wang Y, Ru H, Shaw N, Jiang Y, et al. Structural analysis of the STING adaptor protein reveals a hydrophobic dimer interface and mode of cyclic di-GMP binding. *Immunity.* (2012) 36:1073–86. doi: 10.1016/j.immuni.2012.03.019
68. Burdette DL, Vance RE. STING and the innate immune response to nucleic acids in the cytosol. *Nat Immunol.* (2013) 14:19–26. doi: 10.1038/ni.2491
69. Tsuchiya Y, Jounai N, Takeshita F, Ishii KJ, Mizuguchi K. Ligand-induced Ordering of the C-terminal Tail Primes STING for Phosphorylation by TBK1. *EBioMedicine.* (2016) 9:87–96. doi: 10.1016/j.ebiom.2016.05.039
70. De Oliveira Mann CC, Orzalli MH, King DS, Kagan JC, Lee ASY, Kranzusch PJ. Modular architecture of the STING C-terminal tail allows interferon and NF-kappaB signaling adaptation. *Cell Rep.* (2019) 27:1165–75.e65. doi: 10.1016/j.celrep.2019.03.098
71. Ergun SL, Li L. Structural Insights into STING Signaling. *Trends Cell Biol.* (2020) 30:399–407. doi: 10.1016/j.tcb.2020.01.010
72. Shu C, Yi G, Watts T, Kao CC, Li P. Structure of STING bound to cyclic di-GMP reveals the mechanism of cyclic dinucleotide recognition by the immune system. *Nat Struct Mol Biol.* (2012) 19:722–4. doi: 10.1038/nsmb.2331
73. Gao P, Ascano M, Zillinger T, Wang W, Dai P, Serganov AA, et al. Structure-function analysis of STING activation by c[G(2′,5′)pA(3′,5′)p] and targeting by antiviral DMXAA. *Cell.* (2013) 154:748–62. doi: 10.1016/j.cell.2013.07.023
74. Hiller B, Hornung V. STING Signaling the enERGIC Way. *Cell Host Microbe.* (2015) 18:137–9. doi: 10.1016/j.chom.2015.07.014
75. Ramanjulu JM, Pesiridis GS, Yang J, Concha N, Singhaus R, Zhang SY, et al. Design of amidobenzimidazole STING receptor agonists with systemic activity. *Nature.* (2018) 564:439–43. doi: 10.1038/s41586-018-0705-y
76. Li T, Chen ZJ. The cGAS-cGAMP-STING pathway connects DNA damage to inflammation, senescence, and cancer. *J Exp Med.* (2018) 215:1287–99. doi: 10.1084/jem.20180139
77. Iqbal J, Ansari MA, Kumar B, Dutta D, Roy A, Chikoti L, et al. Histone H2B-IFI16 recognition of nuclear herpesviral genome induces cytoplasmic interferon-beta responses. *PLoS Pathog.* (2016) 12:e1005967. doi: 10.1371/journal.ppat.1005967
78. Gui X, Yang H, Li T, Tan X, Shi P, Li M, et al. Autophagy induction via STING trafficking is a primordial function of the cGAS pathway. *Nature.* (2019) 567:262–6. doi: 10.1038/s41586-019-1006-9
79. Che X, Zhang J, Zhu Y, Yang L, Quan H, Gao YQ. Structural flexibility and conformation features of cyclic dinucleotides in aqueous solutions. *J Phys Chem B.* (2016) 120:2670–80. doi: 10.1021/acs.jpcb.5b11531
80. Zhang X, Shi H, Wu J, Zhang X, Sun L, Chen C, et al. Cyclic GMP-AMP containing mixed phosphodiester linkages is an endogenous high-affinity ligand for STING. *Mol Cell.* (2013) 51:226–35. doi: 10.1016/j.molcel.2013.05.022
81. Gallego-Marin C, Schrum JE, Andrade WA, Shaffer SA, Giraldo LF, Lasso AM, et al. Cyclic GMP-AMP synthase is the cytosolic sensor of plasmodium falciparum genomic DNA and activates type I IFN in malaria. *J Immunol.* (2018) 200:768–74. doi: 10.4049/jimmunol.1701048
82. Sun L, Wu J, Du F, Chen X, Chen ZJ. Cyclic GMP-AMP synthase is a cytosolic DNA sensor that activates the type I interferon pathway. *Science.* (2013) 339:786–91. doi: 10.1126/science.1232458
83. Abe T, Marutani Y, Shoji I. Cytosolic DNA-sensing immune response and viral infection. *Microbiol Immunol.* (2019) 63:51–64. doi: 10.1111/1348-0421.12669
84. Tanaka Y, Chen ZJ. STING specifies IRF3 phosphorylation by TBK1 in the cytosolic DNA signaling pathway. *Sci Signal.* (2012) 5:ra20. doi: 10.1126/scisignal.2002521
85. Wang PH, Fung SY, Gao WW, Deng JJ, Cheng Y, Chaudhary V, et al. A novel transcript isoform of STING that sequesters cGAMP and dominantly inhibits innate nucleic acid sensing. *Nucleic Acids Res.* (2018) 46:4054–71. doi: 10.1093/nar/gky186
86. Chen H, Pei R, Zhu W, Zeng R, Wang Y, Wang Y, et al. An alternative splicing isoform of MITA antagonizes MITA-mediated induction of type I IFNs. *J Immunol.* (2014) 192:1162–70. doi: 10.4049/jimmunol.1300798
87. Stetson DB, Medzhitov R. Recognition of cytosolic DNA activates an IRF3-dependent innate immune response. *Immunity.* (2006) 24:93–103. doi: 10.1016/j.immuni.2005.12.003
88. Pokatayev V, Yang K, Tu X, Dobbs N, Wu J, Kalb RG, et al. Homeostatic regulation of STING protein at the resting state by stabilizer TOLLIP. *Nat Immunol.* (2020) 21:158–67. doi: 10.1038/s41590-019-0569-9
89. Rueckert C, Rand U, Roy U, Kasmapour B, Strowig T, Guzman CA. Cyclic dinucleotides modulate induced type I IFN responses in innate immune cells by degradation of STING. *FASEB J.* (2017) 31:3107–15. doi: 10.1096/fj.201601093R
90. Gonugunta VK, Sakai T, Pokatayev V, Yang K, Wu J, Dobbs N, et al. Trafficking-mediated STING degradation requires sorting to acidified endolysosomes and can be targeted to enhance anti-tumor response. *Cell Rep.* (2017) 21:3234–42. doi: 10.1016/j.celrep.2017.11.061
91. Cai X, Chiu YH, Chen ZJ. The cGAS-cGAMP-STING pathway of cytosolic DNA sensing and signaling. *Mol Cell.* (2014) 54:289–96. doi: 10.1016/j.molcel.2014.03.040
92. Lei Z, Deng M, Yi Z, Sun Q, Shapiro RA, Xu H, et al. cGAS-mediated autophagy protects the liver from ischemia-reperfusion injury independently of STING. *Am J Physiol Gastrointest Liver Physiol.* (2018) 314:G655–67. doi: 10.1152/ajpgi.00326.2017
93. Rasmussen SB, Horan KA, Holm CK, Stranks AJ, Mettenleiter TC, Simon AK, et al. Activation of autophagy by alpha-herpesviruses in myeloid cells is mediated by cytoplasmic viral DNA through a mechanism dependent on stimulator of IFN genes. *J Immunol.* (2011) 187:5268–76. doi: 10.4049/jimmunol.1100949
94. Liang Q, Seo GJ, Choi YJ, Kwak MJ, Ge J, Rodgers MA, et al. Crosstalk between the cGAS DNA sensor and Beclin-1 autophagy protein shapes innate

antimicrobial immune responses. *Cell Host Microbe.* (2014) 15:228–38. doi: 10.1016/j.chom.2014.01.009
95. Watson RO, Bell SL, MacDuff DA, Kimmey JM, Diner EJ, Olivas J, et al. The Cytosolic sensor cGAS detects mycobacterium tuberculosis DNA to induce type i interferons and activate autophagy. *Cell Host Microbe.* (2015) 17:811–9. doi: 10.1016/j.chom.2015.05.004
96. Li L, Yin Q, Kuss P, Maliga Z, Millan JL, Wu H, et al. Hydrolysis of 2′3′-cGAMP by ENPP1 and design of nonhydrolyzable analogs. *Nat Chem Biol.* (2014) 10:1043–8. doi: 10.1038/nchembio.1661
97. Eaglesham JB, Pan Y, Kupper TS, Kranzusch PJ. Viral and metazoan poxins are cGAMP-specific nucleases that restrict cGAS-STING signalling. *Nature.* (2019) 566:259–63. doi: 10.1038/s41586-019-0928-6
98. Taguchi T, Mukai K. Innate immunity signalling and membrane trafficking. *Curr Opin Cell Biol.* (2019) 59:1–7. doi: 10.1016/j.ceb.2019.02.002
99. Sun W, Li Y, Chen L, Chen H, You F, Zhou X, et al. ERIS, an endoplasmic reticulum IFN stimulator, activates innate immune signaling through dimerization. *Proc Natl Acad Sci USA.* (2009) 106:8653–8. doi: 10.1073/pnas.0900850106
100. Dobbs N, Burnaevskiy N, Chen D, Gonugunta VK, Alto NM, Yan N. Sting activation by translocation from the ER is associated with infection and autoinflammatory disease. *Cell Host Microbe.* (2015) 18:157–68. doi: 10.1016/j.chom.2015.07.001
101. Fu YZ, Su S, Gao YQ, Wang PP, Huang ZF, Hu MM, et al. Human cytomegalovirus tegument protein UL82 inhibits STING-mediated signaling to evade antiviral immunity. *Cell Host Microbe.* (2017) 21:231–43. doi: 10.1016/j.chom.2017.01.001
102. Ishikawa H, Ma Z, Barber GN. STING regulates intracellular DNA-mediated, type I interferon-dependent innate immunity. *Nature* (2009) 461:788–92. doi: 10.1038/nature08476
103. Saitoh T, Fujita N, Hayashi T, Takahara K, Satoh T, Lee H, et al. Atg9a controls dsDNA-driven dynamic translocation of STING and the innate immune response. *Proc Natl Acad Sci USA.* (2009) 106:20842–6. doi: 10.1073/pnas.0911267106
104. Chen W, Li S, Yu H, Liu X, Huang L, Wang Q, et al. ER Adaptor SCAP Translocates and recruits IRF3 to perinuclear microsome induced by cytosolic microbial DNAs. *PLoS Pathog.* (2016) 12:e1005462. doi: 10.1371/journal.ppat.1005462
105. Ran Y, Xiong MG, Xu ZS, Luo WW, Wang SY, Wang YY. YIPF5 is essential for innate immunity to DNA virus and facilitates COPII-dependent STING trafficking. *J Immunol.* (2019) 203:1560–70. doi: 10.4049/jimmunol.1900387
106. Luo WW, Li S, Li C, Lian H, Yang Q, Zhong B, et al. iRhom2 is essential for innate immunity to DNA viruses by mediating trafficking and stability of the adaptor STING. *Nat Immunol.* (2016) 17:1057–66. doi: 10.1038/ni.3510
107. Liu Y, Jesus AA, Marrero B, Yang D, Ramsey SE, Sanchez GAM, et al. Activated STING in a vascular and pulmonary syndrome. *N Engl J Med.* (2014) 371:507–18. doi: 10.1056/NEJMoa1312625
108. Jeremiah N, Neven B, Gentili M, Callebaut I, Maschalidi S, Stolzenberg MC, et al. Inherited STING-activating mutation underlies a familial inflammatory syndrome with lupus-like manifestations. *J Clin Invest.* (2014) 124:5516–20. doi: 10.1172/JCI79100
109. Brandizzi F, Barlowe C. Organization of the ER-Golgi interface for membrane traffic control. *Nat Rev Mol Cell Biol.* (2013) 14:382–92. doi: 10.1038/nrm3588
110. McIlwain DR, Lang PA, Maretzky T, Hamada K, Ohishi K, Maney SK, et al. iRhom2 regulation of TACE controls TNF-mediated protection against Listeria and responses to LPS. *Science.* (2012) 335:229–32. doi: 10.1126/science.1214448
111. Dewi PD, Kawasaki T, Murase M, Sueyoshi T, Deguchi T, Ori D, et al. PtdIns3P phosphatases MTMR3 and MTMR4 negatively regulate innate immune responses to DNA through modulating STING trafficking. *J Biol Chem.* (2019) 294:8412–23. doi: 10.1074/jbc.RA118.005731
112. Margolis SR, Wilson SC, Vance RE. Evolutionary origins of cGAS-STING signaling. *Trends Immunol.* (2017) 38:733–43. doi: 10.1016/j.it.2017.03.004
113. Yoshida Y, Suzuki K, Yamamoto A, Sakai N, Bando M, Tanimoto K, et al. YIPF5 and YIF1A recycle between the ER and the Golgi apparatus and are involved in the maintenance of the Golgi structure. *Exp Cell Res.* (2008) 314:3427–43. doi: 10.1016/j.yexcr.2008.07.023
114. Dykstra KM, Pokusa JE, Suhan J, Lee TH. Yip1A structures the mammalian endoplasmic reticulum. *Mol Biol Cell.* (2010) 21:1556–68. doi: 10.1091/mbc.E09-12-1002
115. Kano F, Yamauchi S, Yoshida Y, Watanabe-Takahashi M, Nishikawa K, Nakamura N, et al. Yip1A regulates the COPI-independent retrograde transport from the Golgi complex to the ER. *J Cell Sci.* (2009) 122(Pt 13):2218–27. doi: 10.1242/jcs.043414
116. Wei J, Guo W, Lian H, Yang Q, Lin H, Li S, et al. SNX8 mediates IFNgamma-triggered non-canonical signaling pathway and host defense against Listeria monocytogenes. *Proc Natl Acad Sci USA.* (2017) 114:13000–5. doi: 10.1073/pnas.1713462114
117. Johannes L, Wunder C. The SNXy flavours of endosomal sorting. *Nat Cell Biol.* (2011) 13:884–6. doi: 10.1038/ncb2300
118. Wei J, Lian H, Guo W, Chen YD, Zhang XN, Zang R, et al. SNX8 modulates innate immune response to DNA virus by mediating trafficking and activation of MITA. *PLoS Pathog.* (2018) 14:e1007336. doi: 10.1371/journal.ppat.1007336
119. Zhang L, Mo J, Swanson KV, Wen H, Petrucelli A, Gregory SM, et al. NLRC3, a member of the NLR family of proteins, is a negative regulator of innate immune signaling induced by the DNA sensor STING. *Immunity.* (2014) 40:329–41. doi: 10.1016/j.immuni.2014.01.010
120. Karki R, Man SM, Malireddi RKS, Kesavardhana S, Zhu Q, Burton AR, et al. NLRC3 is an inhibitory sensor of PI3K-mTOR pathways in cancer. *Nature.* (2016) 540:583–7. doi: 10.1038/nature20597
121. Konno H, Konno K, Barber GN. Cyclic dinucleotides trigger ULK1(ATG1) phosphorylation of STING to prevent sustained innate immune signaling. *Cell.* (2013) 155:688–98. doi: 10.1016/j.cell.2013.09.049
122. Chien Y, Kim S, Bumeister R, Loo YM, Kwon SW, Johnson CL, et al. RalB GTPase-mediated activation of the IkappaB family kinase TBK1 couples innate immune signaling to tumor cell survival. *Cell.* (2006) 127:157–70. doi: 10.1016/j.cell.2006.08.034
123. Sun MS, Zhang J, Jiang LQ, Pan YX, Tan JY, Yu F, et al. TMED2 potentiates cellular IFN responses to DNA viruses by reinforcing MITA dimerization and facilitating its trafficking. *Cell Rep.* (2018) 25:3086–98.e83. doi: 10.1016/j.celrep.2018.11.048
124. Shang J, Xia T, Han QQ, Zhao X, Hu MM, Shu HB, et al. Quantitative proteomics identified TTC4 as a TBK1 interactor and a positive regulator of SeV-induced innate immunity. *Proteomics.* (2018) 18:403. doi: 10.1002/pmic.201700403
125. Liu H, Moura-Alves P, Pei G, Mollenkopf HJ, Hurwitz R, Wu X, et al. cGAS facilitates sensing of extracellular cyclic dinucleotides to activate innate immunity. *EMBO Rep.* (2019) 20:293. doi: 10.15252/embr.201846293
126. Hopfner KP, Hornung V. Molecular mechanisms and cellular functions of cGAS-STING signalling. *Nat Rev Mol Cell Biol.* (2020). 501–521. doi: 10.1038/s41580-020-0244-x
127. Zheng C. Evasion of cytosolic DNA-stimulated innate immune responses by herpes simplex virus 1. *J Virol.* (2018) 92:e00099-17. doi: 10.1128/JVI.00099-17
128. Lau L, Gray EE, Brunette RL, Stetson DB. DNA tumor virus oncogenes antagonize the cGAS-STING DNA-sensing pathway. *Science.* (2015) 350:568–71. doi: 10.1126/science.aab3291
129. Yi G, Wen Y, Shu C, Han Q, Konan KV, Li P, et al. Hepatitis C virus NS4B can suppress STING accumulation to evade innate immune responses. *J Virol.* (2016) 90:254–65. doi: 10.1128/JVI.01720-15
130. Aguirre S, Maestre AM, Pagni S, Patel JR, Savage T, Gutman D, et al. DENV inhibits type I IFN production in infected cells by cleaving human STING. *PLoS Pathog.* (2012) 8:e1002934. doi: 10.1371/journal.ppat.1002934
131. Ma Z, Jacobs SR, West JA, Stopford C, Zhang Z, Davis Z, et al. Modulation of the cGAS-STING DNA sensing pathway by gammaherpesviruses. *Proc Natl Acad Sci USA.* (2015) 112:E4306–15. doi: 10.1073/pnas.1503831112
132. Bodda C, Reinert LS, Fruhwurth S, Richardo T, Sun C, Zhang BC, et al. HSV1 VP1-2 deubiquitinates STING to block type I interferon expression and promote brain infection. *J Exp Med.* (2020) 217:422. doi: 10.1084/jem.20191422
133. Wang J, Yang S, Liu L, Wang H, Yang B. HTLV-1 Tax impairs K63-linked ubiquitination of STING to evade host innate immunity. *Virus Res.* (2017) 232:13–21. doi: 10.1016/j.virusres.2017.01.016

134. Holm CK, Rahbek SH, Gad HH, Bak RO, Jakobsen MR, Jiang Z, et al. Influenza A virus targets a cGAS-independent STING pathway that controls enveloped RNA viruses. *Nat Commun.* (2016) 7:10680. doi: 10.1038/ncomms10680
135. Pan S, Liu X, Ma Y, Cao Y, He B. Herpes simplex virus 1 gamma134.5 protein inhibits STING activation that restricts viral replication. *J Virol.* (2018) 92:e01015-18. doi: 10.1128/JVI.01015-18
136. Garcia-Belmonte R, Perez-Nunez D, Pittau M, Richt JA, Revilla Y. African swine fever virus armenia/07 virulent strain controls interferon beta production through the cGAS-STING pathway. *J Virol.* (2019) 93:e02298-18. doi: 10.1128/JVI.02298-18
137. Hill SM, Wrobel L, Rubinsztein DC. Post-translational modifications of Beclin 1 provide multiple strategies for autophagy regulation. *Cell Death Differ.* (2019) 26:617–29. doi: 10.1038/s41418-018-0254-9
138. Chakraborty S, Bose R, Islam S, Das S, Ain R. Harnessing Autophagic network is essential for trophoblast stem cell differentiation. *Stem Cells Dev.* (2020) 29:682–94. doi: 10.1089/scd.2019.0296
139. Pilli M, Arko-Mensah J, Ponpuak M, Roberts E, Master S, Mandell MA, et al. TBK-1 promotes autophagy-mediated antimicrobial defense by controlling autophagosome maturation. *Immunity.* (2012) 37:223–34. doi: 10.1016/j.immuni.2012.04.015
140. Thurston TL, Ryzhakov G, Bloor S, von Muhlinen N, Randow F. The TBK1 adaptor and autophagy receptor NDP52 restricts the proliferation of ubiquitin-coated bacteria. *Nat Immunol.* (2009) 10:1215–21. doi: 10.1038/ni.1800
141. Watson RO, Manzanillo PS, Cox JS. Extracellular M. tuberculosis DNA targets bacteria for autophagy by activating the host DNA-sensing pathway. *Cell.* (2012) 150:803–15. doi: 10.1016/j.cell.2012.06.040
142. Yang J, Tang X, Nandakumar KS, Cheng K. Autophagy induced by STING, an unnoticed and primordial function of cGAS. *Cell Mol Immunol.* (2019) 16:683–4. doi: 10.1038/s41423-019-0240-2
143. Prabakaran T, Bodda C, Krapp C, Zhang BC, Christensen MH, Sun C, et al. Attenuation of cGAS-STING signaling is mediated by a p62/SQSTM1-dependent autophagy pathway activated by TBK1. *EMBO J.* (2018) 37:858. doi: 10.15252/embj.201797858
144. Liu D, Wu H, Wang C, Li Y, Tian H, Siraj S, et al. STING directly activates autophagy to tune the innate immune response. *Cell Death Differ.* (2019) 26:1735–49. doi: 10.1038/s41418-018-0251-z
145. Chen K, Liu J, Cao X. Regulation of type I interferon signaling in immunity and inflammation: a comprehensive review. *J Autoimmun.* (2017) 83:1–11. doi: 10.1016/j.jaut.2017.03.008
146. Malik A, Afaq S, Alwabli AS, Al-Ghmady K. Networking of predicted post-translational modification(PTM) sites in human EGFR. *Bioinformation.* (2019) 15:448–56. doi: 10.6026/97320630015448
147. Mowen KA, David M. Unconventional post-translational modifications in immunological signaling. *Nat Immunol.* (2014) 15:512–20. doi: 10.1038/ni.2873
148. Liu J, Qian C, Cao X. Post-translational modification control of innate immunity. *Immunity.* (2016) 45:15–30. doi: 10.1016/j.immuni.2016.06.020
149. Ko PJ, Dixon SJ. Protein palmitoylation and cancer. *EMBO Rep.* (2018) 19:666. doi: 10.15252/embr.201846666
150. Kontaxi C, Piccardo P, Gill AC. Lysine-Directed post-translational modifications of tau protein in Alzheimer's disease and related tauopathies. *Front Mol Biosci.* (2017) 4:56. doi: 10.3389/fmolb.2017.00056
151. Swatek KN, Komander D. Ubiquitin modifications. *Cell Res.* (2016) 26:399–422. doi: 10.1038/cr.2016.39
152. Yau R, Rape M. The increasing complexity of the ubiquitin code. *Nat Cell Biol.* (2016) 18:579–86. doi: 10.1038/ncb3358
153. Tsuchida T, Zou J, Saitoh T, Kumar H, Abe T, Matsuura Y, et al. The ubiquitin ligase TRIM56 regulates innate immune responses to intracellular double-stranded DNA. *Immunity.* (2010) 33:765–76. doi: 10.1016/j.immuni.2010.10.013
154. Zhang J, Hu MM, Wang YY, Shu HB. TRIM32 protein modulates type I interferon induction and cellular antiviral response by targeting MITA/STING protein for K63-linked ubiquitination. *J Biol Chem.* (2012) 287:28646–55. doi: 10.1074/jbc.M112.362608
155. Seo GJ, Kim C, Shin WJ, Sklan EH, Eoh H, Jung JU. TRIM56-mediated monoubiquitination of cGAS for cytosolic DNA sensing. *Nat Commun.* (2018) 9:613. doi: 10.1038/s41467-018-02936-3
156. Wang Q, Liu X, Cui Y, Tang Y, Chen W, Li S, et al. The E3 ubiquitin ligase AMFR and INSIG1 bridge the activation of TBK1 kinase by modifying the adaptor STING. *Immunity.* (2014) 41:919–33. doi: 10.1016/j.immuni.2014.11.011
157. Zhong B, Zhang L, Lei C, Li Y, Mao AP, Yang Y, et al. The ubiquitin ligase RNF5 regulates antiviral responses by mediating degradation of the adaptor protein MITA. *Immunity.* (2009) 30:397–407. doi: 10.1016/j.immuni.2009.01.008
158. Qin Y, Zhou MT, Hu MM, Hu YH, Zhang J, Guo L, et al. RNF26 temporally regulates virus-triggered type I interferon induction by two distinct mechanisms. *PLoS Pathog.* (2014) 10:e1004358. doi: 10.1371/journal.ppat.1004358
159. Zhang L, Wei N, Cui Y, Hong Z, Liu X, Wang Q, et al. The deubiquitinase CYLD is a specific checkpoint of the STING antiviral signaling pathway. *PLoS Pathog.* (2018) 14:e1007435. doi: 10.1371/journal.ppat.1007435
160. Hatakeyama S. TRIM family proteins: roles in autophagy, immunity, and carcinogenesis. *Trends Biochem Sci.* (2017) 42:297–311. doi: 10.1016/j.tibs.2017.01.002
161. Wang Y, Lian Q, Yang B, Yan S, Zhou H, He L, et al. TRIM30alpha is a negative-feedback regulator of the intracellular DNA and DNA virus-triggered response by targeting STING. *PLoS Pathog.* (2015) 11:e1005012. doi: 10.1371/journal.ppat.1005012
162. Shi M, Deng W, Bi E, Mao K, Ji Y, Lin G, et al. TRIM30 alpha negatively regulates TLR-mediated NF-kappa B activation by targeting TAB2 and TAB3 for degradation. *Nat Immunol.* (2008) 9:369–77. doi: 10.1038/ni1577
163. Xing J, Zhang A, Zhang H, Wang J, Li XC, Zeng MS, et al. TRIM29 promotes DNA virus infections by inhibiting innate immune response. *Nat Commun.* (2017) 8:945. doi: 10.1038/s41467-017-00101-w
164. Yao X, Wu J, Lin M, Sun W, He X, Gowda C, et al. Increased CD40 expression enhances early STING-mediated type I interferon response and host survival in a rodent malaria model. *PLoS Pathog.* (2016) 12:e1005930. doi: 10.1371/journal.ppat.1005930
165. Ni G, Konno H, Barber GN. Ubiquitination of STING at lysine 224 controls IRF3 activation. *Sci Immunol.* (2017) 2:7119. doi: 10.1126/sciimmunol.aah7119
166. Sun H, Zhang Q, Jing YY, Zhang M, Wang HY, Cai Z, et al. USP13 negatively regulates antiviral responses by deubiquitinating STING. *Nat Commun.* (2017) 8:15534. doi: 10.1038/ncomms15534
167. Levental I, Grzybek M, Simons K. Greasing their way: lipid modifications determine protein association with membrane rafts. *Biochemistry.* (2010) 49:6305–16. doi: 10.1021/bi100882y
168. Linder ME, Deschenes RJ. Palmitoylation: policing protein stability and traffic. *Nat Rev Mol Cell Biol.* (2007) 8:74–84. doi: 10.1038/nrm2084
169. Mukai K, Konno H, Akiba T, Uemura T, Waguri S, Kobayashi T, et al. Activation of STING requires palmitoylation at the Golgi. *Nat Commun.* (2016) 7:11932. doi: 10.1038/ncomms11932
170. Hansen AL, Mukai K, Schopfer FJ, Taguchi T, Holm CK. STING palmitoylation as a therapeutic target. *Cell Mol Immunol.* (2019) 16:236–41. doi: 10.1038/s41423-019-0205-5
171. Haag SM, Gulen MF, Reymond L, Gibelin A, Abrami L, Decout A, et al. Targeting STING with covalent small-molecule inhibitors. *Nature.* (2018) 559:269–73. doi: 10.1038/s41586-018-0287-8
172. Li Z, Liu G, Sun L, Teng Y, Guo X, Jia J, et al. PPM1A regulates antiviral signaling by antagonizing TBK1-mediated STING phosphorylation and aggregation. *PLoS Pathog.* (2015) 11:e1004783. doi: 10.1371/journal.ppat.1004783
173. Zhu Y, An X, Zhang X, Qiao Y, Zheng T, Li X. STING: a master regulator in the cancer-immunity cycle. *Mol Cancer.* (2019) 18:152. doi: 10.1186/s12943-019-1087-y
174. Wang F, Alain T, Szretter KJ, Stephenson K, Pol JG, Atherton MJ, et al. S6K-STING interaction regulates cytosolic DNA-mediated activation of the transcription factor IRF3. *Nat Immunol.* (2016) 17:514–22. doi: 10.1038/ni.3433

175. Jin L, Waterman PM, Jonscher KR, Short CM, Reisdorph NA, Cambier JC. MPYS, a novel membrane tetraspanner, is associated with major histocompatibility complex class II and mediates transduction of apoptotic signals. *Mol Cell Biol.* (2008) 28:5014–26. doi: 10.1128/MCB.00640-08
176. Khan WN, Alt FW, Gerstein RM, Malynn BA, Larsson I, Rathbun G, et al. Defective B cell development and function in Btk-deficient mice. *Immunity.* (1995) 3:283–99. doi: 10.1016/1074-7613(95)90114-0
177. Lee KG, Kim SS, Kui L, Voon DC, Mauduit M, Bist P, et al. Bruton's tyrosine kinase phosphorylates DDX41 and activates its binding of dsDNA and STING to initiate type 1 interferon response. *Cell Rep.* (2015) 10:1055–65. doi: 10.1016/j.celrep.2015.01.039
178. Xia T, Yi XM, Wu X, Shang J, Shu HB. PTPN1/2-mediated dephosphorylation of MITA/STING promotes its 20S proteasomal degradation and attenuates innate antiviral response. *Proc Natl Acad Sci USA.* (2019) 116:20063–9. doi: 10.1073/pnas.1906431116
179. Hwang J, Kang T, Lee J, Choi BS, Han S. Design, synthesis, and biological evaluation of C7-functionalized DMXAA derivatives as potential human-STING agonists. *Org Biomol Chem.* (2019) 17:1869–74. doi: 10.1039/c8ob01798k
180. Corrales L, Glickman LH, McWhirter SM, Kanne DB, Sivick KE, Katibah GE, et al. Direct activation of STING in the tumor microenvironment leads to potent and systemic tumor regression and immunity. *Cell Rep.* (2015) 11:1018–30. doi: 10.1016/j.celrep.2015.04.031
181. Jassar AS, Suzuki E, Kapoor V, Sun J, Silverberg MB, Cheung L, et al. Activation of tumor-associated macrophages by the vascular disrupting agent 5,6-dimethylxanthenone-4-acetic acid induces an effective CD8+ T-cell-mediated antitumor immune response in murine models of lung cancer and mesothelioma. *Cancer Res.* (2005) 65:11752–61. doi: 10.1158/0008-5472.CAN-05-1658
182. Prantner D, Perkins DJ, Lai W, Williams MS, Sharma S, Fitzgerald KA, et al. 5,6-Dimethylxanthenone-4-acetic acid(DMXAA) activates stimulator of interferon gene(STING)-dependent innate immune pathways and is regulated by mitochondrial membrane potential. *J Biol Chem.* (2012) 287:39776–88. doi: 10.1074/jbc.M112.382986
183. Ager CR, Zhang H, Wei Z, Jones P, Curran MA, Di Francesco ME. Discovery of IACS-8803 and IACS-8779, potent agonists of stimulator of interferon genes(STING) with robust systemic antitumor efficacy. *Bioorg Med Chem Lett.* (2019) 29:126640. doi: 10.1016/j.bmcl.2019.126640
184. Siu T, Altman MD, Baltus GA, Childers M, Ellis JM, Gunaydin H, et al. Discovery of a novel cGAMP competitive ligand of the inactive form of STING. *ACS Med Chem Lett.* (2019) 10:92–7. doi: 10.1021/acsmedchemlett.8b00466
185. Lioux T, Mauny MA, Lamoureux A, Bascoul N, Hays M, Vernejoul F, et al. Design, Synthesis, and biological evaluation of novel cyclic adenosine-inosine monophosphate(cAIMP) analogs that activate stimulator of interferon genes(STING). *J Med Chem.* (2016) 59:10253–67. doi: 10.1021/acs.jmedchem.6b01300
186. Flood BA, Higgs EF, Li S, Luke JJ, Gajewski TF. STING pathway agonism as a cancer therapeutic. *Immunol Rev.* (2019) 290:24–38. doi: 10.1111/imr.12765
187. Biswas KK, Bhattacharyya UK, Palchoudhury S, Balram N, Kumar A, Arora R, et al. Dominance of recombinant cotton leaf curl Multan-Rajasthan virus associated with cotton leaf curl disease outbreak in northwest India. *PLoS One.* (2020) 15:e0231886. doi: 10.1371/journal.pone.0231886

Conflict of Interest: The authors declare that the research was conducted in the absence of any commercial or financial relationships that could be construed as a potential conflict of interest.

frontiers in Immunology

REVIEW
published: 01 October 2020
doi: 10.3389/fimmu.2020.568412

Vaccinia Virus Activation and Antagonism of Cytosolic DNA Sensing

*Misbah El-Jesr, Muad Teir and Carlos Maluquer de Motes**

Department of Microbial Sciences, University of Surrey, Guildford, United Kingdom

Cells express multiple molecules aimed at detecting incoming virus and infection. Recognition of virus infection leads to the production of cytokines, chemokines and restriction factors that limit virus replication and activate an adaptive immune response offering long-term protection. Recognition of cytosolic DNA has become a central immune sensing mechanism involved in infection, autoinflammation, and cancer immunotherapy. Vaccinia virus (VACV) is the prototypic member of the family Poxviridae and the vaccine used to eradicate smallpox. VACV harbors enormous potential as a vaccine vector and several attenuated strains are currently being developed against infectious diseases. In addition, VACV has emerged as a popular oncolytic agent due to its cytotoxic capacity even in hypoxic environments. As a poxvirus, VACV is an unusual virus that replicates its large DNA genome exclusively in the cytoplasm of infected cells. Despite producing large amounts of cytosolic DNA, VACV efficiently suppresses the subsequent innate immune response by deploying an arsenal of proteins with capacity to disable host antiviral signaling, some of which specifically target cytosolic DNA sensing pathways. Some of these strategies are conserved amongst orthopoxviruses, whereas others are seemingly unique to VACV. In this review we provide an overview of the VACV replicative cycle and discuss the recent advances on our understanding of how VACV induces and antagonizes innate immune activation via cytosolic DNA sensing pathways. The implications of these findings in the rational design of vaccines and oncolytics based on VACV are also discussed.

Keywords: STING, CGAS, interferons, antiviral signaling, vaccinia virus (VACV)

OPEN ACCESS

Edited by:
Chunfu Zheng,
Fujian Medical University, China

Reviewed by:
Yi-Quan Wu,
National Cancer Institute (NCI), United States
Kai Huang,
University of Texas Medical Branch at Galveston, United States

****Correspondence:***
Carlos Maluquer de Motes
c.maluquerdemotes@surrey.ac.uk

Specialty section:
This article was submitted to Molecular Innate Immunity, a section of the journal Frontiers in Immunology

Received: *01 June 2020*
Accepted: *24 August 2020*
Published: *01 October 2020*

Citation:
El-Jesr M, Teir M and Maluquer de Motes C (2020) Vaccinia Virus Activation and Antagonism of Cytosolic DNA Sensing. Front. Immunol. 11:568412. doi: 10.3389/fimmu.2020.568412

INTRODUCTION

Vaccinia virus (VACV) is the prototypic and the most widely and intensely studied member of the family Poxviridae, a family of cytoplasmic-replicating viruses harboring large ∼200 kbp linear dsDNA genomes. VACV is a very immunogenic virus that served as a vaccine for the eradication of smallpox, the only human disease eradicated so far. The virus causing smallpox, variola virus (VARV), and VACV belong to the genus Orthopoxvirus (OPXV), which also includes several other viral species infecting mammals. The origins and evolution of VACV are complex, but likely to share an ancestor with the now extinct horsepox virus (1). Multiple VACV strains exist and were used during the smallpox vaccination campaign around the globe. Although highly similar, the genetic content of these strains may vary, possibly as a reflection of their historical passage and use (2). In 1990, the group of Enzo Paoletti published the genome sequence of VACV strain

Copenhagen (COP), one of the most studied strains (3). In this review, the COP nomenclature is used to identify VACV genes, but reference is also given to the Western Reserve (WR) strain, which is commonly used as a research tool. Despite the huge potential of using VACV as a vaccine vector for other infectious diseases, the smallpox eradication campaign revealed side-effects and complications derived from the use of live replication-competent VACV strains, and highlighted the need for safer vaccines with safety records conforming with current standards. This need fuelled (i) the search for proteins contributing to virulence, and hence likely to attenuate the virus when removed, and (ii) the use of severely attenuated strains generally obtained after serial passages in cell culture. One of this highly attenuated strains is Modified Vaccinia virus Ankara (MVA), a derivative of the Turkish smallpox vaccine strain chorioallantoic VACV Ankara (CVA) that has lost many immunomodulatory and host range genes and is unable to replicate in human cells. The excellent safety profile of MVA and its rapid induction of immune protective responses has fostered its development as vaccine vector against multiple diseases (4). In addition, MVA has become a great tool to understand how VACV is sensed by the host innate immune system, thereby allowing rational improvement of vaccine design.

As a poxvirus VACV is a very complex virus. It follows an exclusively cytosolic replicative cycle, as opposed to most DNA viruses which replicate in the nucleus. Viral genome replication and assembly of nascent virions takes place in specific areas of the cytoplasm generally known as viral factories (5, 6). Establishment of viral factories is preceded by genome release and expression of early genes, which occurs inside the viral cores before these are dismantled and the genome becomes permissive for replication (7–10). Once produced nascent virions travel through the Golgi apparatus and mature into a double-membraned form known as extracellular virus (EV). EV mediate viral spread to neighboring cells and are critical to establish infection within an individual (11, 12). As the infection progresses, single-membraned virions known as mature virus (MV) accumulate inside the cytosol and are released upon cell lysis. In the host, VACV infection initiates in skin fibroblasts and proceeds to inflammatory monocytes recruited to the site of infection (13, 14), which can contain infection but also spread the virus through the blood stream. A core set of genes conserved amongst OPXV can be identified in the central part of the linear genome and are mostly involved in viral replication and morphogenesis. These conserved genes render OPXV antigenically similar and generate cross-protection after immunization. On the contrary, the genome termini are rich in accessory genes whose function is to modulate the host immune response and determine host range. Most of these genes are therefore specific to each member of the genus and have sometimes followed clear duplication and speciation events. For instance, VACV is rich in genes coding for proteins that resemble the cellular B-cell lymphoma (Bcl)-2 family despite having minimal sequence conservation amongst them (15, 16). Equally, other genus members such as cowpox virus (CPXV) or ectromelia virus (ECTV) are rich in genes coding for proteins containing Ankyrin repeats (17–19). Research on the functions of these proteins indicates strong convergent evolution on suppression of host innate immunity. Most of the VACV immunomodulatory genes are under the control of early promoters and are therefore deployed as soon as infection initiates. Some have been identified into the viral particle and may become immediately available upon entry (20–22). Between one-third and one-half of VACV proteins are estimated to interfere with the host immune response, some by more than one mechanism. Given this arsenal of immunomodulatory proteins it remains puzzling how VACV is such an immunogenic virus and induces potent humoral and cellular responses to self and foreign antigens. A unique property of VACV and poxviruses is to replicate in the cytosol, where most innate pattern recognition receptors (PRR) reside (23, 24). The innate immune system provides a rapid and robust response to invading pathogens that is well-known to impact and shape the subsequent adaptive response clearing the infection. The evolutionary interplay between host innate sensors and viral antagonists in the highly hostile cytosolic niche occupied by VACV is likely to profoundly determine the outcome of infection and therapeutic treatment.

Here, we review the current knowledge on how cells sense VACV infection through its DNA genome and how VACV in turn prevents this recognition. VACV produces several intracellular proteins targeting the core components of host DNA sensing signaling and others targeting components acting downstream. VACV also encodes soluble decoy receptors neutralizing some of the host cytokines induced by DNA sensing pathways such as interferons (IFN) and tumor necrosis factor (TNF)-α, but these are not covered here and we refer the reader to previous reviews on the topic (16, 25–27). Finally, we discuss the implications of VACV DNA sensing in the therapeutic use of VACV as a vaccine vector and oncolytic agent.

OVERVIEW OF ANTIVIRAL CYTOSOLIC DNA SENSING

The presence of foreign RNA and DNA within the cell cytosol is a clear sign of danger. Intracellular DNA is detected by a number of PRR that lead to a robust cellular response characterized by a rapid production of chemokines and cytokines including type I IFN (IFN-I) and the subsequent expression of IFN-stimulated genes (ISG). Induction of this antiviral response mostly relies on transcriptional activation by IFN responsive factors (IRF) and the nuclear factor κ-light-chain-enhancer of activated B cells (NF-κB), although transcription-independent mechanisms exist. This is the case of the Absent in Melanoma (AIM)-2-like receptors, which initiate the release of the potent inflammatory cytokines interleukin (IL)-1β and IL-18 upon recognition of cytosolic DNA (28, 29). Activation of antiviral IRF and NF-κB signaling in response to DNA mostly derive from cytosolic DNA sensors, but also from the membrane-bound Toll-like receptor (TLR)-9 which recognizes DNA contained in endosomal vesicles (30, 31). TLR9 expression is mostly restricted to specialized immune cells and it transduces signal via myeloid differentiation primary response 88 (MyD88) to eventually phosphorylate IRF3 and IRF7 (31, 32). Amongst cytosolic DNA sensors cyclic GMP-AMP

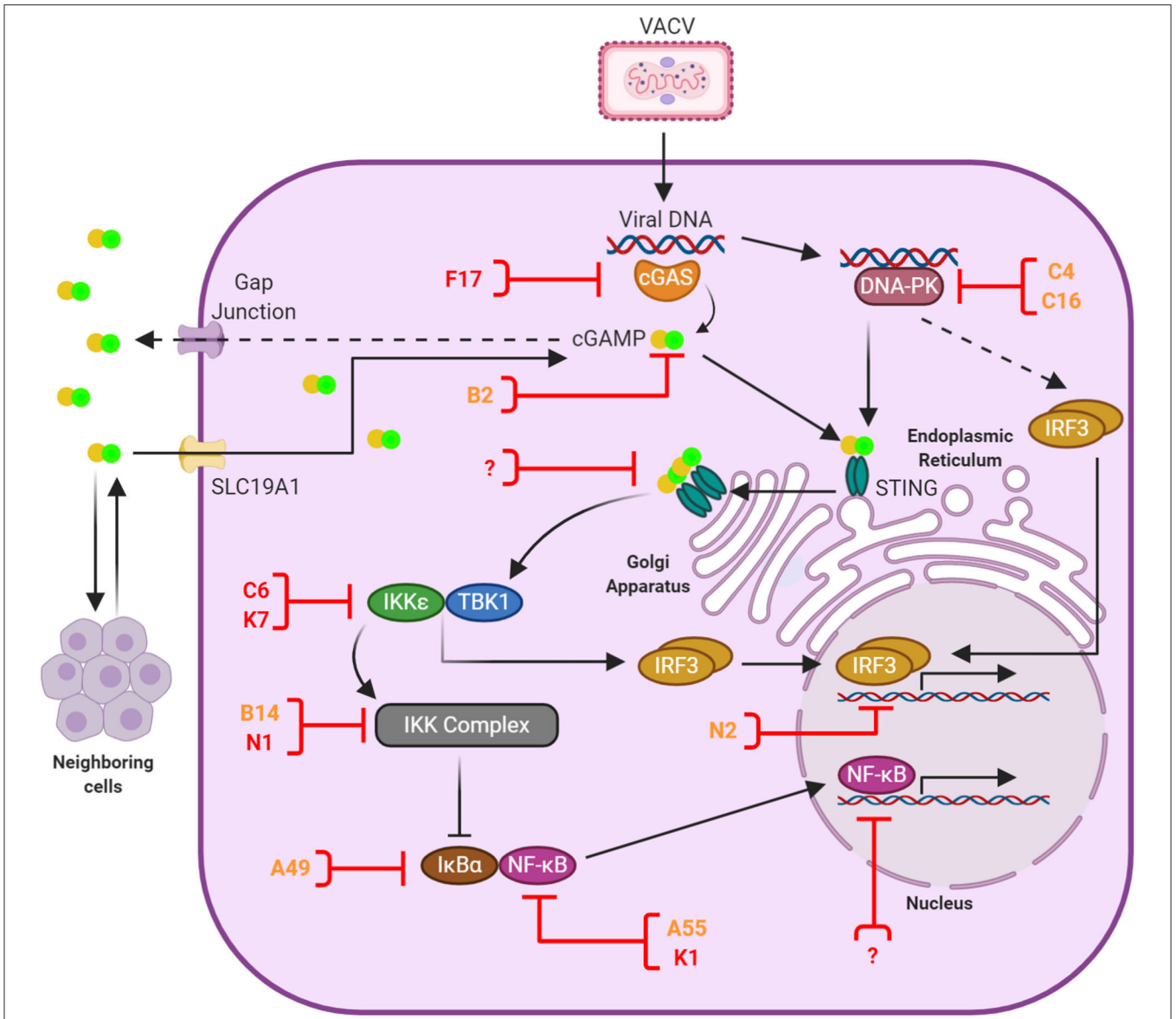

FIGURE 1 | Anti-viral DNA sensing and its antagonism by VACV. Upon infection the VACV genome is released into the cytosol and recognized primarily by cGAS, although other sensors such as DNA-PK play a role in a cell-specific manner. Activated cGAS catalizes the production of 2′ 3′ -cGAMP, which binds and activates STING. In addition, cGAMP is transferred to neighboring cells via gap junctions and imported from the extracellular environment via the transporter SLC19A1. cGAMP-bound STING oligomers mediate the recruitment of TBK1, which subsequently leads to the activation of IRF3 and NF-κB signal transduction and the induction of anti-viral responses. A number of VACV proteins have the capacity to block cytosolic DNA sensing and are shown here in orange or red depending on the level of conservation (see **Table 1**). These proteins counteract multiple stages of the signaling cascade (shown here with a blocked line). Evidence exists for additional inhibitors acting in the cell nucleus, although they remain yet unidentified. At present no VACV inhibitors of STING have been discovered, but this is a convergent signaling point known to be blocked by several viruses. These potential target sites are indicated with a question mark.

synthase (cGAS) stands out as a critical molecule since it appears essential for IFN production in every setting where this has been tested (**Figure 1**). cGAS is a DNA-binding enzyme that produces the small second messenger 2′ 3′ -cyclic GMP-AMP (cGAMP) upon recognition of dsDNA (48–52). cGAS belongs to the family of nucleotydiltransferases, loosely related to the oligoadenylates synthetases (53). The unique phosphodiester linkage in cGAMP (the 2'-OH of GMP binds to the 5′ of AMP and the 3′ -OH of AMP binds to the 5′ phosphate of GMP) confers greater affinity to the stimulator of IFN genes (STING) than other reported cyclic dinucleotides (CDNs) (51, 54, 55). cGAS patrols the cell cytosol as a sensor for abnormal situations revealed by mislocalised DNA either from invading pathogens or cellular stress (56). Its product cGAMP binds to and activates STING to promote IRF and NF-κB activation in the stimulated cell (57–60), but also in unstimulated neighbor cells via intercellular and extracellular transfer (61–64).

Upon cGAMP binding, STING dimers translocate from the endoplasmic reticulum (ER) to Golgi compartments where several post-translational modifications, including palmitoylation and ubiquitylation, take place to establish the STING signalosome (65–68). Here the C-terminal tail of STING interacts with TANK-binding kinase (TBK)-1 to mediate IRF3 activation in a complex trans-phosphorylation process that has recently been enlightened by structural advances (69–71) and has been reviewed in detail elsewhere (72, 73). Phosphorylated IRF3 dimerises and translocates to the cell nucleus to drive expression of IRF-dependent genes including the IFNβ enhanceosome. It is also known that STING oligomerisation induces the subsequent degradation of the inhibitor of κB (IκB)-α and activate, albeit to a lower extent, NF-κB responses including the production of TNFα, IL-1β and IL-6 (57, 58, 74–76). Canonical NF-κB signaling deriving from cytokine receptors or TLR requires the use of TNF receptor-associated factor (TRAF)-6 or TRAF2 to activate the IκBα kinase (IKK) complex, which in turn phosphorylates IκBα and triggers its proteasomal degradation via the E3 ligase β-TrCP. STING responses require the IKK complex, which can be redundantly activated by TBK1 and its homolog IKKε in a manner that may involve the upstream kinase transforming growth factor-β-activated kinase 1 (TAK1) (76, 77). NF-κB would usually be found as the p65/p50 (RelA/NF-κB1) heterodimer, the most common of NF-κB protein dimers (78). Following the degradation of IκBα, NF-κB becomes free to move from the cytoplasm to the nucleus (78, 79). There it can induce the transcription of several target genes, which include immunomodulatory proteins as well as IκBα, which is required to maintain a negative feedback loop (80). There also exists a non-canonical pathway, which comes into play during DNA damage. This pathway involves the activity of ataxia telangiectasia mutated (ATM) and poly ADP-ribose polymerase 1 (PARP-1), initiating an outside signal from within the cell that goes through IFNγ-inducible protein 16 (IFI16) and STING, without the aid of cGAS, and eventually reaches the IKK complex and activates NF-κB (75).

Before and after the discovery of cGAS other molecules were found to affect DNA sensing signaling. Although the specific biochemical pathways used by these molecules are not always deciphered, nearly all of them converge on STING and may act as cofactors, modulators or regulators of the cGAS-cGAMP-STING axis in a species, cell type and/or self- vs. non-self-specific manner. This list includes DNA-dependent activator of interferon (DAI) (81), RNA polymerase III (82, 83), IFI16 (84), the DExD/H-box helicases DHX9, DDX36 (85) and DDX41 (86); the DNA damage proteins Ku70/80 (87), DNA-PK (88), Mre11 (89) and PQBP1 (90); LSM14A (91); and G3BP1 (92). For a detailed review of this topic, we refer the reader to recent publications (72, 73). Two of these molecules, IFI16 and DNA-PK, have been reported to have direct roles in VACV sensing and are discussed below in more detail. One of them, namely DNA-PK, has been recently implicated in STING-independent IFN-I production in response to DNA and involves the downstream signaling of the heat shock protein HSPA8, in what is being referred to as the STING-independent DNA sensing pathway (SIDSP) (93).

DNA SENSING ACTIVATION IN RESPONSE TO VACV

Understanding the interplay between host DNA sensing and VACV is difficult because VACV suppresses cell responses through expression of multiple antagonists acting upstream and downstream of these pathways (16, 94). Insights are therefore usually gained using attenuated VACV strains such as MVA that have lost most of these antagonists or employing live animal models that can reproduce the complex immunological responses generated upon infection. VACV can cause pathology in commonly used mouse breeds such as Balb/c or C57BL/6, so genetically engineered mice lacking specific DNA sensing and innate immune molecules can provide insights into VACV immunity, with the caveat that DNA sensing in mice may differ from humans as it is becoming increasingly reported (93, 95). Inoculation of VACV into transgenic mice deficient for cGAS revealed a mild increase in viral replication and tissue pathology (14, 96) that correlated with reduced IFN-I expression, which was also observed in STING deficient mice (14). Similar experiments performed with ECTV, a mouse-specific virus and the causative agent of mousepox, showed enhanced mortality in STING deficient mice (97), but varied susceptibility in cGAS deficient mice (97, 98). In contrast, mice lacking IFI204 (the mouse ortholog of IFI16) survived ECTV infection and did not exhibit significant differences in viral replication and viral burden (98). Whilst these studies demonstrated the role of cGAS and STING in mounting responses against VACV and ECTV *in vivo*, the observed effects were rather mild. This suggests that VACV and ECTV minimize the activity of this pathway to the point that genetic ablation of an already targeted signaling nodule had reduced effect on the overall response. The discovery of viral inhibitors of DNA sensing (discussed below) has allowed a better assessment of the impact of the cGAS-cGAMP-STING axis and recently, ECTV lacking the viral cGAMP nuclease vSchlafen has shown extreme attenuation in multiple models of infection (99). This has revealed the enormous importance of cGAS-STING in poxvirus immunity.

The use of the highly attenuated VACV strain MVA has proven pivotal in understanding DNA sensing immunity against VACV. The MVA genome is significantly shorter than its parental CVA due to five large deletions and additional mutations in at least 25 genes resulting in truncated proteins (100). Since many of these proteins are non-essential immune modulators, it is not surprising that MVA acts as potent inducer of immune responses in most mammalian cells. Before the discovery of DNA sensing pathways, MVA infection was known to be recognized by TLR dependent and independent pathways including the RNA sensor melanoma differentiation-associated protein (MDA)-5 in macrophages and dendritic cells (101–104). MDA5 converges onto IRF3 signaling and IFN-I production via mitochondrial antiviral signaling protein (MAVS) and recognizes long dsRNA in the cytosol (105, 106), a by-product of poxviral gene expression in this compartment. Subsequently, several studies have shown that IFN-I induction by MVA relies on cGAS and its downstream adaptor STING (88, 94, 107, 108). Deletion or depletion of cGAS or STING in mouse and human cells results in impaired

TABLE 1 | VACV proteins counteracting intracellular DNA sensing pathways.

Protein	Size (kDa)	Conservation[a]	Function	Virulence factor	Key references
A49	18.7	Most OPXV	Targets β-TrCP; NF-κB inhibitor	Yes	(33, 34)
A55	64.6	Most OPXV	NF-κB inhibitor; prevents NF-κB nuclear translocation	Yes	(35)
B2/Poxin	24.6	VACV; vSchlafen in OPXV	2′,3′-cGAMP nuclease	Yes	(36)
B14	17.3	Most OPXV	NF-κB inhibitor; targets IKKβ	Yes	(37, 38)
C4	37.2	Most OPXV	DNA-PK inhibitor; binds to Ku proteins	Yes	(39)
C6	17.3	OPXV	IRF3/7 inhibitor; targets TBK1 adaptors	Yes	(40)
C16	37.5	Most OPXV	DNA-PK inhibitor; binds to Ku protein	Yes	(39, 41)
F17	11.3	OPXV	Dysregulates mTOR; downregulates cGAS and STING	Essential for growth	(42)
K1	32.4	OPXV	NF-κB inhibitor; prevents IκBα degradation	Yes	(43)
K7	17.4	OPXV	IRF3 inhibitor; targets DDX3	Yes	(44)
N1	13.9	OPXV	NF-κB inhibitor	Yes	(37, 45, 46)
N2	20.8	Most OPXV	Nuclear IRF3 inhibitor	Yes	(47)

[a]*Conservation within the OPXV is indicated.*

induction of IFNα, IFNβ, and CXCL10 in response to MVA. These findings are in line with results obtained with other poxviruses and in the context of replicative VACV lacking specific DNA sensing inhibitors (97, 109, 110). In addition to cGAS other DNA sensors have been implicated in VACV immunity: DNA-PK and IFI16. DNA-PK consists of a heterodimer of the DNA-binding proteins Ku70 and Ku80 and DNA-PKcs, its catalytic subunit. DNA-PK is best known for its role in DNA repair and V(D)J recombination (111), but it also acts as a PRR in response to intracellular DNA (88). DNA-PK leads to IRF3 activation and cytokine production including IFN-I in response to cytoplasmic DNA, particularly in fibroblasts. Although the specific biochemical pathway induced by DNA-PK is not as clear as for cGAS, it has been shown to trigger innate immune activation through the cGAS-STING-IRF3 pathway (88, 112) and more recently, in a STING-independent manner (93). DNA-PK is essential for cell viability and this limits its genetic manipulation. Nonetheless, murine fibroblasts deficient for specific DNA-PK components show reduced levels of IFN-I, CXCL10 and IL-6 when infected with MVA whilst retaining complete responsiveness to RNA virus infection, and this correlated with DNA-PK translocation to viral factories (88). IFI16 has also been shown to translocate to viral factories, particularly in keratinocytes, and this correlated with reduced CCL5 and ISGs production in response to MVA (113), although no difference in IFN-I has been observed in macrophages (107), suggesting a cell-specific role for IFI16 in sensing VACV infection. IFI16 is a critical sensor for nuclear DNA viruses and is actively targeted for immune evasion (114, 115). Whilst a VACV inhibitor for IFI16 remains to be discovered, VACV encodes at least 2 molecules preventing DNA-PK-mediated sensing (39, 41).

VACV ANTAGONISTS OF DNA SENSING RESPONSES

VACV employs several strategies to suppress cytosolic DNA sensing. The discovery of these viral inhibitors has served to enlighten these relatively recent innate signaling pathways and provide important insights into their mechanisms of activation and regulation. These inhibitors and strategies are reviewed below and summarized in **Table 1** and **Figure 1**.

Targeting DNA-PK (Proteins C16 and C4)

The first VACV protein reported to suppress cytosolic DNA sensing during infection was C16, first characterized by Fahy et al. (116). It is a 37.5 kDa non-essential protein comprising 331 amino acids, encoded by the *C16L* gene (WR010/209), two copies of which are present in the ITRs on both ends of the VACV genome. C16 is highly conserved among some OPVX members such as VARV, ECTV, and CPXV, while in others such as monkeypox virus (MPXV) or camelpox virus (CMLV) the sequence contains disruptions that alter the reading frame (116). Originally, C16 was found to enhance VACV virulence via an unknown mechanism (116). Only later was its role in DNA sensing inhibition revealed as a DNA-PK inhibitor. During VACV infection C16 binds to the Ku70/80 heterodimer of the DNA-PK complex using its C-terminal domain (41). This prevents the recognition of VACV DNA since the Ku proteins mediate DNA binding. An engineered VACV lacking C16 caused less weight loss and induced higher levels of cytokines and chemokines in mice after intranasal inoculation (41, 116). Furthermore, MVA, which contains a deletion of 5 amino acids in the Ku-binding domain, induced IFN-I production in a DNA-PK-dependent manner (88). It is worth noting that VACV C16 is a multifunctional protein that has also been shown to manipulate hypoxic signaling and reprogramme energy metabolism (117, 118).

More recently, a second VACV protein has been found to target DNA-PK. Protein C4 (WR024) shares 43% identity with C16; it is highly conserved between several members of the OPXV genus; and it is non-essential for virus growth (119). C4 exhibits a similar function to C16 in regards to DNA sensing inhibition (39). C4 uses its C-terminal region to bind the Ku proteins and this reduces IRF3 phosphorylation and cytokine induction. Indeed, the binding of both C16 and C4 to Ku70 has been narrowed to three conserved amino acids. Viruses lacking expression of each of these proteins were attenuated in an intranasal model of infection inducing enhanced recruitment

of immune cells and T cell activation, but remained as virulent as their parental viruses after intradermal inoculation (116, 119). Interestingly, a double deletion virus lacking both C16 and C4 revealed attenuation upon intradermal injection, demonstrating that these proteins had redundant *in vivo* roles in this model of infection (39). Why VACV devotes three genes (two copies of C16L and a copy of C4L) to suppress DNA-PK cytosolic DNA sensing remains unknown, but an explanation might be the high abundance of DNA-PK, particularly in fibroblasts, a primary cell target in the skin. Interestingly, it has been recently shown that DNA-PK can activate a second DNA sensing pathway completely independent of STING activation (93). This could further emphasize the role of C16 and C4 in immunomodulation and DNA sensing inhibition given that these proteins may also inhibit SIDSP.

Targeting cGAS (Protein F17)

Besides the discovery of VACV inhibition of DNA-PK evidence existed that VACV was able to prevent STING activation by other mechanisms (94). One of these was reported by Meade et al. and involved protein F17 (42). F17 (WR056) is a conserved structural protein that constitutes the largest component of the virion lateral bodies and is essential for the formation of infectious virions (120–122). F17 exploits a complex cellular circuit connecting immune sensing and the metabolic rheostat mTOR (mammalian targets of rapamycin). mTOR is composed of two different complex systems, namely mTOR1 and mTOR2, both of which are regulated by distinct subunits conforming a negative feed-back loop (123, 124). F17 sequesters the subunits Raptor and Rictor so their regulatory feed-back is disrupted, allowing VACV to usurp mTOR control from the cell. This leads to overactive mTOR that enhances protein synthesis, but also suppresses innate activation at multiple levels including cGAS downregulation by a process that involves Akt (125) and dysregulation of STING vesicles in the ER (42). These effects suppress IRF3 translocation and trigger a potent suppression of ISG induction in both fibroblasts and macrophages, particularly late during infection in agreement with F17 late expression (42, 109). In the absence of F17 VACV infection leads to detectable ISG expression that depend on cGAS, but not IFI16, presence (109), thus supporting the primordial role of cGAS as a poxvirus DNA sensor. Of note, cGAS deletion did not completely abrogate ISG responses in fibroblasts (109), making room for a second IRF3-activating pathway sensing VACV in these cells. The high conservation of F17 not only across OPXV, but also across most vertebrate poxviruses, highlights the fundamental functions of this protein in poxvirus infections.

Targeting cGAMP (Protein B2)

cGAMP plays a pivotal role in antiviral DNA sensing responses. As a product of activated cGAS it binds STING and triggers innate immune activation in the infected cell. However, it also induces antiviral responses in neighboring cells by multiple mechanisms. cGAMP is transferred to neighboring cells via gap junctions (61) and membrane fusion events (126), is incorporated into exiting viral particles (127, 128) and imported into cells from the extracellular milieu via the transporter SLC19A1 (62, 63). Via these mechanisms cGAMP has the capacity to activate non-infected cells including immune cells and constitutes a potent antiviral signaling molecule. VACV neutralizes the effects of cGAMP by encoding a cGAMP nuclease in gene *B2R* (WR184), discovered by Eaglesham et al. and named poxvirus immune nuclease (poxin) (36). Poxin was identified in a screen for viruses able to destroy cGAMP, which included 24 viruses belonging to 13 different viral families. Only VACV was found to degrade cGAMP, a reflection of its unique nature as a cytosolic replicating virus, and mass spectrometry confirmed the activity to derive from product B2. Poxin binds and linearises cGAMP cleaving the 3′ -5′ bond and converting it into linear Gp[2′ -5′] Ap[3′]. VACV lacking Poxin shows no defect in growth, but displays a significant reduction of viral titer in mice (36). Homologs of Poxin are found in baculovirus and their insect hosts, perhaps revealing a common origin since insect poxviruses and baculoviruses share ecological niches. Within the *Poxviridae*, Poxin is not universally conserved and surprisingly in most OPXV it appears as vSchlafen, a fusion of Poxin with a second protein with high similarity to the mammalian family of Schlafen proteins (also known as gene *B3R* in VACV). Deletion of the entire vSchlafen or only its cGAMP nuclease domain in the context of ECTV renders the virus unable to suppress IRF3 activation during infection and leads to a dramatic 5-log drop in virulence in mice (99), the natural host of ECTV. Despite its critical role in counteracting the antiviral effects of cGAMP both *B2R* and *B3R* are swarmed with inactivating mutations in VARV. Poxin and vSchlafen are early genes, a class of genes expressed from within intact cytoplasmic viral cores (8–10). This allows production of early immune evasion factors before the viral genomic DNA is released and exposed to DNA sensors, and in conjunction with late factors like F17, it ensures complete suppression of innate activation throughout the entire life cycle.

Downstream IRF3 Inhibitors

Beyond the aforementioned, VACV possesses several different non-essential immunomodulatory proteins, most of which were reported when our knowledge on cytosolic DNA sensing was in its infancy. The discovery of DNA sensing pathways provides now a new dimension to their seemingly redundant roles. In most cases the function of these molecules as DNA sensing modulators has not been formally proven, but when the molecular mechanism of action has been elucidated, their antagonistic role can be anticipated. VACV proteins acting downstream of STING, and therefore expected to antagonize DNA sensing, include protein C6, which acts at the level of TBK1/IKKε. C6 binds to the cellular proteins TANK, NF-κB-activating protein (NAP)-1 and similar to NAP1 TBK1 adaptor (SINTBAD) (40). All three molecules work as adaptors for TBK1 and share a conserved TBK1/IKKε-binding domain (129). TBK1 and its adaptors act as a convergence point for TLRs, RNA and DNA sensing pathways and consistent with this, C6 is able to suppress IFN-I induction in response to poly(I:C), poly(dA-dT) and RNA virus infection, but did not affect NF-κB activation. VACV lacking C6 expression replicated normally in cell culture, but was significantly attenuated in mice (40). C6 was also shown to suppress IFN-I signaling (130, 131).

Given this multifunctionality C6 becomes an important VACV IFN antagonist and its deletion increases immunogenicity in mice both in the context of virulent and avirulent VACV such as MVA where C6 is not inactivated (132–136). The related VACV protein K7 also targets the TBK1/IKKε complex to inhibit IRF3 activation. As well as possessing the ability to inhibit NF-κB activation (137), K7 binds to and inhibits the DEAD-box RNA helicase DDX3, a TBK1 adaptor and substrate required for optimal IRF responses (44, 138). K7 binds to the N-terminal region of DDX3 to inhibit its function, ensuring a decreased TBK1/IKKε-dependent IFN-β promoter induction (44, 139). Like C6, K7 contributes to VACV virulence in mice and its removal leads to enhanced immunogenicity and memory immune responses (132, 134). Finally, the VACV Bcl-2 protein N2 acts as an IRF3 inhibitor in the nucleus, although its specific target remains elusive (47). N2 is dispensable for virus growth, but contributes to virulence (47), and MVA deleted for gene N2L enhances immunogenicity and the immune response to infection, marked by an increase in the production INF-β and other pro-inflammatory cytokines immune activation (140).

Downstream NF-κB Inhibitors

Multiple studies have demonstrated that production of inflammatory cytokines via STING-dependent DNA sensing requires NF-κB responses that depend on the IKK complex and the NF-κB heterodimer. VACV encodes multiple immunomodulators known to suppress NF-κB activation and detailed molecular mechanisms of action exist for several of them (16). VACV protein B14 is a Bcl-2-like protein encoded by the VACV *B14R* gene that is well-conserved among OPXV such as VARV and CPXV and contributes to virulence (37, 141). B14 binds to the N-terminal kinase domain and the scaffolding and dimerisation domain of IKKβ, and prevents its phosphorylation and activation, which in turn prevents the phosphorylation and subsequent degradation of IκBα (38, 142). This interaction is mediated by a surface of B14 that is otherwise utilized for dimerisation (37, 143). B14 can also activate the mitogen-activated protein kinase (MAPK)/activator protein 1 (AP-1) pathway (144) and is inactivated in MVA (145), confirming its non-essential role in virus growth. The related VACV protein N1 is a potent virulence factor that serves a dual role as inhibitor of apoptosis and inflammatory signaling (37, 45, 46, 107, 146, 147). Both functions map to different binding interfaces of the protein (45) and the ability to block NF-κB activation correlates with an impaired CD8 T cell effector and memory response (148). Although its exact mechanism of action for suppressing innate immune activation remains unknown, the inhibitory action of N1 on NF-κB signaling is believed to be downstream of the TRAFs. N1 is also known to be modified by ubiquitylation during infection, but this did not affect its ability to suppress NF-κB activation (149). A third VACV Bcl-2 protein evolved to suppress NF-κB signaling is A49, which contains an N-terminal region that mimics the IκBα degron sequence that mediates its proteasomal destruction (33, 150). A49 is phosphorylated by IKKβ and subsequently recognized by the E3 ubiquitin ligase β-TrCP, but unlike IκBα it is spared because it lacks the ubiquitin acceptor sites located upstream of the degron (33, 150). Using this mechanism A49 binds tightly to β-TrCP only when IKKβ is activated and canonical β-TrCP targets including IκBα and β-catenin accumulate in their phosphorylated forms and are not processed (33, 150, 151). A49 antagonism of NF-κB contributes to virulence (33, 34), but mutant A49 viruses unable to bind β-TrCP retain some degree of virulence suggesting the existence of other β-TrCP-independent functions, perhaps mediated by a second product identified in the A49 ORF (34, 152). In addition to these proteins, several VACV proteins including K1 and A55 have been shown to act at the level of the NF-κB heterodimer preventing their translocation or their normal processing (35, 43, 153). Thus, they also have the potential to suppress STING-induced NF-κB activation. Lastly, evidence exists that VACV downregulates NF-κB-dependent gene expression after p65 translocation by yet unidentified viral strategies (154).

IMPLICATIONS FOR THE THERAPEUTIC USE OF VACV

VACV-based therapeutics involve the use of VACV as a vaccine vector and oncolytic agent, as well as the use of VACV-derived proteins and peptides as biologicals. The development of VACV as a vaccine and for virotherapy holds promise and some forms of the virus are now in clinical studies, whereas the development of VACV-derived biologicals is at a much less advanced stage. VACV strain ACAM2000 (a derivative of Wyeth's Dryvax vaccine) and MVA (marketed as Jynneos) are approved by the USA Food and Drug Administration (FDA) for their use against smallpox and monkeypox, and various VACV strains have been engineered to carry heterologous antigens for diseases such as AIDS, malaria or tuberculosis amongst others (2). Enhancing immunogenicity and/or attenuating the virus remain desirable goals to increase VACV safety profile, elicit stronger immunological memory and reduce dosage and administration regimes. The discovery of DNA sensing pathways and their critical biological roles creates novel opportunities for the improvement of VACV as a therapeutic agent. The recognition of foreign incoming DNA in the cytosol triggers a potent immune and inflammatory reaction that includes IFN-I and IFN-III responses known to be beneficial for immune activation. Therefore, strategies aimed at increasing recognition of the VACV genome and boost intracellular DNA sensing signaling are likely to enhance vaccine efficacy and immunogenicity. These may include the deletion of immunomodulatory virulence factors from the virus or the co-administration of STING agonists. Evidence exists for the enhancement of immunogenicity and memory immunity upon removal of VACV immunomodulators [recently reviewed in (155)]. Some of these immunomodulators are listed above as viral DNA sensing antagonists. Therefore, this strategy seems logical to enhance IFN and cytokine production. An important aspect of consideration is whether removal of these viral immunomodulatory proteins is expected to impact on cGAMP levels. cGAMP triggers a STING-dependent, but cGAS-independent induction of cytokines when transferred between cells. Horizontal transfer of cGAMP during infection therefore has the potential to boost and shape the adaptive response.

Indeed, deletion of ECTV cGAMP nuclease vSchlafen led to a marked IFN-I signature in the draining lymph node and spleen that correlated with enhanced NK cell activation and survival to an otherwise lethal infection (99). Furthermore, studies have reported how the cGAS-STING axis promotes the generation of cytotoxic T cells (CTL) via the expression of IFN-I and the cross-presentation of antigens by dendritic cells (DC), in some cases after administration of exogenous cGAMP (156–159). Therefore, preventing the degradation of cGAMP by, for instance, removal of Poxin/B2 from VACV is likely to contribute favorably to the outcome of vaccination. A similar beneficial outcome may derive from the removal of VACV DNA-PK antagonists so DNA-PK-mediated innate immunity responses are unleashed.

A second positive prospect from these studies is the value of STING agonists as adjuvants and anti-virals. Although smallpox was eradicated 40 years ago, the importance of compounds with anti-OPXV activity is increasing due to the emergence of zoonotic OPXV infections, particularly by MPXV. MPXV causes human monkeypox, an emerging zoonotic smallpox-like disease that has a mortality rate of 5–10% and has caused several outbreaks with hundreds of cases in Central and West Africa and outbound travelers (160, 161). At present, ST-246 (marketed as tecovirimat) is the only FDA-approved drug for the treatment of OPXV infections and although it has good activity range against multiple OPXV species including VARV (162–164), alternative strategies are still desirable. Administration of exogenous cGAMP has been shown to elicit strong immune responses and protect mice against lethal ECTV infection (98, 99). This suggests that STING immunity is an attractive antiviral therapeutic target, although further experimentation is needed to determine the effects and specificity of cGAMP delivery pre- and post-infection as well as through different routes of inoculation.

A similar beneficial outcome in enhancing cGAS-STING signaling by either removal of viral immunosuppressive strategies or delivery of STING agonists might be expected in the context of oncolytic VACV. Oncolytic viruses are those that can selectively infect and/or grow in tumor cells leading to their destruction. VACV is a popular oncolytic virus for multiple reasons including its wide cell tropism and cytotoxicity, its ability to grow in hypoxic environments, the possibility for stable transgene expression and the fact that it does not integrate its DNA in the genome of the cell (165–167). Like tumor cells, VACV exploits multiple strategies to suppress cell death (168), some of which might be redundant with cancerous cells. However, whereas cancers tend to establish an immunosuppressive tumor microenvironment, VACV is immunogenic and is capable of altering the immune landscape, co-stimulating acquired anti-tumor immunity following replication within tumor tissues. In the case of immunogenic tumors, it has been reported that their recognition by the host immune system relies on STING-dependent cytosolic DNA sensing (156, 159). It has also been shown that intratumoral injection of MVA generated adaptive anti-tumor immunity in melanoma and colon cancer that was dependent on STING (169) and a GM-CSF (granulocyte-macrophage colony-stimulating factor)-secreting vaccine showed increased anti-tumor efficacy when formulated with STING CDN agonists (170). In addition, susceptibility of certain cancers to viral oncolysis correlates with STING and STING signaling (171, 172). Collectively, these studies demonstrate the importance of the cGAS-cGAMP-STING axis in immunotherapy and offer scope for the improvement of oncolytic VACV and its therapeutic potential.

Finally, a number of human diseases have been connected with cytosolic DNA sensing. Mutations in several human genes result in the accumulation and mislocalisation of DNA molecules leading cGAS activation, and this is best exemplified in the form of the Aicardi-Goutières syndrome (AGS), a rare devastating disease characterized by systemic inflammation (173). The persistent stimulation of cGAS-STING signaling has also recently been associated with systemic lupus erythematosus (SLE) (174), a much more prevalent disease associated with IFN-I dysregulation. Our increased knowledge on VACV antagonism of cytosolic DNA sensing may identify novel components or regulatory mechanisms of these cellular pathways and may reveal novel strategies to counteract the functions of these attractive therapeutic targets. For instance, detailed mechanistic and structural insights into VACV DNA sensing antagonists can allow the development of small molecule inhibitors mimicking the mode of action of the viral proteins. A proof of principle for these approaches is provided by the design of peptides deriving from VACV TLR inhibitors A46 and A52 (175, 176).

CONCLUSIONS

As our knowledge on nucleic acid immunity and inflammation expands it is becoming increasingly clear that the activation and regulation of intracellular DNA sensing has broad implications for human health and disease. VACV is a fantastic tool for discovery in human biology and virus pathogenesis as well as an important therapeutic tool. VACV has already proven pivotal in the discovery of cellular mechanisms for regulation of DNA sensing including uncovering the existence of viral and cellular cGAMP nucleases. VACV targets innate immune signaling at multiple levels and given the importance of DNA sensing for a cytosolic replicating virus it is likely that new viral inhibitors remain to be identified. Further research is also needed to address how VACV is sensed as the virion uncloaks and is recognized by cellular sensors. The identity and relative importance of these in the different cell types that are relevant for VACV infection and spread is also a necessary area of investigation. These findings need to be reciprocated in other poxviruses and can enlighten similar processes in viruses with similar biology such as the African Swine Fever virus and intracellular bacteria. Furthermore, many questions remain unanswered about how cells launch cell intrinsic defense mechanisms against VACV that involve recognition of its genome. Importantly, this knowledge is crucial to increasing the potential of VACV-based therapeutics both in the form of vaccines and oncolytic virus.

AUTHOR CONTRIBUTIONS

Conceptualization and funding acquisition: CM. Writing: ME-J, MT, and CM. All authors contributed to the article and approved the submitted version.

FUNDING

Work in the Maluquer Lab was supported by the UK Biotechnology and Biological Science Research Council (BBSRC grants BB/M003647/1 and BB/T006501/1).

REFERENCES

1. Esparza J, Schrick L, Damaso CR, Nitsche A. Equination (inoculation of horsepox): an early alternative to vaccination (inoculation of cowpox) and the potential role of horsepox virus in the origin of the smallpox vaccine. *Vaccine.* (2017) 35:7222–30. doi: 10.1016/j.vaccine.2017.11.003
2. Sanchez-Sampedro L, Perdiguero B, Mejias-Perez E, Garcia-Arriaza J, Di Pilato M, Esteban M. The evolution of poxvirus vaccines. *Viruses.* (2015) 7:1726–803. doi: 10.3390/v7041726
3. Goebel SJ, Johnson GP, Perkus ME, Davis SW, Winslow JP, Paoletti E. The complete DNA sequence of vaccinia virus. *Virology.* (1990) 179:247–66, 517–63. doi: 10.1016/0042-6822(90)90294-2
4. Volz A, Sutter G. Modified vaccinia virus ankara: history, value in basic research, and current perspectives for vaccine development. *Adv Virus Res.* (2017) 97:187–243. doi: 10.1016/bs.aivir.2016.07.001
5. Moss B. Poxviridae: the viruses and their replication. In: Knipe DM, editor. *Fields Virology*. Philadelphia, PA: Lippincott Williams and Wilkins (2007).
6. Condit RC, Moussatche N, Traktman P. In a nutshell: structure and assembly of the vaccinia virion. *Adv Virus Res.* (2006) 66:31–124. doi: 10.1016/S0065-3527(06)66002-8
7. Joklik WK. The Intracellular uncoating of poxvirus DNA. II. The molecular basis of the uncoating process. *J Mol Biol.* (1964) 8:277–88. doi: 10.1016/s0022-2836(64)80137-6
8. Kates JR, McAuslan BR. Messenger RNA synthesis by a coated viral genome. *Proc Natl Acad Sci USA.* (1967) 57:314–20. doi: 10.1073/pnas.57.2.314
9. Munyon W, Paoletti E, Grace JT Jr. RNA polymerase activity in purified infectious vaccinia virus. *Proc Natl Acad Sci USA.* (1967) 58:2280–7. doi: 10.1073/pnas.58.6.2280
10. Woodson B. Vaccinia mRNA synthesis under conditions which prevent uncoating. *Biochem Biophys Res Commun.* (1967) 27:169–75. doi: 10.1016/s0006-291x(67)80057-3
11. Payne LG. Significance of extracellular enveloped virus in the *in vitro* and *in vivo* dissemination of vaccinia. *J Gen Virol.* (1980) 50:89–100. doi: 10.1099/0022-1317-50-1-89
12. Roberts KL, Smith GL. Vaccinia virus morphogenesis and dissemination. *Trends Microbiol.* (2008) 16:472–9. doi: 10.1016/j.tim.2008.07.009
13. Hickman HD, Reynoso GV, Ngudiankama BF, Rubin EJ, Magadan JG, Cush SS, et al. Anatomically restricted synergistic antiviral activities of innate and adaptive immune cells in the skin. *Cell Host Microbe.* (2013) 13:155–68. doi: 10.1016/j.chom.2013.01.004
14. Parekh NJ, Krouse TE, Reider IE, Hobbs RP, Ward BM, Norbury CC. Type I interferon-dependent CCL4 is induced by a cGAS/STING pathway that bypasses viral inhibition and protects infected tissue, independent of viral burden. *PLoS Pathog.* (2019) 15:e1007778. doi: 10.1371/journal.ppat.1007778
15. Gonzalez JM, Esteban M. A poxvirus Bcl-2-like gene family involved in regulation of host immune response: sequence similarity and evolutionary history. *Virol J.* (2010) 7:59. doi: 10.1186/1743-422X-7-59
16. Smith GL, Benfield CTO, Maluquer de Motes C, Mazzon M, Ember SWJ, Ferguson BJ, Sumner RP. Vaccinia virus immune evasion: mechanisms, virulence and immunogenicity. *J Gen Virol.* (2013) 94(Pt 11):2367–92. doi: 10.1099/vir.0.055921-0
17. Burles K, van Buuren N, Barry M. Ectromelia virus encodes a family of Ankyrin/F-box proteins that regulate NFkappaB. *Virology.* (2014) 468–70, 351–62. doi: 10.1016/j.virol.2014.08.030
18. Herbert MH, Squire CJ, Mercer AA. Poxviral ankyrin proteins. *Viruses.* (2015) 7:709–38. doi: 10.3390/v7020709
19. Odon V, Georgana I, Holley J, Morata J, Maluquer de Motes C. Novel class of viral ankyrin proteins targeting the host E3 ubiquitin ligase cullin-2. *J Virol.* (2018) 92:e01374-18. doi: 10.1128/JVI.01374-18
20. Chung CS, Chen CH, Ho MY, Huang CY, Liao CL, Chang W. Vaccinia virus proteome: identification of proteins in vaccinia virus intracellular mature virion particles. *J Virol.* (2006) 80:2127–40. doi: 10.1128/JVI.80.5.2127-2140.2006
21. Resch W, Hixson KK, Moore RJ, Lipton MS, Moss B. Protein composition of the vaccinia virus mature virion. *Virology.* (2007) 358:233–47. doi: 10.1016/j.virol.2006.08.025
22. Doellinger J, Schaade L, Nitsche A. Comparison of the cowpox virus and vaccinia virus mature virion proteome: analysis of the species- and strain-specific proteome. *PLoS ONE.* (2015) 10:e0141527. doi: 10.1371/journal.pone.0141527
23. Goubau D, Deddouche S, Reis e Sousa C. Cytosolic sensing of viruses. *Immunity.* (2013) 38:855–69. doi: 10.1016/j.immuni.2013.05.007
24. Rathinam VA, Fitzgerald KA. Cytosolic surveillance and antiviral immunity. *Curr Opin Virol.* (2011) 1:455–62. doi: 10.1016/j.coviro.2011.11.004
25. Seet BT, Johnston JB, Brunetti CR, Barrett JW, Everett H, Cameron C, et al. Poxviruses and immune evasion. *Annu Rev Immunol.* (2003) 21:377–423. doi: 10.1146/annurev.immunol.21.120601.141049
26. Alcami A. Viral mimicry of cytokines, chemokines and their receptors. *Nat Rev Immunol.* (2003) 3:36–50 doi: 10.1038/nri980
27. Hernaez B, Alcami A. Virus-encoded cytokine and chemokine decoy receptors. *Curr Opin Immunol.* (2020) 66:50–56. doi: 10.1016/j.coi.2020.04.008
28. Fernandes-Alnemri T, Yu JW, Datta P, Wu J, Alnemri ES. AIM2 activates the inflammasome and cell death in response to cytoplasmic DNA. *Nature.* (2009) 458:509–13. doi: 10.1038/nature07710
29. Hornung V, Ablasser A, Charrel-Dennis M, Bauernfeind F, Horvath G, Caffrey DR, et al. AIM2 recognizes cytosolic dsDNA and forms a caspase-1-activating inflammasome with ASC. *Nature.* (2009) 458:514–8. doi: 10.1038/nature07725
30. Hemmi H, Takeuchi O, Kawai T, Kaisho T, Sato S, Sanjo H, et al. A Toll-like receptor recognizes bacterial DNA. *Nature.* (2000) 408:740–5. doi: 10.1038/35047123
31. Kawai T, Akira S. The role of pattern-recognition receptors in innate immunity: update on toll-like receptors. *Nat Immunol.* (2010) 11:373–84. doi: 10.1038/ni.1863
32. Kawai T, Sato S, Ishii KJ, Coban C, Hemmi H, Yamamoto M, et al. Interferon-alpha induction through toll-like receptors involves a direct interaction of IRF7 with MyD88 and TRAF6. *Nat Immunol.* (2004) 5:1061–8. doi: 10.1038/ni1118
33. Mansur DS, Maluquer de Motes C, Unterholzner L, Sumner RP, Ferguson BJ, Ren H, et al. Poxvirus targeting of E3 ligase beta-TrCP by molecular mimicry: a mechanism to inhibit NF-kappaB activation and promote immune evasion and virulence. *PLoS Pathog.* (2013) 9:e1003183. doi: 10.1371/journal.ppat.1003183
34. Neidel S, Ren H, Torres A, Smith GL. NF-kappaB activation is a turn on for vaccinia virus phosphoprotein A49 to turn off NF-kappaB activation. *Proc Natl Acad Sci USA.* (2019) 116:5699–704. doi: 10.1073/pnas.1813504116
35. Pallett MA, Ren H, Zhang RY, Scutts SR, Gonzalez L, Zhu Z, et al. Vaccinia virus BBK E3 ligase adaptor A55 targets importin-dependent NF-kappaB activation and inhibits CD8(+) T-cell memory. *J Virol.* (2019) 93:e00051–19. doi: 10.1128/JVI.00051-19
36. Eaglesham JB, Pan Y, Kupper TS, Kranzusch PJ. Viral and metazoan poxins are cGAMP-specific nucleases that restrict cGAS-STING signalling. *Nature.* (2019) 566:259–63. doi: 10.1038/s41586-019-0928-6

37. Graham SC, Bahar MW, Cooray S, Chen RA, Whalen DM, Abrescia NG, et al. Vaccinia virus proteins A52 and B14 Share a Bcl-2-like fold but have evolved to inhibit NF-kappaB rather than apoptosis. *PLoS Pathog.* (2008) 4:e1000128. doi: 10.1371/journal.ppat.1000128
38. Chen RA, Ryzhakov G, Cooray S, Randow F, Smith GL. Inhibition of IkappaB kinase by vaccinia virus virulence factor B14. *PLoS Pathog.* (2008) 4:e22. doi: 10.1371/journal.ppat.0040022
39. Scutts SR, Ember SW, Ren H, Ye C, Lovejoy CA, Mazzon M, et al. DNA-PK is targeted by multiple Vaccinia virus proteins to inhibit DNA sensing. *Cell Rep.* (2018) 25:1953–65 e4. doi: 10.1016/j.celrep.2018.10.034
40. Unterholzner L, Sumner RP, Baran M, Ren H, Mansur DS, Bourke NM, et al. Vaccinia virus protein C6 is a virulence factor that binds TBK-1 adaptor proteins and inhibits activation of IRF3 and IRF7. *PLoS Pathog.* (2011) 7:e1002247. doi: 10.1371/journal.ppat.1002247
41. Peters NE, Ferguson BJ, Mazzon M, Fahy AS, Krysztofinska E, Arribas-Bosacoma R, et al. A mechanism for the inhibition of DNA-PK-mediated DNA sensing by a virus. *PLoS Pathog.* (2013) 9:e1003649. doi: 10.1371/journal.ppat.1003649
42. Meade N, Furey C, Li H, Verma R, Chai Q, Rollins MG, et al. Poxviruses evade cytosolic sensing through disruption of an mTORC1-mTORC2 regulatory circuit. *Cell.* (2018) 174:1143–57 e17. doi: 10.1016/j.cell.2018.06.053
43. Shisler JL, Jin XL. The vaccinia virus K1L gene product inhibits host NF-kappaB activation by preventing IkappaBalpha degradation. *J Virol.* (2004) 78:3553–60. doi: 10.1128/jvi.78.7.3553-3560.2004
44. Schroder M, Baran M, Bowie AG. Viral targeting of DEAD box protein 3 reveals its role in TBK1/IKKepsilon-mediated IRF activation. *EMBO J.* (2008) 27:2147–57. doi: 10.1038/emboj.2008.143
45. Maluquer de Motes C, Cooray S, Ren H, Almeida GM, McGourty K, Bahar MW, et al. Inhibition of apoptosis and NF-kappaB activation by vaccinia protein N1 occur via distinct binding surfaces and make different contributions to virulence. *PLoS Pathog.* (2011) 7:e1002430. doi: 10.1371/journal.ppat.1002430
46. DiPerna G, Stack J, Bowie AG, Boyd A, Kotwal G, Zhang Z, et al. Poxvirus protein N1L targets the I-kappaB kinase complex, inhibits signaling to NF-kappaB by the tumor necrosis factor superfamily of receptors, and inhibits NF-kappaB and IRF3 signaling by toll-like receptors. *J Biol Chem.* (2004) 279:36570–8. doi: 10.1074/jbc.M400567200
47. Ferguson BJ, Benfield CTO, Ren H, Lee VH, Frazer GL, Strnadova P, et al. Vaccinia virus protein N2 is a nuclear IRF3 inhibitor that promotes virulence. *J Gen Virol.* (2013) 94(Pt 9):2070–81. doi: 10.1099/vir.0.054114-0
48. Ablasser A, Goldeck M, Cavlar T, Deimling T, Witte G, Rohl I, et al. cGAS produces a 2'-5'-linked cyclic dinucleotide second messenger that activates STING. *Nature.* (2013) 498:380–4. doi: 10.1038/nature12306
49. Diner EJ, Burdette DL, Wilson SC, Monroe KM, Kellenberger CA, Hyodo M, et al. The innate immune DNA sensor cGAS produces a noncanonical cyclic dinucleotide that activates human STING. *Cell Rep.* (2013) 3:1355–61. doi: 10.1016/j.celrep.2013.05.009
50. Gao P, Ascano M, Wu Y, Barchet W, Gaffney BL, Zillinger T, et al. Cyclic [G(2',5')pA(3',5')p] is the metazoan second messenger produced by DNA-activated cyclic GMP-AMP synthase. *Cell.* (2013) 153:1094–107. doi: 10.1016/j.cell.2013.04.046
51. Sun L, Wu J, Du F, Chen X, Chen ZJ. Cyclic GMP-AMP synthase is a cytosolic DNA sensor that activates the type I interferon pathway. *Science.* (2013) 339:786–91. doi: 10.1126/science.1232458
52. Wu J, Sun L, Chen X, Du F, Shi H, Chen C, et al. Cyclic GMP-AMP is an endogenous second messenger in innate immune signaling by cytosolic DNA. *Science.* (2013) 339:826–30. doi: 10.1126/science.1229963
53. Hornung V, Hartmann R, Ablasser A, Hopfner KP. OAS proteins and cGAS: unifying concepts in sensing and responding to cytosolic nucleic acids. *Nat Rev Immunol.* (2014) 14:521–8. doi: 10.1038/nri3719
54. Zhang X, Shi H, Wu J, Zhang X, Sun L, Chen C, et al. Cyclic GMP-AMP containing mixed phosphodiester linkages is an endogenous high-affinity ligand for STING. *Mol Cell.* (2013) 51:226–35. doi: 10.1016/j.molcel.2013.05.022
55. Shang G, Zhang C, Chen ZJ, Bai XC, Zhang X. Cryo-EM structures of STING reveal its mechanism of activation by cyclic GMP-AMP. *Nature.* (2019) 567:389–93. doi: 10.1038/s41586-019-0998-5
56. Ablasser A, Chen ZJ. cGAS in action: expanding roles in immunity and inflammation. *Science.* (2019) 363:eaat8657. doi: 10.1126/science.aat8657
57. Ishikawa H, Barber GN. STING is an endoplasmic reticulum adaptor that facilitates innate immune signalling. *Nature.* (2008) 455:674–8. doi: 10.1038/nature07317
58. Ishikawa H, Ma Z, Barber GN. STING regulates intracellular DNA-mediated, type I interferon-dependent innate immunity. *Nature.* (2009) 461:788–92. doi: 10.1038/nature08476
59. Zhong B, Yang Y, Li S, Wang YY, Li Y, Diao F, et al. The adaptor protein MITA links virus-sensing receptors to IRF3 transcription factor activation. *Immunity.* (2008) 29:538–50. doi: 10.1016/j.immuni.2008.09.003
60. Burdette DL, Monroe KM, Sotelo-Troha K, Iwig JS, Eckert B, Hyodo M, et al. STING is a direct innate immune sensor of cyclic di-GMP. *Nature.* (2011) 478:515–8. doi: 10.1038/nature10429
61. Ablasser A, Schmid-Burgk JL, Hemmerling I, Horvath GL, Schmidt T, Latz E, et al. Cell intrinsic immunity spreads to bystander cells via the intercellular transfer of cGAMP. *Nature.* (2013) 503:530–4. doi: 10.1038/nature12640
62. Luteijn RD, Zaver SA, Gowen BG, Wyman SK, Garelis NE, Onia L, et al. SLC19A1 transports immunoreactive cyclic dinucleotides. *Nature.* (2019) 573:434–8. doi: 10.1038/s41586-019-1553-0
63. Ritchie C, Cordova AF, Hess GT, Bassik MC, Li L. SLC19A1 is an importer of the immunotransmitter cGAMP. *Mol Cell.* (2019) 75:372–81 e5. doi: 10.1016/j.molcel.2019.05.006
64. Zhou C, Chen X, Planells-Cases R, Chu J, Wang L, Cao L, et al. Transfer of cGAMP into bystander cells via LRRC8 volume-regulated anion channels augments STING-mediated interferon responses and anti-viral immunity. *Immunity.* (2020) 52:767–81 e6. doi: 10.1016/j.immuni.2020.03.016
65. Mukai K, Konno H, Akiba T, Uemura T, Waguri S, Kobayashi T, et al. Activation of STING requires palmitoylation at the Golgi. *Nat Commun.* (2016) 7:11932. doi: 10.1038/ncomms11932
66. Tsuchida T, Zou J, Saitoh T, Kumar H, Abe T, Matsuura Y, et al. The ubiquitin ligase TRIM56 regulates innate immune responses to intracellular double-stranded DNA. *Immunity.* (2010) 33:765–6. doi: 10.1016/j.immuni.2010.10.013
67. Zhang J, Hu MM, Wang YY, Shu HB. TRIM32 protein modulates type I interferon induction and cellular antiviral response by targeting MITA/STING protein for K63-linked ubiquitination. *J Biol Chem.* (2012) 287:28646–55. doi: 10.1074/jbc.M112.362608
68. Wang Q, Liu X, Cui Y, Tang Y, Chen W, Li S, et al. The E3 ubiquitin ligase AMFR and INSIG1 bridge the activation of TBK1 kinase by modifying the adaptor STING. *Immunity.* (2014) 41:919–33. doi: 10.1016/j.immuni.2014.11.011
69. Liu S, Cai X, Wu J, Cong Q, Chen X, Li T, et al. Phosphorylation of innate immune adaptor proteins MAVS, STING, and TRIF induces IRF3 activation. *Science.* (2015) 347:2630. doi: 10.1126/science.aaa2630
70. Zhao B, Du F, Xu P, Shu C, Sankaran B, Bell SL, ET AL. A conserved PLPLRT/SD motif of STING mediates the recruitment and activation of TBK1. *Nature.* (2019) 569:718–722. doi: 10.1038/s41586-019-1228-x
71. Zhang C, Shang G, Gui X, Zhang X, Bai XC, Chen ZJ. Structural basis of STING binding with and phosphorylation by TBK1. *Nature.* (2019) 567:394–8. doi: 10.1038/s41586-019-1000-2
72. Ablasser A, Hur S. Regulation of cGAS- and RLR-mediated immunity to nucleic acids. *Nat Immunol.* (2020) 21:17–29. doi: 10.1038/s41590-019-0556-1
73. Hu MM, Shu HB. Innate immune response to cytoplasmic DNA: mechanisms and diseases. *Annu Rev Immunol.* (2020) 38:79–98. doi: 10.1146/annurev-immunol-070119-115052
74. Abe T, Barber GN. Cytosolic-DNA-mediated, STING-dependent proinflammatory gene induction necessitates canonical NF-kappaB activation through TBK1. *J Virol.* (2014) 88:5328–41. doi: 10.1128/JVI.00037-14
75. Dunphy G, Flannery SM, Almine JF, Connolly DJ, Paulus C, Jonsson KL, ET AL. Non-canonical activation of the DNA sensing adaptor STING by ATM and IFI16 mediates NF-kappaB signaling after nuclear DNA damage. *Mol Cell.* (2018) 71:745–60 e5. doi: 10.1016/j.molcel.2018.07.034
76. Fang R, Wang C, Jiang Q, Lv M, Gao P, Yu X, et al. NEMO-IKKbeta are essential for IRF3 and NF-kappaB activation in the cGAS-STING Pathway. *J Immunol.* (2017) 199:3222–33. doi: 10.4049/jimmunol.1700699

77. Balka KR, Louis C, Saunders TL, Smith AM, Calleja DJ, D'Silva DB, et al. TBK1 and IKKepsilon act redundantly to mediate STING-induced NF-kappaB responses in myeloid cells. *Cell Rep.* (2020) 31:107492. doi: 10.1016/j.celrep.2020.03.056
78. Oeckinghaus A, Ghosh S. The NF-kappaB family of transcription factors and its regulation. *Cold Spring Harb Perspect Biol.* (2009) 1:a000034. doi: 10.1101/cshperspect.a000034
79. Liu T, Zhang L, Joo D, Sun SC. NF-kappaB signaling in inflammation. *Signal Transduct Target Ther.* (2017) 2:17023. doi: 10.1038/sigtrans.2017.23
80. Giridharan S, Srinivasan M. Mechanisms of NF-kappaB p65 and strategies for therapeutic manipulation. *J Inflamm Res.* (2018) 11:407–19. doi: 10.2147/JIR.S140188
81. Takaoka A, Wang Z, Choi MK, Yanai H, Negishi H, Ban T, et al. DAI (DLM-1/ZBP1) is a cytosolic DNA sensor and an activator of innate immune response. *Nature.* (2007) 448:501–5. doi: 10.1038/nature06013
82. Ablasser A, Bauernfeind F, Hartmann G, Latz E, Fitzgerald KA, Hornung V. RIG-I-dependent sensing of poly(dA:dT) through the induction of an RNA polymerase III-transcribed RNA intermediate. *Nat Immunol.* (2009) 10:1065–72. doi: 10.1038/ni.1779
83. Chiu YH, Macmillan JB, Chen ZJ. RNA polymerase III detects cytosolic DNA and induces type I interferons through the RIG-I pathway. *Cell.* (2009) 138:576–91. doi: 10.1016/j.cell.2009.06.015
84. Unterholzner L, Keating SE, Baran M, Horan KA, Jensen SB, Sharma S, et al. IFI16 is an innate immune sensor for intracellular DNA. *Nat Immunol.* (2010) 11:997–1004. doi: 10.1038/ni.1932
85. Kim T, Pazhoor S, Bao M, Zhang Z, Hanabuchi S, Facchinetti V, et al. Aspartate-glutamate-alanine-histidine box motif (DEAH)/RNA helicase A helicases sense microbial DNA in human plasmacytoid dendritic cells. *Proc Natl Acad Sci USA.* (2010) 107:15181–6. doi: 10.1073/pnas.1006539107
86. Zhang Z, Yuan B, Bao M., Lu N, Kim T, Liu YJ. The helicase DDX41 senses intracellular DNA mediated by the adaptor STING in dendritic cells. *Nat Immunol.* (2011) 12:959–65. doi: 10.1038/ni.2091
87. Zhang X, Brann TW, Zhou M, Yang J, Oguariri RM, Lidie KB, et al. Cutting edge: Ku70 is a novel cytosolic DNA sensor that induces type III rather than type I IFN. *J Immunol.* (2011) 186:4541–5. doi: 10.4049/jimmunol.1003389
88. Ferguson BJ, Mansur DS, Peters NE, Ren H, Smith GL. DNA-PK is a DNA sensor for IRF-3-dependent innate immunity. *Elife.* (2012) 1:e00047. doi: 10.7554/eLife.00047
89. Kondo T, Kobayashi J, Saitoh T, Maruyama K, Ishii KJ, Barber GN, et al. DNA damage sensor MRE11 recognizes cytosolic double-stranded DNA and induces type I interferon by regulating STING trafficking. *Proc Natl Acad Sci USA.* (2013) 110:2969–74. doi: 10.1073/pnas.1222694110
90. Yoh M, Schneider M, Seifried J, Soonthornvacharin S, Akleh RE, Olivieri KC, et al. PQBP1 is a proximal sensor of the cGAS-dependent innate response to HIV-1. *Cell.* (2015) 161:1293–305. doi: 10.1016/j.cell.2015.04.050
91. Li Y, Chen R, Zhou Q, Xu Z, Li C, Wang S, et al. LSm14A is a processing body-associated sensor of viral nucleic acids that initiates cellular antiviral response in the early phase of viral infection. *Proc Natl Acad Sci USA.* (2012) 109:11770–5. doi: 10.1073/pnas.1203405109
92. Liu ZS, Cai H, Xue W, Wang M, Xia T, Li WJ, et al. G3BP1 promotes DNA binding and activation of cGAS. *Nat Immunol.* (2019) 20:18–28. doi: 10.1038/s41590-018-0262-4
93. Burleigh K, Maltbaek JH, Cambier S, Green R, Gale M Jr, James R. Human DNA-PK activates a STING-independent DNA sensing pathway. *Sci Immunol.* (2020) 5:4219. doi: 10.1126/sciimmunol.aba4219
94. Georgana I, Sumner RP, Towers GJ, Maluquer de Motes C. Virulent poxviruses inhibit DNA sensing by preventing STING activation. *J Virol.* (2018) 92:e02145–17. doi: 10.1128/JVI.02145-17
95. Haag SM, Gulen MF, Reymond L, Gibelin A, Abrami L, Decout A, et al. Targeting STING with covalent small-molecule inhibitors. *Nature.* (2018) 559:269–73. doi: 10.1038/s41586-018-0287-8
96. Schoggins JW, MacDuff DA, Imanaka N, Gainey MD, Shrestha B, Eitson JL, et al. Pan-viral specificity of IFN-induced genes reveals new roles for cGAS in innate immunity. *Nature.* (2014) 505:691–5. doi: 10.1038/nature12862
97. Cheng WY, He XB, Jia HJ, Chen GH, Jin QW, Long ZL, et al. The cGas-sting signaling pathway is required for the innate immune response against ectromelia virus. *Front Immunol.* (2018) 9:1297. doi: 10.3389/fimmu.2018.01297
98. Wong EB, Montoya B, Ferez M, Stotesbury C, Sigal LJ. Resistance to ectromelia virus infection requires cGAS in bone marrow-derived cells which can be bypassed with cGAMP therapy. *PLoS Pathog.* (2019) 15:e1008239. doi: 10.1371/journal.ppat.1008239
99. Hernaez B, Alonso G, Georgana I, El-Jesr M, Martin R, Shair KHY, et al. Viral cGAMP nuclease reveals the essential role of DNA sensing in protection against acute lethal virus infection. *Sci Adv.* (2020) 6:eabb4565. doi: 10.1126/sciadv.abb4565
100. Antoine G, Scheiflinger F, Dorner F, Falkner FG. The complete genomic sequence of the modified vaccinia Ankara strain: comparison with other orthopoxviruses. *Virology.* (1998) 244:365–96. doi: 10.1006/viro.1998.9123
101. Delaloye J, Roger T, Steiner-Tardivel QG, Le Roy D, Knaup Reymond M, Akira S, et al. Innate immune sensing of modified vaccinia virus Ankara (MVA) is mediated by TLR2-TLR6, MDA-5 and the NALP3 inflammasome. *PLoS Pathog.* (2009) 5:e1000480. doi: 10.1371/journal.ppat.1000480
102. Guerra S, Najera JL, Gonzalez JM, Lopez-Fernandez LA, Climent N, Gatell JM, et al. Distinct gene expression profiling after infection of immature human monocyte-derived dendritic cells by the attenuated poxvirus vectors MVA and NYVAC. *J Virol.* (2007) 81:8707–21. doi: 10.1128/JVI.00444-07
103. Barbalat R, Lau L, Locksley RM, Barton GM. Toll-like receptor 2 on inflammatory monocytes induces type I interferon in response to viral but not bacterial ligands. *Nat Immunol.* (2009) 10:1200–7. doi: 10.1038/ni.1792
104. Zhu J, Martinez J, Huang X, Yang Y. Innate immunity against vaccinia virus is mediated by TLR2 and requires TLR-independent production of IFN-beta. *Blood.* (2007) 109:619–25. doi: 10.1182/blood-2006-06-027136
105. Andrejeva J, Childs KS, Young DF, Carlos TS, Stock N, Goodbourn S, et al. The V proteins of paramyxoviruses bind the IFN-inducible RNA helicase, mda-5, and inhibit its activation of the IFN-beta promoter. *Proc Natl Acad Sci USA.* (2004) 101:17264–9. doi: 10.1073/pnas.0407639101
106. Kumar H, Kawai T, Kato H, Sato S, Takahashi K, Coban C, et al. Essential role of IPS-1 in innate immune responses against RNA viruses. *J Exp Med.* (2006) 203:1795–803. doi: 10.1084/jem.20060792
107. Dai P, Wang W, Cao H, Avogadri F, Dai L, Drexler I, et al. Modified vaccinia virus Ankara triggers type I IFN production in murine conventional dendritic cells via a cGAS/STING-mediated cytosolic DNA-sensing pathway. *PLoS Pathog.* (2014) 10:e1003989. doi: 10.1371/journal.ppat.1003989
108. Takahama M, Fukuda M, Ohbayashi N, Kozaki T, Misawa T, Okamoto T, et al. The RAB2B-GARIL5 complex promotes cytosolic dna-induced innate immune responses. *Cell Rep.* (2017) 20:2944–54. doi: 10.1016/j.celrep.2017.08.085
109. Meade N, King M, Munger J, Walsh D. mTOR dysregulation by Vaccinia virus F17 controls multiple processes with varying roles in infection. *J Virol.* (2019) 93:e00784–19. doi: 10.1128/JVI.00784-19
110. Liu F, Niu Q, Fan X, Liu C, Zhang J, Wei Z, et al. Priming and activation of inflammasome by canarypox virus vector ALVAC via the cGAS/IFI16-STING-type I IFN pathway and AIM2 sensor. *J Immunol.* (2017) 199:3293–305. doi: 10.4049/jimmunol.1700698
111. Lieber MR. The mechanism of double-strand DNA break repair by the nonhomologous DNA end-joining pathway. *Annu Rev Biochem.* (2010) 79:181–211. doi: 10.1146/annurev.biochem.052308.093131
112. Morchikh M, Cribier A, Raffel R, Amraoui S, Cau J, Severac D, et al. HEXIM1 and NEAT1 Long non-coding RNA form a multi-subunit complex that regulates DNA-mediated innate immune response. *Mol Cell.* (2017) 67:387–99 e5. doi: 10.1016/j.molcel.2017.06.020
113. Almine JF, O'Hare CA, Dunphy G, Haga IR, Naik RJ, Atrih A, et al. IFI16 and cGAS cooperate in the activation of STING during DNA sensing in human keratinocytes. *Nat Commun.* (2017) 8:14392. doi: 10.1038/ncomms14392
114. Orzalli MH, Broekema NM, Diner BA, Hancks DC, Elde NC, Cristea IM, et al. cGAS-mediated stabilization of IFI16 promotes innate signaling during herpes simplex virus infection. *Proc Natl Acad Sci USA.* (2015) 112:E1773–81. doi: 10.1073/pnas.1424637112
115. Orzalli MH, DeLuca NA, Knipe DM. Nuclear IFI16 induction of IRF-3 signaling during herpesviral infection and degradation of IFI16 by the viral ICP0 protein. *Proc Natl Acad Sci USA.* (2012) 109:E3008–17. doi: 10.1073/pnas.1211302109
116. Fahy AS, Clark RH, Glyde EF, Smith GL. Vaccinia virus protein C16 acts intracellularly to modulate the host response and promote virulence. *J Gen Virol.* (2008) 89(Pt 10):2377–87. doi: 10.1099/vir.0.2008/004895-0

117. Mazzon M, Peters NE, Loenarz C, Krysztofinska EM, Ember SW, Ferguson BJ, et al. A mechanism for induction of a hypoxic response by vaccinia virus. *Proc Natl Acad Sci USA.* (2013) 110:12444–9. doi: 10.1073/pnas.1302140110
118. Mazzon M, Castro C, Roberts LD, Griffin JL, Smith GL. A role for vaccinia virus protein C16 in reprogramming cellular energy metabolism. *J Gen Virol.* (2015) 96(Pt 2):395–407. doi: 10.1099/vir.0.069591-0
119. Ember SWJ, Ren H, Ferguson BJ, Smith GL. Vaccinia virus protein C4 inhibits NF-kappaB activation and promotes virus virulence. *J Gen Virol.* (2012) 93(Pt 10):2098–108. doi: 10.1099/vir.0.045070-0
120. Hiller G, Weber K. A phosphorylated basic vaccinia virion polypeptide of molecular weight 11,000 is exposed on the surface of mature particles and interacts with actin-containing cytoskeletal elements. *J Virol.* (1982) 44:647–57. doi: 10.1128/JVI.44.2.647-657.1982
121. Wickramasekera NT, Traktman P. Structure/function analysis of the vaccinia virus F18 phosphoprotein, an abundant core component required for virion maturation and infectivity. *J Virol.* (2010) 84:6846–60. doi: 10.1128/JVI.00399-10
122. Zhang YF, Moss B. Vaccinia virus morphogenesis is interrupted when expression of the gene encoding an 11-kilodalton phosphorylated protein is prevented by the Escherichia coli lac repressor. *J Virol.* (1991) 65:6101–10.
123. Kim J, Guan K. L. mTOR as a central hub of nutrient signalling and cell growth. *Nat Cell Biol.* (2019) 21:63–71. doi: 10.1038/s41556-018-0205-1
124. Liu GY, Sabatini DM. mTOR at the nexus of nutrition, growth, ageing and disease. *Nat Rev Mol Cell Biol.* (2020) 21:183–203. doi: 10.1038/s41580-019-0199-y
125. Seo GJ, Yang A, Tan B, Kim S, Liang Q, Choi Y, et al. Akt kinase-mediated checkpoint of cGAS DNA sensing pathway. *Cell Rep.* (2015) 13:440–9. doi: 10.1016/j.celrep.2015.09.007
126. Xu S, Ducroux A, Ponnurangam A, Vieyres G, Franz S, Musken M, et al. cGAS-mediated innate immunity spreads intercellularly through HIV-1 Env-induced membrane fusion sites. *Cell Host Microbe.* (2016) 20:443–57. doi: 10.1016/j.chom.2016.09.003
127. Bridgeman A, Maelfait J, Davenne T, Partridge T, Peng Y, Mayer A, etal. Viruses transfer the antiviral second messenger cGAMP between cells. *Science.* (2015) 349:1228–32. doi: 10.1126/science.aab3632
128. Gentili M, Kowal J, Tkach M, Satoh T, Lahaye X, Conrad C, et al. Transmission of innate immune signaling by packaging of cGAMP in viral particles. *Science.* (2015) 349:1232–6. doi: 10.1126/science.aab3628
129. Ryzhakov G, Randow F. SINTBAD, a novel component of innate antiviral immunity, shares a TBK1-binding domain with NAP1 and TANK. *EMBO J.* (2007) 26:3180–90. doi: 10.1038/sj.emboj.7601743
130. Stuart JH, Sumner RP, Lu Y, Snowden JS, Smith GL. Vaccinia virus protein C6 inhibits type I IFN signalling in the nucleus and binds to the transactivation domain of STAT2. *PLoS Pathog.* (2016) 12:e1005955. doi: 10.1371/journal.ppat.1005955
131. Lu Y, Stuart JH, Talbot-Cooper C, Agrawal-Singh S, Huntly B, Smid AI, et al. Histone deacetylase 4 promotes type I interferon signaling, restricts DNA viruses, and is degraded via vaccinia virus protein C6. *Proc Natl Acad Sci USA.* (2019) 116:11997–2006. doi: 10.1073/pnas.1816399116
132. Sumner RP, Ren H, Ferguson BJ, Smith GL. Increased attenuation but decreased immunogenicity by deletion of multiple vaccinia virus immunomodulators. *Vaccine.* (2016) 34:4827–34. doi: 10.1016/j.vaccine.2016.08.002
133. Sumner RP, Ren H, Smith GL. Deletion of immunomodulator C6 from vaccinia virus strain Western Reserve enhances virus immunogenicity and vaccine efficacy. *J Gen Virol.* (2013) 94(Pt 5):1121–6. doi: 10.1099/vir.0.049700-0
134. Garcia-Arriaza J, Arnaez P, Gomez CE, Sorzano CO, Esteban M. Improving adaptive and memory immune responses of an hiv/aids vaccine candidate mva-b by deletion of vaccinia virus genes (C6L and K7R) blocking interferon signaling pathways. *PLoS ONE.* (2013) 8:e66894. doi: 10.1371/journal.pone.0066894
135. Garcia-Arriaza J, Najera JL, Gomez CE, Tewabe N, Sorzano CO, Calandra T, et al. A candidate HIV/AIDS vaccine (MVA-B) lacking vaccinia virus gene C6L enhances memory HIV-1-specific T-cell responses. *PLoS ONE.* (2011) 6:e24244. doi: 10.1371/journal.pone.0024244
136. Marin MQ, Perez P, Gomez CE, Sorzano COS, Esteban M, Garcia-Arriaza J. Removal of the C6 vaccinia virus interferon-beta inhibitor in the hepatitis C vaccine candidate MVA-HCV elicited in mice high immunogenicity in spite of reduced host gene expression. *Viruses.* (2018) 10:414. doi: 10.3390/v10080414
137. Benfield CTO, Ren H, Lucas SJ, Bahsoun B, Smith GL. Vaccinia virus protein K7 is a virulence factor that alters the acute immune response to infection. *J Gen Virol.* (2013) 94(Pt 7):1647–57. doi: 10.1099/vir.0.052670-0
138. Soulat D, Burckstummer T, Westermayer S, Goncalves A, Bauch A, Stefanovic A, et al. The DEAD-box helicase DDX3X is a critical component of the TANK-binding kinase 1-dependent innate immune response. *EMBO J.* (2008) 27:2135–46. doi: 10.1038/emboj.2008.126
139. Kalverda AP, Thompson GS, Vogel A, Schroder M, Bowie AG, Khan AR, et al. Poxvirus K7 protein adopts a Bcl-2 fold: biochemical mapping of its interactions with human DEAD box RNA helicase DDX3. *J Mol Biol.* (2009) 385:843–53. doi: 10.1016/j.jmb.2008.09.048
140. Garcia-Arriaza J, Gomez CE, Sorzano CO, Esteban M. Deletion of the vaccinia virus N2L gene encoding an inhibitor of IRF3 improves the immunogenicity of modified vaccinia virus Ankara expressing HIV-1 antigens. *J Virol.* (2014) 88:3392–410. doi: 10.1128/JVI.02723-13
141. Chen RA, Jacobs N, Smith GL. Vaccinia virus strain Western Reserve protein B14 is an intracellular virulence factor. *J Gen Virol.* (2006) 87(Pt 6):1451–8. doi: 10.1099/vir.0.81736-0
142. Tang Q, Chakraborty S, Xu G. Mechanism of vaccinia viral protein B14-mediated inhibition of IkappaB kinase beta activation. *J Biol Chem.* (2018) 293:10344–52. doi: 10.1074/jbc.RA118.002817
143. Benfield CT, Mansur DS, McCoy LE, Ferguson BJ, Bahar MW, Oldring AP, et al. Mapping the IkappaB kinase beta (IKKbeta)-binding interface of the B14 protein, a vaccinia virus inhibitor of IKKbeta-mediated activation of nuclear factor kappaB. *J Biol Chem.* (2011) 286:20727–35. doi: 10.1074/jbc.M111.231381
144. Torres AA, Albarnaz JD, Bonjardim CA, Smith GL. Multiple Bcl-2 family immunomodulators from vaccinia virus regulate MAPK/AP-1 activation. *J Gen Virol.* (2016) 97:2346–51. doi: 10.1099/jgv.0.000525
145. McCoy LE, Fahy AS, Chen RA, Smith GL. Mutations in modified virus Ankara protein 183 render it a non-functional counterpart of B14, an inhibitor of nuclear factor kappaB activation. *J Gen Virol.* (2010) 91(Pt 9):2216–20. doi: 10.1099/vir.0.022343-0
146. Cooray S, Bahar MW, Abrescia NG, McVey CE, Bartlett NW, Chen RA, et al. Functional and structural studies of the vaccinia virus virulence factor N1 reveal a Bcl-2-like anti-apoptotic protein. *J Gen Virol.* (2007) 88(Pt 6):1656–66. doi: 10.1099/vir.0.82772-0
147. Veyer DL, Maluquer de Motes C, Sumner RP, Ludwig L, Johnson BF, Smith GL. Analysis of the anti-apoptotic activity of four vaccinia virus proteins demonstrates that B13 is the most potent inhibitor in isolation and during viral infection. *J Gen Virol.* (2014) 95(Pt 12):2757–68. doi: 10.1099/vir.0.068833-0
148. Ren H, Ferguson BJ, Maluquer de Motes C, Sumner RP, Harman LE, Smith GL. Enhancement of CD8(+) T-cell memory by removal of a vaccinia virus nuclear factor-kappaB inhibitor. *Immunology.* (2015) 145:34–49. doi: 10.1111/imm.12422
149. Maluquer de Motes C, Schiffner T, Sumner RP, Smith GL. Vaccinia virus virulence factor N1 can be ubiquitylated on multiple lysine residues. *J Gen Virol.* (2014) 95(Pt 9):2038–49. doi: 10.1099/vir.0.065664-0
150. Neidel S, Maluquer de Motes C, Mansur DS, Strnadova P, Smith GL, Graham SC. Vaccinia virus protein A49 is an unexpected member of the B-cell Lymphoma (Bcl)-2 protein family. *J Biol Chem.* (2015) 290:5991–6002. doi: 10.1074/jbc.M114.624650
151. Maluquer de Motes C, Smith GL. Vaccinia virus protein A49 activates Wnt signalling by targetting the E3 ligase beta-TrCP. *J Gen Virol.* (2017) 98:3086–92. doi: 10.1099/jgv.0.000946
152. Neidel S, Torres AA, Ren H, Smith GL. Leaky scanning translation generates a second A49 protein that contributes to vaccinia virus virulence. *J Gen Virol.* (2020) 10: 533–41. doi: 10.1099/jgv.0.001386
153. Bravo Cruz AG, Shisler JL. Vaccinia virus K1 ankyrin repeat protein inhibits NF-kappaB activation by preventing RelA acetylation. *J Gen Virol.* (2016) 97:2691–702. doi: 10.1099/jgv.0.000576

154. Sumner RP, Maluquer de Motes C, Veyer DL, Smith GL. Vaccinia virus inhibits NF-kappaB-dependent gene expression downstream of p65 translocation. *J Virol.* (2014) 88:3092–102. doi: 10.1128/JVI.02627-13
155. Albarnaz JD, Torres AA, Smith GL. Modulating vaccinia virus immunomodulators to improve immunological memory. *Viruses.* (2018) 10:101. doi: 10.3390/v10030101
156. Deng L, Liang H, Xu M, Yang X, Burnette B, Arina A, et al. STING-Dependent cytosolic DNA sensing promotes radiation-induced type I interferon-dependent antitumor immunity in immunogenic tumors. *Immunity.* (2014) 41:843–52. doi: 10.1016/j.immuni.2014.10.019
157. Li T, Cheng H, Yuan H, Xu Q, Shu C, Zhang Y, et al. Antitumor activity of cGAMP via stimulation of cGAS-cGAMP-STING-IRF3 mediated innate immune response. *Sci Rep.* (2016) 6:19049. doi: 10.1038/srep19049
158. Wang H, Hu S, Chen X, Shi H, Chen C, Sun L, et al. cGAS is essential for the antitumor effect of immune checkpoint blockade. *Proc Natl Acad Sci USA.* (2017) 114:1637–42. doi: 10.1073/pnas.1621363114
159. Woo SR, Fuertes MB, Corrales L, Spranger S, Furdyna MJ, Leung MY, et al. STING-dependent cytosolic DNA sensing mediates innate immune recognition of immunogenic tumors. *Immunity.* (2014) 41:830–42. doi: 10.1016/j.immuni.2014.10.017
160. Rezza G. Emergence of human monkeypox in West Africa. *Lancet Infect Dis.* (2019) 19:797–9. doi: 10.1016/S1473-3099(19)30281-6
161. Sklenovska N, Van Ranst M. Emergence of monkeypox as the most important orthopoxvirus infection in humans. *Front Public Health.* (2018) 6:241. doi: 10.3389/fpubh.2018.00241
162. Jordan R, Leeds JM, Tyavanagimatt S, Hruby DE. Development of ST-246(R) for treatment of poxvirus infections. *Viruses.* (2010) 2:2409–35. doi: 10.3390/v2112409
163. Mucker EM, Goff AJ, Shamblin JD, Grosenbach DW, Damon IK, Mehal JM, et al. Efficacy of tecovirimat (ST-246) in nonhuman primates infected with variola virus (Smallpox). *Antimicrob Agents Chemother.* (2013) 57:6246–53. doi: 10.1128/AAC.00977-13
164. Grosenbach DW, Honeychurch K, Rose EA, Chinsangaram J, Frimm A, Maiti B, et al. Oral tecovirimat for the treatment of smallpox. *N Engl J Med.* (2018) 379:44–53. doi: 10.1056/NEJMoa1705688
165. Thorne S. H. Immunotherapeutic potential of oncolytic vaccinia virus. *Immunol Res.* (2011) 50:286–93. doi: 10.1007/s12026-011-8211-4
166. Chan WM, McFadden G. Oncolytic poxviruses. *Annu Rev Virol.* (2014) 1:119–141. doi: 10.1146/annurev-virology-031413-085442
167. Guo ZS, Lu B, Guo Z, Giehl E, Feist M, Dai E, et al. Vaccinia virus-mediated cancer immunotherapy: cancer vaccines and oncolytics. *J Immunother Cancer.* (2019) 7:6. doi: 10.1186/s40425-018-0495-7
168. Veyer DL, Carrara G, Maluquer de Motes C, Smith G. L. Vaccinia virus evasion of regulated cell death. *Immunol Lett.* (2017) 186:68–80. doi: 10.1016/j.imlet.2017.03.015
169. Dai P, Wang W, Yang N, Serna-Tamayo C, Ricca JM, Zamarin D, et al. Intratumoral delivery of inactivated modified vaccinia virus Ankara (iMVA) induces systemic antitumor immunity via STING and Batf3-dependent dendritic cells. *Sci Immunol.* (2017) 2:eaal1713. doi: 10.1126/sciimmunol.aal1713
170. Fu J, Kanne DB, Leong M, Glickman LH, McWhirter SM, Lemmens E, et al. STING agonist formulated cancer vaccines can cure established tumors resistant to PD-1 blockade. *Sci Transl Med.* (2015) 7:283ra52. doi: 10.1126/scitranslmed.aaa4306
171. Xia T, Konno H, Ahn J, Barber GN. Deregulation of STING signaling in colorectal carcinoma constrains dna damage responses and correlates with tumorigenesis. *Cell Rep.* (2016) 14:282–97. doi: 10.1016/j.celrep.2015.12.029
172. Xia T, Konno H, Barber GN. Recurrent loss of STING signaling in melanoma correlates with susceptibility to viral oncolysis. *Cancer Res.* (2016) 76:6747–59. doi: 10.1158/0008-5472.CAN-16-1404
173. Rice GI, Forte GM, Szynkiewicz M, Chase DS, Aeby A, Abdel-Hamid MS, et al. Assessment of interferon-related biomarkers in Aicardi-Goutieres syndrome associated with mutations in TREX1, RNASEH2A, RNASEH2B, RNASEH2C, SAMHD1, and ADAR: a case-control study. *Lancet Neurol.* (2013) 12:1159–69. doi: 10.1016/S1474-4422(13)70258-8
174. An J, Durcan L, Karr RM, Briggs TA, Rice GI, Teal TH, et al. Expression of cyclic GMP-AMP synthase in patients with systemic lupus erythematosus. *Arthritis Rheumatol.* (2017) 69:800–807. doi: 10.1002/art.40002
175. Lysakova-Devine T, Keogh B, Harrington B, Nagpal K, Halle A, Golenbock DT, et al. Viral inhibitory peptide of TLR4, a peptide derived from vaccinia protein A46, specifically inhibits TLR4 by directly targeting MyD88 adaptor-like and TRIF-related adaptor molecule. *J Immunol.* (2010) 185:4261–71. doi: 10.4049/jimmunol.1002013
176. McCoy SL, Kurtz SE, Macarthur CJ, Trune DR, Hefeneider SH. Identification of a peptide derived from vaccinia virus A52R protein that inhibits cytokine secretion in response to TLR-dependent signaling and reduces *in vivo* bacterial-induced inflammation. *J Immunol.* (2005) 174:3006–14. doi: 10.4049/jimmunol.174.5.3006

Conflict of Interest: The authors declare that the research was conducted in the absence of any commercial or financial relationships that could be construed as a potential conflict of interest.

frontiers in Immunology

ORIGINAL RESEARCH
published: 14 October 2020
doi: 10.3389/fimmu.2020.567348

Polymorphisms in STING Affect Human Innate Immune Responses to Poxviruses

Richard B. Kennedy[1], Iana H. Haralambieva[1], Inna G. Ovsyannikova[1], Emily A. Voigt[1], Beth R. Larrabee[2], Daniel J. Schaid[2], Michael T. Zimmermann[3], Ann L. Oberg[2] and Gregory A. Poland[1]*

[1] Mayo Clinic Vaccine Research Group, Mayo Clinic, Rochester, MN, United States, [2] Division of Biomedical Statistics and Informatics, Department of Health Science Research, Mayo Clinic, Rochester, MN, United States, [3] Bioinformatics Research and Development Laboratory, Genomics Sciences and Precision Medicine Center, Medical College of Wisconsin, Milwaukee, WI, United States

OPEN ACCESS

Edited by:
Linda F. Van Dyk, University of Colorado Denver, United States

Reviewed by:
Christopher J. A. Duncan, Newcastle University, United Kingdom
Chunfu Zheng, Fujian Medical University, China
Martin R. Jakobsen, Aarhus University, Denmark

***Correspondence:**
Richard B. Kennedy
kennedy.rick@mayo.edu

Specialty section:
This article was submitted to Viral Immunology, a section of the journal Frontiers in Immunology

Received: *29 May 2020*
Accepted: *24 September 2020*
Published: *14 October 2020*

Citation:
Kennedy RB, Haralambieva IH, Ovsyannikova IG, Voigt EA, Larrabee BR, Schaid DJ, Zimmermann MT, Oberg AL and Poland GA (2020) Polymorphisms in STING Affect Human Innate Immune Responses to Poxviruses. Front. Immunol. 11:567348. doi: 10.3389/fimmu.2020.567348

We conducted a large genome-wide association study (GWAS) of the immune responses to primary smallpox vaccination in a combined cohort of 1,653 subjects. We did not observe any polymorphisms associated with standard vaccine response outcomes (e.g., neutralizing antibody, T cell ELISPOT response, or T cell cytokine production); however, we did identify a cluster of SNPs on chromosome 5 (5q31.2) that were significantly associated (p-value: 1.3 x 10^{-12} – 1.5x10^{-36}) with IFNα response to *in vitro* poxvirus stimulation. Examination of these SNPs led to the functional testing of rs1131769, a non-synonymous SNP in *TMEM173* causing an Arg-to-His change at position 232 in the STING protein—a major regulator of innate immune responses to viral infections. Our findings demonstrate differences in the ability of the two STING variants to phosphorylate the downstream intermediates TBK1 and IRF3 in response to multiple STING ligands. Further downstream in the STING pathway, we observed significantly reduced expression of type I IFNs (including IFNα) and IFN-response genes in cells carrying the H232 variant. Subsequent molecular modeling of both alleles predicted altered ligand binding characteristics between the two variants, providing a potential mechanism underlying differences in inter-individual responses to poxvirus infection. Our data indicate that possession of the H232 variant may impair STING-mediated innate immunity to poxviruses. These results clarify prior studies evaluating functional effects of genetic variants in *TMEM173* and provide novel data regarding genetic control of poxvirus immunity.

Keywords: STING, smallpox vaccine, vaccinia, poxvirus, viral vaccines, immunogenetics, innate immunity, genome-wide association study

INTRODUCTION

Until its eradication in 1980, smallpox (caused by the variola virus) was a deadly, debilitating disease estimated to have killed hundreds of millions of individuals over the last two centuries alone (1). Eradication was made possible by using vaccines based on vaccinia virus (1). These live-virus vaccines elicited robust, long-lasting immunity in nearly all vaccine recipients (2, 3). Routine smallpox vaccination was halted in the United States before global eradication due to rare but serious adverse events, including death; however, poxviruses remain a public health issue for several reasons, including zoonotic poxvirus outbreaks (4–7) and concerns regarding the release of variola virus as a biological weapon and novel poxviruses (8). The increasing use of poxviruses as platform vectors for other vaccines and therapeutics has also enhanced our need for a better understanding of poxvirus immunity. While highly effective, the smallpox vaccine has numerous contraindications as well as rare but serious, potentially life-threatening adverse reactions that limit its widespread use, if needed, in the population. Understanding how poxvirus immunity is controlled may assist in the development of safer yet still effective poxvirus-based vaccines and can provide insights into immunity to other DNA viruses/vaccines.

Although seroconversion rates after smallpox vaccination are high (>97%), antibody titers and cellular immune responses vary widely among recipients (1, 9–12). We have previously reported on a small subset of individuals who develop the classical vaccine take (i.e., response) but fail to mount vigorous adaptive immune responses (13). Previous research by our lab and others demonstrates that genetic polymorphisms are correlated with immune outcomes to multiple viral vaccines, including the smallpox vaccine (11, 12, 14, 15). To move beyond statistical genetic associations, functional studies are also needed to elucidate the biologic mechanisms underlying these associations and link them to gain a better understanding of how genomic factors contribute to inter-individual variation in immune response.

Recognition of foreign nucleic acids by the cGAS/STING pathway leads to type I IFN responses and is an important component of the innate response to viral and bacterial infection (16). Cytosolic DNA is recognized by cGAS, leading to the generation of the cyclic dinucleotide 2'3'cGAMP, which, in turn binds to STING. STING is also able to directly recognize bacterially produced cyclic dinucleotides. Both direct activation of STING and indirect activation through cGAS trigger the phosphorylation of TBK1 and IRF3, resulting in the transcription of type I interferons, TNF, IL-6, with subsequent activation of interferon regulated genes and inflammation. STING has been found to mediate the IFN response to bacteria and DNA viruses, including herpes simplex viruses, CMV, HPV, and poxviruses such as vaccinia and ectromelia (17–21).

We have previously reported the findings from the first genome-wide association study (GWAS) examining the association of single nucleotide polymorphisms (SNPs) with immune responses in a cohort of primary smallpox vaccines (11, 12, 15). Here, we report a cluster of SNPs on chromosome 5 (5q31.2) that were significantly associated with IFNα response following *in vitro* stimulation of PBMCs with vaccinia virus. We report the results from the functional testing of rs1131769, which is a non-synonymous SNP in *TMEM173* that introduces an amino acid change from the arginine at position 232 (R232) to histidine (H232) in the STING protein (18–21). Our results indicate that the H232 variant of STING is associated with a significant reduction in the IFNa response and that this effect is independent of the effect previously described for SNPs in the STING *HAQ* haplotype (22). We also report the results of molecular modeling and molecular dynamics (MD) simulations investigating differences in how the H232 and R232 variants interact with the signaling ligand. Overall, our study provides novel and important data regarding genetic control of poxvirus immunity in humans by linking specific genetic polymorphisms in *TMEM173* to differential STING pathway activation during innate immune responses (IFNα) to vaccinia virus. These results may also explain inter-individual variations in the innate immune response to other DNA viruses (e.g., HPV, VZV, HSV-1), which also stimulate the STING pathway, as well as the large number of bacterial pathogens that also activate STING.

MATERIALS AND METHODS

Study Cohorts

Two previously described study cohorts were combined for our analyses (11, 12, 15). Briefly, the San Diego cohort consists of 1,076 Dryvax® recipients (primarily U.S. Navy personnel) recruited in 2003–2006. The U.S. cohort consists of 1,058 ACAM2000® or Dryvax® recipients (primarily U.S. Army personnel) recruited in 2010–2013. For both cohorts, subjects had received their first (and only) smallpox vaccination between 1 and 4 years prior to study enrollment. All participants gave written informed consent for this study. Approval for all study procedures was obtained from the Institutional Review Boards of the Mayo Clinic (Rochester, MN) and the Naval Health Research Center (NHRC; San Diego, CA).

Measurement of Vaccinia-Specific IFN α Responses

Subject PBMC samples were cultured in the presence/absence of inactivated vaccinia virus (NYCBOH) at an MOI of 0.05. Vaccinia virus was inactivated using psoralen (5ug/ml: Sigma Aldrich, P8399) and long-wave UV light (23). The full panel of cytokines included: IL-1β, IL-2, IL-4, IL-6, IL-10, IL-12p40, IL-12 p70, IL-18, IFNα, IFNβ, and TNFα. Interferon alpha (IFNα) production by vaccinia virus-stimulated PBMC samples was measured by commercial ELISA assay (PBL Biomedical Laboratories, Piscataway, NJ), as previously described (15, 24). PHA was used as a viability control. Cells from subjects that were unable to secrete cytokines (e.g., IFNγ, TNFα, IL-2) upon stimulation by PHA were deemed unviable and not included in the analyses.

Genotyping and Fine Mapping

DNA from all subjects was extracted using Gentra Puregene kits (QIAGEN, #158445) (11). Genome-wide genotyping for the study cohort was performed as previously described (11, 12, 15, 25). For the SD cohort (recruited in 2003–2006), subjects were genotyped with either the Illumina 550 array or the Illumina 650 array. Genotype quality control (QC) prior to imputation was conducted separately for each platform. QC for the Illumina 550 and 650 arrays involved removing monomorphic SNPs and those on the Y chromosome. We also removed all SNPs with a call rate <95%, and all subjects with a call rate <95%. SNPs were also excluded if they failed Hardy-Weinberg Equilibration (HWE) test p-value > 10^{-5}. Genetic sex was verified by PLINK. Subjects in the U.S. cohort were recruited in 2010–2013 and genotyped with the Illumina Omni 2.5 array. For the Omni 2.5 array, mitochondrial SNPs, those on the Y chromosome, and monomorphic SNPs were removed. SNPs were required to have a call rate at least 99%, and subjects had a minimum call rate of 95%. No inconsistencies were found between reported sex and genetic-determined sex. Across these cohorts, a total of 2,062 subjects passed QC for genotyping.

The 1000 Genomes cosmopolitan samples (Build 37: African, AFR; American, AMR; Asian, ASN; European, EUR) served as a reference for SNP imputation. Observed SNPs were eliminated prior to imputation if they could not be converted to the forward strand or if more than one SNP mapped to a given position. The reference genome was filtered to exclude SNPs whose minor allele frequency (MAF) was < 0.005. The data were then phased using SHAPEIT (26) and imputed *via* IMPUTE2 (27). SNPs were included in analyses if their imputation dosage allele R^2 was at least 0.3 and their MAF was at least 0.01. These GWAS QC restrictions resulted in a dataset with 6,210,296 SNPs for the HumHap550 array; 6,244,529 SNPs for the HumHap650 array; and 6,243,494 SNPs for the Omni 2.5 array.

Fine mapping on the chromosome 5 region was performed using a custom Illumina iSelect panel that included known SNPs in the following gene regions: *TMEM173, KCNN2, DNAJC18*, and *TRIM36* (the coding region, the intronic regions, and 10kb upstream and downstream in order to capture regulatory regions). We then identified all SNPs highly correlated (r2 > 0.9) with each of the target SNPs of interest based on the GWAS results. SNPs were excluded from the fine-mapping effort for the following reasons: low rank on the Illumina design score metric (indicating a low likelihood of successful genotyping); any Illumina error codes; previously genotyped SNPs; and monomorphic SNPs (based on HapMap and 1000 Genomes data). The resulting list of 2,406 SNPs were included on the Illumina iSelect panel. The genotyping was performed in Mayo Clinic's Clinical Genome Facility on 2,208 subjects: 2,011 subjects from the SD and U.S. cohorts; and 197 subjects used for quality control (55 negative controls, 48 trios of father/mother/child). 1,996 of these subjects passed all QC metrics filters (e.g., call rate at least 99%, duplicates removed, etc.). Of the genotyped SNPs, a total of 580 SNPs were used in the analysis (156 SNPs failed genotyping; 10 SNPs had call rates < 95%; 32 SNPs had HWE p-values < $10E^{-6}$, and 1,500 were monomorphic). For the Caucasian subgroup, an additional 126 SNPs were removed because they were monomorphic in that subgroup.

Genetic Ancestry and Population Stratification

Genotypes from the GWAS arrays were used to assign ancestry groups (i.e., Caucasian, African American, or Asian) to participants using the STRUCTURE software (28) and the 1000 Genomes reference data. Genetic ancestry proportions were estimated within cohorts and arrays (San Diego/550, San Diego/650, US/Omni 2.5), as previously described (11, 15). A linkage disequilibrium (LD) pruning process (29) was utilized to ensure that the SNPs used for STRUCTURE and for sample eigenvectors were not drawn from small clusters within specific locations (30). Resulting SNPs were entered into to the STRUCTURE program (28), and participant ancestry was classified based on the largest ancestry proportion estimated by STRUCTURE.

Within ancestry groups, eigenvectors were estimated for population-stratification purposes. SNPs with a MAF < 0.01 and those with a HWE p-value < 0.001 were excluded, as were insertion/deletions (INDELS). The remaining SNPs were pruned according to the following variance inflation factors: window size of 50 kilobases; step size of 5; and variance inflation factor threshold of 1.05. SmartPCA was used to create the eigenvectors (31) following the procedures implemented in EIGENSTRAT software. Eigenvectors were included as potential covariates if they had a Tracy-Widom p-value < 0.05.

Selection of Covariates to Adjust for Potential Confounders

For analysis purposes, the immune-response trait of interest (IFNα secretion) was calculated by first computing the difference of the mean stimulated and unstimulated values and then transforming to a normal distribution using normal quantiles. In order to combine data from the two cohorts, potential confounder effects for each ancestry group and cohort were adjusted by linear regression models as described (29). Categorical variables with a very large number of categories were binned using hierarchical clustering. This was achieved by using hierarchical clustering on the estimated regression coefficients for the different categories while binning categories with similar regression coefficients. Categorical variables were included in regression models by using indicator variables for categories, treating the most common category as baseline. Residuals from the linear models were used as the primary adjusted traits for GWAS analyses.

GWAS Analysis Strategy

In order to maximize the power to detect SNPs associated with smallpox vaccine immune response phenotypes, data across genotyping arrays and the two cohorts was pooled after preparing the data as described above. The pooled analyses were then performed using the adjusted traits described above in a regression analysis, along with an indicator of cohort as an

additional adjusting covariate. Because the largest ancestry group was Caucasian, we restricted our pooled analysis to the Caucasian subjects (n=1,605). Multiple testing was controlled for by using the standard p-value threshold (p-value< $5x10^{-8}$) to determine genome-wide statistical significance (32, 33). Statistical analyses were performed with the R statistical software and PLINK (34).

Generation of Stably Transduced BJAB Cell Lines

BJAB cell lines, each expressing one of the rs1131769 variants of interest, were created using custom suCMV promoter-based lentivectors containing a Blasticidin resistance gene (GenTarget Inc.; San Diego, CA). Lentiviral particles were produced in 293T packaging cells using the SureTiter™ Lentiviral vector system (GenTarget Inc.; San Diego, CA), in DMEM with 10% FBS at approximately 10^7 IFU/per ml. Transduction with lentiviral particles was performed at MOI of 10 in the presence of Polybrene (Millipore Sigma) at 8 μg/mL, and stable cell clones were selected for using Blasticidin (InvivoGen; San Diego, CA) at 10 μg/mL.

Transfection of Cells With STING Variants

For HEK 293 T cells, transfection was performed with 20 ng of the STING plasmid constructs (pUNO1-hSTING-H232 and pUNO1-hSTING-WT, InvivoGen; San Diego, CA) and with 20 ng cGAS (pUNO1-hcGAS, InvivoGen; San Diego, CA) using Lipofectamine LTX and PLUS™ Reagent (Invitrogen; Carlsbad, CA), according to the manufacturer's instructions.

Cellular Stimulation With STING Ligands

STING allele-expressing BJAB cells were plated at 300,000 cells/mL, 0.5 mL/well in a 24-well plate. 50 ug/mL of 2'3' cGAMP or ddH2O were added to stimulated and mock-stimulated wells, respectively. Stimulated and control cells were harvested at the indicated times after 2'3' cGAMP stimulation and centrifuged 5 min at 5,000 rpm in microcentrifuge tubes. Supernatants were collected and frozen for ELISA analysis. Cells were resuspended in 200 uL RNAProtect (Qiagen; Valencia, CA) and frozen at -20°C.

Protein Phosphorylation (Western Blot)

Protein expression and phosphorylation (for IRF3 and TBK1) was assessed in transiently transfected HEK 293 T cells and lentivirus-transduced stable BJAB cell lines, expressing the STING alleles of interest. For protein expression and western blotting experiments, cells were incubated overnight in antibiotic-free medium and then stimulated with 2'3'cGAMP (Invivogen; 20 μg/mL for the HEK 293 T cells and 100 μg/mL for the BJAB cells) for different timepoints (15 min, 30 min, 1 h, 2 h, and 4 h). The cells were lysed in RIPA lysis buffer (Sigma) containing protease and phosphatase inhibitors (protease inhibitors cOmplete™ and phosphatase inhibitors PhosSTOP™, Roche). Lysates were centrifuged at 16,000 RPM and 4°C for 20 min. Protein concentrations were quantified using the Pierce BCA Protein Assay Kit (ThermoFisher Scientific; Minneapolis, MN), and equal protein amounts (2 to 3μg) were used for western blot analysis. Laemmli buffer (Bio-Rad; Hercules, CA) with β-mercaptoethanol was added to the samples, and the lysates were denatured by incubating at 95°C for 5 min and were centrifuged at 16,000 RPM for 1 min. Samples were loaded onto 4–20% Criterion™ gels (Bio-Rad; Hercules, CA), and then proteins were transferred to Trans-Blot® Turbo Midi PVDF membranes (Bio-Rad; Hercules, CA) using the Trans-Blot® Turbo™ Transfer System (Bio-Rad; Hercules, CA). Blots were blocked with 3% BSA and probed overnight (at 4°C) with primary monoclonal rabbit anti-STING (cat. # 13647), anti-TANK-binding kinase 1 (TBK1, cat. # 3504), anti-pTBK1 (cat. # 5483), anti-interferon regulatory factor 3 (IRF3, cat. # 4302), and anti-pIRF3 antibody (cat. # 4947) (all from Cell Signaling Technologies; Beverly, MA), or mouse monoclonal anti-alpha tubulin antibody (cat. # 40742, Abcam; Cambridge, MA) for loading control. Membranes were washed and incubated for 1 h at room temperature with the appropriate HRP-labeled pre-absorbed goat anti-rabbit (cat. # sc-2054) or anti-mouse (cat. # sc-2055) secondary antibodies (Santa Cruz Biotechnology, Inc.; Dallas, TX). The membranes were washed, developed using Clarity Western ECL Substrate Solution (Bio-Rad; Hercules, CA) for 10 min, and imaged using the ChemiDoc™ Touch Gel Imaging System (Bio-Rad; Hercules, CA). Comparisons were assessed using Student's t-test.

Gene Expression (qPCR)

Total RNA was extracted from frozen cells using Qiagen RNeasy Plus mini kits according to the manufacturer's instructions, and RNA concentrations were normalized between samples. Random-primer reverse transcription was done using RT2 First Strand kits (Qiagen; Valencia, CA), including a genomic DNA removal treatment, according to the manufacturer's instructions. qPCR was then done on each sample using the Qiagen RT2 SYBR Green/ROX qPCR Mastermix system using the following primers (35): IFN-α, 5'-AAATACAGCCCTTG TGCCTGG-3'and 5'-GGTGAGCTGGCATACGAATCA-3'; IFN-β, 5'-AAGGCCAAGGAGTACAGTC-3' and 5'-ATCTT CAGTTTCGGAGGTAA-3'; IFN-λ1, 5'-CGCCTTGGAAG AGTCACTCA-3'; IFN-λ1 5'-GAAGCCTCAGGTCCCAATTC-3'; b-actin, 5'-AAAGACCTGTACGCCAACAC-3'; b-actin 5'-GTCATACTCCTGCTTGCTGAT-3'; STING, Commercial Qiagen RT2 qPCR Primer Assay for Human TMEM173, MxA, Commercial InvivoGen IFNr qRT-Primer set, hOAS1-F and hOAS1-R; OAS1, Commercial InvivoGen IFNr qRT-Primer set, hMX1-F and hMX1-R. Quantitative PCR was done using an ABI ViiA-7 machine at the standard qPCR conditions starting with incubation at 95°C for 10 min, followed by 40 cycles of 95°C for 15 s and 60°C for 1 min. Ct values were normalized to β-actin levels and unstimulated controls by the standard 2ΔΔCT method. Experimental conditions were compared using Student's t-test.

Promoter Reporter Assays

The promoter reporter assays were performed in HEK 293 T cells, stably expressing one of the STING alleles of interest (for rs1131769 – WT/R232 and H232) under blasticidin selection (36). We used pNiFty2-IFNB-SEAP and pNiFty2-56K-SEAP

promoter-reporter plasmids (InvivoGen; San Diego, CA), encoding the INFβ minimal promoter and the ISG-56K promoter, respectively. Co-expression with constitutively activated IRF3 (or IRF7) leads to promoter induction measured by the inducible expression of the secreted embryonic alkaline phosphatase (SEAP) reporter gene. Promoter assays were performed as previously described (36) but with some modifications. Briefly, 2.5 x 10^4 cells per well (stably expressing STING alleles of interest under blasticidin selection) were cultured overnight in 96-well plates in antibiotic-free medium [DMEM (Gibco Invitrogen Corporation; Carlsbad, CA)], containing 10% fetal bovine serum (FBS, HyClone; Logan, UT). On the following day, cells were transfected with Lipofectamine® LTX (Invitrogen; Carlsbad, CA), according to the manufacturer's protocol, using a constant amount of reporter plasmid (100 ng of either pNiFty2-IFNB-SEAP or pNiFty2-56K-SEAP per well), 0.2 μL PLUS™ Reagent (Invitrogen; Carlsbad, CA) per well, and 0.25 μL Lipofectamine LTX per well. After overnight incubation, the medium was switched to Opti-MEM (Gibco Invitrogen Corporation; Carlsbad, CA), and cells were stimulated with one of two STING ligands: 2'3' cGAMP (100 μg/ml), or inactivated vaccinia virus (MOI of 10) at 37°C for different time periods. Promoter induction was measured by the SEAP reporter secretion (quantified at 620 nm following addition of Quanti-Blue™ media, Invivogen, per the manufacturer's instructions). Experimental conditions were compared using Student's t-test.

ELISA Measurement of Secreted Type I and Type III IFNs

IFNα and IFNλ production by 2'3' cGAMP-treated STING-transduced BJAB cells were measured in triplicate using commercial sandwich ELISA assay sets (IFNα: VeriKine-HS™ Human Interferon Alpha All Subtype ELISA Kit, PBL Assay Science; Piscataway, NJ, and IFNλ: Human IL-29/IL-28B [IFN-lambda 1/3] DuoSet ELISA set, R&D Systems; Minneapolis, MN) according to the manufacturer's instructions. Standard protein samples were diluted in cell culture media for accurate standard curve construction and calculations. Recombinant IFNs were used as positive controls while cell culture media served as the negative control. Biological duplicate samples from each timepoint were each assayed in technical duplicate. The level of sensitivity for the IFNα and IFN λ assays were 12.5 and 62.5 pg/mL, respectively.

Molecular Modeling

The atomic structure of the cyclic dinucleotide binding domain of STING has been experimentally solved (37). As is common for crystallographic structures, mobile loops were not resolved in these structures. To initially place residues within these mobile loops, we used the SwissModel server (38) and template PDB structures 4QXP (39) (open conformation with inhibitor bound) and 4F5Y (40) (closed conformation with cdGMP bound). Mutations present in each template were reverted to WT amino acids according to the UniProt sequence of the canonical transcript (Q86WV6-1). Simulations were run for the apo (un-liganded), cdGMP, and cGAMP ligand states.

We used NAMD (41) and the CHARMM27 with the CMAP (42) force field for Generalized Born implicit solvent molecular dynamics (isMD) simulations using previously optimized conditions (43) that included the following: 1) an interaction cutoff of 15Å; 2) strength tapering (switching) starting at 12Å; 3) a 1fs simulation time step with conformations recorded every 2ps; 4) an initial conformation that was energy minimized for 20,000 steps; and 5) heating to 300K over 300ps *via* a Langevin thermostat. From each of the 12 conditions (two initial conformations, two alleles, and three ligand states), 100ns of simulation trajectory was generated and the final 70ns analyzed. Three additional and independent 20ns replicates for each condition were generated using the same procedure. All trajectories were aligned to the initial R232 closed conformation using C^{α} atoms. Trajectories were then evaluated using multiple metrics, including C-alpha Root Mean Squared Deviation (RMSD), Root Mean Squared Fluctuation (RMSF), Principal Component (PC) analysis, alignment-free distance difference matrix (44–46), and distance monitors across the ligand binding site. We quantified variance of atomic C^{α}–C^{α} (**Figure 7A**) distances using median absolute difference (MAD). Analysis was performed using custom scripts on the Bio3D R package (46) and VMD (47).

RESULTS

Overview of Cohorts and IFNα Response

We conducted a GWAS meta-analysis on two cohorts (n=1,076 and 1,058) of smallpox vaccine recipients (11, 12, 15) with immune outcome data and genome-wide SNP-typing. We imputed additional SNPs, as described in *Materials and Methods* section. As the full dataset was available for all subjects, the cohorts were combined to increase statistical power, and a final study sample of 1,653 Caucasian subjects was available for analysis (see **Supplementary Table 1** for demographic information). The actual cohort used in the analysis for each immune outcome varied depending on how many of those 1,653 individuals had data for that specific outcome. Our original intent was to determine whether or not there were genetic polymorphisms associated with markers of vaccine-induced cellular immunity, as had been noted in preliminary reports on the San Diego Cohort (24, 25, 48). VACV was inactivated in order to minimize the immunomodulatory effect of poxvirus-encoded proteins and to allow full development of the cytokine response. Our outcomes of interest included both innate anti-viral outcomes (secretion of IL-1β, IL-6, IFNα) and markers associated with adaptive immune responses (neutralizing antibody titer, IFNγ ELISPOT response in PBMCs, IFNγ ELISPOT in CD8+ T cells, as well as secretion of IL-2, IFNγ, IL-12p40, and TNFα).

Surprisingly, our GWAS analysis found only a strong signal on chromosome 5 associated with IFNα secretion that exceeded the genome-wide significance level (**Figures 1A, B**). There were two suggestive signals: one on chromosome 11 associated with the CD8+ T cell IFNg ELISPOT response and another on

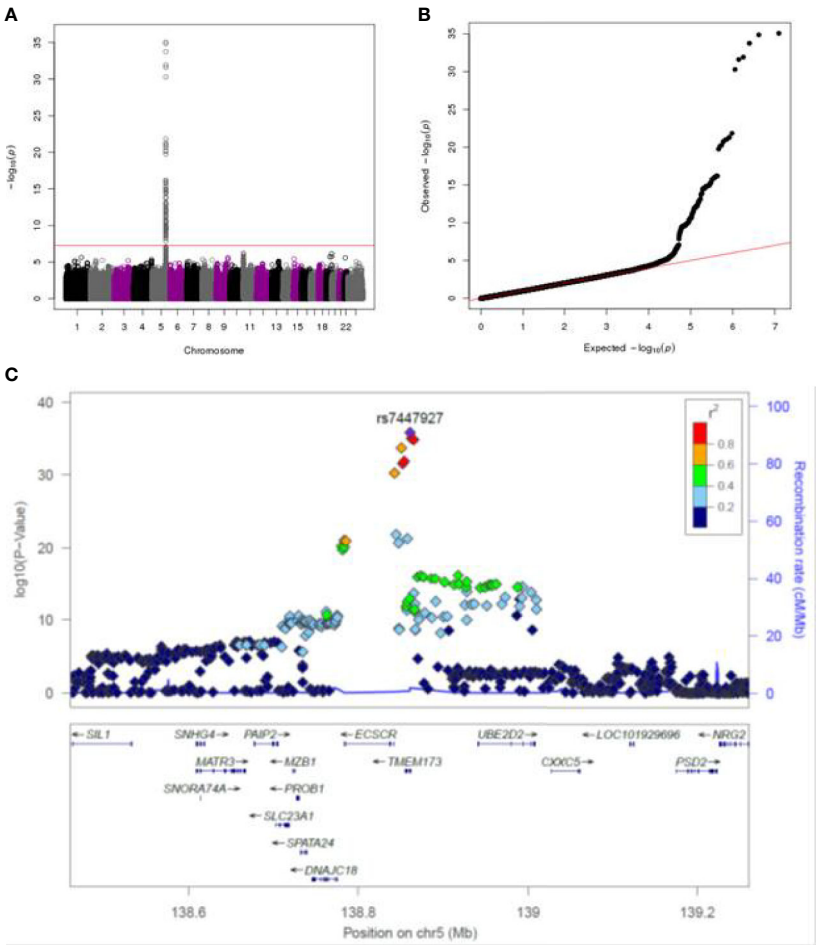

FIGURE 1 | GWAS genotyping results in the combined smallpox vaccine recipient cohort. **(A)** Manhattan plot indicating SNPs associated with IFNα response. **(B)** QQ plot of genome-wide p-values. **(C)** Locus-zoom plot depicting region on chromosome 5 with the strongest association signal. SNP LD is shown in color. The name and location of each gene is shown at the bottom of the panel.

chromosome 9 associated with IFNγ secretion. The remaining outcomes were not associated with any genetic variants. Due to the strength of the IFNα signal and the fact that the other two potential signals did not reach a genome-wide threshold for significance, we focused our efforts on exploring the region on chromosome 5 associated with IFNα secretion.

The locus-zoom plot in **Figure 1C** depicts the SNPs with the strongest statistical association with IFNα response. We used a genome-wide threshold of p-value $<5 \times 10^{-8}$ to establish statistical significance. Further details on the SNPs meeting this threshold are provided in **Table 1**. Of the 1,653 individuals with genotyping available, 1,605 also had IFNα secretion data. This cohort had a median IFNα secretion level of 126 pg/mL (IQR: 48.6–229.6) in PBMC cultures after vaccinia virus stimulation. As illustrated in **Figure 2**, TT homozygotes (H232 STING) had a median IFNα response of 17.7 pg/mL, while individuals homozygous for the R232 STING allele (CC genotype) had an 8-fold higher response (143.6 pg/mL). Heterozygotes had an intermediate phenotype. We did not identify any SNPs in other genes (including those associated with the STING pathway, such as *cGAS*, *TBK1*, or *IRF3*) associated with variations in IFNα secretion.

Several of the SNPs significantly associated with IFNα secretion were located in *TMEM173*, which encodes for STING —an adaptor molecule mediating type I IFN responses to cyclic dinucleotides and double-stranded DNA. STING has previously been shown to play an important role in the innate immune response to poxviruses (20, 49).

A number of additional non-synonymous polymorphisms potentially affecting STING function have previously been identified, including R71H (rs11554776), G230A (rs78233829), R293Q (rs7380824), and R232H (rs1131769) (22, 50). In order to determine which SNPs in the haplotype contributed to the response, while accounting for correlation among SNPs, we used haplo.stats software in R to compute the haplotype frequencies for these four SNPs: rs11554776; rs78233829; rs1131769; and rs7380824 (51).

TABLE 1 | Top SNPs significantly associated with vaccinia virus-specific IFNα secretion.

SNP	ChromosomeLocation	Gene	SNPFunction	GeneLocation	p-value	Minorallele	Majorallele	MAF
rs7447927	138861146	TMEM173	protein-coding	synonymous	1.49E-36	C	G	34.7%
rs13166214	138862744	TMEM173	protein-coding	5'upstream	8.92E-36	A	G	35.3%
rs7444313	138865423	TMEM173	protein-coding	5'upstream	1.41E-35	G	A	34.5%
rs13181561	138850905	TMEM173	protein-coding	3'downstream	1.81E-34	G	A	30.0%
rs55792153	138854203	TMEM173	protein-coding	3'downstream	1.26E-32	A	C	34.2%
rs13153461	138852369	TMEM173	protein-coding	3'downstream	2.61E-32	G	A	31.4%
rs9716069	138842818	ECSCR	protein-coding	5'upstream	5.32E-31	T	A	31.3%
rs28419191	138844599	ECSCR	protein-coding	5'upstream	1.50E-22	T	C	13.2%
rs1131769	***138857919***	***TMEM173***	***protein-coding***	***missense***	**5.25E-22**	***T***	***C***	**14.0%**
rs11954057	138783832	RNU5B-4P	pseudo	3'downstream	8.99E-22	C	G	32.5%
rs36137978	138785565	ECSCR	protein-coding	5'upstream	1.13E-21	C	A	31.6%
rs10875554	138847652	ECSCR	protein-coding	5'upstream	1.99E-21	A	C	15.4%
rs6596479	138780599	RNU5B-4P	pseudo	5'upstream	5.63E-21	C	T	31.9%
rs7446197	138783734	RNU5B-4P	pseudo	3'downstream	7.51E-21	A	G	33.8%
rs10463977	138781765	RNU5B-4P	pseudo	5'upstream	1.80E-20	C	T	32.4%
rs2434576	138917674	UBE2D2	protein-coding	5'upstream	6.57E-17	G	A	30.8%
rs34530489	138873627	LOC642262	pseudo	gene	7.00E-17	G	A	31.4%
rs35779874	138869847	LOC642262	pseudo	5'upstream	1.11E-16	A	G	31.2%
rs7378724	138876953	LOC642262	pseudo	gene	1.13E-16	G	A	30.9%
rs78233829	**138857925**	**TMEM173**	**protein-coding**	**missense**	**3.16E-13**	**G**	**C**	**17.6%**
rs11554776	**138861078**	**TMEM173**	**protein-coding**	**missense**	**1.05E-12**	**T**	**C**	**16.5%**
rs7380824	**138856982**	**TMEM173**	**protein-coding**	**missense**	**1.25E-12**	**T**	**C**	**17.7%**

MAF, minor allele frequency. Bold, italics – SNP studied in this report. Bold – SNPs in HAQ STING haplotype.

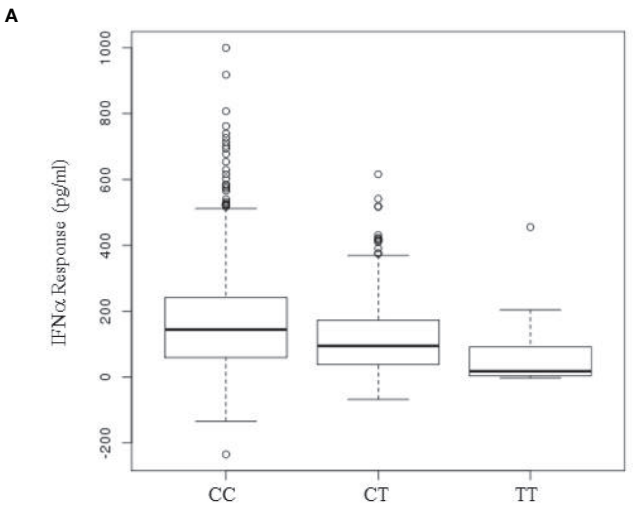

FIGURE 2 | IFNa response in smallpox vaccine recipients displays a dose-dependent association with rs1131769. **(A)** Box and whisker plots for major allele homozygotes (CC), heterozygotes (CT), and homozygous minor allele (TT) subjects. The C allele corresponds to the R232 STING variant and the T allele corresponds to the H232 STING variant. **(B)** Median IFNa response (pg/mL) by rs1131769 genotype group.

The haplotype frequencies were very close between the U.S. and San Diego cohorts; therefore, we proceeded to use the combined sample to evaluate the association of haplotypes with IFNα response. The results presented in **Table 2** illustrate the effects of the haplotypes on IFNα response and the frequencies of the haplotypes. We compare the haplotype CCTC (H232) with the most frequent haplotype CCCC (R232: treated as the baseline in the linear regression model) in order to focus on the effect of the T allele for rs1131769 while controlling for the effects of the other three SNPs on the haplotype, and identified a statistically significant ($p < 2E^{-16}$) decrease in IFNα response. The contrast of the haplotype CCCT with the baseline was not statistically significant, but we had limited power for this comparison because of the low frequency of the haplotype CCCT. We also used likelihood ratio statistics to contrast the effects of the haplotypes CGCT and TGCT, which differed only at the first SNP position, but the effects of these haplotypes were not significantly different (p-value = 0.46), but once again power was limited because of the rarity of haplotype CGCT. These analyses suggest that the SNP rs1131769 is likely the main variant in the haplotype impacting the association with IFNα response. However, the strong association of the haplotype TGCT with IFNα response suggests that there might be additional SNPs in the region that are in linkage disequilibrium with our measured SNPs that are also associated with IFNα response. To further explore this, we computed the dose of the minor allele for each of the four SNPs and performed backward regression, thereby ignoring haplotypes. The two SNPs rs7380824 and rs1131769 remained in the model (each with p-value $< 2E^{-16}$), illustrating that each SNP is strongly associated with IFNα response after adjusting for the other SNPs. The other two SNPs, rs78233829

TABLE 2 | The Effect of rs1131769 on IFNα Response is Independent of the Effect Mediated by the HAQ Haplotype.

Term in Model	Regression Coefficient**	Standard Error of Coefficient	p-value***	Haplotype Frequency
Intercept	0.31	0.037	<2E-16	
Cohort US vs. SD	0.037	0.044	0.40	
Haplotypes*				
CCCC	Baseline			0.683
CCC**T** *(H232)*	–0.011	0.307	0.97	0.002
CC**T**C *(Q293)*	–0.546	0.045	<2e–16	0.139
C**G**C**T** *(AQ)*	–0.281	0.146	0.05	0.011
TGC**T** *(HAQ)*	–0.409	0.042	<2e–16	0.164

**TMEM173 SNPs (haplotype) from left to right: rs11554776 (encodes amino acid/AA change at position 71) —rs78233829 (encodes AA change at position 230) — rs1131769 (encodes AA change at position 232) — rs7380824 (encodes AA change at position 293). In bold are designated the minor alleles defining the respective haplotypes, and in italics are designated the commonly used names of the haplotypes (that are based on encoded amino acid/acids and their position).*

***Regression coefficients from regression analysis of TMEM173 SNP haplotypes with IFNα response. Show the direction and magnitude of the estimated haplotypic effect on IFNα response compared to the haplotype (CCCC) with the greatest population frequency.*

****P-value from regression analysis.*

and rs11554776, were not statistically significant and were both strongly correlated with rs7380824 (Pearson correlations > 0.95).

Promoter Activity of rs1131769 Variants

Two plasmids expressing the secreted embryonic alkaline phosphatase (SEAP) reporter gene, under control of either the INFβ promoter or the interferon stimulated gene (ISG)-56K promoter, were used to measure ligand-stimulated promoter activity in HEK293T cells expressing either R232 or H232 STING (**Figure 3**). Both 293T variant cell lines expressed high levels of STING mRNA (**Figure 3D**) with no significant difference between alleles. Upon 2'3' cGAMP stimulation, IFNβ promoter induction was significantly higher at 10 h post-stimulation in R232 cells compared to cells expressing H232 (**Figure 3A**, p=0.02). Similarly, we observed statistically significant higher induction of the ISG-56K promoter activity in R232 upon stimulation with either 2'3' cGAMP at 4 h and 8 h post-stimulation (**Figure 3B**, p=0.006 and p=0.004, respectively) or inactivated vaccinia virus at 8 h post-stimulation (**Figure 3C**, p=0.002).

In vitro stimulation of our H232 and R232 STING-transfected cells lines with live vaccinia virus resulted in global

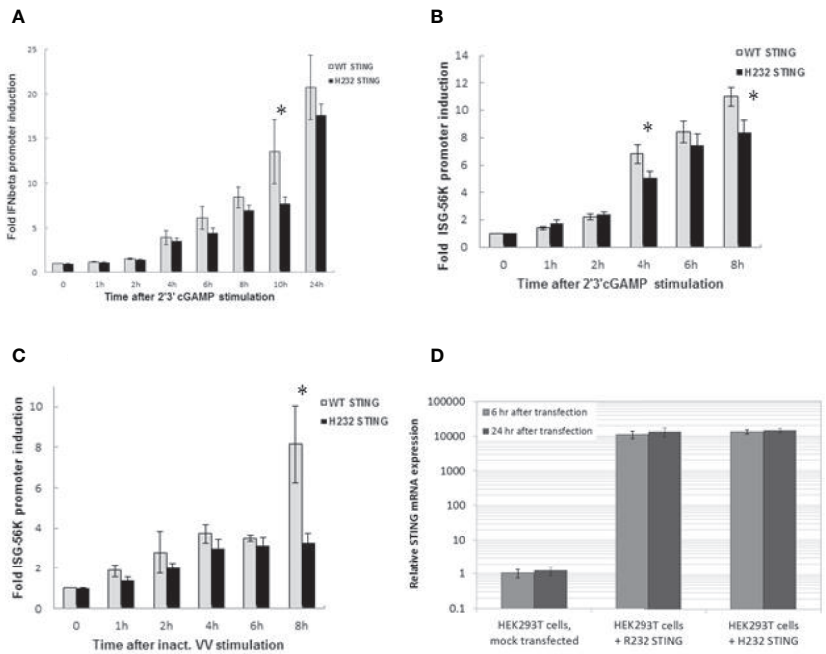

FIGURE 3 | IFNβ and ISG-56K Promoter Activity is Greater in HEK 293T Cells Stably Expressing the R232 STING Variant. **(A)** IFNβ promoter induction following cGAMP stimulation. **(B)** ISG-56K promoter activity after cGAMP stimulation. **(C)** ISG-56K promoter activity after stimulation with inactivated vaccinia virus (inact. VV). Data points for **(A)**, **(B, C)** show the means with error bars representing the standard deviations of three replicates. **(D)** STING expression in HEK293T stably expressing R232 or H232 STING. Data points for **(D)** show the means with error bars representing the standard deviations of eight replicates. A two-tailed t-test* detected significant differences; see text for p-values. Each experiment was performed twice with nearly identical results.

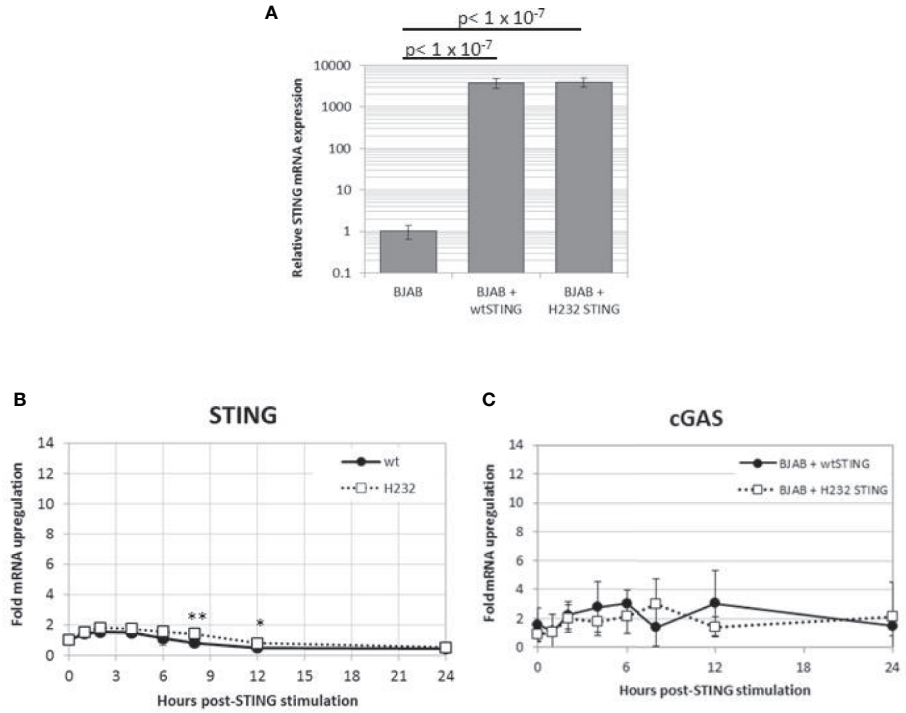

FIGURE 4 | Stable transfection of H232 or R232 STING into BJAB cells results in high level expression that is stable upon cGAMP stimulation. **(A)** Untransduced and stably transduced BJAB cell lines expressing STING alleles were harvested and assayed for STING mRNA using quantitative PCR. Values are shown as fold-levels relative to normal STING expression in untransduced BJAB cells. Data represent means and standard deviations of four biological replicates, assayed with technical duplicates. **(B)** Time course of TMEM173 expression in 2'3' cGAMP-stimulated (50ug/ml) in transduced BJAB cells stably expressing STING variants. **(C)** Time course of cGAS expression in stable BJAB transfectants stimulated with cGAMP. Values are presented as fold-increases over mock-treated cells, normalized to β-actin loading controls. Data points are the average of 8 replicates coming from four biological duplicates. Each experiment was performed twice. Two-tailed t-test: *p < 0.05. **p < 0.005.

downregulation of gene expression, preventing us from examining differential effects between the two STING variants. In order to avoid such confounding issues with viral infection, we stimulated cells with 2'3' cGAMP or inactivated vaccinia virus for all further experiments.

Gene Expression of rs1131769 Variants

mRNA was extracted from PBMCs of individuals homozygous for the CC genotype (R232) and the TT genotype (H232), and the two *TMEM173* variants were PCR amplified and cloned into lentivirus expression vectors. BJAB cells were transduced with these vectors, creating stable cell lines that constitutively overexpress each STING variant. The PCR products and completed expression vectors were both sequenced to verify the insertion of the correct genetic variants. As illustrated in **Figure 4A**, stable transfectants express >1,000-fold higher (and comparable between the two variants) STING mRNA than normal BJAB cells. Expression of both *TMEM173* variants transiently and minimally (less than 2-fold) increased after 2'3' cGAMP stimulation, indicating the STING protein levels of either variant are unlikely to be significantly affected by cGAMP treatment (**Figure 4B**). Finally, we found that *MB21D1* (encoding cGAS, an essential upstream nucleotidyltransferase in the STING pathway that generates cyclic cGAMP) gene expression was not significantly different between the two variants (**Figure 4C**), indicating that signaling pathway function upstream of STING was not affected by the STING gene variants. Note that the HEK293T lines used in this report were also transfected with *MB21D1* as this cell line is known to be deficient in cGAS expression (52).

Effect of rs1131769 Variants on Downstream Phosphorylation

Transiently transfected HEK293T and stably transfected BJAB cells were stimulated with 2'3' cGAMP for the indicated time periods, and phosphorylation of downstream intermediates TBK1 and IRF3 was evaluated (**Figures 5A, B**). In transiently transfected HEK293T cells (also expressing cGAS), H232 STING expression was accompanied by a delay in phosphorylation of both TBK1 and IRF3 until 1 hour after stimulation. Interestingly, we observed substantial pTBK1 and pIRF3 baseline phosphorylation (at timepoint 0) for the R232 STING variant (but not for the H232 variant associated with diminished phosphorylation/activation), which is likely due to STING overexpression. The H232 STING expression at timepoints 0 and 30 min was slightly reduced, but TBK1 and IRF3 protein

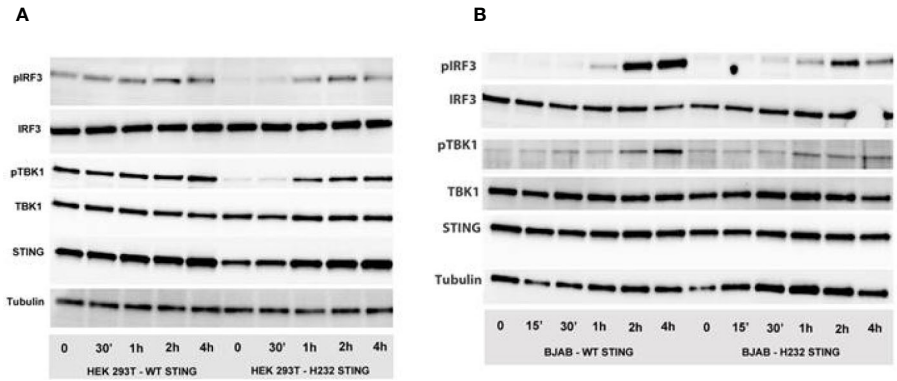

FIGURE 5 | Phosphorylation of IRF3 and TBK1 is delayed and decreased in the presence of H232 STING. **(A)** STING pathway activation (phosphorylation of IRF3 and TBK1) after 2'3' cGAMP stimulation of HEK 293 T cells, transiently expressing WT or H232 STING variants/alleles and cGAS. **(B)** STING pathway activation (phosphorylation of IRF3 and TBK1) after 2'3' cGAMP stimulation of lentivirus-created BJAB cell lines, stably expressing WT or H232 STING variants under Blasticidin selection. Each experiment was conducted three times with two biological duplicates per sample.

expression were similar between the two variants, which demonstrates that the observed differences in phosphorylation/activation are valid. In the stably transduced BJAB line, the delayed phosphorylation was observed with both STING variants and the pattern/kinetics of phosphorylation was similar; however, the magnitude of TBK1 and IRF3 phosphorylation was significantly reduced (in particular at 2h and 4h post-stimulation) in cells expressing H232 compared to cells expressing R232 STING. No major differences in STING protein levels, or in the unphosphorylated forms of either TBK or IRF3, were observed between the cells expressing the two STING variants at the observed timepoints.

Effect of rs1131769 Variants on IFN Response

Reasoning that differences in TBK1 and IRF3 phosphorylation between these variants should have downstream consequences, we decided to examine differential pathway activity mediated by the two STING variants. We stimulated R232 and H232 STING variant-expressing stable BJAB cell lines with 2'3' cGAMP and measured gene expression (qPCR, **Figure 6A**) and protein secretion (ELISA, **Figure 6B**) over time. cGAMP stimulation induced both type I (IFNα, IFNβ) and type III (IFNλ1) interferons, with significantly higher levels of IFNs (mRNA and protein) observed in R232 cells. This effect was consistent regardless of the cGAMP isomer used for stimulation (**Supplementary Figure S1**). Furthermore, the expression of the classical antiviral ISGs, *MX1* and *OAS1*, after 2'3'cGAMP stimulation confirmed the greater STING pathway activation in R232 STING-expressing cells over the H232 STING-expressing cells (**Figure 6C**).

Molecular Modeling of STING Variants

In order to begin elucidating the mechanism underlying the greater STING activity in R232-expressing cells, we used molecular modeling and molecular dynamics simulations to examine structural and functional differences between the R232 and H232 variants. H232 exhibited larger overall deviation from the initial experimental structure, as quantified by RMSD (**Figure 7A**). This greater deviation (a reflection of mobility) occurred both in the presence or absence of ligand. As RMSD is a global measure, we also quantified per-residue mobility using RMSF (**Figure 7B**), which indicated that the ligand-binding loops were more mobile for H232 compared to R232, particularly when the 2'3' cGAMP ligand was bound. We further quantified the displacement of the ligand-binding loops using simple distance measures between residue 232 in each monomer. Regardless of the presence or absence of cGAMP, the ligand-binding loops of H232 were further separated from each other (**Figure 7C**) and from the base of the ligand-binding site (**Figure 8**) compared to R232. Our initial simulations assumed that the ligand-binding loops were closed over the base of the ligand-binding site; structures displayed in **Figures 7D, E** highlight the difference in STING conformation between H232 and R232. Simulations assuming an open ligand-binding loop conformation observed the same effect of H232 compared to R232 (**Supplementary Figure S2**). In summary, H232 exhibited greater structural flexibility and mobility of the ligand-binding loops in both the open or closed conformations and in the presence or absence of cGAMP.

DISCUSSION

Our GWAS across two cohorts of smallpox vaccine recipients, totaling just over 1,600 individuals, identified a highly significant ($p < 1 \times 10^{-30}$) association signal from a region on chromosome 5 that was linked to significant inter-individual variations in IFNα response to *in vitro* stimulation with vaccinia virus. The lack of genetic association with vaccine response markers (e.g., neutralizing antibody titer and IFNg ELISPOT) indicates that the signal observed is likely reflective of an innate response to

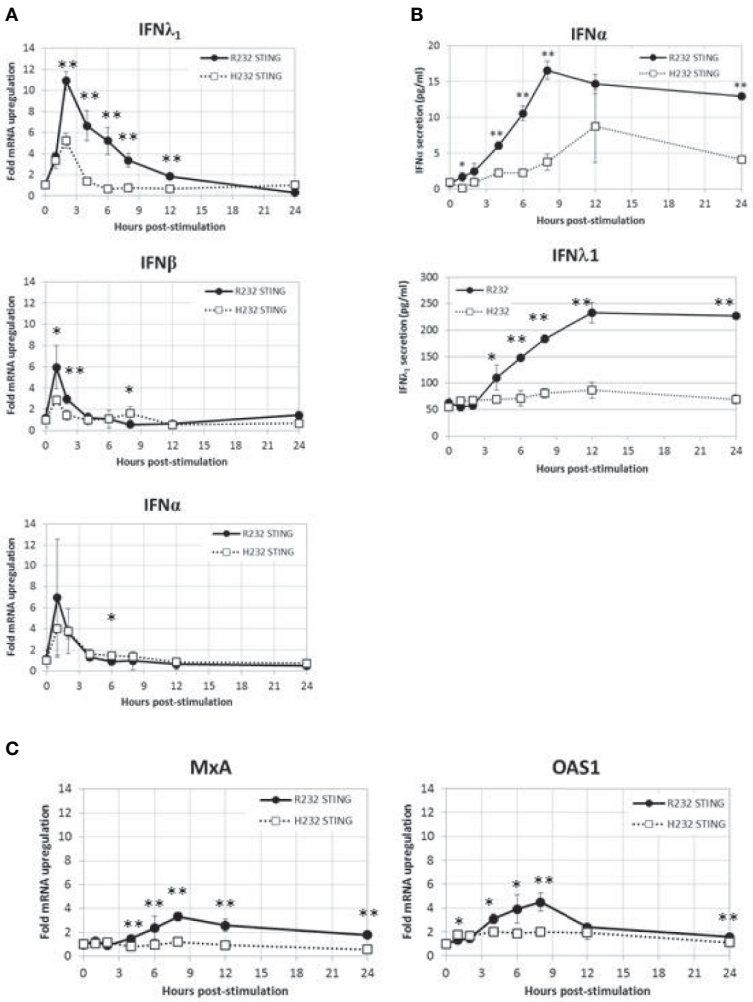

FIGURE 6 | WT and H232 STING-mediated IFN response in stably transduced BJAB cells. **(A)** Time course of *IFNA*, *IFNB*, *IFNL1* gene expression after cGAMP stimulation. **(B)** Time course of cytokine secretion after cGAMP stimulation. **(C)** Activation of representative interferon-stimulated genes after cGAMP stimulation. All data points in **(A, C)** are means and error bars representing the standard deviations of total of eight replicates coming from four biological duplicates. For cytokine secretion **(B)** biological duplicate samples from each timepoint were each assayed in duplicate for a total of four replicates. Each experiment was performed twice. Two-tailed t-test: *$p < 0.05$. **$p < 0.005$.

poxvirus infection rather than a T cell response. This suggests that our findings are broadly applicable to the response to poxvirus infection rather than smallpox vaccination.

Fine-mapping analysis identified a number of putative causal SNPs, including several in *TMEM173*, which encodes for the signaling adaptor protein STING. STING mediates IFN responses to dsDNA and cyclic dinucleotides through a pathway involving cGAS and the phosphorylation of TBK1 and IRF3. Our regression modeling also indicated that multiple SNPs within *TMEM173* have independent effects on the phenotypic outcome. Homozygotes for the H232 allele of rs1131769 in *TMEM173* exhibit a 90% reduction in IFNα secretion compared to R232 homozygotes. This is a highly significant effect that may have significant downstream consequences for poxvirus immunity. We have previously reported that a small percentage of smallpox vaccine recipients have impaired innate immune responses to vaccinia virus and that these same individuals also have suboptimal cellular immunity (13). Our current results provide additional support to existing data (53, 54) suggesting that appropriate innate immune responses are necessary for robust adaptive immunity to vaccinia virus. Further investigation of this effect on smallpox immunity is warranted.

We conducted a series of experiments with the intention of elucidating functional effects of this SNP that might be underlying the identified genotype–phenotype association. We assessed gene expression of both variants of *TMEM137* by PCR and STING expression by western blot and did not detect significant differences between variants in either gene or protein expression. We observed higher promoter activity of

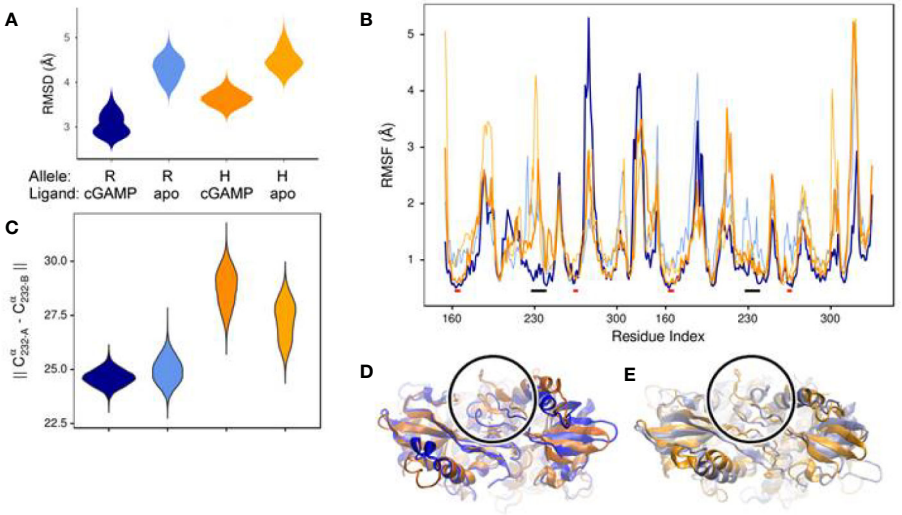

FIGURE 7 | Molecular Simulation ligand binding loop contact with cGAMP in R232 (wt) and H232 STING. **(A)** H232 consistently showed greater deviations from the initial open conformation, both in the presence and absence (marked as: "apo") of cGAMP. Simulation data from R232 is shown in blue, H232 in orange, and cGAMP-bound forms are in a darker shade. This color coding is continued throughout each panel. **(B)** Residues within the ligand binding loops, indicated by black bars, show less difference in mobility between unbound and cGAMP-bound forms. The ligand binding site residues, indicated by red bars, are more comparable in their mobility. **(C)** We monitored the distance between residue 232 from each monomer of the STING dimer as a measure of the separation of the ligand binding loops starting from the closed loop conformation. The separation was greater for H232, compared to R232, in both the unbound and cGAMP-bound forms. **(D)** Representative conformations from the end of cGAMP-bound simulations are shown and the ligand binding loop circled and residue 232 (shown in ball-and-stick representation). The altered conformation of H232 is evident. **(E)** Similar changes to the ligand binding loop conformation were observed in the absence of cGAMP.

downstream IFN-inducible genes in the R232 variant compared to the H232 variant, which suggests that there are differences in activation of the STING pathway. Upon stimulation with 2'3' cGAMP, the R232 STING variant elicited faster phosphorylation of both TBK1 and IRF3 as well as resulted in a greater quantity of phosphorylated TBK1 and IRF3 in the cells. These changes led to a significant increase in IFN and IFN-stimulated gene expression in R232-expressing cells, confirming that the statistical association was rooted in differential biological activity. As is true of most transfection systems, the *TMEM173* gene was overexpressed in our cell lines, with the HEK293T cells expressing ~10,000 times as much *TMEM173* as untransfected cells. The BJAB transfectants also expressed high levels of *TMEM173*, but the overexpression was an order of magnitude lower. More relevant to our results, protein expression was similar to the expression levels of endogenous IRF3, TBK1, and tubulin, suggesting that protein expression was within normal limits despite the upstream overexpression of STING observed at the gene level. We note that the expression (at the gene and protein level) of both variants was consistent; therefore, differences in activity are not a result of differential gene or protein expression between the variants.

Multiple genetic variants of *TMEM173* have been described, including three non-synonymous SNPs: rs1131769 (H232R), which was the focus of our study; rs11554776 (R71H); and rs7380824 (R293Q). R71H and R293Q, together with a fourth SNP, rs78233829 (G230A), form the *HAQ* haplotype (22). Zhang et al. have previously reported that expression of the H232 variant results in reduced IFNβ transcription (55). Our results confirm and extend these initial findings, demonstrating that IFNα secretion is also affected, as is the expression of multiple interferon-stimulated genes. Regarding the 3 alleles in the HAQ haplotype, there has been some controversy over the biological effects of these alleles (56, 57). In one study, cells carrying the G230 variant had fully functional STING activity and the HAQ haplotype effect was attributed to the R71H and R293Q SNPs (50). A similar study evaluating *TMEM173* variants found that the R232H, R293Q, and *AQ* (G230A, R293Q) variants had minimal effects on endogenous STING activity while the reduced STING function of the *HAQ* (R71H, G230A, R293Q) haplotype was attributed to the R71H variant (22). Our analysis supported previous findings that possession of the HAQ haplotype leads to reduced STING activity, demonstrated that the H232 variant also leads to reduced STING activity, and verified that this functional effect is independent of the *HAQ* haplotype. Thus, our haplotype and regression model results indicate that multiple SNPs/haplotypes are independently associated with variations in IFNα secretion. Our study also provides a potential biochemical mechanism for the reduced IFNα activity mediated by the R232H variant; however, further work will be required to tease apart the contributions of each individual SNP to the resulting immune response phenotype.

The crystal structure of STING has been resolved, as has the structure of the H232 variant bound to cGAMP (58). Our molecular modeling simulations, using these structure data, revealed that the ligand-binding loops of STING were more

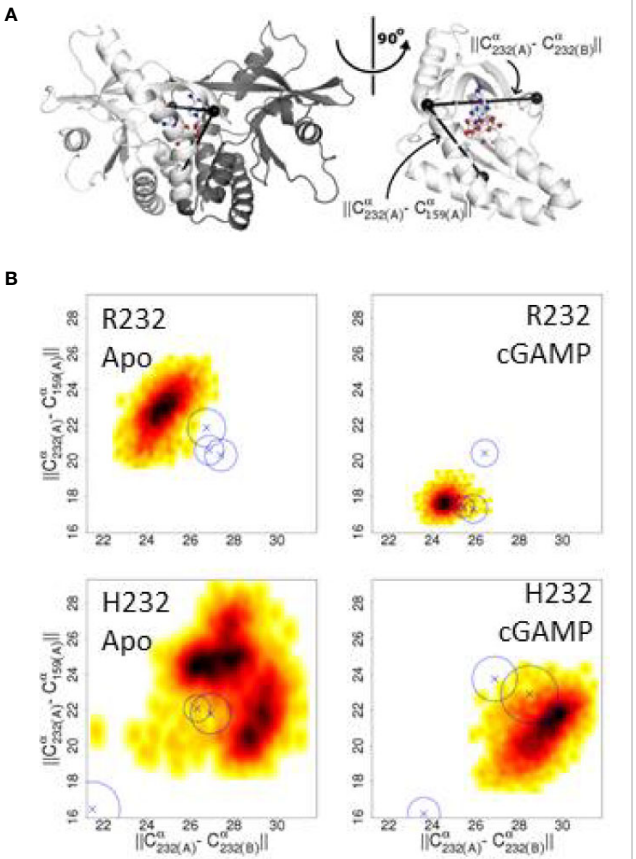

FIGURE 8 | Changes in the ligand binding loop between R232 and H232 are consistent across conditions. **(A)** Diagram of the STING structure showing one monomer of the closed conformation in white and the second monomer in gray, with the three C^{α} atoms used to compute distances marked by black spheres. The bound cGAMP is shown as a ball-and-stick representation. A rotated view, with the second monomer omitted for clarity, more clearly shows the relationship between these C^{α} positions and the ligand binding site. **(B)** H232 lead to a consistent expansion of the distances between the ligand binding loops and from the ligand binding loops to the base of the ligand binding site. Probability density plots are shown with the most frequently sampled regions colored black and scaling through red and yellow as data become more sparse. The medians for additional independent replicates are indicated by Xs and a circle indicating the level of variability.

mobile for H232 compared to WT; that is, H232 loop conformations were more open and flexible than R232, even in the presence of bound cGAMP. We speculate that this may reflect a failure of the ligand-binding loops to either stay closed when beginning from a closed conformation, or to close when beginning from an open conformation. This may be indicative of weaker binding (and/or faster disassociation) between cGAMP and the H232 variant of STING. Our data suggest that the alterations in loop dynamics and weaker affinity of H232 STING for its ligand are the underlying molecular mechanism for the reduced STING activity that we observed for this variant. This hypothesis will require additional experimental data to confirm or refute.

With regard to poxviruses, it has been demonstrated that Modified Vaccinia Ankara (MVA) infection of dendritic cells (DCs) triggers type I IFN production through a STING and cGAS-dependent pathway involving cyclic dinucleotides (49). This type I IFN response is not seen during wild type vaccinia virus infection, likely due to the presence of viral immunomodulatory proteins such as C6L, E3L, and N1L in the wild type virus but not in MVA (20, 21). A recent report confirmed that MVA activated IRF3 in a cGAS- and STING-dependent manner, whereas wild type vaccinia strains failed to do so (19). Our experiments found clear differences in R232 and H232 STING activity in the presence of cyclic dinucleotides and inactivated vaccinia virus. It is possible that possession of the H232 STING variant may alter the effects of viral immunomodulation of this innate immune pathway during infection. This may happen through differential interactions with viral proteins, or indirectly as reduced secretion of type I IFNs may render viral immunomodulation more effective.

We have demonstrated that carriage of the H variant of rs1131769 results in a 90% decrease in innate immune response (secreted IFNα) to vaccinia virus. This data helps resolve prior conflicting reports regarding functional effects of STING polymorphisms. We hypothesize that the effect of this polymorphism is due to different flexibility/mobility in STING H232 loop conformations, which results in reduced ability of H232 STING to phosphorylate downstream signaling intermediates and mediate effective STING pathway activation.

Poxviruses represent a continuing public health concern due to the risk of bioterrorism use, zoonotic outbreaks (e.g., monkeypox, buffalopox, vaccinia-like viruses, and novel poxviruses), the increasing use of poxviruses for oncolytic viral therapy, and their use as vectors for vaccine antigens against HIV, rabies, Ebola, Zika, and other pathogens. STING also plays an essential role in triggering protective innate responses to DNA viruses (e.g., poxviruses, herpes simplex viruses, varicella zoster, EBV, HPV, and others) and multiple bacterial pathogens. Polymorphisms that reduce the effectiveness of the innate response to these threats are likely to enhance disease susceptibility and may have a deleterious effect on vaccine immunogenicity in the ~15% of the population with this genotype. Given the broad potential impact of this pathway, this is an area that merits additional investigation.

Understanding how genetic factors control the immune response to poxviruses will have important clinical implications in how, when, and in whom these vectors can be safely and effectively used. Furthermore, this information may inform the use of adjuvants to overcome this defect and enhance vaccine responses or the development of therapeutic drugs that can be used to enhance the innate antiviral response during an infection.

DATA AVAILABILITY STATEMENT

The datasets presented in this study can be found in online repositories. The names of the repository/repositories and

accession number(s) can be found below: https://immport.niaid.nih.gov, SDY28.

ETHICS STATEMENT

The studies involving human participants were reviewed and approved by Institutional Review Boards of the Mayo Clinic (Rochester, MN) and the Naval Health Research Center (NHRC; San Diego, CA). The patients/participants provided their written informed consent to participate in this study.

AUTHOR CONTRIBUTIONS

RK contributed to the conception and design of the study; participated in the acquisition of data and the analysis and interpretation of the results; prepared the initial draft; revised draft for intellectual content. IH contributed to the study design; participated in data acquisition and interpretation of study results; assisted in drafting the manuscript; revised draft for intellectual content; approved final version. IO contributed to the study design; participated in data acquisition and interpretation of study results; assisted in drafting the manuscript; revised draft for intellectual content; approved final version. EV contributed to the study design; participated in data acquisition and interpretation of study results; assisted in drafting the manuscript; revised draft for intellectual content; approved final version. BL contributed data analysis and interpretation; assisted in drafting the manuscript; revised draft for intellectual content; approved final version. DS supervised and contributed to the data analysis and interpretation; participated in drafting and revising the manuscript; approved final version. MZ contributed to the interpretation of study results, molecular modeling, data analysis, drafting the manuscript; provided critical review; approved final version. AO contributed to the design of the study; participated in data analysis and interpretation; assisted in drafting the manuscript; revised the manuscript for intellectual content; approved the final version. GP contributed to the conception and design of the study; participated in data analysis and interpretation; secured funding for the project; participated in drafting and revising the manuscript; approved final version. All authors contributed to the article and approved the submitted version.

FUNDING

This study was supported by NIH through the NIAID Population Genetics Analysis Program Contract No.HHSN266200400065C and Contract No. HHSN272201000025C, and by the National Center for Research Resources grant 1 UL1 RR024150-01. The content is solely the responsibility of the authors and does not necessarily represent the official views of the National Institutes of Health.

ACKNOWLEDGMENTS

We gratefully thank the study subjects for their participation. We also thank Drs. Megan Ryan and Kevin Russell, as well as the clinical staff at the Naval Health Research Center for assistance with subject recruitment. We thank Nathaniel D. Warner and Krista M. Goergen for statistical and programming assistance and Caroline L. Vitse for proofreading and editorial assistance. This paper has been uploaded to the preprint server bioRxiv (doi: https://doi.org/10.1101/2020.05.28.1216570).

SUPPLEMENTARY MATERIAL

The Supplementary Material for this article can be found online at: https://www.frontiersin.org/articles/10.3389/fimmu.2020.567348/full#supplementary-material

REFERENCES

1. Fenner F, Henderson DA, Arita I, Jezek Z, Ladnyi ID. *Smallpox and its Eradication*. Switzerland: World Health Organization (1988) p. 1–1460 p.
2. Crotty S, Felgner P, Davies H, Glidewell J, Villarreal L, Ahmed R. Cutting edge: Long-term B cell memory in humans after smallpox vaccination. *J Immunol* (2003) 171(10):4969–73. doi: 10.4049/jimmunol.171.10.4969
3. Combadiere B, Boissonnas A, Carcelain G, Lefranc E, Samri A, Bricaire F, et al. Distinct time effects of vaccination on long-term proliferative and IFN-gamma-producing T cell memory to smallpox in humans. *J Exper Med* (2004) 199(11):1585–93. doi: 10.1084/jem.20032083
4. Di Giulio DB, Eckburg PB. Human monkeypox: an emerging zoonosis. *Lancet Infect Dis* (2004) 4(1):15–25. doi: 10.1016/S1473-3099(03)00856-9
5. Essbauer S, Pfeffer M, Meyer H. Zoonotic poxviruses. *Vet Microbiol* (2010) 140(3-4):229–36. doi: 10.1016/j.vetmic.2009.08.026
6. Singh RK, Balamurugan V, Bhanuprakash V, Venkatesan G, Hosamani M. Emergence and reemergence of vaccinia-like viruses: global scenario and perspectives. *Indian J Virol* (2012) 23(1):1–11. doi: 10.1007/s13337-012-0068-1
7. Nagasse-Sugahara TK, Kisielius JJ, Ueda-Ito M, Curti SP, Figueiredo CA, Cruz AS, et al. Human vaccinia-like virus outbreaks in Sao Paulo and Goias States, Brazil: virus detection, isolation and identification. *Rev Inst Med Trop Sao Paulo* (2004) 46(6):315–22. doi: 10.1590/S0036-46652004000600004
8. Breman JG, Arita I, Fenner F. Preventing the return of smallpox. *N Engl J Med* (2003) 348:463–6. doi: 10.1056/NEJMp025175
9. Kennedy RB, Ovsyannikova I, Poland GA. Smallpox vaccines for biodefense. *Vaccine* (2009) 27(Suppl 4):D73–9. doi: 10.1016/j.vaccine.2009.07.103
10. Kennedy RB, Ovsyannikova IG, Jacobson RM, Poland GA. The immunology of smallpox vaccines. *Curr Opin Immunol* (2009) 21(3):314–20. doi: 10.1016/j.coi.2009.04.004
11. Kennedy RB, Ovsyannikova IG, Pankratz VS, Haralambieva IH, Vierkant RA, Jacobson RM, et al. Genome-wide genetic associations with IFNgamma response to smallpox vaccine. *Hum Gen* (2012) 131(9):1433–51. doi: 10.1007/s00439-012-1179-x
12. Ovsyannikova IG, Kennedy RB, O'Byrne M, Jacobson RM, Pankratz VS, Poland GA. Genome-wide association study of antibody response to smallpox vaccine. *Vaccine* (2012) 30(28):4182–9. doi: 10.1016/j.vaccine.2012.04.055
13. Kennedy RB, Poland GA, Ovsyannikova IG, Oberg AL, Asmann YW, Grill DE, et al. Impaired innate, humoral, and cellular immunity despite a take in smallpox vaccine recipients. *Vaccine* (2016) 34(28):3283–90. doi: 10.1016/j.vaccine.2016.05.005

14. Crowe JEJr. Genetic predisposition for adverse events after vaccination. *J Infect Dis* (2007) 196(2):176–7. doi: 10.1086/518800
15. Kennedy RB, Ovsyannikova IG, Shane PV, Haralambieva IH, Vierkant RA, Poland GA. Genome-wide analysis of polymorphisms associated with cytokine responses in smallpox vaccine recipients. *Hum Gen* (2012) 131 (9):1403–21. doi: 10.1007/s00439-012-1174-2
16. Motwani M, Pesiridis S, Fitzgerald KA. DNA sensing by the cGAS-STING pathway in health and disease. *Nat Rev Genet* (2019) 20(11):657–74. doi: 10.1038/s41576-019-0151-1
17. Tan X, Sun L, Chen J, Chen ZJ. Detection of Microbial Infections Through Innate Immune Sensing of Nucleic Acids. *Annu Rev Microbiol* (2018) 72:447–78. doi: 10.1146/annurev-micro-102215-095605
18. Ferguson BJ, Mansur DS, Peters NE, Ren H, Smith GL. DNA-PK is a DNA sensor for IRF-3-dependent innate immunity. *eLife* (2012) 1:e00047. doi: 10.7554/eLife.00047
19. Georgana I, Sumner RP, Towers GJ, Maluquer de Motes C. Virulent poxviruses inhibit DNA sensing by preventing STING activation. *J Virol* (2018) 92(10):e02145–17. doi: 10.1128/JVI.02145-17
20. Unterholzner L, Sumner RP, Baran M, Ren H, Mansur DS, Bourke NM, et al. Vaccinia virus protein C6 is a virulence factor that binds TBK-1 adaptor proteins and inhibits activation of IRF3 and IRF7. *PLoS Pathog* (2011) 7(9): e1002247. doi: 10.1371/journal.ppat.1002247
21. Cao H, Dai P, Wang W, Li H, Yuan J, Wang F, et al. Innate immune response of human plasmacytoid dendritic cells to poxvirus infection is subverted by vaccinia E3 via its Z-DNA/RNA binding domain. *PLoS One* (2012) 7(5): e36823. doi: 10.1371/journal.pone.0036823
22. Yi G, Brendel VP, Shu C, Li P, Palanathan S, Cheng Kao C. Single nucleotide polymorphisms of human STING can affect innate immune response to cyclic dinucleotides. *PLoS One* (2013) 8(10):e77846. doi: 10.1371/journal.pone.0077846
23. Tsung K, Yim JH, Marti W, Buller RM, Norton JA. Gene expression and cytopathic effect of vaccinia virus inactivated by psoralen and long-wave UV light. *J Virol* (1996) 70(1):165–71. doi: 10.1128/JVI.70.1.165-171.1996
24. Ovsyannikova IG, Pankrantz VS, Salk HM, Kennedy RB, Poland GA. HLA alleles associated with the adaptive immune response to smallpox vaccine: a replication study. *Hum Genet* (2014) 133(9):1083–92. doi: 10.1007/s00439-014-1449-x
25. Haralambieva IH, Ovsyannikova IG, Kennedy RB, Larrabee BR, Shane Pankratz V, Poland GA. Race and sex-based differences in cytokine immune responses to smallpox vaccine in healthy individuals. *Hum Immunol* (2013) 74(10):1263–6. doi: 10.1016/j.humimm.2013.06.031
26. Delaneau O, Howie B, Cox AJ, Zagury JF, Marchini J. Haplotype estimation using sequencing reads. *Am J Hum Genet* (2013) 93(4):687–96. doi: 10.1016/j.ajhg.2013.09.002
27. Howie BN, Donnelly P, Marchini J. A flexible and accurate genotype imputation method for the next generation of genome-wide association studies. *PLoS Genet* (2009) 5(6):e1000529. doi: 10.1371/journal.pgen.1000529
28. Pritchard JK, Stephens M, Donnelly P. Inference of population structure using multilocus genotype data. *Genetics* (2000) 155(2):945–59.
29. Ovsyannikova IG, Schaid DJ, Larrabee BR, Haralambieva IH, Kennedy RB, Poland GA. A large population-based association study between HLA and KIR genotypes and measles vaccine antibody responses. *PLoS One* (2017) 12 (2):e0171261. doi: 10.1371/journal.pone.0171261
30. Novembre J, Stephens M. Interpreting principal component analyses of spatial population genetic variation. *Nat Genet* (2008) 40(5):646–9. doi: 10.1038/ng.139
31. Price AL, Patterson NJ, Plenge RM, Weinblatt ME, Shadick NA, Reich D. Principal components analysis corrects for stratification in genome-wide association studies. *Nat Genet* (2006) 38(8):904–9. doi: 10.1038/ng1847
32. Manolio TA. Genomewide association studies and assessment of the risk of disease. *N Engl J Med* (2010) 363(2):166–76. doi: 10.1056/NEJMra0905980
33. Pe'er I, Yelensky R, Altshuler D, Daly MJ. Estimation of the multiple testing burden for genomewide association studies of nearly all common variants. *Genet Epidemiol* (2008) 32(4):381–5. doi: 10.1002/gepi.20303
34. Purcell S, Neale B, Todd-Brown K, Thomas L, Ferreira MA, Bender D, et al. PLINK: a tool set for whole-genome association and population-based linkage analyses. *Am J Hum Genet* (2007) 81(3):559–75. doi: 10.1086/519795
35. Voigt EA, Yin J. Kinetic Differences and Synergistic Antiviral Effects Between Type I and Type III Interferon Signaling Indicate Pathway Independence. *J Interf Cytokine Res* (2015) 35(9):734–47. doi: 10.1089/jir.2015.0008
36. Antoniak S, Owens AP,3, Baunacke M, Williams JC, Lee RD, Weithauser A, et al. PAR-1 contributes to the innate immune response during viral infection. *J Clin Invest* (2013) 123(3):1310–22. doi: 10.1172/JCI66125
37. Huang YH, Liu XY, Du XX, Jiang ZF, Su XD. The structural basis for the sensing and binding of cyclic di-GMP by STING. *Nat Struct Molec Biol* (2012) 19(7):728–30. doi: 10.1038/nsmb.2333
38. Biasini M, Bienert S, Waterhouse A, Arnold K, Studer G, Schmidt T, et al. SWISS-MODEL: modelling protein tertiary and quaternary structure using evolutionary information. *Nucleic Acids Res* (2014) 42(Web Server issue): W252–8. doi: 10.1093/nar/gku340
39. Gao P, Zillinger T, Wang W, Ascano M, Dai P, Hartmann G, et al. Binding-pocket and lid-region substitutions render human STING sensitive to the species-specific drug DMXAA. *Cell Rep* (2014) 8(6):1668–76. doi: 10.1016/j.celrep.2014.08.010
40. Shang G, Zhu D, Li N, Zhang J, Zhu C, Lu D, et al. Crystal structures of STING protein reveal basis for recognition of cyclic di-GMP. *Nat Struct Molec Biol* (2012) 19(7):725–7. doi: 10.1038/nsmb.2332
41. Phillips JC, Braun R, Wang W, Gumbart J, Tajkhorshid E, Villa E, et al. Scalable molecular dynamics with NAMD. *J Comput Chem* (2005) 26 (16):1781–802. doi: 10.1002/jcc.20289
42. Mackerell ADJr., Feig M, Brooks CL3rd. Extending the treatment of backbone energetics in protein force fields: limitations of gas-phase quantum mechanics in reproducing protein conformational distributions in molecular dynamics simulations. *J Comput Chem* (2004) 25(11):1400–15. doi: 10.1002/jcc.20065
43. Sethi S, Dasari S, Plaisier E, Ronco P, Nasr SH, Brocheriou I, et al. Apolipoprotein CII Amyloidosis Associated With p.Lys41Thr Mutation. *Kidney Int Rep* (2018) 3(5):1193–201. doi: 10.1016/j.ekir.2018.04.009
44. Rashin AA, Domagalski MJ, Zimmermann MT, Minor W, Chruszcz M, Jernigan RL. Factors correlating with significant differences between X-ray structures of myoglobin. *Acta Crystallogr D Biol Crystallogr* (2014) 70(Pt 2):481–91. doi: 10.1107/S1399004713028812
45. Holm L, Sander C. Protein structure comparison by alignment of distance matrices. *J Molec Biol* (1993) 233(1):123–38. doi: 10.1006/jmbi.1993.1489
46. Grant BJ, Rodrigues AP, ElSawy KM, McCammon JA, Caves LS. Bio3d: an R package for the comparative analysis of protein structures. *Bioinformatics* (2006) 22(21):2695–6. doi: 10.1093/bioinformatics/btl461
47. Humphrey W, Dalke A, Schulten K. VMD: visual molecular dynamics. *J Molec Graph* (1996) 14(1):33–8, 27-8. doi: 10.1016/0263-7855(96)00018-5
48. Umlauf BJ, Ovsyannikova IG, Haralambieva IH, Kennedy RB, Vierkant RA, Pankratz VS, et al. Correlations between vaccinia-specific immune responses within a cohort of armed forces members. *Viral Immunol* (2011) 24(5):415–20. doi: 10.1089/vim.2011.0029
49. Dai P, Wang W, Cao H, Avogadri F, Dai L, Drexler I, et al. Modified vaccinia virus Ankara triggers type I IFN production in murine conventional dendritic cells via a cGAS/STING-mediated cytosolic DNA-sensing pathway. *PLoS Pathog* (2014) 10(4):e1003989. doi: 10.1371/journal.ppat.1003989
50. Jin L, Xu LG, Yang IV, Davidson EJ, Schwartz DA, Wurfel MM, et al. Identification and characterization of a loss-of-function human MPYS variant. *Genes Immun* (2011) 12(4):263–9. doi: 10.1038/gene.2010.75
51. Schaid DJ, Rowland CM, Tines DE, Jacobson RM, Poland GA. Score tests for association between traits and haplotypes when linkage phase is ambiguous. *Am J Hum Genet* (2002) 70:425–34. doi: 10.1086/338688
52. Sun L, Wu J, Du F, Chen X, Chen ZJ. Cyclic GMP-AMP synthase is a cytosolic DNA sensor that activates the type I interferon pathway. *Science* (2013) 339 (6121):786–91. doi: 10.1126/science.1232458
53. Quigley M, Martinez J, Huang X, Yang Y. A critical role for direct TLR2-MyD88 signaling in CD8 T-cell clonal expansion and memory formation following vaccinia viral infection. *Blood* (2009) 113(10):2256–64. doi: 10.1182/blood-2008-03-148809
54. Zhao Y, De Trez C, Flynn R, Ware CF, Croft M, Salek-Ardakani S. The adaptor molecule MyD88 directly promotes CD8 T cell responses to vaccinia virus. *J Immunol* (2009) 182(10):6278–86. doi: 10.4049/jimmunol.0803682
55. Zhang X, Shi H, Wu J, Sun L, Chen C, Chen ZJ. Cyclic GMP-AMP containing mixed phosphodiester linkages is an endogenous high-affinity ligand for STING. *Molecr Cell* (2013) 51(2):226–35. doi: 10.1016/j.molcel.2013.05.022
56. Patel S, Blaauboer SM, Tucker HR, Mansouri S, Ruiz-Moreno JS, Hamann L, et al. Correction: The Common R71H-G230A-R293Q Human TMEM173 Is a Null Allele. *J Immunol* (2017) 198(11):4547. doi: 10.4049/jimmunol.1700477

57. Patel S, Blaauboer SM, Tucker HR, Mansouri S, Ruiz-Moreno JS, Hamann L, et al. The Common R71H-G230A-R293Q Human TMEM173 Is a Null Allele. *J Immunol* (2017) 198(2):776–87. doi: 10.4049/jimmunol.1601585
58. Gao P, Ascano M, Zillinger T, Wang W, Dai P, Serganov AA, et al. Structure-function analysis of STING activation by c[G(2',5')pA(3',5')p] and targeting by antiviral DMXAA. *Cell* (2013) 154(4):748–62. doi: 10.1016/j.cell.2013.07.023

Conflict of Interest: GP is the chair of a Safety Evaluation Committee for novel investigational vaccine trials being conducted by Merck Research Laboratories. GP offers consultative advice on vaccine development to Merck & Co., Medicago, GlaxoSmithKline, Sanofi Pasteur, Emergent Biosolutions, Dynavax, Genentech, Eli Lilly and Company, Janssen Global Services LLC, Kentucky Bioprocessing, and Genevant Sciences, Inc. GP, RK, and IO hold patents related to vaccinia, influenza, and measles peptide vaccines. GP, RK, and IO have received grant funding from ICW Ventures for preclinical studies on a peptide-based COVID-19 vaccine. RK has received funding from Merck Research Laboratories to study waning immunity to mumps vaccine. These activities and this research have been reviewed by the Mayo Clinic Conflict of Interest Review Board and are conducted in compliance with Mayo Clinic Conflict of Interest policies.

The remaining authors declare that the research was conducted in the absence of any commercial or financial relationships that could be construed as a potential conflict of interest.

frontiers in Immunology

REVIEW
published: 30 November 2020
doi: 10.3389/fimmu.2020.613039

Molecular and Structural Basis of DNA Sensors in Antiviral Innate Immunity

Ayesha Zahid[1,2], *Hazrat Ismail*[3], *Bofeng Li*[1,4*] *and Tengchuan Jin*[1,2,5*]

[1] *Department of Obstetrics and Gynecology, The First Affiliated Hospital of USTC, Division of Life Sciences and Medicine, University of Science and Technology of China, Hefei, China,* [2] *Hefei National Laboratory for Physical Sciences at Microscale, the CAS Key Laboratory of Innate Immunity and Chronic Disease, School of Basic Medical Sciences, Division of Life Sciences and Medicine, University of Science and Technology of China, Hefei, China,* [3] *MOE Key Laboratory for Cellular Dynamics & Anhui Key Laboratory for Chemical Biology, CAS Center for Excellence in Molecular Cell Science, Hefei National Science Center for Physical Sciences at Microscale & University of Science and Technology of China, Hefei, China,* [4] *Department of Medical Oncology, The First Affiliated Hospital of USTC, Division of Life Sciences and Medicine, University of Science and Technology of China, Hefei, China,* [5] *CAS Center for Excellence in Molecular Cell Science, Chinese Academy of Science, Shanghai, China*

OPEN ACCESS

Edited by:
Chunfu Zheng,
Fujian Medical University, China

Reviewed by:
Tsan Sam Xiao,
Case Western Reserve University, United States
Xiaopeng Qi,
Chinese Academy of Sciences, China

***Correspondence:**
Tengchuan Jin
jint@ustc.edu.cn
Bofeng Li
libf@ustc.edu.cn

Specialty section:
This article was submitted to Viral Immunology, a section of the journal Frontiers in Immunology

Received: *01 October 2020*
Accepted: *02 November 2020*
Published: *30 November 2020*

Citation:
Zahid A, Ismail H, Li B and Jin T (2020) Molecular and Structural Basis of DNA Sensors in Antiviral Innate Immunity. Front. Immunol. 11:613039. doi: 10.3389/fimmu.2020.613039

DNA viruses are a source of great morbidity and mortality throughout the world by causing many diseases; thus, we need substantial knowledge regarding viral pathogenesis and the host's antiviral immune responses to devise better preventive and therapeutic strategies. The innate immune system utilizes numerous germ-line encoded receptors called pattern-recognition receptors (PRRs) to detect various pathogen-associated molecular patterns (PAMPs) such as viral nucleic acids, ultimately resulting in antiviral immune responses in the form of proinflammatory cytokines and type I interferons. The immune-stimulatory role of DNA is known for a long time; however, DNA sensing ability of the innate immune system was unraveled only recently. At present, multiple DNA sensors have been proposed, and most of them use STING as a key adaptor protein to exert antiviral immune responses. In this review, we aim to provide molecular and structural underpinnings on endosomal DNA sensor Toll-like receptor 9 (TLR9) and multiple cytosolic DNA sensors including cyclic GMP-AMP synthase (cGAS), interferon-gamma inducible 16 (IFI16), absent in melanoma 2 (AIM2), and DNA-dependent activator of IRFs (DAI) to provide new insights on their signaling mechanisms and physiological relevance. We have also addressed less well-understood DNA sensors such as DEAD-box helicase DDX41, RNA polymerase III (RNA pol III), DNA-dependent protein kinase (DNA-PK), and meiotic recombination 11 homolog A (MRE11). By comprehensive understanding of molecular and structural aspects of DNA-sensing antiviral innate immune signaling pathways, potential new targets for viral and autoimmune diseases can be identified.

Keywords: DNA sensors, pattern-recognition receptors, cyclic GMP-AMP synthase, STING, Toll-like receptor 9, interferon-gamma inducible 16, absent in melanoma 2, RNA polymerase III

INTRODUCTION

Viruses are a threat to humans since ancient times; therefore, many mechanisms exist in the human body to cope with viral infections. A tremendous amount of resources is utilized worldwide to control the spread of viral infections because such infections pose a huge burden to the health sector by resulting in life-threatening diseases. The innate immune system is the body's first line of defense against pathogenic microbes and is essential in conferring antiviral immune responses, which ultimately lead to the pathogen clearance. Numerous innate immune receptors named pattern-recognition receptors (PRRs) are present at the cell surface or within the cells, which are employed by the innate immune defense to detect conserved structural features of the pathogens called pathogen-associated molecular patterns (PAMPs) (1). In the case of viruses, PAMPs include viral genomic material, surface structures such as glycoproteins, capsids, and replication products. Millions of years of evolution have evolved PRRs substantially in three ways: (i) they not only control the infection but also induce cellular senescence (2); (ii) they operate at cellular intrinsic levels and meanwhile are associated with cellular machinery so that a danger signal can be relayed to the local microenvironment when necessary (3, 4); and (iii) they have obtained the capability to detect the presence of non-compartmentalized host nucleic acids (5, 6). Hence, mammalian cells can utilize PPRs to execute a response to the dangerous build-up of endogenous or exogenous nucleic acids. Multiple receptors can recognize a single virus, and one receptor may target different viruses (7). Pathogen-derived nucleic acids as single-stranded (ss) or double-stranded (ds) DNA and RNA serve as the most potent PAMPs that derive antiviral responses that are fundamental for the induction of resulting acquired immunity (8). Over the last decade, several nucleic acid sensors, including members of toll-like receptors (TLRs), RIG-I like receptors (RLRs), NOD-like receptors (NLRs) families, and cyclic GMP-AMP synthase protein families have been identified. Signaling pathways that result in the synthesis of interferons, inflammatory cytokines, and chemokines are triggered by the activation of such receptors and lead to anti-viral inflammatory and cell-mediated immune responses (9–11). Two paradigmatic cytosolic nucleic acid sensing pathways in mammalian cells include the cGAS-STING (cyclic GMP-AMP synthase-stimulator of interferon genes) pathway and RLR-MAVS (RIG-I like receptor-mitochondrial antiviral signaling protein) pathway, which sense cytosolic DNA and RNA respectively (12). **Table 1** lists DNA sensors that detect the nucleic acids of various viruses, bacteria and fungi.

SOURCES OF CYTOTOXIC DNA

The cytosol of eukaryotic cells is deprived of DNA under physiological conditions; nevertheless, multiple factors can contribute to the accumulation of ss or dsDNA in the cytosol, for example, infection by DNA viruses (59), infection by retroviruses which carry out their transcription in the cytosol through the action of viral retro-transcriptase (60), endosomal escape of bacteria (59), activation of regulated cell death (RCD) pathways which results in mitochondrial rupture and consequent release of mitochondrial DNA (mtDNA) into the cytosol (9, 61), reactivation of endogenous retroviral sequences (10), genetic mutations in affecting the activity of the nucleases (12), the formation of micronuclei due to mitotic defects (11, 62, 63), DNA damage following radiation therapy (64) and cytosolic DNA accumulation following phagocytosis, micropinocytosis or uptake of DNA-rich exosomes (65, 66). Hence, there is a continuous risk of cytosolic accumulation of ectopic DNA in both normal and malignant cells, which needs to clear off efficiently to maintain the normal functions of the cells.

DNA SENSORS

DNA sensors are DNA-binding proteins that are component of the innate immune system which are capable of detecting perturbations in DNA homeostasis of the cell and activate the intracellular signaling cascades of the innate immune system as a response (67). DNA sensors can induce a broad range of innate immune responses, and such responses are of particular importance during viral infection when elicitation of type I IFNs is a key immune response that works in a paracrine and autocrine way to confer an anti-viral immunity to the host (4). Type I IFNs, which are induced during the anti-viral immunity, control the viruses in infected cells and restrict their spread to neighboring cells. DNA sensors not only induce type I IFNs but also induce programmed cell death as an innate immune response to the infection. For example, cGAS-STING and TLR9 can induce apoptosis, while IFI16 and AIM2 can induce pyroptosis (68). Although our understanding of the molecular and structural features of DNA sensors has increased significantly over the last few years, however, it is still unclear how various DNA sensing systems are allocated to various locations within the cells and how they cooperate. Differentiating viral and self DNA is very crucial for the host to launch suitable innate responses against viral infections. Based on current knowledge, the signaling specificity of DNA sensors is attributed to various factors such as (i) length, 3D structure and sequence of cytotoxic DNA (8, 69, 70); (ii) subcellular localization of DNA molecules (71); (iii) methylation status of DNA (68) and (iv) association of histones and non-histone chromatin-binding proteins with cytotoxic DNA molecules (8, 71). How the actual source of cytotoxic DNA and each of the factors mentioned above impact the activity of various DNA sensors yet remain to be fully explored.

There exist two broad categories of innate immune DNA sensors based on their expression pattern and subcellular localization. The first category comprises endosomal DNA sensors, such as members of the TLR family. Located in the endosomal membrane of many immune cells such as macrophages, dendritic cells (DCs), and B cells, these TLRs monitor the lumen of lysosomes and endosomes for the

TABLE 1 | A list of DNA sensors which detect the nucleic acids of various viruses, bacteria and fungi.

Pathogen	Genome	Family	Primary host (s)	DNA Sensor(s)	References
Herpes simplex virus (HSV)	dsDNA	Herpesviridae	Human	TLR9, RNA pol III, IFI16, DAI, DHX9, DHX36, DDX41, MRE-11, cGAS	(13–23)
Varicella zoster virus (VZV)	dsDNA	Herpesviridae	Human	TLR9, RNA pol III	(24, 25)
Human cytomegalovirus (HCMV)	dsDNA	Herpesviridae	Human	TLR9, DAI, cGAS	(15, 26, 27)
Murine cytomegalovirus (MCMV)	dsDNA	Herpesviridae	Mouse	AIM2	(28)
Epstein-Barr virus (EBV)	dsDNA	Herpesviridae	Human	TLR9, RNA pol III, cGAS, IFI16	(16, 29–31)
Vaccinia virus (VV)	dsDNA	Poxviridae	Unknown	TLR9, AIM2, DNA-PK, cGAS	(15, 28, 32, 33)
Kaposi's sarcoma-associated herpesvirus (KSHV)	dsDNA	Herpesviridae	Human	TLR9, IFI16, cGAS	(17, 32, 34)
Adenovirus (AdV)	dsDNA	Adenoviridae	Unknown	TLR9, DDX41, cGAS	(15, 18, 35)
Human papilloma virus (HPV)	dsDNA	Herpesviridae	Human	TLR9, cGAS	(15, 36)
Murine gammaherpesvirus 68 (MHV68)	dsDNA	Herpesviridae	Rodent	cGAS	(15)
Ectromelia virus (ECTV)	dsDNA	Poxviridae	Mouse	TLR9	(37)
Human immunodeficiency virus (HIV)	ssRNA	Retroviridae	Human	cGAS, TLR9	(38, 39)
Simian immunodeficiency virus (SIV)	ssRNA	Retroviridae	Non-human primates	cGAS	(39)
Murine leukemia virus (MLV)	ssRNA	Retroviridae	Mouse	cGAS	(39)
West Nile virus (WNV)	ssRNA	Flaviviridae	Human	cGAS	(40)
Dengue virus (DENV)	ssRNA	Flaviviridae	Human	cGAS	(40)
Vesicular stomatitis virus (VSV)	ssRNA	Rhabdoviridae	Cattle, horses, and swine	cGAS, DHX60	(41, 42)
Influenza A virus	dsRNA	Orthomyxoviridae	Birds and mammals	DHX36, DHX9	(43, 44)
Neisseria meningitidis	DNA	Neisseriaceae	Humans	TLR9	(45)
Mycobacterium tuberculosis	DNA	Mycobacteriaceae	Humans	TLR9, AIM2, cGAS	(46–48)
Francisella tularensis	DNA	Francisellaceae	Mammals, birds, amphibians and fish	AIM2	(49)
Francisella novicida	DNA	Francisellaceae	Humans	cGAS, p204	(50)
Streptococcus pneumoniae	DNA	Streptococcaceae	Humans	AIM2, cGAS	(51, 52)
Listeria monocytogenes	DNA	Listeriaceae	Humans and ruminants, etc.	AIM2, IFI16, cGAS	(28, 53)
Mycobacterium bovis	DNA	Mycobacteriaceae	Mammals	p204	(54)
Staphylococcus aureus	DNA	Staphylococcaceae	Humans, dogs, cats, cows and chickens	p204, AIM2	(55, 56)
Aspergillus fumigatus	DNA	Trichocomaceae	Humans	AIM2, TLR9	(57, 58)

AIM2, Absent in melanoma 2; cGAS, cyclic GMP-AMP synthase; DAI, DNA-dependent activator of IRFs; DDX41, DEAD (Asp-Glu-Ala-Asp) box polypeptide 41; DHX9, DEAD/H (Asp-Glu-Ala-Asp/His) box polypeptide 9; DHX36, DEAD/H (Asp-Glu-Ala-Asp/His) box polypeptide 36; DHX60, DEAD/H (Asp-Glu-Ala-Asp/His) box polypeptide 60; IFI16, IFN-gamma-inducible protein 16; DNA-PK, DNA-dependent protein kinase; RNA pol III, RNA polymerase III; MRE-11, meiotic recombination 11 homolog A; TLR9, Toll-like receptor 9.

presence of cytotoxic DNA, e.g., bacterial and viral DNA. The second category accounts for the cytosolic DNA sensors that detect cytoplasmic nucleic acids in virtually all types of cells. **Figure 1** depicts the signaling cascades and resultant immune responses which are triggered by various DNA sensor.

ENDOSOMAL DNA SENSORS

TLR DNA Sensors

Members of the TLR family have the propensity to detect a range of microbial products such as DNA, RNA, and microbial surface molecules. TLRs are type I transmembrane receptors, and they harbor extracellular leucine-rich repeats (LRRs), a transmembrane domain, and a Toll/IL-1 receptor (TIR) domain, which can transduce signals to downstream adaptor molecules such as TIR-domain-containing adapter-inducing interferon-β (TRIF) and myeloid differentiation primary response gene 88 (MyD88) which bring about NF-κB activation. In humans, 10 members of TLRs have been identified, of which five members TLR3, TLR7, TLR8, TLR9, and TLR13 are involved in recognition of pathogenic nucleic acids. These receptors function by utilizing two signaling pathways: TLR7, TLR8, TLR9, and TLR13 mediate the activation of MyD88, while TLR3 activates TRIF (72–74). At present, TLR3, TLR7, TLR8, and TLR9 have been structurally characterized.

TLR9

TLR9 is the only known endosomal localized DNA sensor and was the first reported PPR to detect DNA (68). TLR9 is highly expressed in both plasmacytoid dendritic cells (pDCs) and B cells, and senses un-methylated cytosine–phosphate–guanosine (CpG) motif-containing DNA of viral and bacterial genomes (68, 75, 76) and results in the induction of IFN-α, IFN-λ, many chemokines and cytokines (13, 77–79). The CpG motifs in mammals are methylated at the cytosine base (80), while the bacterial and viral CpG sites are un-methylated; therefore, TLR9 can distinguish between self and non-self to prevent unwanted immune reactivity (81). TLR9 has been reported to detect the DNA of herpes simplex viruses 1 and 2 (HSV-1 and HSV-2), herpes papillomavirus (HPV), varicella-zoster virus (VZV),

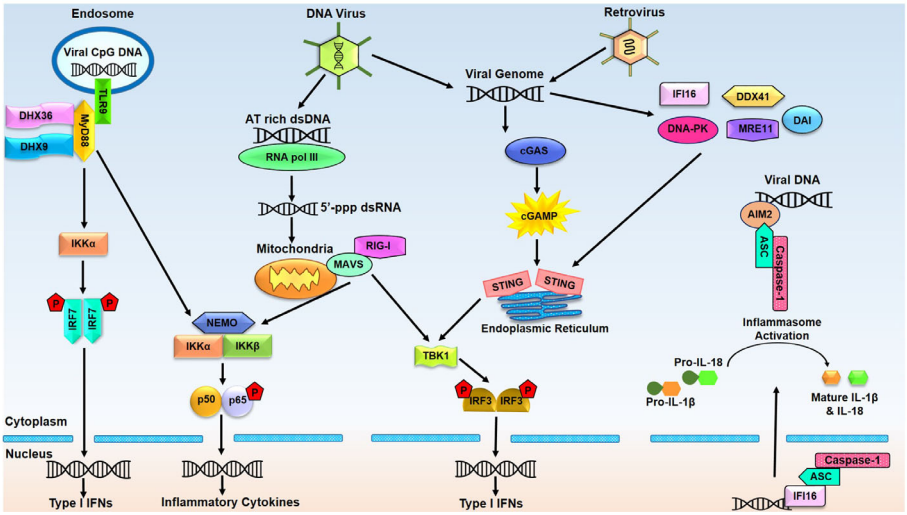

FIGURE 1 | Endosomal and cytosolic DNA sensors and their related signaling pathways. Endosomal DNA sensor TLR9 recognizes the CpG DNA of viral origin and recruits MyD88 leading to activated IRF7 and NF-κB, which mediate induction of type I interferons (IFNs) and inflammatory cytokines. RNA pol III transcribes AT-rich double-stranded DNA (dsDNA) into 5'-triphosphate double-stranded RNA (5'-ppp-dsRNA), leading to the activation of the RIG-I-MAVS signaling pathway. Viral or bacterial DNA can also be detected by cGAS and other putative DNA sensors, all reported to activate the endoplasmic reticulum residing adaptor protein STING. STING travels from the endoplasmic reticulum to the Golgi complex for TBK1-IRF3 and NF-κB activation, triggering the production of type I IFN and inflammatory cytokines. AIM2 and IFI16 detect the viral DNA and respond by forming inflammasome by recruiting ASC and caspase-1 in the cytoplasm and nucleus. Active inflammasome leads to proteolytic cleavage of pro-IL-β and pro-IL-18 to produce mature cytokines. (AIM2, absent in melanoma 2; cGAMP, cyclic GMP-AMP; cGAS, cyclic GMP-AMP synthase; DAI, DNA-dependent activator of IRFs; DDX41, DEAD-box polypeptide 41; DHX9, DEAH-Box Helicase 9; DHX36, DEAH-Box Helicase 36; DNA-PK, DNA-dependent protein kinase; ER, endoplasmic reticulum; IFI16, interferon gamma-inducible protein 16; IFN, interferon; IRF3, Interferon regulatory factor 3; IRF7, Interferon regulatory factor 7; IL-1β, Interleukin-1β; IL-18, Interleukin-18; MAVS, Mitochondrial antiviral-signaling protein; MRE11, meiotic recombination 11 homolog A; NF-κB, Nuclear factor-κB; NEMO, NF-kappa-B essential modulator; RIG-I, Retinoic acid-inducible gene I; STING, Stimulator of interferon genes; TBK-1, TANK-binding kinase 1).

Merkel cell polyomavirus, cytomegalovirus (CMV), Kaposi's sarcoma-associated herpesvirus (KSHV), ectromelia virus (ECTV) and Epstein-Barr virus (EBV) (29, 32, 33, 36, 37, 82). Additionally, a role for TLR9 in the detection of HIV has also been suggested (38).

In unstimulated pDCs, TLR9 is found associated with the endoplasmic reticulum (ER) in its inactive form. Upon the presence of CpG DNA, TLR9 is trafficked to the lysosomes by the action of 12-membrane-spanning ER protein UNC93B, which interacts with TLR9 directly (83). In endolysosomal compartments, the proteolytic cleavage of TLR9 in response to the presence of CpG DNA converts it into active processed form (84). Clathrin-dependent endocytic pathways internalize CpG DNA, which is then translocated to the lysosomes, interacting with active TLR9. It is still ambiguous how TLR9 is triggered to translocate from ER to CpG containing lysosomes. After recognizing CpG DNA, TLR9 interacts with its adaptor protein MyD88, which contains a death domain and a TIR domain (85). MyD88 further interacts with IL-1R associated kinase 1 (IRAK-1), IRAK-4, and IRF-7, which subsequently induces TNF receptor-associated factor 3 (TRAF3) and TRAF6 recruitment, activating the transforming growth factor β-activated kinase 1 (TAK1), mitogen-activated protein kinase (MAPK), and NF-κB ultimately inducing the inflammatory cytokines (85).

Like other TLRs, TLR9 also contains an extracellular LRR domain carrying out ligand recognition, a transmembrane domain, and a cytoplasmic TIR domain that interacts with adaptor proteins and initiates downstream signaling cascades. TLR9 contains 26 LRRs arranged in a ring-shaped structure maintained by multiple interactions (86). A long inserted loop called Z-loop containing about 40 amino acid residues is present in TLR9, whose proteolytic cleavage in endolysosomes is reported to be necessary for the generation of mature functional TLR9. This cleavage also prevents undesired activation of the receptor by the cellular DNA (87). At present, three types of crystal structures of TLR9 are available: unliganded TLR9, CpG-DNA bound TLR9, and inhibitory DNA (iDNA) bound TLR9 (86). These structures have conferred crucial information on the functional mechanism and signaling activities of TLR9. Based on these structures, the activation mechanism of TLR9 has been proposed, which describes that inactive TLR9 is present as a monomer and it dimerizes upon ligand binding to attain an active "m" shaped structure, in which two TLR9 protomers closely position their C-terminal regions as shown in **Figure 2A**. The dimerization of LRR domain regions also induces TIR domain dimerization, which leads to the resultant recruitment of adaptor proteins. The unliganded TLR9 is present in a ring-shaped monomeric form in both

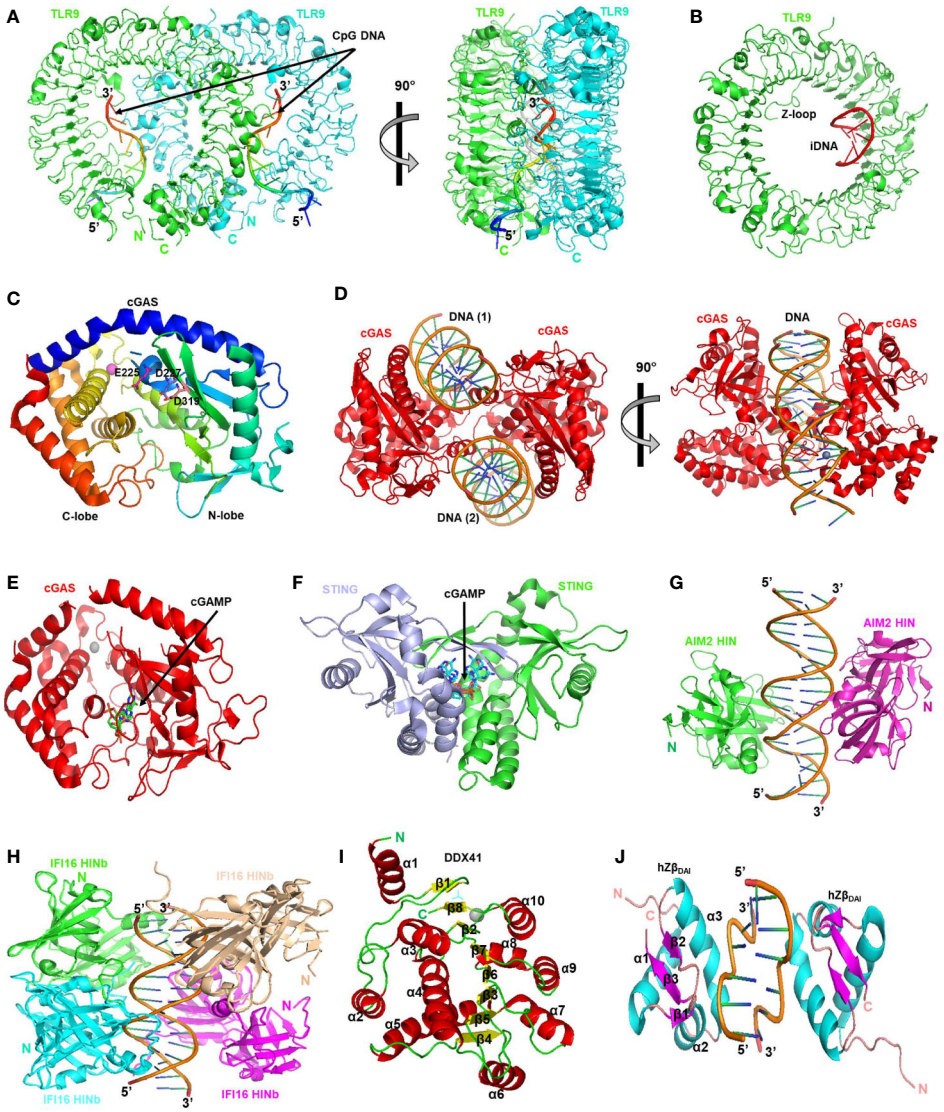

FIGURE 2 | The structures of endosomal and cytosolic DNA sensors. **(A)** TLR9/CpG DNA complex. CpG DNA binding induces the dimerization of TLR9. Two TLR9 molecules are shown in green and cyan colors (PDB code 3WPC) **(B)** TLR9/iDNA complex. iDNA shown in red color forms a stem-loop structure that occupies the interior of ring-shaped TLR9 shown in green color (PDB code 3WPD). **(C)** The overall structure of apo-form of human cGAS. The catalytic residues are shown in the sticks (PDB code 4MKP). **(D)** The structure of human cGAS catalytic domain bound to 18 bp dsDNA. DNA binds to two distinct positively charged surfaces of cGAS, inducing dimerization and conformational rearrangement of cGAS active site (PDB code 4O6A). **(E)** The overall structure of cGAS in complex with 2'3'-cGAMP (PDB code 6MJX). **(F)** The structure of STING bound with cGAMP which is shown as sticks (PDB Code 5CFP). **(G)** The structure of the AIM2 HIN : DNA. HIN domains are represented as green- and magenta-colored ribbons with DNA positioned between them (PDB code 3RN2). **(H)** The structure of the IFI16 HINb: DNA complex is shown as green, cyan, wheat, and magenta ribbons for each HINb domain and orange ribbon for the dsDNA (PDB code 3RNU). **(I)** A ribbon representation of the DEAD domain of DDX41 with secondary structural elements labeled. Helix, sheet, and loop are colored in red, yellow, and green, respectively (PDB code 5H1Y). **(J)** The overall structure of the $hZ\beta_{DAI}$/Z-DNA complex. The protein and DNA are drawn as a ribbon diagram. The N and C termini, the secondary structure elements of $hZ\beta_{DAI}$, and 5′ and 3′ of DNA are labeled. Helix, sheet, and loop are colored in cyan, magenta, and light pink, respectively (PDB code 3EYI). All the images in the figure were drawn by PyMOL molecular graphics system (v1.7.4.0) by using the mentioned PDB IDs which were obtained from Protein Data Bank (https://www.rcsb.org/).

solution and crystal and manifests the inactive form of TLR9 (88). It has been validated through ultracentrifugation, and gel-filtration analysis that cleaved TLR9 dimerizes upon CpG DNA binding (86). Although TLR9 having intact Z-loop has also been shown to bind with CpG DNA, but this binding does not induce dimerization of TLR9; therefore, Z-loop processing, if not necessary for binding with DNA, is essential for mediating the CpG-DNA-induced dimerization of TLR9 (86). In ligand-bound TLR9, a 2:2 complex of TLR9 and CpG-DNA is formed in which CpG-DNA is wedged between the two TLR9 protomers and

stabilizes the structure as shown in **Figure 2A**. In this structure, two C-terminals of TLR9 dimer are located at a proximity of approximately 30 Å from each other. The CpG binding groove formed by the LRR-NT, LLR1, and LLR2 is located at the N-terminus of interface 1 of TLR9, and multiple interactions are formed between cytosine and guanosine of CpG motif and TLR9 in the binding groove. The flanking regions of CpG dinucleotide also contribute the binding, interface 2 of TLR9 involves in recognizing the phosphate backbone of the CpG DNA, and histidine residues in interface 2 establish electrostatic interactions with phosphate groups present in the DNA backbone (86). The binding of TLR9 to CpG DNA is pH-dependent (89), and under acidic conditions, the binding affinity is stronger (86). The crystal structure of the TLR9-iDNA complex depicts that iDNA is present as a stem-loop structure formed through intramolecular base pairing, and it engages the interior of the TLR9 ring structure (**Figure 2B**), and in contrast to the TLR9–CpG–DNA complex, which exhibits 2:2 stoichiometry, TLR9-iDNA is a monomer (86).

DNA SENSORS IN THE CYTOSOL

After endocytosis, many DNA viruses pass through the cytoplasm to reach the nucleus where they release their genomic material. Viral capsid protects the DNA genomes and is not discarded until the viral DNA is injected into the nucleus; therefore, it is worthy of questioning how DNA sensors in the cytosol detect viral DNA under physiological conditions. This question is easier to answer for viruses like smallpox, which replicates in the cytoplasm (90), and polyomavirus simian virus 40, whose capsid is dissembled in the ER and its genomic DNA is released into the cytoplasm (91). Hence, such viruses can trigger the DNA sensing pathways in the cytosol. Nonetheless, many viruses such as herpesviruses expose their DNA only in the nucleus; therefore, there must exist some mechanisms that leak their DNA into the cytoplasm. One explanation for herpesviruses DNA is that it can be sourced from the defective virion particles in the cytoplasm and is ultimately detected by the cytosolic DNA sensors. In HCMV and HSV-1, ubiquitination can label the capsid for proteasomal degradation in the macrophages, leading to the release of their DNA into the cytoplasm (14). Cellular stress-dependent leakage of mtDNA can also occur in the case of herpesviruses, which can lead to the activation of the cGAS-STING pathway (92).

Unlike endosomal sensors for viral sensing, which are limited to TLRs, cytosolic DNA sensors present an array of different PRRs that sense viral nucleic acids and lead to the production of either type I interferons/inflammatory cytokines or caspase 1-dependent secretion of IL-1β. Since type I IFN production is the major anti-viral defense strategy employed by the host, it is the main outcome of DNA sensing in the cytosol. Multiple cytosolic DNA receptors have been identified through intensive investigation of past years such as DAI, RNA polymerase III, cGAS, AIM2, and IFI16, which results in type I IFN production by converging at a common pathway, STING-pathway (59). STING is a transmembrane protein expressed by the outer mitochondrial membrane and ER, and it relocalizes with TANK-binding kinase 1 (TBK1), which executes phosphorylation activation of IRF3 and IRF7 (59, 93). The STING-TBK1 axis is pivotal for driving interferon responses and host resistance against DNA viral infections (59). In the next section, we will discuss major anti-viral cytosolic DNA sensors.

cGAS-STING Pathway

Cyclic GMP-AMP synthase (cGAS) is a DNA-sensing nucleotidyl transferase enzyme that is a member of the nucleotidyltransferase (NTase) family and functions as a cytosolic DNA sensor (41, 94). cGAS is known to recognize various viruses such as DNA viruses, including vaccinia virus, HSV1 and HSV2, cytomegalovirus, adenoviruses, human papillomavirus, and murine gammaherpesvirus 68, which are counteracted by type I IFNs through cGAS–STING pathway (15). Retroviruses such as murine leukemia virus, simian immunodeficiency virus (SIV), human immunodeficiency virus (HIV), West Nile virus, vesicular stomatitis virus (VSV), and Dengue virus have also been reported to be detected by cGAS (40, 41). Besides, it can also sense Gram-positive and Gram-negative bacteria. It is activated by direct binding with DNA, and this binding induces liquid–liquid phase separation to produce liquid droplets acting as a microreactor where the concentration of cGAS is enhanced to increase the synthesis of cyclic GMP-AMP (cGAMP) utilizing ATP and GTP (94, 95). cGAMP has unique mixed phosphodiester linkages between the 2′-hydroxyl group of GMP and the 5′-phosphate of AMP, and also between the 3′-hydroxyl group of AMP and the 5′-phosphate of GMP, forming a unique 2′3′-cGAMP isomer (96, 97). cGAMP's binding to STING yields dimers, tetramers, and higher-order oligomers of STING (98) and activates the STING to produce type I IFNs and NF-κB-dependent proinflammatory cytokines (94).

cGAS can be activated by both self and foreign DNA to induce conformational changes in its structure that are necessary for its enzymatic activity. It can bind to DNA of ~20 bp, but longer dsDNAs of >45 bp result in a ladder-like structure of cGAS dimers, which are more stable and have stronger enzymatic activity (99, 100). The binding affinity of cGAS to dsDNA and ssDNA is *K*d ~87.6 nM and *K*d ~1.5 μM, respectively (101). Many groups have solved the structure of cGAS alone or DNA-bound cGAS (99–104) (**Figures 2C-E**), which provides significant insights about mechanistic aspects of cGAS activation by DNA binding and its enzymatic activity. A substantial conformational change is observed in cGAS upon DNA binding, which induces dimerization and makes its catalytic pocket accessible. The catalytic domain of cGAS possesses a two-lobed structure in which N-lobe exhibits canonical NTase fold while a tight five-helix bundle is present at C-lobe. A deep groove between these two lobes contains the active site, which has three catalytic residues, glutamate 225, aspartate 227, and aspartate 319, crucial for the enzymatic activity of cGAS because their mutations have been shown to abrogate enzymatic activity (99). The C-terminal region of cGAS

contains a conserved zinc ribbon domain, essential for its activity (101, 102). In cGAS dimer, hydrogen bonding between the residues of the zinc-binding loop joins the two molecules of cGAS. cGAS is inactive before DNA binding since its active site presents a scrambled structure, and the NTase domain is destabilized (99). The structure of porcine and mouse cGAS: dsDNA complexes (102, 103) shows that cGAS and dsDNA bind with a 1:1 stoichiometry, and interaction occurs *via* the single binding site. However, two other studies have reported that a 2:2 complex in which each cGAS molecule binds to two dsDNA molecules *via* two binding sites (**Figure 2D**), one of which is the same as reported by previous studies (102, 103), while one binding site is new (99, 100). Both DNA binding sites contain multiple positively charged residues and have shape and charge complementarity with dsDNA (99). After activation of cGAS, a two-step catalytic reaction mediates the formation of cGAMP, and an intermediate pppGpA is formed, and then cyclization of this intermediate yields cGAMP (103). When cGAMP binds with STING, it leads to a conformational change by which two wings of STING are brought to each other in juxtaposition, and the ligand is buried deep in the binding pocket (**Figure 2F**). The binding pocket shows a top lid consists of four antiparallel β-sheet strands, which confer a close confirmation to the structure. A rotation of 180° is observed in ligand-binding pocket upon cGAMP and STING binding, which results from side-by-side packing of STING dimers yielding STING oligomers (105).

Presence of cGAS in the nucleus has been reported by multiple studies (106–108) however, recently it is proposed that tight tethering of chromatin to the cGAS suppresses autoreactivity to self-DNA in the nucleus. The structure of the cGAS catalytic domain bound to a nucleosome has been resolved by many groups, which reveals that cGAS inhibition in the nucleus is mediated by interaction through histone 2A–2B but not through nucleosomal DNA binding. The interaction between cGAS and histone embeds the cGAS DNA-binding site B, and prevents the formation of active cGAS dimers (108–110). Kujirai et al. has reported a cryo-electron microscopy structure with two cGAS molecules bridging two nucleosome core particle (NCP). This configuration shows that all three known cGAS DNA binding sites that are required for cGAS activation become inaccessible, and cGAS dimerization is also inhibited (111). Another structure by Boyer et al. reported the structure of cGAS bound to a single nucleosome. This binding sterically abrogates cGAS oligomerization required to yield functionally active 2:2 cGAS–dsDNA complex (112). These recent findings have provided important information that how cGAS is maintained in an inhibited state in the nucleus.

STING contains four transmembrane helices (TM1–TM4), one folded soluble domain previously assigned as TM5, and a large cytosolic domain (amino acids 173–379) (113, 114). STING is kept in the ER through its binding to Ca^{2+} sensor stromal interaction molecule 1 (STIM1) (115); however, it's binding to cGAMP mediates its trafficking from ER to ER–Golgi intermediate compartment (ERGIC) and the Golgi apparatus by the action of cytoplasmic coat protein complex II (COPII) and ADP-ribosylation factor (ARF) GTPases (116). The palmitoylation of STING takes place in the Golgi apparatus, which is crucial for its activation (117). After translocation to the Golgi apparatus, STING binds with TBK1, which phosphorylates the C-terminal tail region of STING, a docking site for IRF3. TBK1 also phosphorylates IRF3 inducing its activation (104) and activated IRF3 dimerizes and translocate to the nucleus to regulate the transcription of interferon-β (IFNβ) (118), which activates heterodimeric receptor complex comprising IFNα receptor 1 (IFNAR1) and IFNAR2, which further activates the Janus kinase (JAK)-signal transducer and activator of transcription (STAT) signaling pathway to incite the transcription of several ISGs whose protein products ultimately block viral replication, assembly, and release (119). Downstream of the cGAS-STING pathway, programmed cell death, mainly apoptosis, can be activated. Furthermore, the cGAS-STING pathway can induce necroptosis, as well (120).

STING as DNA Sensor

STING has been demonstrated to bind DNA directly, but we still need to fully disclose the physiological relevance of DNA binding by STING (121). A study has reported that amino acids 181–379 in the C-terminal of STING could bind the dsDNA without any stipulation from other proteins; nonetheless, STING bound to dsDNA with only *K*d ∼200–300 μM affinity, which is significantly lower than the binding affinity of the cGAS to DNA (*K*d ∼88 nM). Furthermore, ectopic expression of STING in HEK293T cells, which are deprived of endogenous STING, did not produce IFNβ in response to dsDNA, suggesting that STING cannot execute DNA sensing in cells (94, 122). Therefore, future studies are needed to verify if STING can act as a DNA sensor.

STING polymorphism is suggested to be involved in the pathogenesis of Coronavirus disease 2019 (COVID-19). No data is currently available to demine if COVID-19 alters STING activation during early infection; however, during the second phase of infection, an excessive amount of damaged host DNA activates the STING, which ultimately causes cytokine storm, a characteristic feature of COVID-19 (123).

PYHIN Family Members

PYHIN protein family (pyrin and HIN200 domain-containing proteins, also known as p200 or HIN200 proteins) have been associated with recognizing both microbial and self DNA, resulting in a wide range of innate immune responses. The characteristic features of most family members are the presence of pyrin domain (PYD) at N-terminal capable of mediating protein-protein interactions and one or two C-terminal HIN200 domains, which carry out DNA binding (124). The human genome has been reported to encode 4 PYHIN proteins (124), out of which two proteins, absent in melanoma 2 (AIM2) and IFN-γ inducible 16 (IFI16), are known DNA sensors and have the propensity to execute DNA-induced innate immune responses (16, 125, 126). Structures of PYHIN proteins coordinate with their proposed role as DNA PRRs, and members AIM2, IFI16, and murine protein p204 are now designated to a new family of PRRs termed as AIM2-like receptors (ALRs) (127).

AIM2

AIM2 is mainly expressed in intestinal epithelial cells, keratinocytes, and monocytic lineage (126, 128) and can detect DNA from diverse sources such as self-DNA, bacterial and viral DNA (125, 129, 130). AIM2 is reported to detect vaccinia virus and mouse cytomegalovirus (28). AIM2 contains an N-terminal PYD domain, C-terminal HIN200 domain, which is positively charged and binds with negatively charged DNA. DNA sensing by AIM2 results in the assembly of inflammasome, which is a supramolecular multi-protein complex. The PYD domain of AIM2 establishes interaction with the PYD domain of the adaptor protein of inflammasome known as an apoptosis-associated speck-like protein containing a carboxy-terminal CARD (ASC), while the CARD domain of ASC associates with the CARD domain of pro-caspase-1, leading to the assembly of activated AIM2 inflammasome (126). The autocatalytic cleavage of pro-caspase-1 generates caspase-1, which converts pro-IL-18 and pro-IL-1β into their active forms, which, in turn, mediate downstream inflammatory responses and pyroptosis. AIM2 inflammasome is also known to induce apoptosis (131). AIM2 inflammasome is entirely indispensable for type I IFNs production in response to dsDNA (132, 133), while it is essential to produce active caspase-1 to induce inflammatory responses. This fact underscores that cells use different mechanisms to execute innate immune responses against cytotoxic DNA. Currently, two structures of $AIM2^{PYD}$ are available, one harbors an N-terminal MBP tag, while the other contains surface mutations and these structures reveal that $AIM2^{PYD}$ adopts a six helical bundle shape, which is a characteristic feature of the death domain superfamily (134, 135). It has been proposed that $AIM2^{PYD}$ domain is sequestered by the $AIM2^{HIN}$ domain through intramolecular interactions during the resting state of AIM2; however, upon dsDNA binding, $AIM2^{PYD}$ is displaced from the association of $AIM2^{HIN}$ so that it can interact with PYD domain of ASC (134). However, a later study by Sohn and colleagues reported that acid patch mutant of $AIM2^{PYD}$, which had impaired binding with $AIM2^{HIN}$, also presented loose binding between dsDNA and $AIM2^{HIN}$, thus, ruling out the previously described inhibitory role of $AIM2^{PYD}$.

Furthermore, after reaching a certain threshold concentration, full-length AIM2 was able to self-associate with DNA; therefore, DNA serves as a one-dimension ruler upon which AIM2 clusters itself and increases its local concentration (136). The structure of DNA-bound $AIM2^{HIN}$ domains (**Figure 2G**) reveals that the molecular basis of DNA sensing by AIM2 is sequence-independent because all the interactions of $AIM2^{HIN}$ take place with the phosphate backbone of the dsDNA, not with the individual DNA basis (137). In X-ray crystallographic structure, both strands of B-form DNA are bound by the HIN domain through electrostatic interactions between arginine and lysine of HIN, and sugar and phosphate groups of DNA backbone (134, 137) (**Figure 2G**).

Full activation of AIM2 in cells requires ~80 bp of dsDNA, while isolated $AIM2^{HIN}$ associates with 20-bp dsDNA of ~30 nM affinity, although the footprint of one $AIM2^{HIN}$ is 8–9 bp (137). Even when DNA is present in excess amount, $AIM2^{HIN}$ and $AIM2^{FL}$ both clustered upon the same DNA molecule (136, 138). $AIM2^{PYD}$ does not bind with DNA, but it is involved in the clustering of $AIM2^{HIN}$ on DNA molecules. Moreover, the weak interactions among $AIM2^{HIN}$ protamers also contribute to DNA clustering because mutating the residues involved in HIN: HIN interactions in $AIM2^{HIN}$ and $AIM2^{FL}$ also diminished their cooperative binding with dsDNA (136). Cryo-EM structure has revealed that binding of multiple AIM2 molecules on the same DNA enhances the local concentration of $AIM2^{PYD}$, which then interacts with each other to produce long helical filaments with the core filament being a right-handed one-start hollow filament having an inner diameter of ~20 Å and an outer diameter of ~90 Å (138). ASC^{PYD} subunits assemble to form filaments using AIM2 as a nucleating platform, and it has been demonstrated that $AIM2^{FL}$ + dsDNA and $AIM2^{PYD}$ both promoted the filament formation by ASC^{PYD} subunits (139). Negative stain EM spectra and crystal structure both have reported similarities in subunit organization and diameter of $AIM2^{PYD}$ and ASC^{PYD} (136, 139).

IFI16

The first cytosolic DNA sensor to be reported was IFN γ-inducible protein 16 (IFI16), which induces innate immune responses against ss and ds intracellular cytotoxic DNA (16, 140). It has been reported to sense the DNA of many viruses such as herpesviruses (17, 141), Kaposi's sarcoma herpesvirus (KSHV), cytomegalovirus, and Epstein–Barr virus to mediate STING-dependent IFN-β responses (14, 16, 34). Located predominantly in the nucleus and in small fractions in the cytoplasm, IFI16 can function to activate both type I IFN responses and functional ASC- and CASP1-containing inflammasome (17, 142). For example, during KSHV infection, after recognizing the viral dsDNA, IFI16 forms the AIM2-independent inflammasome complex, which is then transported to the cytoplasm (17); however, details of inflammasome formation by IFI16 are still not fully clear. Furthermore, during HIV infection, IFI16 mediates caspase-1 activation resulting in pyroptosis (143). In contrast, HSV-1 infection leads to IFI16-STING mediated production of IFNβ (16). In macrophages and keratinocytes, IFI16 has been indicated to activate the catalytic activity of cGAS in addition to employing the effectors of STING (144).

The murine PYHIN protein p204 is an orthologue of IFI16 and was crucial for HSV-1 and DNA-induced activation of transcription factor and expression of IFNβ in a macrophage cell line of the mouse (16). It comprises two HIN domains named as HINa and HINb, and contains N-terminal PYD domain that can establish homotypic interactions with other PYD-containing proteins to form higher complexes (145). Due to similarity in domains structure, p204 is suggested to perform similar functions as IFI16, however, further evidience is required to fully establish its role.

IFI16 contains one N-terminal PYD domain, and two tandem HIN200 domains termed as HINa and HINb. The nature of the PYD domain of IFI16 differs from AIM2; thus, it may use a

different mechanism for inflammasome assembly as compared to AIM2. The crystal structure of the HIN domain revealed two interlinked oligonucleotide/oligosaccharide binding (OB) fold domains (146, 147). The structure of both DNA-bound HINa and DNA-bound HINb is available now (137, 148) (**Figure 2H**) which revealed that IFI16 binds to dsDNA in a cooperative and length-dependent manner (142, 149), and scans the dsDNA in one-dimension utilizing its HIN domains (142). HIN domains of IFI16 bind with both ss and dsDNA mainly through electrostatic interactions (16) with the same affinity because dsDNA is recognized as two single strands by HIN domains (148). Although both HINa and HINb can bind to the DNA, they have different affinities for DNA binding (16), and have different DNA binding surfaces (148).

The HIN domains of IFI16 have been proposed to use two distinct modes of DNA binding. The first mode represents AIM2-like DNA binding, in which the linker joining the two OB folds is used as a tether to bind to DNA (137), while the second mode is like p202 HINa binding to DNA in which loops from OB1 and OB2 folds are utilized for DNA binding (150). It has also been suggested that these two distinct modes of DNA binding mediate different immune responses. IFI16 is also implicated to participate in DNA damage response pathways (17); therefore, it is also possible that it can bind with nicks, gaps, and ends of damaged DNA resulting in the initiation of immune responses. Evidence for this feature comes from the ability of the HIN1 domain to recognize different DNA topologies (148). For most of the *in vitro* tested DNA, HINa domain can form complex with DNA relatively faster than HINb, while HINb binds GC-rich DNA more tightly than HINa. One domain of HINb interacts with both strands of DNA, while one domain of HINa binds only one strand of DNA (148). As stated previously, the PYD domain of IFI16 is different from PYD domains of other PYHIN family members; therefore, we need future studies to elucidate the exact mechanism that how the PYD domain of IFI16 interacts with STING to mediate IFN production.

DExD/H-Box Helicase Family Members (DHX9, DHX36, DDX41, DDX60)

DExD/H-Box helicase family has many RNA and DNA helicases involved in DNA-mediated production of type I IFNs. Two subgroups are present in this family, which are the DEAH-box helicases (DHX) and the DEAD-box helicases (DDX) (18, 19). DEAD/H (Asp-Glu-Ala-Asp/His) box polypeptide 9 (DHX9) and DHX36 are involved in the sensing of dsRNA in myeloid DCs and CpG-rich DNA in human pDCs. DHX9 regulates TNF-α expression and induces the activation of NF-κB through MyD88 in human pDCs, whereas DHX36 induces the production of IFN-α and IRF7 activation through MyD88 (19). DDX60 can sense both dsRNA and dsDNA and mediates the expression of CXCL10 and IFN-β. It also augments signals from RIG-I and MDA5 (42).

DDX41

DEAD (Asp-Glu-Ala-Asp) box polypeptide 41 (DDX41) is a cytoplasmic DNA sensor and has been reported to detect the DNA of HSV-1 and adenovirus in myeloid DC and murine bone marrow-derived DC. It can induce type I IFN response through STING-TBK1 signaling after sensing DNA through its DEAD domain. Upon limiting the basal expression of IFI16 *in vitro*, DDX41 served as the initial cytoplasmic DNA sensor and induced the IFN expression; thus, it can be deduced that the expression pattern of different DNA sensors may define their innate response pattern (18).

DDX41 comprises a disordered N-terminal region, a helicase domain, and a DEAD domain. These two domains are conserved among the DEAD-box family members, and they contain multiple conserved motifs, e.g., motif I and Q motif, which are crucial for ATP binding (151). The currently available crystal structure of DDX41 is based on truncated hDDX4 protein and reveals α/β fold found in other DEAD-box family proteins. There are ten α-helices (α1–α10) and a β-sheet organized by eight β-strands (β1–β8) in the overall structure (**Figure 2I**). Helices α1-α5 are present on one side of the β-sheet, whereas helices α6–α10 are positioned on the other side (152). The DEAD domain's crystal structure contains motif Q, P-loop, motif Ia, motif Ib motif II, and motif III positioned at either β-strand-loop or helix loop transitions. Nucleotide-binding is associated with the P-loop (152). Binding with the dsDNA facilitates the interaction of DDX41 with STING, which ultimately induces type I IFN production (148). The dsDNA-bound DEAD domain's docking model suggested that the DNA-binding site involves arginine 267, lysine 304, tyrosine 364, and lysine 381 present at the C-terminal region (151).

Although DDX41 is reported as a DNA sensor by multiple studies, some studies have also reported that RNAi induced depletion of DDX41 resulted in little effect on the induction of IFN-β upon stimulation with DNA virus infection or DNA (121, 153, 154); therefore, further research is indispensable to clarify the exact role of DDX41 as a DNA sensor.

RNA Polymerase III

RNA polymerase III (RNA pol III) serves as a cytosolic dsDNA sensor through produced RNA and transduces signals for RIG-I and MAVS signaling pathways (20, 30). Initially, it was very puzzling that how poly (dA:dT) in some human cell lines could induce IFN-β production through RIG-I/MAVS signaling pathways; however, subsequent research resolved this conundrum by demonstrating that transfected poly (dA:dT) is converted into RNA containing 5'-triphosphate and double-stranded secondary structures by the action of RNA pol III which serves as bona fide trigger of RIG-I (20, 30). This feature gives the host advantage of utilizing the RIG-I-MAVS pathway to detect DNA viruses and bacteria. RNA pol III mediates the synthesis of IFN-inducing small RNA from the DNA of adenovirus in murine bone marrow-derived DCs (155), and inhibition of RNA pol III affected late immune responses during adenovirus infection in murine RAW267.4 cells (156). Although RNA pol III was shown to respond to HSV-1 infection in mouse macrophages (20), the results were challenged by later studies, showing that IFN and cytokine expression are RNA pol

III independent in both human and mouse macrophages (16, 157). Nonetheless, recently it was demonstrated that mutations in RNA pol III during VZV infection in children resulted in reduced IFN production, which could not be compensated by other DNA sensors such as cGAS, DDX41, and IFI16 (24). It can be anticipated that future studies will further elaborate on the role of RNA pol III as a DNA sensor in the innate immune responses.

DAI

DNA-dependent activator of IRFs (DAI, also termed as ZBP1 or DLM1) was the first putative DNA sensor identified by Takaoka et al. and was found to mediate IRF3 activation through TBK1 leading to type I IFNs production (21). Overexpression of DAI resulted in elevated DNA-induced synthesis of type I IFNs, while its inhibition through RNAi suppressed IFN induction in L929 cells. Despite first reports designating DAI as a cytosolic sensor of viral DNA, later studies using DAI-deficient mouse embryonic fibroblasts and mice reported them to induce normal IFN response (158). Therefore, DAI maybe working as an indispensable cytosolic DNA sensor or maybe cell-type specific; nonetheless, future studies are needed to fully decipher its potential as a DNA sensor. N-terminal domain of DAI comprises 2 tandem Z-DNA binding domains (ZBDs or Zα and Zβ) and a third DNA binding region (D3), which binds right-handed B-DNA is present next to the second ZBD. D3 domain has also been shown to bind Z-DNA. C-terminal of DAI interacts with TBK1 after activation (21). The crystal structure of the Zβ domain of human DAI ($hZ\beta_{DAI}$) reported that it shares the same fold as other ZBDs but opts for a unique binding mode to recognize Z-DNA. In $hZ\beta_{DAI,}$ a residue in the first β-strand contributes to the binding with the DNA compared to the residues of β-loop in other ZBDs. This structural data also revealed that both ZBDs of DAI could simultaneously bind the DNA and are required for complete B to Z conversion. It can be expected that the binding of both ZBDs to the same dsDNA may assist in DAI's dimerization (159). The NMR structure of $hZ\beta_{DAI}$ reports conformation deviations from its crystal structure, such as the β-sheet wing movement, which disengages the β-loop of the wing from the Z-DNA movement of the recognition helix. The N-terminal of α3 recognition helix contains charged residues, which seems important for recognizing both B- and Z-conformations of DNA (160).

DNA-PK and MRE-11

DNA-dependent protein kinase (DNA-PK) is a protein involved in DNA damage response and implicated in cytosolic DNA sensing. It comprises three subunits, Ku70, Ku80, and the catalytic subunit DNA-PKcs. Affinity pull-down assays in HEK293T cells have revealed the DNA sensing potential of this protein. Mouse embryonic fibroblasts and mice lacking DNA-PKcs exhibited attenuated cytokine production upon stimulation with viral DNA (161). Furthermore, its subunit Ku70 was also reported to induce IFN-λ1 production upon stimulation with cytosolic DNA in HEK293T cells (22). A very recent study has reported that DNA-PK uses the STING-independent DNA sensing pathway (SIDSP) to exert its functions because the DNA-sensing ability of DNA-PK is not impaired in STING-deficient cells (162). We can anticipate that future updates will render important information on the significance of this new signaling axis.

Meiotic recombination 11 homolog A (MRE-11) is also proposed as a cytosolic DNA sensor that activates the STING pathway (163). MRE-11 is implicated in dsDNA break repair, homologous recombination, and telomere length maintenance. This protein possesses 3' to 5' exonuclease activity and endonuclease activity and interacts with RAD50 for non-homologous DNA end-joining (164). Cryo-EM structures of the *E. coli* MRE11-Rad50 homolog SbcCD reveals that in the resting state of MRE11, ATP-Rad50 blocks its nuclease domain. When DNA is bound, its nuclease domain is freed, and it assembles a DNA cutting channel to carryout nuclease reaction on the DNA end (165). Future studies are required to disclose the complete details of its DNA sensing function.

CONCLUDING REMARKS AND FUTURE DIRECTIONS

In the last decade, research in the field of innate immune sensing of pathogen-derived nucleic acids has witnessed fruitful progress and disclosed important signaling cascades such as a cGAS-STING pathway for the detection of cytosolic DNA and RLR-MAVS pathway for sensing cytoplasmic RNA. Furthermore, many DNA sensors' structural information has undoubtedly yielded important data regarding critical events by which these sensors function. These structural data have advanced our understanding of DNA sensors' regulatory mechanisms, their ligand-binding sites, proteolytic processing, and how they interact and bind DNA. Further updates in this direction are anticipated to elucidate the potential targets for antiviral therapy. Despite the current progress, many crucial questions are still lacking answers. For example, the cellular compartments are guarded by various innate immune receptors to cope with viral infections and given the fact that many viruses replicate in the nucleus, then there must exist receptors for nuclear surveillance, as IFI16 is predominantly located in the nucleus. It needs to be investigated how the nucleus maintains immune surveillance against viruses and which mechanisms are employed.

Furthermore, there is significant redundancy among the cytosolic DNA sensors with multiple sensors contributing to the antiviral immunity; however, we need to decipher the biological importance of this redundancy and crosstalk between them. Besides, the role of inflammasomes in DNA sensing of viruses yet needs to be fully discovered since only a few inflammasomes are known to participate in viral DNA sensing, while for other pathogens such as bacteria, many different inflammasomes are known. Therefore, there is a possibility that viral DNA may be activating some novel yet unknown inflammasomes. Moreover, we lack comprehensive structural data for many DNA sensors, and it is important to understand the complete structural basis of DNA recognition by these sensors, which can point out important targets for drug development. Finally, it will be of immense

significance to know if these DNA sensors detect only naked viral DNA or can sense DNA-associated proteins as well.

AUTHOR CONTRIBUTIONS

AZ wrote the manuscript. HI proofread and helped with figure illustrations. TJ and BL provided the guidance and revised the manuscript. All authors contributed to the article and approved the submitted version.

FUNDING

This work was supported by the Strategic Priority Research Program of the Chinese Academy of Sciences (Grant No. XDB29030104), the National Natural Science Foundation of China (Grant Nos.: 31870731, 31971129 and U1732109), the Fundamental Research Funds for the Central Universities, and the 100 Talents Programme of The Chinese Academy of Sciences. AZ is supported by CAS-TWAS president fellowship. HI is supported by Chinese government scholarship.

REFERENCES

1. Li Y, Li Y, Cao X, Jin X, Jin T. Pattern recognition receptors in zebrafish provide functional and evolutionary insight into innate immune signaling pathways. *Cell Mol Immunol* (2017) 14(1):80–9. doi: 10.1038/cmi.2016.50
2. Jorgensen I, Rayamajhi M, Miao EA. Programmed cell death as a defence against infection. *Nat Rev Immunol* (2017) 17(3):151. doi: 10.1038/nri.2016.147
3. Zitvogel L, Galluzzi L, Kepp O, Smyth MJ, Kroemer G. Type I interferons in anticancer immunity. *Nat Rev Immunol* (2015) 15(7):405–14. doi: 10.1038/nri3845
4. McNab F, Mayer-Barber K, Sher A, Wack A, O'garra A. Type I interferons in infectious disease. *Nat Rev Immunol* (2015) 15(2):87–103. doi: 10.1038/nri3787
5. Galluzzi L, Buqué A, Kepp O, Zitvogel L, Kroemer G. Immunogenic cell death in cancer and infectious disease. *Nat Rev Immunol* (2017) 17(2):97. doi: 10.1038/nri.2016.107
6. Roers A, Hiller B, Hornung V. Recognition of endogenous nucleic acids by the innate immune system. *Immunity* (2016) 44(4):739–54. doi: 10.1016/j.immuni.2016.04.002
7. Ma Z, Ni G, Damania B. Innate sensing of DNA virus genomes. *Annu Rev Virol* (2018) 5:341–62. doi: 10.1146/annurev-virology-092917-043244
8. Andreeva L, Hiller B, Kostrewa D, Lässig C, de Oliveira Mann CC, Drexler DJ, et al. cGAS senses long and HMGB/TFAM-bound U-turn DNA by forming protein–DNA ladders. *Nature* (2017) 549(7672):394–8. doi: 10.1038/nature23890
9. McArthur K, Whitehead LW, Heddleston JM, Li L, Padman BS, Oorschot V, et al. BAK/BAX macropores facilitate mitochondrial herniation and mtDNA efflux during apoptosis. *Science* (2018) 359(6378):eaao6047. doi: 10.1126/science.aao6047
10. Kassiotis G, Stoye JP. Immune responses to endogenous retroelements: taking the bad with the good. *Nat Rev Immunol* (2016) 16(4):207–19. doi: 10.1038/nri.2016.27
11. Bakhoum SF, Ngo B, Laughney AM, Cavallo J-A, Murphy CJ, Ly P, et al. Chromosomal instability drives metastasis through a cytosolic DNA response. *Nature* (2018) 553(7689):467–72. doi: 10.1038/nature25432
12. Chen Q, Sun L, Chen ZJ. Regulation and function of the cGAS–STING pathway of cytosolic DNA sensing. *Nat Immunol* (2016) 17(10):1142–9. doi: 10.1038/ni.3558
13. Lund J, Sato A, Akira S, Medzhitov R, Iwasaki A. Toll-like receptor 9–mediated recognition of herpes simplex virus-2 by plasmacytoid dendritic cells. *J Exp Med* (2003) 198(3):513–20. doi: 10.1084/jem.20030162
14. Horan KA, Hansen K, Jakobsen MR, Holm CK, Søby S, Unterholzner L, et al. Proteasomal degradation of herpes simplex virus capsids in macrophages releases DNA to the cytosol for recognition by DNA sensors. *J Immunol* (2013) 190(5):2311–9. doi: 10.4049/jimmunol.1202749
15. Tan X, Sun L, Chen J, Chen ZJ. Detection of microbial infections through innate immune sensing of nucleic acids. *Annu Rev Microbiol* (2018) 72:447–78. doi: 10.1146/annurev-micro-102215-095605
16. Unterholzner L, Keating SE, Baran M, Horan KA, Jensen SB, Sharma S, et al. IFI16 is an innate immune sensor for intracellular DNA. *Nat Immunol* (2010) 11(11):997–1004. doi: 10.1038/ni.1932
17. Kerur N, Veettil MV, Sharma-Walia N, Bottero V, Sadagopan S, Otageri P, et al. IFI16 acts as a nuclear pathogen sensor to induce the inflammasome in response to Kaposi Sarcoma-associated herpesvirus infection. *Cell host Microbe* (2011) 9(5):363–75. doi: 10.1016/j.chom.2011.04.008
18. Zhang Z, Yuan B, Bao M, Lu N, Kim T, Liu Y-J. The helicase DDX41 senses intracellular DNA mediated by the adaptor STING in dendritic cells. *Nat Immunol* (2011) 12(10):959–65. doi: 10.1038/ni.2091
19. Kim T, Pazhoor S, Bao M, Zhang Z, Hanabuchi S, Facchinetti V, et al. Aspartate-glutamate-alanine-histidine box motif (DEAH)/RNA helicase A helicases sense microbial DNA in human plasmacytoid dendritic cells. *Proc Natl Acad Sci* (2010) 107(34):15181–6. doi: 10.1073/pnas.1006539107
20. Chiu Y-H, MacMillan JB, Chen ZJ. RNA polymerase III detects cytosolic DNA and induces type I interferons through the RIG-I pathway. *Cell* (2009) 138(3):576–91. doi: 10.1016/j.cell.2009.06.015
21. Takaoka A, Wang Z, Choi MK, Yanai H, Negishi H, Ban T, et al. DAI (DLM-1/ZBP1) is a cytosolic DNA sensor and an activator of innate immune response. *Nature* (2007) 448(7152):501–5. doi: 10.1038/nature06013
22. Zhang X, Brann TW, Zhou M, Yang J, Oguariri RM, Lidie KB, et al. Cutting edge: Ku70 is a novel cytosolic DNA sensor that induces type III rather than type I IFN. *J Immunol* (2011) 186(8):4541–5. doi: 10.4049/jimmunol.1003389
23. Krug A, Luker GD, Barchet W, Leib DA, Akira S, Colonna M. Herpes simplex virus type 1 activates murine natural interferon-producing cells through toll-like receptor 9. *Blood* (2004) 103(4):1433–7. doi: 10.1182/blood-2003-08-2674
24. Ogunjimi B, Zhang S-Y, Sørensen KB, Skipper KA, Carter-Timofte M, Kerner G, et al. Inborn errors in RNA polymerase III underlie severe varicella zoster virus infections. *J Clin Invest* (2017) 127(9):3543–56. doi: 10.1172/JCI92280
25. Yu H-R, Huang H-C, Kuo H-C, Sheen J-M, Ou C-Y, Hsu T-Y, et al. IFN-α production by human mononuclear cells infected with varicella-zoster virus through TLR9-dependent and-independent pathways. *Cell Mol Immunol* (2011) 8(2):181–8. doi: 10.1038/cmi.2010.84
26. Varani S, Cederarv M, Feld S, Tammik C, Frascaroli G, Landini MP, et al. Human cytomegalovirus differentially controls B cell and T cell responses through effects on plasmacytoid dendritic cells. *J Immunol* (2007) 179 (11):7767–76. doi: 10.4049/jimmunol.179.11.7767
27. DeFilippis VR, Alvarado D, Sali T, Rothenburg S, Früh K. Human cytomegalovirus induces the interferon response via the DNA sensor ZBP1. *J Virol* (2010) 84(1):585–98. doi: 10.1128/JVI.01748-09
28. Rathinam VA, Jiang Z, Waggoner SN, Sharma S, Cole LE, Waggoner L, et al. The AIM2 inflammasome is essential for host defense against cytosolic bacteria and DNA viruses. *Nat Immunol* (2010) 11(5):395. doi: 10.1038/ni.1864
29. Fiola S, Gosselin D, Takada K, Gosselin J. TLR9 contributes to the recognition of EBV by primary monocytes and plasmacytoid dendritic cells. *J Immunol* (2010) 185(6):3620–31. doi: 10.4049/jimmunol.0903736
30. Ablasser A, Bauernfeind F, Hartmann G, Latz E, Fitzgerald KA, Hornung V. RIG-I-dependent sensing of poly (dA: dT) through the induction of an RNA polymerase III–transcribed RNA intermediate. *Nat Immunol* (2009) 10 (10):1065–72. doi: 10.1038/ni.1779
31. Lim WH, Kireta S, Russ GR, Coates PTH. Human plasmacytoid dendritic cells regulate immune responses to Epstein-Barr virus (EBV) infection and delay EBV-related mortality in humanized NOD-SCID mice. *Blood* (2007) 109(3):1043–50. doi: 10.1182/blood-2005-12-024802
32. West JA, Gregory SM, Sivaraman V, Su L, Damania B. Activation of plasmacytoid dendritic cells by Kaposi's sarcoma-associated herpesvirus. *J Virol* (2011) 85(2):895–904. doi: 10.1128/JVI.01007-10
33. Zhao Y, De Trez C, Flynn R, Ware CF, Croft M, Salek-Ardakani S. The adaptor molecule MyD88 directly promotes CD8 T cell responses to vaccinia virus. *J Immunol* (2009) 182(10):6278–86. doi: 10.4049/jimmunol.0803682

34. Roy A, Dutta D, Iqbal J, Pisano G, Gjyshi O, Ansari MA, et al. Nuclear innate immune DNA sensor IFI16 is degraded during lytic reactivation of Kaposi's sarcoma-associated herpesvirus (KSHV): role of IFI16 in maintenance of KSHV latency. *J Virol* (2016) 90(19):8822–41. doi: 10.1128/JVI.01003-16
35. Appledorn DM, Patial S, McBride A, Godbehere S, Van Rooijen N, Parameswaran N, et al. Adenovirus vector-induced innate inflammatory mediators, MAPK signaling, as well as adaptive immune responses are dependent upon both TLR2 and TLR9 in vivo. *J Immunol* (2008) 181 (3):2134–44. doi: 10.4049/jimmunol.181.3.2134
36. Hasan UA, Bates E, Takeshita F, Biliato A, Accardi R, Bouvard V, et al. TLR9 expression and function is abolished by the cervical cancer-associated human papillomavirus type 16. *J Immunol* (2007) 178(5):3186–97. doi: 10.4049/jimmunol.178.5.3186
37. Samuelsson C, Hausmann J, Lauterbach H, Schmidt M, Akira S, Wagner H, et al. Survival of lethal poxvirus infection in mice depends on TLR9, and therapeutic vaccination provides protection. *J Clin Invest* (2008) 118 (5):1776–84. doi: 10.1172/JCI33940
38. Beignon A-S, McKenna K, Skoberne M, Manches O, DaSilva I, Kavanagh DG, et al. Endocytosis of HIV-1 activates plasmacytoid dendritic cells via Toll-like receptor–viral RNA interactions. *J Clin Invest* (2005) 115(11):3265–75. doi: 10.1172/JCI26032
39. Motwani M, Pesiridis S, Fitzgerald KA. DNA sensing by the cGAS–STING pathway in health and disease. *Nat Rev Genet* (2019) 20(11):657–74. doi: 10.1038/s41576-019-0151-1
40. Sun B, Sundström KB, Chew JJ, Bist P, Gan ES, Tan HC, et al. Dengue virus activates cGAS through the release of mitochondrial DNA. *Sci Rep* (2017) 7 (1):1–8. doi: 10.1038/s41598-017-03932-1
41. Franz KM, Neidermyer WJ, Tan Y-J, Whelan SP, Kagan JC. STING-dependent translation inhibition restricts RNA virus replication. *Proc Natl Acad Sci* (2018) 115(9):E2058–E67. doi: 10.1073/pnas.1716937115
42. Miyashita M, Oshiumi H, Matsumoto M, Seya T. DDX60, a DEXD/H box helicase, is a novel antiviral factor promoting RIG-I-like receptor-mediated signaling. *Mol Cell Biol* (2011) 31(18):3802–19. doi: 10.1128/MCB.01368-10
43. Zhang Z, Yuan B, Lu N, Facchinetti V, Liu Y-J. DHX9 pairs with IPS-1 to sense double-stranded RNA in myeloid dendritic cells. *J Immunol* (2011) 187(9):4501–8. doi: 10.4049/jimmunol.1101307
44. Zhang Z, Kim T, Bao M, Facchinetti V, Jung SY, Ghaffari AA, et al. DDX1, DDX21, and DHX36 helicases form a complex with the adaptor molecule TRIF to sense dsRNA in dendritic cells. *Immunity* (2011) 34(6):866–78. doi: 10.1016/j.immuni.2011.03.027
45. Sjölinder H, Mogensen TH, Kilian M, Jonsson A-B, Paludan SR. Important role for Toll-like receptor 9 in host defense against meningococcal sepsis. *Infect Immun* (2008) 76(11):5421–8. doi: 10.1128/IAI.00615-08
46. Bafica A, Scanga CA, Feng CG, Leifer C, Cheever A, Sher A. TLR9 regulates Th1 responses and cooperates with TLR2 in mediating optimal resistance to Mycobacterium tuberculosis. *J Exp Med* (2005) 202(12):1715–24. doi: 10.1084/jem.20051782
47. Saiga H, Kitada S, Shimada Y, Kamiyama N, Okuyama M, Makino M, et al. Critical role of AIM2 in Mycobacterium tuberculosis infection. *Int Immunol* (2012) 24(10):637–44. doi: 10.1093/intimm/dxs062
48. Watson RO, Bell SL, MacDuff DA, Kimmey JM, Diner EJ, Olivas J, et al. The cytosolic sensor cGAS detects Mycobacterium tuberculosis DNA to induce type I interferons and activate autophagy. *Cell host Microbe* (2015) 17 (6):811–9. doi: 10.1016/j.chom.2015.05.004
49. Jones JW, Kayagaki N, Broz P, Henry T, Newton K, O'Rourke K, et al. Absent in melanoma 2 is required for innate immune recognition of Francisella tularensis. *Proc Natl Acad Sci* (2010) 107(21):9771–6. doi: 10.1073/pnas.1003738107
50. Storek KM, Gertsvolf NA, Ohlson MB, Monack DM. cGAS and Ifi204 cooperate to produce type I IFNs in response to Francisella infection. *J Immunol* (2015) 194(7):3236–45. doi: 10.4049/jimmunol.1402764
51. Feng S, Chen T, Lei G, Hou F, Jiang J, Huang Q, et al. Absent in melanoma 2 inflammasome is required for host defence against Streptococcus pneumoniae infection. *Innate Immun* (2019) 25(7):412–9. doi: 10.1177/1753425919860252
52. Ruiz-Moreno JS, Hamann L, Jin L, Sander LE, Puzianowska-Kuznicka M, Cambier J, et al. The cGAS/STING pathway detects Streptococcus pneumoniae but appears dispensable for antipneumococcal defense in mice and humans. *Infect Immun* (2018) 86(3):e00849-17. doi: 10.1128/IAI.00849-17
53. Hansen K, Prabakaran T, Laustsen A, Jørgensen SE, Rahbæk SH, Jensen SB, et al. Listeria monocytogenes induces IFNβ expression through an IFI16-, cGAS-and STING-dependent pathway. *EMBO J* (2014) 33(15):1654–66. doi: 10.15252/embj.201488029
54. Chunfa L, Xin S, Qiang L, Sreevatsan S, Yang L, Zhao D, et al. The central role of IFI204 in IFN-β release and autophagy activation during Mycobacterium bovis infection. *Front Cell Infect Microbiol* (2017) 7:169. doi: 10.3389/fcimb.2017.00169
55. Chen W, Yu S-X, Zhou F-H, Zhang X-J, Gao W-Y, Li K-Y, et al. DNA sensor IFI204 contributes to host defense against Staphylococcus aureus infection in mice. *Front Immunol* (2019) 10:474. doi: 10.3389/fimmu.2019.00474
56. Hanamsagar R, Aldrich A, Kielian T. Critical role for the AIM 2 inflammasome during acute CNS bacterial infection. *J Neurochem* (2014) 129(4):704–11. doi: 10.1111/jnc.12669
57. Karki R, Man SM, Malireddi RS, Gurung P, Vogel P, Lamkanfi M, et al. Concerted activation of the AIM2 and NLRP3 inflammasomes orchestrates host protection against Aspergillus infection. *Cell host Microbe* (2015) 17 (3):357–68. doi: 10.1016/j.chom.2015.01.006
58. Carvalho A, Pasqualotto A, Pitzurra L, Romani L, Denning D, Rodrigues F. Polymorphisms in toll-like receptor genes and susceptibility to pulmonary aspergillosis. *J Infect Diseases* (2008) 197(4):618–21. doi: 10.1086/526500
59. Ishikawa H, Ma Z, Barber GN. STING regulates intracellular DNA-mediated, type I interferon-dependent innate immunity. *Nature* (2009) 461(7265):788–92. doi: 10.1038/nature08476
60. Yan N, Regalado-Magdos AD, Stiggelbout B, Lee-Kirsch MA, Lieberman J. The cytosolic exonuclease TREX1 inhibits the innate immune response to human immunodeficiency virus type 1. *Nat Immunol* (2010) 11(11):1005–13. doi: 10.1038/ni.1941
61. Galluzzi L, Kepp O, Kroemer G. Mitochondria: master regulators of danger signalling. *Nat Rev Mol Cell Biol* (2012) 13(12):780–8. doi: 10.1038/nrm3479
62. Harding SM, Benci JL, Irianto J, Discher DE, Minn AJ, Greenberg RA. Mitotic progression following DNA damage enables pattern recognition within micronuclei. *Nature* (2017) 548(7668):466–70. doi: 10.1038/nature23470
63. Mackenzie KJ, Carroll P, Martin C-A, Murina O, Fluteau A, Simpson DJ, et al. cGAS surveillance of micronuclei links genome instability to innate immunity. *Nature* (2017) 548(7668):461–5. doi: 10.1038/nature23449
64. Vanpouille-Box C, Alard A, Aryankalayil MJ, Sarfraz Y, Diamond JM, Schneider RJ, et al. DNA exonuclease Trex1 regulates radiotherapy-induced tumour immunogenicity. *Nat Commun* (2017) 8:15618. doi: 10.1038/ncomms15618
65. Woo S-R, Fuertes MB, Corrales L, Spranger S, Furdyna MJ, Leung MY, et al. STING-dependent cytosolic DNA sensing mediates innate immune recognition of immunogenic tumors. *Immunity* (2014) 41(5):830–42. doi: 10.1016/j.immuni.2014.10.017
66. Xu MM, Pu Y, Han D, Shi Y, Cao X, Liang H, et al. Dendritic cells but not macrophages sense tumor mitochondrial DNA for cross-priming through signal regulatory protein α signaling. *Immunity* (2017) 47(2):363–73. e5. doi: 10.1016/j.immuni.2017.07.016
67. Ablasser A, Chen ZJ. cGAS in action: Expanding roles in immunity and inflammation. *Science* (2019) 363(6431):eaat8657. doi: 10.1126/science.aat8657
68. Hemmi H, Takeuchi O, Kawai T, Kaisho T, Sato S, Sanjo H, et al. A Toll-like receptor recognizes bacterial DNA. *Nature* (2000) 408(6813):740–5. doi: 10.1038/35047123
69. Li Y, Berke IC, Modis Y. DNA binding to proteolytically activated TLR9 is sequence-independent and enhanced by DNA curvature. *EMBO J* (2012) 31 (4):919–31. doi: 10.1038/emboj.2011.441
70. Schwartz T, Behlke J, Lowenhaupt K, Heinemann U, Rich A. Structure of the DLM-1–Z-DNA complex reveals a conserved family of Z-DNA-binding proteins. *Nat Struct Biol* (2001) 8(9):761–5. doi: 10.1038/nsb0901-761
71. Lande R, Gregorio J, Facchinetti V, Chatterjee B, Wang Y-H, Homey B, et al. Plasmacytoid dendritic cells sense self-DNA coupled with antimicrobial peptide. *Nature* (2007) 449(7162):564–9. doi: 10.1038/nature06116
72. Bell JK, Mullen GE, Leifer CA, Mazzoni A, Davies DR, Segal DM. Leucine-rich repeats and pathogen recognition in Toll-like receptors. *Trends Immunol* (2003) 24(10):528–33. doi: 10.1016/S1471-4906(03)00242-4
73. Matsushima N, Tanaka T, Enkhbayar P, Mikami T, Taga M, Yamada K, et al. Comparative sequence analysis of leucine-rich repeats (LRRs) within

vertebrate toll-like receptors. *BMC Genomics* (2007) 8(1):124. doi: 10.1186/1471-2164-8-124
74. Fitzgerald KA, Kagan JC. Toll-like receptors and the control of immunity. *Cell* (2020) 180(6):1044–66. doi: 10.1016/j.cell.2020.02.041
75. Yasuda K, Richez C, Uccellini MB, Richards RJ, Bonegio RG, Akira S, et al. Requirement for DNA CpG content in TLR9-dependent dendritic cell activation induced by DNA-containing immune complexes. *J Immunol* (2009) 183(5):3109–17. doi: 10.4049/jimmunol.0900399
76. Ohto U, Shimizu T. Structural aspects of nucleic acid-sensing Toll-like receptors. *Biophys Rev* (2016) 8(1):33–43. doi: 10.1007/s12551-015-0187-1
77. Hochrein H, Schlatter B, O'Keeffe M, Wagner C, Schmitz F, Schiemann M, et al. Herpes simplex virus type-1 induces IFN-α production via Toll-like receptor 9-dependent and-independent pathways. *Proc Natl Acad Sci* (2004) 101(31):11416–21. doi: 10.1073/pnas.0403555101
78. Megjugorac NJ, Young HA, Amrute SB, Olshalsky SL, Fitzgerald-Bocarsly P. Virally stimulated plasmacytoid dendritic cells produce chemokines and induce migration of T and NK cells. *J Leukocyte Biol* (2004) 75(3):504–14. doi: 10.1189/jlb.0603291
79. Megjugorac NJ, Gallagher GE, Gallagher G. Modulation of human plasmacytoid DC function by IFN-λ1 (IL-29). *J Leukocyte Biol* (2009) 86 (6):1359–63. doi: 10.1189/jlb.0509347
80. Smith ZD, Meissner A. DNA methylation: roles in mammalian development. *Nat Rev Genet* (2013) 14(3):204–20. doi: 10.1038/nrg3354
81. Bauer S, Kirschning CJ, Häcker H, Redecke V, Hausmann S, Akira S, et al. Human TLR9 confers responsiveness to bacterial DNA via species-specific CpG motif recognition. *Proc Natl Acad Sci* (2001) 98(16):9237–42. doi: 10.1073/pnas.161293498
82. Shahzad N, Shuda M, Gheit T, Kwun HJ, Cornet I, Saidj D, et al. The T antigen locus of Merkel cell polyomavirus downregulates human Toll-like receptor 9 expression. *J Virol* (2013) 87(23):13009–19. doi: 10.1128/JVI.01786-13
83. Tabeta K, Hoebe K, Janssen EM, Du X, Georgel P, Crozat K, et al. The Unc93b1 mutation 3d disrupts exogenous antigen presentation and signaling via Toll-like receptors 3, 7 and 9. *Nat Immunol* (2006) 7(2):156–64. doi: 10.1038/ni1297
84. Ewald SE, Lee BL, Lau L, Wickliffe KE, Shi G-P, Chapman HA, et al. The ectodomain of Toll-like receptor 9 is cleaved to generate a functional receptor. *Nature* (2008) 456(7222):658–62. doi: 10.1038/nature07405
85. Iwasaki A, Medzhitov R. Regulation of adaptive immunity by the innate immune system. *science* (2010) 327(5963):291–5. doi: 10.1126/science.1183021
86. Ohto U, Shibata T, Tanji H, Ishida H, Krayukhina E, Uchiyama S, et al. Structural basis of CpG and inhibitory DNA recognition by Toll-like receptor 9. *Nature* (2015) 520(7549):702–5. doi: 10.1038/nature14138
87. Park B, Brinkmann MM, Spooner E, Lee CC, Kim Y-M, Ploegh HL. Proteolytic cleavage in an endolysosomal compartment is required for activation of Toll-like receptor 9. *Nat Immunol* (2008) 9(12):1407. doi: 10.1038/ni.1669
88. Tanji H, Ohto U, Shibata T, Miyake K, Shimizu T. Structural reorganization of the Toll-like receptor 8 dimer induced by agonistic ligands. *Science* (2013) 339(6126):1426–9. doi: 10.1126/science.1229159
89. Rutz M, Metzger J, Gellert T, Luppa P, Lipford GB, Wagner H, et al. Toll-like receptor 9 binds single-stranded CpG-DNA in a sequence-and pH-dependent manner. *Eur J Immunol* (2004) 34(9):2541–50. doi: 10.1002/eji.200425218
90. Xu R-H, Wong EB, Rubio D, Roscoe F, Ma X, Nair S, et al. Sequential activation of two pathogen-sensing pathways required for type I interferon expression and resistance to an acute DNA virus infection. *Immunity* (2015) 43(6):1148–59. doi: 10.1016/j.immuni.2015.11.015
91. Spooner RA, Smith DC, Easton AJ, Roberts LM, Lord MJ. Retrograde transport pathways utilised by viruses and protein toxins. *Virol J* (2006) 3 (1):1–10. doi: 10.1186/1743-422X-3-26
92. West AP, Khoury-Hanold W, Staron M, Tal MC, Pineda CM, Lang SM, et al. Mitochondrial DNA stress primes the antiviral innate immune response. *Nature* (2015) 520(7548):553–7. doi: 10.1038/nature14156
93. Hornung V, Latz E. Intracellular DNA recognition. *Nat Rev Immunol* (2010) 10(2):123–30. doi: 10.1038/nri2690
94. Wu J, Sun L, Chen X, Du F, Shi H, Chen C, et al. Cyclic GMP-AMP is an endogenous second messenger in innate immune signaling by cytosolic DNA. *Science* (2013) 339(6121):826–30. doi: 10.1126/science.1229963
95. Du M, Chen ZJ. DNA-induced liquid phase condensation of cGAS activates innate immune signaling. *Science* (2018) 361(6403):704–9. doi: 10.1126/science.aat1022
96. Ablasser A, Goldeck M, Cavlar T, Deimling T, Witte G, Röhl I, et al. cGAS produces a 2′-5′-linked cyclic dinucleotide second messenger that activates STING. *Nature* (2013) 498(7454):380–4. doi: 10.1038/nature12306
97. Diner EJ, Burdette DL, Wilson SC, Monroe KM, Kellenberger CA, Hyodo M, et al. The innate immune DNA sensor cGAS produces a noncanonical cyclic dinucleotide that activates human STING. *Cell Rep* (2013) 3(5):1355–61. doi: 10.1016/j.celrep.2013.05.009
98. Shang G, Zhang C, Chen ZJ, Bai X-C, Zhang X. Cryo-EM structures of STING reveal its mechanism of activation by cyclic GMP–AMP. *Nature* (2019) 567(7748):389–93. doi: 10.1038/s41586-019-0998-5
99. Li X, Shu C, Yi G, Chaton CT, Shelton CL, Diao J, et al. Cyclic GMP-AMP synthase is activated by double-stranded DNA-induced oligomerization. *Immunity* (2013) 39(6):1019–31. doi: 10.1016/j.immuni.2013.10.019
100. Zhang X, Wu J, Du F, Xu H, Sun L, Chen Z, et al. The cytosolic DNA sensor cGAS forms an oligomeric complex with DNA and undergoes switch-like conformational changes in the activation loop. *Cell Rep* (2014) 6(3):421–30. doi: 10.1016/j.celrep.2014.01.003
101. Kranzusch PJ, Lee AS-Y, Berger JM, Doudna JA. Structure of human cGAS reveals a conserved family of second-messenger enzymes in innate immunity. *Cell Rep* (2013) 3(5):1362–8. doi: 10.1016/j.celrep.2013.05.008
102. Civril F, Deimling T, de Oliveira Mann CC, Ablasser A, Moldt M, Witte G, et al. Structural mechanism of cytosolic DNA sensing by cGAS. *Nature* (2013) 498(7454):332–7. doi: 10.1038/nature12305
103. Gao P, Ascano M, Wu Y, Barchet W, Gaffney BL, Zillinger T, et al. Cyclic [G (2′, 5′) pA (3′, 5′) p] is the metazoan second messenger produced by DNA-activated cyclic GMP-AMP synthase. *Cell* (2013) 153(5):1094–107. doi: 10.1016/j.cell.2013.04.046
104. Liu S, Cai X, Wu J, Cong Q, Chen X, Li T, et al. Phosphorylation of innate immune adaptor proteins MAVS, STING, and TRIF induces IRF3 activation. *Science* (2015) 347(6227):eaat8657. doi: 10.1126/science.aaa2630
105. Shang G, Zhu D, Li N, Zhang J, Zhu C, Lu D, et al. Crystal structures of STING protein reveal basis for recognition of cyclic di-GMP. *Nat Struct Mol Biol* (2012) 19(7):725. doi: 10.1038/nsmb.2332
106. Volkman HE, Cambier S, Gray EE, Stetson DB. Tight nuclear tethering of cGAS is essential for preventing autoreactivity. *Elife* (2019) 8:e47491. doi: 10.7554/eLife.47491
107. Gentili M, Lahaye X, Nadalin F, Nader GP, Lombardi EP, Herve S, et al. The N-terminal domain of cGAS determines preferential association with centromeric DNA and innate immune activation in the nucleus. *Cell Rep* (2019) 26(9):2377–93.e13. doi: 10.1016/j.celrep.2019.01.105
108. Jiang H, Xue X, Panda S, Kawale A, Hooy RM, Liang F, et al. Chromatin-bound cGAS is an inhibitor of DNA repair and hence accelerates genome destabilization and cell death. *EMBO J* (2019) 38(21):e102718. doi: 10.15252/embj.2019102718
109. Pathare GR, Decout A, Glück S, Cavadini S, Makasheva K, Hovius R, et al. Structural mechanism of cGAS inhibition by the nucleosome. *Nature* (2020), 1–8. doi: 10.1038/s41586-020-2750-6
110. Michalski S, de Oliveira Mann CC, Stafford C, Witte G, Bartho J, Lammens K, et al. Structural basis for sequestration and autoinhibition of cGAS by chromatin. *Nature* (2020), 1–8. doi: 10.1038/s41586-020-2748-0
111. Kujirai T, Zierhut C, Takizawa Y, Kim R, Negishi L, Uruma N, et al. Structural basis for the inhibition of cGAS by nucleosomes. *Science* (2020) 370(6515):455–8. doi: 10.1126/science.abd0237
112. Boyer JA, Spangler CJ, Strauss JD, Cesmat AP, Liu P, McGinty RK, et al. Structural basis of nucleosome-dependent cGAS inhibition. *Science* (2020) 370(6515):450–4. doi: 10.1126/science.abd0609
113. Ishikawa H, Barber GN. STING is an endoplasmic reticulum adaptor that facilitates innate immune signalling. *Nature* (2008) 455(7213):674–8. doi: 10.1038/nature07317
114. Ouyang S, Song X, Wang Y, Ru H, Shaw N, Jiang Y, et al. Structural analysis of the STING adaptor protein reveals a hydrophobic dimer interface and mode of cyclic di-GMP binding. *Immunity* (2012) 36(6):1073–86. doi: 10.1016/j.immuni.2012.03.019
115. Srikanth S, Woo JS, Wu B, El-Sherbiny YM, Leung J, Chupradit K, et al. The Ca 2+ sensor STIM1 regulates the type I interferon response by retaining the signaling adaptor STING at the endoplasmic reticulum. *Nat Immunol* (2019) 20(2):152–62. doi: 10.1038/s41590-018-0287-8
116. Gui X, Yang H, Li T, Tan X, Shi P, Li M, et al. Autophagy induction via STING trafficking is a primordial function of the cGAS pathway. *Nature* (2019) 567(7747):262–6. doi: 10.1038/s41586-019-1006-9

117. Mukai K, Konno H, Akiba T, Uemura T, Waguri S, Kobayashi T, et al. Activation of STING requires palmitoylation at the Golgi. *Nat Commun* (2016) 7:11932. doi: 10.1038/ncomms11932
118. Agalioti T, Lomvardas S, Parekh B, Yie J, Maniatis T, Thanos D. Ordered recruitment of chromatin modifying and general transcription factors to the IFN-β promoter. *Cell* (2000) 103(4):667–78. doi: 10.1016/S0092-8674(00)00169-0
119. Schneider WM, Chevillotte MD, Rice CM. Interferon-stimulated genes: a complex web of host defenses. *Annu Rev Immunol* (2014) 32:513–45. doi: 10.1146/annurev-immunol-032713-120231
120. Brault M, Olsen TM, Martinez J, Stetson DB, Oberst A. Intracellular nucleic acid sensing triggers necroptosis through synergistic type I IFN and TNF signaling. *J Immunol* (2018) 200(8):2748–56. doi: 10.4049/jimmunol.1701492
121. Abe T, Harashima A, Xia T, Konno H, Konno K, Morales A, et al. STING recognition of cytoplasmic DNA instigates cellular defense. *Mol Cell* (2013) 50(1):5–15. doi: 10.1016/j.molcel.2013.01.039
122. Burdette DL, Monroe KM, Sotelo-Troha K, Iwig JS, Eckert B, Hyodo M, et al. STING is a direct innate immune sensor of cyclic di-GMP. *Nature* (2011) 478(7370):515–8. doi: 10.1038/nature10429
123. Berthelot J-M, Lioté F. COVID-19 as a STING disorder with delayed over-secretion of interferon-beta. *EBioMedicine* (2020) 56:102801–. doi: 10.1016/j.ebiom.2020.102801
124. Cridland JA, Curley EZ, Wykes MN, Schroder K, Sweet MJ, Roberts TL, et al. The mammalian PYHIN gene family: phylogeny, evolution and expression. *BMC Evol Biol* (2012) 12(1):1–17. doi: 10.1186/1471-2148-12-140
125. Hornung V, Ablasser A, Charrel-Dennis M, Bauernfeind F, Horvath G, Caffrey DR, et al. AIM2 recognizes cytosolic dsDNA and forms a caspase-1-activating inflammasome with ASC. *Nature* (2009) 458(7237):514–8. doi: 10.1038/nature07725
126. Bürckstümmer T, Baumann C, Blüml S, Dixit E, Dürnberger G, Jahn H, et al. An orthogonal proteomic-genomic screen identifies AIM2 as a cytoplasmic DNA sensor for the inflammasome. *Nat Immunol* (2009) 10(3):266. doi: 10.1038/ni.1702
127. Paludan SR, Bowie AG. Immune sensing of DNA. *Immunity* (2013) 38 (5):870–80. doi: 10.1016/j.immuni.2013.05.004
128. Di Micco A, Frera G, Lugrin J, Jamilloux Y, Hsu E-T, Tardivel A, et al. AIM2 inflammasome is activated by pharmacological disruption of nuclear envelope integrity. *Proc Natl Acad Sci* (2016) 113(32):E4671–E80. doi: 10.1073/pnas.1602419113
129. Choubey D, Panchanathan R. Absent in Melanoma 2 proteins in SLE. *Clin Immunol* (2017) 176:42–8. doi: 10.1016/j.clim.2016.12.011
130. Muruve DA, Pétrilli V, Zaiss AK, White LR, Clark SA, Ross PJ, et al. The inflammasome recognizes cytosolic microbial and host DNA and triggers an innate immune response. *Nature* (2008) 452(7183):103–7. doi: 10.1038/nature06664
131. Gaidt MM, Ebert TS, Chauhan D, Ramshorn K, Pinci F, Zuber S, et al. The DNA inflammasome in human myeloid cells is initiated by a STING-cell death program upstream of NLRP3. *Cell* (2017) 171(5):1110–24.e18. doi: 10.1016/j.cell.2017.09.039
132. Fischer H, Tschachler E, Eckhart L. Cytosolic DNA sensing through cGAS and STING is inactivated by gene mutations in pangolins. *Apoptosis* (2020) 25(7):474–80. doi: 10.1007/s10495-020-01614-4
133. Fernandes-Alnemri T, Yu JW, Datta P, Wu J, Alnemri ES. AIM2 activates the inflammasome and cell death in response to cytoplasmic DNA. *Nature* (2009) 458(7237):509–13. doi: 10.1038/nature07710
134. Jin T, Perry A, Smith P, Jiang J, Xiao TS. Structure of the absent in melanoma 2 (AIM2) pyrin domain provides insights into the mechanisms of AIM2 autoinhibition and inflammasome assembly. *J Biol Chem* (2013) 288 (19):13225–35. doi: 10.1074/jbc.M113.468033
135. Lu A, Kabaleeswaran V, Fu T, Magupalli VG, Wu H. Crystal structure of the F27G AIM2 PYD mutant and similarities of its self-association to DED/DED interactions. *J Mol Biol* (2014) 426(7):1420–7. doi: 10.1016/j.jmb.2013.12.029
136. Morrone SR, Matyszewski M, Yu X, Delannoy M, Egelman EH, Sohn J. Assembly-driven activation of the AIM2 foreign-dsDNA sensor provides a polymerization template for downstream ASC. *Nat Commun* (2015) 6(1):1–13. doi: 10.1038/ncomms8827
137. Jin T, Perry A, Jiang J, Smith P, Curry JA, Unterholzner L, et al. Structures of the HIN domain: DNA complexes reveal ligand binding and activation mechanisms of the AIM2 inflammasome and IFI16 receptor. *Immunity* (2012) 36(4):561–71. doi: 10.1016/j.immuni.2012.02.014
138. Lu A, Li Y, Yin Q, Ruan J, Yu X, Egelman E, et al. Plasticity in PYD assembly revealed by cryo-EM structure of the PYD filament of AIM2. *Cell Discovery* (2015) 1(1):15013. doi: 10.1038/celldisc.2015.13
139. Lu A, Magupalli VG, Ruan J, Yin Q, Atianand MK, Vos MR, et al. Unified polymerization mechanism for the assembly of ASC-dependent inflammasomes. *Cell* (2014) 156(6):1193–206. doi: 10.1016/j.cell.2014.02.008
140. Jakobsen MR, Bak RO, Andersen A, Berg RK, Jensen SB, Jin T, et al. IFI16 senses DNA forms of the lentiviral replication cycle and controls HIV-1 replication. *Proc Natl Acad Sci* (2013) 110(48):E4571–E80. doi: 10.1073/pnas.1311669110
141. Dutta D, Dutta S, Veettil MV, Roy A, Ansari MA, Iqbal J, et al. BRCA1 regulates IFI16 mediated nuclear innate sensing of herpes viral DNA and subsequent induction of the innate inflammasome and interferon-β responses. *PloS Pathogens* (2015) 11(6):e1005030. doi: 10.1371/journal.ppat.1005030
142. Stratmann SA, Morrone SR, van Oijen AM, Sohn J. The innate immune sensor IFI16 recognizes foreign DNA in the nucleus by scanning along the duplex. *Elife* (2015) 4:e11721. doi: 10.7554/eLife.11721
143. Doitsh G, Galloway NL, Geng X, Yang Z, Monroe KM, Zepeda O, et al. Cell death by pyroptosis drives CD4 T-cell depletion in HIV-1 infection. *Nature* (2014) 505(7484):509–14. doi: 10.1038/nature12940
144. Jønsson K, Laustsen A, Krapp C, Skipper K, Thavachelvam K, Hotter D, et al. IFI16 is required for DNA sensing in human macrophages by promoting production and function of cGAMP. *Nat Commun* (2017) 8(1):1–17. doi: 10.1038/ncomms14391
145. Zhao H, Gonzalezgugel E, Cheng L, Richbourgh B, Nie L, Liu C. The roles of interferon-inducible p200 family members IFI16 and p204 in innate immune responses, cell differentiation and proliferation. *Genes Diseases* (2015) 2 (1):46–56. doi: 10.1016/j.gendis.2014.10.003
146. Liao JC, Lam R, Brazda V, Duan S, Ravichandran M, Ma J, et al. Interferon-inducible protein 16: insight into the interaction with tumor suppressor p53. *Structure* (2011) 19(3):418–29. doi: 10.1016/j.str.2010.12.015
147. Yan H, Dalal K, Hon BK, Youkharibache P, Lau D, Pio F. RPA nucleic acid-binding properties of IFI16-HIN200. *Biochim Biophys Acta (BBA) Proteins Proteomics* (2008) 1784(7-8):1087–97. doi: 10.1016/j.bbapap.2008.04.004
148. Ni X, Ru H, Ma F, Zhao L, Shaw N, Feng Y, et al. New insights into the structural basis of DNA recognition by HINa and HINb domains of IFI16. *J Mol Cell Biol* (2016) 8(1):51–61. doi: 10.1093/jmcb/mjv053
149. Morrone SR, Wang T, Constantoulakis LM, Hooy RM, Delannoy MJ, Sohn J. Cooperative assembly of IFI16 filaments on dsDNA provides insights into host defense strategy. *Proc Natl Acad Sci* (2014) 111(1):E62–71. doi: 10.1073/pnas.1313577111
150. Ru H, Ni X, Zhao L, Crowley C, Ding W, Hung L-W, et al. Structural basis for termination of AIM2-mediated signaling by p202. *Cell Res* (2013) 23 (6):855–8. doi: 10.1038/cr.2013.52
151. Omura H, Oikawa D, Nakane T, Kato M, Ishii R, Ishitani R, et al. Structural and Functional Analysis of DDX41: a bispecific immune receptor for DNA and cyclic dinucleotide. *Sci Rep* (2016) 6(1):1–11. doi: 10.1038/srep34756
152. Jiang Y, Zhu Y, Qiu W, Liu Y-J, Cheng G, Liu Z-J, et al. Structural and functional analyses of human DDX41 DEAD domain. *Protein Cell* (2017) 8 (1):72–6. doi: 10.1007/s13238-016-0351-9
153. Lam E, Stein S, Falck-Pedersen E. Adenovirus detection by the cGAS/STING/TBK1 DNA sensing cascade. *J Virol* (2014) 88(2):974–81. doi: 10.1128/JVI.02702-13
154. Sun L, Wu J, Du F, Chen X, Chen ZJ. Cyclic GMP-AMP synthase is a cytosolic DNA sensor that activates the type I interferon pathway. *Science* (2013) 339(6121):786–91. doi: 10.1126/science.1232458
155. Yamaguchi T, Kawabata K, Kouyama E, Ishii KJ, Katayama K, Suzuki T, et al. Induction of type I interferon by adenovirus-encoded small RNAs. *Proc Natl Acad Sci* (2010) 107(40):17286–91. doi: 10.1073/pnas.1009823107
156. Stein SC, Falck-Pedersen E. Sensing adenovirus infection: activation of interferon regulatory factor 3 in RAW 264.7 cells. *J Virol* (2012) 86 (8):4527–37. doi: 10.1128/JVI.07071-11
157. Melchjorsen J, Rintahaka J, Søby S, Horan KA, Poltajainen A, Østergaard L, et al. Early innate recognition of herpes simplex virus in human primary macrophages is mediated via the MDA5/MAVS-dependent and MDA5/MAVS/RNA polymerase III-independent pathways. *J Virol* (2010) 84 (21):11350–8. doi: 10.1128/JVI.01106-10

158. Ishii KJ, Kawagoe T, Koyama S, Matsui K, Kumar H, Kawai T, et al. TANK-binding kinase-1 delineates innate and adaptive immune responses to DNA vaccines. *Nature* (2008) 451(7179):725–9. doi: 10.1038/nature06537
159. Ha SC, Kim D, Hwang H-Y, Rich A, Kim Y-G, Kim KK. The crystal structure of the second Z-DNA binding domain of human DAI (ZBP1) in complex with Z-DNA reveals an unusual binding mode to Z-DNA. *Proc Natl Acad Sci* (2008) 105(52):20671–6. doi: 10.1073/pnas.0810463106
160. Kim K, Khayrutdinov BI, Lee C-K, Cheong H-K, Kang SW, Park H, et al. Solution structure of the Zβ domain of human DNA-dependent activator of IFN-regulatory factors and its binding modes to B-and Z-DNAs. *Proc Natl Acad Sci* (2011) 108(17):6921–6. doi: 10.1073/pnas.1014898107
161. Ferguson BJ, Mansur DS, Peters NE, Ren H, Smith GL. DNA-PK is a DNA sensor for IRF-3-dependent innate immunity. *elife* (2012) 1:e00047. doi: 10.7554/eLife.00047
162. Burleigh K, Maltbaek JH, Cambier S, Green R, Gale M, James RC, et al. Human DNA-PK activates a STING-independent DNA sensing pathway. *Sci Immunol* (2020) 5(43):eaba4219. doi: 10.1126/sciimmunol.aba4219
163. Kondo T, Kobayashi J, Saitoh T, Maruyama K, Ishii KJ, Barber GN, et al. DNA damage sensor MRE11 recognizes cytosolic double-stranded DNA and induces type I interferon by regulating STING trafficking. *Proc Natl Acad Sci* (2013) 110(8):2969–74. doi: 10.1073/pnas.1222694110
164. Yuan S-SF, Hou M-F, Hsieh Y-C, Huang C-Y, Lee Y-C, Chen Y-J, et al. Role of MRE11 in cell proliferation, tumor invasion, and DNA repair in breast cancer. *J Natl Cancer Institute* (2012) 104(19):1485–502. doi: 10.1093/jnci/djs355
165. Käshammer L, Saathoff J-H, Lammens K, Gut F, Bartho J, Alt A, et al. Mechanism of DNA end sensing and processing by the Mre11-Rad50 complex. *Mol Cell* (2019) 76(3):382–94.e6. doi: 10.1016/j.molcel.2019.07.035

Conflict of Interest: The authors declare that the research was conducted in the absence of any commercial or financial relationships that could be construed as a potential conflict of interest.

frontiers in Immunology

HYPOTHESIS AND THEORY
published: 01 December 2020
doi: 10.3389/fimmu.2020.607069

Lymphocyte Changes in Severe COVID-19: Delayed Over-Activation of STING?

Jean-Marie Berthelot[1]*, *Frédéric Lioté*[2], *Yves Maugars*[1] and *Jean Sibilia*[3,4]

[1] Rheumatology Department, Nantes University Hospital, Nantes, France, [2] Rheumatology Department & Inserm UMR 1132 (centre Viggo Petersen), Hôpital Lariboisière, Université de Paris, Paris, France, [3] Service de rhumatologie, Hopitaux Universitaires de Strasbourg, RESO: Centre de Reference des Maladies Autoimmunes Systemiques Rares Est Sud-Ouest, Strasbourg, France, [4] INSERM UMR_S1109, Universite de Strasbourg, Strasbourg, France

Upon recognition of microbial DNA or self-DNA, the cyclic-GMP-AMP synthase (cGAS) of the host catalyzes the production of the cyclic dinucleotide cGAMP. cGAMP is the main activator of STING, stimulator of interferon genes, leading to interferon synthesis through the STING-TBK1-IRF3 pathway. STING is also a hub for activation of NF-κB and autophagy. The present review details the striking similarities between T and B cell responses in severe coronavirus disease 2019 (COVID-19) and both animal or human models of STING gain of function (SAVI syndromes: STING-associated vasculopathy with onset in infancy). Those similarities may be further clues for a delayed activation of STING in severe COVID-19 patients, due to DNA damages following severe acute respiratory syndrome coronaviruses (SARS-CoV-2) infection and unusual role of STING in SARS-CoV-2 control. In early stages, Th2 differentiation are noticed in both severe COVID-19 and SAVI syndromes; then, CD4+ and CD8+ T cells functional exhaustion/senescent patterns due to TCR hyper-responsiveness are observed. T cell delayed over-responses can contribute to pneumonitis and delayed cytokine secretion with over-production of IL-6. Last, STING over-activation induces progressive CD4+ and CD8+ T lymphopenia in SAVI syndromes, which parallels what is observed in severe COVID-19. ACE2, the main receptor of SARS-CoV-2, is rarely expressed in immune cells, and it has not been yet proven that some human lymphocytes could be infected by SARS-CoV-2 through CD147 or CD26. However, STING, expressed in humans T cells, might be triggered following excessive transfer of cGAMP from infected antigen presenting cells into activated CD4+ and CD8+ T cells lymphocytes. Indeed, those lymphocytes highly express the cGAMP importer SLC19A1. Whereas STING is not expressed in human B cells, B cells counts are much less affected, either in COVID-19 or SAVI syndromes. The recognition of delayed STING over-activation in severe COVID-19 patients could prompt to target STING with specific small molecules inhibitors already designed and/or aspirin, which inhibits cGAS.

Keywords: SARS-CoV-2, cGAMP, lymphopenia, interferon, STING, COVID-19, lymphocyte, aspirin

OPEN ACCESS

Edited by:
Chunfu Zheng,
Fujian Medical University, China

Reviewed by:
Jianzhong Zhu,
Yangzhou University, China
François JMA Meurens,
UMR INRAE-Oniris 1300 Oniris—Nantes Atlantic National College of Veterinary Medicine, France
Markus Maeurer,
Champalimaud Foundation, Portugal

***Correspondence:**
Jean-Marie Berthelot
jeanmarie.berthelot@chu-nantes.fr

Specialty section:
This article was submitted to Viral Immunology, a section of the journal Frontiers in Immunology

Received: *16 September 2020*
Accepted: *03 November 2020*
Published: *01 December 2020*

Citation:
Berthelot J-M, Lioté F, Maugars Y and Sibilia J (2020) Lymphocyte Changes in Severe COVID-19: Delayed Over-Activation of STING? Front. Immunol. 11:607069. doi: 10.3389/fimmu.2020.607069

INTRODUCTION

To account for the quite different outcomes of coronavirus disease 2019 (COVID-19), including in young people, as well as the lower prognosis of male, obese, and aged patients, we previously put forward the hypothesis that a delayed over-activation of the stimulator of interferon (IFN) genes (STING) pathway, could be central to the pathogenesis of severe COVID-19 (1, 2). This delayed over-activation could be the consequence of gain of function in the cGAS-STING axis, and/or cytosolic damages induced by severe acute respiratory syndrome coronaviruses (SARS-CoV-2) in epithelial, endothelial, or innate cells (1, 2). This hypothesis was partly deduced from the observation that bats withstand SARS-CoV viruses, thanks to a loss of function mutation of STING, associated with higher synthesis of IFN-α and much lower synthesis of IFN-β (3).

This hypothesis would fit with the Kawasaki-like features and high thrombosis rate observed in severe COVID-19 (2). Indeed, over-activation of the STING pathway can lead to the release of IFNβ and tissue factor (through induction of pyroptosis by the STING-gasdermin pathway) in infected epithelial cells and/or endothelium (2).

As functional consequences of DNA sensing by the cGAS-STING pathway differ according to antigen presenting cells or lymphocytes (4), which had not been the focus of previous articles (1, 2), the present review aims: i) to study arguments for a possible contribution of over-activation of the cGAS-STING pathways to the disturbances of T and B cell responses observed in previous SARS-CoV, and in severe COVID-19 (**Table 1**); ii) to raise further hypotheses to test in COVID-19 (**Table 2**).

In Vivo Infection of T Cells by SARS-CoV-2 Has Not Yet Been Demonstrated

SARS-CoV-2 invades most host cells *via* binding of its structural spike glycoprotein to angiotensin-converting enzyme 2 (ACE2) (5, 6). Although ACE2 is upregulated by type I IFN and IFN-γ, and to a lesser extent type II IFNs (7), but not type III IFN (8), it is usually not expressed in immune cells (5, 6), especially in T and B cells.

TABLE 1 | Similarities in T and B cells features in severe coronavirus disease 2019 (COVID-19), and STING over-activation, including SAVI (STING-associated vasculopathy with onset in infancy) syndromes.

	Severe COVID-19	STING overactivation
Differentiation at onset	Th2	Th2
T cells phenotype	Exhausted	Exhausted
T cell counts	Marked lymphopenia	Marked lymphopenia
T cell apoptosis	Increased	Increased
Tregs	Reduced number	Reduced number
B cell counts	Declined	Declined
Antibodies	Poorly efficient	Deficiency (in mice)
Myeloid cells	Expansion	Expansion
IL-6 levels	High	High
Pneumonitis	Worsened by T cells	Worsened by T cells

Nevertheless, it was shown that some immune cells, including T cells, can be infected by the SARS-CoVs and middle-east respiratory syndrome coronavirus (MERS-CoVs) (9, 10) [although they poorly replicate in lymphocytes (9)]. This suggests that other receptors can contribute to entry of those SARS-CoVs in some lymphocytes. A first possibility could be CD147 [also known as basigin (5, 11)]. CD147 is strongly expressed in whole blood, neutrophils, classical monocytes, macrophages, plasmacytoid dendritic cells, NK cells, naïve CD4+ T cells, terminal effector CD4+ T cells, naïve CD8+ T cells, effector memory CD8+ T cells, naïve B cells, and plasmablasts (5, 12). It has also been suggested that CD147 could act as a secondary receptor for SARS-CoV-2 in T cell lines (10) (**Table 2**).

CD26 (DPP4) is another receptor important in SARS-CoV infections, described in MERS-CoV, and potentially recognizing SARS-CoV-2 (13). Similar to CD147, CD26 is expressed in nearly all immune cells, but, contrary to CD147, not in B cells (5).

However, contributions of CD147 and CD26 to COVID-19 still remain unproven, and ACE2 should be still considered as the only receptor for SARS-CoV-2 (14) (**Figure 1**).

The STING Pathway Modulate Various T Cells Functions

STING Is the Major Sensor of Self and Foreign Cytosolic DNA

STING is a pattern recognition receptor localized in the endoplasmic reticulum (ER) membrane. The cGAS-STING pathway plays a central role in sensing cytosolic DNA upon infection with DNA from bacteria and DNA-viruses (including endogenous retroviruses). Lack of expression of STING by some cell types contribute to preferential homing of DNA viruses. For instance, hepatitis B virus has a tropism for human hepatocytes, which have undetectable levels of STING protein (15).

Those DNA viruses can reduce STING signaling by increasing autophagy-mediated turnover of STING or interfering with STING trafficking. They can also interfere with IRF signaling and antiviral IFN I responses, rather than with NF-κB responses. For instance, herpes-virus 1 (HSV-1), reduce the ratio of full-length human STING/truncated STING isoforms,

Abbreviations: ACE2, angiotensin-converting enzyme 2; AhR, aryl hydrocarbon receptor; BCR, B cell receptor; cGAS, protein cyclic GMP-AMP synthase; CIVD, common variable immune deficiencies; cTfh, circulating T follicular helper cells; COVID-19, coronavirus disease 2019; EBV, Epstein-Barr virus; ER, endoplasmic reticulum; GATA-3, GATA3 binding protein; ICU, intensive care units; IDO, indoleamine 2,3 dioxygenase; IFIT3, IFN induced protein with tetratricopeptide repeats 3; IFN, interferon; ISG, IFN-stimulated genes; MAVS, mitochondrial antiviral signaling protein; MDA-5, melanoma differentiation-associated protein 5; MERS-CoV, middle-east respiratory syndrome coronavirus; mTORC1, mammalian target of rapamycin complex 1; NETs, neutrophil extracellular traps; NFκB, nuclear factor-kappa B; NKG2A, NK group 2 member A receptor; NKRF, NF-κB-repressing factor; nsp, non-structural proteins; PAMPs, pathogens-associated molecular patterns; PD-1, programmed cell death 1; PHEV, porcine hemagglutinating encephamomyelitis virus; RIG-1, retinoic acid-inducible gene; SARS-CoV, severe acute respiratory syndrome coronaviruses; SAVI syndrome, STING-associated vasculopathy with onset in infancy; STIM1, Ca2+ sensor stromal interaction molecule 1; STING, stimulator of interferon genes; TBK1, TANK-binding kinase 1; TCR, T cell receptor; TIM-3, T-cell immunoglobulin and mucin containing protein-3; ULK1, Unc-51 like autophagy activating kinase 1; UPR, unfolded protein response.

TABLE 2 | Questions and hypotheses to address.

1. Can some subsets of T cells be infected by SARS-CoV-2, following expression of CD147 or CD26, especially activated and exhausted memory T cells?
2. Does SARS-CoV-2 reduce the ratio of full-length wild-type human STING/truncated STING isoforms in antigen presenting cells at early stages of COVID-19?
3. Does SARS-CoV-2 activate aryl hydrocarbon receptor, like α-coronaviruses do?
4. In COVID-19, is IFN-β more detrimental than helpful when given to patients already admitted in ICU units?
5. Do Jak-inhibitors enhance or reduce the replication of SARS-Cov2 *in vitro* and *in vivo* together with the α and β IFNs levels?
6. Is the subdomain within the C terminus domain (CTT) of STING (miniCTT) different in patients with severe COVID-19?
7. Are GM-CSF+ CD4 T cells capable of prodigious ex vivo IL-6 and IFN-γ production in critically ill COVID-19 patients infected by SARS-CoV-2?
8. Is IL-6 negative feedback on cGAS-STING activation abolished in severe SARS-Cov infections by inhibition of ULK1 (and autophagy) by the SARS-CoV viruses?
9. Is this defect increased by concurrent infections by herpes-viruses?
10. Which mechanisms are mostly responsible for the down-regulation of STING activity in T and B cells, as compared to myeloid immune cells and non-immune cells: trafficking, degradation, miRNA-mediated repression, or post-translational modifications?
11. Are Tregs even more prone to exhaustion and/or lymphopenia than effector T cells in mouse or humans with gain of function mutations of STING?
12. Does gain of function and/or activation of some STING-pathways in helper T cells, including Tfh, lead to their premature apoptosis and contribute to the rather short duration of antibodies towards SARS-CoV infections?
13. Is the functionality of some STING pathways impaired in subsets of memory B and T cells in SAVI syndromes and COVID-19?
14. Does concurrent EBV and SARS-CoV-2 infections in B cells increase the exhaustion of T lymphocytes by over-activated presenting B cells?
15. Is miR-576-3p deficient in T cells from severe COVID-19?

induced by alternative splicing of STING RNAs. The three STING truncated isoforms fail to induce IFN-β, and they act as selective pathway inhibitors of full-length STING, even in combination with upstream inducer cyclic-di-GMP-AMP synthase (16).

Importantly, although mainly a DNA sensor, STING is also necessary for full control of enveloped RNA viruses, like influenza virus and coronaviruses, independently of cGAS. Indeed, sensing of lipid membrane fusion through STING also contributes to the antiviral response against enveloped RNA viruses, so that complete protection against RNA viruses also relies on STING (17). STING can also participate in viral RNA sensing through its interaction with the mitochondrial antiviral signaling protein (MAVS) (17). STING further transduces the signaling induced by RNA-derived PAMPs through retinoic acid-inducible gene (RIG-I)-like sensors (RIG-I and melanoma differentiation-associated protein 5 (MDA-5) (17) (**Figure 1**).

Multiple *Flaviviridae* (including zikaviruses, dengue virus, West Nile virus, Japanese encephalitis virus) and hepatitis C virus disrupt STING-mediated signaling (18). Some do so by cleaving STING or cGAS, but others only interfere with the STING-TBK1 interaction (18), explaining why the IFN axis can be affected but not the NF-κB axis (19).

So far, there is no evidence that betacoronaviruses increase autophagy-mediated turnover of STING, interfere with STING trafficking, or cleave STING or cGAS. However, it has been shown that various SARS-CoV-2 protases [non structural protein 3 (NSP3) and NSP16] strongly inhibit the downstream STING-TBK1-IRF3 pathway and IFN synthesis (20). Conversely, SARS-CoV-2 NSP9 and NSP10 protases still increase signaling and IL-6 production by inhibition of NKRF, an endogenous NF-κB repressor (21) (**Figure 1**).

Importantly, STING also senses intra-cellular damaged self-DNA [mitochondrial DNA, and self-dsDNA released in extra-cellular space, including dsDNA from neutrophil extracellular traps (NETs) (22)] secondary to bacterial or viral infections. Therefore, at late stages of RNA viruses infection, the evasion of STING by RNA viruses can be counterbalanced by its activation following released of damaged self-DNA (**Figure 1**).

Upon recognition of non-self (microbial) DNA or self-DNA, the cyclic-GMP-AMP synthase (cGAS) of the host catalyzes the production of cyclic dinucleotides, like cGAMP (from GMPs and AMPs) (**Figure 1**). The length of DNA, rather than its sequence, determines its ability to generate cGAMP following recognition by cGAS (23). Since the endogenous DNA fragments are often short in size, whereas viral and bacterial DNA fragments are generally much longer, this can partly permit discrimination between self and non-self DNA. However, a large amount of self-DNA in cytoplasm outside of the nucleus or mitochondria can also activate the cGAS-STING pathway.

Once activated, STING recruits TANK-binding-kinase (TBK1), which can activate and phosphorylate IFN-regulatory factor 3 (IRF3), to induce type-I IFNs. Those type I IFN then engage the IFN I receptor, thereby activating the JAK/STAT pathways and inducing the transcription of IFN-stimulated genes (ISGs) (23). As the STING gene is itself an ISG, a positive feedback loop can ensue (24). This STING-TBK1-IRF3 axis can be selectively inhibited by viral protease in COVID-19 (20).

However, STING is also a cytosolic hub for other pathways, which can be activated independently of the IFN-TBK1-IRF3 axis. For instance, downstream signaling of STING also lead to NF-κB and/or inflammasomes activation, and secretion of various cytokines, like IL-6 and TNF (1, 16), as also observed in COVID-19 (21) (**Figure 1**).

STING is highly conserved throughout evolution, being observed >500 million years ago, and has also other primitive functions than secretion of IFN-I and cytokines to fight viruses or intra-cellular bacteria (23, 25, 26).

First, it activates the process of autophagy (critical for the elimination of DNA and viruses in the cytosol of innate immune cells), independently of TBK1 activation and IFN-I signals (25) (**Figure 1**).

Second, if foreign nucleic acids accumulate despite autophagy, further activation of the STING pathway can lead to growth arrest, up to apoptosis or pyroptosis (23), which can contribute to increase the risk of thrombosis (Figure) (2). Those STING-mediated cell deaths might be critical for preventing pathogen dissemination (23, 26).

Reciprocally, some bacterial pathogens (and possibly some DNA viruses) have learned to exploit those STING-induced deaths to impair T cell response (27). They sort their DNAs into

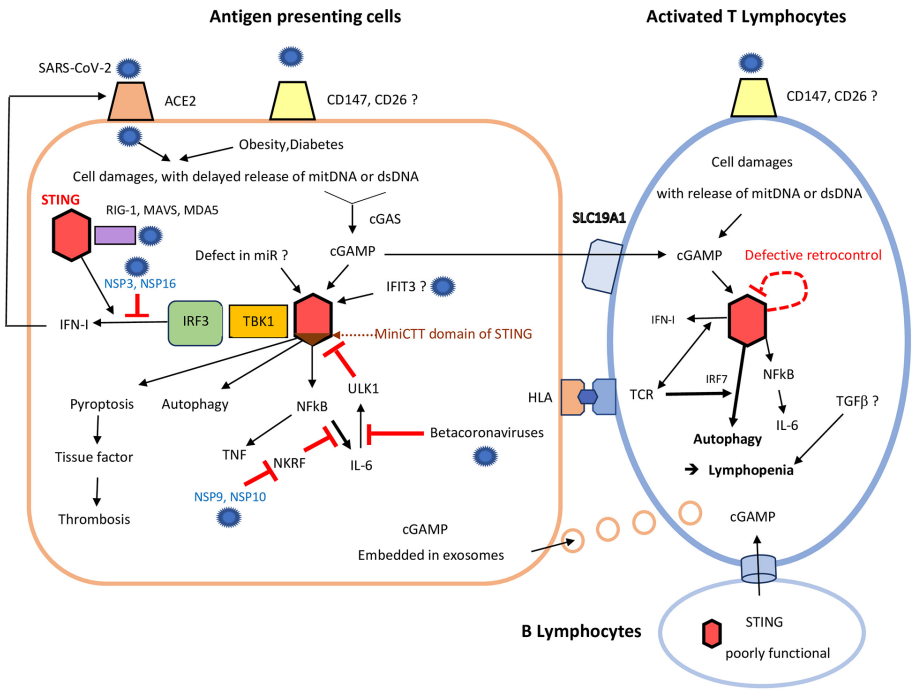

FIGURE 1 | Consequences of STING over-activation on antigen presenting cells and T cells following severe acute respiratory syndrome coronaviruses (SARS-CoV-2) infection. In antigen presenting cells (left), due to poor virus control by RNA sensors (including RIG-1, and MDA5) and despite the help of STING (red hexagon), SARS-CoV-2 induces delayed cell damages, with mitochondrial DNA and dsDNA release. It can add to damaged self-DNA secondary to ageing and/or obesity/diabetes. cGAS catalyzes those self-DNA in cyclic nucleotides, mainly cGAMP, which in turn activates STING (red hexagon). This activation of STING may be enhanced by: i) a lack of miRNAs, (like miR-576-3p, which normally suppress STING translation); ii) excess of IFIT3, which interacts with STING gene to promote its expression. Binding of cGAMP to STING first induces activation of the STING-TBK1-IRF3 pathway, leading to IFN-I synthesis. In COVID-19, the SARS-CoV-2 NSP 3 and 16 lower this IFN secretion, but IFN enhances expression of ACE2 on cell membrane. cGAMP, which can be released to by-stander cells through viral exosomes, can also be transmitted by B cells (low), to activated T cells (right), through specific channels. Independently of the STING-TBK1-IRF3 pathway, binding of cGAMP to STING can also: i) induce pyroptosis; ii) promote autophagy and lymphopenia; iii) activate NF-κB and both TNF and IL-6 synthesis. SARS-CoV-2 NSP 9 and 10 still enhances IL-6 release through inhibition of NKRF. Some beta-coronaviruses can also impede ULK1 and its negative feed-back loop, further enhancing IL-6 secretion. Excess of cGAMP can be internalized by by-stander activated CD4+ and CD8+T cells, which highly express the cGAMP importer SLC19A1. Therefore, even without infection of T lymphocytes, STING activation could also occur in activated T lymphocytes, especially those already stressed by a continuous activation by their hyper-responsive TCR. Defective retro-control of STING (dashed red loop) by IL-6 (see above) could still enhance STING activation in severe COVID-19. In activated T cells, STING overactivation leads to autophagy, up to lymphocyte death. This contributes much to the lymphopenia observed in rodent and human gain of function of STING models, and perhaps also in COVID-19, with subsequent poor virus control.

extracellular vesicles and deliver them to T cells, to excessively stimulate the cGAS-STING pathway, after ingestion, which primes those T cells for apoptosis (27, 28). In HSV-1 infections, STING can also be directly transferred to previously uninfected cells through exosomes (29) (**Figure 1**) in order to force those cells to detect earlier their invasion by HSV-1.

This strategy should less apply to the SARS-CoVs, since they are RNA viruses, less directly recognized by cGAS-STING. However, SARS-CoVs could indirectly tease T cell response through the cGAS-STING pathway. Indeed, viral-induced DNA damage in by-stander cells of T cells (including B cells) can lead to cGAMP synthesis in those neighbor cells (**Figure 1**). Transfer of this cGAMP to T cells can also activate the cGAS-STING pathway in activated CD4+ and CD8+ T cells. Indeed, those activated T cells highly express the cGAMP importer SLC19A1 (whereas naïve T cells do not) (**Figure 1**) (28).

SLC19A1 is a folate-organic phosphate antiporter, and the major transporter of CDNs like cGAMP through the cell membranes, of activated T cells (30). Interestingly, in human cell lines and primary cells *ex vivo*, CDN uptake through SLC19A1 is inhibited by both folates and two anti-folates medications of rheumatoid arthritis and other inflammatory rheumatisms: sulfasalazine and methotrexate (30). Accordingly, the outcome of rheumatoid arthritis with severe COVID-19 treated or not by methotrexate or sulfasalazine could be worth to study, although methotrexate as only limited efficacy against SAVI (STING-associated vasculopathy with onset in infancy) syndromes.

Consequences of cGAS-STING Activation in Murine and Human T Cells

STING Is a Co-Signal Which Modulates Many T Cell Function in Mice

STING is strongly expressed in most cells, except human B cells, and recent studies showed that mouse CD4+ T cells express even higher amounts of STING protein than macrophages and

dendritic cells (28). The activation of mouse T cells upon T cell receptor (TCR) recognition of antigen peptide-MHC is regulated by STING (23, 31), which can modulate various T cell functions, such as cytokine production, cell growth, and differentiation (23). STING can make the mouse T lymphocytes more responsive to ER stress induced by T cell receptor (TCR) signaling. It also leads to lymphocytes death following excessive triggering of TCR, in cells with other sources of ER stress (32, 33).

Some Features of STING Signaling Seem Less Efficient in Human T Cells

In humans, key components of the DNA sensing machinery are expressed in activated T cells, including STING itself (34). However, as compared with other cells (including myeloid immune cell types and non-immune cells), STING seems much less functional in human T cells, at least regarding IFN secretion (**Figure 1**) (18). It has been highlighted in the most recent review on STING that lack of an IFN I response downstream of STING in human T and B lymphocytes is in line with the observation that functional DNA sensing pathway in T and B lymphocytes would lead to continuous IFN I production in those highly proliferative cells and detrimental auto-inflammatory diseases (18).

A compromised expression of the cGAS-STING cascade has also been confirmed in CD8+T cells from cancer patients, with reduced stem-like central memory CD8+T cells subsets (35). This is a selective advantage for survival and growth for cancers (36). Several studies showed that STING re-activation can stimulate antitumor immune responses in numerous cancers, including leukemia, melanoma, glioma, and hepatocellular carcinoma (37).

In HIV patients, resting CD4+ T cells, some of which harbor HIV, are also defective in STING-dependent IFN I production (34). A defective STING pathway may render human T cells vulnerable to other pathogens, due to low production of IFN, including other retroviruses (e.g., human T-lymphotropic virus type 1), or viruses (e.g., VZV and HHV 6) that replicate through a DNA (18). Conversely, other downstream signaling of STING than IFN, like NFκB, are less affected in human T cells, as shown in HIV-1 lymphocytes (38). This is also observed in SAVI syndromes (induced by gain of function of STING), where over-activation of STING by viruses can lead to T cell hyper-responsiveness with IL-6 secretion (as well as T cell exhaustion, and autophagy-induced lymphopenia).

Sources of Activation of STING Within T Lymphocytes

The final sources of cGAMP for the activation of STING in T cells should differ according to the possibility (or not) of a direct infection of T cells by SARS-CoV-2 through CD147 or CD26. Such infection has not yet been demonstrated, but might be searched in subsets of activated T cells of severe COVID-19) (**Table 2**), including memory T cells which upon activation exhibit much greater up-regulation of CD147 than naïve T cells (39) (**Figure 1**).

In such event, STING might be activated by: i) cGAMP incorporated into viral particles during encapsidation in antigen presenting cells, to accelerate STING activation in neighboring T cells and their apoptosis; ii) endogenous cGAMP synthetized from damaged cytosolic self-DNA within T cells, including virally damaged mitochondrial self-DNA, as shown for dengue virus infected cells (40) (T cells are permissive for dengue virus); iii) a non-canonical mechanism involving lipid membrane alterations, as observed following influenza virus infection in mouse embryonic fibroblast cells (41).

However, even if T cells are not infected by SARS-CoV-2, STING could still be activated within T cells by: iv) exogenous cGAMP released in extra-cellular spaces by dying cells, and internalized by activated CD4+ and CD8+T cells (15) (which highly express the cGAMP importer SLC19A1); v) cGAMP transmitted by B cells to T cells *via* other cellular channels; vi) DNA damages occurring in T cells themselves, including oxidized mitochondrial-DNA (**Figure 1**).

T Cell Responses Observed in Coronavirus Disease 2019 and Following STING Activation

Th2 Differentiation at Early Stages

A Th2 Immune Response Is Observed at Onset of Coronavirus Disease 2019

At 24h after the first clinical signs of COVID-19, interleukins (IL-1α, IL-1β, IL-6, IL-10), and IFNs (IFN-α2, IFN-β1, IFN-II) are significantly elevated, but the cellular sources of those cytokines are probably more epithelial and innate cells than T lymphocytes (42). After several days, naïve lymphocytes differentiate in Th2, in line with the role of eosinophils in fighting RNA viruses [ascribed to the RNAses inside their granules (43)]. Such Th2 profile had previously been described in SARS patients, and lethal outcomes correlated with elevated Th2 cell serum cytokines (44).

A Th2 Immune Response Is Also Induced by STING Activation

The main ligand for STING, cGAMP, can also preferentially induce a Th2 differentiation (23, 45). Co-stimulation of antigen presenting cells and T cells by foreign or self-DNA similarly suppresses T-bet expression, followed by the induction of GATA-3 and Th2 cytokines (23, 45). The extra-cellular self dsDNA of neutrophil extracellular traps (NETs) induced by rhinovirus infection of upper airways is associated with a preferential Th2 response (46). Accordingly, the shift towards a Th2 response in early stages of COVID-19 would fit with STING activation (**Table 1**).

However, the expression of the aryl hydrocarbon receptor (AhR) on T cells following CD28 activation can later shift Th1/Th2 balance towards a Th1 response (45). This could explain why, in lungs of mice models of SAVI syndromes, Th1, rather than Th2, seem to play a critical role in tissue damage and the persistence of inflammation (47). Whether SARS-CoV-2 could activate AhR has not been addressed so far (**Table 2**), but a murine coronavirus does it, contributing to cytokine modulation and viral infection (48).

Exhausted/Senescent Phenotypes Are Observed in Severe Coronavirus Disease 2019, But Also Following STING Over-Activation

In most patients, COVID-19 is a benign and even asymptomatic infection, and recognition of some viral peptides by T cells (including some memory T cells already primed by previous encounter with human or animal coronaviruses) could help innate cells to clear SARS-CoV2. Recent findings using immunospot essay assessing IFNγ production, showed that 6/8 contacts of index patients developed a SARS-Cov-2 specific T cell response lasting up to 80 days against structural and/or accessory SARS-CoV-2 proteins, although none developed antibodies, and all were tested negative by PCR (49).

Conversely, due to genetically encoded differences in innate and/or T cells, or epigenetic changes acquired during life, innate and/or adaptive cells could remain inefficient to clear SARS-CoV-2 in the minor subset of patients with severe COVID-19. Those genetically encoded differences might be loss of function mutations polymorphisms: inborn errors of TLR3- and IRF7-dependent type I IFN immunity have been found in 3.5% of life-threatening COVID-19 pneumonia in patients with no prior severe infections (50). However, gain of function mutations in other genes, including genes of the STING pathways, should also be searched, since delayed over-reaction to virus damage might be as important as poor initial control of SARS-CoV-2.

Exhaustion of T Cell Lymphocytes With Delayed Secretion of IL-6 in Severe Coronavirus Disease 2019

Increased presence of strongly activated T cells, characterized by expression of HLA-DR, CD38, CD69, CD25, CD44, and Ki-67 has been reported in several studies on COVID-19 (51). In intensive care (ICU) units, both virus-specific CD4 and CD8 T cells were detected in all COVID-19 patients (at average frequencies of 1.4 and 1.3%, respectively), with phenotypes suggestive of either CD4 central memory, or CD8 effector memory T cells (52).

Although SARS-CoV-2 restrains antigen presentation by down-regulating MHC class I and II molecules, CD4+ T cells, and even more CD8+ T cells (20, 53), exhibit functional exhaustion/senescent patterns (51). The expression of NK group 2 member A receptor (NKG2A), programmed cell death 1 (PD-1), and T-cell immunoglobulin and mucin containing protein-3 (TIM-3) (51) increased as patients progressed from prodromal to overtly symptomatic stages (54). In critically ill patients, cellular functionality was also shown to be impaired in CD4 and CD8 T cells (20). This could explain why, despite initial over-activation of lymphocytes, at autopsy, patients who succumbed to infection all had high virus levels in the respiratory tract and other tissues (55).

Elevations in CRP (C-reactive protein), strongly associated to interleukin (IL)-6 levels, appear to be unique to COVID-19 patients when compared to other viral infections (20). Those elevated IL-6 levels are associated with ICU admission, respiratory failure, and poor prognosis (20). Various activated and expanded antigen presenting cells, including macrophages and dendritic cells, seem usually responsible for the cytokine storm with high IL-6 secretion, and for the high serum levels of CRP (54). This is in line with previous studies on other betacoronaviruses human infections (SARS-CoV and MERS-CoV). Indeed, most of the exhausted T cells express less cytokines than innate cells, and T cell numbers are negatively correlated to serum IL-6, IL-10, and TNF-α concentration. However, IL-6 increases fairly late during the disease's course | 20] [which much reduces its prognostic value at earlier stages (56)].

A first hypothesis for this delayed raise of IL-6 could be the deferred re-expression of ACE2 receptor (57) on previously infected epithelial cells, following IFN secretion, leading to re-activation of macrophages and dendritic cells (**Figure 1**). A second hypothesis is an increased peripheral blood frequency of a subset of polyclonal GM-CSF+ CD4 T cells capable of prodigious *ex-vivo* IL-6 and IFN-γ production, which has been described in COVID-19, although only in critically ill patients (58).

Over-Activation of the STING-Pathway Can Also Activate T Lymphocytes, and Lead to Secretion of IL-6

Unlike in innate immune cells, cGAMP alone does not induce IFN-I production by mouse naïve CD4+ and CD8+ T cells, since both TCR stimulation and STING activation are required (23). Conversely, in effector CD4+ and CD8+ T cells, the STING activation by cGAMP can lead to IFN-I and probably various cytokines production, even without TCR co-stimulation (although cGAMP-induced IFN-I production is further increased by IL-2 and TCR binding) (23). The amount of IFN-I produced by mouse effector Th1 and activated CD8+ T cells in response to co-stimulation with TCR and cGAMP is even higher than in dendritic cells (23). This is in line with the much greater ability of previously activated T cells to internalize cGAMP from neighbor cells, as compared to naïve T cells (22).

This continuous secretion of IFNs by effector T cells help to clear intra-cellular pathogens at the early stages of viral infections. Early or preventive treatment by IFN-α or IFN-β improved the outcomes of SARS-CoV and MERS-CoV infection in mice and in non-human primates. However, some viruses, including SARS-CoVs, not only can lower IFN production, but can also take advantage of some subtypes of IFN, like IFN-β, to persist in the host at later stages (7). This could explain why in humans, survival rates in MERS-CoV infection were not increased, possibly because those drugs were given too late (59). At this stage, the delayed IFN-β response in some murine models of severe acute respiratory syndrome (SARS) is, on the opposite, associated with excessive influx of pathogenic inflammatory monocytes-macrophages and a much worse prognosis (60) (**Table 2**).

STING over-activation might similarly paradoxically enhance SARS-CoV-2 replication in lung monocytes-macrophages through transient increase secretion of IFN-β. This contributes to T lymphocyte exhaustion up to final fall of IFN-I secretion. Indeed, following infection by gamma-herpesvirus 68 (γHV68), the increased secretion of IFN-I also promoted the replication of this virus in cultured macrophages of a mouse model of gain of

function of STING (N153S) (61). Furthermore, IFN-β can also induce up-regulation of ACE2 in airway epithelia (7) (**Figure 1**). This might fuel new infections by SARS-CoV2, and impair antigen-specific T cell responses to SARS-CoV antigens (60).

The contribution of IFN-β to COVID-19 remains quite uncertain however in humans, since: i) IFN-I over-secretion induced early by STING activation in infected cells is quickly counterbalanced by a strong inhibition of the downstream STING-TBK1-IRF3 pathway by various SARS-CoV-2 protases (**Figure 1**) (20); ii) IFN-I, II and III expression was seemingly not significantly increased in lung tissues infected with SARS-CoV-2 (62); iii) although an increased expression of IFN-I, and IFN-I related genes, were observed in human blood during the first stages of COVID-19, they declined when the patient got worse (63).

Nevertheless, STING activation can lead to nuclear-factor kappa B (NFκB) and cytokine secretion, including IL-6, independently of IFN secretion. First, SARS-CoV-2 non-structural protein (NSP)9 and NSP10 still increase IL-6 production, by inhibition of NF-κB-repressing factor (NKRF), an endogenous NF-κB repressor (21) (**Figure 1**). Second, whereas the induction of IFN-response genes are maximally up-regulated in PBMCs from SAVI patients (exposure to cGAMP brought about no change), conversely, transcription of the genes encoding tumor necrosis factor (TNF) and IL-6 was elevated in unstimulated peripheral blood mononuclear cells (PBMCs) from SAVI patients, and was still augmented on exposure to cGAMP (64). This is reminiscent of what is observed in severe COVID-19 patients (**Table 1**) (65).

A subdomain within the C terminus domain (CTT) of STING (mini_CTT), appears to be required for STING-mediated, TBK1/IRF3-independent, NF-κB activation in a human system (31). This mini_CTT domain might also be required for cGAMP-induced inhibition of mammalian target of rapamycin complex 1 (mTORC1) signals in T cells (**Figure 1**). Accordingly, gain of function of this subdomain of STING could be preferentially studied in young patients with severe COVID-19 (**Table 2**).

Lymphopenia Is an Early Prognosis Factor in Coronavirus 2019, and Is Also Induced by STING Over-Activation

T Cell Lymphopenia and Severe Coronavirus 2019

In COVID-19, a sustained decrease in CD4+ and CD8+ T cells, especially $CD8^+$ T cells, is observed, despite an increase in IL-6, IL-10, IL-2, IFN-γ levels, and neutrophil counts. This fall is even more pronounced in patients requiring ICU (54), whatever the age (42). Decreased counts of NK cells, eosinophils (53), and γδ-T cells (66), are also observed in severe cases (53). In most severe COVID-19, this lymphopenia is associated with atrophy of lymphoid organs (67). Regulatory T cells are moderately increased at the onset of mild COVID-19, but similarly later decline in severe cases (68).

In mild cases, this lymphopenia might partly reflect redistribution of lymphocytes to lymphoid organs and tissues, since IFN-I, IL-6, and TNF-α can promote retention of activated lymphocyte in lymphoid organs (54). However, although some autopsy study showed extensive lymphocyte infiltration in the lungs (55), others observed only found neutrophilic infiltration in the lung (69), or death of lymphocytes in spleen and lymph nodes (70).

This T cell lymphopenia appears to predict morbidity and mortality, even at early stages, while elevated levels of CRP, LDH, D-dimer, as well as decreased blood platelets are only late prognosis factors (20).Therefore, rather than a cytokine storm induced by NF-κB stimulation, a marked and widespread virus-induced lymphopenia may be the real cause of death in many patients (71).

Excess of TGF-Signaling Could Contribute to This Lymphopenia

Among the numerous mechanisms for the functional exhaustion/senescent patterns of T lymphocytes in severe COVID-19, the release of TGF-β1 could contribute to impair T cell function (and may also be responsible for switch in IgG to IgA production observed in COVID-19 patients). TGF-β1 levels are indeed associated with more severe COVID-19 (72). Similar observations were previously made in patients with severe acute respiratory syndrome (SARS): TGF-β1 was continuously up-regulated during the entirety of SARS, and its prolonged over-production was associated with severity of SARS and memory TCD8 depletion (73). Whether STING also increase TGF-β1 signaling has not been directly addressed in humans, but in rodents STING deficiency in liver effectively reduced the severity of hepatic fibrosis, which was closely associated with the inhibition of TGF-β1 signaling (74). Therefore, STING activation could also reinforce some TGF-β functions in humans (75) and contribute to lymphopenia (**Figure 1**).

But T Cell Lymphopenia Is Also a Direct Consequence of STING Over-Activation

In humans, a marked lymphopenia with reduced memory CD4 + and CD8+ T cells in the periphery (23) is a major feature of SAVI syndrome (76). In a knock-in model carrying an amino acid substitution (V154M) in mouse STING (corresponding to a mutation seen in human patients), the mice also developed a severe combined immunodeficiency disease affecting B, T, and NK cells, with a significant compensatory expansion of monocytes and granulocytes (77). This phenotype is reminiscent of what is observed in severe COVID-19 (**Table 1**).

B- and T-cell developments were blocked since early immature stages, either in bone marrow or thymus (77). Excess of IFN-I (31) does not contribute to this lymphopenia. Signs of inflammation in lungs and kidneys were also IFN-independent (77), and probably driven by over-reactivity of the TCR (32, 78). This is in line with the observation that in mice STING-associated vasculopathy, STING regulates T cell proliferation in cell culture, independently of IRF3 (32).

Radiations chimeras confirmed that T cell lymphopenia depends on T cell intrinsic expression of the SAVI mutation (79). Co-stimulation of CD4+ T cells by STING and TCR

activation can induce growth arrest and lymphopenia by inhibiting mammalian target of rapamycin complex 1 (mTORC1) activation (**Table 1**). This STING-mediated inhibition of mTORC1 signals following TCR activation is partly dependent on both IFN regulatory factor 3 (IRF3) and IFN regulatory factor 7 (IRF7) (**Figure 1**), but not on TBK1 and IKKε (23). The identification of this unique pathway in T cells is critical for the development of new therapeutic strategies for targeting STING in T cells, and to prevent lymphopenia (23).

STING mutants also induce chronic activation of ER stress and unfolded protein response (UPR) within T lymphocytes. STING-N154S disrupts calcium homeostasis in T cells, and primes them to become hyper-responsive to T cell receptor signaling induced ER stress, leading to cell death, both in CD4+ and CD8+ T cells (32, 78). The mouse CD4+ and CD8+ T cell death through ER stress can be restored (as well as lung disease) by changing TCR specificity (36).

cGAMP-induced STING activation can also lead to the inhibition of IL-2 signaling pathways, which decreases the synthesis of regulatory T cells (Tregs) (23) (**Table 1**).

This T Cell Lymphopenia Can Be Partly Reversed by IL-7

Interleukin 7 (IL-7) is essential for lymphocyte survival and expansion (80). IL-7 therapy has been shown to restore lymphocyte counts and functional activity, leading to decreased viral load and clinical improvement in several life-threatening viral infections (71). The effect of compassionate use of IL-7 in 12 critically ill patients with COVID-19 and severe lymphopenia was compared to the outcome of 13 matched controls who did not benefited from IL-7. IL-7 was associated with a restored lymphocyte count, with the IL-7 group having levels more than two-fold greater than the control group (71). However, functional defects of the exhausted lymphocytes could persist, since at day 30, mortality was 42 and 46%, respectively.

The Human STING-Associated Vasculopathy With Onset in Infancy Syndromes, Induced by Gain of Function Mutation of STING, Share Other Features Than T Cell Exhaustion and Lymphopenia, With Severe Coronavirus 2019, Including Pneumonitis

SAVI syndromes share other striking similarities with COVID-19: a variable combination of fever, rashes, an inflammatory vasculopathy mimicking lupus chilblains, up to vaso-occlusive process and acral necrosis, and pulmonary inflammation leading to interstitial lung disease (64).

In STING N153S SAVI-like mice model, mice lacking adaptive immunity had no lung disease, and T-cell receptor β chain $(Tcrb)^{-/-}$ STING N153S animals only had mild disease (79). Therefore, T cell over-response seems important for lung disease induction, despite the concurrent lymphopenia induced by STING over-activation (79). Crossing those mice to animals lacking cGAS, IRF3/IRF7, IFN-alpha/beta receptor alpha chain (IFNAR1), adaptive immunity, αβ T cells, and mature B cells, showed that lung disease developed independently of cGAS, IRF3/IRF7, and IFNAR1, suggesting that other triggers than cyclic dinucleotides (the ligands of cGAS) and/or IFN, contribute to STING over-activation within T cells (79). A defective retro-control of STING (**Figure 1**) might be one explanation for those findings, either in patients with gain of function of STING, and/or severe COVID-19.

In normal cells, IL-6 is a negative feed-back regulator of STING induced by double-stranded DNA, since IL-6 promotes STING degradation by activating/dephosphorylating UNC-51-like kinase (ULK1) (65) (**Figure 1**). It would be worth testing the hypothesis that this feedback is mitigated in severe COVID-19 by modulation of autophagy (81), and inhibition of molecules like ULK1 by SARS-CoVs (**Table 2**), in as much they can infect activated/memory T cells expressing CD147. Indeed, HSV-1 can inhibit ULK1 to escape the autophagy process (82), and previous studies on other betacoronaviruses showed that, upon cell infection, these viruses inhibit macro-autophagy (83). For instance, the porcine hemagglutinating encephalomyelitis (PHEV) betacoronavirus inhibits the expression of the ULK1 protein (84). Such virally induced lack of negative feedback on STING expression might indeed contribute, together with gain of function variants of the cGAS-STING pathway variants, to a delayed increase of STING activation in activated CD4+ or CD8+ memory T cells following infection by betacoronaviruses, and worse pneumonitis.

The paradoxical poor control of virus in lung macrophages of SAVI models is partly due to excess of IFN-I and II, as deduced by a strong increase of expression of IFN-stimulated genes, which leads to ACE2 over-expression (**Figure 1**). The over-response of some T cell subsets to viral antigens in the lung of SAVI and COVID-19, with subsequent fibrosis (61), could also be the consequence of an imbalance between effector T cells and Tregs. Normally, cytosolic DNA sensing *via* the STING/IFN-β pathway also induces indoleamine 2,3 dioxygenase (IDO). IDO then catabolizes tryptophan to suppress effector and helper T-cell responses and activate Foxp3-lineage CD4(+) Tregs (85). However, Tregs might be even more prone to exhaustion and/or lymphopenia than effector T cells in mouse or humans with over-activation of cGAS-STING, since marked decreases of Tregs have been reported in severe COVID-19 (51) (**Table 2**).

B Cell Responses

B Cell Responses in Coronavirus Disease 2019

Like T cells counts, blood B cells count decline with COVID-19 severity [lower counts being associated with increased length of virus shedding (86)], albeit B cell lymphopenia is much less pronounced than T cell lymphopenia (25, 87).

Like T cell, B cells are markedly activated, with highly oligoclonal B cell populations, and profound CD27+CD38+ plasmablasts expansion in some patients. This plasmablast expansion is uncorrelated with decreases in memory B cell subsets, or with the limited changes observed in the circulating T follicular helper cells (cTfh) compartment (87). Long-term studies on serology kinetics in SARS-CoV and MERS-CoV

infections, showed that most IgG were neutralizing but waned over time, and usually in less than 3 years, with longer durations of detectable antibody associated with more severe symptoms (88). Whether gain of function and/or activation of STING in subsets of cTfh cells leading to their premature apoptosis due to hyperresponsiveness to TCR signals, contribute to this rather short duration of antibodies towards SARS-CoV infections has not been addressed so far (**Table 2**).

Sero-conversion occurs between 7 and 14 days after the onset, but this robust antibody response alone is insufficient to avoid severe COVID-19 (20). The high levels of anti-SARS-CoV-2 antibodies in aged COVID-19 do not prevent from severe clinical outcomes, and COVID-19 ICU patients often have high titers SARS-CoV-2 specific antibodies (89).

Another argument suggesting that antibodies might be less important than T cells to control SARS-CoV-2 is the possibility of only mild COVID-19 in patients with severe hypogammaglobulinemia. In a report on seven patients (32 to 79 years-old) with primary antibody deficiencies and COVID-19, five had common variable immune deficiencies (CVIDs) (dysfunctional B lymphocytes), and two had agammaglobulinemia (lacking B lymphocytes). All were substituted and had similar immunoglobulins levels. Whereas the two patients with agammaglobulinemia had a benign COVID-19 course, the five patients with CVIDs presented with a severe form of COVID-19, requiring treatment with multiple drugs, including IL-6–blocking drugs and mechanical ventilation (90). This suggests an active contribution of over-activated but pathogenic subsets of T-bet+ B cells in severe COVID-19 (87), in line with the observation that the granulomatous-lymphocytic interstitial lung diseases occurring in 10% of patients with CVID are partially reversed by B-cell–depleting drugs (90).

B Cell Responses and STING

In Mice

B cell receptor (BCR) and STING signaling pathways act synergistically to promote antibodies responses independent of type I IFN (91). However, STING functions autonomously in B cells responding to CDNs, and can be activated by cGAMP without the need of previous BCR ligation (91). This can lead to IFN-β production (92), while IFN-I expression by B cells induces an altered polarization of macrophages toward a regulatory/anti-inflammatory profile, at least *in vitro*, that might benefit to some pathogens (93).

Mitochondria-mediated apoptosis induced by STING is also more pronounced in normal mouse B cells than in other cells, since upon stimulation, STING is degraded less efficiently in B cells (94).

In Humans

Activation of MHC class II in human B cells is associated with enhancement of STING signaling (95). However, whereas STING is strongly expressed in mice B cells, in resting humans B cells, STING is poorly expressed and dysfunctional (**Figure 1**), despite the detection of DNA sensing and signaling proteins of the STING pathway [cGAS, gamma-IFN-inducible protein (IFI16), TBK1 and IRF3] (96). The very poor expression of STING in human SAVI B cells could explain why in humans SAVI severe B lymphopenia and hypo-gammaglobulinemia are not observed [whereas in knock-in mice poor B cell development and an almost complete lack of antibodies are found (77)].

This lack of STING signaling in human B cells might be an explanation for the use of B cells as a reservoir for persistent infection by Epstein-Barr virus (EBV), and other human gamma-herpesviruses (96). Consequently, although human B cells appear equipped to sense invading DNA viruses by other sensors than cGAS-STING, yet they fail to induce an IFN-I response upon cytoplasmic DNA exposure in EBV-negative B cells. EBV-transformed B cell lines do express STING, but these lines, as well as STING-reconstituted EBV-negative B cells, do not produce more IFN-I upon dsDNA or cGAMP stimulation than EBV-negative lines, showing that the cytoplasmic cGAS-STING pathway remains dysfunctional, even in EBV-positive human B cells (96).

Of note, a similar abrogation of signal transduction downstream of STING phenomenon has been reported for some subsets of activated human T lymphocytes that produce substantial levels of STING protein (34), and it might also be worth to study the functionality of the STING pathway in all subsets of memory B and T cells in COVID-19 (**Table 2**).

Although they poorly express STING, B lymphocytes could indirectly contribute to activate STING in other T cells in COVID-19. Indeed, to alert other cells of viral infections, triggering of cGAS in infected B cells can result in cGAMP production and packaging, and subsequent transfer of this danger message to other cells, including activated T cells (97) (**Figure 1**).

Consequently, B cells infected by SARS-CoV might contribute to T cell activation and exhaustion in COVID-19, and possibly more frequently in EBV positive patients, which could also contribute to explain why young children have usually much less severe COVID-19 than adults (**Table 2**).

DISCUSSION: SCENARIO FOR T CELLS AND B CELLS RESPONSE IN COVID-2019

The striking similarities between clinical and biological features of SAVI syndromes and severe COVID-19, as well as other studies on the role of STING on T and B lymphocytes (**Table 1**), support the hypothesis of some delayed over-signaling downstream of cGAS-STING in severe COVID-19, despite initial inhibition of the STING-TBK1-IRF3 axis (and IFN secretion) by papain-like-proteases contained within the NSP3 and NSP16 proteins (98) (**Figure 1**).

A lower IFNα/IFN-β ratio downstream of STING could also promote the replication of SARS-CoV, including SARS-CoV-2, as observed in mice models of SARS-CoV and MERS-CoV (60, 99). Parallel activation of macrophages, dendritic cells, and B cell up to exhaustion, might also lead to excessive triggering of TCR and STING from CD4+ and CD8+ and NK cells, leading to their exhaustion and deaths, and further spreading of SARS-CoV-2.

Cases of severe COVID-19 in very young children suggest that some genetically encoded, and perhaps not yet described, gain of function mutations of the cGAS-STING pathway could be a first explanation for severe SARS-CoV-2 infections in the young. However, most old patients with severe COVID-19 never exhibited previous features of SAVI syndromes, so that other explanations than mutations of cGAS-STING must be discussed, which might also be more specific for SARS-CoV infections.

The first one is mutants in various other molecules controlling the STING pathways. For instance, the Ca2+ sensor stromal interaction molecule 1 (STIM1) ensures correct localization of STING at the ER, and its down-regulation should enhance STING activation (100). A more attractive candidate is IFN induced protein with tetratricopeptide repeats 3 (IFIT3) (**Figure 1**), which is highly up-regulated in SARS-CoV-2 infected bronchial epithelial cells (101): IFIT3 interacts with both STING and TANK-binding kinase 1 genes, and activate them in some disorders like lupus (102).

The second explanation could be poor control of STING expression levels by microRNAs (miRNAs) (**Figure 1**). Induction of miR-576-3p (only present in higher primates: humans, chimpanzee, bonobos, gorilla, and orangutan) by IRF3 and IFN-β triggers a feedback mechanism to suppress STING translation and reduce IFN expression (103). During RNA and DNA virus infections, miR-576-3p sets an antiviral response threshold to likely avoid excessive inflammation (103). Deficient production of miR-576-3p has not yet been searched in severe COVID-19 (**Table 2**).

Therefore, the third and most attractive hypothesis so far is a delayed over-activation of the cGAS-STING pathway, due to a rebound effect following initial STING inhibition by viral proteases. This could occur when damaged self-DNA and mitochondrial DNA [especially in elderly patients, or patients with metabolic disorders (1, 104)], combine with STING over-activation induced by transfer of cGAMP and/or STING from infected antigen presenting cells to T cells (**Table 2**) (**Figure 1**).

This rebound effect might be even more severe in patients with mitigated negative feed-back of STING activation by IL-6, induced by disturbances of the autophagy processes, secondary to ULK1 inhibition by beta-coronaviruses, especially in T cells (65, 81) (**Figure 1**). Lymphopenia, a predictor of poor prognostic, is reversed in 1 week by tocilizumab injection (105). The T CD4+, T CD8+, and NK cells reduced anti-viral cytokine production capabilities and cytotoxic potential, are also partially restored by inhibition of IL-6 by tocilizumab (53). However, inhibition of IL-6 has not yet demonstrated its ability to reduce the death rate in severe COVID-19, although it was associated with seemingly better outcomes of COVID-19 in patients who survived (106). A defect of the negative feed-back of STING activation by IL-6 in most severe cases might contribute to explain those observations.

Confirmation of a delayed over-activation of the STING pathways in severe COVID-19 would prompt to test drugs already designed to specifically and timely control STING activation (107), like endogenous nitro-conjugated linoleic acid (NO2-cLA) (108). Although a reduced release of IFN-I has already been confirmed, those drugs should be tested first in animal models of STING gain of function, to make sure that they also correct STING-induced lymphopenia and NFκB over-activation (108). They may be added to vitamin-D and aspirin, which probably also prevent STING over-activation (2).

STING is indeed a "hub" of the immune response, not restricted to the TBK1-IRF3 pathway, and a driver of cell death, including T lymphocytes death. Directly targeting STING might be more efficient to restrain the delayed cytokine storm and prevent lymphopenia, pneumonitis, and vasculopathy, than blocking only a single cytokine like IL-6. Direct inhibition of STING delayed over-activation in severe COVID-19 might also better protect from premature apoptosis of memory central T cells, and early (109), or late recurrences of SARS-CoV-2 infections, even in young patients.

The striking similarities noticed between SAVI syndromes and signs of severe COVID-19 including pneumonitis (1), inflammatory vasculopathies with acral thrombosis or Kawasaki-like features (2), and the lymphocyte changes described above, are not evidences that the cGAS-STING axis plays a central role in COVID-19 pathogenesis. However, those numerous analogies could prompt to study the contribution of STING activation in T and B cells changes observed during severe COVID-19, and to address some of the questions listed in **Table 2**.

This could reinforce the rationale of using drugs preventing from over-activation of STING to treat COVID-19, including as cheap and well tolerated drugs as vitamin-D and aspirin (2). Interestingly, in a large retrospective study performed in American ICUs, even low-dose aspirin seemed to decrease by half mechanical ventilation, ICU admission, and in-hospital mortality in hospitalized patients with COVID-19 (110). If confirmed by prospective studies, this finding would have major consequences on the future of the COVID-19 pandemic.

DATA AVAILABILITY STATEMENT

The original contributions presented in the study are included in the article/supplementary material. Further inquiries can be directed to the corresponding author.

AUTHOR CONTRIBUTIONS

J-MB and JS had the original idea, and J-MB wrote the first draft of the article. JS, YM, and FL extensively corrected it and suggested new references. All authors contributed to the article and approved the submitted version.

ACKNOWLEDGMENTS

To Prof. Pierre Youinou for further incentive.

REFERENCES

1. Berthelot JM, Lioté F. COVID-19 as a STING Disorder With Delayed Over-Secretion of Interferon-Beta. *EBioMedicine* (2020) 23(56):102801. doi: 10.1016/j.ebiom.2020.102801
2. Berthelot JM, Drouet L, Lioté F. Kawasaki-like Diseases and Thrombotic Coagulopathy in COVID-19: Delayed Over-Activation of the STING Pathway? *Emerg Microbes Infect* (2020) 23:1–26. doi: 10.1080/22221751.2020.1785336
3. Xie J, Li Y, Shen X, Goh G, Zhu Y, Cui J, et al. Dampened STING-Dependent Interferon Activation in Bats. *Cell Host Microbe* (2018) 23:297–301.e4. doi: 10.1016/j.chom.2018.01.006
4. Huang L, Li L, Lemos H, Chandler PR, Pacholczyk G, Baban B, et al. Cutting Edge: DNA Sensing via the STING Adaptor in Myeloid Dendritic Cells Induces Potent Tolerogenic Responses. *J Immunol* (2013) 191(7):3509–13. doi: 10.4049/jimmunol.1301419
5. Radzikowska U, Ding M, Tan G, Zhakparov D, Peng Y, Wawrzyniak P, et al. Distribution of ACE2, CD147, CD26 and Other SARS-CoV-2 Associated Molecules in Tissues and Immune Cells in Health and in Asthma, COPD, Obesity, Hypertension, and COVID-19 Risk Factors. *Allergy* (2020) 75:2829–45. doi: 10.1111/all.14429
6. Sun SH, Chen Q, Gu HJ, Yang G, Wang YX, Huang XY, et al. A Mouse Model of SARS-CoV-2 Infection and Pathogenesis. *Cell Host Microbes* (2020) 2020:S1931–3128(20)30302-4. doi: 10.1016/j.chom.2020.05.020
7. Ziegler CGK, Allon SJ, Nyquist SK, Mbano IM, Miao VN, Tzouanas CN, et al. SARS-CoV-2 Receptor ACE2 Is an Interferon-Stimulated Gene in Human Airway Epithelial Cells and Is Detected in Specific Cell Subsets across Tissues. *Cell* (2020) 181:1016–35.e19. doi: 10.1016/j.cell.2020.04.035
8. Busnadiego I, Fernbach S, Pohl MO, Karakus U, Huber M, Trkola A, et al. Antiviral Activity of Type I, II, and III Interferons Counterbalances ACE2 Inducibility and Restricts SARS-CoV-2. *mBio* (2020) 11(5):e01928–20. doi: 10.1128/mBio.01928-20
9. Chu H, Zhou J, Wong BHY, Li C, Chan JFW, Cheng ZS, et al. Middle East Respiratory Syndrome Coronavirus Efficiently Infects Human Primary T Lymphocytes and Activates the Extrinsic and Intrinsic Apoptosis Pathways. *J Infect Dis* (2016) 213(6):904–14. doi: 10.1093/infdis/jiv380
10. Gu J, Gong E, Zhang B, Zheng J, Gao Z, Zhong H, et al. Multiple organ infection and the pathogenesis of SARS. *J Exp Med* (2005) 202(3):415–24. doi: 10.1084/jem.20050828
11. Wang K, Chen W, Zhou YS, Lian JQ, Zhang Z, Du P, et al. SARS-CoV-2 invades host cells via a novel route: CD147-spike protein. *BioRxiv Preprint* (2020). doi: 10.1101/2020.03.14.988345
12. Uhlen M, Fagerberg L, Hallstrom BM, Lindskog C, Oksvold P, Mardinoglu A, et al. Proteomics. Tissue-based map of the human proteome. *Science* (2015) 347(6220):1260419. doi: 10.1126/science.1260419
13. Huang W, Luo WJ, Zhu P, Tang J, Yu XL, Cui YC, et al. Modulation of CD147-induced matrix metalloproteinase activity: role of CD147 N-glycosylation. *Biochem J* (2013) 449(2):437–48. doi: 10.1042/BJ20120343
14. Letko M, Marzi A, Munster V. Functional Assessment of Cell Entry and Receptor Usage for SARS-CoV-2 and Other Lineage B Betacoronaviruses. *Nat Microbiol* (2020) 5(4):562–9. doi: 10.1038/s41564-020-0688-y
15. Thomsen MK, Nandakumar R, Stadler D, Malo A, Valls RM, Wang F, et al. Lack of immunological DNA sensing in hepatocytes facilitates hepatitis B virus infection. *Hepatology* (2016) 64:746–59. doi: 10.1002/hep.28685
16. Rodríguez-García E, Olagüe C, Ríus-Rocabert S, Ferrero R, Llorens C, Larrea E, et al. TMEM173 Alternative Spliced Isoforms Modulate Viral Replication Through the STING Pathway. *Immunohorizons* (2018) 11:363–76. doi: 10.4049/immunohorizons.1800068
17. Ishikawa H, Barber GN. STING is an endoplasmic reticulum adaptor that facilitates innate immune signalling. *Nature* (2008) 455:674–8. doi: 10.1038/nature07317
18. Landman SL, Ressing ME, van der Veen AG. Balancing STING in antimicrobial defense and autoinflammation. *Cytokine Growth Factor Rev* (2020) 55:1–14. doi: 10.1016/j.cytogfr.2020.06.004.doi.org/10.1016/j.cytogfr.2020.06.004
19. Sun L, Xing Y, Chen X, Zheng Y, Yang Y, Nichols DB, et al. Coronavirus papain-like proteases negatively regulate antiviral innate immune response through disruption of STING-mediated signaling. *PLoS One* (2012) 7:e30802 (2012). doi: 10.1371/journal.pone.0030802
20. Vabret N, Britton GJ, Gruber C, Hegde S, Kim J, Kuksin M, et al. Immunology of COVID-19: Current State of the Science. *Immunity* (2020) 52:910–41. doi: 10.1016/j.immuni.2020.05.002
21. Li J, Guo M, Tian X, Liu C, Wang X, Yang X, et al. Virus-host interactome and proteomic survey of PMBCs from COVID-19 patients reveal potential virulence factors influencing SARS-CoV-2 pathogenesis. *bioRxiv* (2020). doi: 10.1101/2020.03.31.019216
22. Wang H, Hu S, Chen X, Shi H, Chen C, Sun L, et al. cGAS is essential for the antitumor effect of immune checkpoint blockade. *Proc Natl Acad Sci U S A* (2017) 114:1637–42. doi: 10.1073/pnas.1621363114
23. Imanishi T, Saito T. T Cell Co-stimulation and Functional Modulation by Innate Signals. *Trends Immunol* (2020) 41:200–12. doi: 10.1016/j.it.2020.01.003
24. Ma F, Li B, Yu Y, Iver SS, Sun M, Cheng G. Positive Feedback Regulation of Type I Interferon by the Interferon-Stimulated Gene STING. *EMBO Rep* (2015) 16:202–12. doi: 10.15252/embr.201439366
25. Gui X, Yang H, Li T, Tan X, Shi P, Li M, et al. Autophagy induction via STING trafficking is a primordial function of the cGAS pathway. *Nature* (2019) 567:262–6. doi: 10.1038/s41586-019-1006-9
26. Yap JKY, Moriyama M, Iwasaki A. Inflammasomes and Pyroptosis as Therapeutic Targets for COVID-19. *J Immunol* (2020) 205:307–12. doi: 10.4049/jimmunol.2000513
27. Nandakumar R, Tschismarov R, Meissner F, Prabakaran T, Krissanaprasit A, Farahani E, et al. Intracellular Bacteria Engage a STING-TBK1-MVB12b Pathway to Enable Paracrine cGAS-STING Signalling. *Nat Microbiol* (2019) 4:701–13. doi: 10.1038/s41564-019-0367-z
28. Imanishi T, Unno M, Kobayashi W, Yoneda N, Matsuda S, Ikeda K, et al. Reciprocal Regulation of STING and TCR Signaling by mTORC1 for T-cell Activation and Function. *Life Sci Alliance* (2019), e201800282. doi: 10.26508/lsa.201800282
29. Kalamvoki M, Du T, Roizman B. Cells infected with herpes simplex virus 1 export to uninfected cells exosomes containing STING, viral mRNAs, and microRNAs. *Proc Natl Acad Sci U S A* (2014) 111:E4991–6. doi: 10.1073/pnas.1419338111
30. Luteijn RD, Zaver SA, Gowen BG, Wyman SK, Garelis NE, Onia L, et al. SLC19A1 transports immunoreactive cyclic dinucleotides. *Nature* (2019) 573(7774):434–8. doi: 10.1038/s41586-019-1553-0
31. Cerboni S, Jeremiah N, Gentili M, Gehrmann U, Conrad C, Stolzenberg MC, et al. Intrinsic antiproliferative activity of the innate sensor STING in T lymphocytes. *J Exp Med* (2017) 214:1769–85. doi: 10.1084/jem.20161674
32. Wu J, Chen YJ, Dobbs N, Sakai T, Liou J, Miner JJ, et al. STING-mediated Disruption of Calcium Homeostasis Chronically Activates ER Stress and Primes T Cell Death. *J Exp Med* (2019) 216:867–83. doi: 10.1084/jem.20182192
33. Gulen MF, Koch U, Haag SM, Schuler F, Apetoh L, Villunger A, et al. Signalling strength determines proapoptotic functions of STING. *Nat Commun* (2017) 8:1–10. doi: 10.1038/s41467-017-00573-w
34. Berg RK, Rahbek SH, Kofod-Olsen E, Holm CK, Melchjorsen J, Jensen DG, et al. T cells detect intracellular DNA but fail to induce type I IFN responses: implications for restriction of HIV replication. *PLoS One* (2014) 9:e84513. doi: 10.1371/journal.pone.0084513.10.1371/journal.pone.0084513
35. Li W, Lu L, Lu J, Wang X, Yang C, Jin J, et al. cGAS-STING–mediated DNA sensing maintains $CD8^+$ T cell stemness and promotes antitumor T cell therapy. *Sci Transl Med* (2020) 12:eaay9013. doi: 10.1126/scitranslmed.aay9013
36. Konno H, Yamauchi S, Berglund A, Putney RM, Mule JJ, Barber GN, et al. Suppression of STING signaling through epigenetic silencing and missense mutation impedes DNA damage mediated cytokine production. *Oncogene* (2018) 37:2037–51. doi: 10.1038/s41388-017-0120-0
37. Zheng J, Mo J, Zhu T, Zhuo W, Yi Y, Hu S, et al. Comprehensive elaboration of the cGAS-STING signaling axis in cancer development and immunotherapy. *Mol Cancer* (2020) 19(1):133. doi: 10.1186/s12943-020-01250-1
38. Palermo E, Acchioni C, Di Carlo D, Zevini A, Muscolini M, Ferrari M, et al. Activation of latent HIV-1 T cell reservoirs with a combination of innate

immune and epigenetic regulators. *J Virol* (2019) 93:e01194–19. doi: 10.1128/jvi.01194-19
39. Guo N, Ye S, Zhang K, Yu X, Cui H, Yang X, et al. Critical epitope in CD147 facilitates memory $CD4^+$ T-cell hyper-activation in rheumatoid arthritis. *Cell Mol Immunol* (2019) 16:568–79. doi: 10.1038/s41423-018-0012-4
40. Aguirre S, Luthra P, Sanchez-Aparicio MT, Maestre AM, Patel J, Lamothe F, et al. Dengue virus NS2B protein targets cGAS for degradation and prevents mitochondrial DNA sensing during infection, Nat. *Microbiol* (2017) 2:1–11. doi: 10.1038/nmicrobiol.2017.37
41. Holm CK, Rahbek SH, Gad HH, Bak RO, Jakobsen MR, Jiang Z, et al. Influenza A virus targets a cGAS-independent STING pathway that controls enveloped RNA viruses. *Nat Commun* (2016) 7:1–9. doi: 10.1038/ncomms10680
42. Yao Z, Zheng Z, Wu K, Junhua Z. Immune Environment Modulation in Pneumonia Patients Caused by Coronavirus: SARS-CoV, MERS-CoV and SARS-CoV-2. *Aging (Albany NY)* (2020) 12:7639–51. doi: 10.18632/aging.103101
43. Roncati L, Nasillo V, Lusenti B, Riva G. Signals of T_h2 immune response from COVID-19 patients requiring intensive care. *Hematol* (2020) 99:1419–20. doi: 10.1007/s00277-020-04066-7
44. Li CKF, Wu H, Yan H, Ma S, Wang L, Zhang M, et al. T cell responses to whole SARS coronavirus in humans. *J Immunol* (2008) 181:5490–500. doi: 10.4049/jimmunol.181.8.5490
45. Negishi T, Kato Y, Ooneda O, Mimura J, Takada T, Mochizuki H. Effects of Aryl Hydrocarbon Receptor Signaling on the Modulation of TH1/TH2 Balance. *J Immunol* (2005) 175:7348–56. doi: 10.4049/jimmunol.175.11.7348
46. Toussaint M, Jackson DJ, Swieboda D, Guedán A, Tsourouktsoglou TD, Ching YM, et al. Host DNA Released by NETosis Promotes Rhinovirus-Induced type-2 Allergic Asthma Exacerbation. *Nat Med* (2017) 23:681–91. doi: 10.1038/nm.4332
47. Nündel K, Marshak-Rothstein A. The Role of Nucleic Acid Sensors and Type I IFNs in Patient Populations and Animal Models of Autoinflammation. *Curr Opin Immunol* (2019) 61:74–9. doi: 10.1016/j.coi.2019.08.003
48. Grunewald ME, Shaban MG, Mackin SR, Fehr AR, Perlman S. Murine Coronavirus Infection Activates the Aryl Hydrocarbon Receptor in an Indoleamine 2,3-Dioxygenase-Independent Manner, Contributing to Cytokine Modulation and Proviral TCDD-Inducible-PARP Expression. *J Virol* (2020) 94:e01743–19. doi: 10.1128/JVI.01743-19
49. Gallais F, Velay A, Wendling MJ, Nazon C, Partisani M, Sibilia J, et al. Intrafamilial exposure to SARS-CoV-2 induced cellular immune response without seroconversion. *medRxiv* (2020). doi: 10.1101/2020.06.21.20132449
50. Zhang Q, Bastard P, Liu Z, Le Pen J, Moncada-Velez M, Chen J, et al. Inborn errors of type I IFN immunity in patients with life-threatening COVID-19. *Science* (2020) 370:eabd4570. doi: 10.1126/science.abd4570
51. Paces J, Strizova Z, Smrz D, Cerny J. COVID-19 and the Immune System. *Physiol Res* (2020) 69:379–88. doi: 10.33549/physiolres.934492
52. Weiskopf D, Schmitz KS, Raadsen MP, Grifoni A, Okba NMA, Endeman H, et al. Phenotype of SARS-CoV-2-specific T-cells in COVID-19 patients with acute respiratory distress syndrome. *Sci Immunol* (2020) 5(48):eabd2071. doi: 10.1126/sciimmunol.abd2071
53. Mazzoni A, Salvati L, Maggi L, Capone M, Vanni A, Spinicci M, et al. Impaired Immune Cell Cytotoxicity in Severe COVID-19 Is IL-6 Dependent. *J Clin Invest* (2020) 28:138554. doi: 10.1172/JCI138554
54. Diao B, Wang C, Tan Y, Chen X, Liu Y, Ning L, et al. Reduction and functional exhaustion of T Cells in patients with coronavirus disease 2019 (COVID-19). *Front Immunol* (2020) 11:827. doi: 10.3389/fimmu.2020.00827
55. Xu Z, Shi L, Wang Y, Zhang J, Huang L, Zhang C, et al. Pathological findings of COVID-19 associated with acute respiratory distress syndrome. *Lancet Respir Med* (2020) 8:420–2. doi: 10.1016/S2213-2600(20)30076-X
56. Zhou F, Yu T, Du R, Fan G, Liu Y, Liu Z, et al. Clinical course and risk factors for mortality of adult inpatients with COVID-19 in Wuhan, China: a retrospective cohort study. *Lancet* (2020) 395:1054–62. doi: 10.1016/S0140-6736(20)30566-3
57. Hirano T, Murakami M. COVID-19: A New Virus, but a Familiar Receptor and Cytokine Release System. *Immunity* (2020) 52:731–3. doi: 10.1016/j.immuni.2020.04.003
58. Zhou Y, Fu B, Zheng X, Wang D, Zhao C, Qi Y, et al. Pathogenic T cells and inflammatory monocytes incite inflammatory storm in severe COVID-19 patients. *Natl Sci Rev* (2020), 2020. doi: 10.1093/nsr/nwaa041
59. Shalhoub S, Farahat F, Al-Jiffri A, Simhairi R, Shamma O, Siddiqi N, et al. IFN-alpha 2a or IFN-beta1a in combination with ribavirin to treat Middle East respiratory syndrome coronavirus pneumonia: A retrospective study. *J Antimicrob Chemother* (2015) 70:2129–32. doi: 10.1093/jac/dkv085
60. Channappanavar R, Fehr AR, Vijay R, Mack M, Zhao J, Meyerholz DK, et al. Dysregulated type I interferon and inflammatory monocyte-macrophage responses cause lethal pneumonia in SARS-CoV-infected mice. *Cell Host Microbe* (2016) 19:181–93. doi: 10.1016/j.chom.2016.01.007
61. Bennion BG, Ingle H, Ai TL, Miner CA, Platt DJ, Smith AM, et al. A Human Gain-of-Function STING Mutation Causes Immunodeficiency and Gammaherpesvirus-Induced Pulmonary Fibrosis in Mice. *J Virol* (2019) 93:e01806–18. doi: 10.1128/JVI.01806-18
62. Chu H, Chan JFW, Wang Y, Yuen TTT, Chai Y, Hou Y, et al. Comparative replication and immune activation profiles of SARS-CoV-2 and SARS-CoV in human lungs: An ex vivo study with implications for the pathogenesis of COVID-19. *Clin Infect Dis* (2020) 71:1400–9. doi: 10.1093/cid/ciaa410
63. Hadjadj J, Yatim N, Barnabei L, Corneau A, Boussier J, Pere H, et al. Impaired type I interferon activity and exacerbated inflammatory responses in severe Covid-19 patients. *Science* (2020) 369:718–24. doi: 10.1126/science.abc6027
64. Liu Y, Jesus AA, Marrero B, Yang D, Ramsey SE, Sanchez GAM, et al. Activated STING in a vascular and pulmonary syndrome. *N Engl J Med* (2014) 371:507–18. doi: 10.1056/NEJMoa1312625
65. Wu X, Yang J, Na T, Zhang K, Davidoff AM, Yuan BZ, et al. RIG-I and IL-6 Are Negative-Feedback Regulators of STING Induced by Double-Stranded DNA. *PLoS One* (2017) 12:e0182961. doi: 10.1371/journal.pone.0182961
66. Lei L, Qian H, Yang X, Zhou X, Zhang X, Zhang D, et al. The phenotypic changes of gamma-delta T cells in COVID-19 patients. *J Cell Mol Med* (2020) 24:11603–6. doi: 10.1111/jcmm.15620
67. Terpos E, Ntanasis-Stathopoulos I, Elalamy I, Kastritis E, Sergentanis TN, Politou M, et al. Hematological findings and complications of COVID-19. *Am J Hematol* (2020). doi: 10.1002/ajh.25829
68. Qin C, Zhou L, Hu Z, Zhang S, Yang S, Tao Y, et al. Dysregulation of Immune Response in Patients With Coronavirus 2019 (COVID-19) in Wuhan, China. *Clin Infect Dis* (2020) 71:762–8. doi: 10.1093/cid/ciaa248
69. Tian S, Xiong Y, Liu H, Niu L, Guo J, Liao M, et al. Pathological study of the 2019 novel coronavirus disease (COVID-19) through postmortem core biopsies. *Mod Pathol* (2020) 33:1007–14. doi: 10.1038/s41379-020-0536-x
70. Chen Y, Feng Z, Diao B, Wang R, Wang G, Wang C, et al. The Novel Severe Acute Respiratory Syndrome Coronavirus 2 (SARS-CoV-2) Directly Decimates Human Spleens and Lymph Nodes. *medRxiv* (2020). doi: 10.1101/2020.03.27.20045427
71. Laterre PF, François B, Collienne C, Hantson P, Jeannet R, Remy KE, et al. Association of Interleukin 7 Immunotherapy With Lymphocyte Counts Among Patients With Severe Coronavirus Disease 2019 (COVID-19). *JAMA Netw Open* (2020) 3(7):e2016485. doi: 10.1001/jamanetworkopen.2020.16485
72. Ghazavi A, Ganji A, Keshavarzian N, Rabiemajd S, Mosayebi G. Cytokine profile and disease severity in patients with COVID-19. *Cytokine* (2020) 137:155323. doi: 10.1016/j.cyto.2020.155323
73. Huang JL, Huang J, Duan ZH, Wei J, Min J, Luo XH, et al. Th2 predominance and CD8+ memory T cell depletion in patients with severe acute respiratory syndrome. *Microbes Infect* (2005) 7:427–36. doi: 10.1016/j.micinf.2004.11.017
74. Luo X, Li H, Ma L, Zhou J, Guo X, Woo SL, et al. Expression of STING is increased in liver tissues from patients with NAFLD and promotes macrophage-mediated hepatic inflammation and fibrosis in mice. *Gastroenterology* (2018) 155:1971–1984.e4. doi: 10.1053/j.gastro.2018.09.010
75. Zhang Y, Chen W, Wang Y. STING is an essential regulator of heart inflammation and fibrosis in mice with pathological cardiac hypertrophy via endoplasmic reticulum (ER) stress. *Biomed Pharmacother* (2020) 125:110022. doi: 10.1016/j.biopha.2020.110022
76. Chia J, Eroglu FK, Özen S, Orhan D, Montealegre-Sanchez G, de Jesus AA, et al. Failure to thrive, interstitial lung disease, and progressive digital necrosis with onset in infancy. *J Am Acad Dermatol* (2016) 74:186–9. doi: 10.1016/j.jaad.2015.10.007

77. Bouis D, Kirstetter P, Arbogast F, Lamon D, Delgado V, Jung S, et al. Severe Combined Immunodeficiency in Stimulator of Interferon Genes (STING) V154M/wild-type Mice. *J Allergy Clin Immunol* (2019) 143:712–725.e5. doi: 10.1016/j.jaci.2018.04.034
78. Luksch H, Stinson WA, Platt DJ, Qian W, Kalugotla G, Miner CA, et al. STING-associated Lung Disease in Mice Relies on T Cells but Not Type I Interferon. *J Allergy Clin Immunol* (2019) 144:254–66.e8. doi: 10.1016/j.jaci.2019.01.044
79. Motwani M, Pawaria S, Bernier J, Moses S, Henry K, Fang T, et al. Hierarchy of Clinical Manifestations in SAVI N153S and V154M Mouse Models. *Proc Natl Acad Sci U S A* (2019) 116:7941–50. doi: 10.1073/pnas.1818281116
80. Barata JT, Durum SK, Seddon B. Flip the coin: IL-7 and IL-7R in health and disease. *Nat Immunol* (2020) 20:1584–93. doi: 10.1038/s41590-019-0479-x
81. Carmona-Guttierez D, Bauer MA, Zimmermann A, Kainz K, Hofer SJ, Kroemer G, et al. Digesting the crisis: autophagy and coronaviruses. *Microb Cell* (2020) 7:119–28. doi: 10.15698/mic2020.05.715
82. Rubio RM, Mohr I. Inhibition of ULK1 and Beclin1 by an α-herpesvirus Akt-like Ser/Thr Kinase Limits Autophagy to Stimulate Virus Replication. *Proc Natl Acad Sci U S A* (2019) 116:26941–50. doi: 10.1073/pnas.1915139116
83. Shojaei S, Suresh M, Klionsky DJ, Labouta HI, Ghavami S. Autophagy and SARS-CoV-2 Infection: A possible Smart Targeting of the Autophagy Pathway. *Virulence* (2020) 11:805–10. doi: 10.1080/21505594.2020.1780088
84. Li Z, Zhao K, lv X, Lan Y, Hu S, Shi J, et al. Ulk1 Governs Nerve Growth Factor/TrkA Signaling by Mediating Rab5 GTPase Activation in Porcine Hemagglutinating Encephalomyelitis Virus-Induced Neurodegenerative Disorders. *J Virol* (2018) 92:e00325–18. doi: 10.1128/JVI.00325-18
85. Lemos H, Huang L, McGaha TL, Mellor AL. Cytosolic DNA Sensing via the Stimulator of Interferon Genes Adaptor: Yin and Yang of Immune Responses to DNA. *Eur J Immunol* (2014) 44:2847–53. doi: 10.1002/eji.201344407
86. Hao S, Lian J, Lu Y, Jia H, Hu J, Yu G, et al. Decreased B cells on admission was associated with prolonged viral RNA shedding from respiratory tract in Coronavirus Disease 2019: a case control study. *J Infect Dis* (2020) 31:jiaa311. doi: 10.1093/infdis/jiaa311
87. Mathew D, Giles JR, Baxter AE, Greenplate AR, Wu JE, Alanio C, et al. Deep Immune Profiling of COVID-19 Patients Reveals Patient Heterogeneity and Distinct Immunotypes With Implications for Therapeutic Interventions. *Science* (2020) 369:eabc8511. doi: 10.1126/science.abc8511
88. Huang AT, Garcia-Carreras B, Hitchings MDT, Yang B, Katznelnik LC, Rattigan SM, et al. A systematic review of antibody mediated immunity to coronaviruses: antibody kinetics, correlates of protection, and association of antibody responses with severity of disease. *Nat Commun* (2020) 11(1):4704. doi: 10.1038/s41467-020-18450-4
89. Shen C, Wang Z, Zhao F, Yang Y, Li J, Yuan J, et al. Treatment of 5 Critically Ill Patients With COVID-19 With Convalescent Plasma. *JAMA* (2020) 323:1582–9. doi: 10.1001/jama.2020.4783
90. Quinti I, Lougaris V, Milito C, Cinetto F, Pecoraro A, Mezzaroma I, et al. A Possible Role for B Cells in COVID-19? Lesson From Patients With Agammaglobulinemia. *J Allergy Clin Immunol* (2020) 146:211–13e4. doi: 10.1016/j.jaci.2020.04.013
91. Walker MM, Crute BW, Cambier JC, Getahun A. B Cell-Intrinsic STING Signaling Triggers Cell Activation, Synergizes With B Cell Receptor Signals, and Promotes Antibody Responses. *J Immunol* (2018) 201:2641–53. doi: 10.4049/jimmunol.1701405
92. Marcus A, Mao AJ, Lensink-Vasan M, Wang LA, Vance RE, Raulet DH. Tumor-Derived cGAMP Triggers a STING-Mediated Interferon Response in Non-tumor Cells to Activate the NK Cell Response. *Immunity* (2018) 49:754–63.e4. doi: 10.1016/j.immuni.2018.09.016
93. Bénard A, Sakwa I, Schierloh P, Colom A, Mercier I, Tailleux L, et al. B Cells Producing Type I IFN Modulate Macrophage Polarization in Tuberculosis. *Am J Respir Crit Care Med* (2018) 197:801–13. doi: 10.1164/rccm.201707-1475OC
94. Tang CHA, Zundell JA, Ranatunga S, Lin C, Nefedova Y, Del Valle JR. Agonist-Mediated Activation of STING Induces Apoptosis in Malignant B Cells. *Cancer Res* (2016) 76:2137–52. doi: 10.1158/0008-5472.CAN-15-1885
95. Katikaneni DS, Jin L. B Cell MHC Class II Signaling: A Story of Life and Death. *Hum Immunol* (2019) 80:37–43. doi: 10.1016/j.humimm.2018.04.013
96. Gram AM, Sun C, Landman SL, Oosenbrug T, Koppejan HJ, Kwakkenbos MJ. Human B Cells Fail to Secrete Type I Interferons Upon Cytoplasmic DNA Exposure. *Mol Immunol* (2017) 91:225–37. doi: 10.1016/j.molimm.2017.08.025
97. Bridgeman A, Maelfait J, Davenne T, Partridge T, Peng Y, Mayer A, et al. Viruses Transfer the Antiviral Second Messenger cGAMP Between Cells. *Science* (2015) 349:1228–32. doi: 10.1126/science.aab3632
98. Nelemans T, Kikkert M. Viral Innate Immune Evasion and the Pathogenesis of Emerging RNA Virus Infections. *Viruses* (2019) 11:E961. doi: 10.3390/v11100961
99. Oh HLJ, Gan SKE, Bertoletti A, Tan YJ. Understanding the T Cell Immune Response in SARS Coronavirus Infection. *Emerg Microbes Infect* (2012) 1:e23. doi: 10.1038/emi.2012.26
100. Srikanth S, Woo JS, Wu B, El-Sherbiny YM, Leung J, Chupradit K, et al. The Ca 2+ sensor STIM1 regulates the type I interferon response by retaining the signaling adaptor STING at the endoplasmic reticulum. *Nat Immunol* (2019) 20:152–62. doi: 10.1038/s41590-018-0287-8
101. Vishnubalaii R, Shaath H, Alaiez NM. Protein Coding and Long Noncoding RNA (lncRNA) Transcriptional Landscape in SARS-CoV-2 Infected Bronchial Epithelial Cells Highlight a Role for Interferon and Inflammatory Response. *Genes (Basel)* (2020) 7(11):E760. doi: 10.3390/genes11070760
102. Wang J, Dai M, Cui Y, Hou G, Deng J, Gao X, et al. Association of Abnormal Elevations in IFIT3 With Overactive Cyclic GMP-AMP Synthase/Stimulator of Interferon Genes Signaling in Human Systemic Lupus Erythematosus Monocytes. *Arthritis Rheumatol* (2018) 70:2036–45. doi: 10.1002/art.40576
103. Yarbrough ML, Zhang K, Sakthivel R, Forst CV, Posner BA, Barber GN, et al. Primate-specific miR-576-3p sets host defense signalling threshold. *Nat Commun* (2014) 5:1–10. doi: 10.1038/ncomms5963
104. Hamann L, Szwed M, Mossakowska M, Chudek J, Puzianowska-Kuznicka M. First evidence for STING SNP R293Q being protective regarding obesity-associated cardiovascular disease in age-advanced subjects – a cohort study. *Immun Ageing* (2020) 17:7. doi: 10.1186/s12979-020-00176-y
105. Giamarellos-Bourboulis EJ, Netea MG, Rovina N, Akinosoglou K, Antoniadou A, Antonakos ND, et al. Complex Immune Dysregulation in COVID-19 Patients With Severe Respiratory Failure. *Cell Host Microbe* (2020) 27(6):992–1000.e3. doi: 10.1016/j.chom.2020.04.009
106. Xu X, Han M, Li T, Sun W, Wang D, Fu B, et al. Effective treatment of severe COVID-19 patients with tocilizumab. *Proc Natl Acad Sci USA* (2020) 117:10970–5. doi: 10.1073/pnas.2005615117
107. Cui X, Zhang R, Cen S, Zhou J. STING modulators: Predictive significance in drug discovery. *Eur J Med Chem* (2019) 182:111591. doi: 10.1016/j.ejmech.2019.111591
108. Hansen AL, Buchan GJ, Ruhl M, Mukai K, Salvatore SR, Ogawa E, et al. Nitro-fatty acids are formed in response to virus infection and are potent inhibitors of STING palmitoylation and signaling. *Proc Natl Acad Sci U S A* (2018) 115:E7768–75. doi: 10.1073/pnas.1806239115
109. Lafaie L, Célarier T, Goethals L, Pozzetto B, Grange S, Ojardias E, et al. Recurrence or Relapse of COVID-19 in Older Patients: A Description of Three Cases. *J Am Geriatr Soc* (2020). doi: 10.1111/jgs.16728
110. Chow JH, Khanna AK, Kethireddy S, Yamane D, Levine A, Jackson AM, et al. Aspirin Use is Associated with Decreased Mechanical Ventilation, ICU Admission, and In-Hospital Mortality in Hospitalized Patients with COVID-19. *Anesth Analg* (2020). doi: 10.1213/ANE.0000000000005292

Conflict of Interest: The authors declare that the research was conducted in the absence of any commercial or financial relationships that could be construed as a potential conflict of interest.

frontiers in Immunology

REVIEW
published: 11 January 2021
doi: 10.3389/fimmu.2020.624556

Function and Regulation of Nuclear DNA Sensors During Viral Infection and Tumorigenesis

Fan Zhang[1,2†], *Yi Yuan*[1,2,3†] *and Feng Ma*[1,2*]

[1] Key Laboratory of Synthetic Biology Regulatory Elements, Chinese Academy of Medical Sciences & Peking Union Medical College, Beijing, China, [2] Suzhou Institute of Systems Medicine, Suzhou, China, [3] Department of Laboratory Medicine, Shanghai Tongji Hospital, School of Medicine of Tongji University, Shanghai, China

IFI16, hnRNPA2B1, and nuclear cGAS are nuclear-located DNA sensors that play important roles in initiating host antiviral immunity and modulating tumorigenesis. IFI16 triggers innate antiviral immunity, inflammasome, and suppresses tumorigenesis by recognizing double-stranded DNA (dsDNA), single-stranded DNA (ssDNA), damaged nuclear DNA, or cooperatively interacting with multiple tumor suppressors such as p53 and BRCA1. hnRNPA2B1 initiates interferon (IFN)-α/β production and enhances STING-dependent cytosolic antiviral signaling by directly binding viral dsDNA from invaded viruses and facilitating N^6-methyladenosine (m^6A) modification of cGAS, IFI16, and STING mRNAs. Nuclear cGAS is recruited to double-stranded breaks (DSBs), suppresses DNA repair, and promotes tumorigenesis. This review briefly describes the nuclear functions of IFI16, hnRNPA2B1, and cGAS, and summarizes the transcriptional, post-transcriptional, and post-translational regulation of these nuclear DNA sensors.

Keywords: nuclear DNA sensor, IFI16, hnRNPA2B1, cGAS, p53, type I interferon, tumorigenesis

OPEN ACCESS

Edited by:
Chunfu Zheng,
Fujian Medical University, China

Reviewed by:
Kislay Parvatiyar,
Tulane University, United States
Wei Zhao,
Shandong University, China

***Correspondence:**
Feng Ma
maf@ism.pumc.edu.cn

†These authors have contributed equally to this work

Specialty section:
This article was submitted to Molecular Innate Immunity, a section of the journal Frontiers in Immunology

Received: *31 October 2020*
Accepted: *25 November 2020*
Published: *11 January 2021*

Citation:
Zhang F, Yuan Y and Ma F (2021) Function and Regulation of Nuclear DNA Sensors During Viral Infection and Tumorigenesis. Front. Immunol. 11:624556. doi: 10.3389/fimmu.2020.624556

INTRODUCTION

The first line of host defense against pathogenic threats is orchestrated by the innate immune system, which relies on the ability of immune cells to recognize the presence of extracellular or intracellular pathogen-associated molecular patterns (PAMPs) through germline-encoded pattern recognition receptors (PRRs) (1). Viral nucleic acids are the main PAMPs generated during viral infection. Once infected, the interactions between PRRs and viral nucleic acids evoke a series of signaling transduction cascades that lead to the initiation of cell defense to eliminate viruses. For instance, recognition of viral DNA by cytosolic DNA sensors like cyclic GMP-AMP synthase (cGAS) elicits the activation of the adaptor protein stimulator of interferon genes (STING), which further recruits and activates TANK-binding kinase 1 (TBK1) and interferon-regulatory factor 3 (IRF3) (2–4). STING also activates the transcription factor nuclear factor-κB (NF-κB), which subsequently collaborates with IRF3 to promote the expression of type I IFNs (IFN-Is) and proinflammatory cytokines (5–7). Additionally, cytosolic DNA binds to the receptor absent in melanoma 2 (AIM2), leading to the recruitment of the apoptosis-associated speck-like protein containing CARD (ASC) and pro-caspase-1 to assemble a multi-protein complex termed inflammasome, which constitutes a group of PRRs and plays essential roles in response to viral infection (8). Once assembled, the AIM2 inflammasome complex further promotes the proteolytic

maturation and secretion of proinflammatory cytokines, including interleukin 1 beta (IL-1β) and IL-18, thereby initiating the inflammatory cascade (9).

Although the stimulation of cytosolic nucleic acid sensors by viral nucleic acids is critical for host antiviral defense, multiple viruses replicate in the nucleus with much less or no opportunities for cytosolic engagement of viral nucleic acids. In the past few years, accumulating evidence has demonstrated that nuclear DNA sensors, such as IFN-γ-inducible protein 16 (IFI16), heterogeneous nuclear ribonucleoprotein A2/B1 (hnRNPA2B1), and nuclear cGAS, also exert critical roles in initiating host antiviral immunity (10). However, compared to the wealth of knowledge about cytosolic DNA sensors and the other PRRs, studies for the roles and underlying mechanisms of nuclear DNA sensors are only just emerging (11–13). Recent evidence indicates that nuclear DNA sensors are also involved in tumor development beyond pathogenic DNA recognition. Aberrant or damaged self-DNA species generated due to genomic instability serve as ligands to engage these nuclear DNA sensors during tumorigenesis.

This review focuses on the latest findings to provide a more comprehensive understanding of the functions of nuclear DNA sensors during viral infection and tumorigenesis. It also summarizes the regulation of these nuclear DNA sensors, including transcriptional, post-transcriptional, and post-translational regulation during viral infection and tumorigenesis.

NUCLEAR DNA SENSORS FACILITATE ANTIVIRAL IMMUNITY

IFI16 is a member of the pyrin and HIN200 domain-containing protein family (PYHIN) that contains a pyrin domain and two DNA-binding HIN domains. It has been identified as a nuclear DNA sensor that mediates the induction of IFN-Is (14). Upon detecting viral DNA in the nucleus, IFI16 translocates to the cytoplasm where it oligomerizes and relays signals through adaptor molecule STING, engaging the TBK1-IRF3 axis and the NF-κB pathway to induce the transcription of IFN-Is (2, 15, 16). IFI16 has also been shown to interact with Kaposi's sarcoma-associated herpesvirus (KSHV) genomic DNA in the nucleus, leading to the formation of a functional inflammasome. Different from the cytosolic AIM2 inflammasome, the IFI16 inflammasome complex is initially assembled in the nucleus and subsequently translocates to the cytoplasm, suggesting a nucleus-associated inflammasome sensor component against KSHV infection (17, 18). The overexpression of IFI16 with other inflammasome components in HEK293T cells is of note as it exhibits a low-level production of IL-1β. When these cells are infected by KSHV, an elevated level of IL-1β is observed, implying that the IFI16 inflammasome requires additional cofactors for optimal activation. The work of Brunette et al. further supports this notion that IFI16 and its mouse homolog p204 are poor activators of either STING-dependent IFNs or ASC-inflammasome, while AIM2 robustly activates both IFNs and the inflammasome in an experimental overexpression system (19).

hnRNPA2B1 is a member of the hnRNP family and has been recently identified as a nuclear DNA sensor (12). Upon sensing viral DNA in the nucleus, hnRNPA2B1 dimerizes and is demethylated by arginine demethylase JMJD6, which results in the cytoplasmic translocation of hnRNPA2B1. The cytoplasmic hnRNPA2B1 dimers interact with STING and activate the TBK1-IRF3 signal transduction cascade to facilitate the transcription of downstream IFN-Is. Moreover, hnRNPA2B1 can disassociate with fat mass and obesity-associated protein (FTO) after virus infection, leading to the promotion of N^6-methyladenosine (m^6A) modification, nucleocytoplasmic trafficking, and translation of cGAS, STING, and IFI16 mRNAs to amplify the activation of IFN-Is in antiviral innate immune response (20). A recent study shows that hnRNPA2B1 plays a vital role in transporting herpes simplex virus 1 (HSV-1) from the envelopment site to the extracellular environment (21). Interestingly, hnRNPA2B1 facilitates the replication of hepatitis E virus (HEV), an ssRNA virus, though hnRNPA2B1 is initially identified as a DNA sensor (22).

cGAS is a member of the nucleotidyltransferase family, the binding of cytoplasmic pathogenic DNA to cGAS induces a phase transition to liquid-like droplets, promoting the production of the secondary messenger cyclic guanosine monophosphate–adenosine monophosphate (cGAMP) and subsequent induction of IFN-Is through the STING-TBK1-IRF3 signaling axis (23, 24). cGAS mainly localizes in the cytoplasm, yet cGAS expresses in interphase and may translocate to the nucleus due to nuclear envelope rupture or mitosis (24, 25). Nuclear cGAS usually maintains a suppressed state by chromatin tethering to limit reactivity against self-DNA (26, 27). A recent study reveals that upon nuclear entry of the human immunodeficiency virus (HIV), NONO, an innate immune sensor of the viral capsid proteins is associated with cGAS in the nucleus and is required to retain cGAS in the nucleus but has no impact on the cytosolic pool of cGAS. The crosstalk between NONO and cGAS in the nucleus enables the sensing of DNA intermediate during HIV infection. The detection of the nuclear viral capsid by NONO promotes DNA sensing by cGAS and reveals an innate strategy of distinguishing viruses from self in the nucleus (28).

IFI16 SUPPRESSES VIRAL REPLICATION AS A TRANSCRIPTIONAL REPRESSOR

Several studies have reported that IFI16 functions as a transcriptional repressor (29). For instance, IFI16 has been described as a restriction factor for human cytomegalovirus (HCMV) replication on account of suppressing the transcriptional activity of the viral DNA polymerase gene (UL54) (30). Besides, IFI16 transcriptionally represses HSV-1 gene expression such as the immediate-early proteins (ICP0 and ICP4), the early proteins (ICP8 and TK), and the late proteins (GB and Us11), and limits viral replicative capacity (31, 32). IFI16 has also been demonstrated to function as a restriction factor for human papillomavirus 18 (HPV18) replication

through histone modifications (33). A recent study shows that IFI16 limits HIV-1 transcription and latency reactivation by targeting the transcription factor Sp1 (34). Overall, these data identify IFI16 as a transcriptional repressor for various DNA viruses in the nucleus, of which the mechanisms still need deeper investigation.

Most studies suggest that IFI16 modulates transcription mainly through association with transcription factors or promoters. As mentioned above, IFI16 binds to the transcription factor Sp1 to suppress HIV-1 transcription (34). Similarly, Cristea et al. show that IFI16 interacts with the major immediate-early promoter (MIEP), and participates in controlling the viral immediate-early gene transcription by HCMV virion protein pUL83 (35). In addition to associating with transcription factors or promoters directly, IFI16 prevents transcription factors from interacting with their promoters. For instance, IFI16 has been shown to inhibit the association of some transcription factors such as Sp1 with the HCMV promoter (30).

Additionally, a study shows that IFI16 blocks the interaction of transcription factors, TATA-binding protein (TBP), and Octamer-Binding Transcription Factor 1 (Oct 1), with HSV-1 promoters (31). Meanwhile, the study also suggests that IFI16 may facilitate global histone modifications by modulating the formation of heterochromatin and euchromatin for both viral and cellular genes. Consequently, IFI16 may modulate transcription through chromatin modification. Another study also suggests that IFI16 promotes the addition of heterochromatin marks and the reduction of euchromatin marks on viral chromatin, thereby inhibiting viral gene expression and replication (36). Furthermore, IFI16 promotes the assembly of heterochromatin on HPV DNA, thus reducing both viral replication and transcription (33). Altogether, IFI16 is involved in transcriptional repression through association with transcription factors or promoters, preventing transcription factors from binding to their promoters and inducing changes in chromatin markers.

NUCLEAR DNA SENSORS REGULATE TUMORIGENESIS

Despite the essential roles of nuclear DNA sensors in the host antiviral defense, studies on these PRRs have also been well documented in the absence of infection. IFI16 acts as a DNA damage amplifier by interacting with p53 through its C-terminal domain and consequently promotes the accumulation and activation of p53 caused by DNA damage (37, 38). Increased levels of IFI16 promote the transcription of known p53 target genes, such as the cell cycle kinase inhibitor p21 and the proapoptotic Bcl-2 family member Bax, inducing p53-mediated cell cycle arrest and apoptosis in human cancer cells (38, 39). Decreased IFI16 mRNA expression is observed in numerous breast cell lines, which results in dysfunction of p53-mediated apoptosis and leads to cancer development (38). Subsequently, Lin et al. show that IFI16 functions as a tumor suppressor in hepatocellular carcinoma (HCC) by activating the p53 signaling pathway and inflammasome (40). In turn, functional activation of p53 stimulates the transcription of IFI16 through associating with the regulatory region of the IFI16 gene in the cells treated with DNA-damaging agents, suggesting a positive feedback loop between p53 and IFI16 (41). A recent research indicates that IFI16 positively regulates programmed cell death 1 ligand 1 (PD-L1) in cervical cancer cells by activating the STING-TBK1-NF-κB pathway, which can interact with the proximal region of the PD-L1 promoter to facilitate PD-L1 expression, and promoting the progression of cervical cancer (42).

Studies have also provided evidence that hnRNPA2B1 functions as a putative proto-oncogene in some cancers such as glioblastoma, pancreatic cancer, liver cancer, and pancreatic ductal adenocarcinoma (PDAC) (43–46). The upregulated expression of hnRNPA2B1 facilitates the malignant phenotypes of cancer cells by modulating many downstream target genes. hnRNPA2B1 is also overexpressed in a variety of other tumors. For instance, the expression of hnRNPA2B1 in human ovarian cancer tissues is significantly higher than that in normal ovarian epithelium tissues, and increased hnRNPA2B1 level is related to the poor prognosis of ovarian cancer patients (47). hnRNPA2B1 also serves as a diagnostic marker for the early detection of lung cancer (48–50).

Another recent study by Liu et al. confirms that DNA damage triggers nuclear translocation of cGAS and leads to the recruitment of cGAS to the site of double-stranded breaks, suppressing homologous recombination DNA repair (HR) and increasing genomic instability and, consequently, tumorigenesis (51). This observation is further supported by a study by Jiang et al., which found that nuclear cGAS inhibits HR in a STING-independent manner (52). These findings suggest that nuclear cGAS is a tumor enhancer by modulating the DNA damage response and influencing genome stability, indicating potential implications for inhibitors that block the nuclear translocation of cGAS for cancer intervention. The above studies suggest that nuclear DNA sensors play critical roles in tumorigenesis and might be a valuable prognostic marker for malignancy development and patient survival.

The functions of nuclear DNA sensors in regulating antiviral immunity, inflammasome activation, transcriptional repression, and tumorigenesis are summarized in **Figure 1**. Due to their important functions, the expression and cellular location of nuclear DNA sensors are tightly regulated (**Figure 2**).

TRANSCRIPTIONAL REGULATION OF NUCLEAR DNA SENSORS

IFI16 mRNA is induced by both IFN-I (IFN-α and IFN-β) and IFN-II (IFN-γ) in multiple human cell lines such as human myeloid leukemia cells and fibrosarcoma cells (53, 54). IFNs are key molecules that contribute to the pathogenesis of systemic lupus erythematosus (SLE), and overproduction of IFN-I is always observed in patients with SLE (55–57). Consistently, the IFI16 transcripts in peripheral blood monocytes (PBMCs) of patients with SLE are significantly higher than that of healthy people (58). Infection with DNA viruses such as vaccinia virus

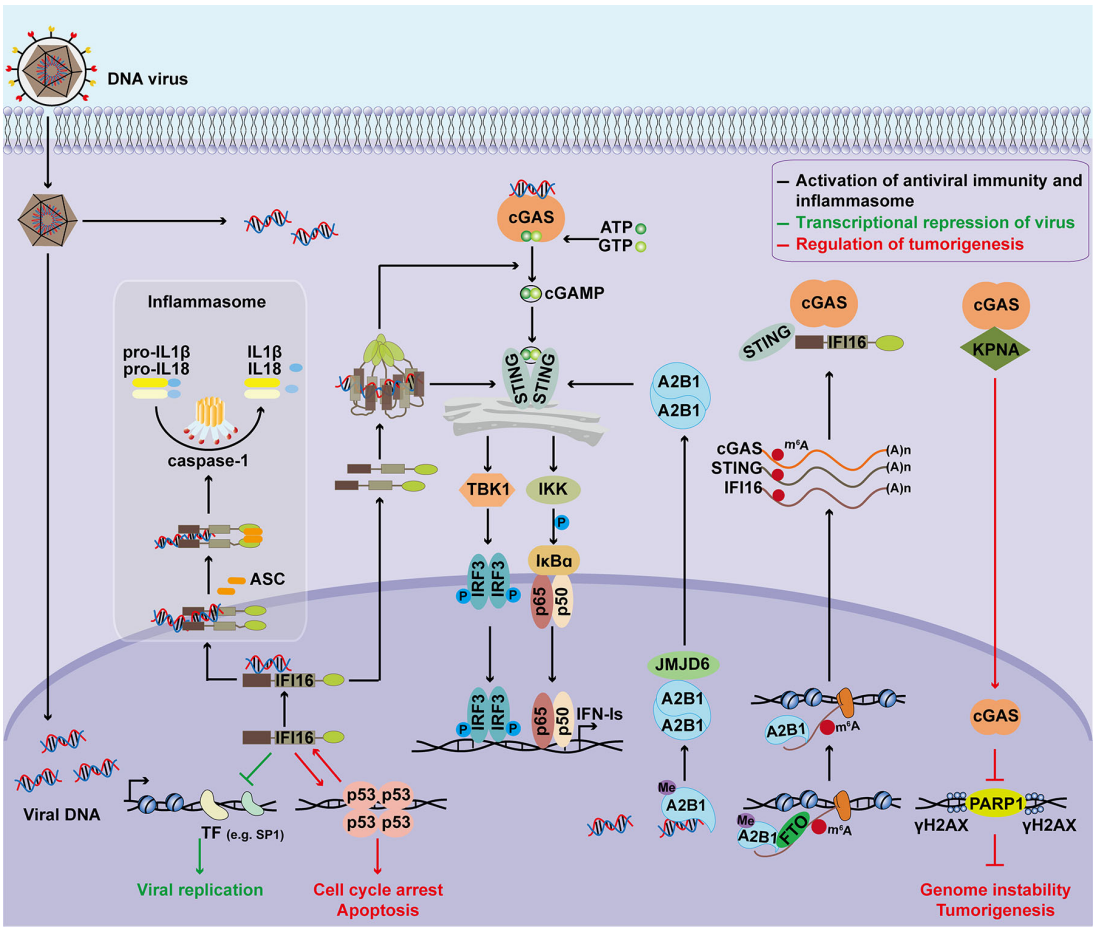

FIGURE 1 | Major functions of nuclear DNA sensors. Upon detecting nuclear viral DNA, IFI16 is transported to the cytoplasm to activate the STING signaling cascade, inducing IFN-Is expression through the TBK1-IRF3 and NF-κB axis. IFI16 also activates inflammasome to promote IL-1β and IL-18 maturation. Additionally, IFI16 functions as a transcriptional repressor to restrict viral replication by associating with transcription factors or promoters, preventing transcription factors from binding to promoters, and inducing chromatin marker changes. Nuclear hnRNPA2B1 dimerizes and is demethylated by JMJD6 after binding to viral dsDNA, resulting in the cytoplasmic translocation of hnRNPA2B1. The cytoplasmic hnRNPA2B1 activates the STING-TBK1-IRF3 signal to facilitate the transcription of IFN-Is. Moreover, demethylated hnRNPA2B1 enhances nucleocytoplasmic trafficking and translates cGAS, STING, and IFI16 mRNAs to amplify the antiviral immune response. Besides, the roles of nuclear DNA sensors during tumorigenesis have also been investigated. IFI16 is shown to act as a tumor suppressor in several types of cancers by interacting with p53 and enhancing p53-mediated transcriptional activation. In turn, functional activation of p53 stimulate the transcription of IFI16 through associating with the regulatory region of the *IFI16* promoter. DNA damage triggers nuclear translocation of cGAS. Nuclear cGAS promotes tumorigenesis by modulating the DNA damage response and increasing genomic instability. ASC, apoptosis-associated speck-like protein containing a CARD; STING, stimulator of interferon genes; TBK1, TANK-binding kinase 1; IKK, IκB kinase; IRF3, interferon regulatory factor 3; IFN-I, type I interferon; A2B1, hnRNPA2B1; JMJD6, jumonji domain containing 6; Me, methylation; m^6A, N^6-Methyladenosine; FTO, fat mass and obesity-associated protein; KPNA, karyopherin alpha; PARP1, Poly (ADP-Ribose) Polymerase 1. γH2AX, phosphorylated H2A histone family member X (H2AX) on serine 139.

(VACV), HSV-1, and human T-lymphotropic virus type 1 (HTLV-1) induces IFI16 expression dramatically (15, 20, 59, 60). IFI16 mRNA expression is correlated with high viral load and low $CD4^+$T cell counts in HIV patients (61). IFI16 epigenetically suppresses hepatitis B virus (HBV) covalently closed circular DNA (cccDNA) by targeting an interferon-sensitive response element (ISRE) located in cccDNA. However, HBV infection downregulates the mRNA expression of IFI16 in the hepatocytes and liver tissues of patients with chronic hepatitis B (62). In addition to being tightly controlled transcriptionally during viral infection, IFI16 expression is precisely regulated during tumorigenesis. For instance, as mentioned above, IFI16 directly binds to the C-terminal region of p53 and enhances p53-mediated transcriptional activation (37, 38). Moreover, p53 also facilitates IFI16 transcription by directly binding to the promoter region of IFI16 and thus provides positive feedback regulation of p53 signaling (41). The IL-6/JAK/STAT3 pathway plays a key role in the growth and development of many human cancers (63). IL-6 treatment induces STAT3 phosphorylation and drives IFI16 transcription in a STAT3-dependent manner in human adenocarcinoma cell lines (64). The oncogene ZNF217 acts as a transcriptional repressor and plays an important role during

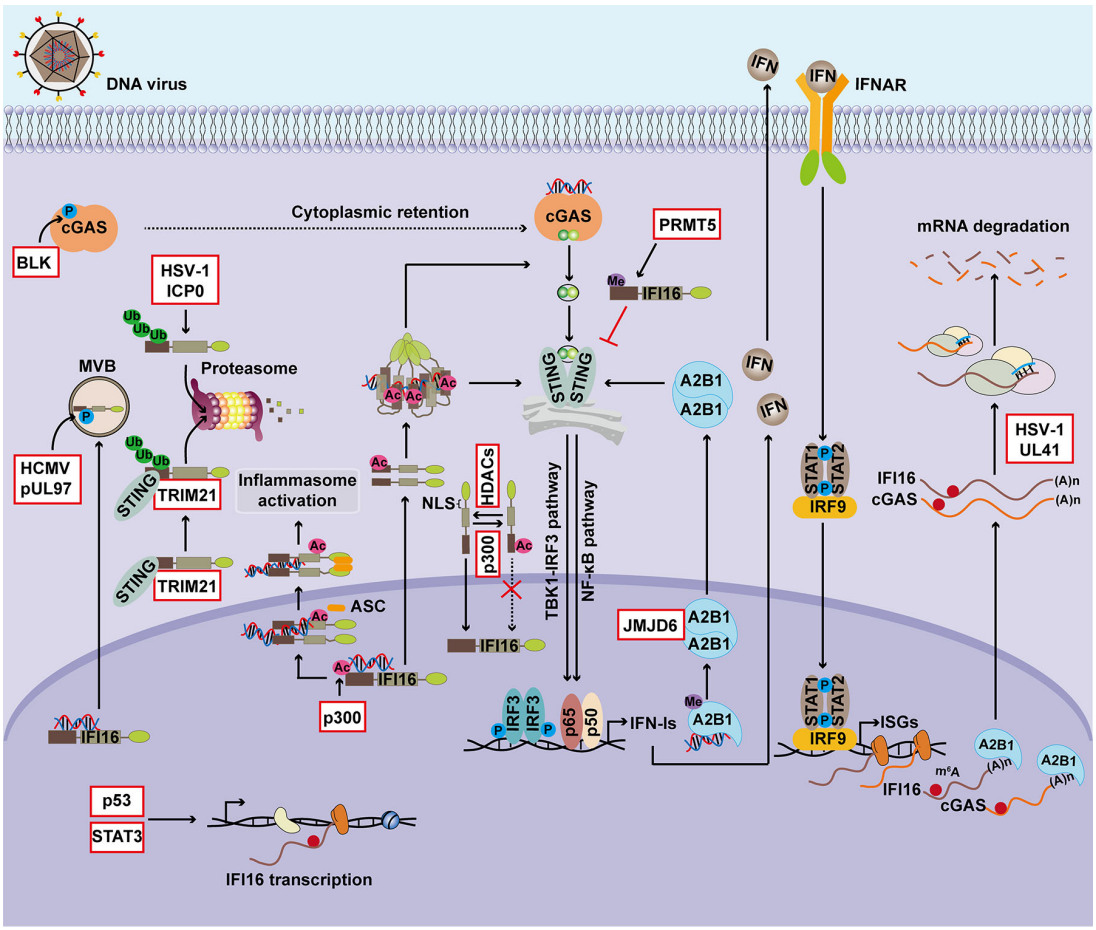

FIGURE 2 | Regulation of nuclear DNA sensors. The expression and activation of DNA sensors are finely controlled during viral infection and tumorigenesis. p53 facilitates IFI16 transcription by directly binding to the promoter region of IFI16, and IL-6 drives IFI16 transcription in a STAT3-dependent manner. Post-transcriptional regulation also involves modulating the expression of nuclear DNA sensors. During DNA virus infection, hnRNPA2B1 functions as an m^6A modulator to promote nucleocytoplasmic trafficking of cGAS and IFI16 mRNAs. UL41 from HSV-1 significantly reduces the expression of cGAS and IFI16 by degrading their transcripts. Furthermore, PTMs, particularly the phosphorylation, ubiquitination, acetylation, and methylation, play critical roles in regulating the activity and stability of nuclear DNA sensors. Phosphorylation of IFI16 controls its subcellular localization, and related antiviral immunity and BLK-mediated phosphorylation of cGAS facilitates its cytosolic retention. ICP0 from HSV-1 induces the ubiquitination and proteasome-dependent degradation of IFI16 and thus suppresses inflammasome activation. STING promotes IFI16 degradation via the ubiquitin-proteasome system by TRIM21. The acetyltransferase p300 mediates acetylation of IFI16 during HSV-1 infection, an essential step for inflammasome assembly and cytoplasmic translocation, activation of cytoplasmic STING signaling, and downstream IFN-β production. The sensing ability of IFI16 is modulated by acetylation of Lys99 and Lys128 within its NLS, and this PTM of IFI16 promotes the cytoplasmic translocation of IFI16, whereas HDACs promotes its nuclear import. hnRNPA2B1 is demethylated by JMJD6 in the HSV-1-infected cells, which consequently initiates IFN-α/β production and enhances STING-dependent cytoplasmic antiviral signaling. BLK, B-lymphoid tyrosine kinase; MVB, multivesicular bodies; ICP0, human HSV-1 infected cell polypeptide 0; TRIM21, tripartite motif-containing protein 21; Ub, Ubiquitination; Ac, Acetylation; Me, Methylation; STAT3, signal transducer and activator of transcription 3; NLS, nuclear localization signal; HDAC, histone deacetylase; PRMT5, protein arginine N-methyltransferase 5.

neoplastic transformation (65–67). Consistent with its oncogenic role, ZNF217 represses the transcription of IFI16 (68).

hnRNPA2B1 mRNA levels are constitutively expressed during viral infection (20). By contrast, it is overexpressed in various malignant tumor tissues and cancer cell lines (69–72). For example, increased mRNA level of hnRNPA2B1 has been found in breast cancer cell lines deficient for breast cancer susceptibility gene 1 (BRCA1) expression. The restoration of BRCA1 expression reverts hnRNPA2B1 upregulation, implying the involvement of BRCA1 in the regulation of hnRNPA2B1 (73). Long non-coding RNA (lncRNA) CACNA1G-AS1 promotes the expression of hnRNPA2B1 in non-small cell lung cancer (NSCLC) cell lines, inducing malignant cell invasion, migration, and epithelial-mesenchymal transformation (EMT) (74). cGAS is an interferon-stimulated gene (ISG), and two adjacent ISREs in the promoter region of cGAS mediate the induction of cGAS by IFN-Is (75). The cGAS mRNA is upregulated in the PBMCs from patients with SLE (76). Both HSV-1 infection and IFN-α treatment induce cGAS mRNA expression in neonatal PBMCs from 1-month-old infants (77).

LncRNA NEAT1 epigenetically inhibits cGAS expression to regulate the malignant phenotype of cancer cells and cytotoxic T cell infiltration in lung cancer (78).

POST-TRANSCRIPTIONAL REGULATION OF NUCLEAR DNA SENSORS

Post-transcriptional regulation also plays a key role in modulating the expression of nuclear DNA sensors and related host antiviral immunity and tumorigenesis. Three isoforms of IFI16, isoform-A, B, and C, are widely detected in multiple cell lines and primary cells due to IFI16 pre-mRNA alternative splicing (79, 80). The spliceosome-associated factor, CTNNBL1, regulates the expression and alternative splicing of IFI16 and promotes proliferation and invasion in ovarian cancer (81). A novel transcript isoform of IFI16, which contains two HIN domains but lacks the PYD domain, interacts with AIM2 to impede the formation of a functional AIM2-ASC complex and inhibits AIM2 inflammasome (82). hnRNPA2B1 is a nuclear m^6A reader and mediates m^6A-dependent primary microRNA processing events (83). During DNA virus infection, hnRNPA2B1 functions as an m^6A modulator to promote the m^6A modification and nucleocytoplasmic trafficking of cGAS and IFI16 mRNAs after viral DNA recognition by hnRNPA2B1 (20). In addition to alternative splicing and m^6A modification, viral proteins control IFI16 and cGAS mRNAs stability. UL41 from HSV-1 significantly degrades cGAS mRNA in HSV-1-infected human foreskin fibroblast (HFF) cells abrogating cGAS-STING-mediated IFN-I production dependent on its RNase activity (84). UL41 also reduces the expression of IFI16 by degrading its transcripts (85).

POST-TRANSLATIONAL MODIFICATION OF NUCLEAR DNA SENSORS

Post-translational modifications (PTMs) play important roles in regulating the activity, stability, and folding of targeted proteins by inducing their covalent linkage to new functional groups, such as phosphate, methyl group, and acetate (86). PTMs including phosphorylation, ubiquitination, methylation, and acetylation have been shown to influence PRR-dependent antiviral immunity and inflammatory responses by targeting the innate sensors and downstream signaling molecules, including receptors, adaptors, enzymes, and transcription factors (1, 86, 87). Moreover, PTMs dynamically change the compartmentalization, trafficking, and physical interaction of key molecules that control immunological processes. Here, this review summarizes the PTMs involved in the positive and negative regulation of the nuclear DNA sensors during viral infection and tumorigenesis, and a summary of the post-translational modifications of nuclear DNA sensors are listed in **Table 1**.

Phosphorylation is the most extensively investigated PTM type in antiviral innate immunity (87, 94). IFI16 contains a CcN motif that targets a heterologous protein to the nucleus and subsequently undergoes phosphorylation, particularly by the CcN-motif-phosphorylating protein kinase (CK2). The IFI16 CK2 phosphorylation site enhances nuclear import by facilitating binding to a nuclear component, and the nuclear-import characteristics of the IFI16 CcN motif were consistent with those of the HIV-1 Tat nuclear target signal (95). The viral protein kinase pUL97 of HCMV, which binds and phosphorylates nuclear IFI16, contributes to the nucleocytoplasmic translocation of IFI16 to overcome the restriction activity of IFI16 (88). These studies indicate that the phosphorylation of IFI16 controls IFI16 cellular location and relates antiviral immunity. Up until recently, there was no direct evidence indicating that IFI16 can be phosphorylated at specific sites upon inflammasome assembly.

Although IFI16 is required for the maximal phosphorylation and activation of p53 induced by ionizing radiation (38), it is unclear whether phosphorylation of IFI16 is also critical for its pro-apoptosis and antitumor role during tumorigenesis. DNA damage induces the nuclear translocation of cGAS, which suppresses DNA repair and promotes tumorigenesis by interacting with PARP (51). However, the B-lymphoid tyrosine kinase (BLK)-mediated phosphorylation of cGAS at Tyr215 facilitates the cytosolic retention of cGAS, which may be important for its antiviral role as a cytosolic DNA sensor (51).

Ubiquitination is also a key regulatory mechanism for nuclear DNA sensors, particularly for IFI16. The protein ubiquitination of target substrates involves a stepwise catalyzation by three enzymes, ubiquitin-activating enzyme (E1), ubiquitin-

TABLE 1 | PTMs of nuclear DNA sensors.

Target sensors	Regulators for PTM	PTMs	Mechanisms	References
IFI16	pUL97	Phosphorylation	pUL97 phosphorylates IFI16 during viral replication and re-localizes it from the nucleus to multivesicular bodies to overcome the restriction activity of IFI16	(88)
IFI16	ICP0	Ubiquitination	ICP0 promotes the ubiquitination and proteasome-dependent degradation of IFI16	(89)
IFI16	TRIM21	Ubiquitination	STING directly interacts with IFI16 and facilitates IFI16 ubiquitination and degradation via the ubiquitin-proteasome pathway by recruiting E3 ligase TRIM21	(90)
IFI16	p300	Acetylation	Acetylated IFI16 is essential for IFI16 cellular redistribution, inflammasome assembly in the cytoplasm, and activation of STING	(91, 92)
IFI16	HDACs	Deacetylation	HDACs activity promotes the nuclear import of IFI16	(91)
IFI16	PRMT5	Methylation	Methylated IFI16 suppresses dsDNA activation of STING pathways and attenuates IFN-I expression	(93)
cGAS	BLK	Phosphorylation	Phosphorylation of cGAS at Tyr205 by BLK facilitates its cytosolic retention	(51)
hnRNPA2B1	JMJD6	Demethylation	hnRNPA2B1 is demethylated by JMJD6 in the HSV-1-infected cells, which initiates IFN-I production	(20)

conjugating enzyme (E2), and ubiquitin ligase (E3) (96, 97), resulting in mono-ubiquitination. Ubiquitin can be further conjugated to additional ubiquitin moieties via the same three-step process, yielding polyubiquitin chains. Ubiquitin undergoes ubiquitination itself at its seven lysine residues (K6/K11/K27/K29/K33/K48/K63) or its amino-terminal methionine, which generates different types of ubiquitin chains with distinct functions (98). For instance, the K48-linked ubiquitin chain often induces the proteasomal degradation of targeted proteins, while the K63-linked ubiquitin chain is involved in the transduction of signaling pathways (99, 100). In addition to inducing IFN-I production as a DNA sensor, IFI16 induces the assembly of inflammasome complexes in response to DNA viruses, which is essential in immune protection against viral infections (17, 101). To counter IFI16-triggered antiviral immune responses, HSV-1 expresses an immediate-early protein, infected cell protein 0 (ICP0), an E3 ubiquitin ligase. After HSV-1 infection, ICP0 promotes the ubiquitination and proteasome-dependent degradation of IFI16 and suppresses inflammasome activation (89). Moreover, a previous study showed that the viral ICP0 protein leads to nuclear re-localization and the degradation of IFI16, resulting in the downstream inhibition of IRF3 signaling during HSV-1 infection (102). However, another study indicates that ICP0 is neither sufficient nor necessary for the degradation of IFI16 during HSV-1 infection (103). Due to these controversial results, the role of IFI16 ubiquitination mediated by ICP0 in antiviral immunity needs to be further clarified. Furthermore, it was recently found that STING facilitates ubiquitination on the first three lysines in the N-terminal region of IFI16 and promotes IFI16 degradation via the ubiquitin-proteasome pathway by recruiting the ubiquitin E3 ligase TRIM21 and restricting IFN-I overproduction during host antiviral immunity (90).

The acetylation of lysine residues, which is inversely regulated by acetyltransferases and deacetylases, occurs commonly in the proteome and plays an important role in numerous biological processes, such as chromatin remodeling, nuclear transport, and innate immunity (104). The sensing ability of IFI16 is modulated by acetylation of Lys99 and Lys128 within its nuclear localization signal (NLS), and the PTM of IFI16 promotes the translocation of IFI16 from the nucleus to the cytoplasm, whereas histone deacetylases (HDACs) promotes its nuclear import (91). The acetyltransferase p300 mediates acetylation of IFI16 during HSV-1 infection, which is essential for IFI16-inflammasome assembly in the nucleus and cytoplasmic translocation, activation of STING in the cytoplasm, and IFN-β production (92). Another relevant study also reported that IFI16 in complex with BRCA1-H2B or with BRCA1 recognizes the viral genome, leading to BRCA1 mediated p300 recruitment, interaction with IFI16, acetylation of IFI16 and H2B by p300, and the cytoplasmic transport of acetylated IFI16-H2B-BRCA1 via Ran GTP during KSHV or HSV-1 infection (105).

The methylation of lysine or arginine residues, which is inversely regulated by methyltransferases and demethylases, plays an important role in innate immune responses (106). A recent study demonstrated that IFI16 is methylated by protein arginine methyltransferase 5 (PRMT5) and suppresses the activation of the STING pathway (93). Moreover, a newly identified nuclear DNA sensor, hnRNPA2B1, is methylated in the resting cells. However, hnRNPA2B1 is demethylated by JMJD6 in the HSV-1-infected cells. Demethylated hnRNPA2B1 initiates IFN-α/β production and enhances STING-dependent cytoplasmic antiviral signaling (20).

Together, PTMs, particularly the phosphorylation, ubiquitination, acetylation, and methylation of nuclear DNA sensors, play a vital role in controlling antiviral immunity and tumorigenesis.

CONCLUSION AND FUTURE PERSPECTIVES

Despite rapid advances in understanding of the functions and mechanisms of cytosolic DNA sensors in regulating host antiviral and antitumor immunity, studies that identify novel key nuclear DNA sensors and elucidate these functions are only just emerging. Given the important roles of nuclear DNA sensors during viral infection and tumorigenesis, it is critical to control expression. In this review, we briefly describe the nuclear functions of IFI16, hnRNPA2B1, and cGAS, and summarize the transcriptional, post-transcriptional, and post-translational regulation of these nuclear DNA sensors. However, several intriguing and important topics require further investigation.

The cytosolic DNA sensor, cGAS, has been found to translocate to the nucleus and is recruited to chromatin double-stranded breaks after DNA damage, where it suppresses homologous-recombination-mediated repair and promotes tumor growth (51, 52). Similarly, DNA-dependent protein kinase (DNA-PK) plays a critical role in the nucleus, where it is necessary for non-homologous end joining (NHEJ) and repairing double-strand DNA breaks. DNA-PK was recently identified as a cytosolic DNA sensor that activates a STING-independent DNA sensing pathway (107–109). These studies show that DNA-PK functions as a DNA sensor in the cytoplasm. However, considering that it predominantly localizes in the nucleus, it may also sense viral DNA in the nucleus and trigger an antiviral immune response like that of nuclear DNA sensors. Since all the three nuclear DNA sensors IFI16, hnRNPA2B1, and cGAS shuttle between cytoplasm and nucleus, all of them are involved in regulating both IFN-I-dependent antiviral immunity and tumorigenesis and newly identified nuclear DNA sensors may possess functions both in cytoplasm and nucleus.

The presence of host self-DNA generally in the nucleus was believed to be an immune-privileged cellular compartment. It is essential to understand how nuclear DNA sensors escape self-DNA-triggered activation in the immune response. cGAS has been reported to maintain an inhibitory state in the nucleus by binding nucleosome tighter to prevent autoreactivity to self-DNA (27, 110–112). A circular RNA named cia-cGAS has been identified to suppress nuclear cGAS by blocking its enzymatic activity, thereby preventing cGAS from sensing self-DNA to maintain host homeostasis (113). The multiple layers of

regulation of nuclear DNA sensors may participate in avoiding inappropriate sensing self-DNA.

Invaded HSV-1 regulates IFI16 at multiple levels. HSV-1 infection-triggered IFN-I production induces IFI16 transcription (15, 20, 59, 60). UL41 protein from HSV-1 degrades IFI16 mRNA via its RNase activity and suppresses IFI16 expression post-transcriptionally (85). The ICP0 protein of HSV-1 degrades IFI16 post-translationally (89). HBV infection also downregulates the IFI16 mRNA level, which is worthy of further investigation (62). Several models have been proposed for the HBV-mediated inhibition of IFI16 expression: 1) HBV may suppress IFI16 transcription by promoting hypermethylation of IFI16 promoters; 2) HBV may stimulate the production of some non-coding RNAs to directly degrade the IFI16 mRNA or target the cellular factors responsible for IFI16 transcription; 3) HBV may actively suppress some innate immune signaling, which is important for IFI16 expression (62). There is always a race between host antiviral innate immunity and the immune evasion strategies of viruses (114). The novel regulation mechanism of nuclear DNA sensors by viral components will be an interesting focus in future studies.

PTMs, including phosphorylation, ubiquitination, methylation, and acetylation, have been shown to regulate the expression and activity of nuclear DNA sensors. Other PTMs, such as glutamylation, SUMOylation, and lactylation, also potentially regulate nuclear DNA sensors during antiviral immunity and tumorigenesis. Hence, three main aspects should be extensively investigated in the next few years: 1) the identification of more important nuclear DNA sensors; 2) elucidation of the novel strategies used by invaded viruses to inhibit the expression and function of nuclear DNA sensors; and, 3) the observation of more PTMs of nuclear DNA sensors and elucidation of related mechanisms.

AUTHOR CONTRIBUTIONS

FM conceived the idea. FZ, YY, and FM drafted the manuscript and created the figures. FM revised the manuscript and approved the submitted version.

FUNDING

This work was supported by grants from the National Key Research and Development Program of China (2018YFA0900803), the National Natural Science Foundation of China (31670883, 31870912, and 82002222), and the Natural Science Foundation of Jiangsu Province (BK20200004).

ACKNOWLEDGMENTS

We thank Haiping Yao and Jing Zhu for editing.

REFERENCES

1. Cao X. Self-regulation and cross-regulation of pattern-recognition receptor signalling in health and disease. *Nat Rev Immunol* (2016) 16(1):35–50. doi: 10.1038/nri.2015.8
2. Ishikawa H, Barber GN. STING is an endoplasmic reticulum adaptor that facilitates innate immune signalling. *Nature* (2008) 455(7213):674–8. doi: 10.1038/nature07317
3. Chen Q, Sun L, Chen ZJ. Regulation and function of the cGAS-STING pathway of cytosolic DNA sensing. *Nat Immunol* (2016) 17(10):1142–9. doi: 10.1038/ni.3558
4. Galluzzi L, Vanpouille-Box C, Bakhoum SF, Demaria S. SnapShot: CGAS-STING Signaling. *Cell* (2018) 173(1):276–276.e1. doi: 10.1016/j.cell.2018.03.015
5. Fitzgerald KA, McWhirter SM, Faia KL, Rowe DC, Latz E, Golenbock DT, et al. IKKepsilon and TBK1 are essential components of the IRF3 signaling pathway. *Nat Immunol* (2003) 4(5):491–6. doi: 10.1038/ni921
6. Hayden MS, Ghosh S. Shared principles in NF-kappaB signaling. *Cell* (2008) 132(3):344–62. doi: 10.1016/j.cell.2008.01.020
7. Sato M, Suemori H, Hata N, Asagiri M, Ogasawara K, Nakao K, et al. Distinct and essential roles of transcription factors IRF-3 and IRF-7 in response to viruses for IFN-alpha/beta gene induction. *Immunity* (2000) 13 (4):539–48. doi: 10.1016/s1074-7613(00)00053-4
8. Evavold CL, Kagan JC. Inflammasomes: Threat-Assessment Organelles of the Innate Immune System. *Immunity* (2019) 51(4):609–24. doi: 10.1016/j.immuni.2019.08.005
9. Wang L, Sun L, Byrd KM, Ko CC, Zhao Z, Fang J. AIM2 Inflammasome's First Decade of Discovery: Focus on Oral Diseases. *Front Immunol* (2020) 11:1487. doi: 10.3389/fimmu.2020.01487
10. Diner BA, Lum KK, Cristea IM. The emerging role of nuclear viral DNA sensors. *J Biol Chem* (2015) 290(44):26412–21. doi: 10.1074/jbc.R115.652289
11. Komatsu T, Nagata K, Wodrich H. The Role of Nuclear Antiviral Factors against Invading DNA Viruses: The Immediate Fate of Incoming Viral Genomes. *Viruses* (2016) 8(10):290. doi: 10.3390/v8100290
12. Zhang X, Flavell RA, Li HB. hnRNPA2B1: a nuclear DNA sensor in antiviral immunity. *Cell Res* (2019) 29(11):879–80. doi: 10.1038/s41422-019-0226-8
13. Lum KK, Howard TR, Pan C, Cristea IM. Charge-Mediated Pyrin Oligomerization Nucleates Antiviral IFI16 Sensing of Herpesvirus DNA. *mBio* (2019) 10(4):e01428-19. doi: 10.1128/mBio.01428-19
14. Chan YK, Gack MU. Viral evasion of intracellular DNA and RNA sensing. *Nat Rev Microbiol* (2016) 14(6):360–73. doi: 10.1038/nrmicro.2016.45
15. Unterholzner L, Keating SE, Baran M, Horan KA, Jensen SB, Sharma S, et al. IFI16 is an innate immune sensor for intracellular DNA. *Nat Immunol* (2010) 11(11):997–1004. doi: 10.1038/ni.1932
16. Almine JF, O'Hare CA, Dunphy G, Haga IR, Naik RJ, Atrih A, et al. IFI16 and cGAS cooperate in the activation of STING during DNA sensing in human keratinocytes. *Nat Commun* (2017) 8:14392. doi: 10.1038/ncomms14392
17. Kerur N, Veettil MV, Sharma-Walia N, Bottero V, Sadagopan S, Otageri P, et al. IFI16 acts as a nuclear pathogen sensor to induce the inflammasome in response to Kaposi Sarcoma-associated herpesvirus infection. *Cell Host Microbe* (2011) 9(5):363–75. doi: 10.1016/j.chom.2011.04.008
18. Singh VV, Kerur N, Bottero V, Dutta S, Chakraborty S, Ansari MA, et al. Kaposi's sarcoma-associated herpesvirus latency in endothelial and B cells activates gamma interferon-inducible protein 16-mediated inflammasomes. *J Virol* (2013) 87(8):4417–31. doi: 10.1128/JVI.03282-12
19. Brunette RL, Young JM, Whitley DG, Brodsky IE, Malik HS, Stetson DB. Extensive evolutionary and functional diversity among mammalian AIM2-like receptors. *J Exp Med* (2012) 209(11):1969–83. doi: 10.1084/jem.20121960
20. Wang L, Wen M, Cao X. Nuclear hnRNPA2B1 initiates and amplifies the innate immune response to DNA viruses. *Science* (2019) 365(6454): eaav0758. doi: 10.1126/science.aav0758
21. Zhou X, Wang L, Zou W, Chen X, Roizman B, Zhou GG. hnRNPA2B1 Associated with Recruitment of RNA into Exosomes Plays a Key Role in Herpes Simplex Virus 1 Release from Infected Cells. *J Virol* (2020) 94(13): e00367-20. doi: 10.1128/jvi.00367-20

22. Pingale KD, Kanade GD, Karpe YA. Heterogeneous Nuclear Ribonucleoproteins Participate in Hepatitis E Virus Replication. *J Mol Biol* (2020) 432(7):2369–87. doi: 10.1016/j.jmb.2020.02.025
23. Sun L, Wu J, Du F, Chen X, Chen ZJ. Cyclic GMP-AMP synthase is a cytosolic DNA sensor that activates the type I interferon pathway. *Science* (2013) 339(6121):786–91. doi: 10.1126/science.1232458
24. Zhong L, Hu MM, Bian LJ, Liu Y, Chen Q, Shu HB. Phosphorylation of cGAS by CDK1 impairs self-DNA sensing in mitosis. *Cell Discovery* (2020) 6:26. doi: 10.1038/s41421-020-0162-2
25. Denais CM, Gilbert RM, Isermann P, McGregor AL, te Lindert M, Weigelin B, et al. Nuclear envelope rupture and repair during cancer cell migration. *Science* (2016) 352(6283):353–8. doi: 10.1126/science.aad7297
26. Zhao B, Xu P, Rowlett CM, Jing T, Shinde O, Lei Y, et al. The Molecular Basis of Tight Nuclear Tethering and Inactivation of cGAS. *Nature* (2020) 587(7835):673–7. doi: 10.1038/s41586-020-2749-z
27. Kujirai T, Zierhut C, Takizawa Y, Kim R, Negishi L, Uruma N, et al. Structural basis for the inhibition of cGAS by nucleosomes. *Science* (2020) 370(6515):455–8. doi: 10.1126/science.abd0237
28. Lahaye X, Gentili M, Silvin A, Conrad C, Picard L, Jouve M, et al. NONO Detects the Nuclear HIV Capsid to Promote cGAS-Mediated Innate Immune Activation. *Cell* (2018) 175(2):488–501.e22. doi: 10.1016/j.cell.2018.08.062
29. Johnstone RW, Kerry JA, Trapani JA. The human interferon-inducible protein, IFI 16, is a repressor of transcription. *J Biol Chem* (1998) 273 (27):17172–7. doi: 10.1074/jbc.273.27.17172
30. Gariano GR, Dell'Oste V, Bronzini M, Gatti D, Luganini A, De Andrea M, et al. The intracellular DNA sensor IFI16 gene acts as restriction factor for human cytomegalovirus replication. *PloS Pathog* (2012) 8(1):e1002498. doi: 10.1371/journal.ppat.1002498
31. Johnson KE, Bottero V, Flaherty S, Dutta S, Singh VV, Chandran B. IFI16 restricts HSV-1 replication by accumulating on the hsv-1 genome, repressing HSV-1 gene expression, and directly or indirectly modulating histone modifications. *PloS Pathog* (2014) 10(11):e1004503. doi: 10.1371/journal.ppat.1004503
32. Diner BA, Lum KK, Toettcher JE, Cristea IM. Viral DNA Sensors IFI16 and Cyclic GMP-AMP Synthase Possess Distinct Functions in Regulating Viral Gene Expression, Immune Defenses, and Apoptotic Responses during Herpesvirus Infection. *mBio* (2016) 7(6):e01553-16. doi: 10.1128/mBio.01553-16
33. Lo Cigno I, De Andrea M, Borgogna C, Albertini S, Landini MM, Peretti A, et al. The Nuclear DNA Sensor IFI16 Acts as a Restriction Factor for Human Papillomavirus Replication through Epigenetic Modifications of the Viral Promoters. *J Virol* (2015) 89(15):7506–20. doi: 10.1128/JVI.00013-15
34. Hotter D, Bosso M, Jonsson KL, Krapp C, Sturzel CM, Das A, et al. IFI16 Targets the Transcription Factor Sp1 to Suppress HIV-1 Transcription and Latency Reactivation. *Cell Host Microbe* (2019) 25(6):858–72.e13. doi: 10.1016/j.chom.2019.05.002
35. Cristea IM, Moorman NJ, Terhune SS, Cuevas CD, O'Keefe ES, Rout MP, et al. Human cytomegalovirus pUL83 stimulates activity of the viral immediate-early promoter through its interaction with the cellular IFI16 protein. *J Virol* (2010) 84(15):7803–14. doi: 10.1128/JVI.00139-10
36. Orzalli MH, Conwell SE, Berrios C, DeCaprio JA, Knipe DM. Nuclear interferon-inducible protein 16 promotes silencing of herpesviral and transfected DNA. *Proc Natl Acad Sci USA* (2013) 110(47):E4492–501. doi: 10.1073/pnas.1316194110
37. Choubey D, Panchanathan R. IFI16, an amplifier of DNA-damage response: Role in cellular senescence and aging-associated inflammatory diseases. *Ageing Res Rev* (2016) 28:27–36. doi: 10.1016/j.arr.2016.04.002
38. Fujiuchi N, Aglipay JA, Ohtsuka T, Maehara N, Sahin F, Su GH, et al. Requirement of IFI16 for the maximal activation of p53 induced by ionizing radiation. *J Biol Chem* (2004) 279(19):20339–44. doi: 10.1074/jbc.M400344200
39. De Andrea M, Gioia D, Mondini M, Azzimonti B, Reno F, Pecorari G, et al. Effects of IFI16 overexpression on the growth and doxorubicin sensitivity of head and neck squamous cell carcinoma-derived cell lines. *Head Neck* (2007) 29(9):835–44. doi: 10.1002/hed.20611
40. Lin W, Zhao Z, Ni Z, Zhao Y, Du W, Chen S. IFI16 restoration in hepatocellular carcinoma induces tumour inhibition via activation of p53 signals and inflammasome. *Cell Prolif* (2017) 50(6):e12392. doi: 10.1111/cpr.12392
41. Song LL, Alimirah F, Panchanathan R, Xin H, Choubey D. Expression of an IFN-inducible cellular senescence gene, IFI16, is up-regulated by p53. *Mol Cancer Res* (2008) 6(11):1732–41. doi: 10.1158/1541-7786.Mcr-08-0208
42. Cai H, Yan L, Liu N, Xu M, Cai H. IFI16 promotes cervical cancer progression by upregulating PD-L1 in immunomicroenvironment through STING-TBK1-NF-kB pathway. *BioMed Pharmacother* (2020) 123:109790. doi: 10.1016/j.biopha.2019.109790
43. Golan-Gerstl R, Cohen M, Shilo A, Suh SS, Bakàcs A, Coppola L, et al. Splicing factor hnRNP A2/B1 regulates tumor suppressor gene splicing and is an oncogenic driver in glioblastoma. *Cancer Res* (2011) 71(13):4464–72. doi: 10.1158/0008-5472.Can-10-4410
44. Dai S, Zhang J, Huang S, Lou B, Fang B, Ye T, et al. HNRNPA2B1 regulates the epithelial-mesenchymal transition in pancreatic cancer cells through the ERK/snail signalling pathway. *Cancer Cell Int* (2017) 17:12. doi: 10.1186/s12935-016-0368-4
45. Chen T, Gu C, Xue C, Yang T, Zhong Y, Liu S, et al. LncRNA-uc002mbe.2 Interacting with hnRNPA2B1 Mediates AKT Deactivation and p21 Up-Regulation Induced by Trichostatin in Liver Cancer Cells. *Front Pharmacol* (2017) 8:669. doi: 10.3389/fphar.2017.00669
46. Barceló C, Etchin J, Mansour MR, Sanda T, Ginesta MM, Sanchez-Arévalo Lobo VJ, et al. Ribonucleoprotein HNRNPA2B1 interacts with and regulates oncogenic KRAS in pancreatic ductal adenocarcinoma cells. *Gastroenterology* (2014) 147(4):882–92.e8. doi: 10.1053/j.gastro.2014.06.041
47. Yang Y, Wei Q, Tang Y, Yuanyuan W, Luo Q, Zhao H, et al. Loss of hnRNPA2B1 inhibits malignant capability and promotes apoptosis via down-regulating Lin28B expression in ovarian cancer. *Cancer Lett* (2020) 475:43–52. doi: 10.1016/j.canlet.2020.01.029
48. Zhou J, Mulshine JL, Unsworth EJ, Scott FM, Avis IM, Vos MD, et al. Purification and characterization of a protein that permits early detection of lung cancer. Identification of heterogeneous nuclear ribonucleoprotein-A2/B1 as the antigen for monoclonal antibody 703D4. *J Biol Chem* (1996) 271 (18):10760–6. doi: 10.1074/jbc.271.18.10760
49. Fielding P, Turnbull L, Prime W, Walshaw M, Field JK. Heterogeneous nuclear ribonucleoprotein A2/B1 up-regulation in bronchial lavage specimens: a clinical marker of early lung cancer detection. *Clin Cancer Res* (1999) 5(12):4048–52.
50. Tauler J, Zudaire E, Liu H, Shih J, Mulshine JL. hnRNP A2/B1 modulates epithelial-mesenchymal transition in lung cancer cell lines. *Cancer Res* (2010) 70(18):7137–47. doi: 10.1158/0008-5472.CAN-10-0860
51. Liu H, Zhang H, Wu X, Ma D, Wu J, Wang L, et al. Nuclear cGAS suppresses DNA repair and promotes tumorigenesis. *Nature* (2018) 563(7729):131–6. doi: 10.1038/s41586-018-0629-6
52. Jiang H, Xue X, Panda S, Kawale A, Hooy RM, Liang F, et al. Chromatin-bound cGAS is an inhibitor of DNA repair and hence accelerates genome destabilization and cell death. *EMBO J* (2019) 38(21):e102718. doi: 10.15252/embj.2019102718
53. Dawson MJ, Trapani JA. IFI 16 gene encodes a nuclear protein whose expression is induced by interferons in human myeloid leukaemia cell lines. *J Cell Biochem* (1995) 57(1):39–51. doi: 10.1002/jcb.240570106
54. Der SD, Zhou A, Williams BR, Silverman RH. Identification of genes differentially regulated by interferon alpha, beta, or gamma using oligonucleotide arrays. *Proc Natl Acad Sci USA* (1998) 95(26):15623–8. doi: 10.1073/pnas.95.26.15623
55. Hooks JJ, Moutsopoulos HM, Geis SA, Stahl NII, Decker JL, Notkins AL. Immune interferon in the circulation of patients with autoimmune disease. *N Engl J Med* (1979) 301(1):5–8. doi: 10.1056/NEJM197907053010102
56. Banchereau J, Pascual V. Type I interferon in systemic lupus erythematosus and other autoimmune diseases. *Immunity* (2006) 25(3):383–92. doi: 10.1016/j.immuni.2006.08.010
57. Oke V, Gunnarsson I, Dorschner J, Eketjall S, Zickert A, Niewold TB, et al. High levels of circulating interferons type I, type II and type III associate with distinct clinical features of active systemic lupus erythematosus. *Arthritis Res Ther* (2019) 21(1):107. doi: 10.1186/s13075-019-1878-y
58. Kimkong I, Avihingsanon Y, Hirankarn N. Expression profile of HIN200 in leukocytes and renal biopsy of SLE patients by real-time RT-PCR. *Lupus* (2009) 18(12):1066–72. doi: 10.1177/0961203309106699
59. Thompson MR, Sharma S, Atianand M, Jensen SB, Carpenter S, Knipe DM, et al. Interferon gamma-inducible protein (IFI) 16 transcriptionally regulates

type i interferons and other interferon-stimulated genes and controls the interferon response to both DNA and RNA viruses. *J Biol Chem* (2014) 289 (34):23568–81. doi: 10.1074/jbc.M114.554147
60. Yang B, Song D, Liu Y, Cui Y, Lu G, Di W, et al. IFI16 regulates HTLV-1 replication through promoting HTLV-1 RTI-induced innate immune responses. *FEBS Lett* (2018) 592(10):1693–704. doi: 10.1002/1873-3468.13077
61. Nissen SK, Hojen JF, Andersen KL, Kofod-Olsen E, Berg RK, Paludan SR, et al. Innate DNA sensing is impaired in HIV patients and IFI16 expression correlates with chronic immune activation. *Clin Exp Immunol* (2014) 177 (1):295–309. doi: 10.1111/cei.12317
62. Yang Y, Zhao X, Wang Z, Shu W, Li L, Li Y, et al. Nuclear Sensor Interferon-Inducible Protein 16 Inhibits the Function of Hepatitis B Virus Covalently Closed Circular DNA by Integrating Innate Immune Activation and Epigenetic Suppression. *Hepatology* (2020) 71(4):1154–69. doi: 10.1002/hep.30897
63. Johnson DE, O'Keefe RA, Grandis JR. Targeting the IL-6/JAK/STAT3 signalling axis in cancer. *Nat Rev Clin Oncol* (2018) 15(4):234–48. doi: 10.1038/nrclinonc.2018.8
64. Ni Z, Bremner R. Brahma-related gene 1-dependent STAT3 recruitment at IL-6-inducible genes. *J Immunol* (2007) 178(1):345–51. doi: 10.4049/jimmunol.178.1.345
65. Collins C, Rommens JM, Kowbel D, Godfrey T, Tanner M, Hwang SII, et al. Positional cloning of ZNF217 and NABC1: genes amplified at 20q13.2 and overexpressed in breast carcinoma. *Proc Natl Acad Sci USA* (1998) 95 (15):8703–8. doi: 10.1073/pnas.95.15.8703
66. Iwabuchi H, Sakamoto M, Sakunaga H, Ma YY, Carcangiu ML, Pinkel D, et al. Genetic analysis of benign, low-grade, and high-grade ovarian tumors. *Cancer Res* (1995) 55(24):6172–80.
67. Bar-Shira A, Pinthus JH, Rozovsky U, Goldstein M, Sellers WR, Yaron Y, et al. Multiple genes in human 20q13 chromosomal region are involved in an advanced prostate cancer xenograft. *Cancer Res* (2002) 62(23):6803–7.
68. Krig SR, Jin VX, Bieda MC, O'Geen H, Yaswen P, Green R, et al. Identification of genes directly regulated by the oncogene ZNF217 using chromatin immunoprecipitation (ChIP)-chip assays. *J Biol Chem* (2007) 282 (13):9703–12. doi: 10.1074/jbc.M611752200
69. von Eckardstein KL, Patt S, Zhu J, Zhang L, Cervos-Navarro J, Reszka R. Short-term neuropathological aspects of in vivo suicide gene transfer to the F98 rat glioblastoma using liposomal and viral vectors. *Histol Histopathol* (2001) 16(3):735–44. doi: 10.14670/HH-16.735
70. Yan-Sanders Y, Hammons GJ, Lyn-Cook BD. Increased expression of heterogeneous nuclear ribonucleoprotein A2/B1 (hnRNP) in pancreatic tissue from smokers and pancreatic tumor cells. *Cancer Lett* (2002) 183 (2):215–20. doi: 10.1016/s0304-3835(02)00168-4
71. Lee CL, Hsiao HH, Lin CW, Wu SP, Huang SY, Wu CY, et al. Strategic shotgun proteomics approach for efficient construction of an expression map of targeted protein families in hepatoma cell lines. *Proteomics* (2003) 3 (12):2472–86. doi: 10.1002/pmic.200300586
72. Lee CH, Lum JH, Cheung BP, Wong MS, Butt YK, Tam MF, et al. Identification of the heterogeneous nuclear ribonucleoprotein A2/B1 as the antigen for the gastrointestinal cancer specific monoclonal antibody MG7. *Proteomics* (2005) 5(4):1160–6. doi: 10.1002/pmic.200401159
73. Santarosa M, Del Col L, Viel A, Bivi N, D'Ambrosio C, Scaloni A, et al. BRCA1 modulates the expression of hnRNPA2B1 and KHSRP. *Cell Cycle* (2010) 9(23):4666–73. doi: 10.4161/cc.9.23.14022
74. Yu PF, Kang AR, Jing LJ, Wang YM. Long non-coding RNA CACNA1G-AS1 promotes cell migration, invasion and epithelial-mesenchymal transition by HNRNPA2B1 in non-small cell lung cancer. *Eur Rev Med Pharmacol Sci* (2018) 22(4):993–1002. doi: 10.26355/eurrev_201802_14381
75. Ma F, Li B, Liu SY, Iyer SS, Yu Y, Wu A, et al. Positive feedback regulation of type I IFN production by the IFN-inducible DNA sensor cGAS. *J Immunol* (2015) 194(4):1545–54. doi: 10.4049/jimmunol.1402066
76. An J, Durcan L, Karr RM, Briggs TA, Rice GII, Teal TH, et al. Expression of Cyclic GMP-AMP Synthase in Patients With Systemic Lupus Erythematosus. *Arthritis Rheumatol* (2017) 69(4):800–7. doi: 10.1002/art.40002
77. Wang ZS, Liu YL, Mi N, Duan DY. Intracellular DNA sensing pathway of cGAS-cGAMP is decreased in human newborns and young children. *Mol Immunol* (2017) 87:76–85. doi: 10.1016/j.molimm.2017.04.007
78. Ma F, Lei YY, Ding MG, Luo LH, Xie YC, Liu XL. LncRNA NEAT1 Interacted With DNMT1 to Regulate Malignant Phenotype of Cancer Cell and Cytotoxic T Cell Infiltration via Epigenetic Inhibition of p53, cGAS, and STING in Lung Cancer. *Front Genet* (2020) 11:250. doi: 10.3389/fgene.2020.00250
79. Johnstone RW, Kershaw MH, Trapani JA. Isotypic variants of the interferon-inducible transcriptional repressor IFI 16 arise through differential mRNA splicing. *Biochemistry* (1998) 37(34):11924–31. doi: 10.1021/bi981069a
80. Veeranki S, Choubey D. Interferon-inducible p200-family protein IFI16, an innate immune sensor for cytosolic and nuclear double-stranded DNA: regulation of subcellular localization. *Mol Immunol* (2012) 49(4):567–71. doi: 10.1016/j.molimm.2011.11.004
81. Li Y, Guo H, Jin C, Qiu C, Gao M, Zhang L, et al. Spliceosome-associated factor CTNNBL1 promotes proliferation and invasion in ovarian cancer. *Exp Cell Res* (2017) 357(1):124–34. doi: 10.1016/j.yexcr.2017.05.008
82. Wang PH, Ye ZW, Deng JJ, Siu KL, Gao WW, Chaudhary V, et al. Inhibition of AIM2 inflammasome activation by a novel transcript isoform of IFI16. *EMBO Rep* (2018) 19(10):e45737. doi: 10.15252/embr.201845737
83. Alarcon CR, Goodarzi H, Lee H, Liu X, Tavazoie S, Tavazoie SF. HNRNPA2B1 Is a Mediator of m(6)A-Dependent Nuclear RNA Processing Events. *Cell* (2015) 162(6):1299–308. doi: 10.1016/j.cell.2015.08.011
84. Su C, Zheng C. Herpes Simplex Virus 1 Abrogates the cGAS/STING-Mediated Cytosolic DNA-Sensing Pathway via Its Virion Host Shutoff Protein, UL41. *J Virol* (2017) 91(6):e02414-16. doi: 10.1128/JVI.02414-16
85. Orzalli MH, Broekema NM, Knipe DM. Relative Contributions of Herpes Simplex Virus 1 ICP0 and vhs to Loss of Cellular IFI16 Vary in Different Human Cell Types. *J Virol* (2016) 90(18):8351–9. doi: 10.1128/JVI.00939-16
86. Deribe YL, Pawson T, Dikic I. Post-translational modifications in signal integration. *Nat Struct Mol Biol* (2010) 17(6):666–72. doi: 10.1038/nsmb.1842
87. Liu J, Qian C, Cao X. Post-Translational Modification Control of Innate Immunity. *Immunity* (2016) 45(1):15–30. doi: 10.1016/j.immuni.2016.06.020
88. Dell'Oste V, Gatti D, Gugliesi F, De Andrea M, Bawadekar M, Lo Cigno I, et al. Innate nuclear sensor IFI16 translocates into the cytoplasm during the early stage of in vitro human cytomegalovirus infection and is entrapped in the egressing virions during the late stage. *J Virol* (2014) 88(12):6970–82. doi: 10.1128/JVI.00384-14
89. Johnson KE, Chikoti L, Chandran B. Herpes simplex virus 1 infection induces activation and subsequent inhibition of the IFI16 and NLRP3 inflammasomes. *J Virol* (2013) 87(9):5005–18. doi: 10.1128/JVI.00082-13
90. Li D, Wu R, Guo W, Xie L, Qiao Z, Chen S, et al. STING-Mediated IFI16 Degradation Negatively Controls Type I Interferon Production. *Cell Rep* (2019) 29(5):1249–60.e4. doi: 10.1016/j.celrep.2019.09.069
91. Li T, Diner BA, Chen J, Cristea IM. Acetylation modulates cellular distribution and DNA sensing ability of interferon-inducible protein IFI16. *Proc Natl Acad Sci U.S.A.* (2012) 109(26):10558–63. doi: 10.1073/pnas.1203447109
92. Ansari MA, Dutta S, Veettil MV, Dutta D, Iqbal J, Kumar B, et al. Herpesvirus Genome Recognition Induced Acetylation of Nuclear IFI16 Is Essential for Its Cytoplasmic Translocation, Inflammasome and IFN-beta Responses. *PloS Pathog* (2015) 11(7):e1005019. doi: 10.1371/journal.ppat.1005019
93. Kim H, Kim H, Feng Y, Li Y, Tamiya H, Tocci S, et al. PRMT5 control of cGAS/STING and NLRC5 pathways defines melanoma response to antitumor immunity. *Sci Transl Med* (2020) 12(551):eaaz5683. doi: 10.1126/scitranslmed.aaz5683
94. Zhou Y, He C, Wang L, Ge B. Post-translational regulation of antiviral innate signaling. *Eur J Immunol* (2017) 47(9):1414–26. doi: 10.1002/eji.201746959
95. Briggs LJ, Johnstone RW, Elliot RM, Xiao CY, Dawson M, Trapani JA, et al. Novel properties of the protein kinase CK2-site-regulated nuclear-localization sequence of the interferon-induced nuclear factor IFI 16. *Biochem J* (2001) 353(Pt 1):69–77. doi: 10.1042/bj3530069
96. Komander D, Rape M. The ubiquitin code. *Annu Rev Biochem* (2012) 81:203–29. doi: 10.1146/annurev-biochem-060310-170328

97. Swatek KN, Komander D. Ubiquitin modifications. *Cell Res* (2016) 26 (4):399–422. doi: 10.1038/cr.2016.39
98. Walczak H, Iwai K, Dikic I. Generation and physiological roles of linear ubiquitin chains. *BMC Biol* (2012) 10:23. doi: 10.1186/1741-7007-10-23
99. Jiang X, Chen ZJ. The role of ubiquitylation in immune defence and pathogen evasion. *Nat Rev Immunol* (2011) 12(1):35–48. doi: 10.1038/nri3111
100. Heaton SM, Borg NA, Dixit VM. Ubiquitin in the activation and attenuation of innate antiviral immunity. *J Exp Med* (2016) 213(1):1–13. doi: 10.1084/jem.20151531
101. Ansari MA, Singh VV, Dutta S, Veettil MV, Dutta D, Chikoti L, et al. Constitutive interferon-inducible protein 16-inflammasome activation during Epstein-Barr virus latency I, II, and III in B and epithelial cells. *J Virol* (2013) 87(15):8606–23. doi: 10.1128/JVI.00805-13
102. Orzalli MH, DeLuca NA, Knipe DM. Nuclear IFI16 induction of IRF-3 signaling during herpesviral infection and degradation of IFI16 by the viral ICP0 protein. (2012) *Proc Natl Acad Sci U S A* (2012) 109(44):E3008-17. doi: 10.1073/pnas.1211302109
103. Cuchet-Lourenco D, Anderson G, Sloan E, Orr A, Everett RD. The viral ubiquitin ligase ICP0 is neither sufficient nor necessary for degradation of the cellular DNA sensor IFI16 during herpes simplex virus 1 infection. *J Virol* (2013) 87(24):13422–32. doi: 10.1128/JVI.02474-13
104. Choudhary C, Kumar C, Gnad F, Nielsen ML, Rehman M, Walther TC, et al. Lysine acetylation targets protein complexes and co-regulates major cellular functions. *Science* (2009) 325(5942):834–40. doi: 10.1126/science.1175371
105. Iqbal J, Ansari MA, Kumar B, Dutta D, Roy A, Chikoti L, et al. Histone H2B-IFI16 Recognition of Nuclear Herpesviral Genome Induces Cytoplasmic Interferon-beta Responses. *PloS Pathog* (2016) 12(10):e1005967. doi: 10.1371/journal.ppat.1005967
106. Beaver JE, Waters ML. Molecular Recognition of Lys and Arg Methylation. *ACS Chem Biol* (2016) 11(3):643–53. doi: 10.1021/acschembio.5b00996
107. Lieber MR, Ma Y, Pannicke U, Schwarz K. Mechanism and regulation of human non-homologous DNA end-joining. *Nat Rev Mol Cell Biol* (2003) 4 (9):712–20. doi: 10.1038/nrm1202
108. Ferguson BJ, Mansur DS, Peters NE, Ren H, Smith GL. DNA-PK is a DNA sensor for IRF-3-dependent innate immunity. *Elife* (2012) 1:e00047. doi: 10.7554/eLife.00047
109. Burleigh K, Maltbaek JH, Cambier S, Green R, Gale M Jr., James RC, et al. Human DNA-PK activates a STING-independent DNA sensing pathway. *Sci Immunol* (2020) 5(43):eaba4219. doi: 10.1126/sciimmunol.aba4219
110. Michalski S, de Oliveira Mann CC, Stafford CA, Witte G, Bartho J, Lammens K, et al. Structural basis for sequestration and autoinhibition of cGAS by chromatin. *Nature* (2020). 587(7835):678–82. doi: 10.1038/s41586-020-2748-0
111. Boyer JA, Spangler CJ, Strauss JD, Cesmat AP, Liu P, McGinty RK, et al. Structural basis of nucleosome-dependent cGAS inhibition. *Science* (2020) 370(6515):450–4. doi: 10.1126/science.abd0609
112. Pathare GR, Decout A, Glück S, Cavadini S, Makasheva K, Hovius R, et al. Structural mechanism of cGAS inhibition by the nucleosome. *Nature* (2020) 587(7835):668–72. doi: 10.1038/s41586-020-2750-6
113. Xia P, Wang S, Ye B, Du Y, Li C, Xiong Z, et al. A Circular RNA Protects Dormant Hematopoietic Stem Cells from DNA Sensor cGAS-Mediated Exhaustion. *Immunity* (2018) 48(4):688–701.e7. doi: 10.1016/j.immuni.2018.03.016
114. Zhu H, Zheng C. The Race between Host Antiviral Innate Immunity and the Immune Evasion Strategies of Herpes Simplex Virus 1. *Microbiol Mol Biol Rev* (2020) 84(4):e00099-20. doi: 10.1128/MMBR.00099-20

Conflict of Interest: The authors declare that the research was conducted in the absence of any commercial or financial relationships that could be construed as a potential conflict of interest.

frontiers in Immunology

MINI REVIEW
published: 29 January 2021
doi: 10.3389/fimmu.2020.613799

Herpes Simplex Virus and Pattern Recognition Receptors: An Arms Race

Jun Zhao, Chao Qin, Yongzhen Liu, Youliang Rao and Pinghui Feng**

Section of Infection and Immunity, Herman Ostrow School of Dentistry, Norris Comprehensive Cancer Center, University of Southern California, Los Angeles, CA, United States

Herpes simplex viruses (HSVs) are experts in establishing persistent infection in immune-competent humans, in part by successfully evading immune activation through diverse strategies. Upon HSV infection, host deploys pattern recognition receptors (PRRs) to recognize various HSV-associated molecular patterns and mount antiviral innate immune responses. In this review, we describe recent advances in understanding the contributions of cytosolic PRRs to detect HSV and the direct manipulations on these receptors by HSV-encoded viral proteins as countermeasures. The continuous update and summarization of these mechanisms will deepen our understanding on HSV-host interactions in innate immunity for the development of novel antiviral therapies, vaccines and oncolytic viruses.

Keywords: herpes simplex virus, pattern recognition receptors, RIG-I/MDA5, CGAS, IFI16, AIM2, DAI, PKR

OPEN ACCESS

Edited by:
Junji Xing,
Houston Methodist Research Institute, United States

Reviewed by:
Angello Retamal-Diaz,
Universidad de Antofagasta, Chile
Maria Kalamvoki,
University of Kansas Medical Center, United States

****Correspondence:***
Jun Zhao
junz@usc.edu
Pinghui Feng
pinghuif@usc.edu

Specialty section:
This article was submitted to Viral Immunology, a section of the journal Frontiers in Immunology

Received: *03 October 2020*
Accepted: *14 December 2020*
Published: *29 January 2021*

Citation:
Zhao J, Qin C, Liu Y, Rao Y and Feng P (2021) Herpes Simplex Virus and Pattern Recognition Receptors: An Arms Race. Front. Immunol. 11:613799. doi: 10.3389/fimmu.2020.613799

INTRODUCTION

Herpesviridae is a family of large DNA viruses that establish persistent infection within their immune-competent host. Members of the family are further grouped into three subfamilies, i.e., alpha-, beta-, and gamma-herpesviruses based on their genome organization, biological characteristics, and cell tropism (1, 2). Herpes simplex virus type 1 (HSV-1 or human herpesvirus 1, HHV-1) and type 2 (HSV-2 or human herpesvirus 2, HHV-2) belong to the alpha-herpesvirus subfamily and the genera simplex virus. They are neurotropic viruses that establish latent infection in the trigeminal ganglia (TG) and dorsal root ganglia (DRG) for the entire life of the host (3). Seropositive for HSV are high, averaging nearly 70% in the general population and approaching 100% in senior citizens of 65-year or older (4, 5). Clinical manifestations of HSV-1 infections include various mucocutaneous diseases, such as herpes labialis, genital herpes, herpetic whitlow, and keratitis (6). It can cause encephalitis that is often life-threatening, in a small portion of the infected individuals who are immune-compromised (6). HSV-2 infection frequently causes genital sores (7).

HSV-1 and HSV-2 are structurally closely related. Herpes simplex virions are spherical particles with a diameter of 186 nm, with glycoprotein protrusions on the surface, making the full diameter approximately 225 nm (8). Both viruses contain a linear double-stranded DNA (dsDNA) genome that is ~150 kilobase (kb) in size and encodes more than 70 open reading frames (ORFs). The viral genomes are caged by a 125 nm icosahedral capsid, which is surrounded by an amorphous layer called tegument (9). Packaged within the tegument compartment, a large number of viral structural proteins are released into the infected cell to establish an environment that is conducive for viral

replication. The tegument is enveloped by a lipid bilayer within which multiple viral glycoproteins are embedded. These surface glycoproteins mediate the entry and fusion of the virus with the target cell (10).

HSV-1 and HSV-2 share almost identical replication cycles. Viral entry into host cells is mediated by the interactions between cellular receptors and viral glycoproteins anchored within the virion envelope. The initial binding occurs through the binding of envelope glycoprotein C (gC) and/or gB to heparan sulfate proteoglycan, which is immediately followed by gD association with one of the three known receptors to initiate virus entry (11). The receptors involved are cell-type dependent. While nectin-1 is the main receptor of epithelial cells, neuronal cells and fibroblasts (12), HVEM is the main receptor of T cells and cornea epithelial cells, for HSV infection (13, 14). Upon fusion of the virion envelope with the host cell membrane, tegument proteins are released into the cytoplasm of the infected cells to facilitate capsid trafficking and evade host antiviral immunity. The de-enveloped nucleocapsid is transported along microtubules to the nuclear pore, where the viral genome is injected into the nucleus. At this point, HSVs adopt two modes of infection. In neuronal cells located at the peripheral ganglia region and lab-isolated primary neurons, the viral genome stays as a circularized episome with no active gene transcription except for the latent-associated transcripts (LATs) (15). LATs do not encode proteins, but two major RNA species and several small non-coding RNAs that regulate cell survival and viral lytic gene expression (16). Therefore, this stage is termed as viral latency with no clear clinical manifestation. However, the virus can be periodically reactivated and enters the lytic cycle, largely due to stress responses and other stimuli not fully understood. During the lytic cycle, the viral genome serves as the template for transcription, leading to the sequential production of viral messenger RNAs and polypeptides of the immediate early (IE), early (E), and late (L) phases (17). Tegument protein VP16 and cellular factors promote transcription of IE genes [e.g., infected cell polypeptide 0 (ICP0), ICP4, ICP22, ICP27 and ICP47]. IE proteins then promote transcription and translation of E genes, which produce the necessary components for viral DNA replication. Replicated viral genomes collaborate with transcription factors to promote the expression of L proteins that are structural components of HSV virions (such as glycoproteins and capsid proteins VP5, VP21, VP23, VP24 and VP26), thereby maximizing viral protein production in preparation for viral assembly and egress. Nucleocapsids assemble in the nucleus, undergo envelopment and de-envelopment at the nuclear membrane, and re-envelopment in the TGN to acquire their tegument and glycoprotein-embedded membrane, en route to the maturation and release of amplified virion progeny (18). Importantly, viral latency, reactivation and lytic replication collectively contribute to the life-long 'persistent infection' of HSV in an immune-competent host, leading to the recurrent pathogenesis associated with the virus.

Upon infection, host cells sense invading viruses *via* cellular pattern-recognition receptors (PRRs) to initiate the antiviral innate immune defense. Structurally, PRRs can be generally classified into several major families, including Toll-like receptors (TLRs), RIG-I like receptor (RLRs), NOD-like receptors (NLRs), C-type lectin receptors (CLRs), AIM2-like receptors (ALRs), and cyclic GMP-AMP synthase (cGAS). These PRRs can recognize various pathogen-associated molecular patterns (PAMPs) from bacteria, viruses, fungi and protozoa. Microbial PAMPs can be lipoproteins, carbohydrates, lipopolysaccharides and nucleic acids. PRRs also recognize endogenous damage- or danger-associated molecular patterns (DAMP) from the host, which are related to immune homeostasis and autoimmune diseases. Among PAMPs, the nucleic acid RNA and DNA have attracted much attention. PRRs recognizing the nucleic acids include: DNA sensors such as endosomal Toll-Like Receptor 9 (TLR9), cytosolic Absent In Melanoma 2 (AIM2), Interferon Gamma Inducible Protein 16 (IFI16), DNA-dependent Activator of Interferon-regulatory factors (DAI) and cyclic GMP-AMP synthase (cGAS); RNA sensors TLR3, TLR7, TLR8, and cytosolic Retinoic acid-Inducible Gene I (RIG-I), Melanoma Differentiation-Associated protein 5 (MDA5), NLR Family Pyrin Domain Containing 3 (NLRP3), and Nucleotide-binding Oligomerization Domain-containing protein 2 (NOD2) (19). TLRs are transmembrane receptors, while cytosolic or nuclear receptors are soluble within their corresponding compartments. After sensing PAMPs or DAMPs, PRRs activate their adaptors and downstream Interferon Regulatory Factors (IRFs) and Nuclear Factor kappa-light-chain-enhancer of activated B cells (NF-κB), leading to the transcription and translation of cytokines, chemokines, MHC, and co-stimulatory molecules. In addition, PRRs can trigger signal transduction and induce cellular processes that do not rely on transcription, such as phagocytosis, autophagy, cell death, and inflammasome activation. These processes work in concert with innate immune response to mesh a network of antiviral host defense (19). In this review, we will summarize the recent findings on the contribution of cytosolic PRRs to sense HSV in host defense, and the counteractive measures deployed by HSV to deflect these PRRs to establish persistent infection.

THE RIG-I- AND MDA5-MAVS PATHWAY

RLRs, including RIG-I (20), MDA5 (21, 22), and probable ATP-dependent RNA helicase DHX58 (LGP2), are cytoplasmic PRRs that recognize virus-derived or viral infection-associated cellular double-stranded RNA (dsRNA). RIG-I recognizes short, blunt-ended dsRNA carrying terminal 5'-triphosphate or 5'-diphosphate moieties (23), while MDA5 prefers longer dsRNA independent of its terminal phosphate groups.

Upon engaging viral dsRNA, RIG-I and MDA-5 hydrolyze ATP to induce their oligomerization on the dsRNA, thereby exposing their N-terminal caspase activation and recruitment domains (CARDs) to relay immune activation *via* seeding the oligomerization of the adaptor protein MAVS (also known as IPS-1, CARDIF, and VISA) (24–28). LGP2 lacks the CARD domain and is reported to inhibit RIG-I-mediated antiviral responses. Once activated, MAVS forms prion-like oligomers on the outer membrane of mitochondria (29), which further

recruits the tank-binding kinase-1(TKB1) and IκB kinase (IKK) complex to activate IRF and NF-κB transcription factors, respectively. Therefore, RIG-I and MDA5 exhibit antiviral activities to a broad spectrum of RNA viruses, including influenza A virus, hepatitis C virus, dengue virus, encephalomyocarditis virus, coronavirus, etc (30). Post-translational modifications, such as phosphorylation and ubiquitination, are discovered to tightly regulate the activation of RIG-I (31–35).

Unlike RNA viruses, genomes of DNA viruses such as herpes simplex viruses (HSV-1 and -2) do not carry the structural features required for binding to RLRs. Remarkably, RLRs demonstrate antiviral activities against HSVs. During HSV-1 latency, two small non-coding RNAs (sncRNAs) coded by the LAT, sncRNA1 and sncRNA2, were shown to interact with and activate RIG-I in neuronal cells, resulting in type I interferon induction and NF-κB activation that promote viral latency and neuronal survival (36). Upon viral entry, early studies have shown that RIG-I and MDA5 non-redundantly activate type I IFN genes upon cytosolic DNA stimulation (37). In support of this, DNA-dependent RNA polymerase III (Pol III) is reported to convert cytosolic DNA to 5'-ppp RNA that activates RIG-I (38). Regarding the source of cytosolic DNA, in macrophages, HSV-1 capsid is found to be degraded by the ubiquitin-mediated proteasome system, thereby releasing viral DNA into the cytosol (39). As such, RIG-I and TLR9 is reported can cooperate to enable the production of type I IFN in HSV-2–infected mouse macrophages (40). However, MDA5 mediates a Pol III-independent pathway to sense HSVs in primary human macrophages (41). The identity of viral RNA or other ligands activating MDA5 remains unknown. In nonimmune cells infected with HSV, studies have detected dsRNA localized in the cytosol, which activates the RIG-I-mediated IFN induction (42). It is proposed that dsRNA molecules originated from the complementary transcription of HSV activate RIG-I. Interestingly, transcripts derived from a cellular 5S ribosomal RNA pseudogene are found to be unmasked by HSV-1 to induce RIG-I activation (43). These findings collectively support the role of RIG-I and MDA5 to sense herpes simplex viruses and induce IFN response.

To counteract RIG-I- and MDA-mediated type I IFN responses, HSV has evolved strategies to directly target these receptors. HSV-2 virion host shutoff (Vhs) protein selectively suppresses the expression of TLR2, TLR3, RIG-I and MDA-5 in human vaginal epithelial cells (44). Given that Vhs is not a sequence-specific endonuclease, it remains unknown how Vhs selectively targets these mRNAs of innate immune function for destruction. It was shown that Vhs targets mRNA for degradation, *via* associating with translation initiation factors (45, 46). Thus, infection-induced translational activation of mRNAs of immune function may be preferentially degraded by Vhs. US11, a dsRNA-binding protein packaged in the virion, binds to RIG-I and MDA5 in a manner independent of its RNA-binding domain and inhibits their interactions with MAVS (47). Released from the tegument upon infection, UL37 displays an intrinsic enzyme activity to deamidate RIG-I during HSV-1 infection (42). Deamidation of two asparagine residues in the helicase domain of RIG-I abrogates its binding to dsRNA and subsequent RNA-stimulated helicase activity. As such, recombinant HSV-1 containing a point mutation that abolishes UL37 deamidase activity triggers more robust RIG-I activation and potent IFN responses than wild-type HSV-1. This recombinant HSV-1 is highly attenuated *in vitro* and in mice.

THE cGAS-STING-IFN Pathway

Stimulator of interferon genes (STING), also known as Met-Pro-Tyr-Ser (MPYS), mediator of IRF3 activation (MITA) (48), Endoplasmic Reticulum IFN stimulator (ERIS) (49), transmembrane protein 173 (TMEM173), is an endoplasmic reticulum adaptor that mediates innate immune activation in response to cyclic dinucleotides (CDNs) (48, 50). These CDNs include cyclic-di-AMP, cyclic-di-GMP, and cyclic-GMP-AMP. Upon activation, STING oligomerizes and translocates to the trans-Golgi network (TGN) where STING recruits TBK1 and IKK kinase complex to activate IRF and NF-κB, leading to the production of type I interferons and inflammatory cytokines. Notably, K27- and K63-linked polyubiquitin chains of STING are essential for the activation of the transcription activity of IRF3 (51).

In response to HSV-1 infection, STING is required for IFN production in multiple cell lines, including murine embryonic fibroblasts, macrophages and dendritic cells (52). Moreover, STING protects mice from HSV-1 lethal infection *via* intravenous and intracerebral routes, while mucosal infection of HSV-1 in *STING*$^{-/-}$ mice results in the increased corneal and trigeminal ganglia viral titers, demonstrating the importance of STING in host defense against HSV-1 *in vivo* (53). As one of the countermeasures, HSV-1 deploys UL36 (also known as VP1–2) to deubiquitinate STING, thus impeding the activation of TBK1 and IRF3. UL36 is the largest protein encoded within HSV and likely provides a scaffold for tegument protein incorporation (54). In fact, HSV-1 ΔDUB mutant induces more robust IFN induction in microglia and shows reduced replication in the brain compared with wild-type HSV-1 (55). Besides UL36, $_{\gamma 1}$34.5 (ICP34.5) interacts with STING and disrupts its translocation from endoplasmic reticulum to Golgi apparatus, a step that is essential for STING to transduce innate immune signals (56). Lastly, ICP27, expressed during HSV-1 *de novo* infection in macrophages, interacts with the activated TBK1-STING signalosome to inhibit IRF3 activation (57), thereby evading immune response downstream of STING.

Paradoxically, in several cell lines, including HEp-2 and HeLa, STING is found to be stabilized by HSV-1 viral proteins, and depletion of STING impedes HSV-1 productive infection (58). The mechanism by which STING enhances HSV-1 replication in these cell lines remains unclear. Nevertheless, these findings suggest the opposing function of STING in host defense is cell type-dependent. One possibility is that the STING-dependent immune defense pathway is rewired by the tumor cell to promote proliferation or growth, which is usurped by HSV-1.

Cyclic guanosine monophosphate (GMP)-adenosine monophosphate (AMP) synthase (cGAS), is a sensor that binds to virus or cell-associated DNA in a sequence-independent manner (59). cGAS is previously demonstrated to mainly reside in the cytoplasm to detect cytoplasmic DNA as it represents a danger signal. Recent finding also suggests that cGAS enters the nucleus to inhibit DNA double-stranded breaks and promotes tumorigenesis (60). The binding of cGAS to DNA induces its oligomerization and concomitant conformational changes, enabling its enzymatic domain to catalyze the synthesis of a second messenger, cyclic GMP-AMP (cGAMP), from cellular GTP and ATP. cGAMP serves as a ligand to activate STING and the downstream IRF and NF-κB branched pathways (61). Therefore, the cGAS-STING pathway plays pivotal roles in inducing type I IFNs and cytokines to mount innate immune responses against bacterial, DNA viruses, cellular genome instability and other related danger signals.

Soon after its discovery, the contribution of cGAS to antagonize HSV-1 was demonstrated by that $cGAS^{-/-}$ mice were more susceptible to HSV-1 challenge than wild-type mice (62). cGAS deficiency also led to impaired IFN expression in microglia, thus resulting in the susceptibility of the mice to herpes simplex encephalitis (HSE) upon ocular infection (63). As cGAS senses HSV-1 DNA to trigger innate immune responses, it is not surprising that HSV-1 evolved diverse strategies to antagonize this pattern recognition receptor and its downstream signaling. HSV-1 tegument protein UL41, an mRNA-specific endonuclease, downregulates the mRNA and protein level of cGAS to abrogate cGAS- and STING-mediated signaling (64). In addition, another tegument protein VP22 is found to interact with cGAS and directly inhibit its enzymatic activity (65). β-catenin is found to be required for the optimal induction of IFN induced by cGAS. As such, HSV-1 US3 phosphorylates β-catenin at Thr556 and blocks its nuclear translocation to dampen cGAS-dependent host antiviral responses (66). We identify that HSV-1 tegument deamidase UL37 targets cGAS, in addition to RIG-I, for deamidation (67). Deamidation of N210, which is in close proximity to the catalytic triad of cGAS, abolishes its catalytic activity to synthesize cGAMP, thereby shutting down cGAMP production and downstream signaling. Interestingly, deamidation does not impair DNA-binding and oligomerization of cGAS, implying the dominant negative effect of deamidated cGAS on the cGAS-IFN pathway. Importantly, non-human primates are resistant to HSV-1 infection and their cGAS proteins contain histine or arginine at the equivalent location of residue 210, which makes cGAS resistant to HSV-1–induced deamidation (67). These findings suggest that cGAS deamidation contributes to the host susceptibility of HSV-1. Altogether, our studies highlight the utmost immune evasion functions of UL37 by targeting multiple sensors for deamidation.

IFI16

IFI16 belongs to the IFN-inducible PYHIN-200 gene family. Members in this family carry the signature HIN domain (IFI16 has two) that binds to dsDNA or ssDNA in a sequence-independent manner. In addition to a DNA-binding domain, IFI16 contains a PYRIN domain (PYD) that mediates protein-protein interactions. Binding to DNA can trigger two distinct signaling pathways, i.e., IFN signaling and inflammasome signaling, depending on the nature of the stimulating signal (68). During viral infection, IFI16 is proposed to bind viral DNA and trigger the activation of STING and induction of IFN, although the detailed mechanism remains unknown (68).

Depletion of IFI16 in the cornea by *in vivo* siRNA transfection results in the decrease of IRF3 phosphorylation and correspondingly increase of HSV-1 viral replication, while $MyD88^{-/-}$ and $Trif^{-/-}$ double knockout mice demonstrate similar IFN production compared to WT controls. This result suggests that IFI16, rather than TLRs, mediates the innate immune response in corneal epithelium against HSV-1 (69). Unlike the cornea, IFI16 is largely dispensable for host defense against HSV-2 in the urogenital system, while TLR2, TLR9, and DAI are essential for IFN and cytokine production (70). In primary human foreskin fibroblasts (HFFs), nuclear resident IFI16 senses the HSV-1 DNA to induce IFN production in a STING-dependent manner, while cGAS promotes IFI16-mediated IFN induction *via* stabilizing IFI16 protein (71). However, how nuclear IFI16 triggers STING activation remains to be addressed. Another study reports a different mechanism of IFI16 to restrict HSV-1 replication in multiple cell lines, where IFI16 selectively binds to HSV-1 transcription start sties to block viral gene transcription *via* inducing repressive histone modifications (72). These studies demonstrate multiple functions of IFI16 to restrict HSV-1 replication. The controversy on IFI16 and cGAS as the HSV-1 sensor could be explained by the differential compartmentalization of the two sensors. For example, cGAS plays major roles in sensing HSV-1 DNA in macrophages, where viral DNA is exposed in the cytosol due to capsid degradation (39). In contrast, IFI16 may detect and mount innate immune response in cells where DNA is delivered into the nucleus. However, a number of recent studies reported that part of the cGAS resides in the nucleus (60, 73), adding to the complexity of the nuclear DNA-sensing mechanism against HSV-1. Following the sensing of nuclear DNA, an immediate question is how nuclear signal of activated IFI16 is relayed to the cytoplasmic STING and downstream signaling events. These questions call for further investigation.

To counteract IFI16, HSV-1 encodes ICP0, a E3 ligase, to induce IFI16 degradation in a proteasome-dependent manner (74). Interesting, ICP0 reduces IFI16 protein in HFFs and oral keratinocytes (NOKs), whereas HSV-1–induced loss in IFI16 protein is dependent on Vhs-mediated mRNA decay (75). These findings highlight distinct mechanisms by which HSV-1 antagonizes the expression of IFI16 in a cell type-specific fashion.

AIM2

Transfection of bacterial, viral and cellular DNA into macrophages leads to the formation of inflammasomes (76, 77). The inflammasome is a protein complex formed in response to the activation of several sensors, including the

NLR (NOD-like receptor) or PYHIN (containing pyran and HIN domains) proteins upon recognizing varieties of viral PAMPs (78). Genetic manipulation *via* RNA interference in cultured cells and knockout in mice demonstrates that AIM2 is a cytosolic DNA sensor (79–84). AIM2 consists of a C-terminal HIN-200 domain and an N-terminal pyrin domain, which form an intramolecular loop to establish a self-repressing state (85). Upon stimulation, the HIN-200 domain binds directly to the sugar-phosphate backbone of dsDNA, releasing the pyrin domain which forms homotypic interaction with the pyrin domain of apoptosis-associated speck-like protein containing a carboxy-terminal CARD (ASC) (86). The CARD of ASC then interacts with the CARD of pro-caspase-1 to activate caspase-1 and form the AIM2 inflammasome. Finally, the activated caspase-1 cleaves the pro-IL-1β and pro-IL-18 and induces the release of the mature IL-1β and IL-18 from the cell (85, 87). Importantly, the expression of the sensors and the cytokine precursors requires a priming step that is stimulated by pro-inflammatory signals such as LPS. Besides cytokine releasing, activated AIM2 inflammasome also induces an inflammatory cell death to protect infected host from invading pathogens, including intracellular bacteria (88, 89), vaccinia virus (79, 89), and murine cytomegalovirus (a beta-herpesvirus) (89). In the absence of microbial infection, AIM2 also plays an important role in sensing damage-associated molecular patterns (DAMPs) released by distressed or damaged cells (90). The cellular DNA, as one of the DAMPs produced by nuclear DNA damage or immunogenic cell death, activates AIM2 and initiates inflammasome assembly to promote the secretion of IL-1β and IL-18 (91–93). It was reported that inhibition of potassium efflux inhibited the secretion of IL-1β mediated by AIM2 (94), suggesting that like NLRP3, AIM2 inflammasome activation may depend on distinct ion fluxes and concentrations (95).

Because viral DNA can be released into the cytoplasm during HSV-1 infection in macrophages, it should engage cytoplasmic DNA sensors such as AIM2 (39, 96). However, HSV-1 infection of macrophages induces inflammasome activation independent of AIM2, in stark contrast to murine cytomegalovirus that efficiently induces AIM2-dependent inflammasome activation (89). Based on this observation, it is hypothesized that HSV-1 may have evolved a mechanism(s) to evade AIM2-dependent inflammasome activation. Indeed, HSV-1 tegument protein VP22 was reported to inhibit AIM2-dependent inflammasome activation and IL-1β secretion in infected macrophages (97). VP22 interacts with AIM2 and prevents its oligomerization, an essential step in AIM2 inflammasome activation. Consequently, recombinant VP22-deficient HSV-1 (HSV-1ΔVP22) potently induces AIM2 inflammasome activation and subsequent secretion of IL-1β and IL-18. Similarly, HSV-2 and PRV VP22 homologues also demonstrate inhibitory effect on AIM2-dependent inflammasome activation (97). Interestingly, KSHV tegument protein ORF63 interacts with an inflammasome sensor NLRP1 and prevents its oligomerization to block inflammasome activation in ways similar to VP22 (98). Collectively, these findings reveal a mechanism that the inhibition of AIM2-dependent inflammasome activation appears to be shared by diverse herpesviruses.

DAI

DNA-dependent activator of IRFs (DAI, also known as ZBP-1) is the first putative cytosolic DNA receptor identified (99). DAI recruits TBK1 and IRF3, and induces type I IFN production after binding to dsDNA. HSV-1 induces DAI activation in the murine fibroblast cell line L929 (99). Structurally, DAI contains tandem amino-terminal Z-DNA-binding domains, Zα1 and Zα2 (also called Zβ), which binds double-stranded Z-form DNA (99, 100). In addition to Z-DNA-binding domains, DAI also contains RIP homotypic interaction motifs (RHIMs) that trigger necroptosis and activate NF-κB pathway by interacting with the receptor-interacting kinase-3 (RIPK3) (101, 102). RIPK3 and its downstream substrate Mixed Lineage Kinase domain-Like protein (MLKL) contributes to the programmed necrotic cell death, which curtails viral replication and restricts dissemination of virions (103, 104). In this pathway, DAI acts as a nucleic acid sensor to detect viral RNA transcripts rather than the cytoplasmic viral DNA during the infection of influenza (105–108), vaccinia (109), MCMV (110, 111), and HSV1 (112, 113), and triggers necroptosis. On the other hand, these viruses manage to inhibit necroptosis by encoding gene products to target DAI-mediated signaling (109, 114, 115). MCMV M45 inhibits virus-induced necroptosis by blocking DAI-dependent oligomerization and activation of RIPK3 (115), while HSV-1 deploys ICP6 (UL39) to prevent the formation of DAI-RIPK3-MLKL complex induced by virus infection (116). Therefore, MCMV and HSV1 deploy similar strategies to block DAI-mediated necroptosis and maintain the viability of the infected cells.

PKR

DsRNA-dependent protein kinase R (PKR), an interferon-stimulated serine/threonine kinase, is a potent antiviral protein whose activity depends on dsRNA binding (117, 118). PKR consists of two dsRNA-binding domains (dsRBDs) and a kinase domain (119). Encountering dsRNA, DsRBDs bind to the backbone of a RNA in a sequence-independent manner, thus triggering a conformational change and subsequent oligomerization of PKR (120). PKR undergoes cis-phosphorylation within the activation loop by its kinase domain (121). Once activated, PKR phosphorylates the translation initiation factor eIF2α, leading to the suppression of eIF2 in cap-dependent translation and a global shutdown of translation (122). As such, PKR exerts its antiviral activity on a broad spectrum of DNA and RNA viruses by blocking the translation of cellular and viral mRNAs. Besides inhibiting protein synthesis, PKR was reported to promote the RLR-mediated type I interferon signaling *via* phosphorylation of IκB (123) and stabilization of mRNAs of type I interferon genes (124). Nevertheless, the molecular mechanism underpinning the PKR-dependent amplification of interferon signaling is not fully understood.

In HSV-1–infected cells, PKR is shown to be activated, which is required for the activation of NF-κB (125). It remains unclear

whether dsRNAs activating PKR originate from HSV-1–encoded symmetrical transcripts or the HSV-1–infected host genome. Interestingly, HSV-1 may activate PKR *via* a cellular protein activator known as PACT (126). To escape PKR-mediated antiviral responses, HSV-1 deploys $\gamma_1$34.5 (ICP34.5) to recruit cellular protein phosphatase 1α (PP1) that counteracts PKR-mediated eIF2α phosphorylation and restores translation (127–129). Moreover, ICP34.5 antagonizes Beclin 1-mediated autophagy, an antiviral process that is dependent on PKR (130). US11, a tegument protein, directly binds PKR to inhibit its conformational change and activation by PACT (126). It was later demonstrated that virion-associated US11, rather than its expression during replication, mediates the inhibition of PKR autophosphorylation (131). Additionally, Vhs degrades RNAs to block PKR activation during early stages of HSV-1 infection (132). These diverse viral strategies to antagonize PKR further emphasize the importance of PKR as a potent anti-HSV molecule.

DISCUSSION

In the current review, we summarized the recent findings on the contribution of cytosolic PRRs in sensing HSVs and the direct countermeasures evolved by these viruses (**Figure 1**). During HSV-1 infection, diverse molecular patterns throughout the virus life cycle, including viral DNA genome, transcription-derived RNA species, unmasked cellular RNA, etc., are dynamically sensed by the PRRs to trigger innate immune signaling. On the other side of the coin, HSV develops various countermeasures, ranging from transcription shutoff, protein degradation, interaction competition to enzymatic activity disruption, to escape PRR detection. These lessons learnt from our characterization of HSV-PRR interactions deepen the understanding of the nature and regulations of PRR-mediated innate immune signaling, and may lead to the discovery of novel antiviral modalities. Importantly, strategies interfering with these manipulations can be potentially developed into novel antiviral therapies, while immune modulatory-deficient HSV mutants are good candidates for vaccine and oncolytic virus strains, further highlighting the translational value of the basic research.

One of the knowledge gaps to fill is on the functional redundancy of the PRRs in sensing HSV, as controversy remains on defining the 'true' sensor for HSV. While a simple explanation is that such redundancy may have been evolved by the host as backup protections during the arms races with the virus, emerging studies have implicated these PRRs have unique roles in mounting immune responses and antagonizing HSV-1 infection in a temporal and cell/tissue-specific manner. Notably, part of the previous studies relies heavily on a single model cell line, sometimes cancer cell lines, to characterize HSV-PRR interactions, which limits the scope of the findings as some PRRs or signaling pathways may be missing. Thus, more investigations are needed to systematically address the

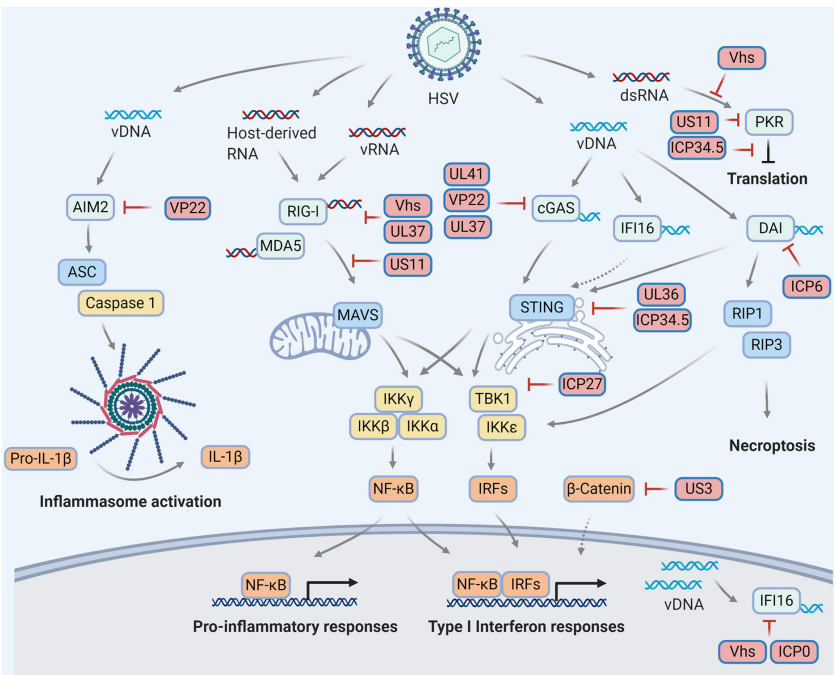

FIGURE 1 | HSV manipulations on the cytosolic pattern recognition receptors. Viral infection derives molecular patterns (DNAs and RNAs) which activate pattern recognition receptors (light blue) to transduce innate immune signaling through distinct adaptor proteins (blue) and ultimately trigger antiviral responses, including but not limited to cytokine production, inflammasome activation, translational inhibition and necroptosis. To escape innate immune surveillance, HSV encode viral proteins (red) to manipulate multiple steps of each signaling pathway *via* diverse mechanisms, resulting in a complex HSV-host interaction network on innate immunity.

contributions of PRRs, including more *in vivo* studies of HSV infection using tissue-specific knockout mouse models.

Interestingly, 'functional redundancy' applies to the virus too, because HSVs deploy multiple proteins to target the same sensor, e.g. RIG-I and cGAS, though *via* distinct molecular mechanism. One possibility is that these viral proteins sequentially work on the sensor throughout the HSV life cycle to maintain constant immune evasion. Alternatively, these viral proteins are cooperating to synergistically antagonize PRR functions or operate in a tissue-specific manner. It will require more work to define the 'major players' in these viral proteins that potently antagonize innate immune responses, as efforts in manipulating such proteins confer the greatest susceptibility of the virus to immune response and thus could serve as the best antiviral strategy.

AUTHOR CONTRIBUTIONS

JZ and PF conceived the paper. JZ, CQ, YL, YR, and PF wrote the paper. All authors contributed to the article and approved the submitted version.

FUNDING

Work in the Feng laboratory is supported by grants from National Institute of Health (DE027556, DE026003 and CA221521 to PF and DE028973 to JZ) and startup funds from the Herman Ostrow School of Dentistry of University of Southern California.

REFERENCES

1. Sehrawat S, Kumar D, Rouse BT. Herpesviruses: Harmonious Pathogens but Relevant Cofactors in Other Diseases? *Front Cell Infect Microbiol* (2018) 8:177. doi: 10.3389/fcimb.2018.00177
2. Sharma V, Mobeen F, Prakash T. Comparative Genomics of Herpesviridae Family to Look for Potential Signatures of Human Infecting Strains. *Int J Genomics* (2016) 2016:9543274. doi: 10.1155/2016/9543274
3. Steiner I, Benninger F. Update on herpes virus infections of the nervous system. *Curr Neurol Neurosci Rep* (2013) 13:414. doi: 10.1007/s11910-013-0414-8
4. Looker KJ, Magaret AS, May MT, Turner KM, Vickerman P, Gottlieb SL, et al. Global and Regional Estimates of Prevalent and Incident Herpes Simplex Virus Type 1 Infections in 2012. *PLoS One* (2015) 10:e0140765. doi: 10.1371/journal.pone.0140765
5. Looker KJ, Magaret AS, Turner KM, Vickerman P, Gottlieb SL, Newman LM. Global estimates of prevalent and incident herpes simplex virus type 2 infections in 2012. *PLoS One* (2015) 10:e114989. doi: 10.1371/journal.pone.0114989
6. Danastas K, Miranda-Saksena M, Cunningham AL. Herpes Simplex Virus Type 1 Interactions with the Interferon System. *Int J Mol Sci* (2020) 21 (14):5150. doi: 10.3390/ijms21145150
7. Tognarelli EI, Palomino TF, Corrales N, Bueno SM, Kalergis AM, Gonzalez PA. Herpes Simplex Virus Evasion of Early Host Antiviral Responses. *Front Cell Infect Microbiol* (2019) 9:127. doi: 10.3389/fcimb.2019.00127
8. Grünewald K, Desai P, Winkler DC, Heymann JB, Belnap DM, Baumeister W, et al. Three-dimensional structure of herpes simplex virus from cryo-electron tomography. *Science* (2003) 302:1396–8. doi: 10.1126/science.1090284
9. Wu W, Newcomb WW, Cheng N, Aksyuk A, Winkler DC, Steven AC. Internal Proteins of the Procapsid and Mature Capsids of Herpes Simplex Virus 1 Mapped by Bubblegram Imaging. *J Virol* (2016) 90:5176–86. doi: 10.1128/JVI.03224-15
10. Kukhanova MK, Korovina AN, Kochetkov SN. Human herpes simplex virus: life cycle and development of inhibitors. *Biochem (Mosc)* (2014) 79:1635–52. doi: 10.1134/S0006297914130124
11. Wirtz L, Möckel M, Knebel-Mörsdorf D. Invasion of Herpes Simplex Virus 1 into Murine Dermis: Role of Nectin-1 and Herpesvirus Entry Mediator as Cellular Receptors during Aging. *J Virol* (2020) 94(5):e02046–19. doi: 10.1128/JVI.02046-19
12. Petermann P, Thier K, Rahn E, Rixon FJ, Bloch W, Ozcelik S, et al. Entry mechanisms of herpes simplex virus 1 into murine epidermis: involvement of nectin-1 and herpesvirus entry mediator as cellular receptors. *J Virol* (2015) 89:262–74. doi: 10.1128/JVI.02917-14
13. Wang K, Tomaras GD, Jegaskanda S, Moody MA, Liao HX, Goodman KN, et al. Monoclonal Antibodies, Derived from Humans Vaccinated with the RV144 HIV Vaccine Containing the HVEM Binding Domain of Herpes Simplex Virus (HSV) Glycoprotein D, Neutralize HSV Infection, Mediate Antibody-Dependent Cellular Cytotoxicity, and Protect Mice from Ocular Challenge with HSV-1. *J Virol* (2017) 91(19):e00411–17. doi: 10.1128/JVI.00411-17
14. Montgomery RI, Warner MS, Lum BJ, Spear PG. Herpes simplex virus-1 entry into cells mediated by a novel member of the TNF/NGF receptor family. *Cell* (1996) 87:427–36. doi: 10.1016/S0092-8674(00)81363-X
15. Stevens JG, Wagner EK, Devi-Rao GB, Cook ML, Feldman LT. RNA complementary to a herpesvirus alpha gene mRNA is prominent in latently infected neurons. *Science* (1987) 235:1056–9. doi: 10.1126/science.2434993
16. Nicoll MP, Proenca JT, Efstathiou S. The molecular basis of herpes simplex virus latency. *FEMS Microbiol Rev* (2012) 36:684–705. doi: 10.1111/j.1574-6976.2011.00320.x
17. Radtke K, Kieneke D, Wolfstein A, Michael K, Steffen W, Scholz T, et al. Plus- and minus-end directed microtubule motors bind simultaneously to herpes simplex virus capsids using different inner tegument structures. *PLoS Pathog* (2010) 6:e1000991. doi: 10.1371/journal.ppat.1000991
18. Alandijany T. Host Intrinsic and Innate Intracellular Immunity During Herpes Simplex Virus Type 1 (HSV-1) Infection. *Front Microbiol* (2019) 10:2611. doi: 10.3389/fmicb.2019.02611
19. Chen N, Xia P, Li S, Zhang T, Wang TT, Zhu J. RNA sensors of the innate immune system and their detection of pathogens. *IUBMB Life* (2017) 69:297–304. doi: 10.1002/iub.1625
20. Yoneyama M, Kikuchi M, Natsukawa T, Shinobu N, Imaizumi T, Miyagishi M, et al. The RNA helicase RIG-I has an essential function in double-stranded RNA-induced innate antiviral responses. *Nat Immunol* (2004) 5:730–7. doi: 10.1038/ni1087
21. Kang DC, Gopalkrishnan RV, Wu Q, Jankowsky E, Pyle AM, Fisher PB. mda-5: An interferon-inducible putative RNA helicase with double-stranded RNA-dependent ATPase activity and melanoma growth-suppressive properties. *Proc Natl Acad Sci USA* (2002) 99:637–42. doi: 10.1073/pnas.022637199
22. Andrejeva J, Childs KS, Young DF, Carlos TS, Stock N, Goodbourn S, et al. The V proteins of paramyxoviruses bind the IFN-inducible RNA helicase, mda-5, and inhibit its activation of the IFN-beta promoter. *Proc Natl Acad Sci USA* (2004) 101:17264–9. doi: 10.1073/pnas.0407639101
23. Schlee M, Roth A, Hornung V, Hagmann CA, Wimmenauer V, Barchet W, et al. Recognition of 5' triphosphate by RIG-I helicase requires short blunt double-stranded RNA as contained in panhandle of negative-strand virus. *Immunity* (2009) 31:25–34. doi: 10.1016/j.immuni.2009.05.008
24. Seth RB, Sun L, Ea CK, Chen ZJ. Identification and characterization of MAVS, a mitochondrial antiviral signaling protein that activates NF-kappaB and IRF 3. *Cell* (2005) 122:669–82. doi: 10.1016/j.cell.2005.08.012
25. Xu LG, Wang YY, Han KJ, Li LY, Zhai Z, Shu HB. VISA is an adapter protein required for virus-triggered IFN-beta signaling. *Mol Cell* (2005) 19:727–40. doi: 10.1016/j.molcel.2005.08.014
26. Kawai T, Takahashi K, Sato S, Coban C, Kumar H, Kato H, et al. IPS-1, an adaptor triggering RIG-I- and Mda5-mediated type I interferon induction. *Nat Immunol* (2005) 6:981–8. doi: 10.1038/ni1243

27. Meylan E, Curran J, Hofmann K, Moradpour D, Binder M, Bartenschlager R, et al. Cardif is an adaptor protein in the RIG-I antiviral pathway and is targeted by hepatitis C virus. *Nature* (2005) 437:1167–72. doi: 10.1038/nature04193
28. Peisley A, Wu B, Xu H, Chen ZJ, Hur S. Structural basis for ubiquitin-mediated antiviral signal activation by RIG-I. *Nature* (2014) 509:110–4. doi: 10.1038/nature13140
29. Hou F, Sun L, Zheng H, Skaug B, Jiang QX, Chen ZJ. MAVS forms functional prion-like aggregates to activate and propagate antiviral innate immune response. *Cell* (2011) 146:448–61. doi: 10.1016/j.cell.2011.06.041
30. Loo YM, Gale M Jr. Immune signaling by RIG-I-like receptors. *Immunity* (2011) 34:680–92. doi: 10.1016/j.immuni.2011.05.003
31. Gack MU, Shin YC, Joo CH, Urano T, Liang C, Sun L, et al. TRIM25 RING-finger E3 ubiquitin ligase is essential for RIG-I-mediated antiviral activity. *Nature* (2007) 446:916–20. doi: 10.1038/nature05732
32. Oshiumi H, Matsumoto M, Hatakeyama S, Seya T. Riplet/RNF135, a RING finger protein, ubiquitinates RIG-I to promote interferon-beta induction during the early phase of viral infection. *J Biol Chem* (2009) 284:807–17. doi: 10.1074/jbc.M804259200
33. Gack MU, Nistal-Villan E, Inn KS, Garcia-Sastre A, Jung JU. Phosphorylation-mediated negative regulation of RIG-I antiviral activity. *J Virol* (2010) 84:3220–9. doi: 10.1128/JVI.02241-09
34. Wies E, Wang MK, Maharaj NP, Chen K, Zhou S, Finberg RW, et al. Dephosphorylation of the RNA sensors RIG-I and MDA5 by the phosphatase PP1 is essential for innate immune signaling. *Immunity* (2013) 38:437–49. doi: 10.1016/j.immuni.2012.11.018
35. Zeng W, Sun L, Jiang X, Chen X, Hou F, Adhikari A, et al. Reconstitution of the RIG-I pathway reveals a signaling role of unanchored polyubiquitin chains in innate immunity. *Cell* (2010) 141:315–30. doi: 10.1016/j.cell.2010.03.029
36. da Silva LF, Jones C. Small non-coding RNAs encoded within the herpes simplex virus type 1 latency associated transcript (LAT) cooperate with the retinoic acid inducible gene I (RIG-I) to induce beta-interferon promoter activity and promote cell survival. *Virus Res* (2013) 175:101–9. doi: 10.1016/j.virusres.2013.04.005
37. Choi MK, Wang Z, Ban T, Yanai H, Lu Y, Koshiba R, et al. A selective contribution of the RIG-I-like receptor pathway to type I interferon responses activated by cytosolic DNA. *Proc Natl Acad Sci USA* (2009) 106:17870–5. doi: 10.1073/pnas.0909545106
38. Chiu YH, Macmillan JB, Chen ZJ. RNA polymerase III detects cytosolic DNA and induces type I interferons through the RIG-I pathway. *Cell* (2009) 138:576–91. doi: 10.1016/j.cell.2009.06.015
39. Horan KA, Hansen K, Jakobsen MR, Holm CK, Soby S, Unterholzner L, et al. Proteasomal degradation of herpes simplex virus capsids in macrophages releases DNA to the cytosol for recognition by DNA sensors. *J Immunol* (2013) 190:2311–9. doi: 10.4049/jimmunol.1202749
40. Rasmussen SB, Jensen SB, Nielsen C, Quartin E, Kato H, Chen ZJ, et al. Herpes simplex virus infection is sensed by both Toll-like receptors and retinoic acid-inducible gene- like receptors, which synergize to induce type I interferon production. *J Gen Virol* (2009) 90:74–8. doi: 10.1099/vir.0.005389-0
41. Melchjorsen J, Rintahaka J, Soby S, Horan KA, Poltajainen A, Ostergaard L, et al. Early innate recognition of herpes simplex virus in human primary macrophages is mediated via the MDA5/MAVS-dependent and MDA5/MAVS/RNA polymerase III-independent pathways. *J Virol* (2010) 84:11350–8. doi: 10.1128/JVI.01106-10
42. Zhao J, Zeng Y, Xu S, Chen J, Shen G, Yu C, et al. A Viral Deamidase Targets the Helicase Domain of RIG-I to Block RNA-Induced Activation. *Cell Host Microbe* (2016) 20:770–84. doi: 10.1016/j.chom.2016.10.011
43. Chiang JJ, Sparrer KMJ, van Gent M, Lassig C, Huang T, Osterrieder N, et al. Viral unmasking of cellular 5S rRNA pseudogene transcripts induces RIG-I-mediated immunity. *Nat Immunol* (2018) 19:53–62. doi: 10.1038/s41590-017-0005-y
44. Yao XD, Rosenthal KL. Herpes simplex virus type 2 virion host shutoff protein suppresses innate dsRNA antiviral pathways in human vaginal epithelial cells. *J Gen Virol* (2011) 92:1981–93. doi: 10.1099/vir.0.030296-0
45. Feng P, Everly DN Jr., Read GS. mRNA decay during herpesvirus infections: interaction between a putative viral nuclease and a cellular translation factor. *J Virol* (2001) 75:10272–80. doi: 10.1128/JVI.75.21.10272-10280.2001
46. Feng P, Everly DN Jr., Read GS. mRNA decay during herpes simplex virus (HSV) infections: protein-protein interactions involving the HSV virion host shutoff protein and translation factors eIF4H and eIF4A. *J Virol* (2005) 79:9651–64. doi: 10.1128/JVI.79.15.9651-9664.2005
47. Xing J, Wang S, Lin R, Mossman KL, Zheng C. Herpes simplex virus 1 tegument protein US11 downmodulates the RLR signaling pathway via direct interaction with RIG-I and MDA-5. *J Virol* (2012) 86:3528–40. doi: 10.1128/JVI.06713-11
48. Zhong B, Yang Y, Li S, Wang YY, Li Y, Diao F, et al. The adaptor protein MITA links virus-sensing receptors to IRF3 transcription factor activation. *Immunity* (2008) 29:538–50. doi: 10.1016/j.immuni.2008.09.003
49. Sun W, Li Y, Chen L, Chen H, You F, Zhou X, et al. ERIS, an endoplasmic reticulum IFN stimulator, activates innate immune signaling through dimerization. *Proc Natl Acad Sci USA* (2009) 106:8653–8. doi: 10.1073/pnas.0900850106
50. Ishikawa H, Barber GN. STING is an endoplasmic reticulum adaptor that facilitates innate immune signalling. *Nature* (2008) 455:674–8. doi: 10.1038/nature07317
51. Tsuchida T, Zou J, Saitoh T, Kumar H, Abe T, Matsuura Y, et al. The ubiquitin ligase TRIM56 regulates innate immune responses to intracellular double-stranded DNA. *Immunity* (2010) 33:765–76. doi: 10.1016/j.immuni.2010.10.013
52. Ishikawa H, Ma Z, Barber GN. STING regulates intracellular DNA-mediated, type I interferon-dependent innate immunity. *Nature* (2009) 461:788–92. doi: 10.1038/nature08476
53. Parker ZM, Murphy AA, Leib DA. Role of the DNA Sensor STING in Protection from Lethal Infection following Corneal and Intracerebral Challenge with Herpes Simplex Virus 1. *J Virol* (2015) 89:11080–91. doi: 10.1128/JVI.00954-15
54. Cardone G, Newcomb WW, Cheng N, Wingfield PT, Trus BL, Brown JC, et al. The UL36 tegument protein of herpes simplex virus 1 has a composite binding site at the capsid vertices. *J Virol* (2012) 86:4058–64. doi: 10.1128/JVI.00012-12
55. Bodda C, Reinert LS, Fruhwurth S, Richardo T, Sun C, Zhang BC, et al. HSV1 VP1-2 deubiquitinates STING to block type I interferon expression and promote brain infection. *J Exp Med* (2020) 217(7):e20191422. doi: 10.1084/jem.20191422
56. Pan S, Liu X, Ma Y, Cao Y, He B. Herpes Simplex Virus 1 gamma134.5 Protein Inhibits STING Activation That Restricts Viral Replication. *J Virol* (2018) 92(20):e01015–18. doi: 10.1128/JVI.01015-18
57. Christensen MH, Jensen SB, Miettinen JJ, Luecke S, Prabakaran T, Reinert LS, et al. HSV-1 ICP27 targets the TBK1-activated STING signalsome to inhibit virus-induced type I IFN expression. *EMBO J* (2016) 35:1385–99. doi: 10.15252/embj.201593458
58. Kalamvoki M, Roizman B. HSV-1 degrades, stabilizes, requires, or is stung by STING depending on ICP0, the US3 protein kinase, and cell derivation. *Proc Natl Acad Sci USA* (2014) 111:E611–7. doi: 10.1073/pnas.1323414111
59. Sun L, Wu J, Du F, Chen X, Chen ZJ. Cyclic GMP-AMP synthase is a cytosolic DNA sensor that activates the type I interferon pathway. *Science* (2013) 339:786–91. doi: 10.1126/science.1232458
60. Liu H, Zhang H, Wu X, Ma D, Wu J, Wang L, et al. Nuclear cGAS suppresses DNA repair and promotes tumorigenesis. *Nature* (2018) 563:131–6. doi: 10.1038/s41586-018-0629-6
61. Wu J, Sun L, Chen X, Du F, Shi H, Chen C, et al. Cyclic GMP-AMP is an endogenous second messenger in innate immune signaling by cytosolic DNA. *Science* (2013) 339:826–30. doi: 10.1126/science.1229963
62. Li XD, Wu J, Gao D, Wang H, Sun L, Chen ZJ. Pivotal roles of cGAS-cGAMP signaling in antiviral defense and immune adjuvant effects. *Science* (2013) 341:1390–4. doi: 10.1126/science.1244040
63. Reinert LS, Lopusna K, Winther H, Sun C, Thomsen MK, Nandakumar R, et al. Sensing of HSV-1 by the cGAS-STING pathway in microglia orchestrates antiviral defence in the CNS. *Nat Commun* (2016) 7:13348. doi: 10.1038/ncomms13348
64. Su C, Zheng C. Herpes Simplex Virus 1 Abrogates the cGAS/STING-Mediated Cytosolic DNA-Sensing Pathway via Its Virion Host Shutoff Protein, UL41. *J Virol* (2017) 91(6):e02414–16. doi: 10.1128/JVI.02414-16
65. Huang J, You H, Su C, Li Y, Chen S, Zheng C. Herpes Simplex Virus 1 Tegument Protein VP22 Abrogates cGAS/STING-Mediated Antiviral Innate Immunity. *J Virol* (2018) 92(15):e00841–18. doi: 10.1128/JVI.00841-18

66. You H, Lin Y, Lin F, Yang M, Li J, Zhang R, et al. beta-Catenin Is Required for the cGAS/STING Signaling Pathway but Antagonized by the Herpes Simplex Virus 1 US3 Protein. *J Virol* (2020) 94(5):e01847–19. doi: 10.1128/JVI.01847-19
67. Zhang J, Zhao J, Xu S, Li J, He S, Zeng Y, et al. Species-Specific Deamidation of cGAS by Herpes Simplex Virus UL37 Protein Facilitates Viral Replication. *Cell Host Microbe* (2018) 24:234–48.e5. doi: 10.1016/j.chom.2018.07.004
68. Unterholzner L, Keating SE, Baran M, Horan KA, Jensen SB, Sharma S, et al. IFI16 is an innate immune sensor for intracellular DNA. *Nat Immunol* (2010) 11:997–1004. doi: 10.1038/ni.1932
69. Conrady CD, Zheng M, Fitzgerald KA, Liu C, Carr DJ. Resistance to HSV-1 infection in the epithelium resides with the novel innate sensor, IFI-16. *Mucosal Immunol* (2012) 5:173–83. doi: 10.1038/mi.2011.63
70. Triantafilou K, Eryilmazlar D, Triantafilou M. Herpes simplex virus 2-induced activation in vaginal cells involves Toll-like receptors 2 and 9 and DNA sensors DAI and IFI16. *Am J Obstet Gynecol* (2014) 210:122.e1–122e10. doi: 10.1016/j.ajog.2013.09.034
71. Orzalli MH, Broekema NM, Diner BA, Hancks DC, Elde NC, Cristea IM, et al. cGAS-mediated stabilization of IFI16 promotes innate signaling during herpes simplex virus infection. *Proc Natl Acad Sci USA* (2015) 112:E1773–81. doi: 10.1073/pnas.1424637112
72. Johnson KE, Bottero V, Flaherty S, Dutta S, Singh VV, Chandran B. IFI16 restricts HSV-1 replication by accumulating on the hsv-1 genome, repressing HSV-1 gene expression, and directly or indirectly modulating histone modifications. *PloS Pathog* (2014) 10:e1004503. doi: 10.1371/journal.ppat.1004503
73. Volkman HE, Cambier S, Gray EE, Stetson DB. Tight nuclear tethering of cGAS is essential for preventing autoreactivity. *Elife* (2019) 8:e47491. doi: 10.7554/eLife.47491
74. Orzalli MH, DeLuca NA, Knipe DM. Nuclear IFI16 induction of IRF-3 signaling during herpesviral infection and degradation of IFI16 by the viral ICP0 protein. *Proc Natl Acad Sci USA* (2012) 109:E3008–17. doi: 10.1073/pnas.1211302109
75. Orzalli MH, Broekema NM, Knipe DM. Relative Contributions of Herpes Simplex Virus 1 ICP0 and vhs to Loss of Cellular IFI16 Vary in Different Human Cell Types. *J Virol* (2016) 90:8351–9. doi: 10.1128/JVI.00939-16
76. Muruve DA, Petrilli V, Zaiss AK, White LR, Clark SA, Ross PJ, et al. The inflammasome recognizes cytosolic microbial and host DNA and triggers an innate immune response. *Nature* (2008) 452:103–7. doi: 10.1038/nature06664
77. Stacey KJ, Ross IL, Hume DA. Electroporation and DNA-dependent cell death in murine macrophages. *Immunol Cell Biol* (1993) 71(Pt 2):75–85. doi: 10.1038/icb.1993.8
78. Rathinam VA, Fitzgerald KA. Inflammasome Complexes: Emerging Mechanisms and Effector Functions. *Cell* (2016) 165:792–800. doi: 10.1016/j.cell.2016.03.046
79. Hornung V, Ablasser A, Charrel-Dennis M, Bauernfeind F, Horvath G, Caffrey DR, et al. AIM2 recognizes cytosolic dsDNA and forms a caspase-1-activating inflammasome with ASC. *Nature* (2009) 458:514–8. doi: 10.1038/nature07725
80. Fernandes-Alnemri T, Yu JW, Datta P, Wu J, Alnemri ES. AIM2 activates the inflammasome and cell death in response to cytoplasmic DNA. *Nature* (2009) 458:509–13. doi: 10.1038/nature07710
81. Burckstummer T, Baumann C, Bluml S, Dixit E, Durnberger G, Jahn H, et al. An orthogonal proteomic-genomic screen identifies AIM2 as a cytoplasmic DNA sensor for the inflammasome. *Nat Immunol* (2009) 10:266–72. doi: 10.1038/ni.1702
82. Roberts TL, Idris A, Dunn JA, Kelly GM, Burnton CM, Hodgson S, et al. HIN-200 proteins regulate caspase activation in response to foreign cytoplasmic DNA. *Science* (2009) 323:1057–60. doi: 10.1126/science.1169841
83. Jin T, Perry A, Jiang J, Smith P, Curry JA, Unterholzner L, et al. Structures of the HIN domain:DNA complexes reveal ligand binding and activation mechanisms of the AIM2 inflammasome and IFI16 receptor. *Immunity* (2012) 36:561–71. doi: 10.1016/j.immuni.2012.02.014
84. Jin T, Perry A, Smith P, Jiang J, Xiao TS. Structure of the absent in melanoma 2 (AIM2) pyrin domain provides insights into the mechanisms of AIM2 autoinhibition and inflammasome assembly. *J Biol Chem* (2013) 288:13225–35. doi: 10.1074/jbc.M113.468033
85. Man SM, Karki R, Kanneganti TD. AIM2 inflammasome in infection, cancer, and autoimmunity: Role in DNA sensing, inflammation, and innate immunity. *Eur J Immunol* (2016) 46:269–80. doi: 10.1002/eji.201545839
86. Man SM, Kanneganti TD. Regulation of inflammasome activation. *Immunol Rev* (2015) 265:6–21. doi: 10.1111/imr.12296
87. Brunette RL, Young JM, Whitley DG, Brodsky IE, Malik HS, Stetson DB. Extensive evolutionary and functional diversity among mammalian AIM2-like receptors. *J Exp Med* (2012) 209:1969–83. doi: 10.1084/jem.20121960
88. Kalantari P, DeOliveira RB, Chan J, Corbett Y, Rathinam V, Stutz A, et al. Dual engagement of the NLRP3 and AIM2 inflammasomes by plasmodium-derived hemozoin and DNA during malaria. *Cell Rep* (2014) 6:196–210. doi: 10.1016/j.celrep.2013.12.014
89. Rathinam VA, Jiang Z, Waggoner SN, Sharma S, Cole LE, Waggoner L, et al. The AIM2 inflammasome is essential for host defense against cytosolic bacteria and DNA viruses. *Nat Immunol* (2010) 11:395–402. doi: 10.1038/ni.1864
90. Matzinger P. Tolerance, danger, and the extended family. *Annu Rev Immunol* (1994) 12:991–1045. doi: 10.1146/annurev.iy.12.040194.005015
91. Komada T, Chung H, Lau A, Platnich JM, Beck PL, Benediktsson H, et al. Macrophage Uptake of Necrotic Cell DNA Activates the AIM2 Inflammasome to Regulate a Proinflammatory Phenotype in CKD. *J Am Soc Nephrol* (2018) 29:1165–81. doi: 10.1681/ASN.2017080863
92. Hu B, Jin C, Li HB, Tong J, Ouyang X, Cetinbas NM, et al. The DNA-sensing AIM2 inflammasome controls radiation-induced cell death and tissue injury. *Science* (2016) 354:765–8. doi: 10.1126/science.aaf7532
93. Lian Q, Xu J, Yan S, Huang M, Ding H, Sun X, et al. Chemotherapy-induced intestinal inflammatory responses are mediated by exosome secretion of double-strand DNA via AIM2 inflammasome activation. *Cell Res* (2017) 27:784–800. doi: 10.1038/cr.2017.54
94. Fernandes-Alnemri T, Yu JW, Juliana C, Solorzano L, Kang S, Wu J, et al. The AIM2 inflammasome is critical for innate immunity to Francisella tularensis. *Nat Immunol* (2010) 11:385–93. doi: 10.1038/ni.1859
95. Latz E, Xiao TS, Stutz A. Activation and regulation of the inflammasomes. *Nat Rev Immunol* (2013) 13:397–411. doi: 10.1038/nri3452
96. Morrison EE, Wang YF, Meredith DM. Phosphorylation of structural components promotes dissociation of the herpes simplex virus type 1 tegument. *J Virol* (1998) 72:7108–14. doi: 10.1128/JVI.72.9.7108-7114.1998
97. Maruzuru Y, Ichinohe T, Sato R, Miyake K, Okano T, Suzuki T, et al. Herpes Simplex Virus 1 VP22 Inhibits AIM2-Dependent Inflammasome Activation to Enable Efficient Viral Replication. *Cell Host Microbe* (2018) 23:254–65.e7. doi: 10.1016/j.chom.2017.12.014
98. Gregory SM, Davis BK, West JA, Taxman DJ, Matsuzawa S, Reed JC, et al. Discovery of a viral NLR homolog that inhibits the inflammasome. *Science* (2011) 331:330–4. doi: 10.1126/science.1199478
99. Takaoka A, Wang Z, Choi MK, Yanai H, Negishi H, Ban T, et al. DAI (DLM-1/ZBP1) is a cytosolic DNA sensor and an activator of innate immune response. *Nature* (2007) 448:501–5. doi: 10.1038/nature06013
100. Wang Z, Choi MK, Ban T, Yanai H, Negishi H, Lu Y, et al. Regulation of innate immune responses by DAI (DLM-1/ZBP1) and other DNA-sensing molecules. *Proc Natl Acad Sci USA* (2008) 105:5477–82. doi: 10.1073/pnas.0801295105
101. Kuriakose T, Kanneganti TD. ZBP1: Innate Sensor Regulating Cell Death and Inflammation. *Trends Immunol* (2018) 39:123–34. doi: 10.1016/j.it.2017.11.002
102. Rebsamen M, Heinz LX, Meylan E, Michallet MC, Schroder K, Hofmann K, et al. DAI/ZBP1 recruits RIP1 and RIP3 through RIP homotypic interaction motifs to activate NF-kappaB. *EMBO Rep* (2009) 10:916–22. doi: 10.1038/embor.2009.109
103. Kaiser WJ, Upton JW, Mocarski ES. Receptor-interacting protein homotypic interaction motif-dependent control of NF-kappa B activation via the DNA-dependent activator of IFN regulatory factors. *J Immunol* (2008) 181:6427–34. doi: 10.4049/jimmunol.181.9.6427
104. Ishii KJ, Kawagoe T, Koyama S, Matsui K, Kumar H, Kawai T, et al. TANK-binding kinase-1 delineates innate and adaptive immune responses to DNA vaccines. *Nature* (2008) 451:725–9. doi: 10.1038/nature06537
105. Kuriakose T, Zheng M, Neale G, Kanneganti TD. IRF1 Is a Transcriptional Regulator of ZBP1 Promoting NLRP3 Inflammasome Activation and Cell

Death during Influenza Virus Infection. *J Immunol* (2018) 200:1489–95. doi: 10.4049/jimmunol.1701538
106. Thapa RJ, Ingram JP, Ragan KB, Nogusa S, Boyd DF, Benitez AA, et al. DAI Senses Influenza A Virus Genomic RNA and Activates RIPK3-Dependent Cell Death. *Cell Host Microbe* (2016) 20:674–81. doi: 10.1016/j.chom.2016.09.014
107. Kuriakose T, Man SM, Malireddi RK, Karki R, Kesavardhana S, Place DE, et al. ZBP1/DAI is an innate sensor of influenza virus triggering the NLRP3 inflammasome and programmed cell death pathways. *Sci Immunol* (2016) 1 (2):aag2045. doi: 10.1126/sciimmunol.aag2045
108. Kesavardhana S, Kuriakose T, Guy CS, Samir P, Malireddi RKS, Mishra A, et al. ZBP1/DAI ubiquitination and sensing of influenza vRNPs activate programmed cell death. *J Exp Med* (2017) 214:2217–29. doi: 10.1084/jem.20170550
109. Koehler H, Cotsmire S, Langland J, Kibler KV, Kalman D, Upton JW, et al. Inhibition of DAI-dependent necroptosis by the Z-DNA binding domain of the vaccinia virus innate immune evasion protein, E3. *Proc Natl Acad Sci USA* (2017) 114:11506–11. doi: 10.1073/pnas.1700999114
110. Sridharan H, Ragan KB, Guo H, Gilley RP, Landsteiner VJ, Kaiser WJ, et al. Murine cytomegalovirus IE3-dependent transcription is required for DAI/ZBP1-mediated necroptosis. *EMBO Rep* (2017) 18:1429–41. doi: 10.15252/embr.201743947
111. Maelfait J, Liverpool L, Bridgeman A, Ragan KB, Upton JW, Rehwinkel J. Sensing of viral and endogenous RNA by ZBP1/DAI induces necroptosis. *EMBO J* (2017) 36:2529–43. doi: 10.15252/embj.201796476
112. Guo H, Gilley RP, Fisher A, Lane R, Landsteiner VJ, Ragan KB, et al. Species-independent contribution of ZBP1/DAI/DLM-1-triggered necroptosis in host defense against HSV1. *Cell Death Dis* (2018) 9:816. doi: 10.1038/s41419-018-0868-3
113. Pham TH, Kwon KM, Kim YE, Kim KK, Ahn JH. DNA sensing-independent inhibition of herpes simplex virus 1 replication by DAI/ZBP1. *J Virol* (2013) 87:3076–86. doi: 10.1128/JVI.02860-12
114. Upton JW, Kaiser WJ, Mocarski ES. DAI/ZBP1/DLM-1 complexes with RIP3 to mediate virus-induced programmed necrosis that is targeted by murine cytomegalovirus vIRA. *Cell Host Microbe* (2012) 11:290–7. doi: 10.1016/j.chom.2012.01.016
115. Upton JW, Kaiser WJ, Mocarski ES. Virus inhibition of RIP3-dependent necrosis. *Cell Host Microbe* (2010) 7:302–13. doi: 10.1016/j.chom.2010.03.006
116. Wang X, Li Y, Liu S, Yu X, Li L, Shi C, et al. Direct activation of RIP3/MLKL-dependent necrosis by herpes simplex virus 1 (HSV-1) protein ICP6 triggers host antiviral defense. *Proc Natl Acad Sci USA* (2014) 111:15438–43. doi: 10.1073/pnas.1412767111
117. Roberts WK, Hovanessian A, Brown RE, Clemens MJ, Kerr IM. Interferon-mediated protein kinase and low-molecular-weight inhibitor of protein synthesis. *Nature* (1976) 264:477–80. doi: 10.1038/264477a0
118. Sen GC, Taira H, Lengyel P. Interferon, double-stranded RNA, and protein phosphorylation. Characteristics of a double-stranded RNA-activated protein kinase system partially purified from interferon treated Ehrlich ascites tumor cells. *J Biol Chem* (1978) 253:5915–21.
119. Nanduri S, Carpick BW, Yang Y, Williams BR, Qin J. Structure of the double-stranded RNA-binding domain of the protein kinase PKR reveals the molecular basis of its dsRNA-mediated activation. *EMBO J* (1998) 17:5458–65. doi: 10.1093/emboj/17.18.5458
120. Dey M, Cao C, Dar AC, Tamura T, Ozato K, Sicheri F, et al. Mechanistic link between PKR dimerization, autophosphorylation, and eIF2alpha substrate recognition. *Cell* (2005) 122:901–13. doi: 10.1016/j.cell.2005.06.041
121. Dey M, Mann BR, Anshu A, Mannan MA. Activation of protein kinase PKR requires dimerization-induced cis-phosphorylation within the activation loop. *J Biol Chem* (2014) 289:5747–57. doi: 10.1074/jbc.M113.527796
122. Hovanessian AG. The double stranded RNA-activated protein kinase induced by interferon: dsRNA-PK. *J Interferon Res* (1989) 9:641–7. doi: 10.1089/jir.1989.9.641
123. Zamanian-Daryoush M, Mogensen TH, DiDonato JA, Williams BR. NF-kappaB activation by double-stranded-RNA-activated protein kinase (PKR) is mediated through NF-kappaB-inducing kinase and IkappaB kinase. *Mol Cell Biol* (2000) 20:1278–90. doi: 10.1128/MCB.20.4.1278-1290.2000
124. Schulz O, Pichlmair A, Rehwinkel J, Rogers NC, Scheuner D, Kato H, et al. Protein kinase R contributes to immunity against specific viruses by regulating interferon mRNA integrity. *Cell Host Microbe* (2010) 7:354–61. doi: 10.1016/j.chom.2010.04.007
125. Taddeo B, Luo TR, Zhang W, Roizman B. Activation of NF-kappaB in cells productively infected with HSV-1 depends on activated protein kinase R and plays no apparent role in blocking apoptosis. *Proc Natl Acad Sci USA* (2003) 100:12408–13. doi: 10.1073/pnas.2034952100
126. Peters GA, Khoo D, Mohr I, Sen GC. Inhibition of PACT-mediated activation of PKR by the herpes simplex virus type 1 Us11 protein. *J Virol* (2002) 76:11054–64. doi: 10.1128/JVI.76.21.11054-11064.2002
127. Mohr I, Gluzman Y. A herpesvirus genetic element which affects translation in the absence of the viral GADD34 function. *EMBO J* (1996) 15:4759–66. doi: 10.1002/j.1460-2075.1996.tb00853.x
128. Chou J, Roizman B. Herpes simplex virus 1 gamma(1)34.5 gene function, which blocks the host response to infection, maps in the homologous domain of the genes expressed during growth arrest and DNA damage. *Proc Natl Acad Sci USA* (1994) 91:5247–51. doi: 10.1073/pnas.91.12.5247
129. He B, Gross M, Roizman B. The gamma(1)34.5 protein of herpes simplex virus 1 complexes with protein phosphatase 1alpha to dephosphorylate the alpha subunit of the eukaryotic translation initiation factor 2 and preclude the shutoff of protein synthesis by double-stranded RNA-activated protein kinase. *Proc Natl Acad Sci USA* (1997) 94:843–8. doi: 10.1073/pnas.94.3.843
130. Orvedahl A, Alexander D, Talloczy Z, Sun Q, Wei Y, Zhang W, et al. HSV-1 ICP34.5 confers neurovirulence by targeting the Beclin 1 autophagy protein. *Cell Host Microbe* (2007) 1:23–35. doi: 10.1016/j.chom.2006.12.001
131. Ishioka K, Ikuta K, Sato Y, Kaneko H, Sorimachi K, Fukushima E, et al. Herpes simplex virus type 1 virion-derived US11 inhibits type 1 interferon-induced protein kinase R phosphorylation. *Microbiol Immunol* (2013) 57:426–36. doi: 10.1111/1348-0421.12048
132. Sciortino MT, Parisi T, Siracusano G, Mastino A, Taddeo B, Roizman B. The virion host shutoff RNase plays a key role in blocking the activation of protein kinase R in cells infected with herpes simplex virus 1. *J Virol* (2013) 87:3271–6. doi: 10.1128/JVI.03049-12

Conflict of Interest: The authors declare that the research was conducted in the absence of any commercial or financial relationships that could be construed as a potential conflict of interest.

frontiers in Immunology

ORIGINAL RESEARCH
published: 01 February 2021
doi: 10.3389/fimmu.2020.613079

Chicken cGAS Senses Fowlpox Virus Infection and Regulates Macrophage Effector Functions

Marisa Oliveira[1], Damaris Ribeiro Rodrigues[2], Vanaique Guillory[3], Emmanuel Kut[3], Efstathios S. Giotis[4,5], Michael A. Skinner[4], Rodrigo Guabiraba[3†], Clare E. Bryant[2†] and Brian J. Ferguson[1†]*

[1] Department of Pathology, University of Cambridge, Cambridge, United Kingdom, [2] Department of Veterinary Medicine, University of Cambridge, Cambridge, United Kingdom, [3] ISP, INRAE, Université de Tours, Nouzilly, France, [4] Department of Infectious Diseases, Imperial College London, London, United Kingdom, [5] School of Life Sciences, University of Essex, Colchester, United Kingdom

The anti-viral immune response is dependent on the ability of infected cells to sense foreign nucleic acids. In multiple species, the pattern recognition receptor (PRR) cyclic GMP-AMP synthase (cGAS) senses viral DNA as an essential component of the innate response. cGAS initiates a range of signaling outputs that are dependent on generation of the second messenger cGAMP that binds to the adaptor protein stimulator of interferon genes (STING). Here we show that in chicken macrophages, the cGAS/STING pathway is essential not only for the production of type-I interferons in response to intracellular DNA stimulation, but also for regulation of macrophage effector functions including the expression of MHC-II and co-stimulatory molecules. In the context of fowlpox, an avian DNA virus infection, the cGAS/STING pathway was found to be responsible for type-I interferon production and MHC-II transcription. The sensing of fowlpox virus DNA is therefore essential for mounting an anti-viral response in chicken cells and for regulation of a specific set of macrophage effector functions.

Keywords: DNA, fowlpox, chicken, macrophages, cyclic GMP-AMP synthase, stimulator of interferon genes, pattern recognition receptor

OPEN ACCESS

Edited by:
Chunfu Zheng,
Fujian Medical University, China

Reviewed by:
Henrique De Paula Lemos,
Newcastle University, United Kingdom
Lei Huang,
Newcastle University, United Kingdom

****Correspondence:***
Brian J. Ferguson
bf234@cam.ac.uk

†These authors share senior authorship

Specialty section:
This article was submitted to Molecular Innate Immunity, a section of the journal Frontiers in Immunology

Received: *01 October 2020*
Accepted: *16 December 2020*
Published: *01 February 2021*

Citation:
Oliveira M, Rodrigues DR, Guillory V, Kut E, Giotis ES, Skinner MA, Guabiraba R, Bryant CE and Ferguson BJ (2021) Chicken cGAS Senses Fowlpox Virus Infection and Regulates Macrophage Effector Functions. Front. Immunol. 11:613079. doi: 10.3389/fimmu.2020.613079

INTRODUCTION

The ability of virally infected cells to mount an effective innate immune response is dependent on the intracellular sensing of nucleic acids by pattern recognition receptors (1). The PRRs that sense and respond to intracellular DNA are well characterized in a number of mammalian and non-mammalian organisms but are less studied in avian species, including chickens (2). The PRR cyclic cAMP-GMP (cGAMP) synthase (cGAS) binds intracellular viral DNA and, *via* production of the second-messenger 2'3'-cGAMP, triggers a range of signaling outputs including type-I interferon (IFN-I) production, cell death and cellular senescence (3). The absence of cGAS or the adaptor protein, stimulator of interferon genes (STING), which binds cGAMP, results in the susceptibility to DNA virus infection in knockout mice and impairs IFN-I production by cells infected with DNA viruses or transfected with linear double stranded DNA (4). Through its ability to sense mislocalized self-DNA, the cGAS/STING signaling axis is also a potent regulator of

autoinflammatory and anti-tumor immune responses (5, 6). People with activating mutations in STING or loss-of function mutations in the 5'-3' exonuclease TREX1, which removes excess cytoplasmic dsDNA, suffer from interferonopathies (7).

The ability of cGAS/STING signaling to drive multiple downstream signaling outputs is dependent on the activation of a number of distinct signaling mechanisms, some of which are better defined than others. The production of IFN-I in this context is dependent on STING recruiting and facilitating activation of TANK-binding kinase-1 (TBK1) and the transcription factor interferon regulatory factor-3 (IRF3) (8). IRF3 phosphorylation, dimerization, and translocation to the nucleus results in IFN-I transcription. The mechanism or mechanisms by which STING can promote cell death are less well described, but include inflammasome activation (9) and apoptosis of various cell types including myeloid and T cells (10, 11). cGAS can also activate a programme of cellular senescence in fibroblasts by sensing damaged self-DNA (12). It is not currently clear in what contexts these disparate signaling outputs are activated by cGAS/STING and to what extent they cross-talk with each other.

Chickens are economically important livestock birds that are infected by numerous viruses including fowlpox virus (FWPV). Fowlpox is a virus from the *poxviridae* family that replicates its double stranded DNA genome in the cytoplasm of infected cells. The infection is characterized by proliferative lesions in the skin that progress to thick scabs (cutaneous form) and by lesions in the upper GI and respiratory tracts (diphtheritic form) (13). Transmitted mechanically by biting insects, it causes significant losses to all forms of poultry production systems (from backyard, through extensive to intensive commercial flocks). It is particularly challenging in tropical climes where control of biting insects is difficult. FWPV is also used as a live recombinant vaccine vector in avian and mammalian species (14). Like other poxviruses the cytoplasmic replication cycle of FWPV exposes large amounts of foreign DNA to intracellular DNA sensing PRRs, making cGAS a likely candidate for sensing FWPV infection and making FWPV a potentially useful tool for delineating nucleic acid sensing mechanisms in avian systems. The mechanisms by which FWPV is sensed by PRRs during infection have not, however, been described.

In this study we show the existence of a cGAS/STING pathway in chicken macrophages and determine its downstream signaling outputs. Using cGAS and STING CRISPR/Cas9 knockout HD11 cells and pharmacological inhibitors of STING and TBK1 in primary macrophages, we show that the activation of cGAS by intracellular DNA induces an IFN-I response and that this response can be enhanced by priming cells with IFNα. As well as driving IFN-I production, we show that cGAS/STING signaling in macrophages can enhance transcription of specific immune recognition molecules including genes encoding the class II major histocompatibility complex (MHC-II) and co-stimulatory proteins, but without altering phagocytosis. Using FWPV mutants that are deficient in specific immunomodulators we are able to overcome the immunosuppression of wild type FWPV and show that this virus is sensed by cGAS, resulting in IFN-I and MHC-II transcription. These data show that the cGAS/STING/TBK1 pathway senses viral DNA in chicken macrophages and that this pathway regulates not only the antiviral interferon response but also modulates specific components of macrophage effector function machinery.

MATERIALS AND METHODS

Reagents

Calf Thymus (CT) DNA (Sigma), Herring Testes (HT) DNA (Sigma), polyinosinic-polycytidylic acid (poly(I:C), Invivogen), 2'3'-cGAMP (Invivogen) and chicken interferon alpha (Yeast-derived Recombinant Protein, Kingfisher Biotech, Inc) were diluted in nuclease-free water (Ambion, ThermoFisher). H-151 and BX795 (Invivogen) were diluted in DMSO, following the manufacturer's protocols.

Cell Culture

HD11 cells, an avian myelocytomatosis virus (MC29)-transformed chicken macrophage-like cell line (15), were incubated at 37°C, 5% CO_2. They were grown in RPMI (Sigma-Aldrich, Germany) complemented with 2.5% volume per volume (v/v) heat-inactivated foetal bovine serum (FBS; Sera Laboratories International Ltd), 2.5% volume per volume (v/v) chicken serum (New Zealand origin, Gibco, Thermo Fisher Scientific), 10% Tryptose Phosphate Broth solution (Gibco, Thermo Fisher Scientific), 2 mM L-glutamine (Gibco, Thermo Fisher Scientific), 50 μg/ml of penicillin/streptomycin (P/S; Gibco, Thermo Fisher Scientific).

Chicken embryonic fibroblasts (CEFs) (Pirbright Institute, Woking) were incubated at 37°C, 5% CO_2 and were grown in Dulbecco's Modified Eagle Medium (DMEM) -F12 with Glutamax (Gibco), 5% v/v FBS, and 50 μg/ml P/S.

Knock-Out HD11 Cell Line Generation by CRISPR-Cas9

CRISPR Guide Design

According to the *MB21D1* (cGAS) and *TMEM137* (STING) sequences obtained from the Ensembl database (release 94), single guide (sg)RNA sequences (**Table 1**) were designed targeting the catalytic domain (residues 11-13 and 109) and start of the open reading frame, for cGAS and STING, respectively.

TABLE 1 | CRISPR/Cas9 guide RNAs.

Gene	Target	Guide	Sequence
cGAS	Catalytic Domain	sgRNA1	CTCTTTCTCGCATATCGAGA
		sgRNA2	ACGGCCTCAACATAGAATGC
		sgRNA3	TTTGGTTCAGATATCTGCAA
		sgRNA4	ACTGTGAAAAGGAAAAAGCG
STING	Coding Region	sgRNA1	GTAGCCGATGTAGTAGGAC
		sgRNA2	GTGCAGACGCTGCGGATGA

Knock-Out Cell Lines Generation Using CRISPR-Cas9

Genome editing of HD11 was performed using ribonucleoprotein (RNP) delivery. tracrRNA was mixed with the target specific sgRNA (**Table 1**), followed by an incubation at 95°C. To form the RNP complex, the tracrRNA/sgRNA mix was incubated with the Cas9 protein (IDT, Leuven, Belgium) and electroporation enhancer at 21°C.

To generate knockout cells, $1x10^6$ cells per guide were electroporated with the corresponding RNP complex using Lonza Electroporation Kit V (Lonza). After 48 h, the cells were expanded for future experiments and their DNA were extracted using the PureLink Genomic DNA Kit (Thermo Scientific, Waltham, MA, USA). The knockout efficiency was evaluated by genotyping the polyclonal cell populations using MiSeq (Illumina) according to a published method (16). The primers used for the sequencing are listed **Table 2**.

The successfully edited populations (using guides cGAS sg3 and STING sg1) were diluted to a concentration of 0.5 cell/well and seeded in 96-well plates. Individual clones were sequenced by MiSeq and the confirmed knockout clones were expanded for experiments.

Primary Macrophages

Chicken bone marrow derived macrophages (BMDM) were generated as previously described (17). Briefly, femurs and tibias of 4 week-old immunologically mature White Leghorn (PA12 line) outbred chickens were removed, both ends of the bones were cut and the bone marrow was flushed with RPMI supplemented with P/S. Cells were then washed and re-suspended in RPMI, loaded onto an equal volume of Histopaque-1077 (Sigma-Aldrich, Germany), and centrifuged at 400 g for 20 min. Cells at the interface were collected and washed twice in RPMI. Purified cells, pooled from three homozygous chickens, were seeded in triplicates at 1×10^6 cells/ml in sterile 60 mm bacteriological petri dishes in RPMI supplemented with 10% FBS, 25 mM HEPES, 2 mM L-glutamine, P/S and 25 ng/ml recombinant chicken colony stimulating factor 1 (CSF-1) (Kingfisher Biotech, Inc) at 41°C and 5% CO2. Half of the medium was replaced with fresh medium containing CSF-1 at day 3. At day 6, adherent cells were harvested and cultured in RPMI supplemented with 10% FBS, 25 mM HEPES, 2 mM L-glutamine, and P/S prior to stimulation. Procedures were performed in strict compliance with legal dispositions applicable in France, which state that animal euthanasia for the only purpose of organ or tissue use is not considered as an experimental procedure with obligation of submission to ethics committee for approval (Ordinance 2013-118, article R.214-89, published in the Journal Officiel de la République Française # 0032 of the February 7, 2013, pp. 2199).

Stimulation Assays

HD11 (WT, cGAS and STING knockouts) were seeded in 12-well plates at a density of 3×10^5 cells/well. In the following day, the cells were transfected using TransIT-LT1 (Mirus Bio, USA) with HT-DNA (1, 2, or 5 μg/ml), CT-DNA (1, 2, or 5 μg/ml) or Poly(I:C) (1 μg/ml), and harvested 6 or 16 h post-transfection. In the priming assays, IFNα (200 ng/ml) was added 16 h prior to transfection. 2'3' cGAMP was added at a concentration of 2.5 μg/ml and cells were harvested 6 h post-treatment.

BMDM were seeded in 6-well plates at $8x10^5$ cells/ml. In the following day, cells were transfected using TransIT-LT1 with HT-DNA (2 μg/ml), CT-DNA (2 μg/ml), or Poly(I:C) (1 μg/ml), and harvested 6 h post-transfection. In the priming assays, IFNα (50 ng/ml) was added 16 h prior transfection to the cells supernatants. 2'3' cGAMP was added to cells supernatants at the concentration of 10 μg/ml and the cells were harvested 6 h post-treatment.

Chicken IFN-I Bioassay

The presence of IFN-I in supernatants of stimulated BMDM was measured indirectly using a luciferase-based Mx-reporter bioassay (18). Briefly, cells from the quail fibroblast cell line CEC32 carrying the luciferase gene under the control of chicken Mx promoter (kindly provided by Prof. Peter Stäheli, University of Freiburg, Germany) were seeded at 2.5×10^5 cells/well in 24-well plates and incubated at 41°C under 5% CO_2. The next day, cells were incubated for 6 h with the diluted supernatants (1/10 of total volume). Medium was removed and cells were washed twice with PBS. Cells were lysed using the Cell Culture Lysis Reagent (Promega, USA), according to the manufacturer's instructions, and luciferase activity was measured using the Luciferase assay reagent (Promega, USA) and a GloMax-Multi Detection System (Promega, USA).

Cell Viability

BMDM or HD11 viability following different stimuli was assessed using the fluorescent DNA intercalator 7-aminoactinomycin D (7-AAD, BD Biosciences, USA). Briefly, following stimulations, supernatants were discarded, and the cells were harvested and washed in PBS. Cells were stained according to the manufacturer's protocol and the viability was analyzed by flow cytometry (BD FACS Calibur). Data were expressed as the percentage of 7AAD positive cells over total acquired events (50,000 cells).

TABLE 2 | Illumina sequencing primers.

Gene	Guide	Forward primer	Reverse primer
cGAS	sgRNA1	CTATTTAAATCTCGTGCTCACCCC	CTCACTCCCTGTTCTAAATAACG
	sgRNA2	GTGTTTCTTCTGTTATGGAAAAGG	GCTTGGCCACTAAGTAAATTGG
	sgRNA3	CCACTTGAATGCACATCAGTCTGG	CCAGTGTCGTCACTCTCATCTAGCT
STING	sgRNA1	TCCACAGGGCCACCACT	TGCAGGAGCCGTTTCCATCT
	sgRNA2	CAACCAGGAGCAGCCCTGCT	CTGGAGTGCAGGTGGAAGATCTCC

RNA Extraction

Cells were lysed by overlaying with 250 µl of lysis buffer containing 4 M guanidine thiocyanate, 25 mM Tris pH 7, and 143 mM 2-mercaptoethanol. As a second step, 250 µl of ethanol was added, and the solution was transferred to a silica column (Epoch Life Science, Inc., Sugar Land, TX, USA) and centrifuged; all centrifugation steps were performed for 90 s at 16,600 *g*. The bound RNA was washed by centrifugation with 500 µl of buffer containing 1 M guanidine thiocyanate, 25 mM Tris pH 7, and 10% ethanol, followed by a double washing step with 500 µl of wash buffer 2 [25 mM Tris pH 7 and 70% (v/v) ethanol]. RNA was eluted by centrifugation in 30 µl of nuclease-free water and the concentration was measured using a NanoDrop 2000 Spectrophotometer (Thermo Scientific, Waltham, MA, USA).

cDNA and qPCR

Using 500 ng of RNA extracted from HD11 cells, cDNA was produced using SuperScript III reverse transcriptase, following the manufacture's protocol (Thermo Scientific, Waltham, MA, USA). Samples were diluted in nuclease-free water in a 1:2.5 ratio. One µl of the diluted product was used for quantitative PCR (qPCR) in a final volume of 10 µl. qPCR was performed using SybrGreen Hi-Rox (PCR Biosystems Inc.) using primers described in **Table 3**. Fold change in mRNA expression was calculated by relative quantification using hypoxanthine phosphoribosyltransferase (HPRT) as endogenous control.

Total RNA (up to 1 µg per reaction) from BMDM was reverse transcribed with iScript cDNA synthesis kit (Bio-Rad, USA). Quantitative PCR was performed using 1 µl of cDNA, 5 µl of iQ SYBR Green Supermix (Bio-Rad, USA), 0.25 µl of each primer pair and 3.5 µl of nuclease-free water in a total reaction volume of 10 µl. Fold-increase in gene expression was calculated by relative quantification using HPRT and Glyceraldehyde 3-phosphate dehydrogenase (GAPDH) as endogenous controls.

Phagocytosis Assay by Flow Cytometry

HD11 WT cells were seeded at a confluence of $3x10^5$ cells/ml in 12-well plates. The cells were primed with IFNα for 16 h and then with transfected exogenous DNA (HT- and CT-DNA – 2 µg/ml) or treated with 2'3'cGAMP (5 µg/ml) for 6 h. After this, the cells were incubated with Zymosan coated beads conjugated with FITC at a ratio of 30 beads to 1 cell for all conditions for 40 min at 37°C. The cells were wash two times in PBS and fixed in suspension using the solution (missing ref; BD Biosciences) with 4% PFA. Cell populations were counted by analysis on a CytoFLEX cytometer.

TABLE 3 | qRT-PCR primer sequences.

Gene	Forward primer	Reverse primer
HPRT	TGGTGGGGATGACCTCTCAA	GGCCGATATCCCACACTTCG
IFNB	TCCTGCAACCATCTTCGTCA	CACGTCTTGTTGTGGGCAAG
ISG12-2	TGACCAGAACGTCCACAAAGCCG	ACCTGCTCCTGGACCGATGCTT
BLB1	GTGAGCCGCAAGCTGAATAC	ACCGTGAAGGACTCCACAAC
BLB2	ATGAATGAAGTGGACAGGGTCT	TTCAGGAACCACTTCACCTCG
DMB1	CGAGGTGAAGTGGTTCCTGA	CAGTCCCCGTTCTGCATCA
DMB2	CATGTTCGCCATCCCCAATG	GAGCACGTGTAGGTGTCCC
CD40	AGCCATGCCACTTCTGGAC	ATCGGAAGTGTTCGTCCCTT
CD86	TATGCACGTGGACAAGGGAC	AACCTCCGCTGGAAGAACAG
STING	AGCTCCCTACCTCCATCAGGA	TCTGGAAAACCCCAGCATCTC
IRF7	TGCCTCAGGCGTCCCCAATG	TGTGTGCCCACAGGGTTGGC
FPV094	TATAATGAATGGCGCTGTGT	GTTTTGCTATCTTGGCTGT
FPV168	ACCTCAAACAACCTCATC	GTTAATACTTGTGACTGCTG

Fowlpox Virus Growth and Titration

Fowlpox WT (FP9) and mutants [FPV012 (19) and FPV184 (20)] were propagated in primary chicken embryonic fibroblasts (CEFs) and grown in DMEM-F12 (Thermo Fisher Scientific, Waltham, MA, USA) containing 1% FBS and 5% P/S, and harvested 5 days later. Ten-fold dilutions of cell supernatants were prepared in serum-free DMEM-F12 and used to inoculate confluent monolayers of CEFs for 1.5 h at 37°C. Cells were then overlaid with 2xMEM : CMC (1/1 ratio). The foci were counted 7 days later after staining with Toluidine Blue.

Fowlpox Virus Infection

HD11 cells were seeded in 12-well plates in the day prior infection. Fowlpox viruses were diluted in serum-free DMEM-F12 at a multiplicity of infection (MOI) of 3 and added in the cells (1 ml per well). Infected cells and supernatants were collected from infections at 8 and 24 h post-infection.

Statistical Analysis

Prism 7 (GraphPad) was used to generate graphs and perform statistical analysis. Data were analyzed using an unpaired t test with Welch's correction unless stated otherwise. Data with $P < 0.05$ was considered significant and 2-tailed P-value were calculated and presented as: $^*p < 0.05$, $^{**}p < 0.01$, $^{***}p < 0.001$; $^{****}p < 0.0001$. Each experiment has at least two biological replicates unless stated.

RESULTS

Intracellular DNA Activates an IFN-I Response in Chicken Macrophages

In order to assess the ability of chicken macrophages to sense and respond to intracellular DNA, we used a combination of the monocytic cell line HD11 and primary bone marrow derived macrophages (BMDM). Transfection of CT DNA, increasing doses of HT-DNA or the RNA analogue poly(I:C) into HD11 cells resulted in transcription of chicken interferon-β (IFNβ) and the interferon stimulated gene (ISG) ISG12.2, an orthologue of mammalian IFI6 (**Figure 1A**). A dose-dependent response to DNA was observed. Transfection of DNA into primary BMDMs also resulted in IFNβ and ISG12.2 transcription (**Figure 1B**) and IFN-I secretion as measured by a bioassay (**Figure 1C**), indicating that this response is present in both primary macrophages and the transformed monocytic HD11 cell line.

Since in mammalian systems STING is recognized as an interferon stimulated gene (ISG) (21), we sought to understand the effect of IFN-I priming of macrophages on the response to intracellular DNA. Pre-treatment of HD11 or BMDM with chIFNα resulted in an enhancement of IFNβ transcription

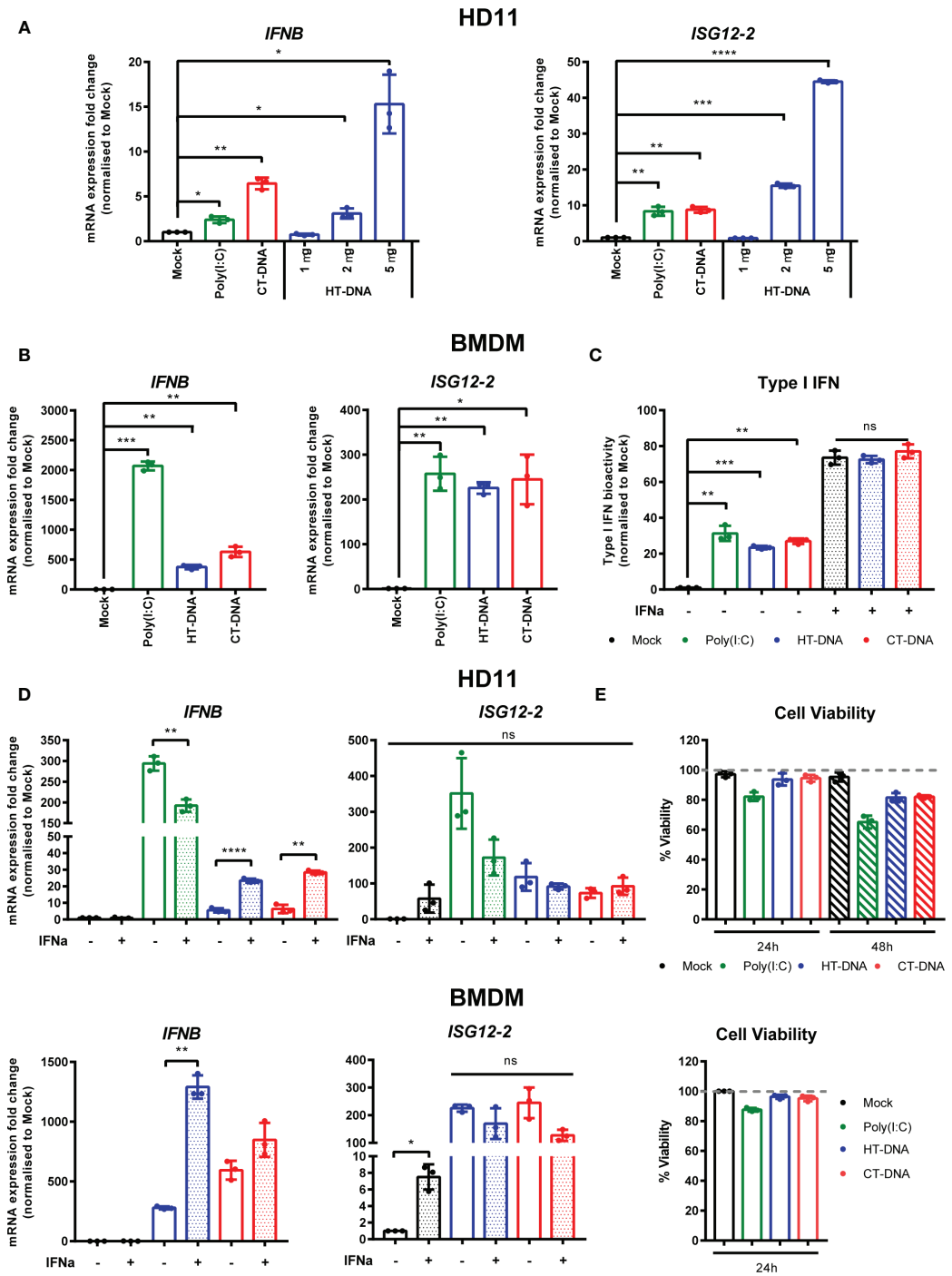

FIGURE 1 | Intracellular DNA activates an IFN-I response in chicken macrophages. **(A)** HD11 cells were transfected with HT-DNA (1, 2, and 5 µg/ml), CT-DNA (5 µg/ml) or Poly(I:C) and transcription of IFNB and ISG12.2 measured by qRT-PCR 6 h later. **(B)** Chicken BMDM were transfected with HT- DNA, CT-DNA (2 µg/ml) or Poly(I:C) (1 µg/ml) and transcription of IFNB and ISG12.2 measured by qRT-PCR 6 h later. **(C)** Resting BMDMs or BMDMs primed with IFNα for 6 h were transfected with HT- DNA, CT-DNA (2 µg/ml) or Poly(I:C) (1 µg/ml) and interferon activity in the supernatants was measured after 24 h using a bioassay. IFNα stimulation is a positive control in this assay. **(D)** HD11 or BMDM were primed with IFNα for 6 h, transfected with HT-DNA, CT-DNA, or Poly(I:C) and transcription of IFNB and ISG12.2 measured by qRT-PCR 6 h later. **(E)** HD11 (top) or IFNα-primed BMDM (bottom) were transfected with HT-DNA, CT-DNA, or Poly(I:C) and cell viability measured by 7AAD staining 24 or 48 h later. *p < 0.05, **p < 0.01, ***p < 0.001; ****p < 0.0001; ns: no significant difference. Data is representative of two or more replicates.

following DNA stimulation and confirmed ISG12.2 as an ISG (**Figure 1D**). This signaling enhancement might be explained by increased transcription of STING and/or IRF7 following IFNα treatment (**Supplementary Figure 1**). Across all HD11 and BMDM DNA stimulations we found that there was little observable or measurable cell death (**Figure 1E**), indicating that, in chicken macrophages, cell death is likely not a specific output of STING signaling.

Intracellular DNA Stimulates Transcription of MHC-II and Co-Stimulatory Molecules

The sensing of both intracellular and extracellular pathogens activates macrophages, causing up-regulation or enhancement of effector functions designed to combat infection. We hypothesized that DNA transfection, mimicking the presence of intracellular infection, might result in direct effects on the molecules that contribute to T cell stimulation. In chickens, there are two classical MHC-II genes encoded by BLB1 and BLB2, as well as a DM system that includes the DMB1 and DMB2 genes encoding class II-specific chaperones or peptide editors (22), all of which were transcriptionally upregulated by DNA stimulation in chicken BMDMs (**Figure 2A**). In HD11 cells, only BLB1 transcription was upregulated by DNA stimulation, while BLB2 transcription was upregulated only by IFNα pre-treatment (**Supplementary Figure 2**) and DMB1/2 were not altered by any stimuli (not shown), highlighting possible differences between primary and transformed cells in this specific context (**Figure 2B**). CD86 and CD40 are key co-stimulatory molecules in T cell activation. In BMDM CD86 and CD40 transcription was upregulated in response to DNA stimulation (**Figure 2A**). There was, however, no measurable impact of DNA stimulation on phagocytosis as measured by bead-uptake assays in HD11 cells (**Figure 2C**). As such, key molecules involved in T cell activation by macrophages are regulated by DNA stimulation, but not all macrophage effector functions are equally enhanced by this signal.

STING and TBK1 Contribute to DNA-Driven Transcriptional Responses in Chicken BMDMs

In order to dissect the signaling pathway downstream of intracellular DNA sensing, we first used the ligand 2'3'-cGAMP, the enzymatic product of cGAS that directly binds and activates STING (23). Treatment of BMDMs or HD11 cells with 2'3'-cGAMP led to increased transcription levels of IFNb, ISG12.2, BLB1, BLB2, CD86, and CD40 (**Figures 3A, B**). This response, and the response to DNA and cGAMP stimulation, could be reduced by small molecule inhibitors of STING (H151) and the kinase TBK1 (BX795), indicating the existence of a STING and TBK1-dependent signaling pathway in chicken macrophages and evidencing the cross-species utility of these two pharmacological inhibitors (**Figures 3C, D**). As with DNA stimulation, there was no measurable impact of cGAMP treatment on phagocytosis in HD11 cells (**Figure 3E**).

cGAS Is Essential for Intracellular DNA-Dependent IFN-I and MHC-II Transcription in HD11 Cells

To address the possibility that cGAS is a principle PRR responsible for sensing intracellular DNA in chicken macrophages, we generated HD11 knockout cell lines using CRISPR/Cas9 genome editing. To do this, we analyzed the annotated cGAS sequence in the current release of the *Gallus gallus* genome and designed gRNA sequences targeting regions of the gene which exhibited high conservation across multiple orthologues. By sequencing single cell clones we generated multiple cGAS knockout cell lines with two different gRNAs. By sequencing across the gRNA PAM target sites, we characterized indels to confirm the knockout status in these clones (e.g., **Figure 4A**). Stimulation of multiple cGAS knockout HD11 clones, each with a different indel, with DNA resulted in an abrogation of IFN-I and ISG transcription indicating that cGAS is a key PRR for sensing intracellular DNA in chicken macrophages (**Figure 4B** and **Supplementary Figure 3**). cGAS knockout also abrogated the upregulation of DNA-driven BLB1 stimulation, indicating the cGAS-dependent signaling is responsible for regulation of MHC class II transcription in this context (**Figure 4B**). These data were independent of IFNα pre-treatment, which enhanced IFN-I and BLB1 transcription in WT DNA-stimulated cells, but did not affect cGAS KO cells (**Figure 4C**). Consistent with the mammalian cGAS mechanism, stimulation of WT or cGAS KO cells with 2'3'-cGAMP resulted in robust IFN-I transcription, indicating IFN-I production by direct STING ligation was not affected by cGAS KO (**Figure 4D**). These data confirm the intracellular DNA PRR function of cGAS in chicken macrophages.

STING Is Essential for Intracellular DNA-Dependent IFN-I Transcription in HD11 Cells

In parallel, using the same methodology, we generated multiple STING knockout HD11 cell lines (**Figure 5A**). Stimulation of these cells with DNA phenocopied the cGAS knockout lines, and neither STING or cGAS KO altered tonic IFNB transcription, confirming the function of chicken STING downstream of cGAS in the intracellular DNA sensing pathway (**Figure 5B**, **Supplementary Figures 4** and **5**). These data are consistent with the presence of a cGAS/STING pathway in HD11 cells and, in concert with the data using H151 in BMDMs, indicate the function of STING as a critical adaptor protein for intracellular DNA sensing in chicken macrophages.

Fowlpox Triggers a cGAS/STING Dependent DNA Sensing Pathway in HD11 Cells

FWPV replication exposes large quantities of DNA to the cytoplasm of infected cells making it a prime target for intracellular DNA sensing PRRs. Despite this, using the wild-type vaccine strain FP9 we, and others (13, 19), observe little or no IFN-I transcription in infected cells, and indeed a

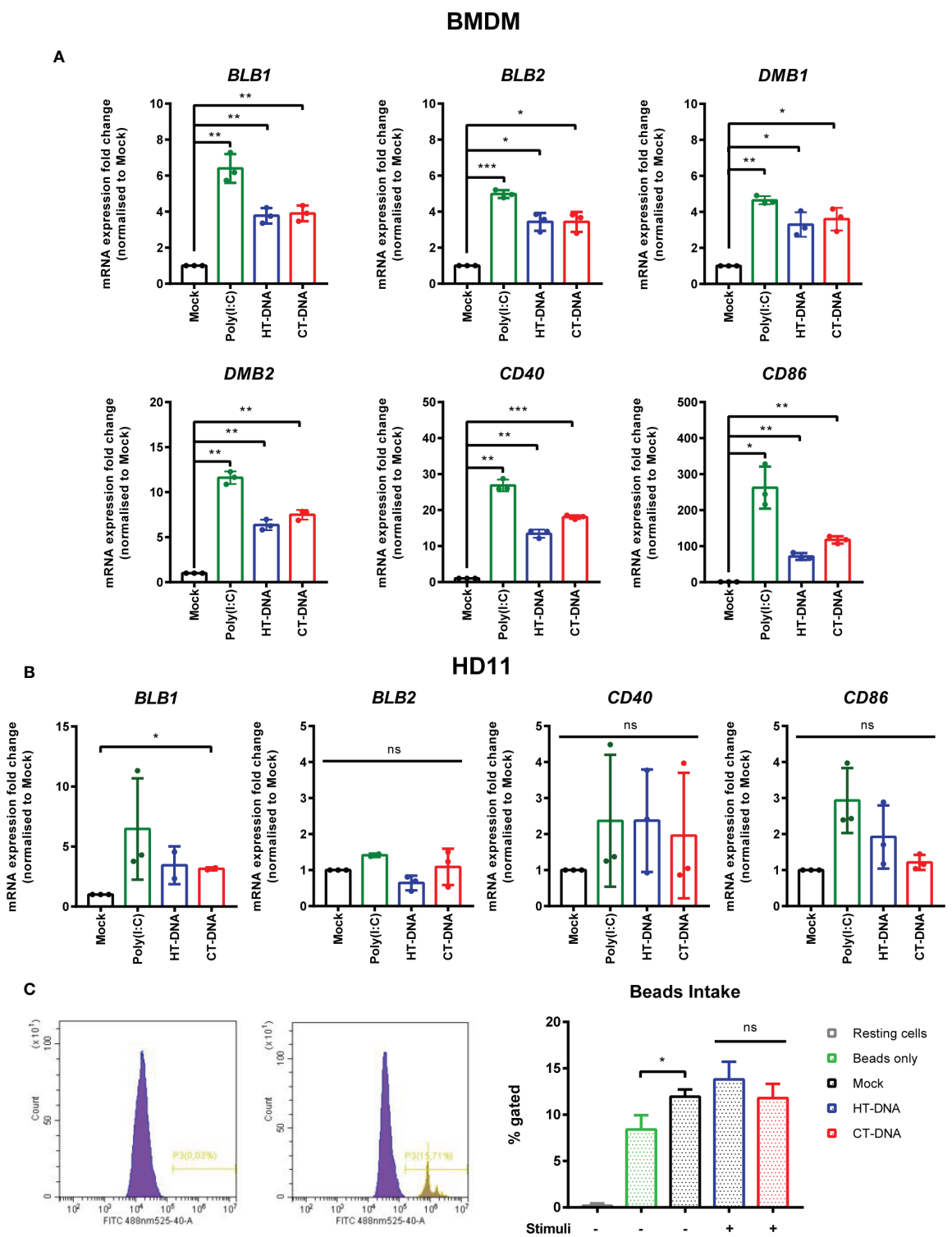

FIGURE 2 | Intracellular DNA stimulates transcription of MHC-II and co-stimulatory molecules. **(A)** BMDMs or **(B)** HD11 cells were transfected with HT-DNA, CT-DNA, or Poly(I:C) and transcription of BLB1, BLB2, DMB1, DMB2, CD40, and CD86 measured by qRT-PCR 6 h later. **(C)** HD11 cells were stimulated with HT-DNA, CT-DNA, or Poly(I:C) and 6 h later phagocytosis was monitored by FITC-conjugated, zymosan coated bead uptake. Histograms of non-treated versus treated cells (left panels) and respective percentages of FITC positive cells for each treatment tested (right panel) are presented. *$p < 0.05$, **$p < 0.01$, ***$p < 0.001$; ns, no significant difference. Data is representative of two or more replicates.

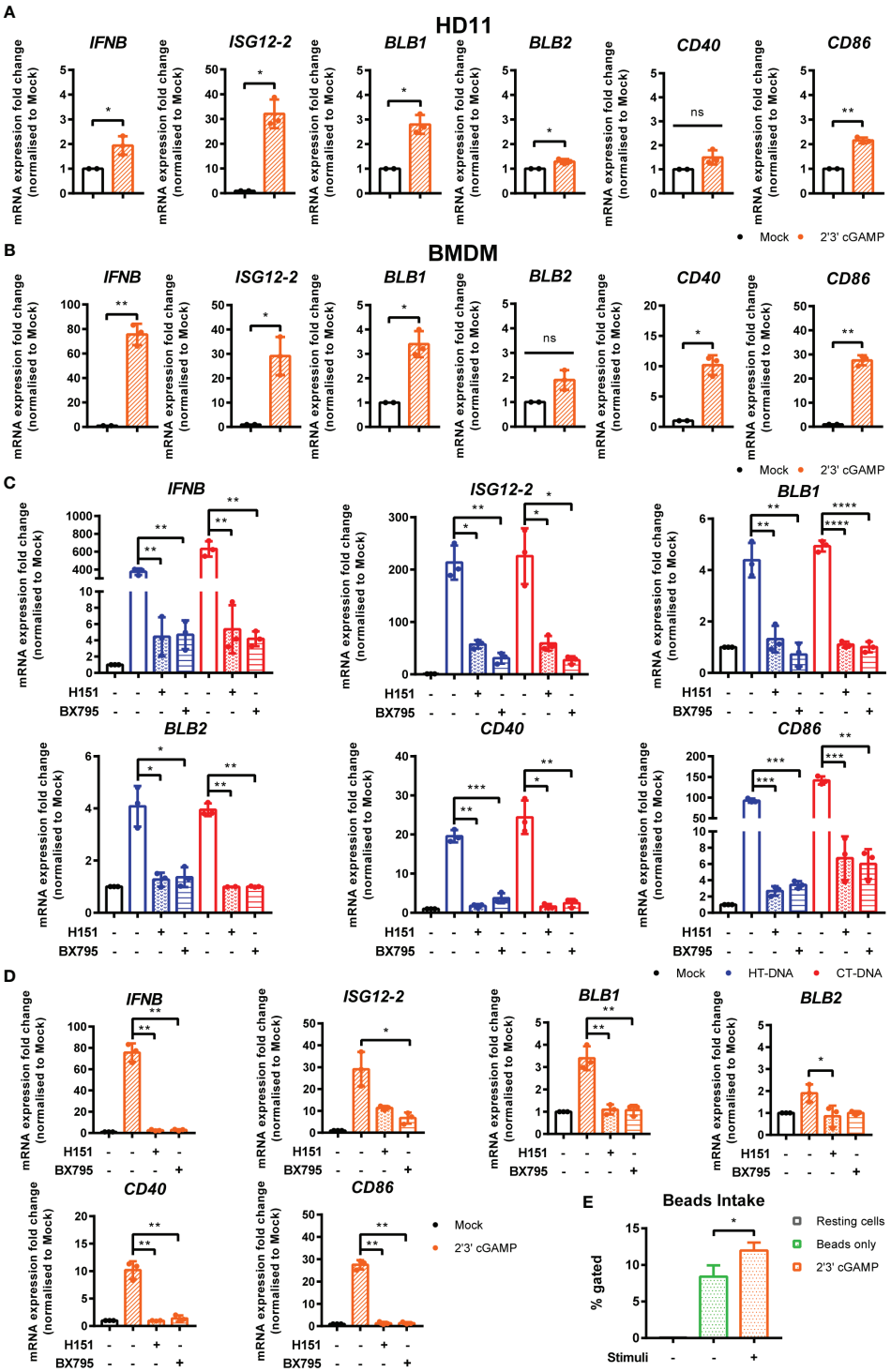

FIGURE 3 | STING and TBK1 contribute to DNA-driven transcriptional responses in chicken BMDMs. **(A)** HD11 and **(B)** BMDM cells were treated with 2'3'cGAMP (10 μg/ml) and qRT-PCR carried out 6 h later for the indicated genes. **(C)** BMDM were treated with the STING inhibitor H-151 (10 uM) or TBK1 inhibitor BX795 (1 uM) for 1 h before transfection with HT-DNA and CT-DNA. Six hours later, RNA was extracted and qRT-PCR carried out for the indicated genes. **(D)** BMDM were treated with the STING inhibitor H-151 (10 uM) or TBK1 inhibitor BX795 (1 uM) for 1 h before treatment with 2'3'cGAMP (10 μg/ml). Six hours later, RNA was extracted and qRT-PCR carried out for the indicated genes. **(E)** HD11 cells were treated with 2'3'cGAMP (2.5 μg/ml) 6 h later phagocytosis was monitored by FITC-conjugated, zymosan coated bead uptake. *p < 0.05, **p < 0.01, ***p < 0.001; ****p < 0.0001; ns: no significant difference. Data is representative of two or more replicates.

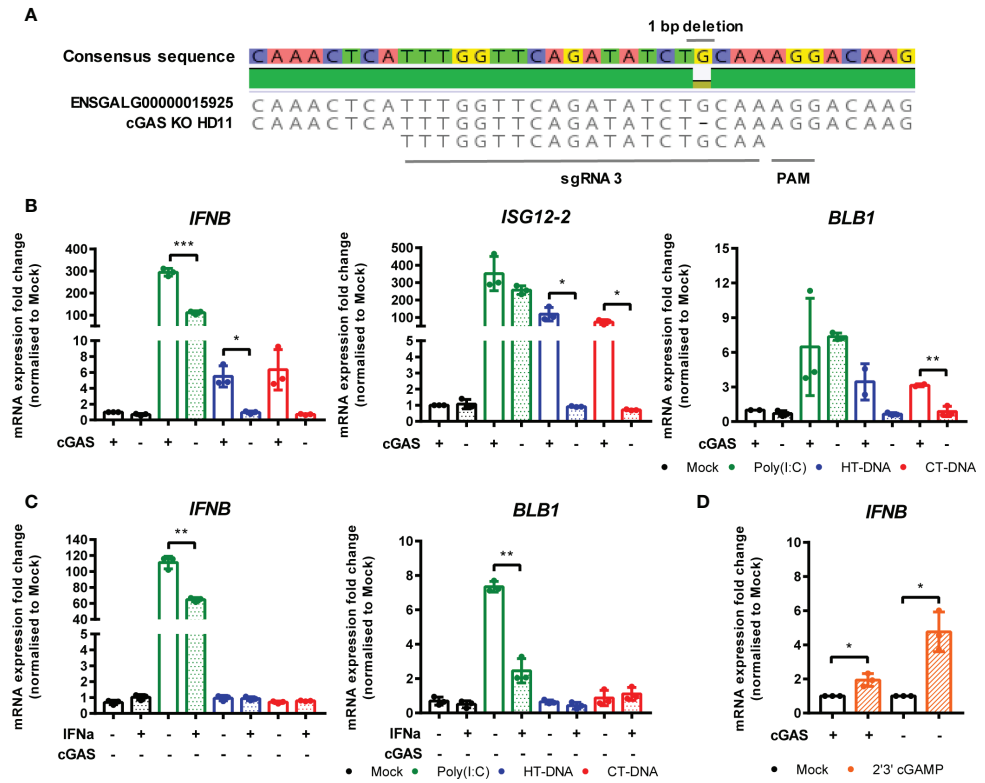

FIGURE 4 | cGAS is essential for intracellular DNA-dependent IFN-I and MHC-II transcription in HD11 cells. **(A)** Example of identification of indel in clonally selected HD11 cGAS KO using NGS sequencing. **(B)** WT and cGAS KO HD11 cells were transfected with HT-DNA, CT-DNA (2 μg/ml) or Poly(I:C) (1 μg/ml) for 6 h and transcription of the indicated genes measured by qRT-PCR. **(C)** cGAS KO HD11 cells were primed with IFNα for 6 h, transfected with HT-DNA, CT-DNA, or Poly(I:C) and transcription of IFNB and ISG12.2 measured by qRT-PCR 6 h later **(D)** WT or cGAS KO cells were treated with 2'3'cGAMP (10 μg/ml) and transcription of IFNB measured by qRT-PCR 6 h later. *p < 0.05, **p < 0.01, ***p < 0.001; ns, no significant difference. Data is representative of two or more replicates.

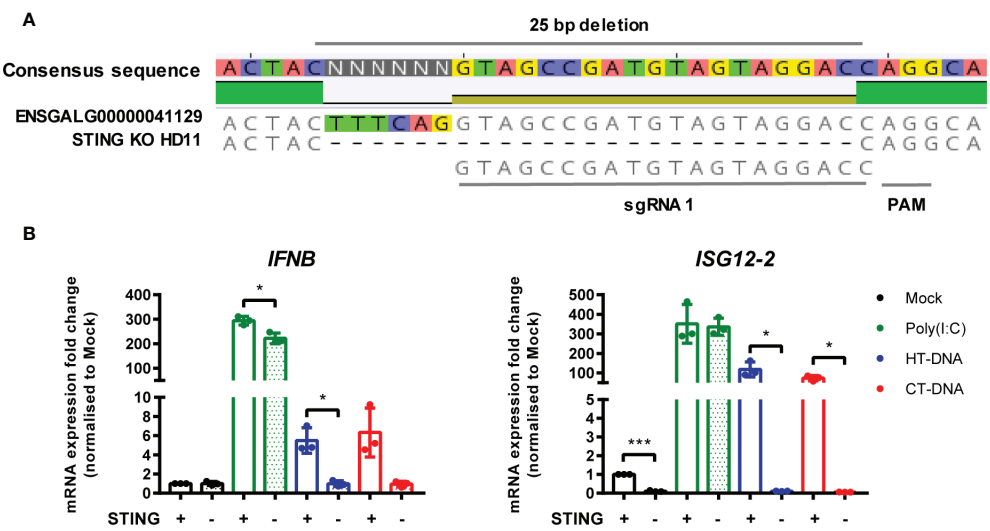

FIGURE 5 | STING is essential for intracellular DNA-dependent IFN-I transcription in HD11 cells. **(A)** Example of identification of indel in clonally selected HD11 STING KO using NGS sequencing. **(B)** WT and STING KO HD11 cells were transfected with HT-DNA, CT-DNA (2 μg/ml) or Poly(I:C) (1 μg/ml) for 6 h and transcription of the indicated genes measured by qRT-PCR 6 h later. *p < 0.05, ***p < 0.001; 2difference. Data is representative of two or more replicates.

downregulation of IFN and MHC transcription (**Figure 6A**). The lack of IFN-I response in poxvirus infected cells is likely due to the presence of numerous virally-encoded suppressors of PRR signaling and IFN-I production (19, 24), hence deletion of specific innate immunomodulators from the viral genome can result in a virus that stimulates host IFN-I signaling. We made use of FWPV mutants FPV012 and FPV184 (19, 20), each deficient in single genes that are proposed immunomodulators, and both of which induce IFN-I production from infected cells (19), including HD11 cells (**Figure 6B**). In the absence of cGAS or STING the transcription of IFN-I, ISG12.2, BLB1 and CD40 by FPV184 or FPV012 was significantly lower at 24 h post infection (**Figures 6B, C**), despite robust infection of HD11 cells by all three virus strains (**Figure 6D**), indicating that FWPV is sensed in infected cells by the DNA sensing PRR cGAS and that the cGAS/STING pathway is responsible for FWPV-induced IFN-I production and MHC-II transcription. Despite its importance for the IFN-I response, in HD11 cells loss of the cGAS/STING pathway did not affect the replicative capacity of the FP9 or mutant viruses (**Figure 6E**).

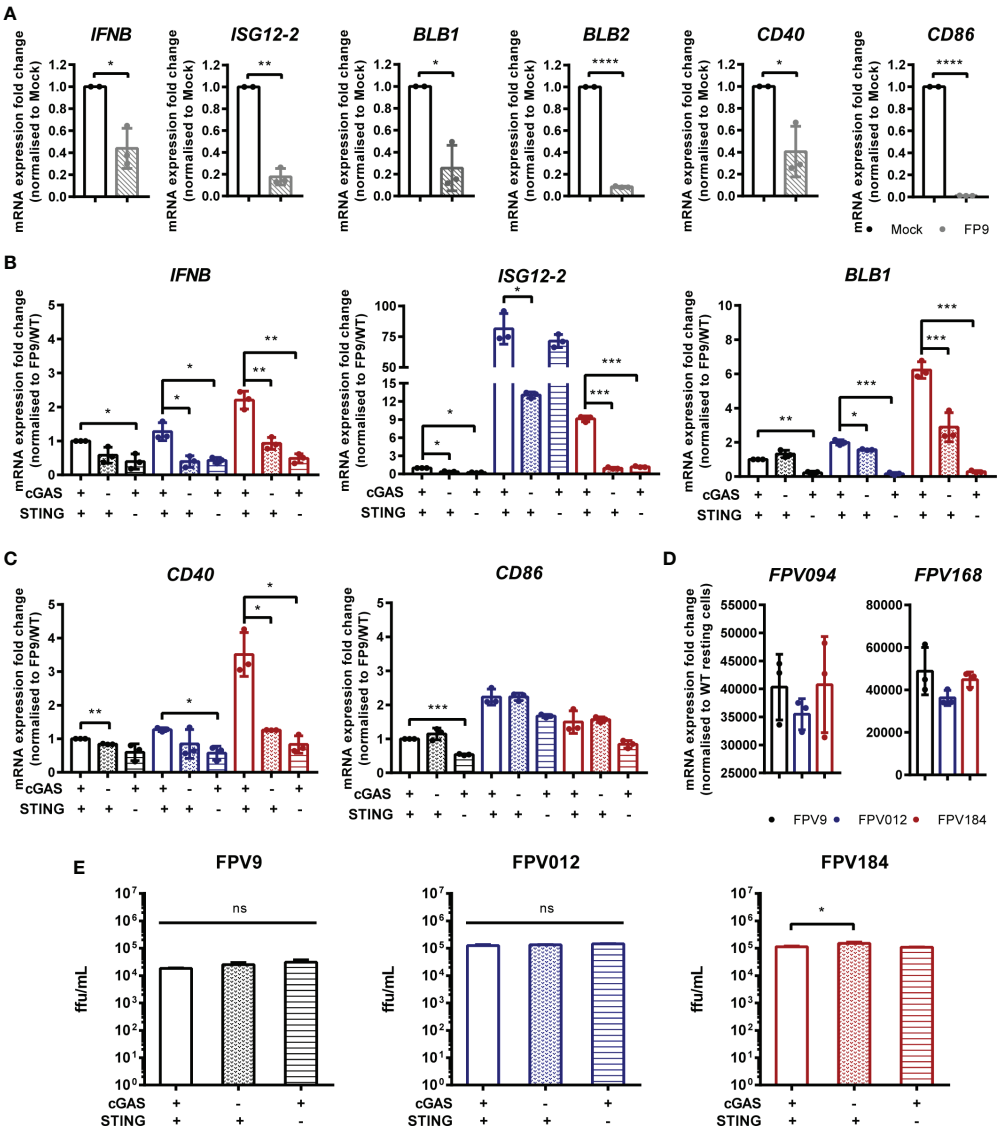

FIGURE 6 | Fowlpox triggers a cGAS/STING dependent DNA sensing pathway in HD11 cells. **(A)** HD11 cells were infected with FWPV strain FP9 at a multiplicity of infection of three. Twenty-four hours later, RNA was extracted and qRT-PCR carried out for the indicated genes. **(B, C)** HD11 WT, cGAS or STING KO cells were infected with FP9 (black bars), FPV012 (blue bars), FPV184 (red bars), at a multiplicity of infection of three. Twenty-four hours later, RNA was extracted and qRT-PCR carried out for the indicated genes. **(D)** HD11 cells were infected with FWPV strain FP9 at a multiplicity of infection of three. Twenty-four hours later, RNA was extracted and qRT-PCR carried out for the indicated FWPV genes. **(E)** HD11 WT, cGAS or STING KO cells were infected with FP9, FPV012, or FPV184 at a multiplicity of infection of three, cell supernatants harvested and released FP9 was titrated on CEFs to measure focus forming units (ffu) per ml. *$p < 0.05$, **$p < 0.01$, ***$p < 0.001$; ****$p < 0.0001$; ns, no significant difference. Data is representative of two or more replicates.

DISCUSSION

The ability of innate immune cells to detect virus infection is dependent on a set of PRRs that directly bind viral nucleic acids. Macrophages act in this context as tissue-resident sentinel sensors of infection that express a broad repertoire of PRRs and mount a rapid and robust innate immune response to viruses and other pathogens. Indeed intracellular DNA sensing was first described in macrophages (25). As well as interferon and cytokine production, activated macrophages use effector functions for pathogen clearance and for activation of adaptive immunity. In mammalian systems the signaling outputs downstream of intracellular DNA detection in macrophages include IRF-dependent IFN and cytokine production and cell death driven by the AIM2 inflammasome. In chicken macrophages, which lack AIM2, we find that intracellular DNA sensing produces IFN but does not result in measurable cell death, rather it upregulates a specific set of antigen presentation machinery including the MHC-II gene BLB1 and co-stimulatory molecules, providing a direct link between anti-viral innate sensing and the initiation of adaptive immunity.

During DNA virus infection, the cGAS/STING-dependent signaling pathway is triggered by viral DNA, resulting in type-I interferon production *via* activation of TBK1 and the IRF family of transcription factors. Although well defined in mammalian systems, the function of chicken cGAS and STING has only more recently been identified (26, 27). FWPV is an avian poxvirus that causes skin lesions and respiratory infections and can infect multiple cell types including macrophages (28). Here we show that the cGAS/STING pathway in chicken macrophages can sense FWPV infection and is responsible for the IFN-I response as well as for upregulation of BLB1.

In order to escape detection and evade host anti-viral responses, poxviruses like FWPV encode a broad range of immunomodulatory proteins that target PRR signaling pathways resulting in these viruses being able to effectively inhibit IFN production from infected cells. These immune evasion mechanisms mask the signaling outputs of PRR signaling during infection with wild type poxviruses. To overcome this issue, we used two mutant FWPVs with deletions in individual genes that block IFN-I production during infection. Infection of cells with FPV184 and FPV012 (29) resulted in interferon and ISG transcription, which was lost in cGAS and STING knockout lines. FWPV DNA is therefore sensed by the cGAS/STING pathway and the downstream signaling response leading to IFN-I production is effectively blocked by the wild type virus. In culture the loss of cGAS or STING didn't lead to significant alterations FWPV's replicative capacity in infected cells (**Figure 6E**), but it remains to be seen how individual PRRs like cGAS contribute to protection against FWPV infection *in vivo*. In mice cGAS/STING are essential for the host response to poxvirus infections such as vaccinia and ectromelia viruses, and the protective effects are meditated *via* IFN-I, despite the presence of large numbers of immunomodulators targeting PRR signaling, including the cGAS/STING systems in these viruses. As such it is likely that cGAS/STING mediated FWPV DNA sensing and IFN-I production has a significant contribution to host defence against FWPV infection in chickens, although mechanistically it remains to be seen exactify how IFN-I mediates this defence against this avian poxvirus.

Birds occupy the same habitats as mammals, have comparable ranges of life span and body mass, and confront similar pathogen challenges, yet birds have a different repertoire of organs, cells, molecules and genes of the immune system compared to mammals (30). It is increasingly evident that the immune system of avian species is rather different from those of model mammalian species. Untested extrapolation from mammalian systems cannot provide the quality of knowledge that is required for understanding host-pathogen relationships in birds. Here, we find that the signaling downstream of chicken cGAS leading to IFN-I transcription is similar to that found in mammalian systems. The presence of orthologues of STING and TBK1 in the chicken genome and their functional inhibition by small molecule compounds (H151 and BX795) is indicative of mechanistic signaling pathway conservation. The chicken genome also contains an orthologue of IRF3, which is the main transcription factor downstream of STING/TBK1 activation, although chicken IRF7 (as this gene is annotated) is not equivalent to mammalian IRF3 or IRF7 and may be considered more as a hybrid these two genes (31). It is likely that chicken IRF7 and TBK1 are recruited by STING following 2'3'-cGAMP ligation and that subsequent phosphorylation, dimerization, and nuclear translocation of IRF7 leads to DNA-induced IFN-I transcription (27, 32). In mammalian systems, the transcription of IFNβ also requires activation of NF-κB, to a greater or lesser extent depending on the species (33, 34). STING can itself be responsible for NF-κB activation following virus infection (35). The extent to which chicken IFNβ transcription downstream of cGAS activation requires NF-κB activity along with IRF7 remains to be explored (32). Recent evidence has implicated chicken cGAS and STING in avian antiviral defence, in particular against Marek's Disease Virus (MDV) and chicken adenovirus 4 (36, 37) in fibroblasts. Using CRISPR/Cas9 technology to knockout STING and cGAS in a transformed monocytic cell line (HD11) and complementing these data in primary macrophages with pharmacological inhibitors we have been able to show this cGAS/STING/TBK1 pathway is active in chicken macrophages. The use of primary cells in this context is important as transformation or immortalization can significantly alter PRR pathways so as to obscure physiological signaling mechanisms.

IFN-I is one of the most effective anti-viral innate immune mediators. Secretion and subsequent ISG transcription induced by autocrine and paracrine IFN receptor signaling sets an anti-viral/inflammatory state in infected and bystander cells. As an example, chicken IFNβ was shown to be an autocrine/paracrine pro-inflammatory mediator in chicken macrophages (17), with direct effects in macrophage effector functions. Nucleic acid sensing PRRs therefore provide a rapid and potent innate response helping to combat infection and reduce viral spread in infected tissues. At the same time, innate immune responses can initiate and amplify adaptive immune responses for example,

by regulating functions of antigen presenting cells (APCs), promoting cross-priming and stimulating antibody production (38–40). In both mammals and birds, macrophages are key regulators of adaptive immunity as principle APCs. By processing and presenting antigen to T and B cells, macrophages directly trigger adaptive responses. The discovery that cGAS/STING signaling can directly regulate the transcription of MHC genes in macrophages provides further evidence linking PRR signaling with the activation of adaptive immunity during infection. It remains to be explored exactly how the transcription of BLB1 and BLB2 is regulated by cGAS/STING signaling. In tissues, macrophages survey the local environment for infection and damage. In this context, macrophage effector functions may be modulated by the presence of innate immune mediators in the tissue. The priming effect of IFNα as an enhancer of macrophage DNA sensing, by upregulating STING expression, suggests a possible mechanism of bystander surveillance. Tissue resident macrophages may respond to signals, including IFN-I and cGAMP, secreted from virally infected stromal cells by enhancing specific effector functions appropriate to defend against viral infection in the tissue (41, 42).

Our data adds to the list of chicken cGAS/STING functions in sensing of avian DNA viruses such as MDV and Adenovirus 4 that replicate in the nucleus or FWPV that replicates in the cytoplasm, and in the regulation of macrophage effector functions. The ability of this pathway to sense a broad range of DNA viruses that replicate in different compartments in avian innate immune cells indicates that this pathway is a primary DNA sensing mechanism for DNA viruses in chickens.

DATA AVAILABILITY STATEMENT

The raw data supporting the conclusions of this article will be made available by the authors, without undue reservation.

AUTHOR CONTRIBUTIONS

BF and CB provided the funding and supervised the work. MO, DR, RG, VG, and EK performed the experiments and statistical analysis. SG and MS generated the mutant fowlpox viruses. BF, CB, RG designed the study and wrote the manuscript. All authors contributed to the article and approved the submitted version.

FUNDING

This work was funded by BBSRC grants BB/S001336/1 (BF and CB), BB/E009956/1, BB/G018545/1, BB/H005323/1 & BB/K002465/1 (MS) and by EUROFERI (Région Centre-Val-de-Loire, France, RG).

ACKNOWLEDGMENTS

This manuscript has been released as a Pre-print at BioRxiv. We thank the experimental facility PFIE (Plateforme d'Infectiologie Expérimentale, Centre INRAE Val de Loire, Nouzilly, France) for providing the animals used for the isolation of primary macrophages.

SUPPLEMENTARY MATERIAL

The Supplementary Material for this article can be found online at: https://www.frontiersin.org/articles/10.3389/fimmu.2020.613079/full#supplementary-material

Supplementary Figure1 | Effect of IFNα priming on expression levels of STING and IRF7 in BMDM and HD11. BMDM or HD11 cells were treated with IFNα for 6 h and transcription of STING and IRF7 measured by qRT-PCR 6 h later. Data is representative of two or more replicates.

Supplementary Figure 2 | BLB2 but not BLB1 is an ISG in HD11 cells. HD11 cells were treated with IFNα for 6 h and the indicated genes were measured by qRT-PCR. Data is representative of two or more replicates.

Supplementary Figure 3 | cGAS is essential for intracellular DNA-dependent IFN-I transcription in HD11 cells. WT or three individual cGAS knockout clones with different indels were stimulated with HT-DNA (2 μg/ml) and IFNB transcription measured by qRT-PCR 6 h later. Data is representative of two or more replicates.

Supplementary Figure 4 | STING is essential for intracellular DNA-dependent IFN-I transcription in HD11 cells. WT or three individual cGAS knockout clones with different indels were stimulated with HT-DNA (2 μg/ml) and IFNB transcription measured by qRT-PCR 6 h later. Data is representative of two or more replicates.

Supplementary Figure 5 | STING or cGAS loss does not significantly alter tonic IFN-I transcription. IFNB transcription measured by qRT-PCR in WT, cGAS KO or STING KO HD11 cells (data shown relative to WT cells).

REFERENCES

1. Mansur DS, Smith GL, Ferguson BJ. Intracellular sensing of viral DNA by the innate immune system. *Microbes Infect* (2014) 16:1002–12. doi:trrex1. doi: 10.1016/j.micinf.2014.09.010
2. Bryant CE, Orr S, Ferguson B, Symmons MF, Boyle JP, Monie TP. International union of basic and clinical pharmacology. XCVI. Pattern recognition receptors in health and disease. *Pharmacol Rev* (2015) 67:462–504. doi: 10.1124/pr.114.009928
3. Li T, Chen ZJ. The cGAS–cGAMP–STING pathway connects DNA damage to inflammation, senescence, and cancer. *J Exp Med* (2018) 215:1287–99. doi: 10.1084/jem.20180139
4. Li X-D, Wu J, Gao D, Wang H, Sun L, Chen ZJ. Pivotal roles of cGAS-cGAMP signaling in antiviral defense and immune adjuvant effects. *Science* (2013) 341:1390–4. doi: 10.1126/science.1244040
5. Mullard A. Can innate immune system targets turn up the heat on "cold" tumours? *Nat Rev Drug Discov* (2017) 2017:171. doi: 10.1038/nrd.2017.264
6. Ablasser A, Hertrich C, Wassermann R, Hornung V. Nucleic acid driven sterile inflammation. *Clin Immunol* (2013) 147:207–15. doi: 10.1016/j.clim.2013.01.003
7. Crow YJ, Rehwinkel J. Aicardi-Goutieres syndrome and related phenotypes: linking nucleic acid metabolism with autoimmunity. *Hum Mol Genet* (2009) 18:R130–6. doi: 10.1093/hmg/ddp293

8. Tanaka Y, Chen ZJ. STING specifies IRF3 phosphorylation by TBK1 in the cytosolic DNA signaling pathway. *Sci Signal* (2012) 5:ra20. doi: 10.1126/scisignal.2002521
9. Gaidt MM, Ebert TS, Chauhan D, Ramshorn K, Pinci F, Zuber S, et al. The DNA Inflammasome in Human Myeloid Cells Is Initiated by a STING-Cell Death Program Upstream of NLRP3. *Cell* (2017) 171:1110–24.e18. doi: 10.1016/j.cell.2017.09.039
10. Gulen MF, Koch U, Haag SM, Schuler F, Apetoh L, Villunger A, et al. Signalling strength determines proapoptotic functions of STING. *Nat Commun* (2017) 8:427. doi: 10.1038/s41467-017-00573-w
11. Sze A, Belgnaoui SM, Olagnier D, Lin R, Hiscott J, Van Grevenynghe J. Host restriction factor SAMHD1 limits human T cell leukemia virus type 1 infection of monocytes via STING-mediated apoptosis. *Cell Host Microbe* (2013) 14:422–34. doi: 10.1016/j.chom.2013.09.009
12. Glück S, Guey B, Gulen MF, Wolter K, Kang TW, Schmacke NA, et al. Innate immune sensing of cytosolic chromatin fragments through cGAS promotes senescence. *Nat Cell Biol* (2017) 19:1061–70. doi: 10.1038/ncb3586
13. Giotis ES, Skinner MA. Spotlight on avian pathology: fowlpox virus. *Avian Pathol* (2019) 48:87–90. doi: 10.1080/03079457.2018.1554893
14. Lousberg EL, Fraser CK, Tovey MG, Diener KR, Hayball JD. Type I interferons mediate the innate cytokine response to recombinant fowlpox virus but not the induction of plasmacytoid dendritic cell-dependent adaptive immunity. *J Virol* (2010) 84:6549–63. doi: 10.1128/JVI.02618-09
15. Beug H, von Kirchbach A, Döderlein G, Conscience JF, Graf T. Chicken hematopoietic cells transformed by seven strains of defective avian leukemia viruses display three distinct phenotypes of differentiation. *Cell* (1979) 18:375–90. doi: 10.1016/0092-8674(79)90057-6
16. Schmidt T, Schmid-Burgk JL, Ebert TS, Gaidt MM, Hornung V. Designer nuclease-mediated generation of knockout THP1 cells. In: *Methods in Molecular Biology*. New York, Humana Press Inc. (2016). p. 261–72. doi: 10.1007/978-1-4939-2932-0_19
17. Garrido D, Alber A, Kut E, Chanteloup NK, Lion A, Trotereau A, et al. The role of type I interferons (IFNs) in the regulation of chicken macrophage inflammatory response to bacterial challenge. *Dev Comp Immunol* (2018) 86:156–70. doi: 10.1016/j.dci.2018.04.025
18. Schwarz H, Harlin O, Ohnemus A, Kaspers B, Staeheli P. Synthesis of IFN-β by Virus-Infected Chicken Embryo Cells Demonstrated with Specific Antisera and a New Bioassay. *J Interferon Cytokine Res* (2004) 24:179–84. doi: 10.1089/107999004322917025
19. Laidlaw SM, Robey R, Davies M, Giotis ES, Ross C, Buttigieg K, et al. Genetic Screen of a Mutant Poxvirus Library Identifies an Ankyrin Repeat Protein Involved in Blocking Induction of Avian Type I Interferon. *J Virol* (2013) 87:5041–52. doi: 10.1128/jvi.02736-12
20. Giotis ES, Laidlaw SM, Bidgood SR, Albrecht D, Burden JJ, Robey RC, et al. Modulation of Early Host Innate Immune Response by an Avipox Vaccine Virus' Lateral Body Protein. *Biomedicines* (2020) 8:634. doi: 10.3390/biomedicines8120634
21. Ma F, Li B, Yu Y, Iyer SS, Sun M, Cheng G. Positive feedback regulation of type I interferon by the interferon-stimulated gene STING. *EMBO Rep* (2015) 16:202–12. doi: 10.15252/embr.201439366
22. Parker A, Kaufman J. What chickens might tell us about the MHC class II system. *Curr Opin Immunol* (2017) 46:23–9. doi: 10.1016/j.coi.2017.03.013
23. Ablasser A, Goldeck M, Cavlar T, Deimling T, Witte G, Röhl I, et al. cGAS produces a 2'-5'-linked cyclic dinucleotide second messenger that activates STING. *Nature* (2013) 498:380–4. doi: 10.1038/nature12306
24. Smith GL, Benfield CTO, Maluquer de Motes C, Mazzon M, Ember SWJ, Ferguson BJ, et al. Vaccinia virus immune evasion: mechanisms, virulence and immunogenicity. *J Gen Virol* (2013) 94:2367–92. doi: 10.1099/vir.0.055921-0
25. Stetson DB, Medzhitov R. Recognition of cytosolic DNA activates an IRF3-dependent innate immune response. *Immunity* (2006) 24:93–103. doi: 10.1016/j.immuni.2005.12.003
26. Vitak N, Hume DA, Chappell KJ, Sester DP, Stacey KJ. Induction of interferon and cell death in response to cytosolic DNA in chicken macrophages. *Dev Comp Immunol* (2016) 59:145–52. doi: 10.1016/j.dci.2016.01.023
27. Gao L, Li K, Zhang Y, Liu Y, Liu C, Zhang Y, et al. Inhibition of DNA-Sensing Pathway by Marek's Disease Virus VP23 Protein through Suppression of Interferon Regulatory Factor 7 Activation. *J Virol* (2018) 93:e01934–18. doi: 10.1128/jvi.01934-18
28. Williams SM, Smith JA, Garcia M, Brinson D, Kiupel M, Hofacre C. Severe histiolymphocytic and heterophilic bronchopneumonia as a reaction to in ovo fowlpox vaccination in broiler chicks. *Vet Pathol* (2010) 47:177–80. doi: 10.1177/0300985809353314
29. Giotis ES, Robey RC, Skinner NG, Tomlinson CD, Goodbourn S, Skinner MA. Chicken interferome: avian interferon-stimulated genes identified by microarray and RNA-seq of primary chick embryo fibroblasts treated with a chicken type I interferon (IFN-α). *Vet Res* (2016) 47:75. doi: 10.1186/s13567-016-0363-8
30. Kaiser P. Advances in avian immunology-prospects for disease control: A review. *Avian Pathol* (2010) 39:309–24. doi: 10.1080/03079457.2010.508777
31. Grant CE, Vasa MZ, Deeley RG. clRF-3, a new member of the interferon regulatory factor (IRF) family that is rapidly and transiently induced by dsRNA. *Nucleic Acids Res* (1995) 23:2137–46. doi: 10.1093/nar/23.12.2137
32. Cheng Y, Zhu W, Ding C, Niu Q, Wang H, Yan Y, et al. IRF7 Is Involved in Both STING and MAVS Mediating IFN-β Signaling in IRF3-Lacking Chickens. *J Immunol* (2019) 203:1930–42. doi: 10.4049/jimmunol.1900293
33. Kim TK, Maniatis T. The mechanism of transcriptional synergy of an in vitro assembled interferon-β enhanceosome. *Mol Cell* (1997) 1:119–29. doi: 10.1016/S1097-2765(00)80013-1
34. Fang R, Wang C, Jiang Q, Lv M, Gao P, Yu X, et al. NEMO–IKKβ Are Essential for IRF3 and NF-κB Activation in the cGAS–STING Pathway. *J Immunol* (2017) 199:3222–33. doi: 10.4049/jimmunol.1700699
35. Stempel M, Chan B, Juranić Lisnić V, Krmpotić A, Hartung J, Paludan SR, et al. The herpesviral antagonist m152 reveals differential activation of STING -dependent IRF and NF-κB signaling and STING's dual role during MCMV infection. *EMBO J* (2019) 38:e100983. doi: 10.15252/embj.2018100983
36. Li K, Liu Y, Xu Z, Zhang Y, Luo D, Gao Y, et al. Avian oncogenic herpesvirus antagonizes the cGAS-STING DNA-sensing pathway to mediate immune evasion. *PloS Pathog* (2019) 15:e1007999. doi: 10.1371/journal.ppat.1007999
37. Wang J, Ba G, Han YQ, Ming SL, Di Wang M, Fu PF, et al. Cyclic GMP-AMP synthase is essential for cytosolic double-stranded DNA and fowl adenovirus serotype 4 triggered innate immune responses in chickens. *Int J Biol Macromol* (2020) 146:497–507. doi: 10.1016/j.ijbiomac.2020.01.015
38. Schulz O, Diebold SS, Chen M, Näslund TI, Nolte MA, Alexopoulou L, et al. Toll-like receptor 3 promotes cross-priming to virus-infected cells. *Nature* (2005) 433:887–92. doi: 10.1038/nature03326
39. Desmet CJ, Ishii KJ. Nucleic acid sensing at the interface between innate and adaptive immunity in vaccination. *Nat Rev Immunol* (2012) 12:479–91. doi: 10.1038/nri3247
40. Loré K, Betts MR, Brenchley JM, Kuruppu J, Khojasteh S, Perfetto S, et al. Toll-Like Receptor Ligands Modulate Dendritic Cells to Augment Cytomegalovirus- and HIV-1-Specific T Cell Responses. *J Immunol* (2003) 171:4320–8. doi: 10.4049/jimmunol.171.8.4320
41. Ablasser A, Schmid-Burgk JL, Hemmerling I, Horvath GL, Schmidt T, Latz E, et al. Cell intrinsic immunity spreads to bystander cells via the intercellular transfer of cGAMP. *Nature* (2013) 503:530–4. doi: 10.1038/nature12640
42. Schadt L, Sparano C, Schweiger NA, Silina K, Cecconi V, Lucchiari G, et al. Cancer-Cell-Intrinsic cGAS Expression Mediates Tumor Immunogenicity. *Cell Rep* (2019) 29:1236–48.e7. doi: 10.1016/j.celrep.2019.09.065

Conflict of Interest: The authors declare that the research was conducted in the absence of any commercial or financial relationships that could be construed as a potential conflict of interest.

frontiers in Immunology

ORIGINAL RESEARCH
published: 04 February 2021
doi: 10.3389/fimmu.2020.598884

Poly(dA:dT) Suppresses HSV-2 Infection of Human Cervical Epithelial Cells Through RIG-I Activation

Dan-Dan Shao[1†], Feng-Zhen Meng[1†], Yu Liu[2], Xi-Qiu Xu[1], Xu Wang[2], Wen-Hui Hu[2], Wei Hou[1] and Wen-Zhe Ho[2*]*

[1] School of Basic Medical Sciences, Wuhan University, Wuhan, China, [2] Department of Pathology and Laboratory Medicine, Lewis Katz School of Medicine, Temple University, Philadelphia, PA, United States

Epithelial cells of the female reproductive tract (FRT) participate in the initial innate immunity against viral infections. Poly(dA:dT) is a synthetic analog of B form double-stranded (ds) DNA which can activate the interferon (IFN) signaling pathway-mediated antiviral immunity through DNA-dependent RNA Polymerase III. Here we investigated whether poly(dA:dT) could inhibit herpes simplex virus type 2 (HSV-2) infection of human cervical epithelial cells (End1/E6E7). We demonstrated that poly(dA:dT) treatment of End1/E6E7 cells could significantly inhibit HSV-2 infection. Mechanistically, poly(dA:dT) treatment of the cells induced the expression of the intracellular IFNs and the multiple antiviral IFN-stimulated genes (ISGs), including IFN-stimulated gene 15 (ISG15), IFN-stimulated gene 56 (ISG56), 2'-5'-oligoadenylate synthetase 1 (OAS1), 2'-5'-oligoadenylate synthetase 2 (OAS2), myxovirus resistance protein A (MxA), myxovirus resistance protein B (MxB), virus inhibitory protein, endoplasmic reticulum-associated, IFN-inducible (Viperin), and guanylate binding protein 5 (GBP5). Further investigation showed that the activation of RIG-I was largely responsible for poly(dA:dT)-mediated HSV-2 inhibition and IFN/ISGs induction in the cervical epithelial cells, as RIG-I knockout abolished the poly(dA:dT) actions. These observations demonstrate the importance for design and development of AT-rich dsDNA-based intervention strategies to control HSV-2 mucosal transmission in FRT.

Keywords: herpes simplex virus type 2, human cervical epithelial cells, poly(dA:dT), interferon, interferon-stimulated gene, retinoic acid-inducible gene-I

OPEN ACCESS

Edited by:
Rongtuan Lin,
McGill University, Canada

Reviewed by:
Sampsa Matikainen,
University of Helsinki, Finland
Chunfu Zheng,
Fujian Medical University, China

***Correspondence:**
Wen-Zhe Ho
wenzheho@temple.edu
Wei Hou
houwei@whu.edu.cn

[†]These authors have contributed equally to this work

Specialty section:
This article was submitted to Viral Immunology, a section of the journal Frontiers in Immunology

Received: *25 August 2020*
Accepted: *16 December 2020*
Published: *04 February 2021*

Citation:
Shao D-D, Meng F-Z, Liu Y, Xu X-Q, Wang X, Hu W-H, Hou W and Ho W-Z (2021) Poly(dA:dT) Suppresses HSV-2 Infection of Human Cervical Epithelial Cells Through RIG-I Activation. Front. Immunol. 11:598884. doi: 10.3389/fimmu.2020.598884

INTRODUCTION

Herpes simplex virus type 2 (HSV-2) is the leading cause of genital herpes and the most commonly sexual transmitted virus. It is estimated that 417 million people aged 15–49 (11%) worldwide are infected with HSV-2 infection in 2012 (1). Importantly, the epidemiological and biological studies have shown a strong association between human immunodeficiency virus 1 (HIV-1) and HSV-2 infection. HSV-2 infection increases the risk of HIV-1 acquisition by approximately three-fold (2) and facilitates transmissibility of HIV-1 up to five-fold through genital ulcers (3). In turn, HIV-1

TABLE 1 | Primer sets for real-time PCR.

Primer	Accession No.	Orientation	Sequences	Product (bp)
GAPDH	NM_002046	Sense	5'-GGTGGTCTCCTCTGACTTCAACA-3'	127
		Antisense	5'-GTTGCTGTAGCCAAATTCGTTGT-3'	
HSV-2 ICP0	D10471.1	Sense	5'-GTGCATGAAGACCTGGATTCC-3'	82
		Antisense	5'-GGTCACGCCCACTATCAGGTA-3'	
HSV-2 ICP27	D10471.1	Sense	5'-TTCTGCGATCCATATCCGAGC-3'	101
		Antisense	5'-AAACGGCATCCCGCCAAA-3'	
HSV-2 ICP8	D10658.1	Sense	5'-AGGACATAGAGACCATCGCGTTCA-3'	99
		Antisense	5'-TGGCCAGTTCGCTCACGTTATT-3'	
HSV-2 gC	AJ297389.1	Sense	5'-AAATCCGATGCCGGTTTCCCAA-3'	120
		Antisense	5'-TTACCATCACCTCCTCTAAGCTAGGC-3'	
HSV-2 gD	K02373.1	Sense	5'-ATCCGAACGCAGCCCCGC-3'	142
		Antisense	5'-TCTCCGTCCAGTCGTTTAT-3'	
HSV-2 DNA polymerase	M16321.1	Sense	5'-GCTCGAGTGCGAAAAAACGTTC-3'	215
		Antisense	5'-CGGGGCGCTCGGCTAAC-3'	
IFN-β	NM_002176.4	Sense	5'-GCCGCATTGACCATCTATGAGA-3'	346
		Antisense	5'-GAGATCTTCAGTTTCGGAGGTAAC-3'	
IFN-λ1	NM_172140	Sense	5'-CTTCCAAGCCCACCCCAACT-3'	142
		Antisense	5'-GGCCTCCAGGACCTTCAGC-3'	
IFN-λ2/3	NM_172139	Sense	5'-TTTAAGAGGGCCAAAGATGC-3'	267
		Antisense	5'-TGGGGCTGAGGCTGGATACAG-3'	
IRF3	NM_001571.1	Sense	5'-ACCAGCCGTGGACCAAGAG-3'	65
		Antisense	5'-TACCAAGGCCCTGAGGCAC-3'	
IRF7	NM_001572	Sense	5'-TGGTCCTGGTGAAGCTGGAA-3'	134
		Antisense	5'-GATGTCGTCATAGAGGCTGTTGG-3'	
STAT1	NM_007315	Sense	5'-CCGTGGCACTGCATACAATC-3'	187
		Antisense	5'-ACCATGCCGAATTCCCAAAG-3'	
STAT2	XM_017019904.1	Sense	5'-CCCCATCGACCCCTCATC-3'	69
		Antisense	5'-GAGTCTCACCAGCAGCCTTGT-3'	
STAT3	NM_003150	Sense	5'-CTGCCCCATACCTGAAGACC-3'	162
		Antisense	5'-TCCTCACATGGGGGAGGTAG-3'	
ISG15	NM_005101	Sense	5'-GGCTGGGACCTGACGGTGAAG-3'	492
		Antisense	5'-GCTCCGCCCGCCAGGCTCTGT-3'	
ISG56	NM_001270930	Sense	5'-TTCGGAGAAAGGCATTAGA-3'	85
		Antisense	5'-TCCAGGGCTTCATTCATAT-3'	
OAS1	NM_001032409	Sense	5'-AGAAGGCAGCTCACGAAACC-3'	71
		Antisense	5'-CCACCACCCAAGTTTCCTGTA-3'	
OAS2	XM_011538415.1	Sense	5'-CAGTCCTGGTGAGTTTGCAGT-3'	146
		Antisense	5'-ACAGCGAGGGTAAATCCTTGA-3'	
MxA	XM_005260982.2	Sense	5'-GCCGGCTGTGGATATGCTA-3'	69
		Antisense	5'-TTTATCGAAACATCTGTGAAAGCAA-3'	
MxB	XM_005260983.4	Sense	5'-CAGCAGACGATCAACTTGGTG-3'	159
		Antisense	5'-CATGACGCTTTTCTCAGTGCC-3'	
Viperin	NM_001318443.1	Sense	5'-TGGGTGCTTACACCTGCTG-3'	235
		Antisense	5'-TGAAGTGATAGTTGACGCTGGT-3'	
GBP5	NM_001134486.2	Sense	5'-TGGCAAATCCTACCTGATGA-3'	97
		Antisense	5'-CCATATCCAAATTCCCTTGG-3'	
RIG-I	NM_014314.4	Sense	5'-CTTGGCATGTTACACAGCTGAC-3'	104
		Antisense	5'-GCTTGGGATGTGGTCTACTCA-3'	
IFI16	NM_001376589.1	Sense	5'-CCGTTCATGACCAGCATAGG-3'	106
		Antisense	5'-TCAGTCTTGGTTTCAACGTGGT-3'	
cGAS	NP_612450.2	Sense	5'-GGGAGCCCTGCTGTAACACTTCTTAT-3'	186
		Antisense	5'-CCTTTGCATGCTTGGGTACAAGGT-3'	
STING	NP_938023.1	Sense	5'-ACTGTGGGGTGCCTGATAAC-3'	197
		Antisense	5'-TGGCAAACAAAGTCTGCAAG-3'	
DAI	NM_001160418.2	Sense	5'-CAACAACGGGAGGAAGACAT-3'	499
		Antisense	5'-TCATCTCATTGCTGTGTCCC-3'	
AIM2	NM_004833.3	Sense	5'-TAGCGCCTCACGTGTGTTAG-3'	103
		Antisense	5'-TTGAAGCGTGTTGATCTTCG-3'	
DHX29	NM_001345965.2	Sense	5'-TCAGCACCTGGGAGCTACTT-3'	111
		Antisense	5'-TCTGCATCACTCCACTCCAG-3'	

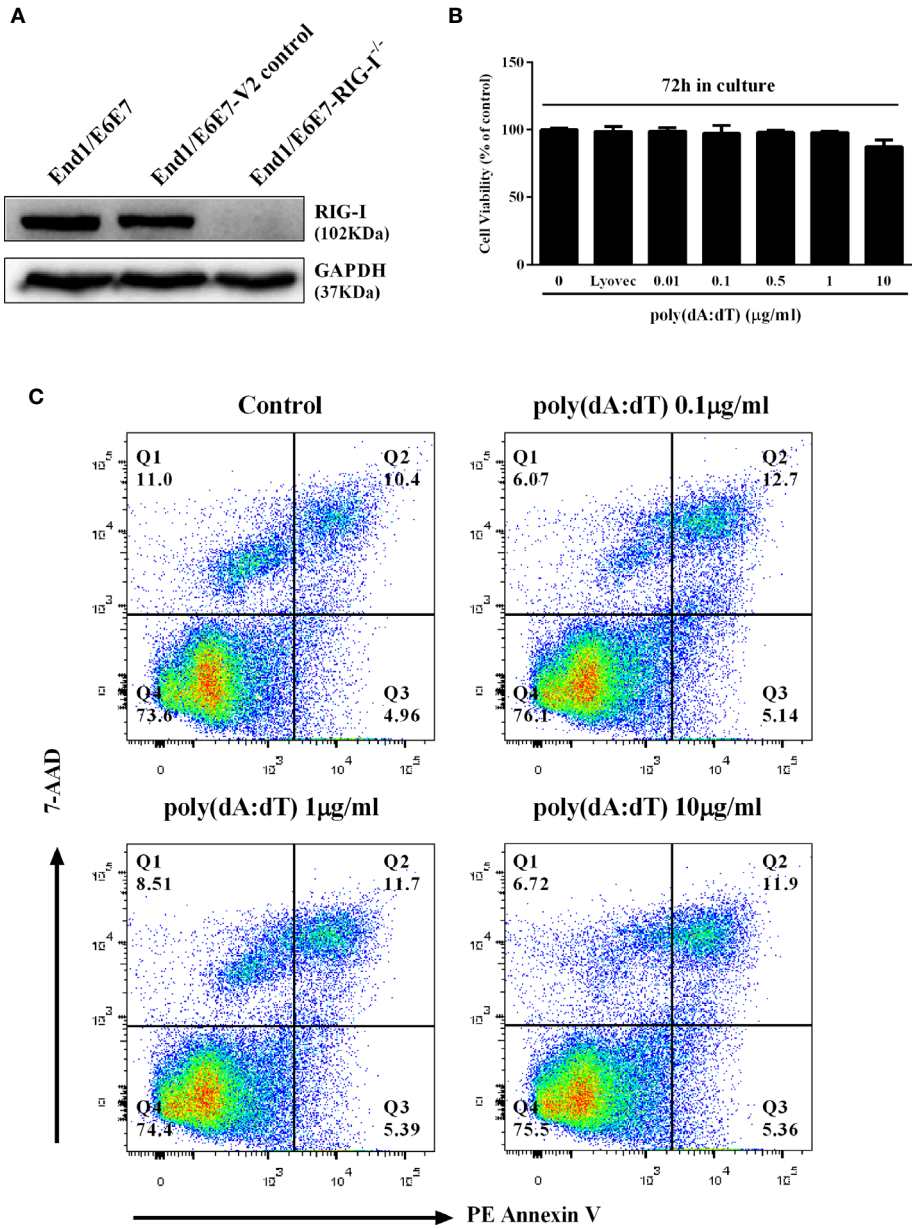

FIGURE 1 | Effect of poly(dA:dT) on End1/E6E7 cells. **(A)** Cell lysates of End1/E6E7 cells, End1/E6E7 V2 control cells and RIG-I knockout End1/E6E7 cells were subjected to Western blot assay for RIG-I expression and GAPDH was used as a protein loading control. **(B, C)** End1/E6E7 cells were treated with poly(dA:dT) at the indicated concentrations, and cell viability was assessed by MTT assay **(B)** and annexin V/7-AAD assay **(C)** 72h post poly(dA:dT) treatment.

infection enhances HSV-2 shedding frequency and quantity (4, 5), people with HIV-1-related immunosuppression can have severe HSV-2 diseases (6, 7).

Epithelial cells in the female reproductive tract (FRT) are the first barrier to pathogen invasion. At cellular level, epithelial cells constitute a unique microenvironment and participate in FRT innate immunity against viral infections, including HSV-2 (8, 9). HSV-2 primarily infects genital epithelium and replicates within the vaginal keratinocytes (10). Human cervical epithelial cells have been extensively used to study FRT-mediated immunity against viral infections (11–14). Studies have shown that these cells could be immunologically activated and produced the multiple antiviral factors against HSV-2 (12) and HIV-1 (15). As the outmost layer cells in FRT, human cervical epithelial cells are the first to contact with invading microbes. Thus, understanding the processes and mechanisms of these cells-mediated innate immunity against viral infections is of importance and significance.

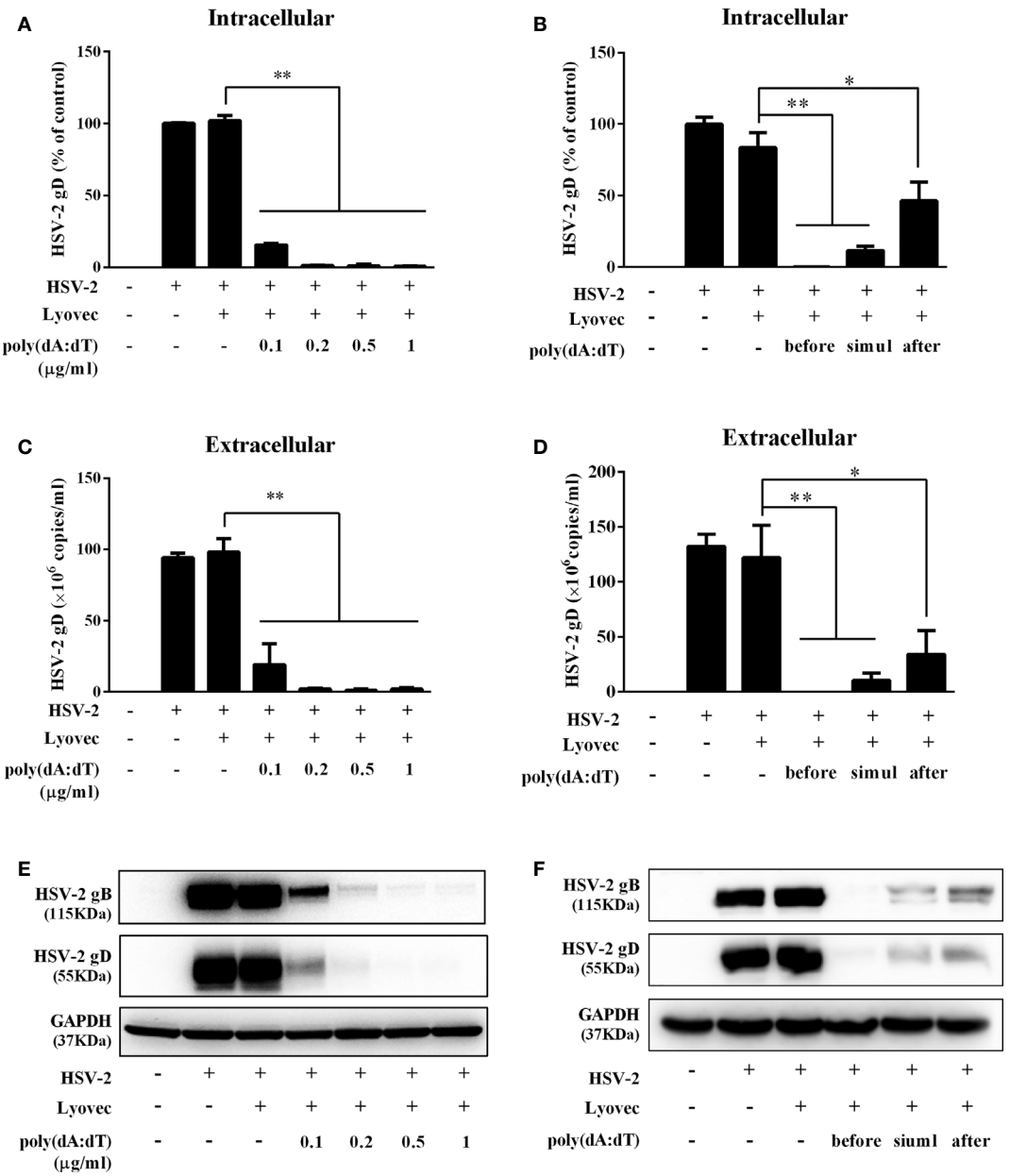

FIGURE 2 | Poly(dA:dT) inhibits HSV-2 infection. **(A, C, E)** End1/E6E7 cells were pretreated with poly(dA:dT) at indicated concentrations for 24h prior to HSV-2 (MOI = 0.001) infection. Forty-eight hours after HSV-2 infection, **(A)** intracellular DNA, **(C)** extracellular DNA, and **(E)** total cellular proteins were collected and subjected to the real-time PCR or Western blot for HSV-2 gene expression. **(B, D, F)** End1/E6E7 cells were treated with either poly(dA:dT) (0.5μg/ml) for 24h prior to HSV-2 (MOI=0.001) infection (before) or poly(dA:dT) and infected with HSV-2 simultaneously (simul) or infected with HSV-2 for 2h prior to poly(dA:dT) treatment (after). At 48h post HSV-2 infection, **(B)** intracellular DNA, **(D)** extracellular DNA, and **(F)** total cellular proteins were collected and analyzed by the real-time PCR or Western blot for HSV-2 gene expression. Data shown are the mean ± SD of three independent experiments. Asterisks indicate statistically significant differences. (*$P < 0.05$, **$P < 0.01$).

DNA-dependent RNA polymerase III (RNA Pol III) is involved in DNA-mediated innate immunity response by converting AT-rich DNA into a RNA intermediate which can be recognized by RIG-I, resulting in the activation of interferon (IFN) signaling pathway. Poly(dA:dT) is a synthetic analog of B form double stranded DNA (dsDNA) can be sensed by the RNA Pol III and then recognized by cytosolic RNA sensor RIG-I, eliciting an intracellular immune response to control virus replication (16–18). IFN regulatory factor 3 (IRF3) and IRF7 are the crucial transcription factors involved in RIG-I signaling

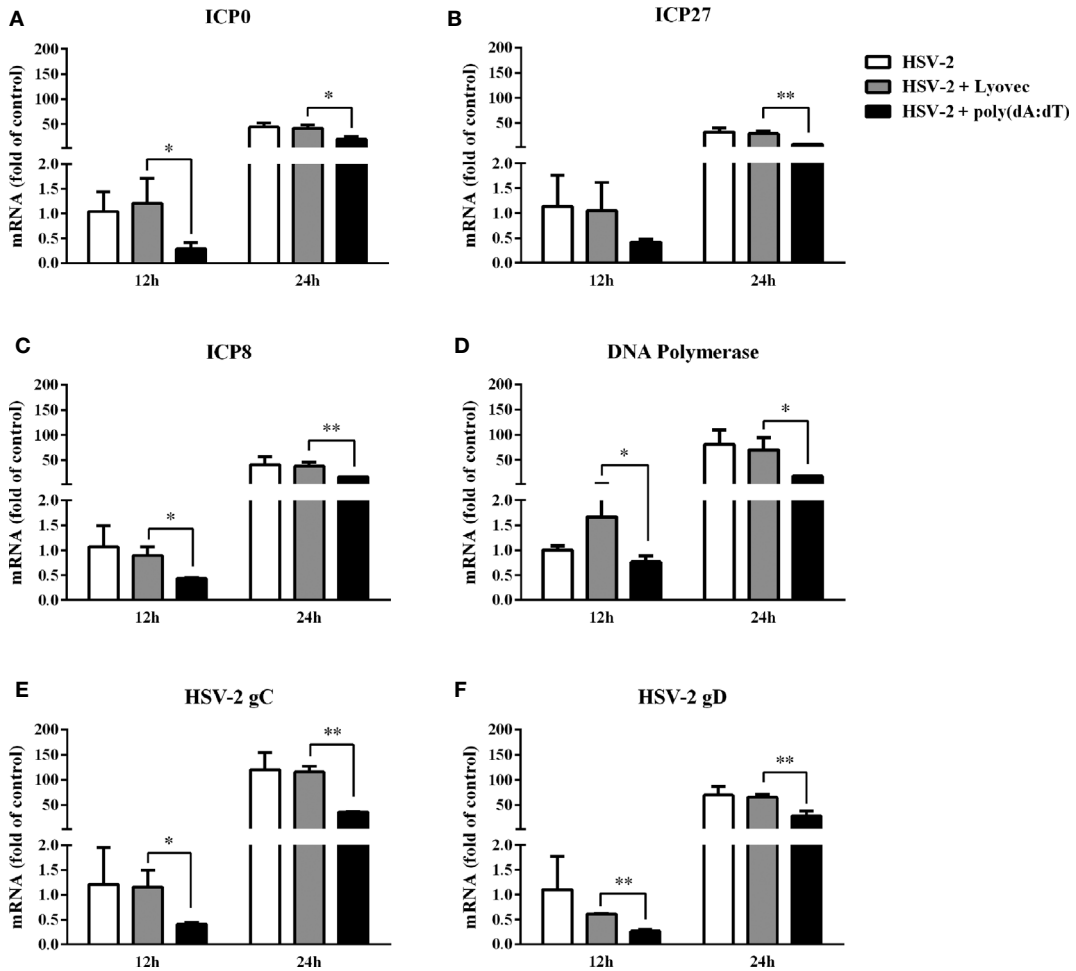

FIGURE 3 | Effect of poly(dA:dT) on HSV-2 gene expression. End1/E6E7 cells were transfected with or without poly(dA:dT) (0.5μg/ml) at indicated concentrations for 24h prior to HSV-2 infection (MOI = 0.001). Cellular RNAs were collected from the virus-infected cells at 12 or 24h post infection and subjected to the real-time PCR for HSV-2 immediate early genes **(A, B)**, early genes **(C, D)** and late genes **(E, F)** expression. The results were measured as HSV-2 gene levels relative (%) to control (without treatment, which is defined as 100%). Data are shown as mean ± SD of three independent experiments. Asterisks indicate statistically significant differences (*$P < 0.05$, **$P < 0.01$).

pathway (19). It has been reported that the association of RIG-I with pre-genomic RNA can induce type III IFN and inhibit hepatitis B virus (20). Type III IFN, also known as IFN lambda (IFN-λ), can induce expression of ISGs and exert antiviral properties similar to type I IFNs (21).

Studies have shown that activation of IFN-dependent innate immune defense through RIG-I signaling pathway is vital in antiviral response of epithelial cells (22–24). However, we know little about whether poly(dA:dT) has the ability to activate the intracellular antiviral immunity of human cervical epithelial cells, an essential component of the mucosal defense mechanisms in the FRT. In this study, we examined whether poly(dA:dT) has the ability to induce the intracellular antiviral factors against HSV-2 infection of human cervical epithelial cells. We also explored the cellular and molecular mechanisms underlying poly(dA:dT)-mediated IFN/ISG induction and HSV-2 inhibition in these cells.

MATERIALS AND METHODS

Cell Lines and Virus

End1/E6E7 cell line was established from normal human endocervical epithelia immortalized by expression of human papillomavirus 16/E6E7. End1/E6E7 cells have exactly the same cytokeratin and involucrin patterns as primary End1 cells and the morphological and immunocytochemical characteristics of the End1/E6E7 cells closely resembled those of origin and primary cultures. Therefore, End1/E6E7 cells provide the basis for valid reproducible *in vitro* models for studies on

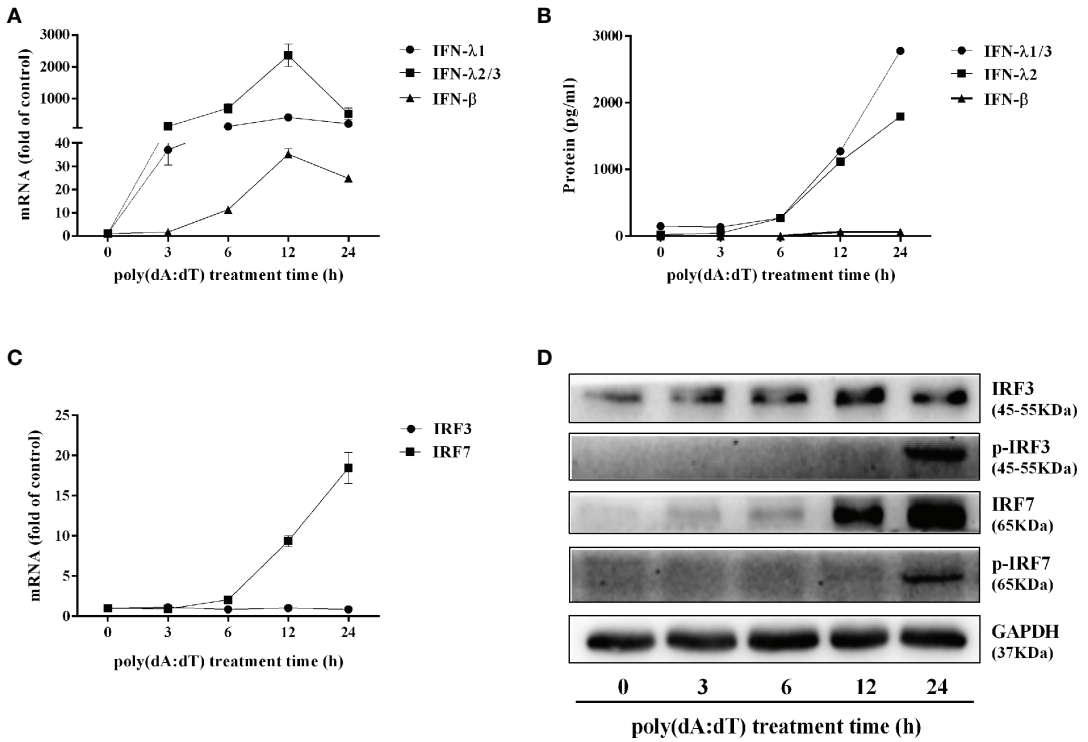

FIGURE 4 | Effect of poly(dA:dT) on IFNs and IRFs expression. End1/E6E7 cells were transfected with or without poly(dA:dT) (0.5μg/ml) for the indicated times. **(A, C)** Total cellular RNAs were extracted and subjected to the real-time PCR for IFN-β, IFN-λ1, IFN-λ2/3, and IRF3, IRF7 expression. **(B)** The cell-free supernatant was subjected to ELISA assay to determine IFN-β, IFN-λ1/3, and IFN-λ2 protein levels. **(D)** Total cellular proteins were collected and subjected to Western blot with the antibodies against IRF3, IRF7, p-IRF3, p-IRF7, and GAPDH. Data are shown as mean ± SD of three independent experiments.

cervicovaginal physiology and infections and for testing pharmacological agents for intravaginal application (25). In addition, End1/E6E7 cell line has been broadly used as an *in vitro* model of human female reproductive tract (13, 26, 27). End1/E6E7 cells were cultured in keratinocyte growth medium (Gibco, USA) supplemented with the provided recombinant epidermal growth factor (0.1ng/ml) and bovine pituitary extract (50μg/ml). African green monkey kidney epithelial cells (Vero) and 293T cells were cultured in Dulbecco's modified Eagle's culture medium (DMEM, Gibco) supplemented with 10% fetal bovine serum (FBS, Gibco) at 37°C in a humidified atmosphere of 5% CO_2. HSV-2 G strain was provided by Dr. Qinxue Hu (State Key Laboratory of Virology, Wuhan Institute of Virology, Chinese Academy of Sciences, China). The HSV-2 G strain was propagated at a low multiplicity of infection (MOI = 0.001) in Vero cells.

Plasmids and Reagents

LentiCRISPRv2-puro, psPAX2, and pMD2.G plasmids were provided by Dr. Jian Huang (Department of Pathology and Laboratory Medicine, Temple University, USA). PE Annexin V Apoptosis Detection Kit I was purchased from BD (Pharmingen, USA). Poly(dA:dT), LyoVec, and puromycin were purchased from InvivoGen (San Diego, CA, USA). Lipofectamine 3000 Reagent was purchased from Thermo Fisher Scientific (Carlsbad, CA, USA). Antibodies against RIG-I, DNA sensors, ISGs, signal transducers and activators of transcription (STATs), and IRFs were purchased from Cell Signaling Technology (Danvers, MA, USA). Antibodies against HSV-1+HSV-2 gD, HSV-1+HSV-2 gB were purchased from Abcam (Cambridge, UK). Antibody to GAPDH was purchased from Proteintech (Chicago, USA).

Cell Viability Assay

The cytotoxic effect of poly(dA:dT) was evaluated by the MTT assay based on the manufacturer's instruction. End1/E6E7 cells were seeded in 96-well plate (1×10^4 cells/well) treated with different concentrations of poly(dA:dT) for 72h. Cells were then incubated with MTT working solution (0.5mg/ml) for 4h at 37°C in darkness. The formation of soluble formazan from MTT was measured by spectrophotometric determination of absorption at 490nm using a 96-well plate reader (SpectraMax i3, Molecular Devices, Sunnyvale, CA, USA).

Flow Cytometry Analysis of Apoptosis

We used Annexin V/7-AAD assay to measure the apoptosis effect of poly(dA:dT) on End1/E6E7 cells. Cells were seeded in 24-well plate (2×10^5 cells/well) and treated with different concentrations of poly(dA:dT) for 72h. Cells were washed

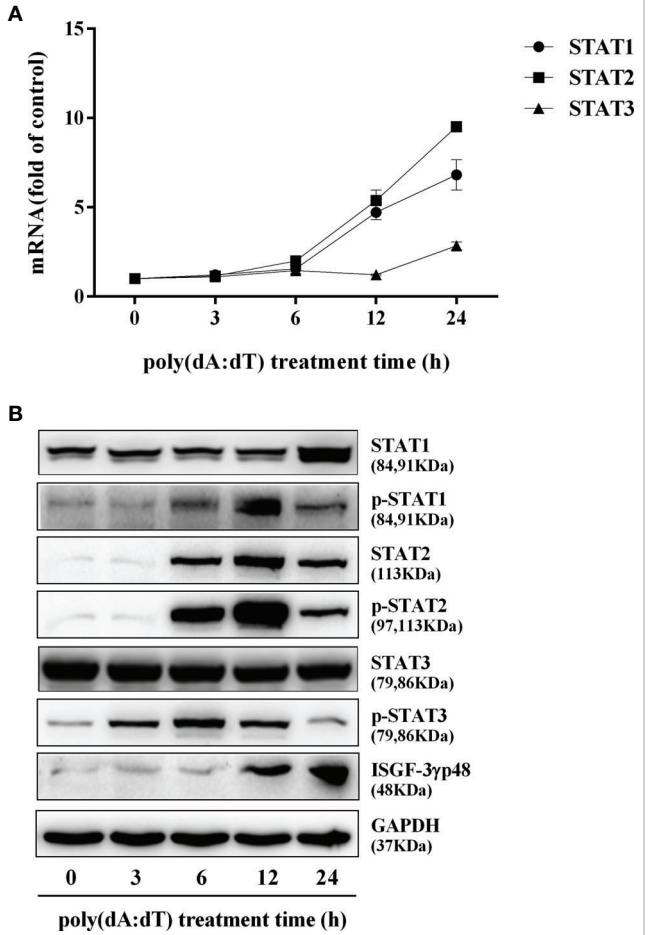

FIGURE 5 | Effect of poly(dA:dT) on JAK/STAT signaling pathway. End1/E6E7 cells were transfected with or without poly(dA:dT) (0.5μg/ml) for the indicated times. **(A)** Total cellular RNAs were extracted and subjected to the real-time PCR for STAT1, STAT2, and STAT3 expression. **(B)** Total cellular proteins were collected and subjected to Western blot with the antibodies against STAT1, STAT2, STAT3, p-STAT1, p-STAT2, p-STAT3, ISGF-3γp48, and GAPDH. Data are shown as mean ± SD of three independent experiments.

twice with cold phosphate-buffered saline (PBS) and then resuspended in 1×binding buffer at a concentration of 1×10^5 cells/ml. Annexin V-PE (2.5μl) and 7-AAD (5μl) were added and then incubated for 15min at room temperature without light, finally analyzed by FCM (FACScan, Becton Dickinson, San Jose, CA).

RNA Extraction and Real-Time PCR

Total cellular RNAs from the cells were extracted using TRI-Reagent® (Molecular Research Center, Cincinnati, OH) according to the manufacturer's instruction. Total RNAs were subjected to reverse transcription reaction using the random primer, dNTPs, M-MLV reverse transcriptase and RNase inhibitor (Promega Co., Madison, WI) to generate complementary DNA (cDNA). cDNA was then used as a template for real-time PCR which was performed with IQ SYBR Green supermix (Bio-Rad Laboratories, Hercules, CA). The level of GAPDH mRNA was used as an endogenous reference to normalize the quantities of target mRNAs. The sequences of oligonucleotide primers are shown in **Table 1**.

In Vitro Antiviral Assay

End1/E6E7 cells were pretreated with poly(dA:dT) for 24h and infected with HSV-2 (MOI = 0.001) for 2h. The cells were then washed to remove unattached viruses and subsequently cultured for 48h. HSV-2 genome DNAs from HSV-2-infected cells and culture supernatant were extracted with DNA lysis buffer as previously described (12) and subjected to the real-time PCR. HSV-2 gD standards with known copy numbers were used to quantify HSV-2 gD copies in the culture supernatant. Total proteins were extracted from End1/E6E7 cells and subjected to the Western blot. In addition, the antiviral effect of poly(dA:dT) under different treatment conditions (before, simultaneously and after HSV-2 infection) was evaluated. Briefly, End1/E6E7 cells were pretreated with poly(dA:dT) (0.5μg/ml) for 24h, then infected with HSV-2 (before); End1/E6E7 cells were simultaneously (simul) treated with poly(dA:dT) and infected with HSV-2; End1/E6E7 cells were first infected with HSV-2 for 2h, then washed and treated with poly(dA:dT) (after). At 48h post infection, both HSV-2 genomic DNA and total proteins were extracted from End1/E6E7 cells and subjected to the real-time PCR or Western blot assay.

CRISPR Cas9

We used the CRISPR Cas9 system to abrogate RIG-I expression in End1/E6E7 cells. Briefly, we designed gRNA (5'-GGGTCTTCCGGGATATAATCC-3') targeting the conserved sites in human RIG-I genomic sequences based on CCTop (https://crispr.cos.uni-heidelberg.de/). The gRNA was then subcloned into the lentiCRISPRv2 plasmid to obtain the lentiCRISPRv2-gRNA clone that expressed both Cas9 and gRNA according to the publications' instruction (28, 29). Then lentiCRISPRv2-gRNA plasmid and two packaging plasmids, psPAX2 and pMD2.G, were co-transfected into 293T cells to obtain lentivirus. LentiCRISPRv2 was used as an empty vector control. Three days after the lentivirus infection, End1/E6E7 cells were cultured with puromycin (0.5μg/ml) containing medium for 14 days. Total cellular proteins were then collected and subjected to Western blot for RIG-I protein expression.

Western Blot

Total cell lysates were prepared with the cell extraction buffer (Invitrogen, Shanghai, China) with 1% protease inhibitor cocktail (Sigma, MO) and 1% phosphatase inhibitor mixture (Applygen, Beijing, China). The total proteins were quantified by a BCA protein assay kit (Beyotime Institute of Biotechnology, Shanghai, China), and equal amount of proteins were separated on SDS-PAGE. After being transferred to a PVDF membrane (Millipore, Germany), non-

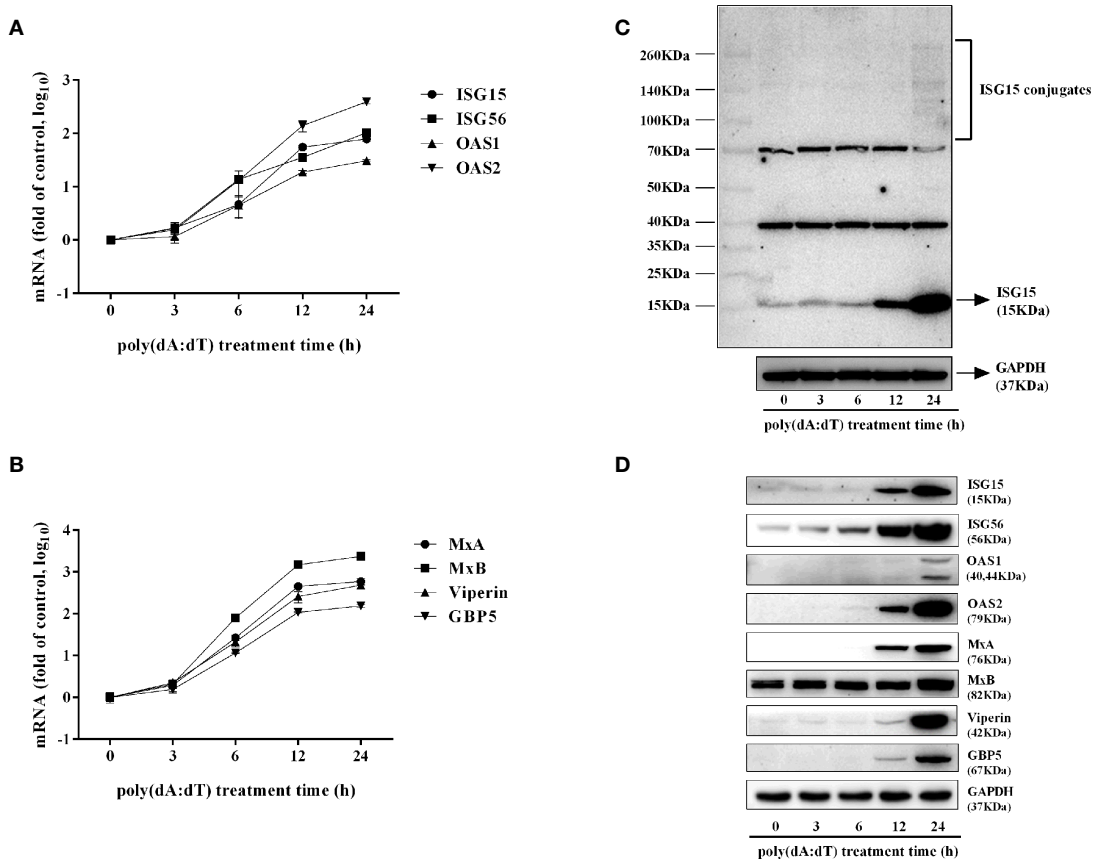

FIGURE 6 | Effect of poly(dA:dT) on ISGs expression. End1/E6E7 cells were transfected with or without poly(dA:dT) (0.5μg/ml) for the indicated times. **(A, B)** Total cellular RNAs were isolated and subjected to the real-time PCR for ISG15, ISG56, OAS1, OAS2, MxA, MxB, viperin, and GBP5 expression. **(C, D)** Total cellular proteins were collected and subjected to Western blot with antibodies against ISG15 and ISG15-conjugates, ISG56, OAS1, OAS2, MxA, MxB, Viperin, GBP5, and GAPDH. Data shown represent the mean ± SD of three independent experiments.

specific sites were blocked with 5% non-fat milk for 3h prior to incubating with primary antibodies at 4°C overnight. The membranes were washed with TBST and further incubated with horseradish peroxidase-conjugated second antibody. Blots were developed with SuperSignal West Pico Chemiluminescent Substrate (Thermo Fisher Scientific, Waltham).

ELISA

IFN-β, IFN-λ1/3, and IFN-λ2 protein levels in cells culture supernatant were measured by ELISA kits (R&D system Inc., MH, USA). The assays were carried out according to the manufacturer's instruction.

Statistical Analysis

Data were presented as mean ± SD from at least three independent experiments, and statistical significance was analyzed by Student's t-test using GraphPad Prism for Windows version 5.0 (GraphPad Software Inc., San Diego, CA). Statistical significance was defined as $P < 0.05$ or $P < 0.01$.

RESULTS

Poly(dA:dT) Has Little Cytotoxicity Effect on End1/E6E7 Cells

We first examined the effect of poly(dA:dT) on the viability and apoptosis of End1/E6E7 cells. As shown in **Figures 1B, C**, little cytotoxic and apoptosis effect was observed in End1/E6E7 cells treated with poly(dA:dT) at the dose as high as 10μg/ml.

Poly(dA:dT) Inhibits HSV-2 Infection of End1/E6E7 Cells

To determine the anti-HSV-2 effect of poly(dA:dT), End1/E6E7 cells were pretreated with poly(dA:dT) for 24h prior to HSV-2 infection. As shown in **Figures 2A, C, E**, cells transfected with poly(dA:dT) had lower levels of intracellular and extracellular HSV-2 DNA/protein than the control cells. This poly(dA:dT)-mediated HSV-2 inhibition was dose-dependent. To further determine the anti-HSV-2 effect of poly(dA:dT), End1/E6E7 cells were treated with poly(dA:dT) under different treatment conditions (before, simultaneously and after HSV-2 infection). As shown in **Figures 2B, D, F**, under all

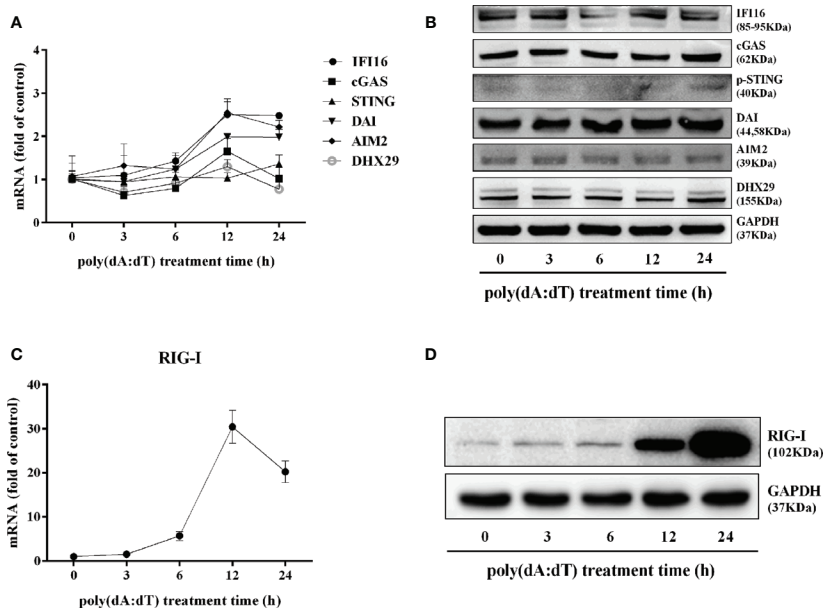

FIGURE 7 | Effect of poly(dA:dT) on the DNA sensors and RIG-I. End1/E6E7 cells were transfected with or without poly(dA:dT) (0.5μg/ml) for the indicated times. **(A)** Total cellular RNAs were extracted and the messenger RNA (mRNA) levels of DNA sensors (IFI16, cGAS, STING, DAI, AIM2, and DHX29) were measured by the real-time PCR. **(B)** Total cellular proteins were collected and subjected to Western blot with the antibodies against IFI16, cGAS, p-STING, DAI, AIM2, DHX29, and GAPDH. **(C)** Total cellular RNAs were extracted and subjected to the real-time PCR for measuring RIG-I mRNA. **(D)** Total cellular proteins were collected and subjected to Western blot with the antibodies against RIG-I and GAPDH. Representative data are the mean ± SD of three independent experiments.

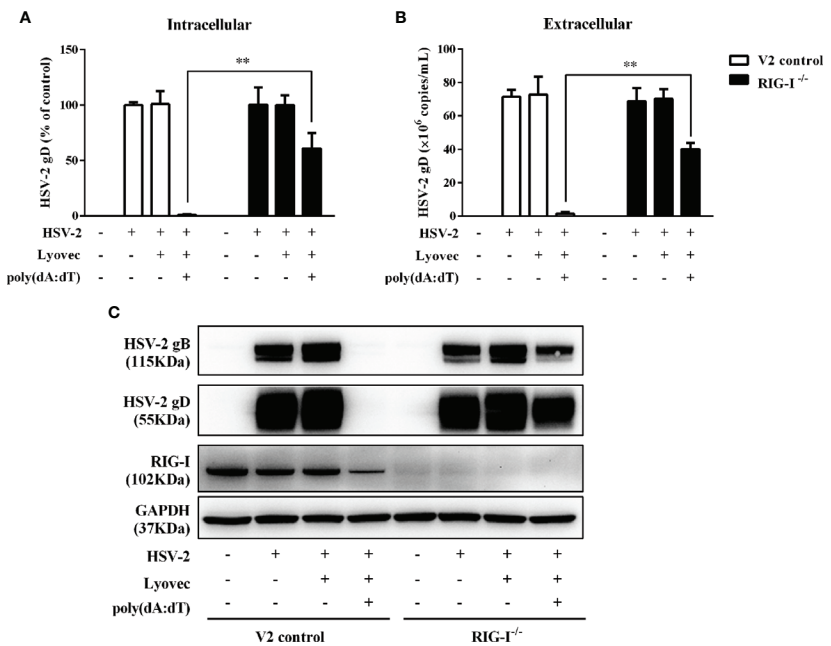

FIGURE 8 | Effect of RIG-I knockout on poly(dA:dT)-mediated HSV-2 inhibition. End1/E6E7 control cells (V2 control) and RIG-I knockout End1/E6E7 cells (RIG-$I^{-/-}$) were transfected with or without poly(dA:dT) (0.5μg/ml) for 24h prior to HSV-2 infection (MOI = 0.001). **(A, B)** Total DNAs extracted from cells (intracellular) and culture supernatant (Extracellular) were measured by the real-time PCR for HSV-2 gD expression. **(C)** Total cellular proteins were collected and subjected to Western blot with antibodies against HSV-2 gB, HSV-2 gD, RIG-I, and GAPDH. The results are the mean ± SD of three independent experiments. Asterisks indicate that the differences between the indicated groups are statistically significant (**$P < 0.01$).

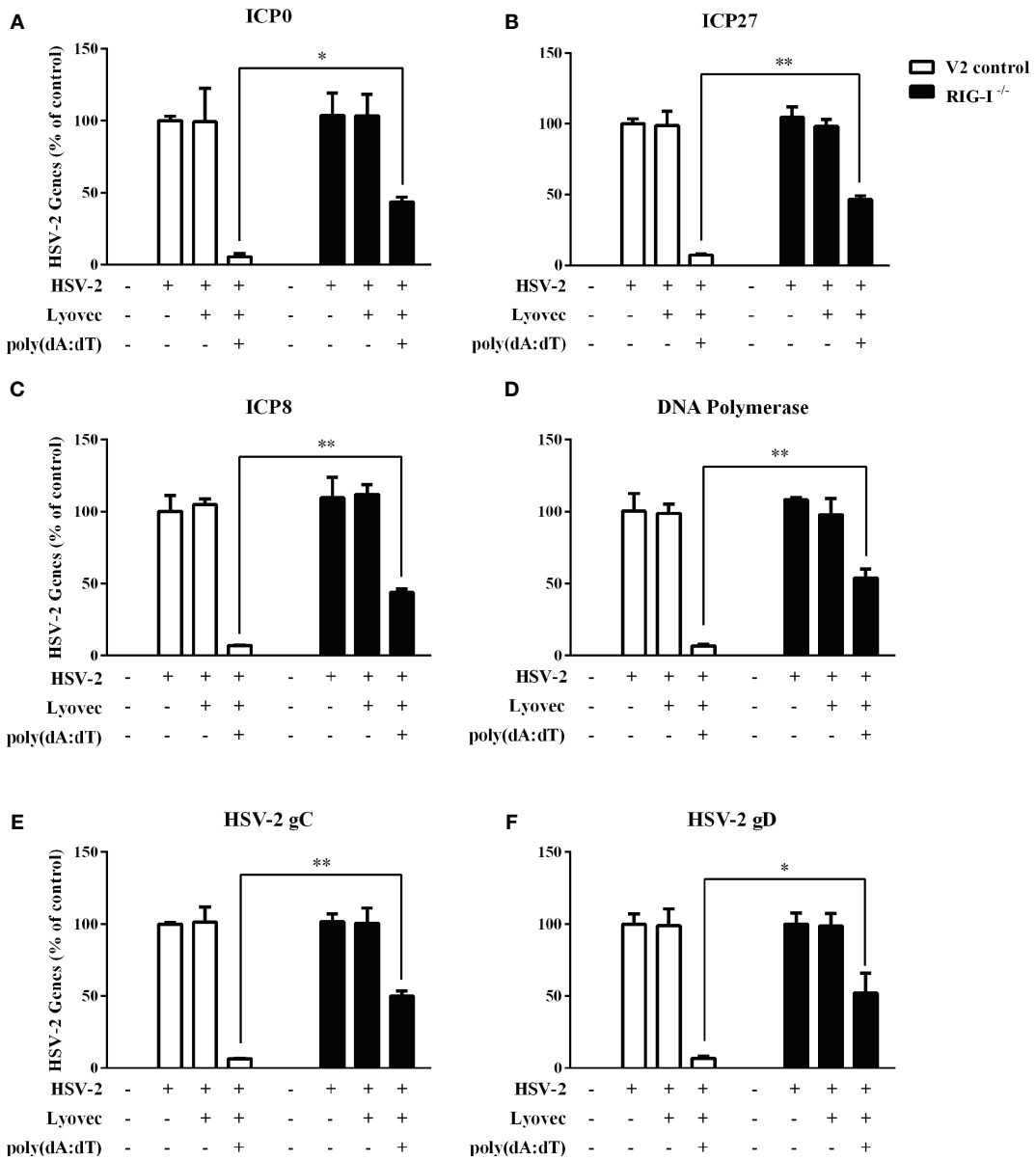

FIGURE 9 | Effect of RIG-I knockout on poly(dA:dT)-mediated inhibtion of HSV-2 gene expression. End1/E6E7 control cells (V2 control) and RIG-I knockout End1/E6E7 cells (RIG-I$^{-/-}$) were transfected with or without poly(dA:dT) (0.5μg/ml) for 24h prior to HSV-2 infection (MOI = 0.001). At 24h post HSV-2 infection, cellular RNAs were collected and subjected to the real-time PCR for HSV-2 immediate early genes **(A, B)**, early genes **(C, D),** and late genes **(E, F)** expression. The results were measured as HSV-2 gene levels relative (%) to control (without treatment, which is defined as 100%). Data are shown as mean ± SD for three independent experiments. Asterisks indicate that the differences between the indicated groups are statistically significant (*$P < 0.05$, **$P < 0.01$).

the three treatment conditions, poly(dA:dT) were able to significantly suppress HSV-2 infection at both DNA and protein levels. Pretreatment of the cells with poly(dA:dT) was the most effective in HSV-2 inhibition (**Figures 2B, D, F**). In addition, we examined the effect of poly(dA:dT) on several key HSV-2 genes, including two immediate early genes (IE: ICP0 and ICP27), two early genes (E: ICP8 and DNA polymerase) and two late genes (L: HSV-2 gC and gD). As shown in **Figure 3**, poly(dA:dT) could significantly inhibit the expression of HSV-2 IE (**Figures 3A, B**), E (**Figures 3C, D**) and L (**Figures 3E, F**) genes in the infected cells.

Poly(dA:dT) Activates the JAK/STAT Signaling Pathway

To determine the mechanisms by which poly(dA:dT) inhibits HSV-2 infection of End1/E6E7 cells (**Figures 2** and **3**), we examined whether poly(dA:dT) could activate IFN-based

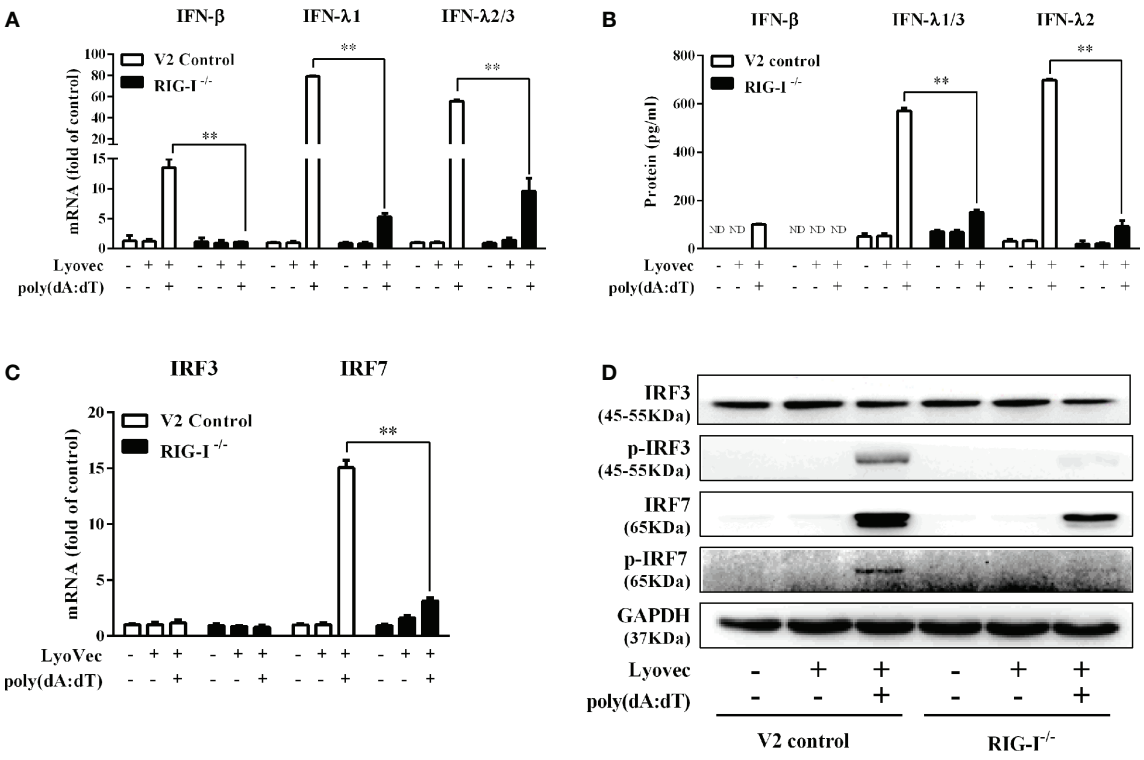

FIGURE 10 | Effect of RIG-I knockout on poly(dA:dT)-induced expression of IFNs and IRFs. End1/E6E7 control cells (V2 control) and RIG-I knockout End1/E6E7 cells (RIG-I$^{-/-}$) were transfected with or without poly(dA:dT) (0.5μg/ml) for 12h. **(A, C)** Total cellular RNAs were extracted and subjected to the real-time PCR for IRF3, IRF7, IFN-β, IFN-λ1, and IFN-λ2/3 mRNA expression. **(B)** The cell-free supernatant was collected and subjected to ELISA assay to determine IFN-β, IFN-λ1/3, and IFN-λ2 protein levels. **(D)** Total cellular proteins were collected and subjected to Western blot with antibodies against IRF3, IRF7, p-IRF3, p-IRF7, and GAPDH. The results are the mean ± SD of three independent experiments. Asterisks indicate that the differences between the indicated groups are statistically significant (ND, not detected, $^{**}P < 0.01$).

immunity in End1/E6E7 cells. As shown in **Figures 4A, B**, poly (dA:dT) induced the expression of IFN-β and IFN-λ at both mRNA (**Figure 4A**) and protein (**Figure 4B**) levels. These effects of poly(dA:dT) on IFN-β and IFN-λ induction were time-dependent. We next studied whether IRF3 and IRF7, the key positive regulators of the IFN signaling pathway, were involved in the IFN-β and IFN-λ induction by poly(dA:dT) in End1/E6E7 cells. As shown in **Figure 4D**, poly(dA:dT) facilitated the phosphorylation of both IRF3 and IRF7 (p-IRF3 and p-IRF7), which were positively associated with the treatment time of poly (dA:dT) in End1/E6E7 cells.

To determine whether the induction of IFN-β and IFN-λ is responsible for the activation of JAK/STAT signaling pathway, we analyzed the impact of poly(dA:dT) on the expression of signal transducers and activators of transcription (STATs). As shown in **Figure 5**, poly(dA:dT) induced the mRNA expression of STAT1, STAT2, STAT3 (**Figure 5A**), and protein expression of p-STAT1, p-STAT2, p-STAT3, IFN-regulated transcription factor 3 (ISGF-3)-γp48 in a time-dependent fashion (**Figure 5B**). In addition, poly(dA:dT) treatment of End1/E6E7 cells also induced the expression of ISG15, ISG56, OAS1, OAS2, MxA, MxB, Viperin, and GBP5 at both mRNA (**Figures 6A, B**) and protein levels (**Figures 6C, D**).

Poly(dA:dT) Induces RIG-I

In addition to the DNA sensors (30–32), RIG-I (16, 17) is involved in sensing cytosolic DNA. We thus examined the effect of poly(dA:dT) on RIG-I expression in End/E6E7 cells. As shown in **Figures 7C, D**, poly(dA:dT) time-dependently enhanced the expression of RIG-I in the cells. In contrast, poly (dA:dT) had little effect on the expression of the key DNA sensors (IFI16, cGAS, phosphor-stimulator of IFN genes (p-STING), DAI, AIM2, and DExH-box helicase 29 (DHX29) (**Figures 7A, B**).

RIG-I Knockout Significantly Compromises Poly(dA:dT)-Mediated HSV-2 Inhibition

To determine whether RIG-I plays a role in poly(dA:dT)-mediated HSV-2 inhibition, we constructed RIG-I knockout End1/E6E7 cells (RIG-I$^{-/-}$) and End1/E6E7 V2 control cells (V2 control) through CRISPR Cas9 system (**Figure 1A**). As shown in **Figures 8A–C**, the levels of both HSV-2 DNA (**Figures 8A, B**) and protein (**Figure 8C**) in RIG-I$^{-/-}$ cells were significantly higher than those in V2 control cells. In addition, we examined the impact of RIG-I knockout on poly(dA:dT)-mediated HSV-2 gene inhibition and

observed that RIG-I$^{-/-}$ cells has higher levels of HSV-2 IE, E and L genes expression than V2 control cells (**Figure 9**). The expression level of RIG-I in HSV-2 infected cells was lower than those in uninfected cells. Especially, the expression level of RIG-I in HSV-2 infected cells which were pretreated with poly(dA:dT) was significantly lower than those in uninfected cells.

RIG-I Knockout Diminishes the Effect of Poly(dA:dT) on the Activation of JAK/STAT Signaling Pathway

To determine whether RIG-I is vital for poly(dA:dT)-mediated IFN induction, we examined the levels of IFN-β and IFN-λ in RIG-I knockout cells (RIG-I$^{-/-}$) and control cells (V2 control) transfected with poly(dA:dT). As shown in **Figures 10A, B**, IFN-β and IFN-λ levels in RIG-I$^{-/-}$ cells were significantly lower than those in V2 control cells. In addition, we examined the impact of RIG-I knockout on the expression of IRF3 and IRF7, the key regulators of IFNs. We observed that there was a significant decrease in the levels of p-IRF3 and p-IRF7 in RIG-I$^{-/-}$ cells as compared to those in V2 control cells (**Figure 10D**). To determine whether the suppression of IFN-β, IFN-λ, and IRFs in RIG-I$^{-/-}$ cells is associated with the inhibition of JAK/STAT signaling pathway, we analyzed the effect of poly(dA:dT) on STATs expression. **Figure 11** demonstrated that poly(dA:dT)-mediated induction of p-STAT1, p-STAT2, and ISGF-3γp48 diminished in RIG-I$^{-/-}$ cells as compared to V2 control cells. In addition, RIG-I$^{-/-}$ cells had lower expression of poly(dA:dT)-stimulated ISGs (ISG15, ISG56, OAS1, OAS2, MxA, MxB, Viperin, and GBP5) than V2 control cells at both mRNA (**Figures 12A, B**) and protein (**Figure 12C**) levels.

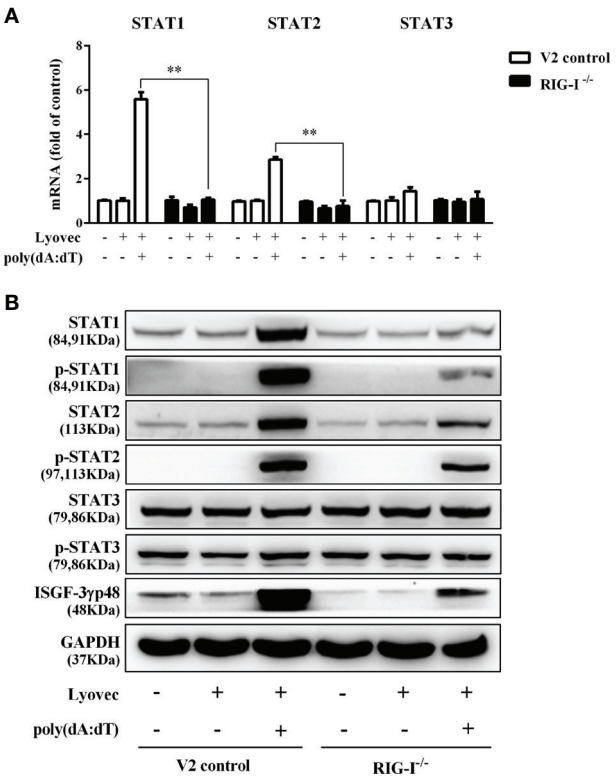

FIGURE 11 | Effect of RIG-I knockout on poly(dA:dT)-induced expression of STATs. End1/E6E7 control cells (V2 control) and RIG-I knockout End1/E6E7 cells (RIG-I$^{-/-}$) were transfected with or without poly(dA:dT) (0.5μg/ml) for 12h. **(A)** Total cellular RNAs were collected and subjected to the real-time PCR for STAT1, STAT2, and STAT3 expression. **(B)** Total cellular proteins were collected and subjected to Western blot with the antibodies against STAT1, STAT2, STAT3, p-STAT1, p-STAT2, p-STAT3, ISGF-3γp48, and GAPDH. The results are the mean ± SD of three independent experiments. Asterisks indicate that the differences between the indicated groups are statistically significant (**$P < 0.01$).

DISCUSSION

As the first line of defense in FRT, human cervical epithelial cells are in direct contact with the virus and thus play an important role in preventing viral infections, including HSV-2. HSV-2 is a dsDNA virus which can be recognized by the cytosolic DNA sensors. There are several cytosolic dsDNA sensors involved in the host cells innate immunity against viral infections, including cGAS, whose secondary messenger cyclic GMP-AMP (cGAMP) can activate downstream sensor protein stimulator of IFN genes (STING). In addition to cGAS (33–35), AIM2, IFI16, and DAI are the cytosolic DNA receptors, activation of which could induce innate immune response to virus infections (36–39). Studies have shown that classical B form dsDNA is a potent immune stimulator when presents in the cytosol (40, 41). In the present study, we examined whether poly(dA:dT) has the ability to activate the intracellular innate immunity against HSV-2 infection of human cervical epithelial cells. We found that poly (dA:dT) could significantly induce the expression of IFNs/the antiviral ISGs (**Figures 4** and **6**) and inhibit HSV-2 replication (**Figure 2**). The investigation on the mechanisms for the induction of IFNs showed (**Figures 4C, D**) that poly(dA:dT) treatment of the cells enhanced the phosphorylation of IRF3 and IRF7, the key and positive regulators of IFNs during viral infections (42). IRF3 and IRF7 phosphorylation is a crucial step in activating the IFNs-mediated antiviral immunity (43). During viral infections, IRF3 is important in the early phase of inducing the transcription of IFN-α and IFN-β, which results in the IRF7 activation. Both IFN-β, IFN-λ1 gene expression is regulated by virus-activated IRF3 and IRF7, whereas IFN-λ2/3 gene expression is mainly controlled by IRF7 (44).

In addition to the positive impact on the IRFs, poly(dA:dT) could also activate the JAK/STAT signaling pathway that is vital for IFN-mediated innate immune response. We observed that poly(dA:dT) not only enhanced the expression of STAT1, STAT2, and STAT3 (**Figure 5A**) but also facilitate the phosphorylation of STAT1, STAT2, STAT3, and ISGF-3γp48 (**Figure 5B**). Several studies (45–47) have shown that comparing with STATs 1 and 2, STAT3 is an acute phase response factor with a transient activation. Therefore, it is likely that activation duration of STAT3 is shorter than that of STAT1 and STAT2.

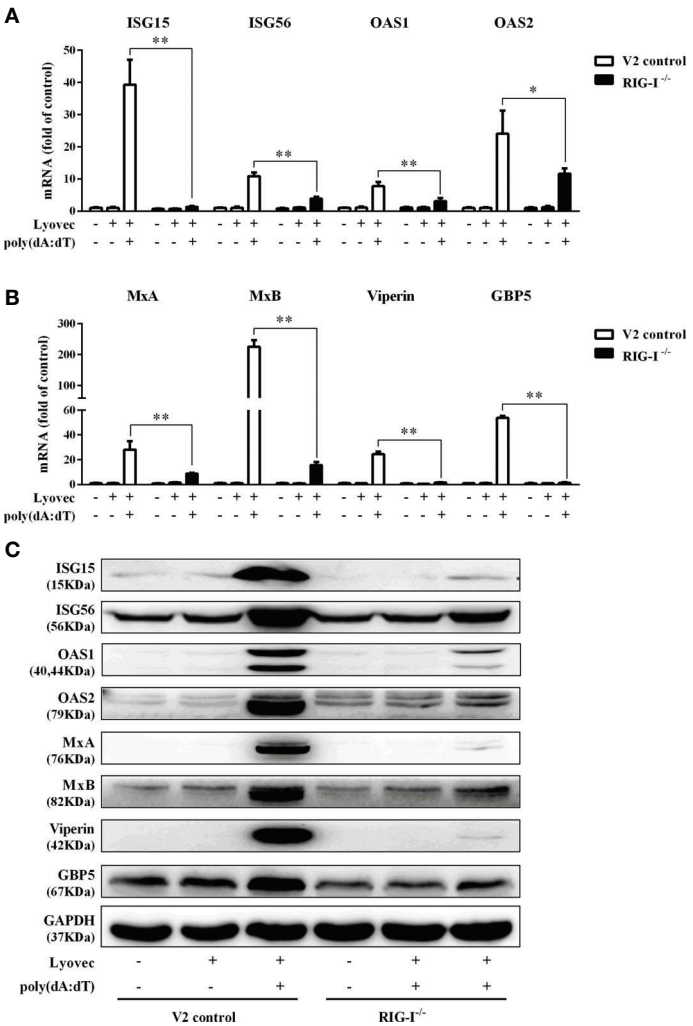

FIGURE 12 | Effect of RIG-I knockout on poly(dA:dT)-induced ISGs expression. **(A, B)** End1/E6E7 control cells (V2 control) and RIG-I knockout End1/E6E7 cells (RIG-I$^{-/-}$) were transfected with or without poly(dA:dT) (0.5μg/ml) for 12h. Total cellular RNAs were extracted and subjected to the real-time PCR for ISG15, ISG56, OAS1, OAS2, MxA, MxB, viperin, and GBP5 expression. **(C)** V2 control and RIG-I$^{-/-}$ cells were transfected with or without poly(dA:dT) (0.5μg/ml) for 24h. Cellular proteins were collected and subjected to Western blot with the antibodies against ISG15, ISG56, OAS1, OAS2, MxA, MxB, viperin, GBP5, and GAPDH, respectively. The results are the mean ± SD of three independent experiments. Asterisks indicate that the differences between the indicated groups are statistically significant (*$P < 0.05$, **$P < 0.01$).

Furthermore, poly(dA:dT) treatment induced the expression of several key antiviral ISGs (**Figure 6**), including ISG15, ISG56, OAS1, OAS2, MxA, MxB, viperin, and GBP5, some of which are known to have the ability to inhibit HSV-2 infection. For example, OAS1 can directly inhibit HSV-2 proliferation (48), MxB interferes with viral replication through blocking the uncoating of viral DNA from the incoming viral capsid (49), ISG15 and ISG15-conjugates have multiple antiviral functions including inhibition of virus release and replication (50, 51). Therefore, the induction of these anti-HSV-2 ISGs provides a sound mechanism for poly(dA:dT)-mediated HSV-2 inhibition.

To determine the initial recognition molecule(s) for the poly (dA:dT) action on HSV-2 inhibition and IFN/ISGs induction, we first examined the effect of poly(dA:dT) on the expression of the DNA sensors. We found that poly(dA:dT) had little effect on the expression of the DNA sensors at both mRNA and protein levels (**Figures 7A, B**). In addition, we failed to identify a specific DNA sensor that plays a major role in poly(dA:dT)-mediated IFN/ISG induction (data not shown). In contrast, poly(dA:dT) could significantly induce the RIG-I expression in the cells (**Figures 7C, D**). Importantly, the vital role of RIG-I in the poly(dA:dT) actions was shown in the experiments using RIG-I$^{-/-}$ and the parental control cells (**Figure 1A**). We observed that while poly (dA:dT) could significantly inhibit HSV-2 replication in the parental control cells, it had little effect on HSV-2 infectivity in RIG-I$^{-/-}$ cells (**Figures 8** and **9**). In addition, RIG-I$^{-/-}$ cells

lacked the effective response to poly(dA:dT) stimulation and expressed significantly lower levels of IFN-β and IFN-λ, p-IRF3 and p-IRF7 than the control cells (**Figure 10**). Similarly, the expression of p-STAT1, p-STAT2, ISGF-3γp48, and the antiviral ISGs was lower in RIG-I$^{-/-}$ cells as compared with that in the control cells (**Figures 11** and **12**). Finally, the important role of RIG-I in the intracellular innate immunity against HSV-2 was also supported by the observation that RIG-I levels in HSV-2-infected cells were lower than those in uninfected cells, particularly in the cells infected and transfected with poly(dA:dT). The decreased expression of RIG-I in the infected cells is likely due to the negative effects of HSV-2 on the intracellular antiviral innate immunity, which is one of the strategies for the virus to escape the host cell immune response. These combined observations indicate that RIG-I is indeed a necessary and key sensor for poly(dA:dT)-mediated activation of IFN/STAT signaling pathways and HSV-2 inhibition. Therefore, it is possible that the interaction of poly(dA:dT) with RIG-I through RNA polymerase (Pol) III is crucial in initiating intracellular anti-HSV-2 innate immunity (**Figure 13**). Chiu et al. (17) reported that poly(dA-dT) serves as a template for the *de novo* synthesis of poly(A-U) RNA by DNA-dependent RNA Pol III. They showed that Pol-III is responsible for the synthesis of the RNA from poly(dA-dT), which binds directly to RIG-I. Cheng et al. also demonstrated that RIG-I is essential for B form (AT-rich) dsDNA signaling pathway as poly(dA-dT) is converted by RNA Pol III of the host cell into a 5' triphosphate RNA intermediate, which can be recognized by RIG-I (52).

Collectively, our study for the first time has demonstrated that the activation of the RIG-I by poly(dA:dT) could effectively inhibit HSV-2 infection of human cervical epithelial cells. While the precise cellular and molecular mechanisms for poly(dA:dT)-mediated HSV-2 inhibition remain to be determined, the induction of IFNs and the multiple antiviral ISGs should be largely responsible for much of poly(dA:dT)-mediated anti-HSV-2 activity. These findings are clinically significant as they indicate that activating the intracellular innate immunity by poly(dA:dT) has potential for the prevention and treatment of HSV-2 infection. However, future *ex vivo* and *in vivo* investigations in animal models and clinical studies are necessary in order to determine whether poly(dA:dT) is effective in activating FRT innate immunity and beneficial for protecting human cervical epithelial cells from HSV-2 infection. These future studies will be crucial for the design and development of AT-rich dsDNA-based intervention strategies to control HSV-2 mucosal transmission in FRT.

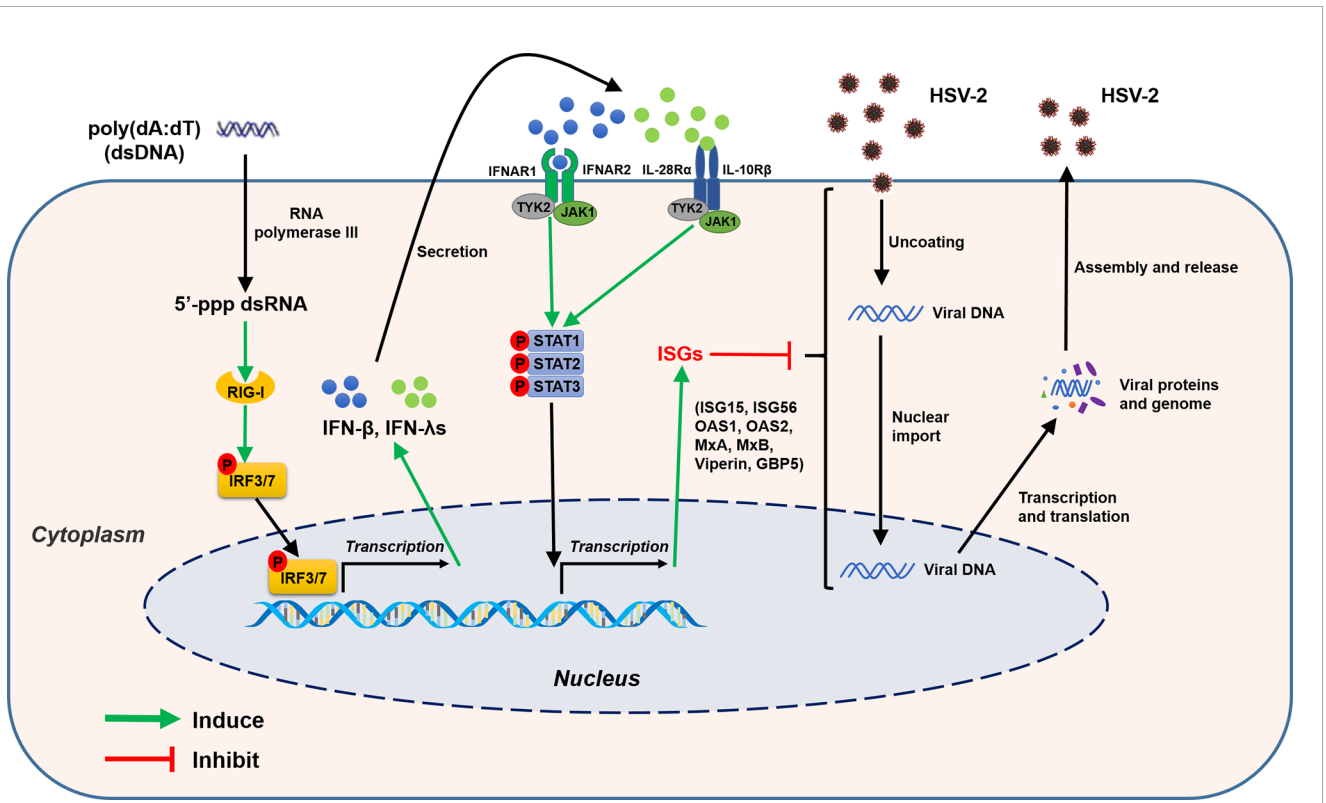

FIGURE 13 | Schematic diagram of mechanisms for poly(dA:dT)-mediated HSV-2 inhibition in human cervical epithelial cells. Poly(dA:dT) can be recognized by RNA polymerase III which then converts DNA into 5'-ppp RNA, the ligand for RIG-I. The activation of RIG-I facilitates the phosphorylation and translocation of IRF3 and IRF7, resulting in the production of IFNs. The released IFNs bind to their corresponding receptors on the cell surface, and trigger JAK/STAT signaling pathway, facilitating STATs phosphorylation and inducing the antiviral ISGs (ISG15, ISG56, OAS1, OAS2, MxA, MxB, viperin, GBP5) which have the ability to block or inhibit HSV-2 at different steps of replication cycle.

DATA AVAILABILITY STATEMENT

The raw data supporting the conclusions of this article will be made available by the authors, without undue reservation.

AUTHOR CONTRIBUTIONS

D-DS and F-ZM performed most experiments and analyzed the data. YL, X-QX, XW, and W-HH helped with some experiments. D-DS, F-ZM, W-ZH, and WH wrote the manuscript. D-DS, F-ZM, W-ZH, and WH reviewed and revised the manuscript. All authors contributed to the article and approved the submitted version.

ACKNOWLEDGMENTS

We thank Qinxue Hu (State Key Laboratory of Virology, Wuhan Institute of Virology, Chinese Academy of Sciences) for providing the HSV-2 G strain.

REFERENCES

1. Looker KJ, Magaret AS, May MT, Turner KM, Vickerman P, Gottlieb SL, et al. Global and Regional Estimates of Prevalent and Incident Herpes Simplex Virus Type 1 Infections in 2012. *PloS One* (2015) 10(10):e0140765. doi: 10.1371/journal.pone.0140765
2. Freeman EE, Weiss HA, Glynn JR, Cross PL, Whitworth JA, Hayes RJ. Herpes simplex virus 2 infection increases HIV acquisition in men and women: systematic review and meta-analysis of longitudinal studies. *Aids* (2006) 20 (1):73–83. doi: 10.1097/01.aids.0000198081.09337.a7
3. Gray RH, Wawer MJ, Brookmeyer R, Sewankambo NK, Serwadda D, Wabwire-Mangen F, et al. Probability of HIV-1 transmission per coital act in monogamous, heterosexual, HIV-1-discordant couples in Rakai, Uganda. *Lancet* (2001) 357(9263):1149–53. doi: 10.1016/S0140-6736(00)04331-2
4. Schacker T, Zeh J, Hu HL, Hill E, Corey L. Frequency of symptomatic and asymptomatic herpes simplex virus type 2 reactivations among human immunodeficiency virus-infected men. *J Infect Dis* (1998) 178(6):1616–22. doi: 10.1086/314486
5. Augenbraun M, Feldman J, Chirgwin K, Zenilman J, Clarke L, DeHovitz J, et al. Increased genital shedding of herpes simplex virus type 2 in HIV-seropositive women. *Ann Intern Med* (1995) 123(11):845–7. doi: 10.7326/0003-4819-123-11-199512010-00006
6. Schiffer JT, Gottlieb SL. Biologic interactions between HSV-2 and HIV-1 and possible implications for HSV vaccine development. *Vaccine* (2019) 37 (50):7363–71. doi: 10.1016/j.vaccine.2017.09.044
7. Looker KJ, Elmes JAR, Gottlieb SL, Schiffer JT, Vickerman P, Turner KME, et al. Effect of HSV-2 infection on subsequent HIV acquisition: an updated systematic review and meta-analysis. *Lancet Infect Dis* (2017) 17(12):1303–16. doi: 10.1016/S1473-3099(17)30405-X
8. Wira CR, Grant-Tschudy KS, Crane-Godreau MA. Epithelial cells in the female reproductive tract: a central role as sentinels of immune protection. *Am J Reprod Immunol* (2005) 53(2):65–76. doi: 10.1111/j.1600-0897.2004.00248.x
9. Blaskewicz CD, Pudney J, Anderson DJ. Structure and function of intercellular junctions in human cervical and vaginal mucosal epithelia. *Biol Reprod* (2011) 85(1):97–104. doi: 10.1095/biolreprod.110.090423
10. Zhao X, Deak E, Soderberg K, Linehan M, Spezzano D, Zhu J, et al. Vaginal submucosal dendritic cells, but not Langerhans cells, induce protective Th1 responses to herpes simplex virus-2. *J Exp Med* (2003) 197(2):153–62. doi: 10.1084/jem.20021109
11. MacDonald EM, Savoy A, Gillgrass A, Fernandez S, Smieja M, Rosenthal KL, et al. Susceptibility of human female primary genital epithelial cells to herpes simplex virus, type-2 and the effect of TLR3 ligand and sex hormones on infection. *Biol Reprod* (2007) 77(6):1049–59. doi: 10.1095/biolreprod.107.063933
12. Zhou L, Li JL, Zhou Y, Liu JB, Zhuang K, Gao JF, et al. Induction of interferon-lambda contributes to TLR3 and RIG-I activation-mediated inhibition of herpes simplex virus type 2 replication in human cervical epithelial cells. *Mol Hum Reprod* (2015) 21(12):917–29. doi: 10.1093/molehr/gav058
13. Xu XQ, Liu Y, Zhang B, Liu H, Shao DD, Liu JB, et al. IL-22 suppresses HSV-2 replication in human cervical epithelial cells. *Cytokine* (2019) 123:154776. doi: 10.1016/j.cyto.2019.154776
14. Liu Y, Xu X-Q, Zhang B, Gu J, Meng F-Z, Liu H, et al. BowmanBirk Inhibitor Suppresses Herpes Simplex Virus Type 2Infection of Human Cervical Epithelial Cells. *Viruses* (2018) 10(10):557. doi: 10.3390/v10100557
15. Xu XQ, Guo L, Wang X, Liu Y, Liu H, Zhou RH, et al. Human Cervical Epithelial Cells Release Antiviral Factors and Inhibit HIV Replication in Macrophages. *J Innate Immun* (2019) 11(1):29–40. doi: 10.1159/000490586
16. Ablasser A, Bauernfeind F, Hartmann G, Latz E, Fitzgerald KA, Hornung V. RIG-I-dependent sensing of poly(dA:dT) through the induction of an RNA polymerase III-transcribed RNA intermediate. *Nat Immunol* (2009) 10 (10):1065–72. doi: 10.1038/ni.1779
17. Chiu YH, Macmillan JB, Chen ZJ. RNA polymerase III detects cytosolic DNA and induces type I interferons through the RIG-I pathway. *Cell* (2009) 138 (3):576–91. doi: 10.1016/j.cell.2009.06.015
18. Bauernfeind F, Ablasser A, Kim S, Bartok E, Hornung V. An unexpected role for RNA in the recognition of DNA by the innate immune system. *RNA Biol* (2010) 7(2):151–7. doi: 10.4161/rna.7.2.11058
19. Paz S, Sun Q, Nakhaei P, Romieu-Mourez R, Goubau D, Julkunen I, et al. Induction of IRF-3 and IRF-7 phosphorylation following activation ofthe RIG-I pathway. *Cell Mol Biol (Noisy-le-Grand France)* (2006) 52:17–28. doi: 10.1170/T694
20. Sato S, Li K, Kameyama T, Hayashi T, Ishida Y, Murakami S, et al. The RNA Sensor RIG-I Dually Functions as an Innate Sensor and Direct Antiviral Factor for Hepatitis B Virus. *Immunity* (2015) 42(1):123–32. doi: 10.1016/j.immuni.2014.12.016
21. Hemann EA, Gale M, Savan R. Interferon Lambda Genetics and Biology in Regulation of Viral Control. *Front Immunol* (2017) 8(1707). doi: 10.3389/fimmu.2017.01707
22. Hirata Y, Broquet AH, Menchen L, Menchen L, Kagnoff MF. Activation of innate immune defense mechanisms by signaling through RIG-I/IPS-1 in intestinal epithelial cells. *J Immunol* (2007) 179(8):5425–32. doi: 10.4049/jimmunol.179.8.5425
23. Chauveau E, Doceul V, Lara E, Adam M, Breard E, Sailleau C, et al. Sensing and control of bluetongue virus infection in epithelial cells via RIG-I and MDA5 helicases. *J Virol* (2012) 86(21):11789–99. doi: 10.1128/JVI.00430-12
24. Le Goffic R, Pothlichet J, Vitour D, Fujita T, Meurs E, Chignard M, et al. Cutting Edge: Influenza A virus activates TLR3-dependent inflammatory and RIG-I-dependent antiviral responses in human lung epithelial cells. *J Immunol* (2007) 178(6):3368–72. doi: 10.4049/jimmunol.178.6.3368
25. Fichorova RN, Rheinwald JG, Anderson DJ. Generation of papillomavirus-immortalized cell lines from normal human ectocervical, endocervical, and vaginal epithelium that maintain expression of tissue-specific differentiation proteins. *Biol Reprod* (1997) 57(4):847–55. doi: 10.1095/biolreprod57.4.847
26. Pandit H, Kale K, Yamamoto H, Thakur G, Rokade S, Chakraborty P, et al. Surfactant Protein D Reverses the Gene Signature of Transepithelial HIV-1 Passage and Restricts the Viral Transfer Across the Vaginal Barrier. *Front Immunol* (2019) 10:264. doi: 10.3389/fimmu.2019.00264
27. Zadora PK, Chumduri C, Imami K, Berger H, Mi Y, Selbach M, et al. Integrated Phosphoproteome and Transcriptome Analysis Reveals Chlamydia-Induced Epithelial-to-Mesenchymal Transition in Host Cells. *Cell Rep* (2019) 26(5):1286–302.e8. doi: 10.1016/j.celrep.2019.01.006

28. Shalem O, Sanjana NE, Hartenian E, Shi X, Scott DA, Mikkelson T, et al. Genome-scale CRISPR-Cas9 knockout screening in human cells. *Science* (2014) 343(6166):84–7. doi: 10.1126/science.1247005
29. Sanjana NE, Shalem O, Zhang F. Improved vectors and genome-wide libraries for CRISPR screening. *Nat Methods* (2014) 11(8):783–4. doi: 10.1038/nmeth.3047
30. Unterholzner L. The interferon response to intracellular DNA: why so many receptors? *Immunobiology* (2013) 218(11):1312–21. doi: 10.1016/j.imbio.2013.07.007
31. Zhang Z, Yuan B, Bao M, Lu N, Kim T, Liu YJ. The helicase DDX41 senses intracellular DNA mediated by the adaptor STING in dendritic cells. *Nat Immunol* (2011) 12(10):959–65. doi: 10.1038/ni.2091
32. Wu J, Sun L, Chen X, Du F, Shi H, Chen C, et al. Cyclic GMP-AMP is an endogenous second messenger in innate immune signaling by cytosolic DNA. *Science* (2013) 339(6121):826–30. doi: 10.1126/science.1229963
33. Ablasser A, Chen ZJ. cGAS in action: Expanding roles in immunity andinflammation. *Science* (2019) 363(6431):eaat8657. doi: 10.1126/science.aat8657
34. Ablasser A, Goldeck M, Cavlar T, Deimling T, Witte G, Röhl I, et al. cGAS produces a 2′-5′-linked cyclic dinucleotide second messenger that activates STING. *Nature* (2013) 498(7454):380–4. doi: 10.1038/nature12306
35. Wu J, Sun L, Chen X, Du F, Shi H, Chen C, et al. Cyclic GMP-AMP Is an Endogenous Second Messenger in Innate Immune Signaling by Cytosolic DNA. *Science* (2013) 339(6121):826. doi: 10.1126/science.1229963
36. Takaoka A, Wang Z, Choi MK, Yanai H, Negishi H, Ban T, et al. DAI (DLM-1/ZBP1) is a cytosolic DNA sensor and an activator of innate immune response. *Nature* (2007) 448(7152):501–5. doi: 10.1038/nature06013
37. Eriksson K, Svensson A, Hait AS, Schluter K, Tunback P, et al. Cutting Edge: Genetic Association between IFI16 Single NucleotidePolymorphisms and Resistance to Genital Herpes Correlates with IFI16 Expression Levels and HSV-2-Induced IFN-beta Expression. *J Immunol* (2017) 199(8):2613–7. doi: 10.4049/jimmunol.1700385
38. Kerur N, Veettil MV, Sharma-Walia N, Bottero V, Sadagopan S, Otageri P, et al. IFI16 acts as a nuclear pathogen sensor to induce the inflammasome in response to Kaposi Sarcoma-associated herpesvirus infection. *Cell Host Microbe* (2011) 9(5):363–75. doi: 10.1016/j.chom.2011.04.008
39. Monroe KM, Yang Z, Johnson JR, Geng X, Doitsh G, Krogan NJ, et al. IFI16 DNA Sensor Is Required for Death of Lymphoid CD4 T Cells Abortively Infected with HIV. *Science* (2014) 343(6169):428. doi: 10.1126/science.1243640
40. Stetson DB, Medzhitov R. Recognition of Cytosolic DNA Activates an IRF3-Dependent Innate Immune Response. *Immunity* (2006) 24(1):93–103. doi: 10.1016/j.immuni.2005.12.003
41. Ishii KJ, Coban C, Kato H, Takahashi K, Torii Y, Takeshita F, et al. A Toll-like receptor–independent antiviral response induced by double-stranded B-form DNA. *Nat Immunol* (2006) 7(1):40–8. doi: 10.1038/ni1282
42. Lazear HM, Nice TJ, Diamond MS. Interferon-lambda: Immune Functions at Barrier Surfaces and Beyond. *Immunity* (2015) 43(1):15–28. doi: 10.1016/j.immuni.2015.07.001
43. Honda K, Takaoka A, Taniguchi T. Type I interferon [corrected] gene induction by the interferon regulatory factor family of transcription factors. *Immunity* (2006) 25(3):349–60. doi: 10.1016/j.immuni.2006.08.009
44. Osterlund PI, Pietila TE, Veckman V, Kotenko SV, Julkunen I. IFN regulatory factor family members differentially regulate the expression of type III IFN (IFN-lambda) genes. *J Immunol* (2007) 179(6):3434–42. doi: 10.4049/jimmunol.179.6.3434
45. Raz R, Durbin JE, Levy DE. Acute phase response factor and additional members of the interferon-stimulated gene factor 3 family integrate diverse signals from cytokines, interferons, and growth factors. *J Biol Chem* (1994) 269(39):24391–5. doi: 10.1016/S0021-9258(19)51096-1
46. Akira S. IL-6-regulated transcription factors. *Int J Biochem Cell Biol* (1997) 29 (12):1401–18. doi: 10.1016/S1357-2725(97)00063-0
47. Tomic J, Lichty B, Spaner DE. Aberrant interferon-signaling is associated with aggressive chronic lymphocytic leukemia. *Blood* (2011) 117(9):2668–80. doi: 10.1182/blood-2010-05-285999
48. Kristiansen H, Scherer CA, McVean M, Iadonato SP, Vends S, Thavachelvam K, et al. Extracellular 2'-5' oligoadenylate synthetase stimulates RNase L-independent antiviral activity: a novel mechanism of virus-induced innate immunity. *J Virol* (2010) 84(22):11898–904. doi: 10.1128/JVI.01003-10
49. Crameri M, Bauer M, Caduff N, Walker R, Steiner F, Franzoso FD, et al. MxB is an interferon-induced restriction factor of human herpesviruses. *Nat Commun* (2018) 9(1):1980–0. doi: 10.1038/s41467-018-04379-2
50. Morales DJ, Lenschow DJ. The antiviral activities of ISG15. *J Mol Biol* (2013) 425(24):4995–5008. doi: 10.1016/j.jmb.2013.09.041
51. Perng Y-C, Lenschow DJ. ISG15 in antiviral immunity and beyond. *Nat Rev Microbiol* (2018) 16(7):423–39. doi: 10.1038/s41579-018-0020-5
52. Cheng G, Zhong J, Chung J, Chisari FV. Double-stranded DNA and double-stranded RNA induce a common antiviral signaling pathway in human cells. *Proc Natl Acad Sci* (2007) 104(21):9035. doi: 10.1073/pnas.0703285104

Conflict of Interest: The authors declare that the research was conducted in the absence of any commercial or financial relationships that could be construed as a potential conflict of interest.

Advantages of publishing in Frontiers

OPEN ACCESS
Articles are free to read for greatest visibility and readership

FAST PUBLICATION
Around 90 days from submission to decision

HIGH QUALITY PEER-REVIEW
Rigorous, collaborative, and constructive peer-review

TRANSPARENT PEER-REVIEW
Editors and reviewers acknowledged by name on published articles

Frontiers
Avenue du Tribunal-Fédéral 34
1005 Lausanne | Switzerland

Visit us: www.frontiersin.org
Contact us: frontiersin.org/about/contact

REPRODUCIBILITY OF RESEARCH
Support open data and methods to enhance research reproducibility

DIGITAL PUBLISHING
Articles designed for optimal readership across devices

FOLLOW US
@frontiersin

IMPACT METRICS
Advanced article metrics track visibility across digital media

EXTENSIVE PROMOTION
Marketing and promotion of impactful research

LOOP RESEARCH NETWORK
Our network increases your article's readership